

UNCLASSIFIED

AD NUMBER
AD110693
NEW LIMITATION CHANGE
TO Approved for public release, distribution unlimited
FROM Distribution authorized to U.S. Gov't. agencies and their contractors; Administrative/Operational Use; Oct 1957. Other requests shall be referred to Wright Air Development Center, Wright-Patterson AFB, OH 45433.
AUTHORITY
USAFAMRL ltr, 3 Jan 1985

THIS PAGE IS UNCLASSIFIED

UNCLASSIFIED

AD 110693

DEFENSE DOCUMENTATION CENTER

FOR

SCIENTIFIC AND TECHNICAL INFORMATION

CAMERON STATION ALEXANDRIA, VIRGINIA



UNCLASSIFIED

NOTICE: When government or other drawings, specifications or other data are used for any purpose other than in connection with a definitely related government procurement operation, the U. S. Government thereby incurs no responsibility, nor obligation whatsoever; and the fact that the Government may have formulated, furnished, or in any way supplied the said drawings, specifications, or other data is not to be regarded by implication or otherwise as in any manner licensing the holder or any other person or corporation, or conveying any right or permission to manufacture, use or sell any patented invention that may in any way be related thereto.

NOTICES

When Government drawings, specifications, or other data are used for any purpose other than in connection with a definitely related Government procurement operation, the United States Government thereby incurs no responsibility nor any obligation whatsoever; and the fact that the Government may have formulated, furnished, or in any way supplied the said drawings, specifications, or other data, is not to be regarded by implication or otherwise as in any manner licensing the holder or any other person or corporation, or conveying any rights or permission to manufacture, use, or sell any patented invention that may in any way be related thereto.

Qualified requesters may obtain copies of this report from the ASTIA Document Service Center, Knott Building, Dayton 2, Ohio.

This report has been released to the Office of Technical Services, U. S. Department of Commerce, Washington 25, D. C., for sale to the general public.

Copies of WADC Technical Reports and Technical Notes should not be returned to the Wright Air Development Center unless return is required by security considerations, contractual obligations, or notice on a specific document.

WADC TECHNICAL REPORT 56-524
ASTIA DOCUMENT NR AD-110693

DYNAMIC RESPONSE OF HUMAN OPERATORS

Duane T. McKuer
CONTROL SPECIALISTS, INC.

Ezra S. Krendel
THE FRANKLIN INSTITUTE

OCTOBER 1957

FLIGHT CONTROL LABORATORY
CONTRACT AF33(616)-3080
PROJECT 1345

AERO MEDICAL LABORATORY
CONTRACT AF33(616)-2804
PROJECT 1182

WRIGHT AIR DEVELOPMENT CENTER
AIR RESEARCH AND DEVELOPMENT COMMAND
UNITED STATES AIR FORCE
WRIGHT-PATTERSON AIR FORCE BASE, OHIO

ABSTRACT

This report presents the results of a concerted effort to arrive at a suitable mathematical description of human operator dynamic response. The investigation has been primarily concerned with operations in which continuous closed-loop control is exerted in a visual input, manual output tracking situation subjected to excitation by random appearing forcing functions.

The basic input to the study was a relatively large body of data on human response characteristics, some available from earlier investigators and some from concurrent experiments. All of the data available, published or unpublished, were considered in arriving at the various descriptions of interest. Generally speaking the best-designed and instrumented experiments yield data in two parts. The first is that portion of the operator output response linearly coherent with his input and generally taking a describing function form which involves amplitude and phase information as a function of frequency. The second is that portion of the operator's response not linearly coherent with his input, the "remnant". This latter part, by its basic nature must be described by statistical quantities. A portion of the report is devoted to an exposition of the mathematical basis for the models derived and measurements taken, and possible sources of the remnant.

All of the quasi-linear describing function data obtained, including some presented for the first time, were curve-fitted to yield simple mathematical expressions which are descriptive of the linear portion of the operator's response for varying machine dynamics and forcing functions. The available remnant data statistics are correlated with task difficulty and an attempt is made to "explain" the remnant in terms of three logically distinct sources, each resulting in equivalent operator output power. On the basis of these correlations and explanations it appears possible to define mathematically, within limits, the dynamic behavior of the operator for the class of tasks considered. The definition becomes increasingly questionable as the demands of the tasks increase. The simple tasks can further be used to define a "preferred" operator describing function form so that definitive criteria for the improvement of a man-controlled machine is established.

PUBLICATION REVIEW

This report has been reviewed and is approved.

FOR THE COMMANDER:

John L. Martin, Jr.
JOHN L. MARTIN, JR.
Colonel, USAF
Chief, Flight Control Laboratory
Directorate of Development

Jack Bollerud
JACK BOLLERUD
Colonel, USAF (MC)
Chief, Aero Medical Laboratory
Directorate of Research

TABLE OF CONTENTS

INTRODUCTION	1
Project Background	1
Description of the Human Operator	3
General Organization and Brief Summary of the Report	4
Section I. TYPES OF MANUAL CONTROL SYSTEMS	7
Section II. GENERAL BACKGROUND FOR HUMAN DYNAMICS RESEARCH	11
A. The Role of Psychology	11
B. The Engineer's Contribution	13
Section III. MATHEMATICAL MODELS FOR MANUAL CONTROL SYSTEMS AND QUASI-LINEARIZATION TECHNIQUES	17
A. Introduction	17
B. Quasi-linear Describing Functions	19
1. Sinusoidal Input Describing Functions	20
2. "n" Input Describing Functions	22
3. Step Input Describing Function	28
C. The Measurement of General System Quasi-linear Describing Characteristics	31
1. Determination of the Open Loop Describing Function, Y	34
2. The Spectral Density of the Remnant	35
3. Power Spectra of the Error and the Mean-squared Error	35
4. Definition of the "Linear Correlation" and the Signal to Noise Ratio	36
5. Possible Sources of the Remnant Term	37
a. Operator Response to Other Inputs	37
b. Nonlinear Transfer Behavior	37
c. Injection of Noise Into the Loop	37
d. Nonsteady Behavior of the Operator	37
Section IV. OPERATOR RESPONSE TO SIMPLE VISUAL INPUTS	45
A. The Operator's Response to Single Visual Step Inputs	45
B. The Operator's Response to a Visual Sequence of Steps	50
C. The Operator's Response to Visual Simple Periodic and other "Completely Predictable" Functions	51
Section V. LINEAR OPERATOR RESPONSE TO RANDOM APPEARING VISUAL FORCING FUNCTIONS IN COMPENSATORY TASKS WITH NO CONTROLLED ELEMENT DYNAMICS	55
A. Introduction	55
B. Human Operator Transfer Characteristics in Compensatory Systems with no Controlled Element Dynamics	56

1. Elkind's Compensatory Experiments	56
a. General Experimental Results on Open Loop Describing Functions	59
1. Experiment II - Amplitude	59
2. Experiment III - Bandwidth	61
3. Experiment IV - Shape	64
b. Analytical Approximations to the Open Loop Describing Function Data	67
c. Relationships Between the Derived Models and Input Characteristics	70
d. Attempts to Apply Conventional Servo Criteria to Elkind's Results	73
2. Russell's Simple Tracker	77
3. The Franklin Institute Simple Tracker	83
C. Human Operator Remnant Characteristics in Compensatory Systems with no Controlled Element Dynamics	87
1. Linear Correlations	87
2. Remnant Data and Attempted Explanations	91
a. Noise Models	92
b. Model Based Upon Nonsteady Operator Behavior	106
c. Comparison of the Simple Tracker Data from the Three Sources	109
 Section VI. LINEARIZED OPERATOR RESPONSE TO RANDOM APPEARING VISUAL FORCING FUNCTIONS IN COMPENSATORY TASKS WITH CONTROLLED ELEMENT DYNAMICS	113
A. Introduction	113
B. The Russell Data	115
1. The Effect of Gain Changes in Controlled Element: $Y_c = K_c$	115
2. Effects of Insertion of a Simple Lag: $Y_c = 1/(Ts + 1)$	115
3. Effect of Insertion of Pure Integration: $Y_c = 1/s$	115
4. Effect of Insertion of Lead-Pure Lag: $Y_c = (T_s + 1)/s$	120
5. Effect of Insertion of Lag-Lead: $Y_c = [a(Ts + 1)/(aTs + 1)]$	120
6. Effect of $1/(Ts + 1)$ in Postfilter and $(Ts + 1)/(Ts + 10)$ in Prefilter Positions	120
7. Effect of a Quadratic Controlled Element: $K_c/[s/\omega_n)^2 + (2\zeta s)/\omega_n + 1]$	123
C. The Tustin Data	123
D. The Franklin Institute F-80A Simulator Data	127
1. The F-80A Simulator	127
2. Experimental Procedure	131
3. The Accuracy of Spectral Estimates	133
4. The Data Reduction Equipment	137
5. Measured Describing Functions	139
6. The Remnant and Tracking Errors	150
 Section VII. THE VARIABILITY OF DESCRIBING FUNCTION DATA	169
A. Introduction	169
B. Variability in Simple Man Generated Time Series	169
C. Variability in Tracking Tasks Without Dynamics	171
D. The Variability in Compensatory Tracking Systems with Dynamics	181
 Section VIII. NONLINEAR MODELS OF HUMAN OPERATORS IN COMPENSATORY TASKS	189
A. Introduction	189

B. Goodyear Stationary Mockup Study	189
C. The Second Goodyear Study - Moving Simulator with Piston Engine Fighter Pilot Subjects	195
D. The Third Goodyear Study - Moving Simulator with Jet Fighter Pilot Subjects	198
E. Comparison of Nonlinear and Quasi-Linear Models of Human Operators in Compensatory Tasks	206
1. Describing Function of Goodyear Analog Pilot for Moving Simulator Case	206
2. Remnant for Goodyear Analog Pilot for Moving Simulator Case	208
 Section IX. HYPOTHETICAL MODEL OF THE HUMAN OPERATOR IN COMPENSATORY TASKS	213
A. Summary of Models	213
B. Hypothetical Transfer or Describing Function Model	213
1. Reaction Time Delay	213
2. Neuromuscular Lags	217
3. Indifference Threshold	217
4. Equalization	218
5. Gain Adjustment and Optimizing Behavior	219
6. Hypothetical Transfer Function Model	220
C. Hypothetical Remnant Models	220
 Section X. PREFERRED FORM OF OPERATOR'S DESCRIBING FUNCTION IN COMPENSATORY TASKS - AN INTERIM BASIS FOR MANUAL CONTROL SYSTEM DESIGN	227
 Section XI. COMPARISON OF COMPENSATORY AND PURSUIT TRACKING	233
A. Introduction	233
B. Compensatory vs. Pursuit Tracking without Human Dynamics Measurements	233
C. Compensatory vs. Pursuit Tracking with Human Dynamics Measurements	234
 REFERENCES	243
 DISTRIBUTION LIST	249

LIST OF ILLUSTRATIONS

Figure

Page

Section I

1	Compensatory and Pursuit Displays.....	8
2	Functional Block Diagrams of Simple Manual Control Systems.....	9
3	Equivalent Block Diagrams of Systems With Linearized Operator.....	10

Section III

4	Linear System Representation.....	17
5	Transfer Characteristic For Limiting With Typical Output for a Sinusoidal Input	20
6	Actual Nonlinear and "Equivalent" Linear Characteristics for Limiting.....	21
7	Amplitude Ratio and Phase Due to Limiting	22
8	Gaussian Input Describing Function for Limiting	25
9	Block Diagram of a Simple Feedback System Containing a Limiter	29
10	Limiter With Actual Input and Output	29
11	Equivalent Limiter Consisting of Describing Function and Remnant.....	30
12	Equivalent Limiter with Remnant Derived From a Linear Operation on the Input	30
13	Equivalent Block Diagram of System with Limiter	30
14	Modified Equivalent Block Diagram of System with Limiter	31
15	Block Diagram Showing Human Operator in Continuous Control Task	33
16	Single and Double Input Systems	38

Section IV

17	Typical Responses in Following Step Displacements of a Moving Line	45
18	Muscle Coordination in the Extension of the Arm	46
19	Cam System and Closed Loop Servo Analogy.....	48
20	Dynamic Portion of the Responses of Subjects to Step Input	49
21	Step Forcing Function Amplitudes	51
22	Response to Closely Spaced, Step-like Irregular Inputs.....	51
23	Typical Parts of the Response to a Simple Sinusoid	52
24	Block Diagrams Representing Phases in the Operator's Response to Sinusoidal Inputs	53

Section V

25	Elkind's Tracking Apparatus	57
26	Types of Power Density Spectra Used in the Elkind Compensatory Study	57
27	Forcing Function Conditions for Elkind's Experiment IV — Shape	59
28	Effect of Amplitude: Mean Closed-Loop Transfer Characteristics	60
29	Experiment III — Open Loop Transfer Characteristics.....	61

Figure

Page

30	Variation of Relative Mean Square Error with Bandwidth of Rectangular Spectra Forcing Function	63
31	Open Loop Transfer Characteristics for RC Filtered Spectra	64
32	Open Loop Transfer Characteristics for Selected Band Forcing Functions	65
33	Example of Data Fitting with Simple Transfer Function	68
34	Gain, K , Versus Frequency of First Break Point, f_0	71
35	Variation of Gain, K , with Cutoff Frequency, f_{co} , For Rectangular Spectra Forcing Functions	71
36	Measured Gain, K , Versus $1/\alpha_f \bar{f}$ for Rectangular Spectra	72
37	Measured Gain, K , Versus $0.39/\alpha_f \bar{f}$ for All Inputs	72
38	Measured Values of $K\alpha_f$ Versus Measured \bar{f} for Bandpass Spectra	72
39	Measured Gain, K , Versus the Parameter $K'_c = 3.8/(\alpha_f e^{7/0.38})$	73
40	Analogous Servosystem to Elkind's Simple Tracker	74
41	Russell's Power Spectra of Low, Medium, and High Speed Forcing Functions and Approximate White Noise Through First Order Filter "Equivalents"	78
42	Russell's Tracking Apparatus	79
43	Block Diagram of Russell's Experimental Setup	79
44	Russell Simple Tracker, Low Speed Forcing Function, Averaged Data	80
45	Russell Simple Tracker, Medium Speed Forcing Function, Averaged Data	81
46	Russell Simple Tracker, High Speed Forcing Function, Averaged Data	82
47	Interior of Cockpit, Franklin Institute Simulator	83
48	Cockpit and Computer Racks, Franklin Institute Simulator	84
49	Franklin F-80A Simulator Characteristics	85
50a	Franklin Simple Tracker, 1 Rad/Sec Forcing Function Bandwidth	86
50b	Franklin Simple Tracker, 2 Rad/Sec Forcing Function Bandwidth	86
51	Linear Correlation Squared, Elkind's Experiment II -- Effect of Forcing Function Amplitude	89
52	Linear Correlation Squared, Elkind's Experiment III -- Effect of Forcing Function Bandwidth	89
53	Linear Correlation Squared, Elkind's Experiment IV -- Effect of Shape (RC Filtered Forcing Functions)	90
54	Linear Correlation Squared, Elkind's Experiment IV -- Effect of Shape (Selected Band Forcing Functions)	90
55	Normalized Remnant for Rectangular Spectra Forcing Functions. Elkind's Experiment III -- Bandwidth	91
56	Remnant Characteristics of the Elkind Compensatory Experiment R.16	94
57	Remnant Characteristics of the Elkind Compensatory Experiment R.24	95
58	Remnant Characteristics of the Elkind Compensatory Experiment R.40	96
59	Remnant Characteristics of the Elkind Compensatory Experiment R.64	97
60	Remnant Characteristics of the Elkind Compensatory Experiment R.96	98
51	Remnant Characteristics of the Elkind Compensatory Experiment R 1.6	99

Figure		Page
62	Remnant Characteristics of the Elkind Compensatory Experiment R 2.4	100
63	Variation of Frequency of First Zero with Cutoff Frequency for Elkind Rectangular Forcing Functions	101
64	Typical Time Variation of Noise and Autocorrelation Function	102
65	Spectrum of $2(T\sigma_n^2)[(\sin \frac{1}{2}\omega T)/(\frac{1}{2}\omega T)]^2$	104
66	Expected Value $\sigma_{\Delta H}^2 = \overline{\Delta H(t)^2}$ vs. Forcing Function Bandwidth, f_{co}	107
67	Sample Variation of the Normalized Autocorrelation	108
68	Comparison of Simple Tracker Data (Franklin and Elkind)	110
69	Comparison of Simple Tracker Data (Franklin and Elkind)	111
70	Comparison of Simple Tracker Data (Franklin and Elkind)	111

Section VI

71	Russell Experimental Characteristics, Before and After Inserting Controlled Element: $Y_c = 1/(s+1)$	116
72	Russell Experimental Characteristics, Before and After Inserting Controlled Element: $Y_c = 1/(s/2+1)$	117
73	Russell Experimental Characteristics, Before and After Inserting Controlled Element: $Y_c = 1/(s/0.2+1)$	118
74	Russell Experimental Characteristics, Before and After Inserting Controlled Element: $Y_c = 1/s$	119
75	Russell Experimental Characteristics, Before and After Inserting Controlled Elements: $Y_c = (s+1)/s$, $Y_c = (s/2+1)/s$	121
76	Russell Experimental Characteristics, Before and After Inserting Controlled Elements: $Y_c = (10rs+10)/(10rs+1)$; $r = 0.5, 2.0$	122
77	Russell Experimental Characteristics, Before and After Inserting Controlled Elements: $Y_c = K_c/[(s/\omega_n)^2 + 2\zeta s/\omega_n + 1]$; $\omega_n = 7.8, 16$; $\zeta = 0.371$	124
78	Tustin Experiments, Controlled Element Dynamics	125
79	Handle Force-Displacement Characteristics for Tustin Data	125
80	Tustin "Aided-Laying" Characteristics	126
81	Tustin Characteristics, "Displacement Speed Control"	126
82	Tustin Residual Data	127
83	The F-80A Simulator Display	128
84	Franklin F-80A Simulator Response in Azimuth	130
85	Franklin F-80A Simulator Response in Elevation	130
86	Block Diagram of the Cross-Spectrum Analyzer	138
87	Cross Spectrum Analyzer	138
88	Comparison of H Computed with H Measured by the Cross Spectrum Analyzer	140
89	A Comparison of H for a Human Operator Measured by Digital and Analog Methods	140
90	F-80A Simulator Open Loop Describing Function for Pilot P-1	141
91	F-80A Simulator Open Loop Describing Function for Pilot P-2	142
92	F-80A Simulator Open Loop Describing Function for Pilot P-3	143

Figure		Page
93	F-80A Simulator Open Loop Describing Function for Pilot P-4	144
94	F-80A Simulator Open Loop Describing Function for Pilot P-5	145
95	F-80A Simulator Open Loop Describing Function for Pilot P-6	146
96	F-80A Simulator Y_p with $\pm\sigma$ Confidence Bands (Lateral; $\omega_{co} = 1$ rad/sec)	148
97	F-80A Simulator Y_p with $\pm\sigma$ Confidence Bands (Lateral; $\omega_{co} = 2$ rad/sec)	149
98	F-80A Simulator Y_p with $\pm\sigma$ Confidence Bands (Longitudinal; $\omega_{co} = 1$ rad/sec)	150
99	F-80A Simulator Y_p with $\pm\sigma$ Confidence Bands (Longitudinal; $\omega_{co} = 2$ rad/sec)	151
100	F-80A Simulator Grand Averages for Y_p in Azimuth Control	152
101	F-80A Simulator Grand Averages for Y_p in Elevation Control	152
102	F-80A Simulator Closed Form Approximations to Y_p for Longitudinal Control	154
103	F-80A Simulator Closed Form Approximations to Y_p for Lateral Control	155
104	Linear Correlations for 6 Pilots with $\pm\sigma$ Confidence Bands (Lateral; $\omega_{co} = 1$ rad/sec)	157
105	Linear Correlations for 6 Pilots with $\pm\sigma$ Confidence Bands (Lateral; $\omega_{co} = 2$ rad/sec)	158
106	Linear Correlations for 6 Pilots with $\pm\sigma$ Confidence Bands (Longitudinal; $\omega_{co} = 1$ rad/sec)	159
107	Linear Correlations for 6 Pilots with $\pm\sigma$ Confidence Bands (Longitudinal; $\omega_{co} = 2$ rad/sec)	160
108	Averaged Linear Correlation for All Pilots with $\pm\sigma$ Confidence Bands	161
109	F-80A Closed Loop Remnant, Lateral Control	162
110	F-80A Closed Loop Remnant, Longitudinal Control	163
111	F-80A Remnant Due to Noise Injected at Operator's Output	163
112	F-80A Remnant Due to Noise Injected at Operator's Input	163
113	Remnant Due to Non-Steady Describing Function	164
114	Averaged Error Spectra, Lateral Control	165
115	Averaged Error Spectra, Longitudinal Control	165
116	Averaged Forcing Function Spectra, Lateral Control	166
117	Averaged Forcing Function Spectra, Longitudinal Control	166

Section VII

118	Smoothed Error Spectra From Indiana Data	173
119a	Input Spectrum For Franklin Step Tracker	174
119b	Franklin Step Input Tracker; The Effect of Instructions	174
120	Russell Simple Tracker; The Effect of Instructions	176
121	A Physiological Cause of Variability	176
122	Elkind's Long Time Variations	178
123	Elkind's Among Subjects Variations	180
124a	Y_p Measured in a Ten Minute Tracking Fatigue Test; Lateral Control ($d = 0.3$ in. rms)	183
124b	Y_p Measured in a Ten Minute Tracking Fatigue Test; Longitudinal Control ($d = 0.3$ in. rms)	183

Figure	Page
124c Relative Closed Loop Remnant, Φ_{nn} , Measured in a Ten Minute Tracking Fatigue Test ($d = 0.3$ in. rms)	184
124d Error Spectrum, Φ_{EE} , Measured in a Ten Minute Tracking Fatigue Test ($d = 0.3$ in. rms)	184
125a Y_p Measured in a Ten Minute Tracking Fatigue Test; Lateral Control ($d = 0.8$ in. rms)	185
125b Y_p Measured in a Ten Minute Tracking Fatigue Test; Longitudinal Control ($d = 0.8$ in. rms)	185
125c Relative Closed Loop Remnant, Φ_{nn} , Measured in a Ten Minute Tracking Fatigue Test ($d = 0.8$ in. rms)	186
125d Error Spectrum, Φ_{EE} , Measured in a Ten Minute Tracking Fatigue Test ($d = 0.8$ in. rms)	186

Section VIII

126 Forcing Function Used in First Goodyear Study	190
127 Record of Forcing Function and Responses from Both a Pilot and the Analog Pilot of Figure 128	192
128 Goodyear "Stationary Mockup" Study, Computer Representation of Human Operator and Controlled Element	193
129 Equivalent Open Loop Bode Plot of Goodyear Computer Set-up, for the Stationary Mockup	194
130 Dynamic Cockpit Mockup Showing Pilot in Position for Roll Studies	196
131 Goodyear Pilot Analog, Dynamic Substitution Test Schematic	197
132 Goodyear Experimental Results for Pilot and Simulator in Parallel	197
133 Goodyear Moving Mockup Controlled Element	199
134 Goodyear Experimental Studies, Power Spectral Density	200
135 Block Diagram of Goodyear Hypothetical Jet Pilot Analog System with Moving Simulator	201
136 Goodyear "Moving Mockup" Study Computer Representation of the Human Operator and Controlled Element	202
137 Phase Shift and Attenuation Characteristics for Pilot Analog Circuit	203
138 Goodyear Experimental Characteristics, Light Plane Pilot with Mockup Pitch	204
139 Goodyear Experimental Characteristics, Proficient Jet Pilot Including Mockup Pitch	204
140 Goodyear Experimental Characteristics, Less Proficient Jet Pilot Including Mockup Pitch	205
141 Goodyear Experimental Characteristics, Less Proficient Jet Pilot with Reduced Aerodynamic Damping	205
142 Goodyear Experimental Characteristics, Less Proficient Jet Pilot with Reduced Aircraft Sensitivity	205
143 Anticipation or Sgn Function Transfer Characteristic	207
144 Threshold Transfer Characteristic	207
145 General Form of Anticipation Circuit Output	208

Section IX

146 Possible Forms of the Operator Model	221
147 Variation of Average Linear Correlation with Task Difficulty (Elkind Rectangular Spectra Forcing Function)	224

Figure**Section XI****Page**

148	Effect of Amplitude: Mean Closed Loop Describing Functions	235
149	Comparison of Closed Loop Describing Functions for Bandwidth Experiment	236
150	Comparison of Closed Loop Describing Functions for Bandwidth Experiment	237
151	Comparison of Closed Loop Describing Functions for Shape Experiment	238
152	Comparison of Closed Loop Describing Functions for Shape Experiment, Selected Bands	239
153	Linear Correlation Squared for Study of an Input Amplitude	240
154	Linear Correlation Squared for Study of Bandwidths	240
155	Pursuit Tracking Configuration with Unity Controlled Element Dynamics	241

LIST OF SYMBOLS

a, A	Constants
a	Defining characteristic of certain-nonlinear transfer elements
$a(t)$	Remnant signal for step inputs
A	Sinusoidal amplitude
b, B	Constants
b_1/A	Weighting function (linear equivalent) for limiting
$c, c(t)$	Operator output
\bar{c}^2	Mean square operator output
C	Transform of operator output
C/E	Russell's open loop operator describing function
d	Forcing function amplitude (rms)
$\Delta e_0(t)$	Operator output discrete response component
E	Transform of error
$E()$	Expected value of ()
f	Frequency
f	Statistical degrees of freedom
f_{co}	Cutoff frequency
f_n	Undamped natural frequency
f_1	Frequency of first zero of a spectrum
$f(t)$	Time function
\bar{f}	Mean frequency of a spectrum
\bar{f}_e	Error spectrum mean frequency
F	Statistical Distribution
F	Transform of time function
\mathfrak{F}	Fourier transformation
\mathfrak{F}^{-1}	Inverse Fourier transformation
$g()$	Arbitrary probability distribution function of ()
$g_n(\omega)$	Polynomial in ω
$G(f), G_1(f)$	Open loop operator describing function (Elkind)
$h(u)$	"Best" weighting function
$h(r)$	Closed loop weighting function; i.e., system time response to impulse function
$h_n(\omega)$	Polynomial in ω
$H, H(s), H(j\omega), H(f)$	Closed loop transfer function
$H(j\omega, t)$	Closed loop, time varying, describing function
$\Delta H(t)$	Time varying component of $H(j\omega, t)$

H_a	Average value of closed loop describing function
$l_0(j\omega)$	Frequency varying component of $H(j\omega, t)$
$i, i(t)$	Forcing function
$l(\omega_c)$	A particular definite integral (abbrev.)
l_2	A particular definite integral (abbrev.)
k	Constant
K, K_p	Human operator transfer function gains
K_c	Calculated gain
K_r	Controlled element gain
\mathcal{L}	Laplace transformation
n	Number of runs used in average
$n, n(t)$	Closed loop remnant
$n(t)$	Operator direct response remnant component
$n_e(t)$	Operator remnant, open loop
$\overline{n^2}$	Mean square closed loop remnant power
N_z	Transform of open loop remnant $\mathcal{Z}\{n_e(t)\}$
p	Airframe rate of roll
p	Pilot (human operator) subscript
$p(x)$	Probability distribution function
$P(n, p)$	Poisson distribution
$P_i(f)$	Pursuit component of operator describing function (Elkind)
q	Airframe rate of pitch
r	Airframe rate of yaw
$r(t)$	System output
R	Correlation function
$R(j\omega), R(s)$	Transform of system output
$R_{cc}(r)$	Output autocorrelation function
$R_{HH}(r, \omega)$	Correlation function of time varying transfer function
$R_{\Delta H \Delta H}$	Autocorrelation of the time varying portion in the closed loop transfer function $H(j\omega, t)$
$R_{ir}(r)$	Forcing function — output cross correlation function
$R_{ii}(r)$	Autocorrelation function of the input
$R_{ir}(r)$	Cross correlation function between input and response
$R_{nn}(r)$	Autocorrelation of the remnant, closed loop
$R_{nne}(r)$	Autocorrelation of the remnant, open loop, at operator's output
$R_{nni}(r)$	Autocorrelation of the remnant, open loop, at operator's input
$R_{ri}(r)$	Cross correlation function between system output and forcing function

$R_{rr}(r)$	Autocorrelation function of the system output
$R_{ee}(0)$	Mean square error
$R_{ee}(r)$	Error autocorrelation
s	Laplace operator
t	Time
T	Time limit of integration
T	Transfer function time constant
T_I	General lag time constant for human operator transfer function
T_L	General lead time constant for human operator transfer function
T_N	General lag time constant (neuromuscular)
T_0, T_1	Elkind forms equivalent to T_I and T_N
U_0	Airframe steady-state forward velocity
v_i	Velocity input
$w(u), w(x), w(r)$	Optimum weighting function
x	Independent (probability) variable
$X(t)$	Statistical random variable
y_c	Controlled element weighting function
y_p	Operator weighting function (1 input compensatory)
y_{pi}	Operator weighting function (2 input pursuit)
y_{pe}	Operator weighting function (2 input pursuit)
Y	Describing function
$Y(j\omega, t)$	General human operator time varying transfer function
$\Delta Y(t)$	Time varying part of $Y(j\omega, t)$
$Y_0(s)$	Transfer function giving $a(t)$ from $t(t)$ for step input in nonlinear system
Y_e	Controlled Element transfer function
Y_F	Bandpass filter transfer function
Y_N	Neuromuscular lag transfer function
Y_p	Operator describing function
Y_{pe}, Y_{pi}, Y_{pt}	Operator's describing function
$Y_{pt}(s)$	Describing function operating on $I(s)$
Y_{pt}	True value, operator's open loop transfer function
$Y_{pe}(s)$	Describing function operating on $E(s)$
$Y_0(j\omega)$	Frequency varying part of $Y(j\omega, t)$
$z(u), z(x), z(r)$	Arbitrary $f(x)$ with continuous derivative $x_0 < x < x_1$

a	Ratio of lead to lag time constants
a, a_c	Ratio of frequency to natural frequency ($a = \omega/\omega_n$, $a_c = \omega_c/\omega_n$)
β_e	Number of axis crossings, per second, of the error signal
$\epsilon, \epsilon(t)$	Error
ϵ_H	Small spectral error quantity
ϵ_{in}	Error between input and remnant
$\epsilon_R + j\epsilon_I$	Complex spectral error
ζ	Damping ratio of second order transfer function
θ	Airframe pitch angle
λ	Small coefficient
ρ	Linear correlation
ρ_a	Average linear correlation
σ	Standard deviation
σ_f	Spectrum standard deviation
σ^2	Variance
$\sigma_{\Delta H \Delta H}^2$	Mean square value of $\Delta H(t)$
σ_f^2	Mean square value of forcing function
σ_I^2	Instrument and computer errors, component of variance
σ_n^2	Mean square value of remnant
σ_s^2	Sampling errors, component of variance
σ_e^2	Variance of the error spectrum
σ_z^2	Sum of the components of variance σ_I^2 and σ_s^2
Σ	Summation
τ	A variable
τ	General finite time interval
τ	Time delay
τ'	Approximate value of τ
ϕ	Phase angle
ϕ_1	Phase component of ϵ_{H1}
Φ	Spectral quantity
$\Phi(x)$	Error function
Φ_{cc}	Operator output spectral density
Φ_{EE}	Error spectra
Φ_{EEH}	Raw or unsmoothed error spectra
Φ_{FF}	Forcing function spectra
$\Phi_{\Delta H}(\omega)$	Power spectral density of $\Delta H(t)$ due to nonsteady behavior

$\Phi_{\Delta H \Delta H}(\omega)$	Power spectral density of $\Delta H(t)$
Φ_{ie}	Cross spectral density function (forcing function — operator's output)
Φ_{ii}	Forcing function power spectral density
$\Phi_{ii}(\omega)$	Forcing function spectral density
$\Phi_{io}(j\omega)$	Cross spectral density (forcing function — system output)
Φ_{io_c}	Cross spectral density function (forcing function — operator's remnant at output)
Φ_{ie}	Cross spectral density function (forcing function — system error)
$\Phi_m(\omega)$	Measured spectrum
Φ_{ni}	Cross spectral density function (remnant — forcing function)
Φ_{nn}	Closed loop remnant
Φ_{nn_c}	Open loop remnant, operator's output
Φ_{nn_e}	Open loop remnant, operator's input
Φ_p	Spectra (jab lags)
$\Phi_t(\omega)$	True spectrum
Φ_{ee}	Power spectral density of the error
χ^2	Chi-square statistical distribution
ψ	Airframe azimuth angle
ω	Angular velocity (frequency) in rad/sec
ω_{co}	Cutoff frequency (rad/sec)
ω_n	Natural frequency
ω_{ny}	Nyquist or folding frequency
$\langle \rangle$	Ensemble average
\angle	Angle
$ $	Magnitude
Δ	Small (differential) element

DYNAMIC RESPONSE OF HUMAN OPERATORS

INTRODUCTION

PROJECT BACKGROUND

At the present time the Aeromedical and Flight Control Laboratories are sponsoring a series of coordinated contracts with the Franklin Institute, Princeton University and Control Specialists, Inc. aimed at the gathering of human response data and the application of these data to aircraft design. The overall task can be divided conveniently into three logically consecutive phases which outline the specific areas of activity engaged in by the three contractors.

- (1) The development of measurement concepts, and the design of experimental procedures, simulator and data reduction equipment, etc., and their application to the direct measurement of human response characteristics in ground based simulators. This activity, together with human response data-reduction for the entire program, is performed by the Franklin Institute under Contract AF 33(616)-2804. In terms of the overall program, the fundamental research result from Franklin is an indication of what pilots do in a ground simulator environment.
- (2) The design of experimental procedures, simulator and flight test equipment, etc., and their application to the direct measurement of human response characteristics in the air and on the ground. This phase is performed by Princeton University under Contract AF 33(616)-2806. The basic research result is expected to be an indication of the differences in pilot behavior on the ground and in the air.
- (3) The compilation, correlation, and codification of human response data, including pertinent handling quality information, and the analytical application of these correlated data (or their logical extension), to aircraft design. This phase is performed by Control Specialists, Inc. under Contract AF 33(616)-3080. The fundamental research results are expected to be:
 - a. A summary and engineering evaluation of available human operator data resulting in applicable mathematical or analog descriptions representing the pilot as a system element.
 - b. A compilation of pertinent handling quality and pilot opinion data obtained from airframe-pilot flight studies, and an attempt to correlate these data with the operator models derived above.
 - c. The development and assessment of practical engineering methods employing these human response data to pilot-airframe systems.

This report presents both the results achieved by Control Specialists in item 3-c above, and some of the results achieved by the Franklin Institute to date.

From the outset, the overall Air Force program has been predicated on the importance of the pilot as a continuous closed loop control device in the pilot-airframe system. The original emphasis on ground simulation did not imply that the pilot responded to visual inputs only, but rather that such inputs were most important for the tracking tasks under study. A validating flight test program to determine the effects of added inputs due to acceleration and orientation changes during flight, and the effect of an actual versus simulated environment on the pilot's control characteristics was envisioned from the very beginning. This report deals, except for one minor exception, with tracking tasks for which the inputs to the man are visual only. The following practical examples of pilot tasks, which can be called tracking, will make our reasons for emphasizing the visual input channel more obvious:

- a. aspects of the collision type courses flown in rocketry and approach situations

b. pursuit courses flown in gunnery

c. "constant range" tracking in formation flying

d. "infinite range" tracking which approximates in many instances such normal flight stabilization and control problems as rough weather flying, horizontal turn entries and so forth.

The foregoing tasks are all characterized by the fact that they may be difficult to perform, especially when externally applied inputs may be tending to drive the aircraft from the desired course. In some of these situations the pilot is extended to his limits of performance, hence it becomes necessary to examine the other components of the pilot-aircraft system in search of possible techniques to compensate for deteriorating manual performance.

This compensation directed toward the improvement of the pilot-aircraft system would proceed as follows: To begin with, a criterion or criteria of system performance would have to be specified. Then one of two procedures could be followed:

1. Theoretical

The various system elements and their interrelations could be described by some compatible mathematical scheme. Then knowing which elements and interrelations would permit modification, the system could be redesigned about the fixed characteristics to approach or equal the specified optimal performance. In the problem of the pilot-aircraft system the straightforward mathematical scheme to apply is linear servomechanism theory. Consequently the key problem in this approach is to determine the feasibility and then the description, if any, of the key fixed element, the pilot, in terms of servo theory.

2. Empirical

The system would be set up, preferably in the air, though possibly some aspects could be studied by the ground simulation, and the various components of the system varied according to some experimental schedule. As in the theoretical approach the fixed element, the pilot, is the key problem. Either a Standard American Pilot must be supplied for the tests, or an adequate, and presumably large, number of pilots must test the system. Also, since there is no description of the range and adaptability of the pilot's performance available, the only way to determine whether the pilot is tracking at the limit of his ability is to ask him.

It would be extreme to claim that the foregoing dichotomy is complete. In usual practice the two approaches are complementary, although one may be favored over the other. The important point about the two approaches is that they are headed toward the same goal. Should they reach different conclusions about the specifications for systems design, it will be necessary to resolve the differences by a painstaking evaluation of the possible causes of difference.

In human pilot-airframe systems studies these two approaches have been roughly separated into human dynamics research, corresponding to the theoretical approach, and handling qualities research, corresponding to the empirical approach. The respective basic questions being: "What does a pilot do?" and "What does a pilot like?"

The question "What does the pilot like?" is not always asked explicitly since excellent performance is sometimes interpreted as evidence of preference. Actually a large number of human operator performance, as distinct from human dynamics, studies are empirical in the sense we have described. Logical consistency demands that the results of studies applying human response data to airframe pilot systems should be highly correlated with handling quality tests. Since handling qualities tests involve rankings and questionnaire analyses these correlations may be qualitative. If this correlation is not forthcoming, the entire sequence of human pilot research (including portions of many of the ground simulator-display-operator systems programs) will have little value in the design of servo systems composed of the airframe-pilot combination; since pilots, not engineers or psychologists, are the final judges of aircraft handling qualities.

At the outset of C.S.I.'s program there had been no extensive attempt to correlate the mass of existing human operator response data with the even more massive flying quality data, although valuable work had been done

in limited and specific areas. Therefore, such a correlation was considered to be an extremely important part of C.S.I.'s effort.

Before the data obtained in the handling qualities and operator response fields could be compared, it was necessary to codify, correlate and summarize the information within each area. Fortunately, this process was not as awesome as it might have been, as previous workers had already made excellent starts. This was particularly true in the handling qualities field, where flight experience along particular lines is almost invariably compared with the results of other efforts. In the human response measurement field some codification and summaries existed, but little work had been done on showing the compatibility of data from diverse sources.

It was therefore decided that C.S.I.'s efforts would be programmed as follows:

- (1) Summarize and attempt to correlate the various human response studies available.
- (2) Compile, and attempt to correlate, pertinent handling-quality and pilot opinion data obtained from airframe-pilot system flight studies.
- (3) Attempt to correlate the data and hypothesis of (1) with the consequences of (2).
- (4) Finally, if (3) was reasonably successful, apply the human response data to pilot-airframe design problems. This final item was considered to be a meaningful (assuming success on item 3), and relatively simple servo analysis problem.

At the present time a major portion of the work involved in summarizing and correlating the individual fields of human response and handling quality items has been accomplished, though only the first is documented here.

DESCRIPTION OF THE HUMAN OPERATOR

Many agencies and individuals, both in the USA and abroad, have contributed substantially to the state of knowledge of human response characteristics. In most instances, however, their data have not been compared, since different means were used to determine the response data, different tasks were set for the operator, different operator inputs were utilized, only small populations were studied, and the data were presented in different forms. A cursory review of the situation indicates that, even though the data are as yet statistically insufficient, reasonable compatibility may be found between the results; and some generalizations about human behavior in particular tasks can be hypothesized.

The type of human response measurements of most concern to this program are those involved in closed loop control tasks yielding pilots' transfer characteristics for particular routine functions, such as stabilization and tracking. A unique transfer characteristic for even these simple tasks cannot be expected, since a formal description of the pilot will depend upon at least the following factors:

- (1) The characteristics of the controlled elements. (The operator, to be successful, must adapt his transfer characteristics to that form required for adequate stability and performance.)
- (2) The particular type of input imposed and its degree of predictability.
- (3) The actual individual reaction times, thresholds, etc., of the human during the particular operation. (There are variations between one individual and another, which depend on the populations sampled, and even with a single individual at various times. Any proposed set of transfer characteristics would certainly have to allow for individual differences.)
- (4) The motivation, attention, previous training, and general psychological and physiological condition of the human at the time of the operation.

From these considerations, it is clear that our hypothetical mathematical model must be able to describe a mechanism which:

- a. adapts itself in some way as a function of the inputs imposed and elements controlled,
- b. may have fairly wide individual variations in the parameters adopted,

c. is capable of manipulation to a certain extent either by training or at the operator's volition.

At present the individual differences in parameters must be largely ignored since there are few data extant dealing with reasonable populations. Similarly we will be able to say very little about the effects of motivation, attention, and training. The adaptability of the transfer characteristics to both inputs and controlled elements is a different matter, and is used here as a basis of classifying past experiments.

The technique for achieving useful transfer characteristics must account for the following. Firstly, in order to be readily applicable, the transfer characteristic must be linearized, and secondly, this characteristic must be generalizable beyond the measuring experiment. Since it is the verdict of past experimenters that the human operator is nonlinear to some extent in any given task, the foregoing present problems of central importance. This report discusses two approaches to these problems:

- a. a linearized transfer function plus a remnant not derivable from the input by any linear operation
- b. the use of analog computer elements to construct the model.

The generalizability of the measurements, always a problem with nonlinearities, is approached by using what is essentially a very general sort of input function. The direct attack using a nonlinear model has yet to be successfully applied to continuous closed loop human operator tracking.

To have a complete picture of the operator from a pure performance standpoint, we need to know the answers to two questions. The first is:

- a. In a given situation how will the operator perform?
- b. From a performance standpoint, is there anything to be gained by having the operator perform in some specified way?

Partial answers are given to both of these questions in this report. The first is answered by the use of an adaptive-optimizing model developed to be consistent with all of the available data. This model can be used, with caution, for stability and limited performance predictions of manual control systems. The second question is answered by defining the preferred operator form and, in a restricted sense, the human's response when operating with this form.

GENERAL ORGANIZATION AND BRIEF SUMMARY OF THE REPORT

While the report has a total of eleven sections, it can be divided more generally into three major parts. The first part (Sections I-III) is primarily background information to give the reader a general idea of the types of manual control systems of interest here, a comprehension of the historical background of human dynamics research, and a feeling for the mathematical models and techniques required to describe the human operator adequately.

The summary conclusions of the first part of this report are:

- a. There are reasons to hope that a linearized transfer function, i.e., describing function, can be found to characterize manual tracking.
- b. Gaussian input signals are the "appropriate" inputs to be used in obtaining describing functions from human operators. In practice, random appearing inputs are adequate.
- c. The linear correlation between the tracker's input and output, obtained as a function of frequency, is a crucial quantity since it determines the magnitude of the remnant term.
- d. The remnant may be described by various theories. Although it is probable that the remnant arises from a combination of sources, it is impossible to decompose a measured remnant into components which may be assigned to specific sources.

The second part (Sections IV-VIII) constitutes a detailed summary of all the presently available relevant human dynamic response data measured under conditions such that only an error signal was displayed, and a detailed examination and attempted explanation of these data in terms of various mathematical models. The first step of importance taken in these sections is the organization of the data of various experimenters into a common form. This is followed by the development of approximate analytical models to fit the data. Finally, an attempt is made to interpret the data from the individual sources.

The summary conclusions of the second major division of this report are as follows:

- a. It is possible, without doing violence to the data, to obtain describing functions which are generally applicable to the results of the many diverse experiments.
- b. The magnitude of the remnant is directly proportional to the task demands. The task demands, in turn, are mainly functions of the input forcing function and the controlled element's dynamics.
- c. Although motivation, instruction, training, and so forth can increase the variability of describing function measurements, the differences in describing functions due to individual differences can be made negligible by both training and selection procedures. Training alone suffices for simple tasks, whereas for complex tasks, such as flying an aircraft, selection of subjects is quite important.
- d. The results of analog computer simulations of the human operator are compatible with the results of direct measurements of describing functions. Each method complements the other in affording insights of the underlying process.

The third major subdivision of the report (Sections IX and X) is concerned with attempted generalizations of the consequences of the individual data. These generalizations take the forms of hypothetical operator models for the tracking tasks examined. These models are in two categories -- a general one attempting to provide the analyst with a mathematical description of the operator for various system conditions; and the other a "preferred form" which can be used to give the analyst an idea of both the upper limit of system performance and the type of modifications which would be required to the system to achieve this "optimum" condition. By having both of these models, the analyst can assess the performances of particular system configurations and compare them with a more or less theoretical optimum which could be obtained if system performance alone were the sole design objective. Since other factors are often as important as dynamic performance, the designer must usually arrive at a compromise based upon judgment. Having information of the degree of performance degradation, based upon some theoretical (and practically obtainable) optimum, offers extremely valuable assistance in attaining a suitable overall design compromise.

In summary this last major division comes to the following conclusions:

- a. The general operator model is that of an adaptive and optimizing device.
 - i. adaptive in that input signals and controlled element influence the choice of parameters
 - ii. optimizing in that parameters are adjusted for best performance consistent with stability requirements.
- b. The preferred form of human operator performance is one in which no lead terms need be generated, and the operator may or may not act as a smoothing circuit with a long time constant.
- c. Whether the system should be designed about the man so that the demands on him are lightened in the sense of (b) must be determined by overall considerations of logistics, reliability, and so forth.

The final section of the report (Section XI) is a general summary of operator response in pursuit tracking; e.g., tracking tasks for which both the input and the operator's response are displayed and their difference is the error signal. From a logical standpoint pursuit systems should be treated in the same fashion as those systems displaying error only, or compensatory systems, of Sections V through X. Unfortunately, however, the study of

transfer characteristics in pursuit systems has been restricted to a very small number of cases and generalizations cannot be made based solely on these data. We do feel that pursuit systems have merit in many applications, so the section has been added to the report for completeness. The conclusions of Section XI are that pursuit tracking, by allowing the operator to predict and therefore decrease his phase lag, enables the operator to use higher gain. The result of this is better dynamic performance and smaller errors.

Section I

TYPES OF MANUAL CONTROL SYSTEMS

The behavior of human beings as elements in company with other components of control systems will depend both upon the capabilities of the human and on the external environment. By his ability to modify his characteristics to match appropriately the many possible control situations, the human must be considered a unique control system component. The very fact of this adaptation makes description of the operator enormously complex when viewed in the large, and makes it desirable to try to set up some simplified, constant situations within which one may have some hope of obtaining a reasonably simple behavioral model.

In order to deal with the control situation with any degree of confidence, therefore, it is necessary that the goals of the controller and the constraints or rules governing his interactions with the system remain reasonably constant over the duration of interest. Thus if we consider the example of a duck hunter scanning a flock of birds, each exciting his interest and making him hesitate in indecision before aiming for a particular bird, we have a problem of resolution of purpose or goal orientation. Similarly, the hunter might be assumed to have a gun whose behavior was unknown to him, its shot spread, range, recoil, or accuracy might vary in an arbitrary manner. This type of problem illustrates an unfamiliarity with the rules governing the controller's interactions with his environment and his problem. In this report we are not interested in either of the above problems. Our emphasis is on that phase of duck hunting where a reasonably experienced hunter is leading a flying duck with his shotgun. We want to be able to describe the hunter's dynamic performance. We never got around to describing duck hunters, but we do attempt to describe the manual processes for minimizing visually perceived errors by exercising continuous control so as to match visually presented input and output signals. This is what we define as tracking. With our interests focused on tracking, we can now attempt to classify tracking problems for our conceptual convenience. Our criteria for classification will be based on the type of information which the stimulus to be tracked and the controller's response present to the controller as a basis for future tracking decisions. In application, these criteria result in three limiting types of classifications, defined as follows:

Precognitive

This condition exists when the operator has complete information about the input's future and a stimulus can trigger off a repertory of practiced, properly sequenced responses. In a sense, the situation itself may be the stimulus. Thus throwing a baseball at a target is precognitive behavior, as is steering a car out of a skid, or navigational flying under VFR conditions. The operator doesn't need to maintain a frequent check on the individual responses in a sequence. Instead end product responses are monitored; such as, "Did I hit the target?", "Am I still skidding?" or "Have I passed over a given fix?" In that continuous close control is not maintained on the perceived error, precognitive behavior is not tracking. However, we have included this behavior because occasionally tracking approaches these conditions. One might call precognitive behavior open loop control.

Pursuit

In pursuit behavior past experience provides the tracker with information about what to expect in a future input, but he must operate in a closed loop fashion with visual feedback about his responses. In this form of tracking the operator's corrective responses can be distinguished from his input. The reader should realize, however, that these responses are displayed *after* they have been modified by the system dynamics. Our duck hunter aiming for a bird using an open sight is an example of pursuit tracking.

Compensatory

Compensatory tracking is the same as pursuit except that the visually displayed effects of the controller's responses are not distinguishable from the system's input. Were our duck hunter aiming for the duck using telescopic sights with a small field of view, we would have compensatory tracking. Since in compensatory tracking the visual display is the system forcing function minus the modified control response, the operator can determine the effects of control motion alone only under zero input conditions.

In this report we shall be concerned only with certain members of the pursuit and compensatory classifications. This study is specifically applied to manual control systems where the operator has the more or less

continuous task of trying to effect some degree of match between a visually displayed input quantity and a visually displayed output quantity being controlled.

For the conditions of concern in this report the classifications above can be conveniently thought of as defining the type of display. Figure 1 illustrates the general nature of pure pursuit and compensatory displays.

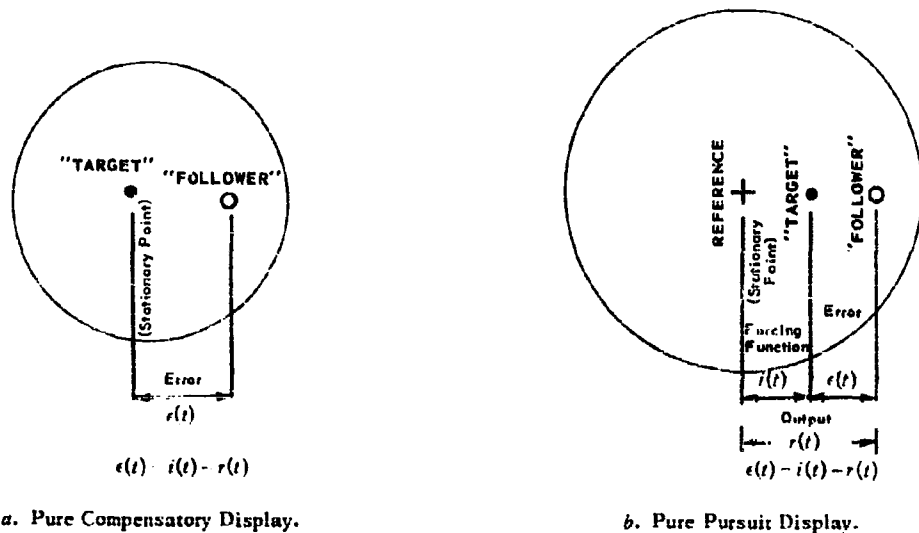


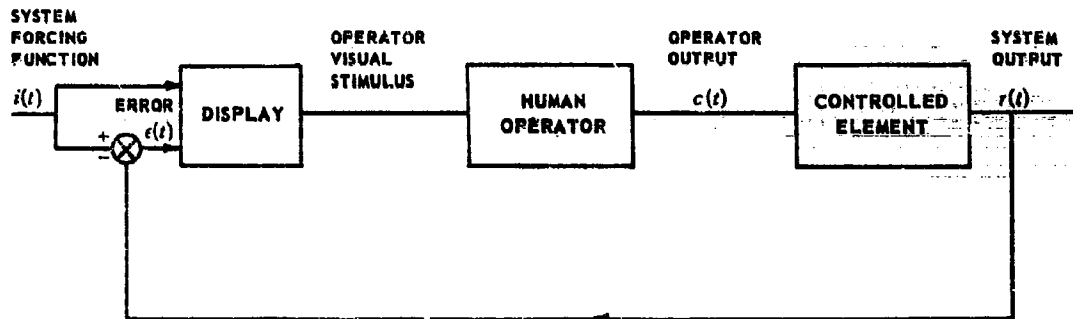
Figure 1. Compensatory and Pursuit Displays.

In the compensatory display the operator is presented with an input consisting only of an indicator showing the difference, or error, $e(t)$, between the forcing function $i(t)$ and the system output, $r(t)$. The operator's task is to minimize the error signal presented by trying to keep the circle superimposed on the stationary dot. In the pursuit display the operator sees both the input and output of the system. Again the operator's task is to minimize the error existing between the location of the dot and the circle, with the general operation being one of pursuing the target with the follower, trying to keep the circle around the dot. For the purposes of this report, then, the input environmental factors operating upon the control system can be essentially reduced to a definition of the type of display presented to the operator. Other fine points are actually involved, but for the nonce these will be deferred to later sections.

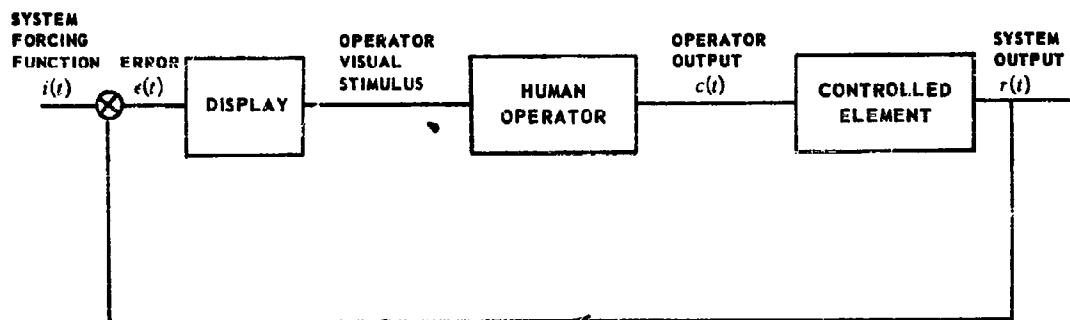
The other fundamental factors in the control situation are the type of element being controlled by the operator, such as an aircraft, automobile, etc., and the actual means of exerting control, such as a control stick or wheel with their associated restraints (springs, dampers, etc.). All of these characteristics will be lumped into the general classification of the "controlled elements." In many cases the controlled element can be described suitably by linear transfer functions, though in others nonlinearities may be present which also require description.

With the controlled element and display type defined, we can now draw functional block diagrams of the two simple control situations considered in this report. These diagrams, Fig. 2, show the human operator as an element of a closed loop system.

If the characteristics of the human operator for a given overall task are assumed to be capable of quasi-linear description, the operator mathematical model will consist of a linear transfer function plus an additional quantity inserted as an input into the system by the operator. Then the functional block diagrams



a. Functional Block Diagram of Simple Pursuit Manual Control System.



b. Functional Block Diagram of Simple Compensatory Manual Control System.

Figure 2.

of Fig. 2 can be made into equivalent block diagrams showing the combined operations of the system. These are shown in Fig. 3. To simplify the structure, the dynamic characteristics of the display are lumped with the controlled element, and the actual forcing function is modified, if necessary, to an equivalent one. The linear transfer characteristics of the human operating on his presented inputs are described by the weighting functions, $y_p(r)$, $y_{pe}(r)$ and $y_e(r)$, or their Laplace transforms $Y_p(s)$, $Y_{pe}(s)$ and $Y_e(s)$. Since all of the operator's output is not described by the action of these transfer characteristics, an additional term, $n_c(t)$, is added at his linear output to form the total operator output $c(t)$. The location of $n_c(t)$ at the operator's output is arbitrary, and does not necessarily imply that such a quantity is physically inserted at that point.

The two block diagrams of Fig. 3 clearly illustrate the servo system characteristics of manual control systems in general tracking tasks. Recognizing this allows us to apply the whole body of servo theory in our attack upon human behavior in such manual control systems. As servo systems with single inputs, the compensatory system is of extremely simple, single unity-feedback form. As a closed loop system, the operator's output and system error are given in terms of Laplace transforms and transfer functions by,

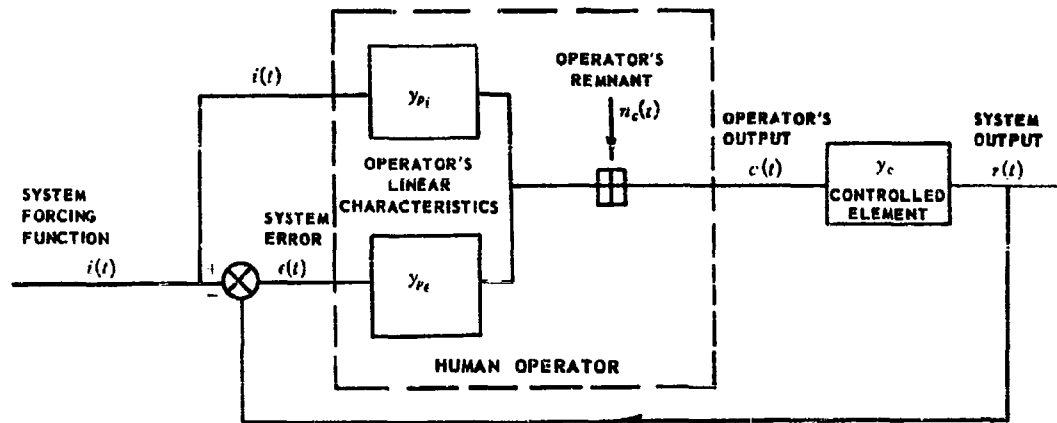
$$C(s) = \frac{Y_p(s)I(s) + N_c(s)}{1 + Y_p(s)Y_c(s)}, \quad E(s) = \frac{I(s) - Y_c(s)N_c(s)}{1 + Y_p(s)Y_c(s)} \quad (I-1)$$

The pursuit system is a somewhat more complex servo, being a particular type of open-cycle, closed-cycle system.* Here the operator's output and system error are given by,

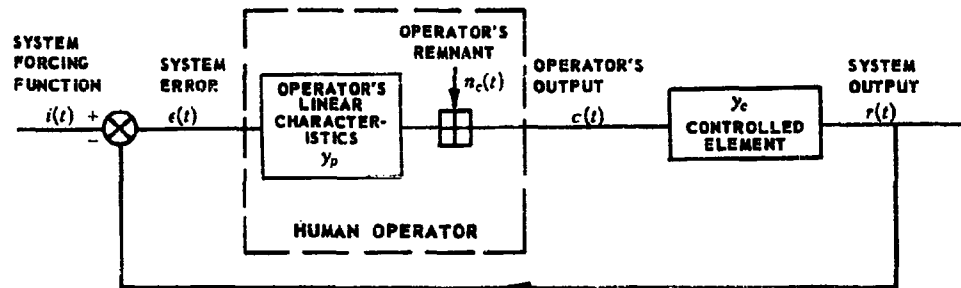
$$C(s) = \frac{[Y_{pi}(s) + Y_{pe}(s)] I(s) + N_c(s)}{1 + Y_{pe}(s) Y_c(s)} \quad (1-2)$$

$$E(s) = \frac{[1 - Y_{pi}(s) Y_c(s)] I(s) - Y_c(s) N_c(s)}{1 + Y_{pe}(s) Y_c(s)}$$

By comparing the error equations of Eq. (1-1) and (1-2), it is quite apparent that the pursuit type of system could result in smaller errors than the compensatory system if the operator is capable of making effective use of the additional information available by the proper adjustment of the transfer function $Y_{pi}(s)$. Therefore, even though most of the available experimental work summarized in this report has been concerned with compensatory systems, the pursuit system offers possible improvements and some aspects of such systems form an important part of this report.



a. Equivalent Block Diagram of Pursuit System with Linearized Operator.



b. Equivalent Block Diagram of Compensatory System with Linearized Operator.

Figure 3.

* See J. R. Moore, Ref. 60.

Section II

GENERAL BACKGROUND FOR HUMAN DYNAMICS RESEARCH

This section will attempt to put human dynamics studies in their historical perspective and to provide a verbal summary, having some psychological content, of the analytic developments which will be presented in greater detail further along in this report.

No pretense is made to either depth or completeness of coverage in this section for we are attempting to equip the reader with adequate familiarity rather than a scholarly knowledge of the tracking field. Any omissions of pertinent human dynamics research that occur are due not to value judgments but ignorance on our part. More details and original references can be found in [28, 48, 56].

A. THE ROLE OF PSYCHOLOGY

Before World War II tracking as such received no attention in the psychological literature. To be sure, experimental psychologists conducted research on many aspects of human sensory and control behavior which were later to be of importance in tracking studies, but their interests were not in tracking performance. Perhaps the earliest tracking devices used by psychologists were pursuitmeters, simple direct manual controlled devices which might have either compensatory or pursuit displays. These pursuitmeters were used from the early 1920's on to study eye-hand coordination under such conditions as degree of alcohol ingestion, different training routines, and different instructions, etc. In addition pursuitmeters were used as components of test batteries designed for the selection of persons possessing a high degree of eye-hand coordination, and as devices for producing boredom by prolonged operation. Many of the foregoing applications of tracking devices are still under active study.

World War II stimulated our present interest in tracking since the host of complicated manual control devices developed for modern fire control problems required a more detailed description of human operator performance than had hitherto existed. No longer could pilots or gunners compute leads in their head, as our duck hunter in Section I was able to do, but now the human operator served as a *sensor* which generated measures of rates, positions, and sometimes ranges of a target; and as a *controller* which fed these data into a computer. Depending on the dynamics of the controlled element, the operator might be coupled with a system which resulted in poor performance or even tended to instability.

At first, in the haste of the war time emergency, little thought was given to the human operator of the various military tracking devices. First in Great Britain, and then in this country, the improvement of the human operator's functioning became recognized as an important research area. As a consequence, research teams consisting mainly of psychologists were organized to improve matters. These men reflected professional attitudes and prior training in their manner of attacking human operator performance problems. Industrial psychologists fragmented the task, performed job analyses, and proceeded to develop test techniques for the selection of personnel who could be expected to excel at the required task. Experimental psychologists took a different tack and directed their efforts toward increasing the number of possible competent operators by studying the complementary possibilities of training and of equipment redesign. The training studies fell rather naturally under such traditional learning rubrics as: transfer problems, part vs. whole learning, massed versus distributed trials and so forth. Equipment redesign efforts were divided into static, kinetic and dynamic studies. The static studies dealt with such matters as anthropometry and the placement of controls, knob and handwheel design, reticle design and so forth. The kinetic studies concerned themselves with control display relationships. Typical of the kinetic questions examined were:

- a. What is the optimal display-control ratio?
- b. What is the optimal tracking handwheel diameter and speed?
- c. What effects do friction, stiction, inertia and so forth have on tracking accuracy?
- d. What are the effects of magnification, retical design, target size, and so forth on tracking accuracy?
- e. What is the subject's reaction time in responding to a step input?

The list could be expanded, but this sampling of topics serves to characterize the type of questions which were of interest.

The dynamic studies are characterized by their emphasis on attempted analytic descriptions of the process by which the human operator exerted control in closed loop tasks. Except for rare instances, we will discuss only dynamic studies in this report. It is difficult to state precisely how and where the need for dynamic studies first arose. It is clear, however, that such studies were originated and stimulated by engineers, not psychologists. Much of the experimentation, however, and the introduction of concepts of psychological or psychophysical content, was due to experimental psychologists. In a sense, the engineers introspected on the problem with the aid of some psychological sophistication. The most complete background data which the experimental psychologists could make available for this introspection dealt with visual processes and with reaction times.

There are data on visual sensory discriminations in referring to the resolving power of the eye, the adaptation of the eye, and the discriminability of displacements, velocities and accelerations. These quantities are often interdependent, and one must recognize the presence of interactions between the size of a visual stimulus, the stimulus' luminous intensity, and the brightness of the surroundings against which it is viewed. Similarly, there are interactions between the degree of structure in the visual field and the perception of displacement, velocity or acceleration. Because of the intimate relation of these data to the measuring situation, the general inadequacy of mathematical models (such as Weber's law) and the ready availability of summary data and handbooks, no attempt will be made to present numbers at this time [28, 69, 79, 94].

On a more highly integrated level in the nervous system the visual sense has been studied to determine the effects on reaction time delays of competing stimuli. Notions such as "span of attention" are pertinent here in the evaluation of tracking displays. The competition among stimuli leads us to the various studies on the increase of reaction time in multiple choice and compound reaction time displays in which a higher mental process, involving selecting and sequencing response decisions, results in a slower reaction time. Some workers have found it useful to describe similar phenomena in an information theory context [43], and as would be expected it has been found that reaction time increases with stimulus information content. It is of interest to note that when a one bit visual signal, i.e., go or no go, is employed as a stimulus to the practiced alerted human operator the reaction time approaches a lower limit of about 0.15 seconds. There are other cases in which the time to respond may approach zero, as in anticipatory behavior, but in these cases we are really redefining the stimulus to which the response takes place, and the reaction time remains at its physiological limit. This brief discussion serves to indicate the critical importance of the context and predictability of the input signal to the operator on his reaction time. In Section IV we will attempt to analyze the reaction time found in tracking in terms of its component parts. Surprising as it may seem, the reaction time exhibited in a serial response problem such as tracking is an elusive quantity. This is because it is difficult to isolate proper stimulus-response pairs in the tracking task as well as the lack of a simple criterion of predictability which could serve as a basis for ranking stimuli. Fein [29] has made measurements which show that the minimum period of free wagging for fingers or limb is a characteristic of the nervous system rather than of the musculoskeletal system. This minimum period is 0.1 to 0.15 seconds and is presumably the lower limit for serial reaction time.

We have discussed delays which might occur in the onset of a response due to organization factors in the visual modality. The operator can and does organize his perceptions around more than just the proper sequencing of responses, for his responses must be appropriate in magnitude as well as direction. An interesting psychological problem arises here since the magnitude of a stimulus is related to the context in which the stimulus is found. The so called range effect provides an example [26, 71, 73, 77, 89] and although small and of little practical importance in actual equipment operation, the presence of this effect is easily verified by experiment (e.g., Figure 21). The effect consists of overestimating a stimulus when it is the shortest and underestimating the same stimulus when it is the largest in a range of stimuli. It is difficult to separate motor from sensory influences in tracking performance, but the compatibility of the "range effect" with such perceptual phenomena as adaptation level provides a consistent framework for discussing the effect in perceptual terms. Best present knowledge indicates that the range effect is asymmetrical in that responses to the smallest displacement are more heavily skewed to the mean of the series of stimuli than are the responses to the largest displacements of the series. It is possible that the explanation of the skewed distributions may reside in the type of scale which the operator uses to subjectively rank stimulus magnitude, with the central tendency effect explainable either perceptually in terms of an adaptation level or on the response side by some sort of least effort principle. For our present purposes the reason for

discussing the "range effect" is to serve as an illustration of the type of stimulus context variables which influence the organization of tracking behavior and which were considered important when human dynamics were first examined.

There are a series of more nebulous psychological factors which, though not readily amenable to description in engineering terms, nevertheless are of importance because of their influence on tracking performance. Aspiration level, motivation, and "set to respond", are the major factors of this type.

The tracker's level of aspiration in the tracking task determines his self imposed level of tracking performance. The tracker who is attempting to minimize an error will not necessarily reduce the error to the limits of his visual acuity, but will reduce the error to that level which he is willing to tolerate. Certain errors may be deemed unavoidable or too small to bother about [40]. Although magnification serves to increase the apparent error, tracking performance does not improve in proportion to increased magnification since the attendant diminution of field size offsets some of the gains attributable to increased magnification. High motivation enables the tracker to overcome fatigue effects, to persist in boring tasks, and to focus his efforts on the task at hand without regard to distractions. The operator's set to respond refers to behavior which may be established by instructions. One could instruct the operator as to the visual cues to expect, or in the manipulative procedures to be used in tracking.

The foregoing general and sketchy remarks are indicative of what the psychologist would consider in formulating a description of human dynamics.

The earliest, basically psychological, formulation of this nature is due to Craik [20] who hypothesized that the human operator in a tracking task emitted corrective responses which were not modifiable by sensory feedback during their execution which was at a frequency of two per second. The 0.5 seconds period between responses was called the refractory period. Smoothing in the tracking system might, however, serve to mask this hypothesized discrete nature of human tracking. In experiments, the refractory period was manifest when the reaction time to the second of two consecutive stimuli increased by as much as 0.3 seconds beyond the normal 0.2 second reaction time to the first stimulus when the stimuli were less than 0.5 seconds apart. There is a voluminous literature on the refractory period, and we have only referenced a few representative papers [21, 25, 41, 46, 59, 87]. The present status of the controversy appears to be that most observers agree that there does appear to be a superimposed ripple of about 2 cycles per second on the tracker's output, but there is considerable disagreement as to the source of this periodicity. Later in this report it will be found that this type periodicity is consistent with three of the remnant models presented. Additionally, the near neutral stability, which it will turn out characterizes many man-machine systems, would also tend to manifest itself as a superimposed ripple when excited by any remnant at all [82]. Whether this ripple is at 2 cycles/second is a function of the control dynamics and input signal.

B. THE ENGINEERS' CONTRIBUTION

The engineers' interest in this problem arose when the human operator was given power controls to manipulate. Direct linkages, or "pointing stick" devices caused no major problems, but when the controlled element (Fig. 2) assumed dynamic characteristics, stability and the criteria of merit for errors became problems. The interest and attitude of engineers can be summarized by quoting Tustin whose early work was the genesis of the major content of this report [82].

"The object of the series of tests described in the present report was to investigate the nature of the layer's response in a number of particular cases and to attempt to find the laws of relationships of movement to error. In particular it was hoped that this relationship might be found (within the range of practical requirements) to be approximately linear and so permit the well-developed theory of 'linear servo-mechanisms' to be applied to manual control in the same way as it is applied to automatic following."

This same attitude and hope had motivated A. Sobczyk, R. S. Phillips and H. K. Weiss [44, 91, 92], but it was Tustin who introduced the concept of measuring a linear operator to describe the human and recognizing a remnant term which expressed that portion of the operator's control behavior which was not ascribable to this linear operation on the input. It is this basic notion which has been extended in this present report. Tustin went further and postulated origins for the remnant. In his earlier work [82] he suggested that an essentially white noise at the operator's output, and not variations of his linear transfer functions parameters, might account for the remnant. This remnant actually accounted for half of the total error.

In a subsequent report [86] he was of a different mind, and believed that the remnant resulted from the existence of a "threshold" in response together with a tendency for the response to be impulsive in form. The evidence for this is weak, being based on a questionable choice of linear transfer function form which yielded the parameters for the human operator's underlying linearized differential equations. The appropriate differential equations in operational form were applied to the error input and to the control response and the two solutions to the equations were plotted and compared. This comparison, over a seven second segment, showed periods of about 0.5 second over which the output was zero followed by an impulsive response of a magnitude which seemed to vary in a random fashion.

Although it is not important for us to dwell on the form of linearized transfer function Tustin extracted (in Section VI we will present some of his data in detail and recompute transfer characteristics), it is of interest to note his findings on the optimizing behavior of Y_p , the human's description. Tustin observed that the operator adjusts his open loop gain to a value such that the controlled element and the operator form a marginally stable system. This finding anticipates a great deal of more extensive future research, and is one of the human operator's most useful characteristics. He can change his characteristics to improve performance consistent with stability considerations.

Another important finding of Tustin's [83] upon which a considerably more elaborate structure has been built is his concept of compensation as applied to man-machine systems. Compensation, of course, is a very old servo system technique which consists of designing such circuits as will provide lead or other equalization for the operator to compensate for his phase lags, and thus allow him to operate at higher gain, while attenuating the relatively high frequency remnant noise as best as possible. Thus compensation is a compromise between lead and lag networks, each dominant over different frequency ranges. The exact specification for the compensation networks is a function of the controlled element and precise knowledge of the remnant's frequency characteristics. Tustin considered aided tracking to be a primitive form of compensation. Tustin advocated doing for the operator what he cannot do well himself, but allowing him to act as an optimizing amplifier, which he can do quite well. This contribution of Tustin's has been modified slightly, but remains essentially unchanged as one of the major conclusions of present human dynamics research.

That the human operator imposes certain requirements on the controlled element was recognized by others as well [44, 91, 92]. Weiss, for example, presented a detailed argument for aided tracking, i.e., the man and his manual control have the transfer characteristic Y_p where

$$Y_p = Y_p \frac{(1+Ts)}{s}$$

T is the aided tracking time constant = the ratio of change in position to the change in velocity of the output as a result of a given change of manual control position. Weiss's position was that aided tracking was by far preferable to velocity tracking, for which the transfer function was $1/s$, since velocity tracking forced the operator to generate high leads with consequent higher errors and the risk of going unstable.

In addition, Weiss advocated so selecting the particular aided tracking time constant with the controlled element dynamics in mind. Thus a controlled element whose transfer function was of the lead-lag form could be coupled with an aided manual control so that the manual control's lead cancelled the controlled element's lag. The result would be equivalent to a controlled element of transfer function equal to unity, and an aided manual control. This new aided manual control would of course have a time constant which was equal to the time constant of the lead term of the controlled element.

This suggestion was also made by a team of engineers and psychologists working at The Franklin Institute during World War II who conducted many large scale simulator experiments to determine the optimum aided tracking time constant for various controlled element dynamics [59, 66]. Not only were the theoretical predictions for the optimum aided tracking constant corroborated by experiment, but the thesis that what the operator is given to work with is more important than his training or selection was demonstrated. This thesis is central to engineering psychology. Untrained college students, secretaries, and engineers were able to out-perform trained gunners on flexible gunnery simulator tests when the naive subjects were provided with optimal controls and the trained gunners used existing equipment.

Weiss, as did Tustin and others, took cognizance of the human's time constant adjustability by suggesting that tracking instructions be determined by the smoothing, i.e., integrating circuits following the man in the control loop. Thus, to be specific, with the M-5 director he advised smooth tracking, i.e., no sudden changes in error, but with the M7A1B1 director he advised quick corrections, since the associated smoothing circuits easily eliminate high frequency errors but pass slow changes. To assess these systems, Weiss advocated measuring the spectral density of the error power from the autocorrelation of the error function so that more effective information on tracking requirements could be supplied to selection and training facilities.

North, in an a priori non-experimental model, elaborated on the applications of spectral density techniques by expressing the system error spectrum in terms of coherent and stochastic influences, thus gaining insight into the remnant's structure. These foregoing suggestions that the spectral density is a useful analytic tool for evaluating tracking will be developed considerably in Section III of this report.

We will not discuss analog computer models of the human operator in this section since the Goodyear group's fine work in this regard will be considered in detail in Section VIII of this report. In addition we will not dwell at any length on the various suggested linearized transfer functions for the human operator [44, 67, 85]. Suffice it to say that most of them were of the general form:

$$\frac{C}{E} = Y_p = \frac{K(1+T_1s)e^{-T_2s}}{(1+T_2s)} \approx \frac{K(1+T_1s)e^{-T_2s}}{s}$$

In Sections V and VI of this report we will derive describing functions (linearized transfer functions in the Tustin sense) for various input and controlled element characteristics, and attempt to bring otherwise disparate results together.

Many of the early workers in the field attempted to develop their human operator models on an a priori basis by postulating such attributes as: proportional, or proportional plus derivative control, or that the musculature (a second order system) was important and could be approximated by a first order term, or that τ was 0.25 or 0.3 or even 0.5 seconds. Actually, these efforts were usually misleading, and as will be seen in Sections V and VI, it is considerably more effective to extract Y_p from the data, while using physical reasoning as a technique for getting insights, not as a closed deductive logic.

There are considerably more historical references than have been discussed in the foregoing. Some of these are in our list of references, others may be found in the summary reports [28, 48, 56]. It was our intent to select material in the foregoing which anticipated in some sense our subsequent development rather than to strive for completeness.

Section III

MATHEMATICAL MODELS FOR MANUAL CONTROL SYSTEMS AND QUASI-LINEARIZATION TECHNIQUES

A. INTRODUCTION

A fundamental problem in dynamic analysis is the mathematical characterization of cause and effect relationships for general system elements. A direct way to specify such information would be to determine the element responses arising from a large variety of inputs, and then to catalog these results as input-response pairs. For all but the simplest elements and conditions this direct procedure would become extremely unwieldy. In order to achieve a simpler specification, we would like to modify the basic question from "What are the effects due to various causes?" to "What is the operation of the system element in modifying a cause into an effect?" In other words, the analyst desires a "mathematical model" of a device which responds to an input in a fashion approximating that of the physical element, and which might be used for several similar types of inputs.

With systems containing only elements which behave in a fashion describable by linear constant-coefficient differential equations, this second question is answered simply by specifying the system's weighting or transfer functions. If the system were represented by the block diagram of Fig. 4, where the weighting function,

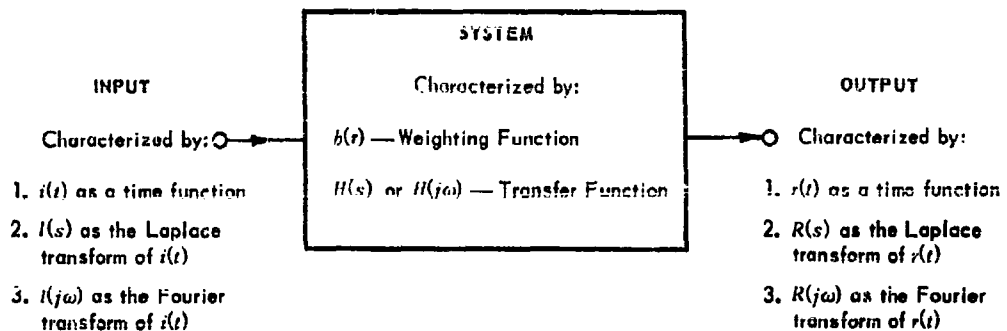


Figure 4. Linear System Representation.

$b(t)$, is the time response of the system when an impulse function is applied at zero time, then the relationship between the response and the input would be given by the so-called superposition or convolution integral,

$$r(t) = \int_{-\infty}^{\infty} b(t) i(t - \tau) d\tau \quad (\text{III-1})$$

Since the response, $r(t)$, to any input, $i(t)$, can be found if $b(t)$ is known, we can dispense with a gigantic tabulation of input-response pairs to describe a linear system's operation, and need specify only the weighting function.

Because algebraic operations are easier to use than integrals like Eq. (III-1), it is usually preferable to work with transforms of the input, response, and weighting functions rather than the time functions. If the Fourier transform is used, the transformation of Eq. (III-1) becomes

$$R(j\omega) = \int_{-\infty}^{\infty} r(t) e^{-j\omega t} dt = H(j\omega) I(j\omega) \quad (\text{III-2})$$

where $R(j\omega)$, $I(j\omega)$, and $H(j\omega)$ are the Fourier transforms of $r(t)$, $i(t)$ and $b(t)$ respectively.

When the conventional unilateral Laplace transform is used, the convolution integral of Eq. (III-1) is first modified to

$$r(t) = \int_0^t b(\tau) i(t-\tau) d\tau; \quad t \geq 0 \quad (\text{III-3})$$

This form of the convolution integral can then be Laplace transformed to give

$$R(s) = \int_0^\infty r(t) e^{-st} dt = H(s) I(s) \quad (\text{III-4})$$

where $R(s)$, $I(s)$, and $H(s)$ are the Laplace transforms of $r(t)$, $i(t)$ and $b(t)$. The transfer function $H(s)$, is essentially the same thing as the transfer function $H(j\omega)$, with $j\omega$ replaced by s .†

The introduction of the weighting function, or its transform, the transfer function, allows us to describe the performance of a *linear* system completely without having to resort to the awkward device of a complete dictionary of input-response pairs. On the other hand, in a general system some of the parameters may not be linear, but may depend, instead, upon the values of the dependent variables which define the system's response. If this is the case, the convolution integral is not valid, and the behavior of the system is a function of the *particular* inputs and initial conditions. This puts the analyst right back to the beginning — forcing him to define system operation by input-response pairs — for the response of a nonlinear system to a particular input is just that! Results of nonlinear analyses are applicable only to the specific situations considered, and the specification of system behavior requires us to give both the input and the response.

Fortunately many nonlinear systems of interest have specific input-specific response pairs which appear to be very similar to input-response pairs for linear systems. This similarity leads immediately to the notion that the performance of some nonlinear elements, for particular inputs, could be approximated by a linear element plus an additional quantity called the remnant.‡ From this general basis the *describing function* technique has been evolved. In this approach nonlinear elements are replaced by "equivalent" linear elements. The equivalent linear element is derived from consideration of the response of the nonlinear element to a particular type or class of input. Since the input type is defined, and the response is the result of a linear operation, it would be expected that this equivalent linear representation would be of considerable value in approximating the actual nonlinear system.

As an example of this concept consider the *sinusoidal input describing function*, which is derived from consideration of the harmonic response of the nonlinear element to a sinusoidal input at various frequencies and amplitudes. Suppose that a sine wave is applied to the input of a nonlinear element having a single input and output. The output very likely will be a nonsinusoidal periodic wave with the same period as the input wave. If the output waveform is analyzed in terms of its Fourier components, the fundamental component will bear a relationship to the input sine wave which can be described in amplitude ratio and phase angle terms. The describing function will be the ratio of the fundamental to the input in the same way as used in a linear system. The remnant will be composed of all the higher harmonics. The output would then be the sum of the describing function times the input plus the remnant.

From the above comments it is apparent that a whole series of describing functions could be defined for a particular nonlinear element simply by considering different types of inputs. The sinusoidal input describing function already noted is exceptionally important and is an oft-used tool in servo analysis. In many problems the type of transient input is fairly well known in analytic form and a *transient describing function* is of value. Of these the most important in this report is the *step input describing function*. Finally, perhaps the most important type of describing function for general systems is one based upon statistical inputs. Such a describing function, particularly for inputs with Gaussian amplitude distributions, is very important in nonlinear control problems

† With some additional restrictions, particularly with regard to the convergence of the Fourier and Laplace transform integrals, the Fourier and Laplace transformations of $i(t)$ and $r(t)$ will be identical for $t \geq 0$ when s replaces $j\omega$. Therefore, even though Fourier transforms are most often used in this report, both forms will appear as dictated by local convenience.

‡ While the notion of molding a nonlinearity into an equivalent linear element is quite old and has been used by many writers, the first instance of major exploitation of the technique was probably by Kryloff and Bogoliuboff [55].

involving the types of inputs used in statistical design techniques, and can be considered a fairly general type of equivalent linearization. This *Gaussian input describing function* is of particular importance in this report.

As a final general comment on describing functions it should be stated that, since the inputs are different, the only thing the various describing functions have in common is the nonlinear system they approximate. If the nonlinearities in the system elements become more linear, the various describing functions tend to approach one another. When the nonlinearities are entirely removed, all of the describing functions become identical to the system's transfer function.

Because the characteristics of the human operator depend strongly on the type of inputs which he is expected to follow, the describing function concept is our only recourse if it is desired to retain the general simplicity of the linear methods. Almost all of the experimental research upon which we shall report, and which attempts to specify operator characteristics in manual control tasks, has been based upon this general approach. Therefore this section is devoted to various aspects of the describing function technique.

Before embarking upon the detailed discussion of the describing function methods useful in approximating human responses, it is necessary to mention some alternate approaches to the nonlinear problem. The most important practical alternate is the use of an operator analog comprised of analog computer elements. Using the very wide range of nonlinear and linear analog elements available, a computer setup can be made by cut and try procedures and adjusted until the "analog operator" responses to particular inputs are similar to those of the actual operator.

If a "perfect" analog were ever achieved, the input type would not be important. In the case of the human operator, however, a separate analog is required for different inputs to achieve a practical and reasonably simple computer setup. In this sense, then, the computer analog represents a nonlinear describing function. The technique is of great value in instances where a point by point prediction of operator response is desired, for studies including nonlinear control effects, and as a means of providing insight into some of the types of nonlinear behavior which might occur in the operator. When nonlinear transfer characteristics become exceedingly important it is probably the only practical approach. The analog technique is fairly straightforward, so no further discussion of the general method need be included in this section.

There are, of course, other approaches to the problem of specifying the characteristics of a general system, such as the phase plane method, various digital computer techniques, decision function models for operator choice behavior, etc. None of these, however, are as yet of much importance in the empirical determination of operator characteristics.¹

In the way of outlining what is to come, this section is divided into two major parts. The first part is devoted to a general explanation of the describing function technique. This part, in turn, is made up of three subsections, one on sinusoidal input describing functions, one on Gaussian input describing functions, and the third on step input describing functions. The second part is concerned with an exposition of the general mathematical terms involved in the measurement of describing functions and remnants, of both the sinusoidal and random input variety. It consists of several topical divisions including the determinations of open loop quasilinear describing functions, the spectral density of the remnant and the system error, and the mean squared error. Other quantities of particular importance, such as linear correlations and signal to noise ratio, are also developed. Finally, the possible general sources of the remnant term are considered in some detail.

The major purpose of this section is to provide the general mathematical background appropriate to the actual types of serve system problems involved. Much of the discussion is therefore fairly academic and a good deal could be skipped by the general reader without too great a loss in understanding of the latter sections.

B. QUASI-LINEAR DESCRIBING FUNCTIONS

In the study of human dynamics the operator characteristics are strong functions of input type, similar to those of many other nonlinear systems. As will be shown later in the review of experimental work, a very important factor to the operator in determining his response characteristics is the general predictability of his input.

¹ These other techniques occasionally offer or bring up useful and interesting side issues — see for example Platzter [62].

Specifically, the operator's mode of response appears to be different for single sine waves (which are essentially completely predictable once started), step functions (which have known final values immediately after initiation of the stimulus), and "random appearing functions." The random appearing inputs are not restricted to functions which are known only by their statistics, but include those which can be made up by as few as three non-harmonically related sine waves. In most of the experimental work, the random appearing inputs have been either such a sum of sine waves, or time functions which had essentially Gaussian amplitude distributions. Therefore the types of describing functions of interest are those for step, sinusoidal and Gaussian inputs. All of these describing functions fall into a category which can be called quasi-linear because they tend to be linear under a fixed set of conditions, such as given inputs, yet nonlinear when changes in these conditions are considered.

1. Sinusoidal Input Describing Functions

In the sinusoidal input describing function technique, an equivalent linear element is derived from consideration of the harmonic response of the nonlinear element to a sinusoidal input at various frequencies and amplitudes.[†] As an example consider the case of a simple limiter, having the transfer characteristic shown in

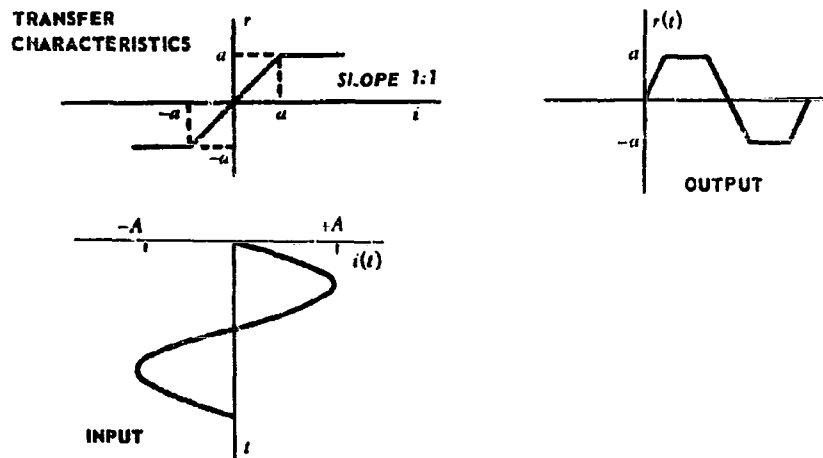


Figure 5. Transfer Characteristic for Limiting with Typical Output for a Sinusoidal Input.

Fig. 5. In this instance, if the input is $i(t) = A \sin \omega t$ the output can be written as a Fourier series

$$r(t) = b_1 \sin \omega t + \sum_{n=3,5,\dots}^{\infty} b_n \sin n\omega t \quad (\text{III-5})$$

where

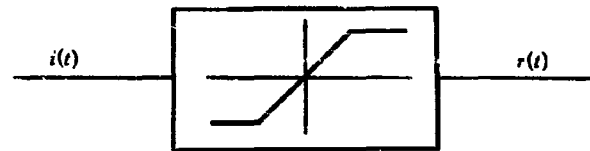
$$b_1 = \frac{1}{\pi} \left[A \left(2 \sin^{-1} \frac{a}{A} - \frac{2a}{A} \sqrt{1 - \left(\frac{a}{A} \right)^2} \right) + 4A \sqrt{1 - \left(\frac{a}{A} \right)^2} \right]$$

[†] The sinusoidal describing function technique has been rather thoroughly exploited in the past ten years because of its extreme importance. One of the first references to the method is to an unpublished 1946 report by Nichols and Kreezer in Greenwood, Holdam and MacRae, page 354 [36]. One of the first published applications appears in Tustin [84]. Later work following the same general lines was done by Kochenburger [47], Johnson [45], McRuer, Halliday and Press [58], and many others.

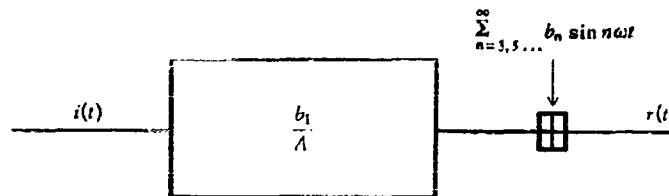
$$b_n = \frac{4}{\pi} \left[\left(\frac{A}{1-n^2} \right) (n \sin B \cos nB - \sin nB \cos B) + \frac{a}{n} \cos nB \right]$$

and $B = \sin^{-1} \frac{a}{A}$

The sinusoidal input describing function is defined, in general, as the ratio of the fundamental of the output to the input. The output fundamental may have a phase shift relative to the input sine wave, thereby giving rise to both an amplitude ratio and a phase angle. In the above case for the limiter, the sinusoidal describing functions will be simply b_1/A , while the remnant includes everything else in the output. In this way the actual nonlinear transfer characteristic of Fig. 6a can be replaced by the "equivalent" linear element plus remnant of Fig. 6b.



a. Actual Nonlinear Transfer Characteristic for Limiting.



b. "Equivalent" Linear Characteristic for Limiting.

Figure 6.

The "amplitude ratio" and "phase angle" for the sinusoidal describing function for limiting is shown in Fig. 7, including those of the output harmonics.† It will be noted that the "phase angle" of the sinusoidal input describing function in this case is zero. This will always be the case when the nonlinearity is dependent only upon the instantaneous value of the input. The describing function is then a pure gain which varies with input amplitude alone. In general, of course, the sinusoidal input describing function can vary with both the amplitude and frequency of the input sine wave.

The sinusoidal input describing function technique can also be interpreted in a slightly different manner. The input is again assumed to be sinusoidal. While the output will not be sinusoidal, it can be approximated by a sinusoidal function with the same frequency as the input but with a different amplitude and phase. The complete output, $r(t)$, can be expanded into a trigonometric series, i.e.,

$$r(t) = \sum_{n=1}^{\infty} a_n e^{jn\omega t} \quad (\text{III-6})$$

It is now desired to determine the values of a_n which give the "best" approximation to $r(t)$, where "best" is

† The "amplitude ratio" of a harmonic to a fundamental is an arbitrary term adopted for convenience in plotting the results. It completely ignores the difference in frequency existing between the harmonic and the fundamental.

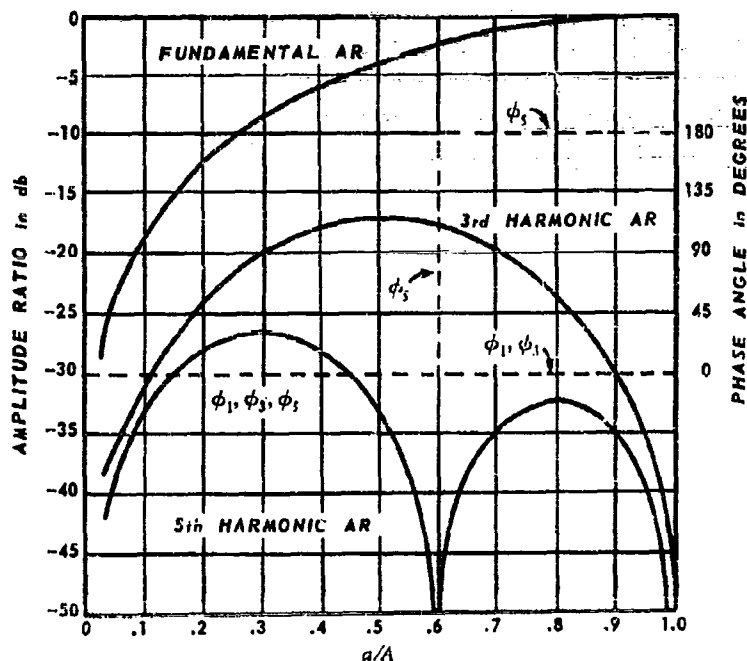


Figure 7. Amplitude Ratio and Phase Due to Limiting.

defined as the result of minimizing the mean square error of approximation. The mean square error in approximation is given, if $r(t)$ is integrable over the range $-\pi$ to $+\pi$, by

$$\bar{\epsilon}^2 = \frac{1}{2\pi} \int_{-\pi}^{\pi} |r(t) - \sum_{n=1}^N a_n e^{jnt}|^2 dt \quad (\text{III-7})$$

It can be shown that $\bar{\epsilon}^2$ will be a minimum when

$$a_n = \frac{1}{2\pi} \int_{-\pi}^{\pi} r(t) e^{-jnt} dt \quad (\text{III-8})$$

which is, of course, the formula for the familiar Fourier coefficient. Since a_1 is the complex number describing the fundamental of the output it can be concluded that the use of this sinusoidal input describing function results in a particular linear equivalent which minimizes the mean square difference between the actual and approximate output.

2. Random Input Describing Functions†

When the input to a nonlinear element is random rather than sinusoidal we can no longer interpret a describing function in terms of fundamental and harmonic quantities, so this aspect of the sinusoidal describing function technique has little carryover into the random input case. On the other hand, an extension of the mean

† Much of the underlying theory and application of random input describing functions is due to Borton [9, 10, 11, 12, 13]. Reference 12 is followed closely here.

square approximation is feasible. For example, if one assumes, for the moment, that the describing function for simple nonlinearities which depend only on the instantaneous value of the input is an amplitude dependent pure gain (as it is in the sinusoidal case), then the error in approximation of the true output $r(t)$ by the equivalent linear output, $Ki(t)$, will be

$$e(t) = r(t) - Ki(t) \quad (\text{III-9})$$

and the error squared will be:

$$e^2(t) = [r(t) - Ki(t)]^2 \quad (\text{III-10})$$

The mean square error can be found by expanding the right hand side and averaging, i.e.,

$$e^2(t) = r^2(t) - 2Ki(t)r(t) + K^2i^2(t) \quad (\text{III-11})$$

$$\begin{aligned} \bar{e}^2 &= \lim_{T \rightarrow \infty} \frac{1}{2T} \int_{-T}^{+T} e^2(t) dt \\ &= \lim_{T \rightarrow \infty} \frac{1}{2T} \left(\int_{-T}^{+T} r^2(t) dt - 2K \int_{-T}^{+T} r(t)i(t) dt + K^2 \int_{-T}^{+T} i^2(t) dt \right) \\ &= \bar{r}^2 - 2K\bar{ir} + K^2\bar{i}^2 \end{aligned} \quad (\text{III-12})$$

The desired value of K is that which minimizes \bar{e}^2 . Therefore since,

$$\frac{d\bar{e}^2}{dK} = -2\bar{ir} + 2K\bar{i}^2 \quad (\text{III-13})$$

then the desired equivalent gain K must be

$$K = \frac{\bar{ir}}{\bar{i}^2} \quad (\text{III-14})$$

If both $r(t)$ and $i(t)$ are assumed to be stationary random functions of one sort or another, the time averaged quantities in Eq. (III-14) can be put into terms of probability characteristics. Because the functions are stationary the expected value, or ensemble average, of a stochastic variable of given distribution function will be equal to the time average for this variable. For example, if $X(t)$ is a random variable having an amplitude distribution

defined by the probability distribution $p(x)$, then the mean or expected value of X is defined by $E[X] = \int_{-\infty}^{+\infty} xp(x)dx$.

When the ergodic hypothesis holds, i.e., when time averages are equal to ensemble averages, this expected value will be equal to the time average $\bar{X} = \lim_{T \rightarrow \infty} \frac{1}{2T} \int_{-T}^{+T} X(t) dt$.

Now, if $g(X)$ is some arbitrary function of the random variable X , the expected value of $g(X)$ will be a probability-weighted average of the values that g can assume. When $x < X < x+dx$ then, the probability weighted average will be $g(x)$ times the probability that X lies in the interval between x and $x+dx$. This will be given approximately by

$$g(x) \text{Pr}\{x < X < x+dx\} \doteq g(x)p(x)dx$$

When integrated over the various values which X can assume, a fundamental theorem is obtained which gives the expected values of $g(X)$ as

$$E[g(X)] = \int_{-\infty}^{+\infty} g(x)p(x)dx \quad (\text{III-15})$$

Eq. (III-15) is essentially in the category of a definition, and is valid for any random process, stationary or otherwise if the integral exists. The concepts of stationarity and the ergodic hypothesis enter into the problem only when it is desired to have the expected value, as computed above, equal the time average.

With the assumption that the ergodic hypothesis holds, it is now possible to use Eq. (III-15) to find the values of the time averages \bar{r} and \bar{i}^2 in terms of the probability characteristics.

To find the value of \bar{r} , consider that the actual transfer characteristic of the nonlinear element is such that the output is a single valued symmetrical function of the input, i.e.,

$$r(t) = f[i(t)] \quad (\text{III-16})$$

Then the arbitrary function of Eq. (III-15) $g(X)$ is recognized as $X/f(X)$, or

$$E[ri] = \int_{-\infty}^{\infty} x/f(x) p(x) dx = \bar{r} \quad (\text{III-17})$$

To determine \bar{i}^2 , the second moment of i , we can identify $i(t)$ as the random variable $X(t)$ with probability distribution $p(x)$, and thus by definition

$$E[i^2] = E[X^2] = \int_{-\infty}^{\infty} x^2 p(x) dx = \overline{i^2(t)} \quad (\text{III-18})$$

We can now substitute Eq. (III-17) and (III-18) into (III-14) to obtain the value of the equivalent gain K in terms of the probability distribution characteristic of the input and the transfer characteristics of the nonlinear element. This will be

$$K = \frac{\int_{-\infty}^{\infty} x/f(x) p(x) dx}{\int_{-\infty}^{\infty} x^2 p(x) dx} \quad (\text{III-19})$$

It should be noted that the only restriction upon the results to this point are those due to the assumption that a pure gain was desired as the approximation to the nonlinearity and that the input and output are stationary processes. While the value of K given above by either Eq. (III-14) or its equivalent (III-19) is the "best" pure number in the sense that it will give a minimum mean square error, it is *not necessarily* the "best" linear operator in that same sense. This will be discussed more thoroughly later.

To solidify the discussion leading to this point consider, as an example, the same limiter described previously. The amplitude of the output is defined by

$$\begin{aligned} f(x) &= -a \quad \text{for } x < -a \\ &= x \quad \text{for } -a < x < a \\ &= a \quad \text{for } x > a \end{aligned} \quad (\text{III-20})$$

Assume that the amplitude of the input time function has a Gaussian probability distribution given by

$$p(x) = \frac{e^{-\frac{x^2}{2\sigma^2}}}{\sigma\sqrt{2\pi}} \quad (\text{III-21})$$

where σ^2 is the variance. The equivalent gain K will then be given by

$$\begin{aligned} K &= \frac{\int_{-\infty}^{+\infty} x f(x) p(x) dx}{\int_{-\infty}^{+\infty} x^2 p(x) dx} = \frac{\int_{-\infty}^{-a} -ax p(x) dx + \int_{-a}^{+a} x^2 p(x) dx + \int_{+a}^{+\infty} ax p(x) dx}{\sigma^2} \\ &= \frac{a[\int_{-\infty}^{-a} -x p(x) dx + \int_{+a}^{+\infty} x p(x) dx] + \int_{-a}^{+a} x^2 p(x) dx}{\sigma^2} \end{aligned}$$

Substituting the expression for $p(x)$ and performing the indicated integration for the bracketed numerator term,

$$K = \frac{\sqrt{\frac{2}{\pi}} a \sigma e^{-\frac{a^2}{2\sigma^2}} + \int_{-\infty}^{\infty} \frac{x^2 e^{-\frac{x^2}{2\sigma^2}} dx}{\sigma^2 \sqrt{2\pi}}$$

Recognizing that the integrand is an even function of x and grouping terms,

$$K = \frac{2}{\sqrt{\pi}} \left(\frac{a}{\sqrt{2}\sigma} \right) e^{-\frac{a^2}{2\sigma^2}} + \frac{2}{\sqrt{\pi}} \int_0^{\infty} \left(\frac{x}{\sqrt{2}\sigma} \right)^2 e^{-\frac{x^2}{2\sigma^2}} \left(\frac{dx}{\sqrt{2}\sigma} \right)$$

Letting $\frac{x}{\sqrt{2}\sigma} = z$

$$K = \frac{2}{\sqrt{\pi}} \left[z e^{-z^2} \right]_0^{\frac{a}{\sqrt{2}\sigma}} + 2 \int_0^{\frac{a}{\sqrt{2}\sigma}} z^2 e^{-z^2} dz = \frac{2}{\sqrt{\pi}} \int_0^{\frac{a}{\sqrt{2}\sigma}} e^{-z^2} dz$$

The last step, above, is a reverse integration by parts. We can thus write,

$$K = \Phi \left(\frac{a}{\sqrt{2}\sigma} \right) \quad (\text{III-22})$$

where Φ is the error function defined by

$$\Phi(z) = \frac{2}{\sqrt{\pi}} \int_0^z e^{-z^2} dz \quad (\text{III-23})$$

The value of K is plotted versus a/σ in Fig. 8. This particular Gaussian input describing function can be compared directly with that for the sinusoidal describing function to obtain a notion of the similarities of the results for this simple case.

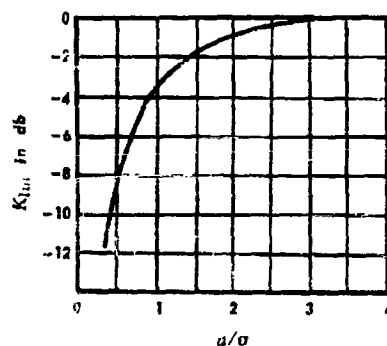


Figure 8. Gaussian Input Describing Function for Limiting.

Having explored the general idea of the statistical input describing function for a simple example, it is now necessary to generalize the development. Conceptually, the generalization is not far removed from the first case considered—the major difference is the desire to have the "best" linear equivalent system rather than merely the closest approach using a pure gain. If the nonlinear element is approximated by some linear weighting function $b(r)$, then the output $r(t)$ will be approximated by $\int_{-\infty}^{\infty} b(\tau) i(t-\tau) d\tau$. This is directly analogous to the situation described in the linear cases discussed prior to Eq. (III-3) except that the $b(r)$ in this case is the "best" linear equivalent weighting function of the general system element rather than being a complete description. If the equivalent linear system weighting function is to be realizable, then $b(r) = 0$ for $r < 0$, so that the approximate output will be $\int_0^{\infty} b(\tau) i(t-\tau) d\tau$. The error in approximation is then

$$e(t) = r(t) - \int_0^{\infty} b(\tau) i(t-\tau) d\tau, \quad t > 0 \quad (\text{III-24})$$

Since a minimum mean squared error is desired, the required $b(r)$ is that linear quantity which minimizes $\overline{e^2(t)}$, or

$$\overline{e^2(t)} = \overline{\left[r(t) - \int_0^{\infty} b(\tau) i(t-\tau) d\tau \right]^2} \quad (\text{III-25})$$

Application of the calculus of variations to this expression will reveal that it will be a minimum when the weighting

function $b(r)$ which characterizes the equivalent system satisfies the integral equation

$$R_{ir}(r) = \int_0^\infty b(u) R_{ii}(r-u) du, \quad \text{for } r > 0 \quad (\text{III-26})$$

where $R_{ir}(r)$ is the cross-correlation function between input and output, and $R_{ii}(t)$ is the autocorrelation function of the input. The results in going from Eq. (III-25) to (III-26) are independent of the type of input process involved. Therefore, the weighting function satisfying Eq. (III-26) yields the "best" linear approximation to the actual output, in the mean-square difference sense, under quite general conditions. At this juncture this general property may appear to be rather innocuous, but it is a valuable item of background information.

While the desired answer to Eq. (III-25) is given in Eq. (III-26), the details of the development will now be considered as an aside. This is largely an academic exercise added for completeness, so the reader may skip over it if he desires. Using the absolute value of the error squared, we can obtain the following directly from Eq. (III-24), where $()^*$ is the complex conjugate of $()$.

$$\begin{aligned} |e(t)|^2 &= e(t) e^*(t) \\ &= [r(t) - \int_0^\infty b(r) i(t-r) dr] [r^*(t) - \int_0^\infty b^*(r) i^*(t-r) dr] \\ &= r(t) r^*(t) - r(t) \int_0^\infty b^*(r) i^*(t-r) dr - r^*(t) \int_0^\infty b(r) i(t-r) dr \\ &\quad + \int_0^\infty dr [b^*(r) i^*(t-r)] \int_0^\infty du [b(u) i(t-u)] \end{aligned} \quad (\text{III-27})$$

Taking the mean square,

$$\begin{aligned} |e(t)|^2 &= \lim_{T \rightarrow \infty} \frac{1}{2T} \left\{ \int_{-T}^T r(t) r^*(t) dt - \int_{-T}^T r(t) \left[\int_0^\infty b^*(r) i^*(t-r) dr \right] dt \right. \\ &\quad \left. - \int_{-T}^T r^*(t) \left[\int_0^\infty b(r) i(t-r) dr \right] dt + \int_{-T}^T \int_0^\infty [b^*(r) i^*(t-r) dr] \left[\int_0^\infty b(u) i(t-u) du \right] dt \right\} \end{aligned} \quad (\text{III-28})$$

By noting the functional dependence of various terms (e.g., $b^*(r) i^*(t-r)$ is not a function of u and so may be included under the second integral of the last term), interchanging the order of integration in places and using appropriate bars to indicate the averaging process,

$$\begin{aligned} |e(t)|^2 &= \overline{r(t) r^*(t)} - \int_0^\infty b^*(r) dr \overline{i(t) i^*(t-r)} - \int_0^\infty b(r) dr \overline{r^*(t) i(t-r)} \\ &\quad + \int_0^\infty dr \int_0^\infty b(r) b^*(u) du \overline{i^*(t-r) i(t-u)} \end{aligned} \quad (\text{III-29})$$

The symbolism can be simplified by noting that the barred expressions on the right are autocorrelation and cross-correlation functions, i.e., the autocorrelations of the response and input are respectively:

$$\begin{aligned} R_{rr}(r) &= \overline{r(t) r^*(t+r)} = \lim_{T \rightarrow \infty} \frac{1}{2T} \int_{-T}^{+T} r(t) r^*(t+r) dt \\ R_{ii}(r) &= \overline{i(t) i^*(t+r)} = \lim_{T \rightarrow \infty} \frac{1}{2T} \int_{-T}^{+T} i(t) i^*(t+r) dt \end{aligned} \quad (\text{III-30})$$

and the cross-correlation functions are,

$$\begin{aligned} R_{ri}(r) &= \overline{r(t) i^*(t+r)} = \lim_{T \rightarrow \infty} \frac{1}{2T} \int_{-T}^{+T} r(t) i^*(t+r) dt \\ R_{ir}(r) &= \overline{i(t) r^*(t+r)} = \lim_{T \rightarrow \infty} \frac{1}{2T} \int_{-T}^{+T} i(t) r^*(t+r) dt \end{aligned} \quad (\text{III-31})$$

Substituting these into the above expression for $|e(t)|^2$ and since $R_{xy}(r) = R_{yx}^*(-r)$, and $R_{xx}(0) = \overline{X^2}$

$$\begin{aligned} |e(t)|^2 &= R_{rr}(0) - \int_0^\infty b^*(r) R_{ir}(r) dr - \int_0^\infty b(r) R_{ri}(r) dr \\ &\quad + \int_0^\infty dr \int_0^\infty du b(r) b^*(u) R_{ii}(r-u) \end{aligned} \quad (\text{III-32})$$

Eq. (III-32) gives the mean square error in terms of the auto and cross correlations of the input and output time functions and the equivalent linear weighting function. The next part of the problem is to find the minimum value of $|e(t)|^2$ with respect to $b(r)$. Looking at Eq. (III-32) it becomes apparent that the usual method of differentiating to find extreme values is not applicable here because:

(1) $b^*(r)$ is not differentiable with respect to $b(r)$.

(2) The unknown function, $b(r)$, appears under the definite integral sign.

We must therefore take recourse to the calculus of variations. The general procedure is simple enough and will be outlined below.

Given the integral $I = \int_{x_0}^{x_1} F[y(x)] dx$, one desires to determine the function $y(x)$ which will make I a minimum. To do this, take a function $y_1(x)$ which is presumed to be close to $y(x)$, so that

$$y_1(x) = y(x) + \lambda z(x)$$

where λ is a small quantity and $z(x)$ is some arbitrary function of x with a continuous derivative in the interval $x_0 \leq x \leq x_1$. The neighboring function $y_1(x)$ can then be substituted into the integral. The integral is then a function of λ and the minimum value of $I(\lambda)$, if $y(x)$ (which equals $y_1(x)$ when λ is zero) is to be the function which makes $I(\lambda)$ a minimum, will be given by the condition

$$\left. \frac{dI(\lambda)}{d\lambda} \right|_{\lambda=0} = 0$$

Applying this to Eq. (III-32), the weighting function $b(r)$ will be set equal to $w(r) + \lambda z(r)$, where $w(r)$ is the optimum weighting function, λ is the small multiplier, and $z(r)$ is the arbitrary function. Eq. (III-32) then becomes

$$\begin{aligned} |e(t)|^2 = & R_{rr}(0) - \int_0^\infty [w^*(r) + \lambda z^*(r)] R_{rr}(r) dr - \int_0^\infty [w(r) + \lambda z(r)] R_{rr}(r) dr \\ & + \int_0^\infty \int_0^\infty du [w^*(r) + \lambda z^*(r)] [w(u) + \lambda z(u)] R_{ii}(r-u) \end{aligned} \quad (\text{III-33})$$

Differentiating Eq. (III-33) with respect to λ , and setting the expression obtained equal to zero, and then setting $\lambda=0$ we obtain

$$\int_0^\infty z^*(r) R_{rr}(r) dr + \int_0^\infty z(r) R_{rr}^*(r) dr - \int_0^\infty \int_0^\infty du R_{ii}(r-u) [z(u) w^*(r) + w(u) z^*(r)] = 0 \quad (\text{III-34})$$

Now $R_{ii}(r-u)$ is an autocorrelation function, and therefore an even function which can be expressed as $R_{ii}(r) = R_{ii}^*(-r)$, even though the conjugate of R_{ii} is just R_{ii} . Therefore, integrals of the form:

$$\begin{aligned} \int_0^\infty \int_0^\infty du R_{ii}(r-u) z(u) w^*(r) &= \int_0^\infty \int_0^\infty du R_{ii}(u-r) z(r) w^*(u) \\ &= \int_0^\infty z(r) dr \int_0^\infty w^*(u) R_{ii}^*(r-u) du \end{aligned} \quad (\text{III-35})$$

Then, Eq. (III-34) will take the form,

$$\int_0^\infty z^*(r) dr [R_{rr}(r) - \int_0^\infty R_{ii}(r-u) w(u) du] + \int_0^\infty z(r) dr [R_{rr}^*(r) - \int_0^\infty R_{ii}^*(r-u) w^*(u) du] = 0 \quad (\text{III-36})$$

Now, if U is defined as

$$U = \int_0^\infty z^*(r) dr [R_{rr}(r) - \int_0^\infty R_{ii}(r-u) w(u) du]$$

then Eq. (III-36) has the form

$$U + U^* = 0 \quad (\text{III-37})$$

If U were a pure imaginary it could satisfy Eq. (III-37), but since U is a function of $z(r)$, which is completely arbitrary, then U must be arbitrary. It follows, therefore, that U must be zero. Then

$$\int_0^\infty z^*(r) dr [R_{rr}(r) - \int_0^\infty R_{ii}(r-u) w(u) du] = 0 \quad (\text{III-38})$$

or, since $z(r)$ is arbitrary,

$$R_{rr}(r) - \int_0^\infty R_{ii}(r-u) w(u) du = 0 \quad \text{for } r \geq 0 \quad (\text{III-39})$$

Finally, replacing $w(u)$ by $b(u)$, with the same definition as the "best" weighting function,

$$R_{rr}(r) = \int_0^\infty b(u) R_{ii}(r-u) du \quad (\text{III-40})$$

which is the same as Eq. (III-26), the previously given answer.

Returning to the main argument, we can compare, for the case of the simple nonlinearity previously considered, the result of the use of this general linearization with the result obtained for the pure gain previously assumed. For a pure gain to be the best linear approximation in this case requires

$$R_{ii}(r) = KR_{ii}(r) \quad (\text{III-41})$$

If the input were a sine wave, Eq. (III-41) would be valid; e.g., the sinusoidal describing function for limiting has already been shown to be a pure gain. Also, since a Gaussian process can be thought of as being the equivalent of a signal consisting of an infinite number of sinusoids of random amplitudes, different frequencies, and random phases, Eq. (III-41) will also be valid for inputs with Gaussian amplitude distributions. For other inputs with different amplitude distributions, Eq. (III-41) will generally not hold, and the best linear approximation may be frequency sensitive. In any event, it is comforting that Gaussian input describing functions for simple nonlinearities will be amplitude, i.e., variance, sensitive pure gains, and that a strong conceptual tie exists between the simple sinusoidal describing function and the more complex one with Gaussian inputs. In particular it is important to note that Gaussian input describing functions for simple nonlinearities can be readily derived from Eq. (III-19), which is repeated below in its proper form for Gaussian inputs.

$$K = \frac{\int_{-\infty}^{\infty} x f(x) p(x) dx}{\int_{-\infty}^{\infty} x^2 p(x) dx} = \frac{\int_{-\infty}^{\infty} x f(x) e^{-\frac{x^2}{2\sigma^2}} dx}{\sqrt{2\pi} \sigma^3} \quad (\text{III-42})$$

For complex nonlinearities, Eq. (III-26) permits a direct approach to the determination of the "best" Gaussian input describing function. It does not, however, provide a completely happy ending. A major problem still exists in the determination of the cross-correlation and autocorrelation functions. In all but a few special cases the cross-correlation is most easily obtained experimentally. Here one comes to the real value of the statistical input describing function since it adds a final piece of information to a wide body of theory upon which an extremely valuable technique for system's evaluation can be based. The general concepts of this method will be discussed in a succeeding sub-section.

Finally, it should be noted that all of the preceding discussion, for both sinusoidal and random input describing functions, has been on the equivalent linearization of a general system containing nonlinearities, where the inputs to the nonlinear elements have been known. When the quasi-linearization technique is applied to a control system employing feedback, the situation is complicated by the fact that the input to the nonlinear element also depends upon its response. To determine the equivalent linear transfer function then requires a knowledge of the probability density function of the actual input to the nonlinearity, and not merely that of the system forcing function. This can lead to a difficult situation. Although a general situation can be very difficult to analyze, considerable simplification is often possible for both the sinusoidal and Gaussian input describing functions. This is due to the happy circumstance that in a linear system having either a sinusoidal or Gaussian input all the other signals in the system are also sinusoidal or Gaussian. If a nonlinearity exists in the system, the sinusoidal or Gaussian nature of the signals is destroyed, but due to the low-pass nature of most control systems the input to the nonlinearity may still be approximately sinusoidal or Gaussian. Therefore, the application of these types of quasi-linearized describing functions is often valid, even when the nonlinearity is strong.

3. The Step Input Describing Function

Essentially the same notions previously applied to the cases of sinusoidal and random appearing inputs can be applied to the case when transient inputs are applied.† Here again one uses the fundamental principle that the quasi-linear representation of the system must be based upon its actual input, or one which approximates the actual input as closely as possible. In the present report, the most important transient describing function is that for step inputs, so it will be the only one discussed in detail.

In the case of the sinusoidal and Gaussian input describing functions we can deal fairly exclusively with single elements rather than with closed loop systems since, in both cases, all of the signals in a linear system

† Much of the early work on transient input describing functions is due to Chen [15].

will have the same form as the input. In the case where transient inputs are used as the basis for the definition of describing functions these considerations are no longer valid. This is due to the fact that the form of a transient input into a nonlinear element depends upon location of the element within the closed loop system to a much greater extent than in the case of sinusoidal or Gaussian inputs. Therefore, a given nonlinear element such as limiting does not have a practically useful, essentially unique, transient describing function. On the other hand, a given control system does have such a transient describing function. To illustrate these ideas and the general method of obtaining transient input describing functions, consider the system of Fig. 9. Here a step function is applied to a closed loop system consisting of a limiter and a pure integration.

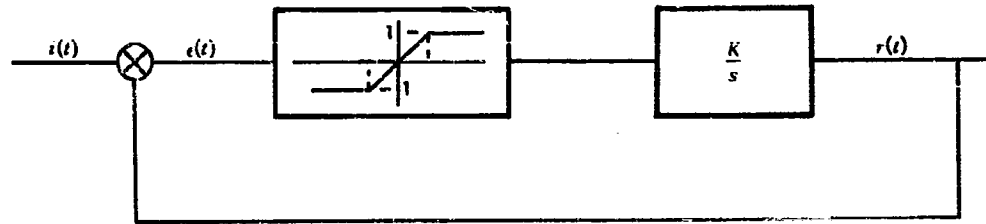


Figure 9. Block Diagram of a Simple Feedback System Containing a Limiter.

If the input, $i(t)$, is a step function of magnitude n , where n is greater than unity, then the limiter output immediately following $t = 0$ will be unity and $r(t)$ will be equal to Kt until a time t equal to $(n-1)/K$. Therefore

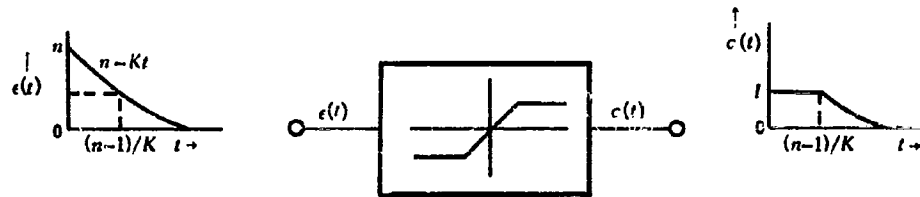


Figure 10. Limiter with Actual Input and Output.

between the times given by $0 < t < (n-1)/K$, the actual input to the nonlinear element is $e(t) = n - Kt$. This can be considered to be the proper signal to use as a "test" of the limiter to determine its output, as shown in Fig. 10. The limiter can then be replaced by an equivalent linear element and an additional input, or remnant, signal. This is shown in Fig. 11, where the linearized transfer characteristic of the limiter is its gain in the unlimited region (unity) and the remnant signal, $a(t)$, accounts for the discrepancy when the limiter operates in the saturated region. The remnant signal, $a(t)$, can be put into a form derivable from the input directly, as shown in Fig. 12. The transfer function giving $a(t)$ from the input, $i(t)$, will be called $Y_a(s)$, and can be seen to be given by:

$$Y_a(s) = \frac{\frac{n-1}{s} - \frac{K}{s^2} \left(1 - e^{-\frac{(n-1)s}{K}} \right)}{n/s} = \frac{n-1}{n} - \frac{K}{ns} \left(1 - e^{-\frac{(n-1)s}{K}} \right) \quad (\text{III-43})$$

One can now replace the nonlinear element by its equivalent linearized blocks, as shown in Fig. 13. Finally, this block diagram can be manipulated to give the equivalent block diagram of Fig. 14. This is the effective linearized system, and shows rather nicely several interesting aspects of nonlinear systems. First, it is noticed that the

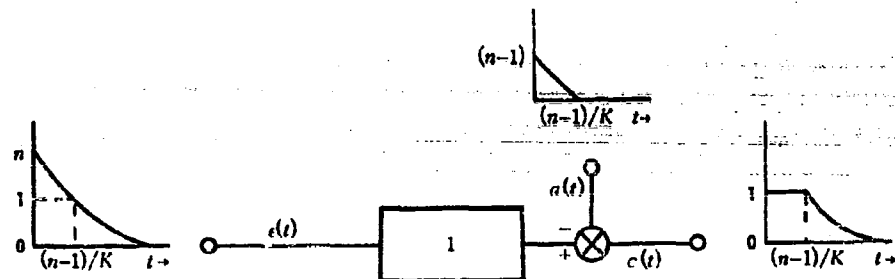


Figure 11. Equivalent Limiter Consisting of Describing Function and Remnant.

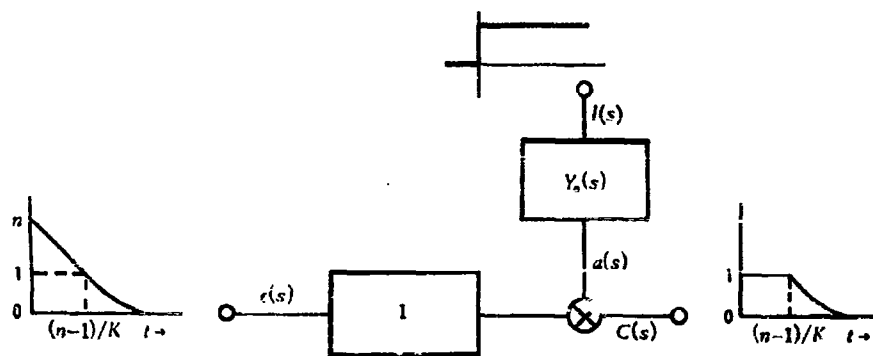


Figure 12. Equivalent Limiter with Remnant Derived from a Linear Operation on the Input.

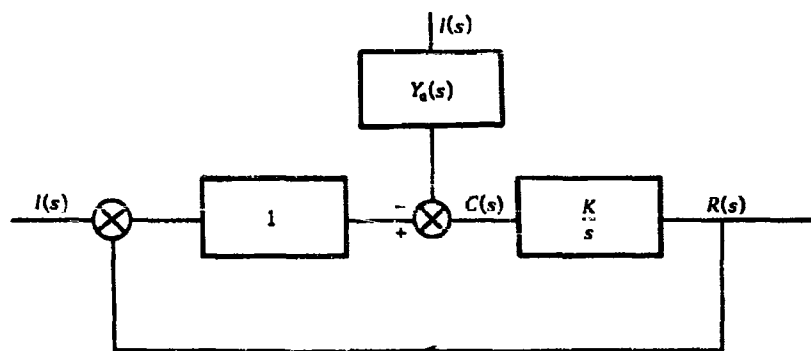


Figure 13. Equivalent Block Diagram of System with Limiter.

effects of the nonlinearity in this case can be approximated by inserting a particular linear network outside the closed loop. Second, it is observed that the characteristics of this linear transfer function are functions of both the input, n , and the characteristics of the system, in this case K . In essence, the effect of the nonlinearity has

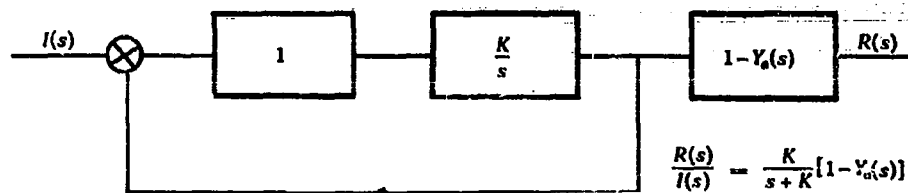


Figure 14 Modified Equivalent Block Diagram of System with Limiter.

been represented by a closed loop linear system operating into a linearized transfer characteristic which depends upon the nonlinear element, the input, and system parameters. In general, this sort of representation will always be possible with systems having single, simple, piecewise-linear elements within the loop. It can often be applied when more than one nonlinear element is present, though the complexity in applying the method increases rapidly with the number of nonlinear elements. The fundamental problem in the method is involved in finding the transfer function, $Y_n(s)$, which relates the output of the linearized closed loop system to the actual approximate output, i.e., that element which gives an "equivalent" effect of the nonlinearity.

When the nonlinearity is a complex one such as hysteresis, backlash, etc., but can still be represented by piecewise-linear characteristics, the problem of a quasi-linearization is much more difficult. Also, in these cases the effect of the nonlinearity cannot, in general, be taken care of by a block external to the closed loop.

C. THE MEASUREMENT OF GENERAL SYSTEM QUASI-LINEAR DESCRIBING CHARACTERISTICS

A primary intent of the last section was to develop general notions about describing functions so that they could be used as fundamental techniques in the description of the human operator for a restricted and specific set of conditions. By utilizing these concepts we can often preserve to some extent the simplicity of linear models without serious sacrifice of accuracy in describing the system characteristics.

As a design tool the sinusoidal input describing function technique has great application in estimating stability with known nonlinear elements and in interpreting harmonic response results. The statistical input describing functions have great value as indicators of performance in situations where the general types of inputs are statistical in nature. But perhaps the greatest merit of statistical input describing functions lies in the fact that they provide a fairly firm theoretical edifice for the measurement and equivalent linearization of quite general systems which may incorporate components having unknown characteristics. As examples of such systems one could include things as complex as the economic system and as simple as an optimizing positional servo. Another excellent example is the problem considered in this report — that of characterizing the dynamics of human operators in various tracking tasks.

Having noted the general usefulness of the describing function as a basis of measurement, it now becomes necessary to develop an abbreviated body of theory upon which to proceed. In the present instance, the chief concern is that of measuring human operator characteristics while operating in a closed loop task with random appearing inputs. The random appearing inputs used in the fundamental measurements have been either several non-harmonically related sine waves or functions having Gaussian amplitude distributions. The following formulation is general enough to apply to either.

Before proceeding with the detailed development of the quantities important in measurement, it is desirable to make some comments about the general form in which these results should be obtained. Most of the development discussed to this point has been in terms of time functions, i.e., auto and cross-correlation functions,

weighting functions, etc. Much of this has been for analytical convenience and to enable the reader to refer easily to the referenced sources. All of the results obtained in terms of time functions can be interpreted equally well in the transform domain, since all of the functions concerned can be considered to have Fourier transforms. For example, the Fourier transform of the autocorrelation and cross-correlation functions are the power spectral density and cross-spectral density, i.e., the spectral density, $\Phi_{ii}(\omega)$, is

$$\Phi_{ii}(\omega) = 2 \int_{-\infty}^{\infty} R_{ii}(\tau) e^{-j\omega\tau} d\tau$$

and the cross-spectral density, $\Phi_{iv}(\omega)$ is

$$\Phi_{iv}(\omega) = 2 \int_{-\infty}^{\infty} R_{iv}(\tau) e^{-j\omega\tau} d\tau$$

Just as the correlation functions are defined in terms of the time signals, the spectra are defined in terms of the Fourier transforms of the time signals. If $I(j\omega)$ and $R(j\omega)$ are the Fourier transforms of $i(t)$ and $r(t)$, then the spectral density Φ_{ii} is

$$\Phi_{ii} = \lim_{T \rightarrow \infty} \frac{1}{T} [I^*(j\omega) I(j\omega)] = \lim_{T \rightarrow \infty} \frac{1}{T} |I(j\omega)|^2$$

and the cross spectrum, $\Phi_{iv}(j\omega)$ is

$$\Phi_{iv} = \lim_{T \rightarrow \infty} \frac{1}{T} [I^*(j\omega) R(j\omega)]$$

Because of this duality between the time and frequency domains, we could conceivably take our measurements using either type of function.† As an aid in deciding which type to use, we can consider three aspects of the problem. These are:

- (1) The desired form of the end result.
- (2) The relative difficulty of data reduction.
- (3) The adequacy of the data in a reduced form.

The answer to the first item is straightforward when part of the final result is to be either a transfer function or a weighting function which is to be further analyzed and interpreted. While these two functions are transforms of one another, the transfer function is by far the easiest to manipulate. When the simple practical advantages of Bode plots are also considered, particularly in terms of one's ability to curve-fit such diagrams, the transfer function is quite definitely the preferred form.

Regarding the second item, the technique chosen for effecting the data analysis, and the amount of computation noise which is tolerable determine the decision. Thus, if one is in a position to use analog filter techniques on the data, the calculation of spectra is indicated since frequency analysis is a straightforward analogue computation, whereas the computation of lagged products is somewhat more difficult. If one is able to use high speed digital machines, and these machines are reasonable for the problem involved, there is little to choose computationally between a frequency or a time domain description of the data. Although procedurally the computation of correlations would precede the computation of spectra on such machines, the added machine manipulations do not constitute a substantial argument. Perhaps the only computational excuse for not computing spectra would arise when individual desk calculators were being used to reduce the data. In such a primitive example, the added labor burden might argue against transforming the correlations. This situation is, however, quite remote.

The third item is the real clincher for the outright reduction of data into spectral form. In any measurement program involving complex operations it is extremely desirable to have some notion of the adequacy of the results. The defining equations for correlations and spectra involve time averages over intervals which in the

† This duality exists precisely only for the complete integrals. In the practical case, with finite limits on the integrals and restricted amounts of data, it is probably wise to compute directly the quantity ultimately required. This avoids, to some extent at least, "the twin dangers of cascaded mathematical approximation and complex propagation of statistical fluctuations." [Tukey, 80.]

limit approach infinity. Clearly then any empirical data must be interpreted as estimates of the true values of the desired quantities. Although the theory for sampling errors in correlation functions results in cumbersome formulations, Tukey and others [4, 8, 37, 38, 65, 75, 80, 81] have developed straightforward techniques for assigning sampling error confidence limits to spectra. Unfortunately, the assignment of confidence limits to cross spectra has not as yet been presented in a reasonably simple way. Heuristic efforts have been made [53] and more rigorous developments are presently nearing completion.[†]

For these reasons, we can conclude that the use of the spectral form of the data is preferable, at least at the present time. The following developments therefore use spectral terms almost entirely.

The fundamental control situation to be considered is illustrated in Fig. 15, where a compensatory system is used for simplicity. In this block diagram, the action of the human is represented by the weighting function, $y_p(r)$, which operates on the error, and a remnant, $n_c(t)$. The input to the operator is the error, $e(t)$, and he

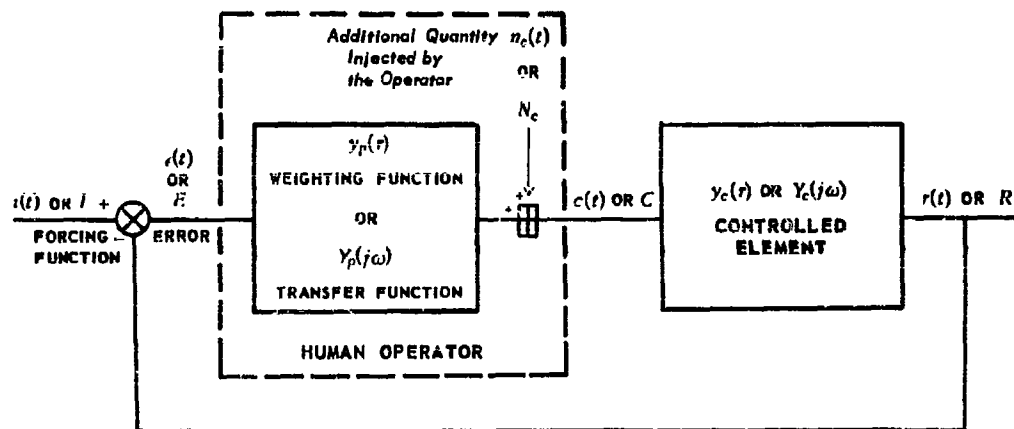


Figure 15. Block Diagram Showing Human Operator in Continuous Control Task.

controls the controlled element which includes the dynamics of everything, other than the operator, that is present in the loop. In the problem at hand the task is to find the characteristics of the operator, i.e., $y_p(r)$ and $n_c(t)$, or some closely related quantities from measurements made from observable signals in the loop. The various signals concerned are recapitulated below, both as time functions and as their transforms. So that the various time functions may be considered to have Fourier transforms it should be understood that the time function used in the transform is identical to the actual time function in the intervals $-T < t < T$, and is zero elsewhere. That is, the Fourier transform of a typical signal, $f_1(t)$, will be used as,

$$F(j\omega) = \int_{-T}^T f(t) e^{-j\omega t} dt; \quad \text{where: } f(t) = f_1(t); \quad -T < t < T$$

$$f(t) = 0 \quad \text{elsewhere}$$

On this basis all of the signals in the loop have Fourier transforms. The principal notation to be used is summarized below.

[†] See also Section VI-D-3 for a more extensive discussion of these points.

Quantity	Time Function	Fourier Transform
System Forcing Function	$i(t)$	$I(j\omega)$ or I
Error Signal of the System; Input to the Operator	$e(t)$	$E(j\omega)$ or E
Operator Output	$c(t)$	$C(j\omega)$ or C
System Output Response	$r(t)$	$R(j\omega)$ or R
Remnant at the Operator's Output	$n_c(t)$	$N_c(j\omega)$ or N_c
Operator's Weighting and Describing Functions	$y_p(r)$	$Y_p(j\omega)$ or Y_p
Controlled Element Weighting and Transfer Functions	$y_c(r)$	$Y_c(j\omega)$ or Y_c

1. Determination of the Open Loop Describing Function, Y_p

From the block diagram it is apparent that the operator's output is given by

$$C = Y_p E + N_c \quad (\text{III-45})$$

and the error is given by

$$E = I - R = I - Y_c C = I - Y_c(Y_p E + N_c) \quad (\text{III-46})$$

so that

$$C = Y_p(I - Y_c C) + N_c \quad (\text{III-47})$$

or

$$C(1 + Y_c Y_p) = Y_p I + N_c \quad (\text{III-48})$$

so that the operator's output becomes

$$C = \frac{Y_p I + N_c}{1 + Y_c Y_p} \quad (\text{III-49})$$

which is the result previously given in Eq. (I-1). Similarly

$$E = \frac{I - Y_c N_c}{1 + Y_c Y_p} \quad (\text{III-50})$$

The cross-spectral density functions Φ_{ic} and Φ_{ie} can be found as follows,

$$\begin{aligned} \Phi_{ic} &= \lim_{T \rightarrow \infty} \frac{1}{T} (I^* C) = \lim_{T \rightarrow \infty} \frac{1}{T} [I(-j\omega) C(j\omega)] \\ &= \lim_{T \rightarrow \infty} \frac{1}{T} \left[\left(\frac{Y_p I + N_c}{1 + Y_c Y_p} \right)^* \right] = \left(\frac{1}{1 + Y_p Y_c} \right) \left[Y_p \lim_{T \rightarrow \infty} \frac{1}{T} (I^* I) + \lim_{T \rightarrow \infty} \frac{1}{T} (N_c^* I) \right] \quad (\text{III-51}) \end{aligned}$$

The quantity, $\lim_{T \rightarrow \infty} \frac{1}{T} (I^* I)$ is recognized as the power spectral density of the forcing function, $\Phi_{ii}(\omega)$. The quantity $\lim_{T \rightarrow \infty} \frac{1}{T} (N_c^* I)$ is similarly recognized as the cross spectral density between the forcing function and the remnant, $\Phi_{in_c}(j\omega)$. This cross spectrum is zero, since by definition N_c has no linear coherence with the forcing function I . Then Eq. (III-51) becomes

$$\Phi_{ic} = \frac{Y_p}{1 + Y_p Y_c} \Phi_{ii} \quad (\text{III-52})$$

Similarly, it can be shown that the cross spectral density between the error and the input is

$$\Phi_{ie} = \frac{1}{1 + Y_p Y_c} \Phi_{ii} \quad (\text{III-53})$$

Consequently, the open loop describing function Y_p is given by

$$Y_p = \frac{\Phi_{ic}}{\Phi_{ie}} \quad (\text{III-54})$$

2. The Spectral Density of the Remnant

In most instances the value of the open loop injected remnant, N_c , as a Fourier transform is not a particularly important piece of information. On the other hand, the spectral density of N_c is often an extremely valuable "property" of an equivalent linear system. To find this quantity we can form the operator output power spectral density, noting, as before, that the forcing function-remnant cross spectra are zero,

$$\begin{aligned} \Phi_{cc} &= \lim_{T \rightarrow \infty} \frac{1}{T} (C^* C) = \lim_{T \rightarrow \infty} \frac{1}{T} \left[\left(\frac{Y_p I + N_c}{1 + Y_c Y_p} \right)^* \left(\frac{Y_p I + N_c}{1 + Y_c Y_p} \right) \right] \\ &= \left| \frac{Y_p}{1 + Y_c Y_p} \right|^2 \lim_{T \rightarrow \infty} \frac{1}{T} (I^* I) + \left| \frac{1}{1 + Y_c Y_p} \right|^2 \lim_{T \rightarrow \infty} \frac{1}{T} (N_c^* N_c) \\ &= \left| \frac{Y_p}{1 + Y_c Y_p} \right|^2 \Phi_{ii} + \left| \frac{1}{1 + Y_c Y_p} \right|^2 \Phi_{nn} \end{aligned} \quad (\text{III-55})$$

In most cases it is easiest to measure the total output power in terms of that portion linearly coherent with the forcing function (the first term above) and a remainder or "closed loop" remnant. Since $Y_p/(1 + Y_c Y_p)$ is recognized as a closed loop describing function, H , and defining $|1/(1 + Y_p Y_c)|^2 \Phi_{nn}$ as the closed loop remnant spectral density Φ_{nn} , we can write Eq. (III-55) as

$$\Phi_{cc} = |H|^2 \Phi_{ii} + \Phi_{nn} \quad (\text{III-56})$$

The possible sources and points of injection of the actual quantities composing the closed loop remnant will be discussed later. For the present, the term Φ_{nn} is preferred since it represents, without regard to origin, the total portion of the operator's output power which is not linearly coherent with the input.

3. Power Spectra of the Error and the Mean Squared Error

The power spectral density of the error can be found in several forms. The most obvious is simply

$$\begin{aligned} \Phi_{ee} &= \lim_{T \rightarrow \infty} \frac{1}{T} (E^* E) = \lim_{T \rightarrow \infty} \frac{1}{T} \left[\left(\frac{I - Y_c N_c}{1 + Y_c Y_p} \right)^* \left(\frac{I - Y_c N_c}{1 + Y_c Y_p} \right) \right] \\ &= \left| \frac{1}{1 + Y_c Y_p} \right|^2 \lim_{T \rightarrow \infty} \frac{1}{T} (I^* I) + \left| \frac{Y_c}{1 + Y_c Y_p} \right|^2 \lim_{T \rightarrow \infty} \frac{1}{T} (N_c^* N_c) \end{aligned} \quad (\text{III-57})$$

which, in terms of the closed loop transfer function, is

$$\Phi_{ee} = \left| \frac{H}{Y_p} \right|^2 \Phi_{ii} + |Y_c|^2 \Phi_{nn} \quad (\text{III-58})$$

An equivalent expression can be found from considering Eq. (III-46). In this instance

$$\begin{aligned}\Phi_{ee} &= \lim_{T \rightarrow \infty} \frac{1}{T} (E^* E) = \lim_{T \rightarrow \infty} \frac{1}{T} [(I - Y_c C)^* (I - Y_c C)] \\ &= \lim_{T \rightarrow \infty} \frac{1}{T} [(I^* I) - Y_c^* (C^* I) - Y_c (I^* C) + |Y_c|^2 (C^* C)] \\ &= \Phi_{ii} + |Y_c|^2 \Phi_{cc} - 2 \operatorname{Re} (Y_c \Phi_{ic})\end{aligned}\quad (\text{III-59})$$

A common performance parameter in many systems is the mean squared error. By definition, the mean squared error is given by

$$\overline{e^2(t)} = \lim_{T \rightarrow \infty} \frac{1}{2T} \int_{-T}^T e^2(t) dt = R_{ee}(0) \quad (\text{III-60})$$

This is related to the spectral density of the error by the expression

$$\overline{e^2(t)} = \int_0^\infty \Phi_{ee}(f) df = \frac{1}{2\pi} \int_0^\infty \Phi_{ee}(\omega) d\omega \quad (\text{III-61})$$

The mean squared error could then be found either by inserting (III-58) or (III-59) into (III-61). Oftentimes the ratio of the mean squared error to the mean square forcing function is an interesting measure of system performance. This quantity will be, using equations (III-59) and (III-61),

$$\frac{\overline{e^2(t)}}{\int_0^\infty \Phi_{ii}(f) df} = 1 + \frac{\int_0^\infty |Y_c(f)|^2 \Phi_{cc}(f) df - 2 \operatorname{Re} \int_0^\infty Y_c(f) \Phi_{ic}(f) df}{\int_0^\infty \Phi_{ii}(f) df} \quad (\text{III-62})$$

4. The Definition of the "Linear Correlation" and the Signal to Noise Ratio

In general, one tends to have the most confidence in the describing function technique when the quasi-linear transfer function, by itself, provides an adequate representation of the system, i.e., when the remnant term is relatively small. In practice this means that if the remnant is small, the analyst can ignore its effect. When the remnant is large, ugly suspicion will arise that some important nonlinear effects may be occurring, and the analyst is then forced into the often difficult task of trying to explain the source of the remnant on a basis consistent with the initial assumptions of quasi-linearity. If this process meets with little success, as would occur when the remnant was large and strongly correlated in a nonlinear fashion with the forcing function, the only recourse is to abandon the describing function concept and attempt to determine nonlinear approximations for the system.

In any event, it is desirable to have a means of relating the amount of linearly correlated output to total output. This fraction, called the linear correlation, can be found directly from Eq. (III-56). The fraction of the linearly correlated output power spectrum to the total output power spectrum is the square of the linear correlation, ρ , and is given by

$$\rho^2 = \frac{|H|^2 \Phi_{ii}}{\Phi_{cc}} = 1 - \frac{\Phi_{nn}}{\Phi_{cc}} \quad (\text{III-63})$$

If one prefers to think in terms of a signal to noise ratio, then since

$$\frac{\Phi_{nn}}{\Phi_{cc}} = 1 - \rho^2 \quad (\text{III-64})$$

the output signal to noise power ratio will be

$$\frac{|H|^2 \Phi_{ii}}{\Phi_{nn}} = \frac{|H|^2 \Phi_{ii}}{\Phi_{cc}} \frac{\Phi_{cc}}{\Phi_{nn}} = \frac{\rho^2}{1 - \rho^2} \quad (\text{III-65})$$

The linear correlation can also be found in terms of the cross-correlation function between the forcing function and operator output, since, by Eq. (III-52),

$$\Phi_{ic} = \frac{Y_p}{1 + Y_p Y_c} \Phi_{ii}, \text{ or } \frac{Y_p}{1 + Y_p Y_c} = H = \frac{\Phi_{ic}}{\Phi_{ii}} \quad (\text{III-66})$$

Then

$$\rho^2 = \frac{|H|^2 \Phi_{ii}}{\Phi_{cc}} = \frac{\Phi_{ic} \Phi_{ic}^* \Phi_{ii}}{(\Phi_{ii})^2 \Phi_{cc}} = \frac{|\Phi_{ic}|^2}{\Phi_{ii} \Phi_{cc}} \quad (\text{III-67})$$

or

$$\rho = \frac{|\Phi_{ic}|}{\sqrt{\Phi_{ii} \Phi_{cc}}} \quad (\text{III-68})$$

In practice, Eq. (III-68) is used to find ρ , which is then normally used to compute the closed loop remnant Φ_{nn} .

5. The Possible Sources of the Remnant Term

That portion of the operator's output which is not linearly coherent with the forcing function can often be a large and significant portion of the operator description. From an experimental point of view the total remnant, due to all sources, is conveniently lumped in the term Φ_{nn} , which we have previously called the closed loop remnant at the operator's output. From the standpoint of the analyst, the possible underlying sources of this remnant are extremely important, so some discussion of these is necessary here.

Fundamentally, the remnant, Φ_{nn} , is the power spectral density of all of the operator's output which is not linearly coherent with the forcing function, i.e., which cannot be "explained" as the result of a linear operation on the system input by the action of the operator. Therefore, in a given situation, components of Φ_{nn} could result from the following sources:

a. *Operator Responses to Other Inputs* — Operator responses to inputs other than the supposed system forcing function could exist in two categories,

- (1) The result of a linear operation by the operator on these other inputs.
- (2) The result of nonlinear operation on these inputs.

b. *Nonlinear Transfer Behavior* — Nonlinear operation by the operator on the forcing function. The portion of the remnant due to this source would be coherent with the forcing function by some nonlinear correlation.

c. *Injection of Noise Into the Loop* — Injection of "noise" into the loop which is completely uncorrelated with the forcing function, i.e., is unexplained by any linear or nonlinear correlation. This noise could be injected at any place within the operator's "block" in the system block diagram, though it is usually most convenient to consider it as being lumped at the input and/or the output of the block representing the linear operation of the operator.

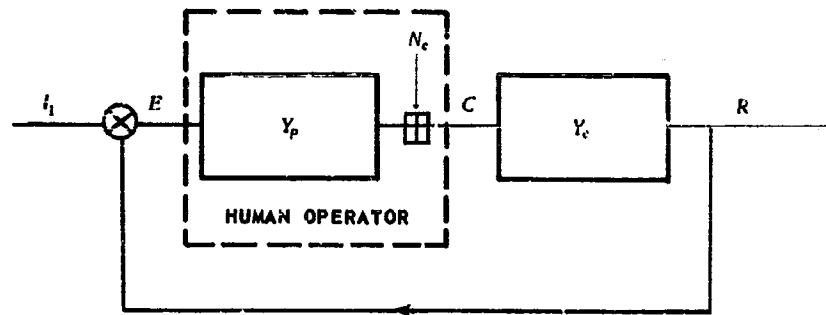
d. *Nonsteady Behavior of the Operator* — The variation, during a measurement run, of the operator's linear transfer characteristics. By necessity, the describing function is found experimentally by the use of fairly long runs, e.g., two to four minutes. In particular portions of these runs the operator may be responding in one linear fashion which is changed to various other linear modes of behavior during other portions of the run. The measured describing function is, of course, a particular kind of "average" of all these characteristics, and hence cannot "explain" all of the actual output power. This type of behavior has sometimes been called "nonstationary" operation of the operator, but in this report it will be called "nonsteady" behavior to avoid confusion with the term nonstationary as applied to time series.

Each of the above sources, with the exception of item a(1), will be considered in more detail in the following discussion.

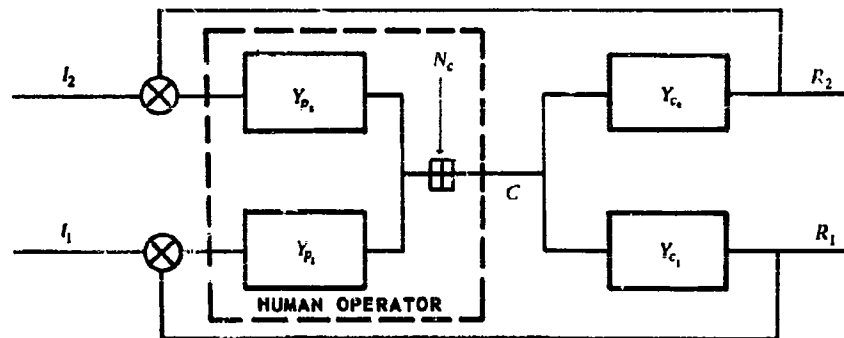
a. Operator Response to Other Inputs

To see the general effects of an additional input on the remnant term consider the two block diagrams of Fig. 16. In the single input system of Fig. 16a the spectral density of the operator's output, Φ_{cc} , is given by

$$\Phi_{cc} = \left| \frac{Y_p}{1 + Y_p Y_c} \right|^2 \Phi_{ii} + \left| \frac{1}{1 + Y_p Y_c} \right|^2 \Phi_{nn_c} \quad (\text{III-69})$$



a. Single Input System.



b. Double Input System.

Figure 16.

In the double input system of Fig. 16b, for which i_1 and i_2 are independent, the spectral density of the operator's output is

$$\Phi_{cc} = \left| \frac{Y_{p1}}{1 + Y_{p1} Y_{c1} + Y_{p2} Y_{c2}} \right|^2 \Phi_{ii_1} + \left| \frac{Y_{p2}}{1 + Y_{p1} Y_{c1} + Y_{p2} Y_{c2}} \right|^2 \Phi_{ii_2} + \left| \frac{1}{1 + Y_{p1} Y_{c1} + Y_{p2} Y_{c2}} \right|^2 \Phi_{nn_c} \quad (\text{III-70})$$

When the measurements are taken on a system such as that in Fig. 16b, but the assumption is made that the system configuration is that of Fig. 16a (which might be done because the existence of the second input, Φ_{ii_2} , is not known), the observed remnants and linear correlation would be

$$\begin{aligned}\Phi_{nn\text{obs}} &= \left| \frac{1}{1 + Y_{p_i} Y_{c_i} + Y_{p_s} Y_{c_s}} \right|^2 (|Y_{p_s}|^2 \Phi_{i i_s} + \Phi_{nn_e}) \\ \rho_{\text{obs}}^2 &= \left| \frac{Y_{p_s}}{1 + Y_{p_i} Y_{c_i} + Y_{p_s} Y_{c_s}} \right|^2 \frac{\Phi_{i i_s}}{\Phi_{nn_e}}\end{aligned}\quad (\text{III-71})$$

The actual remnant and linear correlation of the two-input system would be, of course,

$$\begin{aligned}\Phi_{nn\text{act}} &= \left| \frac{1}{1 + Y_{p_i} Y_{c_i} + Y_{p_s} Y_{c_s}} \right|^2 \Phi_{nn_e} \\ \rho_{\text{act}}^2 &= \left| \frac{1}{1 + Y_{p_i} Y_{c_i} + Y_{p_s} Y_{c_s}} \right|^2 \left(\frac{|Y_{p_i}|^2 \Phi_{i i_i} + |Y_{p_s}|^2 \Phi_{i i_s}}{\Phi_{nn_e}} \right)\end{aligned}\quad (\text{III-72})$$

The ratios of actual to observed remnants and linear correlations are then

$$\begin{aligned}\frac{\Phi_{nn\text{obs}}}{\Phi_{nn\text{act}}} &= 1 + |Y_{p_s}|^2 \frac{\Phi_{i i_s}}{\Phi_{nn_e}} \\ \frac{\rho_{\text{act}}}{\rho_{\text{obs}}} &= \sqrt{1 + \frac{|Y_{p_s}|^2 \Phi_{i i_s}}{|Y_{p_i}|^2 \Phi_{i i_i}}}\end{aligned}\quad (\text{III-73})$$

From Eq. (III-73) it can be seen readily that the operator's apparent remnant could be higher and the linear correlation lower if all the inputs were not taken into proper account. While this statement is almost a truism, improper consideration of all inputs, nonetheless, represents an important source of an observed remnant.

b. Nonlinear Transfer Behavior

With sinusoidal forcing functions the existence of nonlinear transfer characteristics would require harmonics in the output. When the forcing function is Gaussian, an analogous phenomena will occur, with the remnant containing power at all harmonics of the random amplitude and phase sinusoids which can be thought of as making up the Gaussian forcing function. This means that one necessary condition for the existence of nonlinear transfer characteristics is remnant power at frequencies other than those represented at substantial power levels in the forcing function spectrum. However, the mere existence of considerable remnant power outside the effective bandwidth of the forcing function is not a sufficient condition for the existence of nonlinear behavior in the transfer characteristic, since injected noise can lead to the same result.

A necessary and sufficient condition for nonlinear transfer behavior is present when the describing function is dependent upon forcing function amplitude. This possibility may be readily checked experimentally by using more than one amplitude for the forcing function (at equivalent spectrum shapes and bandwidths).

If the describing function for a given forcing function shape and bandwidth does have a distinct amplitude dependence, then the next step is an attempt to isolate the probable causes. This process is essentially one of decomposition of the describing function parameters into those that are dependent on the input amplitude and those that are not. Further examination of the amplitude dependent parameter will then often lead fairly directly to the possible source. For example, if one had a measured transfer function having an approximate analytical model $K(\sigma)/(T_s + 1)$, and plotting $K(\sigma)$ versus σ resulted in a plot that looked similar to Fig. 8, then one would suspect that a limiter was present. This type of detective work can often be used quite successfully, but one should remember that the validity of the procedure depends upon the assumption that the element input signal is essentially Gaussian (if the forcing function is Gaussian).

c. Injection of Noise Into the Loop

A portion of the remnant may result from the injection into the loop, by the operator, of an extraneous signal uncorrelated with the forcing function signal. Its point or points of injection could be almost anywhere

within the human operator block in the block diagram. Since the operator is considered to have only two terminals, i.e., an input and an output, the experimenter can measure only the effects of the extraneous signals at the output. The exact locations and forms of components of this overall signal are therefore impossible to determine by experimental techniques based only upon this type of two terminal model. However, it is often possible to show that suitable models, based upon other data and reasonable assumptions, might result in an effect at the output equivalent to that actually observed. To gain insight into the possible forms of these models it is often valuable to take the measured closed loop remnant data and transcribe it into equivalent open loop data. This is generally done assuming that all of the Φ_{nn} term is due to the injection of an extraneous signal at a particular point in the control loop. For example, if all of the closed loop Φ_{nn} is assumed to be due to noise injected by the operator at his output, then the power spectral density of this open loop output noise will be (see discussion preceding Eq. (III-56))

$$\Phi_{nn_e} = |1 + Y_p Y_c|^2 \Phi_{nn} = \frac{|Y_p|^2}{|H|^2} \Phi_{nn} \quad (\text{III-74})$$

On the other hand, if all of the closed loop Φ_{nn} is assumed to come from noise injected by the operator at his input, then the power spectral density of this open loop operator input noise will be

$$\Phi_{nn_e} = \left| \frac{1 + Y_p Y_c}{Y_p} \right|^2 \Phi_{nn} = \frac{\Phi_{nn}}{|H|^2} \quad (\text{III-75})$$

If the operator's transfer block is broken down into a more detailed block diagram, other sources could also be considered in a similar fashion.

Once the remnant term is placed in one of these open loop forms the analyst can attempt to derive some model which appears to fit the data. This is a powerful technique in many cases, and can often lead to considerable insight into what may actually be occurring in the system.

d. Nonsteady Behavior of the Operator

During any measurement run we would expect the operator to vary his transfer characteristics to some extent, and this variation of transfer characteristics will have a distinct influence on the operator's output power. In other words, we would expect the actual system linear transfer characteristic to be given by some system function $H(j\omega; t)$ instead of simply $H(j\omega)$. This possibility immediately brings up two important problems,

- (i) If the system function is time varying, i.e., given by $H(j\omega; t)$ instead of $H(j\omega)$, what is the output power spectral density?, and
- (ii) What portion of the output spectral density of (i) is linearly coherent with the forcing function, i.e., capable of being "explained" by some transfer characteristic derived from a cross-correlation measurement?

If part of the output power of item (i) is not "linearly" coherent with the forcing function, in the sense mentioned above, then that portion is a possible source of remnant power.

Looking at the second question first, the operator's output, $c(t)$, is given by

$$c(t) = \mathcal{F}^{-1}[H(j\omega; t)I(j\omega)] \quad (\text{III-76})$$

As written, Eq. (III-76) is obviously linear, though the equivalent differential equation would have time varying coefficients. The reader could quite logically comment that any output power due to the transfer characteristic $H(j\omega; t)$ would be "linearly coherent" with the input, since $H(j\omega; t)$ is a linear operator. In the sense used here, however, linear coherence refers to that portion of the output given by the operation, upon the forcing function, of a transfer characteristic derived from cross-correlation measurements. From this point of view it is not obvious that all of the output power due to operation upon the input by a linear system function $H(j\omega; t)$ will be linearly coherent with the input. Exploring this further, the forcing function-operator output cross correlation is

$$\begin{aligned}
R_{ic}(r) &= \lim_{T \rightarrow \infty} \frac{1}{2T} \int_{-T}^{+T} i(t) c(t+r) dt \\
&= \lim_{T \rightarrow \infty} \frac{1}{2T} \int_{-T}^{+T} i(t) [3^{-1} [H(j\omega; t+r)] I(j\omega)] dt \\
&= \lim_{T \rightarrow \infty} \frac{1}{2T} \int_{-T}^{+T} i(t) \left[\frac{1}{2\pi} \int_{-\infty}^{+\infty} H(j\omega; t+r) I(j\omega) e^{j\omega t} d\omega \right] dt \quad (\text{III-77})
\end{aligned}$$

To apply this result directly to our problem, we shall assume that the describing function varies about some average value during a run, thereby becoming a time varying describing function. If we assume that the time variation is separable from an "average" transfer characteristic, which is a frequency function only, then

$$H(j\omega; t) = H_0(j\omega) + \Delta H(t) \quad \text{and} \quad H(j\omega; t+r) = H_0(j\omega) + \Delta H(t+r).$$

Equation (III-77) then becomes,

$$R_{ic}(r) = \lim_{T \rightarrow \infty} \frac{1}{2T} \int_{-T}^{+T} i(t) \left[\frac{1}{2\pi} \int_{-\infty}^{+\infty} H_0(j\omega) I(j\omega) e^{j\omega t} d\omega \right] dt + \lim_{T \rightarrow \infty} \frac{1}{2T} \int_{-T}^{+T} i(t) \left[\frac{1}{2\pi} \int_{-\infty}^{+\infty} \Delta H(t+r) I(j\omega) e^{j\omega t} d\omega \right] dt \quad (\text{III-78})$$

Consider only the second term on the right hand side of Eq. (III-78). This becomes

$$\lim_{T \rightarrow \infty} \frac{1}{2T} \int_{-T}^{+T} i(t) \Delta H(t+r) \left[\frac{1}{2\pi} \int_{-\infty}^{+\infty} I(j\omega) e^{j\omega t} d\omega \right] dt = \lim_{T \rightarrow \infty} \frac{1}{2T} \int_{-T}^{+T} i^2(t) \Delta H(t+r) dt \quad (\text{III-79})$$

or, alternatively,

$$= \frac{1}{2\pi} \int_{-\infty}^{+\infty} I(j\omega) \left[\lim_{T \rightarrow \infty} \frac{1}{2T} \int_{-T}^{+T} i(t) \Delta H(t+r) e^{j\omega t} dt \right] d\omega$$

In examining these integrals, each of which is the time-varying portion of the cross-correlation, there are two interesting cases to consider.

Case 1: $\Delta H(t)$ is an analytic function. $\Delta H(t+r)$ can then be expanded into a Taylor's series as

$$\begin{aligned}
\Delta H(t+r) &= \Delta H(r) + t \Delta H'(r) + \frac{t^2}{2} \Delta H''(r) + \frac{t^3}{3!} \Delta H'''(r) + \dots \\
&= \sum_{n=0}^{\infty} \frac{t^n}{n!} \frac{d^n \Delta H}{dt^n}(r) \quad (\text{III-80})
\end{aligned}$$

Substituting Eq. (III-80) into Eq. (III-79), we can obtain,

$$\sum_{n=0}^{\infty} \frac{1}{n!} \frac{d^n \Delta H}{dt^n}(r) \left[\lim_{T \rightarrow \infty} \frac{1}{2T} \int_{-T}^{+T} t^n i^2(t) dt \right] \quad (\text{III-81})$$

Since $\lim_{T \rightarrow \infty} \frac{1}{2T} \int_{-T}^{+T} t^2 i^2(t) dt$ is a constant, the limit and integral enclosed in the brackets of Eq. (III-81) will (if no further restrictions are placed upon the functions),

- a. diverge if $n > 0$
- b. be equal to 0 if $n = 0$

The instance for $n > 0$ is the important case since for $n = 0$ there is no time variation in the transfer function. Because we always have finite run lengths, however, the term in brackets will generally have a finite value, giving rise to a measured cross-correlation function which is time varying and dependent upon run length.

Case 2: $\Delta H(t)$ is a random function. If $\Delta H(t)$ is a random function there are two possibilities.

a. $\Delta H(t)$ has some coherence with $i^2(t)$ and hence with $i(t)$. In this instance the integral giving the time varying portion of the cross-correlation will have a value, and the cross-correlation measurement will then take it into account.

b. $\Delta H(t)$ has no coherence with $i^2(t)$ and consequently no coherence with $i(t)$.

Here the cross-correlation measurement will not take the time varying characteristic into account. The output power due to such a process will then be in the remnant and the cross-correlation will measure only the "average" transfer function $H_0(j\omega)$.

While the possibility of an analytical time variation in $\Delta H(t)$ is by no means ruled out at present, it is safe to say that it is improbable and so we shall drop it from further consideration. A stochastic $\Delta H(t)$, or a variation over the measurement runs that amount to almost the same thing is quite possible, however, and hence such a form of nonsteady behavior must still be considered.

Proceeding now to the first question above, the answer is readily at hand, for Zadeh has shown [95] that if the system function is $H(j\omega; t)$ instead of $H(j\omega)$, then the output autocorrelation function $R_{cc}(r)$ is given by

$$R_{cc}(r) = \mathfrak{I}^{-1} [R_{HH}(r, \omega) \Phi_{ii}(\omega)] \quad (\text{III-82})$$

Φ_{ii} is the forcing function power spectral density and $R_{HH}(r, \omega)$ is the correlation function of the system function, i.e.,

$$R_{HH}(r, \omega) = \lim_{T \rightarrow \infty} \frac{1}{2T} \int_{-T}^{+T} H(j\omega; t) H(-j\omega; t+r) dt \quad (\text{III-83})$$

Using equation (III-83),

$$\begin{aligned} R_{HH}(r, \omega) &= \lim_{T \rightarrow \infty} \frac{1}{2T} \int_{-T}^{+T} [H_0(j\omega) + \Delta H(t)] [H_0(-j\omega) + \Delta H(t+r)] dt \\ &= \lim_{T \rightarrow \infty} \frac{1}{2T} \int_{-T}^{+T} \{ |H_0|^2 + \Delta H(t) H_0(-j\omega) + H_0(j\omega) \Delta H(t+r) + \Delta H(t) \Delta H(t+r) \} dt \\ &= |H_0|^2 + H_0(-j\omega) \lim_{T \rightarrow \infty} \frac{1}{2T} \int_{-T}^{+T} \Delta H(t) dt + H_0(j\omega) \lim_{T \rightarrow \infty} \frac{1}{2T} \int_{-T}^{+T} \Delta H(t+r) dt + \lim_{T \rightarrow \infty} \frac{1}{2T} \int_{-T}^{+T} \Delta H(t) \Delta H(t+r) dt \quad (\text{III-84}) \end{aligned}$$

The first and second integrals will be zero if $\Delta H(t)$ is a stationary random process of zero mean, and the third integral is just the autocorrelation, $R_{\Delta H \Delta H}(r)$, of $\Delta H(t)$. So Eq. (III-84) becomes

$$R_{HH}(r, \omega) = |H_0|^2 + R_{\Delta H \Delta H}(r) \quad (\text{III-85})$$

The autocorrelation of the operator's output will then be

$$R_{cc}(r) = \mathfrak{I}^{-1} [|H_0|^2 \Phi_{ii}] + \mathfrak{I}^{-1} [R_{\Delta H \Delta H}(r) \Phi_{ii}] \quad (\text{III-86})$$

which, since $R_{\Delta H \Delta H}(r)$ is a function of r only becomes

$$R_{cc}(r) = \mathfrak{I}^{-1} [|H_0|^2 \Phi_{ii}] + R_{\Delta H \Delta H}(r) R_{ii}(r) \quad (\text{III-87})$$

If we desire the output spectral density rather than its autocorrelation, then

$$\begin{aligned} \Phi_{cc}(\omega) &= |H_0|^2 \Phi_{ii} + \mathfrak{I} [R_{\Delta H \Delta H}(r) R_{ii}(r)] \\ &= |H_0|^2 \Phi_{ii} + \int_{-\infty}^{+\infty} \Phi_{ii}(\omega') \Phi_{\Delta H \Delta H}(\omega' - \omega) d\omega' \end{aligned}$$

where $\Phi_{\Delta H \Delta H}(\omega)$ is the power spectral density of $\Delta H(t)$, or the Fourier transform of $R_{\Delta H \Delta H}(r)$. This second term is due to the nonsteady behavior of the operator, and will be denoted by the symbol $\Phi_{\Delta H}$ for convenience, i.e.,

$$\Phi_{\Delta H}(\omega) = 3[R_{\Delta H \Delta H}(r)R_{ii}(r)] = \int_{-\infty}^{\infty} \Phi_{ii}(\omega')\Phi_{\Delta H \Delta H}(\omega-\omega')d\omega' \quad (\text{III-89})$$

Then

$$\Phi_{cc}(\omega) = |H_0|^2 \Phi_{ii} + \Phi_{\Delta H}(\omega) \quad (\text{III-90})$$

Equation (III-90) answers the first question above, giving the output power spectral density due to the assumed sort of nonsteady operator behavior.

In general, probably the simplest technique for examining a remnant term suspected of being largely power due to nonsteady operator behavior is to work with the autocorrelation functions, for then

$$R_{\Delta H \Delta H}(r) = \frac{R_{nn}(r)}{R_{ii}(r)} \quad (\text{III-91})$$

and when $r=0$,

$$\sigma_{\Delta H \Delta H}^2 = \frac{\sigma_n^2}{\sigma_i^2} \quad (\text{III-92})$$

When none of the above possibilities, by themselves, are useful in explaining the origin of a large remnant term, one is reduced to the inevitable conclusion that either a combination of sources exists, or very nonlinear and/or nonsteady behavior is extremely important in the problem. If extreme nonlinear behavior is the answer, the quasi-linearization technique is not too applicable and one must seek a nonlinear approximation. From an analytical standpoint, nonlinear methods analogous to those quasi-linear techniques used to this point are in their infancy or nonexistent. In terms of the effort involved, nonlinear correlation methods make such things as the reduction of data into cross spectra (which is an onerous, time consuming task) appear like child's play. Therefore if the overall system is exceedingly nonlinear, in the sense described above, the most reasonable step may be to adopt a purely empirical approach and attempt to find a suitable nonlinear analog of the operator. When analog computer elements are used in this process, the overall nonlinear problem can often be fairly straightforward.

Section IV OPERATOR RESPONSE TO SIMPLE VISUAL INPUTS

A. THE OPERATOR'S RESPONSE TO SINGLE VISUAL STEP INPUTS

One of the simplest of tracking tasks is the process of following a single step forcing function in a situation where the controlled element has no appreciable dynamics.* Some aspects of the operator's behavior in performing such tasks have been studied by a host of investigators since the dawn of experimental psychology. Most of these investigators have been concerned with various reaction time experiments; a much smaller number have been concerned with examining the problem as a tracking task and applying dynamic analysis methods to the results. It is primarily the latter results which are reviewed here [14, 32, 57, 71, 77, 78].

In terms of experimental results, Fig. 17 shows typical responses [32] to visual step inputs from an experiment in which subjects were to follow a line on moving recording paper which could be viewed through a narrow, transverse slot. The original line drawn on the paper consisted of a step, which served as the forcing function. A line drawn by the subject was the output.

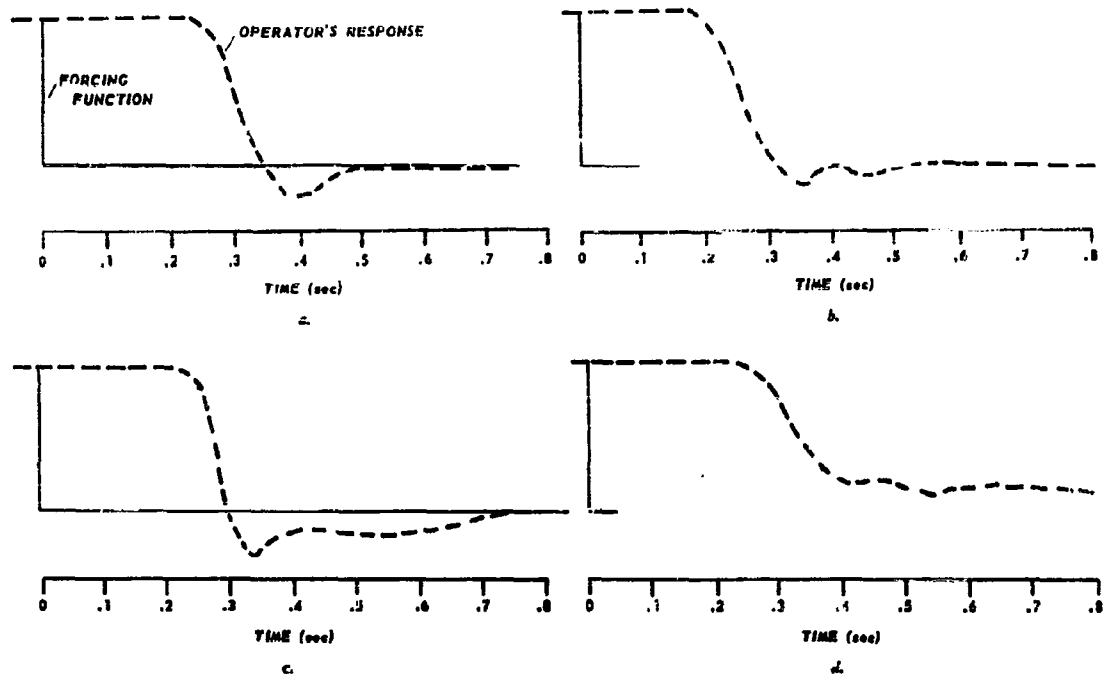


Figure 17. Typical Responses in Following Step Displacements of a Moving Line.
(Ref. 32)

Similar responses have been observed in an experiment in which subjects tracked a target by moving an aircraft type control stick [78]. The target was a dot seen against a vertical line on an oscilloscope. As the

*In the performance of the actual experimental work reviewed here a sequence of steps was supplied. In the sense used above, such a sequence is considered to be essentially a repetition of single step presentation if the time between successive steps is large, and the amplitudes of the steps are constant in magnitude, though possibly of either sign.

jumped to the right or left, the subject was to move the stick to return the dot to the vertical line as quickly as possible.

Reference 21 also describes comparable results in an experiment utilizing a vertically mounted, movable disk with a triangle painted at a point next to the outer edge having its apex pointed toward the center of the disk. The operator was provided with a control wheel linked directly with a pointer. After a step function had been applied to the disk the operator would line up his pointer with the apex of the triangle.

In terms of types of displays, the second mentioned is compensatory, the third pursuit, and the first has aspects of both. We will, however, discuss the results of all three experiments by considering only Fig. 17 since the experimental results are quite similar with respect to the effects in which we are interested at this time.

Inspection of these figures reveals that the response can be separated into two phases. The first phase consists of a dead portion (reaction-time delay) during which the subject makes no movement at all. After this initial period there is the *dynamic portion* of the response, during which the subject moves relatively quickly, ending with a small error (the primary movement of this positioning response); and then sometimes more slowly toward the new position of the line, eliminating the remaining error (the secondary movement).

The average duration of the dead time portion of the responses shown in Fig. 17 is about 0.25 seconds and is well within the range of simple reaction time to visual stimuli given in References 79 and 94. It is not meaningful to present average values for human reaction time to visual stimuli without considerable explanation since these time measurements are functions of such subject centered variables as attention, motor set, training, alertness, and mode of response, and of such stimulus variables as the complexity of the stimulus, the intensity of the stimulus, and the temporal interval between stimulus and alerting signal. A good lower limit for simple reaction time to a visual stimulus for a practiced alerted subject is 0.180 seconds. This total dead time may be analyzed into its components in an approximate fashion. The latencies of the visual process will vary from 0.035 to 0.070 seconds [76], depending on the intensity of the stimulus. Considering synaptic delays and peripheral and central conduction times, the total time for a command to reach the muscle would be 0.01 to 0.02 seconds, and the muscle contraction time would be between 0.02 and 0.04 seconds [69]. The difference between 0.180 and the sum of the lower or higher latencies for the components of the reaction time can be attributed to central organizing processes [57, 69, 78]. Such organizing processes would have to account for between 0.05 and 0.11 seconds for the example given. In Fig. 18 we have muscle action potentials from the biceps and triceps of the arm of a subject who

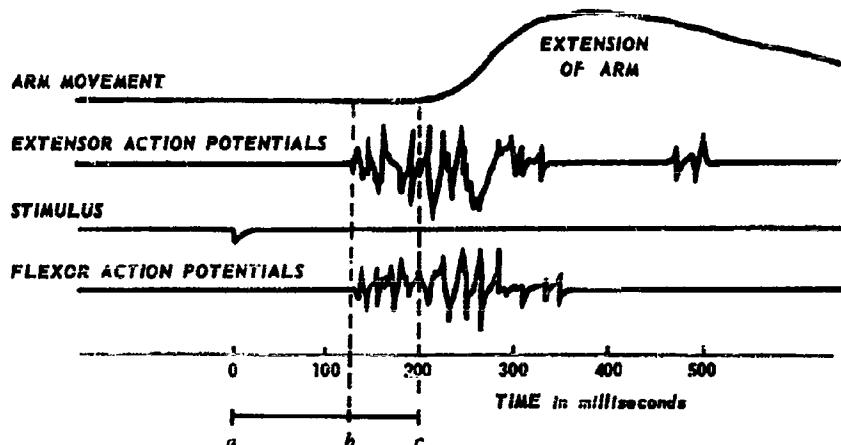


Figure 18. Muscle Coordination in the Extension of the Arm.
(From Ref. 39, p. 9)

was told to extend his arm as quickly as he could after seeing a visual signal. This response was ballistic rather than continuous. Note that the interval $c-a$, which is the reaction time of about 0.200 seconds consists of conduction, synaptic and organizing delays whose sum is 0.140 seconds measured by $b-a$, and a period of muscular contraction and preparation to move the arm of 0.06 seconds which is measured by $c-b$. The purpose in presenting this rather tenuous discussion of neural lags is to acquaint the reader with the physiological limits constraining this control system, and to raise the possibility that in certain types of control tasks the operator may be characterized by latencies which will be considerably shorter than the usual reaction time latencies, if his central organizing process latencies can be cut down by training or the nature of his task.

A movement response to a visual stimulus can be executed without *continual* visual control of the movement, as shown by (b) and (d) of Fig. 17. In these figures, although the line to be followed was suddenly terminated after the step occurred, the proper response continued with but relatively little final error. It is apparent from these results and the experimental setups that the dynamic portion of the response is *not* under a closed-loop type of control in which the eyes are used to continually measure the error. The detailed mechanism used by the human in generating these responses is not yet known, but speculation and some experimental effort has led to the interesting and instructive opposing points of view summarized below.

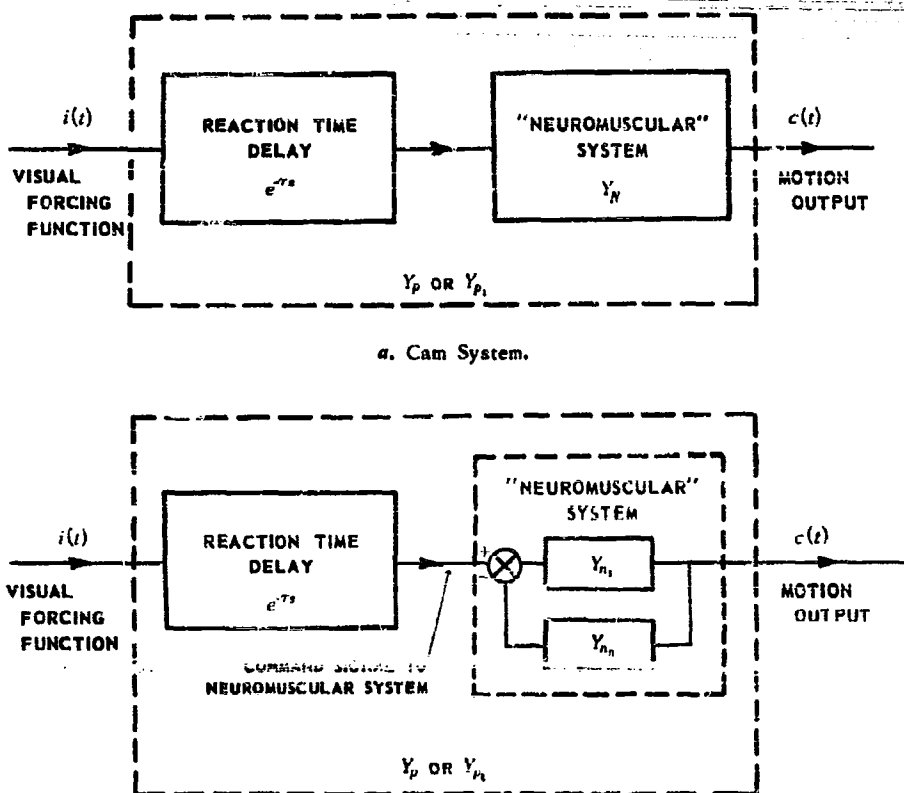
Reference 78 states that the dynamic portion of the response is ballistic with the effectors reacting in an open-loop fashion to the signal from the central nervous system which was set during the reaction-time delay. References 32 and 57, however, point out that such an open loop characteristic might not account for the oscillatory "hunting" which is apparent in some responses to step inputs, such as that in (b) or (c) of Fig. 17; and that an occasional oscillation of this sort could more readily occur if the dynamic portion of the response is made under some type of closed loop control. Since the eyes are apparently not included in this loop, the feedback signal, which is continually subtracted from the "command" signal set in the cerebellum during the dead portion of the response, would then come from the proprioceptive receptors in the effector which makes the response.

The proponents of the "cam action" or ballistic response viewpoints counter [16] part of the "closed loop" argument by experiments on kinesthetic reaction time. The results of these experiments yielded a kinesthetic reaction time of 0.129 seconds before a subject could stop a falling motion of his right arm, which was encased in a splint and initially held horizontally by an electromagnet. It was concluded from these tests that the kinesthetic reaction time was too long to permit continuous voluntary control of short-duration hand and arm movements by kinesthetic information furnished through feedback. Reference 16 also notes that the closed loop, proprioceptive feedback model would require continuous and up to date information on the space position of the body member. It is then stated that physiologists currently believe that the type of feedback underlying the proprioceptive reflexes arises from receptors which indicate the amount of tension within a muscle. The position of the body member is known, but this knowledge is presumably gained by a synthesis of the activity of a large number of receptor organs of different types and in different parts of the body. Such a computation would probably require a length of time comparable to a visual reaction time.

In partial answer to these objections, References 32, 33, and 57 state that a reaction-time delay is not determined by the time required for sensory perception and transmission, but that it is used up mostly in computing and setting the signal sent to the effectors. Then, if a computation and setting up of the response are not required, the time delay imposed on the feedback signal may be very small. This could conceivably be as small as the 0.03 to 0.06 seconds cited above for the combination of nerve conduction and muscle contraction. The hypothesis offered is that the dynamic portion of the response to a step input is made under closed-loop control with the proprioceptive senses, and without reaction-time delay. Support for this position can be found in studies which attempted to determine the rate at which a single motor unit could contract in voluntary contraction and yet have each contraction modified on the basis of its predecessor. Using the higher delay time of 0.06 seconds, one would conservatively expect that muscular contractions in continuously controlled movement would occur at a rate of slightly more than 10 per second. Electromyographic studies of voluntary movements of moderate strength show just such a rate of electrical discharge corresponding to muscle contractions [69].

Getting back to the experimental data, we can readily see that the facts are not describable by either the pure pursuit or pure compensatory block diagrams of Fig. 2 if the visual senses are not in the loop. In terms of an outer loop containing a visual sensor, the response appears to be essentially open loop, feeding through either Y_p in the compensatory case, or Y_{p_i} in the case of pursuit. In either event the result is the same, since both systems reduce to single blocks when viewed in this outer loop sense. The points of view discussed above are not contrary to this, but are concerned rather with the behavior within the blocks, Y_p or Y_{p_i} . This is probably most easily seen by referring to Fig. 19, which illustrates both notions. Since external measurements allow us to

determining only the characteristics of the input and output, we can only determine an equivalent transfer function for the operator of the form $e^{-\tau_s} Y_N(s)$. The transfer function Y_N will be called that of the "neuromuscular system" since both nerves and muscles are involved, regardless of the above stated points of view. The pure time-delay, $e^{-\tau_s}$, represents the effect of the visual reaction time for this type of input, and τ will be of the order of 0.25 sec.



a. Cam System.

b. Closed Loop Servo Analogy.

Figure 19.

To derive a step input describing function which would describe the dynamic portion of the response, curves can be fitted to typical responses to step inputs. Then the Laplace transform of the function representing the fitted curve is taken, multiplied by s (because the forcing function was a step function), and divided by the magnitude of the step. The resulting linear transfer function when multiplied by an $e^{-\tau_s}$ to take into account the reaction time delay, is an approximation to the overall transfer function of the subject in responding to a step function command. Work of this nature is described in detail in References 32, 33, and 57. Figure 20, taken from Reference 57, shows two curves fitted with typical responses. These and similar data were then put into transfer function form [32] giving the quantity $Y_N(s)$, which describes the overall dynamic portion of the operator's response.

If one is inclined to view the neuromuscular system as a closed loop operation, the open loop neuromuscular system transfer function ($Y_n Y_{n_o}$) of Fig. 19 can be readily found from these same data if it is presumed that $Y_{n_o} = \text{unity}$. For frequencies up to 20 rad/sec, polar plots of $Y_N(j\omega)$ were matched by the plots obtained by closing the loop around the function

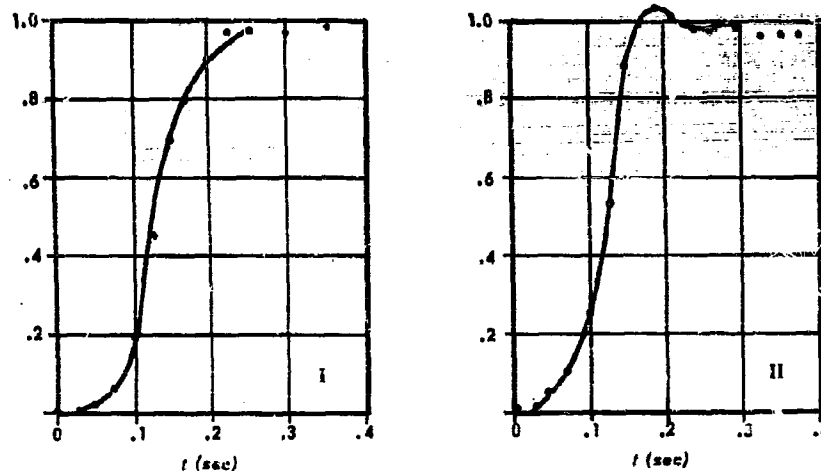


Figure 20. Dynamic Portion of the Responses of Subjects to Step Input (Reaction-Time Delay Omitted).
(Ref. 57)

$$KG(s) = \frac{K}{s(T^2s^2 + 2\zeta Ts + 1)} \quad (IV-1)$$

where $T = 0.042$ sec; ($1/T = 23.8$)

$\zeta = 0.5$

$K = 6.84$ to 7.85 sec^{-1}

Reference 33 contains these Nyquist plots.

Regardless of whether one holds the "closed loop" or "ballistic" point of view regarding the "neuromuscular system," the following transfer function will describe the dynamic portion of the response of a human operator to a step forcing function (to the extent that the data are representative).

$$Y_H(s) = \frac{KG(s)}{1 + KG(s)} \quad (IV-2)$$

where $KG(s)$ is the function given in Eq. (IV-1).

To include the dead portion of the response due to reaction-time delay the factor e^{-Ts} must be included. The linearized data then gives Eq. (IV-3) as the human operator transfer function for the case of hand motion and essentially no controlled element dynamics, when following a visual forcing function consisting of a simple step.

$$Y_P(s)_{\text{STEP}} = e^{-Ts} Y_H(s) = \frac{e^{-Ts}}{\frac{T^2s^3}{K} + \frac{2\zeta Ts^2}{K} + \frac{s}{K} + 1} = \frac{e^{-Ts}}{(s/K) + 1} \div \frac{e^{-Ts}}{T_N s + 1} \quad (IV-3)$$

It will be noted that the last approximation of Eq. (IV-3) is a simple first order lag. This may lead to confusion since the neuromuscular system possesses inertia, thereby requiring at least a second order transfer function. For sufficiently low frequencies, however, the first order lag is a suitable approximation, and it is debatable whether the data should be pushed much further than this.

B. THE OPERATOR'S RESPONSE TO A VISUAL SEQUENCE OF STEPS

The response to a single step was covered above. The topic to be discussed in this sub-section is that of the operator's response when the step command sequence is irregular, i.e., uneven intervals between steps and/or varying step amplitudes.

It would be convenient if the principle of superposition could be applied and hence permit the prediction of the response of a human operator to an irregular sequence of steps simply as the resultant of his responses to the individual steps, using the transfer function for step-function responses obtained above. While the final conclusion of this sub-section will be that one can do essentially this without too much error, there are two special characteristics requiring some consideration. These are the possibility of a refractory phase (a period of time after a stimulus when the operator cannot operate on a subsequent stimulus — analogous to the refractory phase for individual nerves and muscle fibres), and the so-called range effect. Superposition will be inapplicable to the extent that either of these effects exist.

Several investigators, among them Hick [41] and Vince [87], have indicated that a psychological refractory phase may exist, and that a certain minimum time must therefore elapse after a first response before the response to a second stimulus can be made. This time is in addition to the normal reaction-time delay which would be expected to separate the second stimulus and response. The experimental results upon which this tentative conclusion was based showed an increase in response time (used to approximate reaction time) as the time interval was decreased between individual steps in a sequence. It should be noted that these same results can be partially accounted for by considering the operator's bandwidth limitations. In other words, a sequence of steps used as inputs to the transfer function $e^{-Ts}Y_0(s)$, Eq. (IV-3), will give response records where response time values apparently increase, due to a scale effect on the amplitude of transient modes, as the spacing between steps becomes small.

Other investigators, such as Ellson and Hill [25], have performed experiments from which it is possible to infer that no refractory phase exists as such. While the type of experiment performed by Ellson and Hill does not prove positively that there is no refractory phase in the response to a sequence of opposed steps of constant amplitude, it does point strongly in that direction. Therefore, until more definite information is established to the contrary, it can probably be assumed that a practically significant refractory phase does not exist [21].

The range effect is a somewhat different matter, and in the case of certain sequences of steps, the operator's response may be modified slightly in a nonlinear fashion. If a sequence of command steps of about the same relative size is given the test subject, he will tend to overshoot in his response to a smaller step and undershoot in his response to a larger one. In examining this phenomenon Ellson and Wheeler ran two series of tests [26], one with input step amplitudes of 0.25, 0.50, and 1.0 inches and the other with amplitudes of 1.0, 1.5, and 2.0 inches. The subjects tended to overshoot the one inch stimulus when it was the smallest in the series, and undershoot the same stimulus when it was the largest. The tendency is therefore a function of range and not simply a result of the absolute magnitudes of the stimuli.

This range effect can be considered as an example of a type of behavior pattern often found in psychology and termed by some the "central tendency of judgment." In the present case this tendency is definitely present, but as can be seen from Fig. 21 the overall effect is really quite small. We can conclude, therefore, that the range effect is not too severe a deterrent to the assumption of superposition, and that the transfer function given for single steps, Eq. (IV-3), is also reasonably suitable to describe the gross behavior of the operator in tasks involving sequences of steps.

A final point that should be mentioned on visual step sequences is noted in Reference 14. This was the result of an experiment using the pursuit setup previously described (rotary disk for input, control wheel and pointer for output). In this experiment the subjects were asked to respond to inputs consisting primarily of more or less irregular, closely spaced, steps. The input was much closer to a random type of input than simple step sequences, but individual steps and responses were still recognizable as being particular input-response pairs (see Fig. 22). Therefore, the individual reaction time delays could still be measured. The results of this experiment indicated that the reaction-time delay to often-moving, irregular step-like inputs might be slightly less than that to steps where the time between input movements is sufficient for the operator to settle down to a constant position. The average reaction time delay for the irregular inputs was about 0.2 seconds, as opposed to the average of 0.25

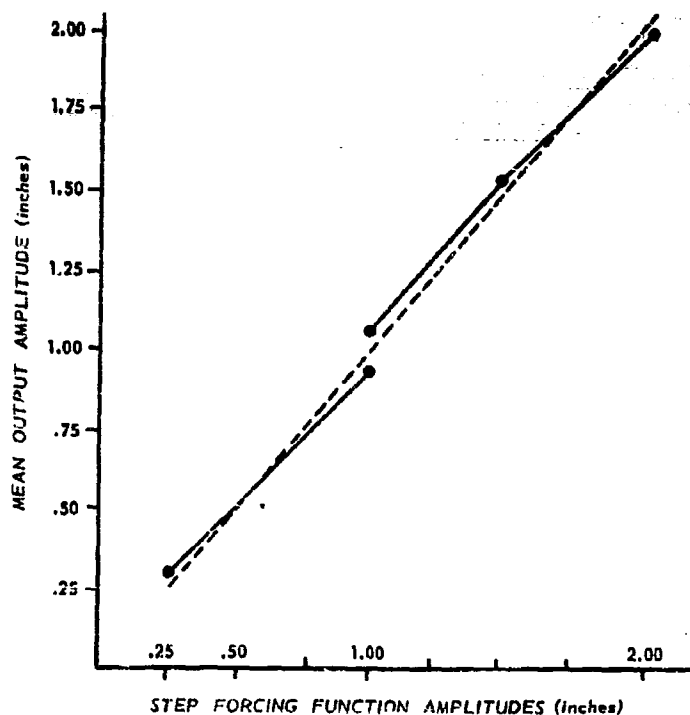


Figure 21.
(Ref. 26, p. 7)

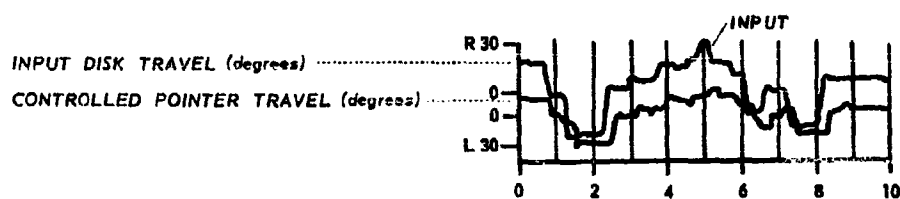


Figure 22. Response to Closely Spaced, Step-like Irregular Inputs.
(Ref. 14, p. 11)

seconds obtained with the same subjects using more widely spaced and less irregular step forcing functions. This result, and similar effects due to warning and motivation found in classical reaction time experiments, is helpful in explaining some of the lower reaction times found in tasks, such as tracking random inputs, where serial rather than solitary responses were demanded of the subject.

C. THE OPERATOR'S RESPONSE TO VISUAL SIMPLE PERIODIC AND OTHER "COMPLETELY PREDICTABLE" FUNCTIONS

The most obvious completely predictable forcing function is the pure sinusoidal oscillation. The response of the operator to this system input form, with no controlled element dynamics, has been thoroughly

studied by several researchers. Notable results have been reported by Mayne [32, 33, 37] and by Ellison and Gray [24], among others.

The Goodyear (Mayne) experiments utilized the recording paper, narrow slit, apparatus touched on previously in the review of operator responses to simple step inputs. Typical results of these studies, which are

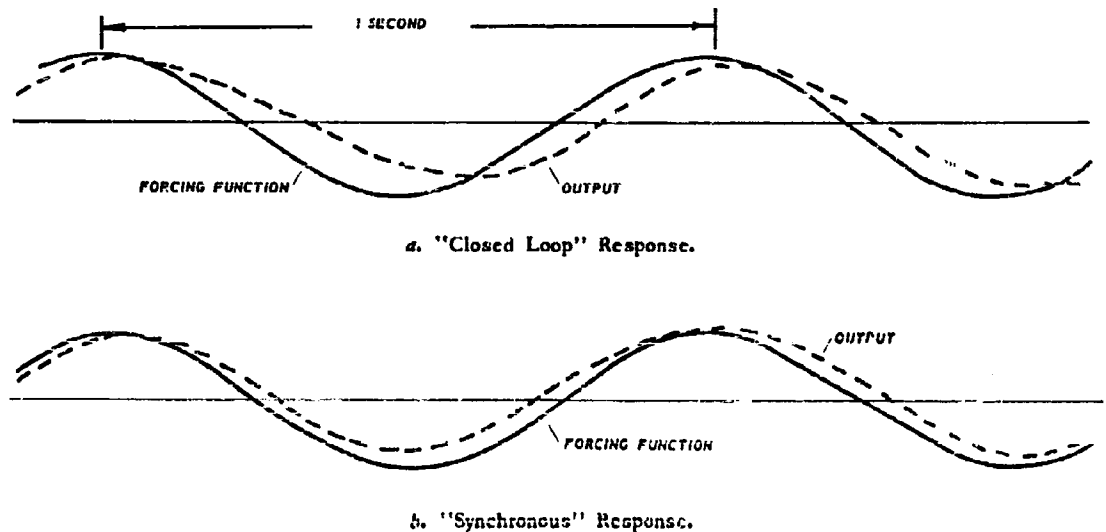


Figure 23. Typical Parts of the Response to a Simple Sinusoid.

comparable with those achieved by others, are illustrated in Fig. 23. The interesting feature is that the response seems to occur in three main parts:

- (1) The very first part of the response (not shown in the figure) contains a reaction time delay. This is followed shortly by
- (2) A "non-synchronous" response, Fig. 23a, which reveals the presence of a phase lag. This lag is too small to be due to a reaction-time delay. (A factor of $e^{-\tau}$ in the transfer function would give a phase lag of 90° at a frequency of 1 cps if τ is taken to be 0.25 sec.)
- (3) Shortly thereafter the response changes to a "synchronous" following of the sine wave with no phase lag and only slight attenuation. This mode can be maintained fairly easily at frequencies of 2.5 to 3 cps. (It should be noted that similar synchronous modes also exist for other forcing functions, such as a square wave.)

After a period in the synchronous mode, the operator tends to drift out of synchronism. When this occurs, he gets back into the synchronous mode by going through the first two response phases noted above, though usually more rapidly than the first time.

Mayne's proposed explanation of the synchronous and nonsynchronous characteristics is summarized as follows: The "non-synchronous" portion of the response displaying the phase lag occurs when the operator is effecting continual closed loop control with the eyes included in the loop. The eyes are exercising continuous control, and no time is required for computation and setting of responses in the cerebellum. (This is

analogous to Mayne's view of the closed loop proprioceptive responses for the step function case.) Since the computation time is a large part of the reaction-time delay, it might be possible to have this continuous control without the additional phase lag due to the whole reaction-time delay. To accomplish the final or "synchronous" mode of response, the operator must have added some sort of prediction to govern his response to eliminate the phase lag entirely. Once started, the synchronous response can be continued, for short periods, without the use of the eyes. Evidently the operator can "set in" to his effectors a certain range of functions which determine his response. The control of this response may or may not be made closed loop using the proprioceptive sense, but in any event requires that the "set in" function take into account the neuromuscular lags.

Our view of the underlying phenomena differs, to some extent, from Mayne's. We feel that, in terms of block diagrams, the three forms of response can probably be adequately represented by the three parts of Figure 24. During the very first part of the response, the narrow slit through which the operator views input and output effectively makes the display a compensatory one, Fig. 24a. This is particularly true at the initial

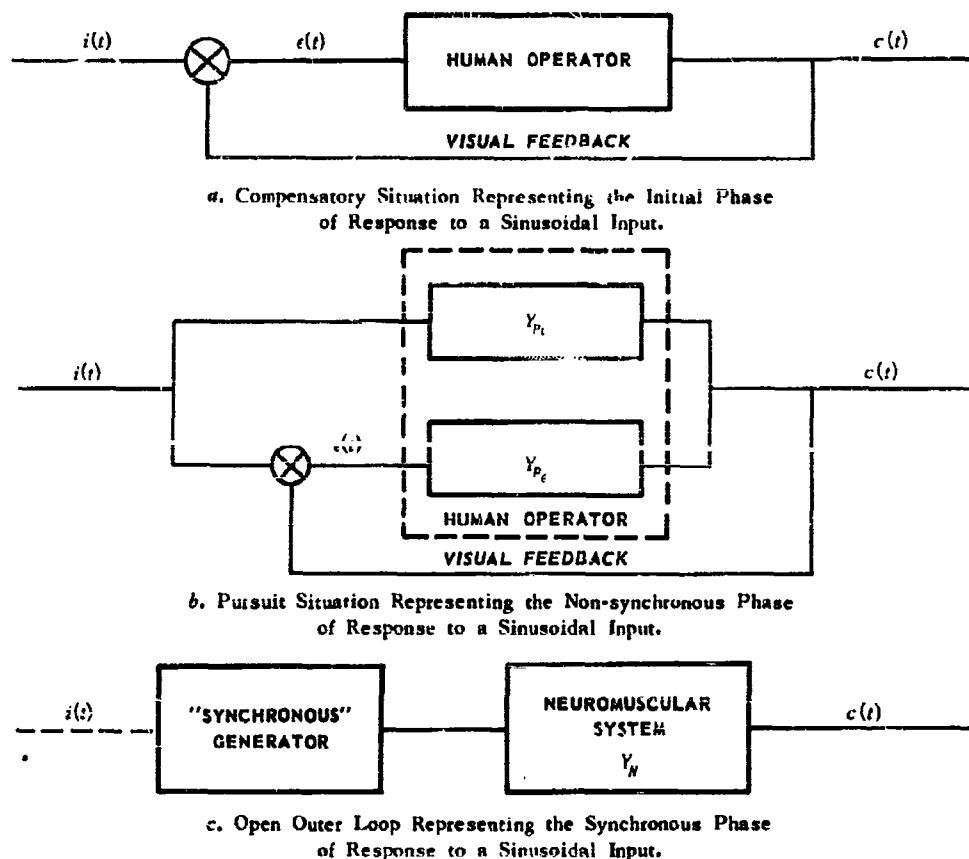


Figure 24. Block Diagrams Representing Phases in the Operator's Response to Sinusoidal Inputs.

instants before the operator has started his response. Shortly after the start of the operator's response, the operator recognizes the periodic nature of the forcing function and the pursuit aspects of the display take over. Here the operator generates a suitable transfer function in Y_{p_i} to overcome visual reaction time, Fig. 24b.* Finally,

* The effective reduction of visual reaction time in simple pursuit situations with no controlled elements is discussed in detail in Section XI.

the operator is able to detect and take advantage of all of the internal coherence and predictability of his input signal (the error). The action of the central nervous system then resembles a programmer or synchronous generator which generates command signals to the neuromuscular system based upon a complete "knowledge" of the forcing function and the operator's lags. This last response is essentially open-loop (in the outer loop, at least) with no visual feedback. As the synchronous motion drifts off or the input frequency is changed, the operator retraces his steps through at least the non-synchronous mode, and "corrects" the "programmer" to get back into the synchronous mode.

If the closed loop operation of a human being were linear for all inputs, it would be possible to express his response to a sine wave by using his transfer function in response to a step forcing function. The experimental results cited above make it clear that the overall operation cannot be considered linear. For example, correlation between the synchronous portion and the response to a step is impossible because the absence of phase in the former would imply an instantaneous response to a step input. On the other hand, the fact that the operator outputs for sine wave forcing functions are also fair sine waves indicates directly that a separate linear transfer function can be defined for each of the particular sine wave cases.

Mayne suggests that the dynamic portion of the response to a step function can be correlated with the non-synchronous response to a sine wave. In this connection, it is worth noting that the 40° phase lag observed in the latter response is approximately equal to the phase lag which would be caused by the transfer function $Y_N(s)$ of Eq. (IV-3) at the frequency of 1 cps.

In the synchronous mode the operator is able to keep forcing function-output phase shift to nearly zero over a wide frequency range, but is not able to maintain unity amplitude ratio at the higher frequencies. Both the input and the output are approximately sinusoidal, so a transfer function could theoretically be defined for this synchronous mode. To match qualitatively the frequency response characteristics mentioned above, using transfer functions made up of rational polynomials, the simplest possible form of such a transfer function would be that of Eq. (IV-4).

$$Y_p(s)_{\text{SYNCHRONOUS}} = \frac{1}{(Ts + 1)(-Ts + 1)} \quad (\text{IV-4})$$

This exhibits an amplitude ratio decrease with frequency but no phase shift. It will be noted that this transfer function is that of an unstable system, giving rise to a divergence, so even though it might be suitable for describing the response, the general form is misleading. Therefore probably the simplest way to represent the synchronous mode is with a describing function which is real but frequency dependent, as in Eq. (IV-5).

$$Y_p(j\omega)_{\text{SYNCHRONOUS}} = K(\omega) \quad (\text{IV-5})$$

Something akin to the synchronous mode appears in other situations where the operator has thoroughly "learned" his inputs and, by experience, seems to provide exactly the required output. Examples of this "total prediction" are a helmsman's ability in "meeting" a turning ship and some pilots' ability to cope with the well known "JC maneuver", by applying a single, properly timed, conditioned output response. Other skilled activities, like catching a ball and tagging a base runner in one continuous motion, counter-punching, serving a tennis ball, etc., are similar examples. All of these may be considered as practical examples of the precognitive situation discussed in Section I.

Apparently a characteristic of total prediction is the pre-setting in the neural centers of an entire response, and the substitution of memory for continuous control by the external senses. In the process of setting up these learned responses, the operator presumably goes through the following stages:

- (1) When the input is first encountered, control is through the external senses, with reaction time delay, etc.
- (2) At some later period, the "system" possibly becomes either a pursuit situation, or retains a compensatory form under closed loop control of the proprioceptive or visual senses but without reaction time delay.
- (3) Finally, the entire response is completely learned, becoming "synchronous" or skilled. In some instances observed experimentally an apparent synchronous mode could conceivably be the same type of control as (2), with the addition of a lead to offset the neuromuscular lag. A true synchronous mode, which can exist without the external senses operating in the loop, cannot be described in this fashion. [By definition!]

Section V

LINEARIZED OPERATOR RESPONSE TO RANDOM APPEARING VISUAL FORCING FUNCTIONS IN COMPENSATORY TASKS WITH NO CONTROLLED ELEMENT DYNAMICS

A. INTRODUCTION

Responses of operators in manual control systems with random appearing inputs exhibit a type of behavior which we shall call "equalization", since its action is directly analogous to that of the equalizing elements inserted into servo systems to improve the overall performance of the system. By its nature, equalization appears to be a continuous operation performed on data continuously observed by the external senses. This property distinguishes it from the "total prediction" which is observed in the synchronous part of the response to a sine wave, and also from the possible cam like action (or the equivalent closed-loop proprioceptive responses without external control) observed in both the initial stages of response to sine wave inputs and the dynamic part of the response to step inputs.

The operator must obviously adapt his equalizing behavior in some way to enable him to handle controlled elements having widely diverse dynamic characteristics. Perhaps the best way to classify his equalizing behavior is on the basis of the controlled elements which "force" the operator's characteristics to take on some particular form consistent with reasonable overall system performance. Therefore the discussion of operator dynamic characteristics in compensatory tasks has been divided into two major parts; the first will treat past experimental data on compensatory systems with no controlled element dynamics, i.e., $Y_c = 1$, and the second will consider systems with various controlled element dynamic characteristics. This section is concerned with compensatory systems of the first type, while those in the second category are considered in Section VI.

The human operator as a component of a manual control system must be considered to be a nonlinear and/or time varying element. This statement implies that two different quantities will generally be required to specify a human operator on a quasi-linear basis. The first quantity will be a describing function which relates the operator's output to the applied system input on a linear basis. The second quantity will be an operator output (or remnant), which is not linearly coherent with the forcing function to the system. These two quantities will be discussed separately; transfer characteristics in the first part of this section, and remnant characteristics in the second.

In all cases considered here the general system situation was the compensatory type shown in Fig. 2b, and the basic task was to track a random appearing forcing function. This general type of forcing function is probably the most fruitful one we can use if results are desired which will be applicable over a wide range of tracking situations. Since, characteristically, the forcing functions to most manual systems in operational use are low in frequency and at least partially stochastic, low frequency Gaussian noise is a natural idealization of actual forcing functions. Low frequency Gaussian noise is also capable of being easily "shaped" in various ways without changing its Gaussian nature. This enables one to study the influence of forcing function characteristics upon operator behavior when all the other system parameters are fixed. For these reasons most of the experimental work on operator transfer characteristics which has been done since the advent of suitable automatic computing devices utilizes Gaussian forcing functions. In some of the earlier work the desirability of using random appearing forcing functions was recognized, so appropriate sums of non-harmonically related sine waves were used to simulate randomness while still allowing the experimenter to reduce his data simply.

The experimental data considered in this section have been taken directly from the efforts of three investigators and their colleagues, specifically J. I. Elkind [22, 23], L. Russell [70], and E. S. Krendel [49, 50, 51, 53]. Using these experimental data as fundamental sources, the authors and their associates have replotted and derived "best fit" describing functions of the operator (and fits for other data) for all cases except the describing functions of Elkind, which were initially presented in suitable form. The describing function fits provide a convenient structuring of the data from which we can determine the influence of the forcing function (and the controlled element, for that matter) upon the transfer characteristics.

In the discussion that follows, the presentation of past experimental results on the operator in simple compensatory tracking tasks is divided into the two previously mentioned major categories, i.e., transfer characteristics and remnant characteristics. The first major subdivision is further broken down into three parts, corresponding

to results obtained on Elkind's, Russell's and the Franklin Institute's "simple trackers". The correlation of Elkind's results with simple servo analysis criteria is also included. A considerable portion of the subsection on Elkind's work with transfer characteristics, which includes the effects of variations in forcing function bandwidth, amplitude, and spectral shape upon the describing function, is taken directly from Reference 23.

The second major subdivision of the section is a detailed discussion of the second part of the operator's description — the remnant. In physical terms the word remnant as used here will normally be considered to mean that part of the operator's output power spectrum which is not linearly coherent with the system forcing function. For much of the historical past of tracking research this quantity has been largely ignored or passed off as a mildly troublesome deterrent to a linear description of the operator. By analogy with linear systems, the transfer characteristics have been granted the major emphasis. This situation cannot continue if the full realization of quasi-linear techniques is to be applied to complex manual control systems — for much evidence points to the fact that the more demanding the task, the more important the remnant. Indeed, in some systems discussed here and in the next section the remnant term is the significant one in terms of operator output power. Considerable attention has therefore been devoted to the exploration of possible sources of the remnant which are still consistent with the assumptions of quasi-linearization. Two of the possible applicable "explanations" are applied to Elkind's data in the second division of this section. The meager data on the remnant from the Russell and Franklin simple trackers is also presented.

In the final subsection we have attempted to summarize the similarities and differences obtained in the three simple tracker experiments.

B. HUMAN OPERATOR TRANSFER CHARACTERISTICS IN COMPENSATORY SYSTEMS WITH NO CONTROLLED ELEMENT DYNAMICS

1. Elkind's Compensatory Experiments

Elkind's experiments involved a very thorough study of the effects of forcing function characteristics upon the response of the simplest possible compensatory system employing a human operator, a display, and a lightweight, essentially frictionless control without spring restraints. The tracking apparatus is illustrated in Fig. 25, and consisted primarily of a "pip-trapper", two oscilloscopes, and associated electronics. The display was the vertically mounted scope with a stationary "target" at the center of the screen and a "follower" (a small circle $\frac{1}{16}$ inch in diameter, generated electronically) which moved about the screen as a direct function of the error. The subject tried to keep the follower circle around the target dot by moving the control (a small pencil-like stylus) on the screen of the lower oscilloscope. The error voltages which drove the "follower" were generated by taking the difference between the input voltage and the X coordinate of the follower position for the horizontal motion, and the Y coordinate of the follower position alone for the vertical motion. This was done since the stylus was free to move in both X and Y directions so that the operator could move his hand in a free and natural motion without external restraint. However, the vertical display Y-axis sensitivity was one-quarter that of the horizontal display. The operator could therefore move in a natural arc without producing significant vertical movement of the follower. The display was then essentially one-dimensional, and the measurements were all taken on this basis, i.e., only horizontal movements of the follower were used. The gain between the X-axis of the pip-trapper horizontal display was equal to that of the horizontal follower motion on the vertical display.

In operation, the subject was seated directly in front of the upper screen and allowed to adjust his viewing distance to whatever value he thought best (20 to 30 inches). The lower oscilloscope was mounted to the right of the operator in a location so that the tracking motions were very similar to those used in writing. An arm rest which supported the entire forearm was provided, and the subject was allowed to use finger, wrist or forearm movements as he desired. This allowed him to adjust to different movement amplitudes by using the muscle group most suitable for that amplitude.

In all of the Elkind experiments discussed in this section the forcing functions were made up of signals generated by summing a large number (40 to 144) of sinusoids of different frequencies and arbitrary phases, with components spaced equally in frequency. Such a signal of different frequency, random phase sinusoids approaches a Gaussian process as the number of sinusoidal components becomes infinite, and allows one to achieve a very sharp, essentially rectangular spectrum cutoff if desired. Other spectral shapes can be obtained by appropriate

filtering. The actual spectral forms used in the various portions of the study are shown in Fig. 26.

Elkind performed four basic experiments on both compensatory and pursuit systems. In this section we are concerned primarily with the compensatory results of his Experiments II, III, and IV, which consisted of test conditions defined as follows:

Experiment II — Amplitude: The forcing functions were three signals identical in all respects except amplitude. Their spectra were rectangular with cutoff frequency of 0.64 cps (4.02 rad/sec). The

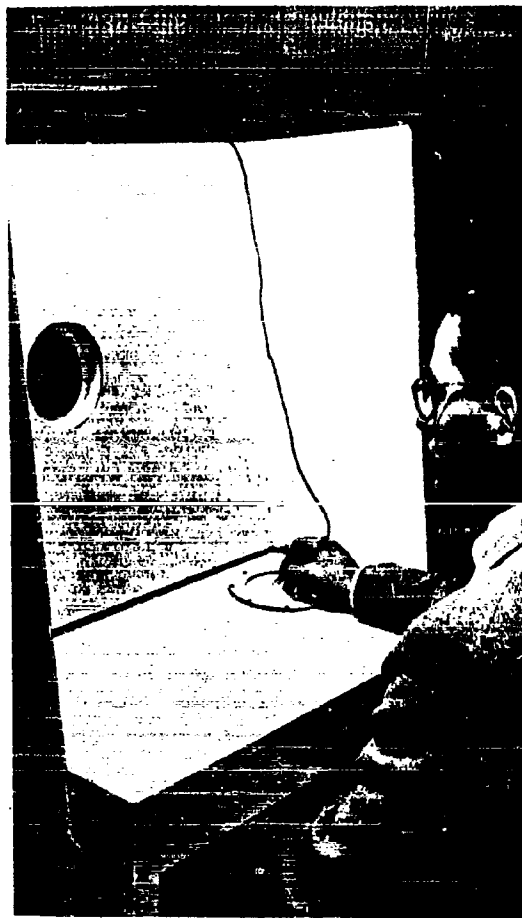


Figure 25. Elkind's Tracking Apparatus.
(Fig. 3-3, Ref. 23)

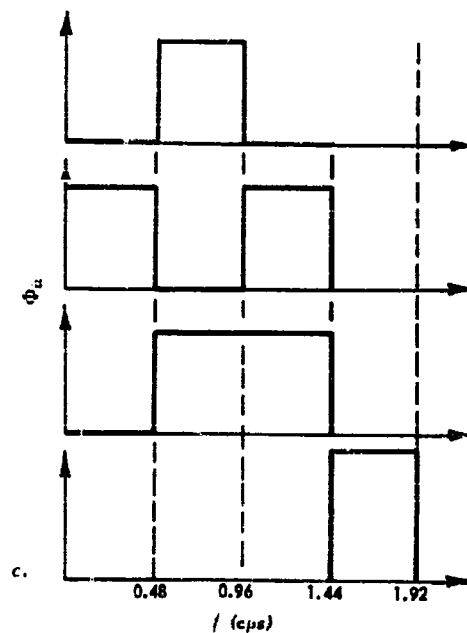
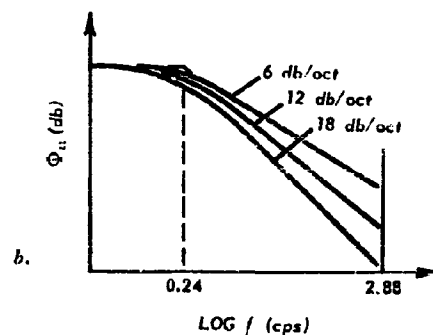
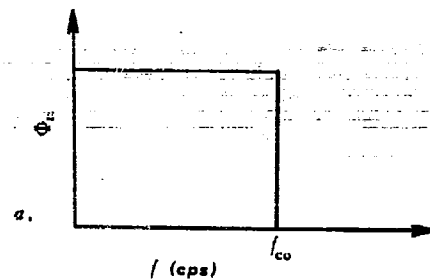


Figure 26. Types of Power Density Spectra
Used in the Elkind Compensatory Study.

amplitudes were 1, 0.32 and 0.10 rms inches. Runs were classified as A1, A2, and A3, corresponding to the amplitudes in descending order.

Experiment III — Bandwidth: The input signals had rectangular spectra of 1 inch rms amplitude and various cutoff frequencies, f_{co} . Runs were classified as follows:

RUN	f_{co} (cps)	ω_{co} (rad/sec)
R .16	0.16	1.00
R .24	0.24	1.51
R .40	0.40	2.51
R .64	0.64	4.02
R .96	0.96	6.03
R 1.6	1.60	10.05
R 2.4	2.40	15.07

An additional frequency of 4.0 cps was available, but was so difficult to track that the subjects were unwilling to try.

Experiment IV — Shape: For this experiment the signals used were RC filtered and selected band spectra, all having 1 inch rms amplitude. Run classification and input spectra shape are indicated in Fig. 27.

One group of three subjects was used in all of the compensatory experiments. They were all members of the staff of MIT and were well acquainted with the objectives of the experiment and the characteristics of the input signals. Before data were recorded, the subjects went through a training period of about thirty 4-minute tracking runs over a period of about one week. All of the subjects achieved high proficiency during the training period.

In the actual data runs the subjects were instructed to keep the center of the follower as close to the target as possible at all times. The input signals were recorded on magnetic tape for all inputs in the entire experimental sequence, Experiments I through IV, and in reverse order (IV through I). The subjects tracked each set twice, first in forward order and then in reverse order. Each tracking run was five minutes in duration, with rest periods of about one minute inserted between runs. The first minute of the five minute run was practice for the subject to adjust to the signal, and the last four minutes constituted the scoring run.

Elkind's experimental results [23] were presented in the forms of

- (1) Linear phase and amplitude ratio plots of the closed-loop describing function $H(f)$.
- (2) Bode plots of the open-loop describing function $Y_p(f)$.
- (3) Linear plots of linear correlation squared, i.e., $\rho^2 = 1 - \Phi_{nn}/\Phi_{ee}$.
- (4) Bode plots of error spectrum relative to mean-square input, $\Phi_{ee}/\int_0^\infty \Phi_{ii} df$.
- (5) Bode plots of the spectrum of the uncorrelated output relative to mean-square input, $\Phi_{nn}/\int_0^\infty \Phi_{ii} df$.
- (6) The relative mean-square tracking error, $\int_0^\infty \Phi_{ee} df / \int_0^\infty \Phi_{ii} df$.

In most of this subsection the item of major concern is the open-loop describing function $Y_p(f)$, though some of the other items will be mentioned from time to time. Our chief concern will be with the analytic form of curves fitted to the $Y_p(f)$ data. The experimental data gathered by Elkind is so significant, however, that a general review of the results applicable to transfer characteristics is in order.

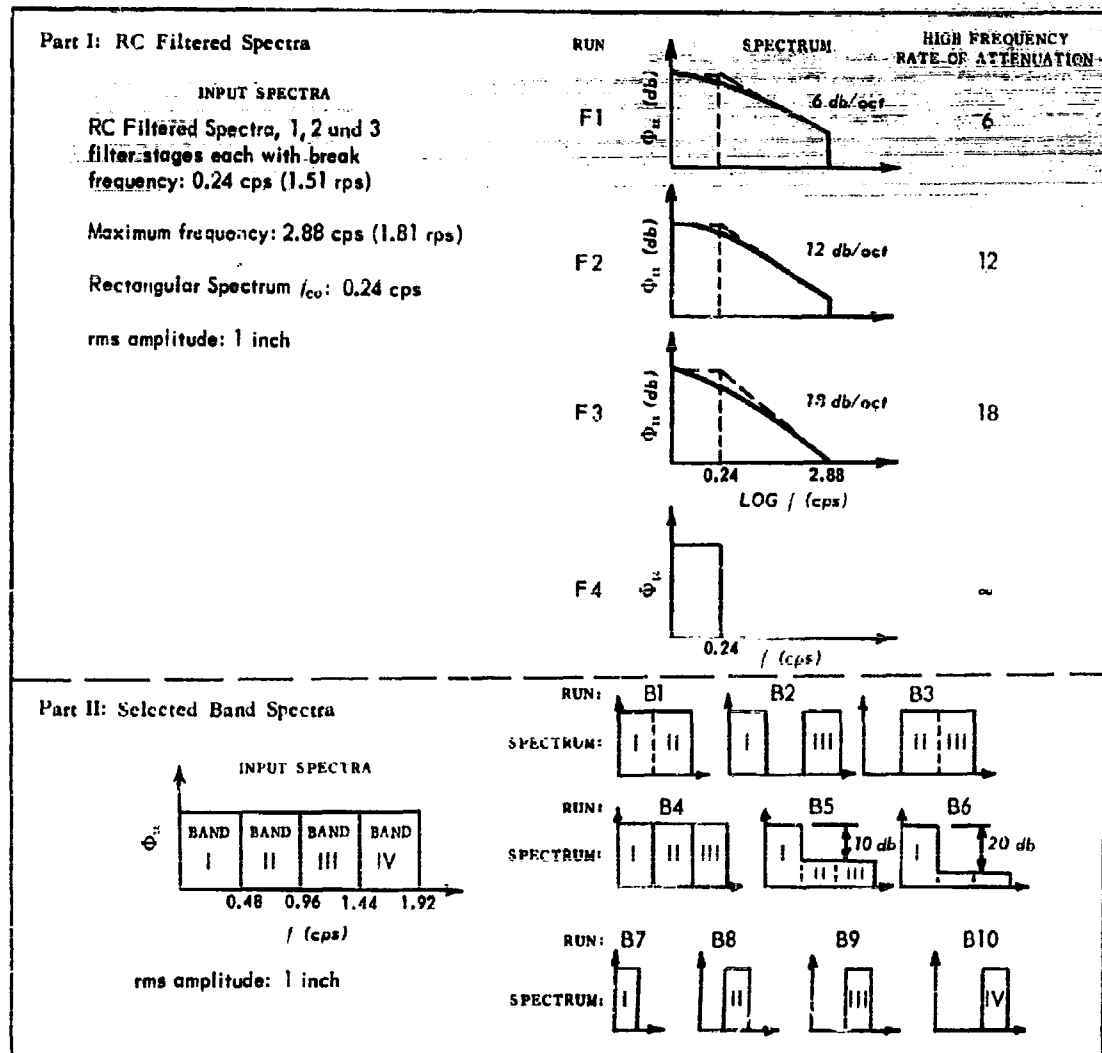


Figure 27. Forcing Function Conditions for Elkind's Experiment IV — Shape.
 (Adapted from Table 3-IV, Ref. 23)

a. General Experimental Results on Open Loop Describing Functions

- (1) **Experiment II — Amplitude:** In this experiment the open-loop transfer functions were not determined, but the results in terms of closed loop describing functions are shown in Fig. 28. Analysis of variance of the real and imaginary parts of $H(f)$ were performed at three representative frequencies to determine whether differences among characteristics were statistically significant. These results indicated that the closed loop human operator characteristics were essentially invariant over the entire range of amplitudes studied in this experiment, that is, from 0.1 inch to 1.0 inch rms. This means that the neuromuscular system is capable of being adjusted to a wide range of movement amplitudes, since the

operators used finger, wrist and forearm movements in making the responses to the various inputs. Small, precise movements required for input A3 were made with the fingers, and large, gross movements required for input A1 were made with wrist and forearm.

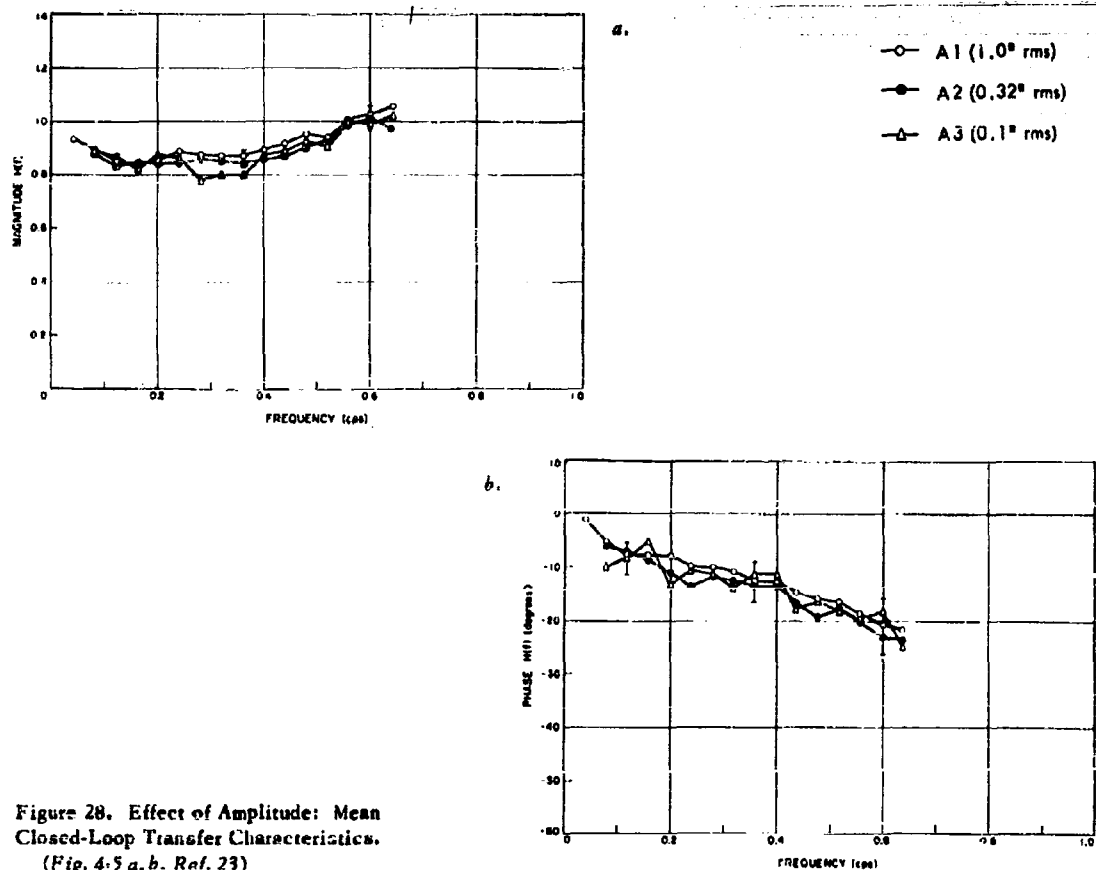


Figure 28. Effect of Amplitude: Mean Closed-Loop Transfer Characteristics. (Fig. 4.5 a, b, Ref. 23)

These results also give us our first chance to observe the possibility of operator nonlinear transfer characteristics. If these were markedly nonlinear we would expect a large difference in the open loop describing functions for the three forcing function mean amplitudes, and somewhat less difference between the three closed loop describing functions. Unfortunately, the open loop data were not presented in Reference 23, so our assessment must be based upon the data shown in Fig. 28. While slight differences are apparent in these data, e.g., magnitude $H(f)_{1.0} > H(f)_{0.32} > H(f)_{0.1}$, the differences are quite small and somewhat inconsistent. To the extent that these slight differences actually exist, one could surmise that the open-loop gain (and possibly some low frequency lag) was a mildly increasing function of rms forcing function amplitude. The most general observation, however, would be that there is little evident nonlinear transfer behavior for the forcing function situations noted.

(2) Experiment III — Bandwidth: The variation with forcing function bandwidth of the amplitude ratios and phases of $Y_p(f)$, the open loop describing function, are shown in Fig. 29. It will be noted that the magnitude and phase lag of $Y_p(f)$ show a general decrease with increasing forcing function bandwidth. In

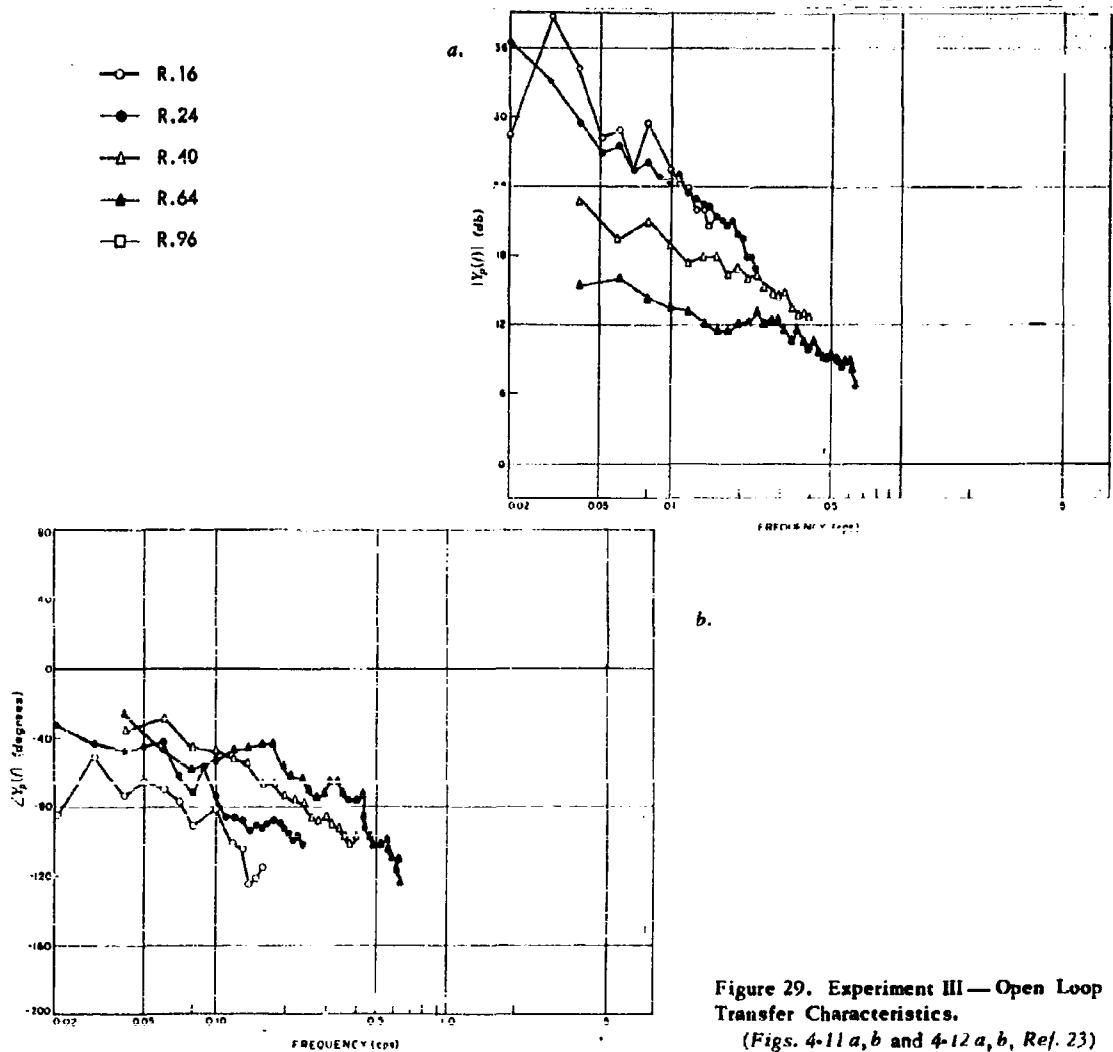
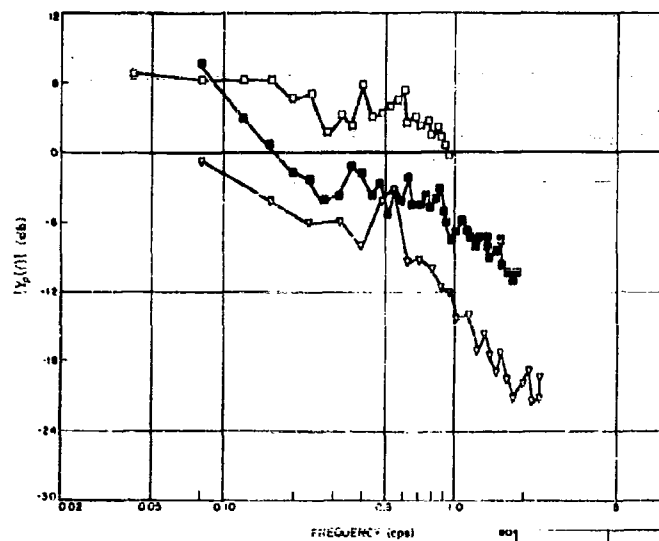


Figure 29. Experiment III — Open Loop Transfer Characteristics.
(Figs. 4-11 a, b and 4-12 a, b, Ref. 23)

terms of the analytical models fitted to these data, we will later see that this general behavior appears to obey quite reasonable "laws".

Another item of importance determined by Elkind in this experiment was the mean square error relative to the mean square input. These results are plotted as Fig. 30. The reader is cautioned that the plot is intended merely as a graphical tabulation and that no particular trend or curve fit is proposed,



C.

□ R.96
■ R1.6
△ R2.4

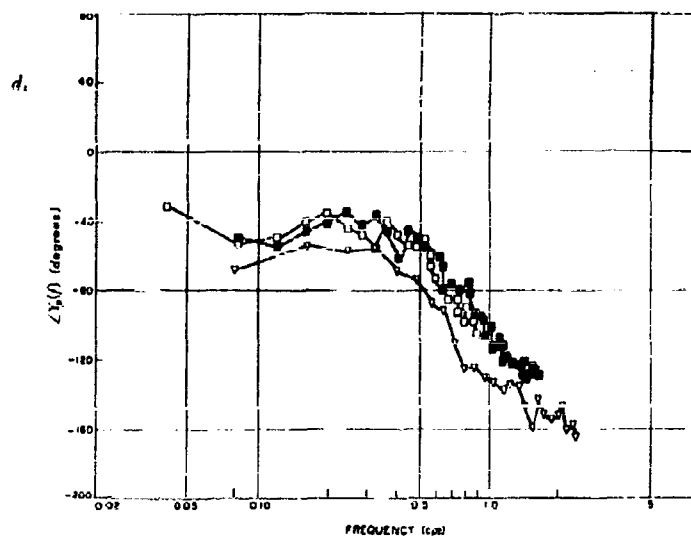


Figure 29. (Continued.)

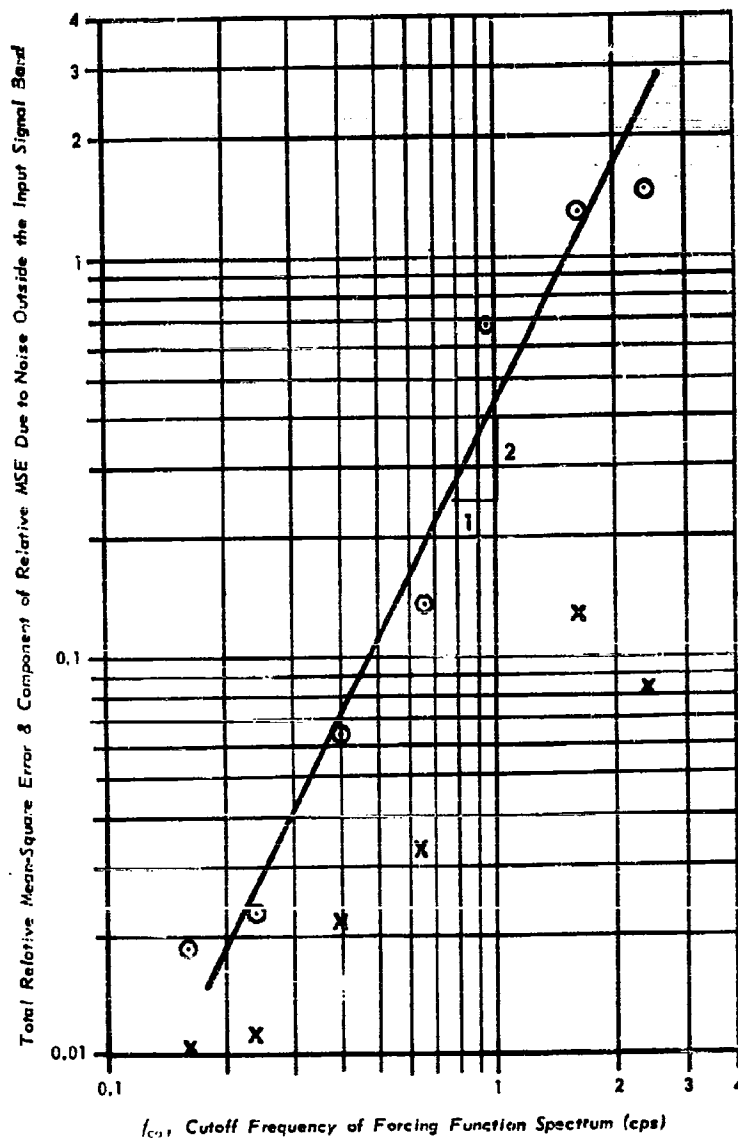


Figure 30. Variation of Relative Mean Square Error with Bandwidth of Rectangular Spectra Forcing Functions.

(Data Source: Table 4-VI, Ref. 23)

(3) **Experiment IV — Shape:** The effects of forcing function spectral shape upon the open loop transfer characteristics are shown in Figures 31 and 32. The results with RC filtered spectra are shown in Fig. 31, and those for the selected band spectra in Fig. 32.

The open loop characteristics for RC filtered forcing functions are similar in many respects to those for rectangular spectra, especially the one with an 18 db/oct high frequency attenuation. This becomes particularly apparent when the data for input R.24 is superimposed upon the plot. Perhaps the most important characteristic to note is the increase in amplitude ratio and phase angle as the forcing function becomes simpler to track, i.e., as the higher forcing function frequencies are more heavily attenuated. Along this same line, the operator adjusts his phase margin downward as the high frequency content of the signal is reduced. For the RC forcing function with the greatest amount of power at high frequencies (F1), the phase margin is about 70 degrees, while for F3 it is only 35 degrees. The smaller phase margins permit the operator to have higher dc gain and hence better low frequency tracking performance.

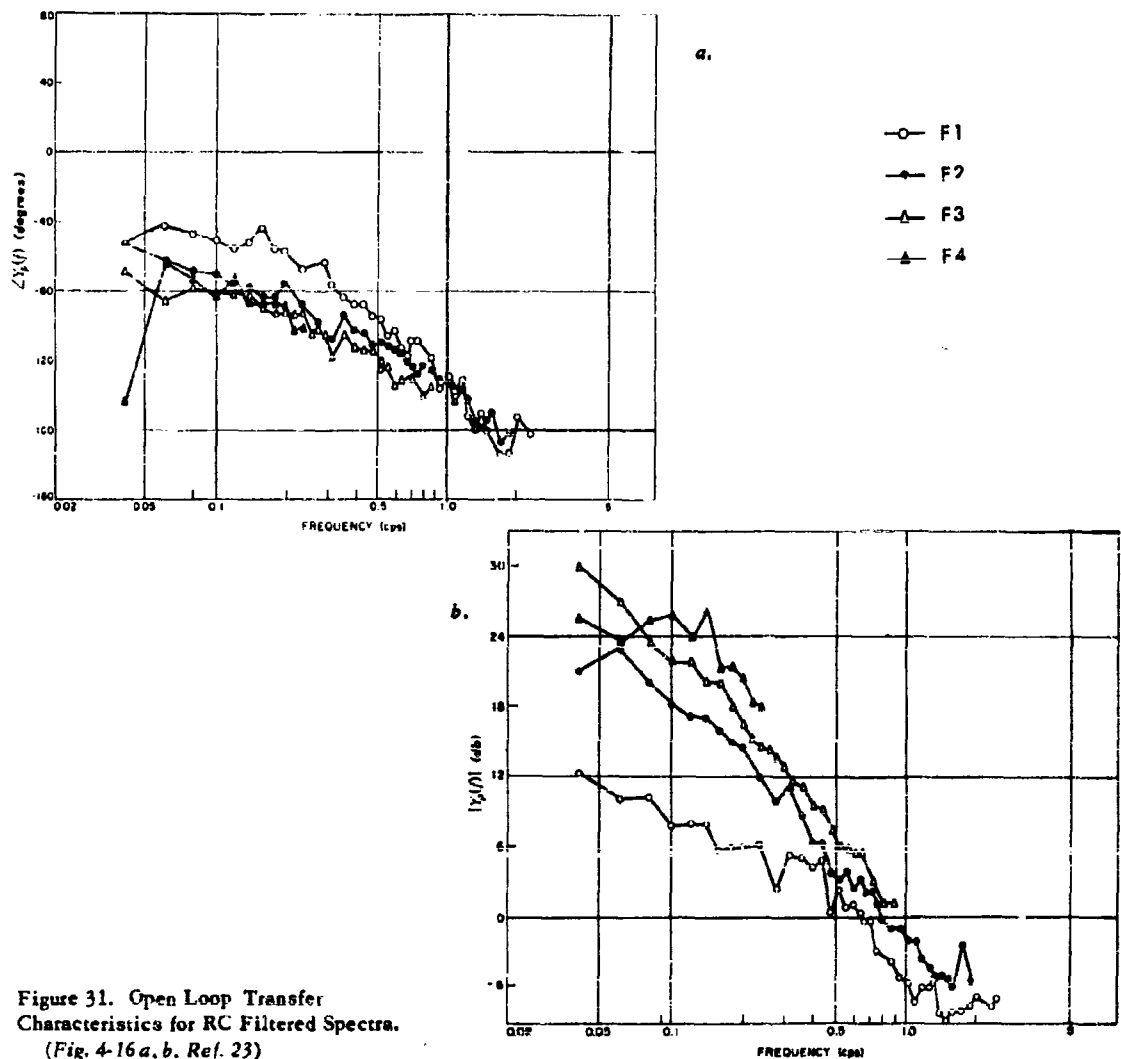
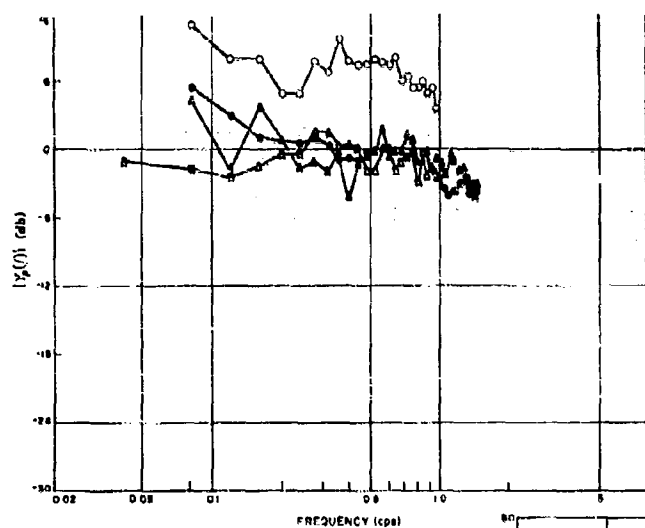
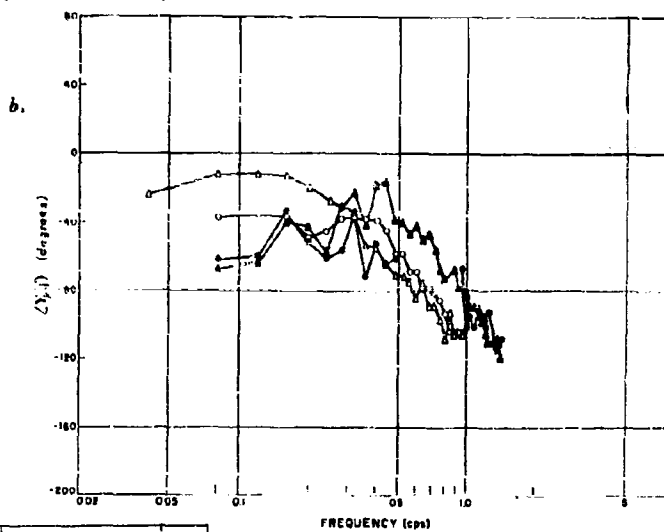


Figure 31. Open Loop Transfer Characteristics for RC Filtered Spectra. (Fig. 4-16 a, b, Ref. 23)

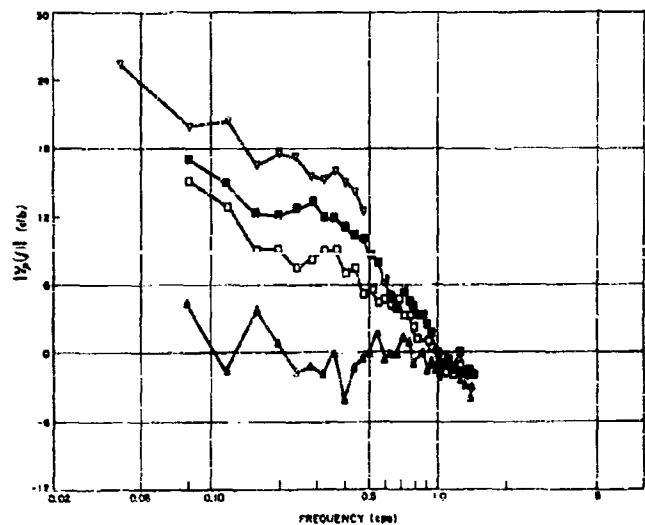


a.

- B1
- B2
- B3
- ▲ B4
- ◊ B5
- B6
- ▼ B7



b.



c.

Figure 32. Open Loop Transfer Characteristics for Selected Band Forcing Functions.

(Figs. 4-23 a, b, 4-24 a, b, and 4-25 a, b, Ref. 23)

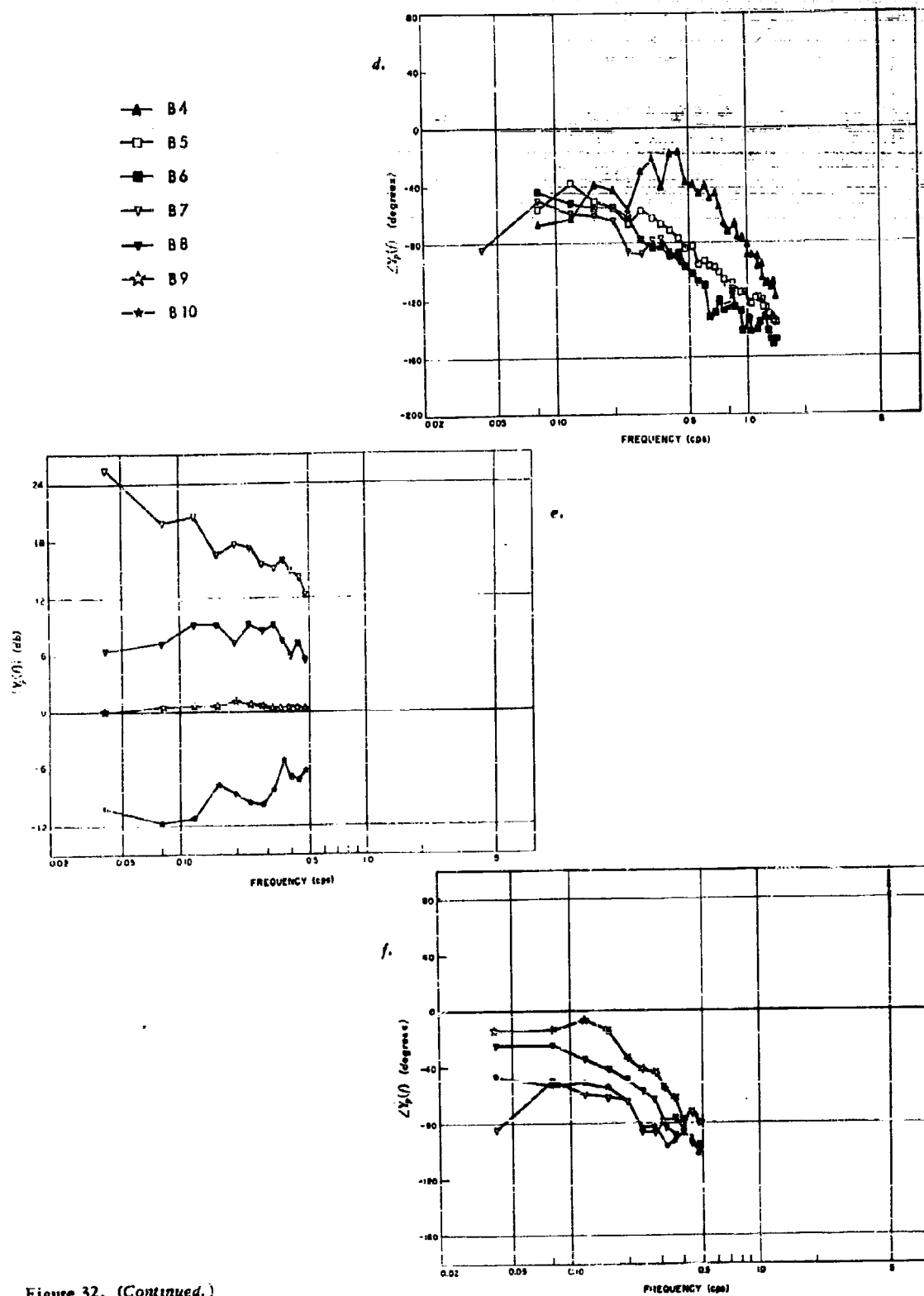


Figure 32. (Continued.)

The open loop describing functions for the selected band spectra are fairly similar to those obtained for the rectangular and RC filtered cases, particularly in the way in which the phase margins obtained with B4, B5 and B6 decrease as power at high frequencies decreases. The data for the band-pass signals (B3, B8, B9, and B10) were translated down the frequency scale so that the lowest frequency component of the forcing function corresponded to the origin on the new frequency scale. To some extent, these translated transfer functions are similar to those associated with the normal low-pass inputs. In other words, the human operator appears to be able to shift his low-pass characteristics up the frequency scale, like a single-sideband modulator, when he is confronted with a bandpass input. However, when he makes these transitions, his gain is reduced and phase lag increased.

b. Analytical Approximations to the Open Loop Describing Function Data

The measured open-loop transfer characteristics of Figures 29, 31, and 32 present the actual linearized describing function model of the human operator for the conditions of the experiments and within the bandwidth of the forcing function. These results are analogous to those obtained when one runs a conventional harmonic response test on a "black box" of unknown characteristics. At this point we would like to obtain analytical models which approximate the data, preferably in a form involving a small number of parameters. Then, with the experimental results approximated by these isolated parameters, and knowing the characteristics of the forcing function, we should be able to summarize conveniently the relationships between the presumed operator parameters and the forcing function characteristics. In this way we can obtain some "laws" of operation of the approximate analytical models. Then, to the extent that the analytical model approximates the operator, we have much greater insight into the "laws" which actually govern the overall behavior of the operator.

In considering the possible types of models which might be used, we should first note that models having nonlinear transfer characteristics capable of being characterized by the same describing functions are not particularly desirable possibilities. After all, the effort involved in taking the data for the quasi-linear describing function should not go for naught. Nonlinear models are therefore placed in the category of last resort.

Considering linear models, we can readily say that the most desirable types are transfer functions made up of ratios of rational polynomials, with the addition of a pure time delay term also being allowed. Such transfer function forms are desirable because they are simple, well understood, and completely adequate for approximating any of a large number of "frequency responses". By allowing the transfer function parameters to change as a function of the input parameters, we can cover the entire range of measured data for a given set of input conditions.

Having decided to use a conventional transfer function form, the next point to be considered must be the degree of approximation to be used in fitting the analytical model to the data. Since the experimental information covers only a restricted frequency range, it is possible to fit analytical transfer functions to the data to any arbitrarily defined degree of accuracy. An extremely accurate fitting procedure appears hardly warranted in this instance because of the data reduction errors and the variation between subjects whose data make up the averages. A conceptual point is also involved in that we would like to have a fairly simple analytical model with a small number of parameters so that they can be readily related to parameters defining the input characteristics. From these considerations we can conclude that the appropriate model to use in fitting a set of data is the simplest transfer function form which is reasonably consistent with the trends of all the data for a given type of forcing function.

As general criteria for the types of fits and forms acceptable we can list the following as consistent with all known human operator data in compensatory tasks of various kinds.

- (1) The operator's describing function should go to zero at infinite frequency, i.e., his transfer characteristics are fundamentally those of a low pass filter.
- (2) The describing function should be finite at zero frequency because of physical limitations.
- (3) A pure time delay, $e^{-\tau s}$, should be included to account for the reaction time delay.*

* Several writers prefer to reserve the term "reaction time delay" for discrete tasks and adopt such nomenclature as "analysis time", etc., for continuous tasks. We prefer to use "reaction time delay" as a term synonymous with an apparent pure time delay. In the sense used here, reaction time will vary with the "discreteness" of the task.

(4) When the experimental closed loop system is stable, the approximate fitted transfer function form should also yield a stable closed loop system.

The simplest transfer function form that satisfies these requirements for much of Elkind's compensatory open loop transfer characteristic data is

$$Y_p = \frac{K e^{\tau_1 j \omega}}{T_0 j \omega + 1} \quad (V-1)$$

where K is the dc gain, τ_1 a pure time delay (analogous to the reaction time delay in tracking discrete inputs), and T_0 is a time constant representing a low frequency lag in the operator's characteristics. The process of using Eq. (V-1) to fit the experimentally determined characteristics is illustrated in Fig. 33. A good fit to the data must be achieved simultaneously in magnitude and phase, so it is usually necessary to shuttle back and forth between these two quantities and adjust the parameters of Y_p to obtain a compromise giving the best fit. Since the pure time delay $e^{\tau_1 j \omega}$ does not affect the amplitude characteristics, the amplitude ratio curves are fitted by

$$|Y_p| = \left| \frac{K}{T_0 j \omega + 1} \right| \quad (V-2)$$

Approximate values for K and T_0 can be determined from these data using templates or other means, with the chief criterion being the visual appearance of a good fit.

The phase associated with the term $(T_0 j \omega + 1)^{-1}$ can then be subtracted from the measured phase to give that hypothetically due to $e^{\tau_1 j \omega}$. On a linear plot of phase versus frequency, the phase lag due to reaction time should be approximately linear, and the slope (expressed in rad/rad/sec) will be the value of $-\tau_1$. Therefore, when the residual phase is not approximately linear, it is necessary to select other values of T_0 (and hence K), and repeat the process until satisfactory results are attained. The parameters defining Elkind's approximate fits using

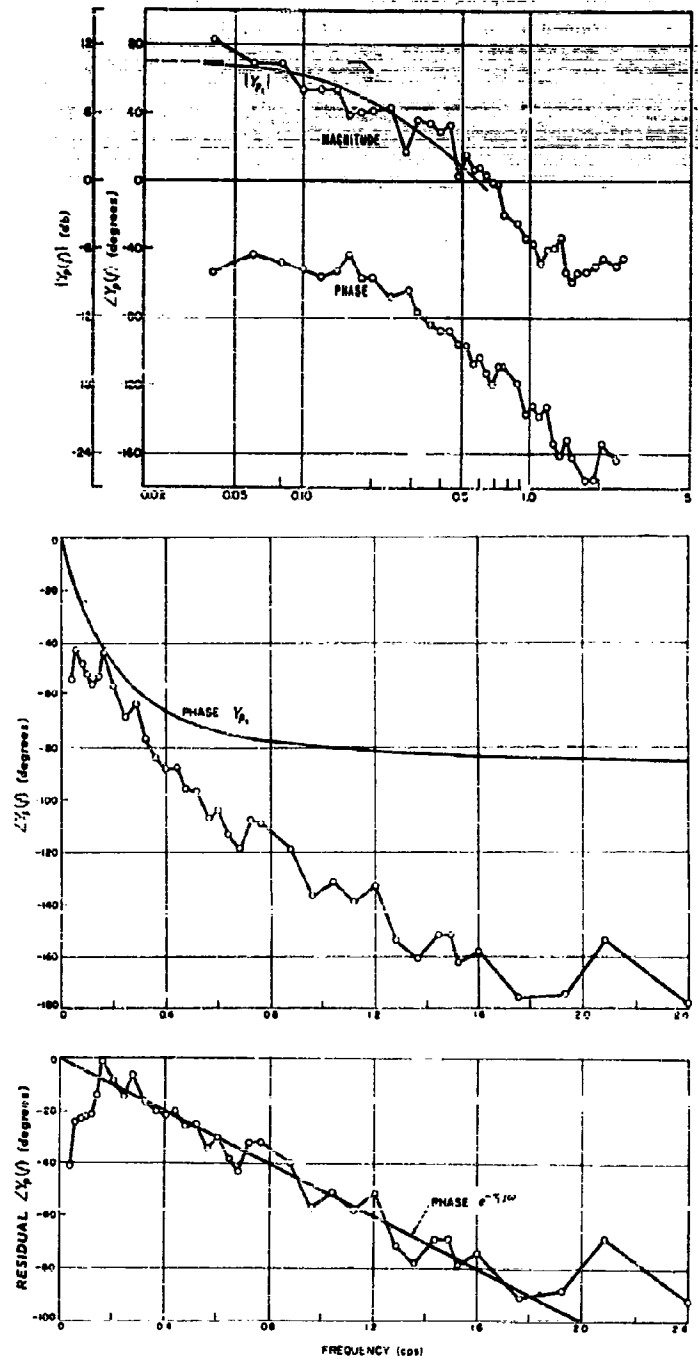


Figure 33. Example of Data Fitting with Simple Transfer Function. (Fig. 5-1 a, b, c, Ref. 23)

this simple transfer function form are given in Table 1.* It should be noted here that Elkind used the parameter f_0 (equal to $\frac{1}{2}\pi T_0$) in his work, so it is also noted in the table.

Table 1. Summary of Parameters of $Y_p(j\omega)$ and $Y_b(j\omega)$.

INPUT	τ_1 sec	f_0 cps	$1/T_0$ rad/sec	K db	r sec	$1/T_1$ rad/sec
R .16	0.64	0.035	0.22	34.5	0.110	1.885
R .24	0.264	0.050	0.314	31.5	0.104	6.22
R .40	0.214	0.125	0.785	22.5	0.133	12.3
R .64	0.183	0.275	1.73	15.0	0.150	30.3
R .96	0.139	0.58	3.65	6.5	0.139	∞
R 1.6	0.122	0.6	3.77	-0.6	0.122	∞
R 2.4	0.116	0.3	1.885	-3.0	0.116	∞
F 1	0.139	0.18	1.13	10.5	0.139	∞
F 2	0.126	0.05	0.314	25.0	0.126	∞
F 3	0.178	0.03	0.1885	33.0	0.178	∞
F 4	0.306	0.056	0.352	31.0	0.102	4.90
B 1	0.153	0.76	4.77	9.0	0.153	∞
B 2	0.107	0.8	5.03	1.5	0.107	∞
B 3	0.278	2.0	12.56	-1.0	0.278	∞
B 4	0.150	2.0	12.56	-0.3	0.150	∞
B 5	0.128	0.30	1.885	11.1	0.128	∞
B 6	0.149	0.16	1.005	17.7	0.149	∞
B 7	0.156	0.14	0.88	23.2	0.100	17.85
B 8	0.388	0.5	3.14	9.0	0.219	6.28
B 9	† 0.39	† 2.0	12.56	0.4	† 0.390	∞
B 10	† 1.14	0.45	2.83	-11.0	† 1.14	∞

† Approximate values.

NOTE: Corresponding nomenclature between Reference 23 and this table are given by:

Table 1	τ_1	r	$1/T_0$	f_0	$1/T_1$	K
Ref. 23	α'	α_{max}	$2\pi f_0$	f_0	$2\pi f_{max}$	K

While the low frequency approximation of Eq. (V-1) fits the data quite well, an analytical closed loop transfer function derived from this equation would indicate an unstable condition at frequencies well beyond the measurement bandwidth for some of the lower cutoff forcing functions. There was no evidence of a closed loop instability in any of the experimental data so we would suppose that the operator introduces more attenuation at high frequencies than would be indicated by the application of Eq. (V-1). While it is not possible to utilize the experimental data to find the high frequency portion of an approximate transfer function, it is possible to "stabilize" the closed loop system by adding a lag to Eq. (V-1), i.e.,

$$Y_p(j\omega) = \frac{K e^{-\tau j\omega}}{(T_0 j\omega + 1)(T_1 j\omega + 1)} \quad (V-3)$$

* The bandpass characteristics B 3, B 8, B 9, and B 10 were translated down the frequency scale before fitting. In this translation, the low frequency cutoffs of the forcing function spectra were set at zero.

If $1/T_1$ is much greater than any of the frequencies measured, then the low frequency behavior of the transfer function of Eq. (V-3) can be made the same as that of (V-1) if $T_1 + r$ is approximately equal to r_1 . This is due to the fact that the term $(T_1 j\omega + 1)^{-1}$, in the region $\omega \ll 1/T_1$, will introduce a phase shift which is essentially linear, and no attenuation. The addition of a simple lag, $T_1 j\omega + 1$, is by no means a unique way to define the possible higher frequency behaviors; any combination of lags and leads leading to a stable system would be suitable if they satisfied the relationships,

$$r + \sum_i T_i - \sum_j T_j = r_1$$

$$\frac{1}{T_1} \gg \omega_{co}; \quad \frac{1}{T_j} \gg \omega_{co} \quad (V-4)$$

where the T_i are lags, the T_j are leads and ω_{co} is the forcing function cutoff frequency (or an approximation thereto) in rad/sec. The single lag represented by T_1 is, however, the simplest form which can be added to Eq. (V-1) to assure stability and consistency with the measured low frequency response.

Unfortunately it is not possible to find unique values of r and T_1 from the low frequency data. By examining the general trends of the higher input bandwidth data, we can conclude that the phase margin for the lower input bandwidths is of the order of zero degrees. Therefore, it would be fairly reasonable to adjust T_1 and r to values just consistent with neutral stability. This procedure can yield only approximate, maximum values of r and $1/T_1$. However, we would have a reasonable amount of confidence in the results if the values for r are near those values of r_1 found for the cases where Eq. (V-1) was both a good fit and led to a stable closed loop system. These values of r and $1/T_1$ are shown in Table 1.

Elkind estimated the accuracy of the parameters obtained on his fits as follows:

$$r = 0.13 \pm .027 \text{ sec}$$

$$K \text{ within } \pm 3 \text{ db} \quad (\text{All low-pass forcing function signals, i.e., B 3, B 8, B 9 and B 10 not included.})$$

$$f_0 \text{ within } \pm 0.2 f_0$$

No consistent pattern of variation that can be related to the parameters of the input signal were present in the values of r . From the general trend of evidence cited in Section IV, i.e., r becoming smaller as the task becomes more "continuous", and similar trends exhibited in classical reaction time experiments with tasks involving either high motivation levels or short time spacing between stimuli [94, 2nd Edition], it is probably reasonable to identify the pure time delay r with the previously defined reaction time delay. This would imply a time for central processes in the interval 0 to 0.08 seconds in tasks of this nature considering the previously cited reaction time components in Section IV and the 0.02 second variability of r .

c. Relationships Between the Derived Models and Input Characteristics

Having obtained analytical describing function models approximating the operator's transfer characteristics, the next important point is to attempt to relate the parameters of these analytical models to forcing function parameters. In this regard, Elkind has found several interesting results tending to show the type of adaptation to forcing function characteristics made by the approximate operator models.

The first relationship of importance is the variation of the product K/f_0 for all the runs. As shown in Fig. 34, K/f_0 is very approximately constant over a wide range of forcing function characteristics, i.e.,

$$K/f_0 \approx 1.5 \quad (V-5)$$

It will be noted in Fig. 34 that the relationship of Eq. (V-5) is fairly good for most of the data points excepting those forcing functions with the larger amounts of power at the high frequencies, such as F 1, F 2, R 1.6 and R 2.4. It will also be noted that all of the high gain ($K \gg 1$), rectangular spectra runs are approximated very closely by

$$K/f_0 \approx 1.3 \quad (\text{R.16, R.24, R.40 and R.64}) \quad (V-6)$$

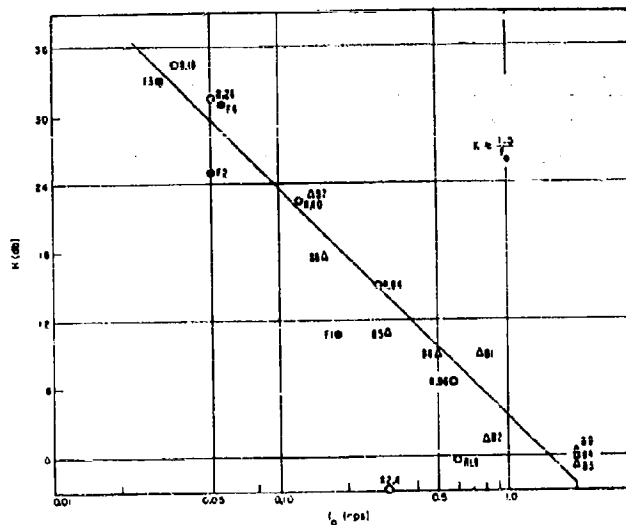


Figure 34. Gain, K , Versus Frequency of First Break Point, f_0 .
(Fig. 5-2, Ref. 23)

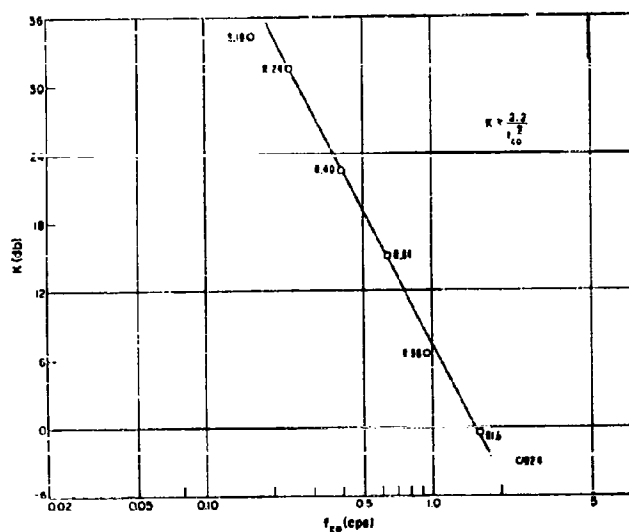


Figure 35. Variation of Gain, K , with Cutoff Frequency, f_{co} ,
for Rectangular Spectra Forcing Functions.
(Fig. 5-3, Ref. 23)

This latter point will be of interest later.

Elkind was also able to develop several very interesting expressions relating the gain to characteristics of the forcing function from his experimental results. These shall be reviewed below.

The simplest input spectra to work with are those having rectangular shapes. Since Elkind's Experiment III showed that input amplitude had small effect on the closed loop transfer characteristics of the operator, H , (at least for inputs between 0.1-1.0 inch rms around a value of f_{co} of .64 cps) it is reasonable to suppose that the major input characteristic of importance for rectangular spectra is the value of the cut-off, f_{co} . A plot of open loop dc gain, K , versus f_{co} , Fig. 35, for the rectangular forcing function spectra shows that K varies approximately inversely with the square of f_{co} , i.e.,

$$K = \frac{2.2}{f_{co}^2} \quad (V-7)$$

The RC filtered and selected band spectra are more complex than the rectangular spectra, and cannot be described in terms of a cutoff frequency alone. In his search for more fundamental measures of forcing function signal characteristics, Elkind noted that the two factors which appeared to have the most important influence on the gain were the predictability of the forcing function and its location on the frequency scale. After trying a series of combinations with the experimental results, he found that the parameters \bar{f} , the mean frequency of the spectrum, and σ_f , its standard deviation, appeared to be appropriate parameters. These are defined by

$$\bar{f} = \frac{\int_0^\infty f \Phi_{ii} df}{\int_0^\infty \Phi_{ii} df}$$

$$\sigma_f = \left[\frac{\int_0^\infty f^2 \Phi_{ii} df}{\int_0^\infty \Phi_{ii} df} - (\bar{f})^2 \right]^{1/2} \quad (V-8)$$

The quantity \bar{f} is a measure of location; σ_f , being related to the spectrum width, is a measure of predictability. The product $\sigma_f \bar{f}$ is directly proportional to f_{co}^2 for rectangular

spectra, and a good fit to the data of K versus $\sigma_f \bar{f}$ for rectangular spectra is (Fig. 36)

$$K = \frac{0.39}{\sigma_f \bar{f}} \quad (V-9)$$

Using Eq. (V-9) to compute a calculated gain, K_c , for all forcing functions resulted in the data of Fig. 37. Here it will be noted that the agreement between measured and computed values is good for forcing functions having low pass characteristics, but is poor for the bandpass spectra (dashed lines).

As the mean frequency \bar{f} of the bandpass forcing functions becomes greater, the difference between K and K_c increases. To explain these differences Elkind developed different weighting values for the various terms in Eq. (V-9) involving \bar{f} by considering the bandpass data alone. The effect of \bar{f} was isolated by plotting the measured values of $K\bar{f}$ against \bar{f} , as shown in Fig. 38. The points from Fig. 38 were then fitted by

$$K = \frac{3.8}{\sigma_f \bar{f}^{1.38}} \quad (V-10)$$

This new expression was then used to compute gains for all inputs, called K'_c , which were compared with the measured values (Fig. 39). This curve provides the best fit to all of the data that Elkind was able to find.

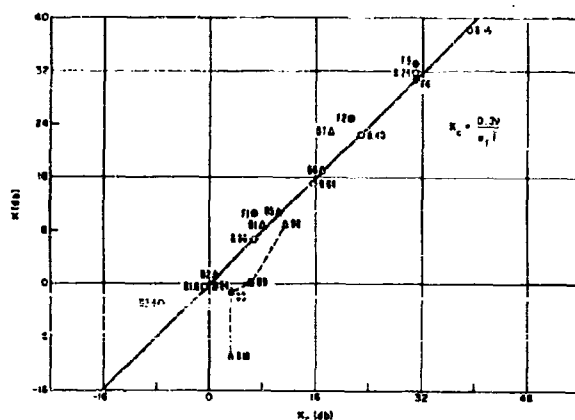


Figure 37. Measured Gain, K , Versus $0.39/(\sigma_f \bar{f})$ for all Inputs. (Fig. 5-5, Ref. 23)

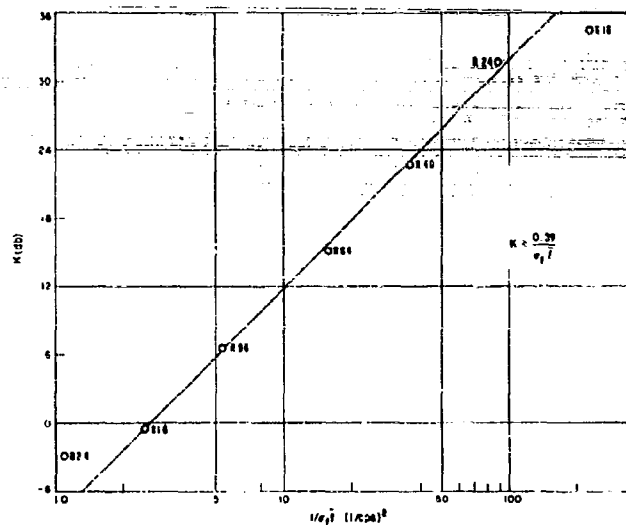


Figure 36. Measured Gain, K , Versus $1/(\sigma_f \bar{f})$ for Rectangular Spectra. (Fig. 5-4, Ref. 23)

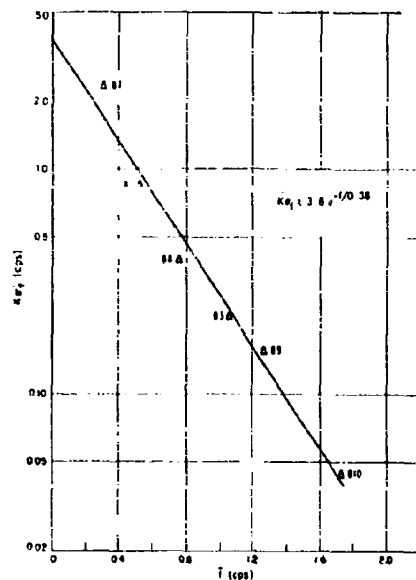


Figure 38. Measured Values of $K\bar{f}$ Versus Measured \bar{f} for Bandpass Spectra. (Fig. 5-6, Ref. 23)

All of the experimental fits obtained by Elkind throw a considerable amount of light on the adaptive behavior of the analytical model. It is comforting to note that such simple expressions define the observed transfer behavior so well. On the other hand, we cannot be sure that other parameters may not be equally "significant" as, say, σ_f and \bar{f} in the role of fundamental parameters defining the forcing function characteristics. Elkind tried many variations, with the best ones being those shown above, but he by no means claims to have been on the receiving handset of a straight line to the Supreme Servomechanist. Therefore, the experimentally derived relationships reviewed above should be considered with due care and caution.

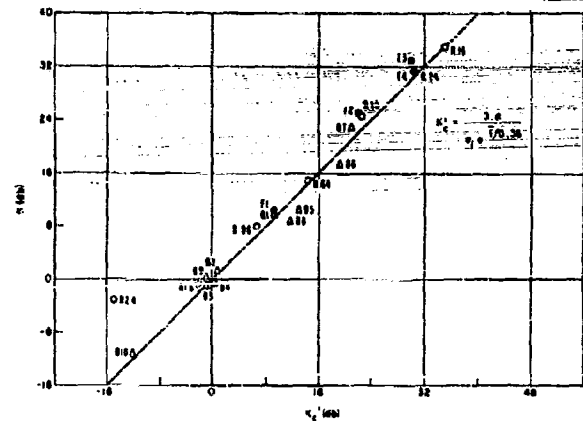


Figure 39. Measured Gain, K , Versus the Parameter $K'_e = 3.8/(\sigma_f e^{7/0.38})$ (Fig. 5-7, Ref. 23)

d. Attempts to Apply Conventional Servo Criteria to Elkind's Results

The experimental results obtained by Elkind are especially significant in that they indicate the general sort of way in which the human operator adjusts his parameters as a function of forcing function conditions when in a compensatory task with no controlled element dynamics. In particular the data express, within the limits of the experimental situation, the results of the operation of some optimizing criterion internal to the human. With these data extant, it is now of great interest to determine the correspondence, if any, between the types of criteria used by servo system designers with those adopted by the operator in adjusting his parameters.

Servo design criteria exist in many different forms, but the type most easily applied to systems analogous to that of the human operator tracking stochastic inputs is one involving the minimization of the root-mean-square error. There is some reason to believe that the human operator may be relatively sensitive to such a criterion since one would suspect that he

- (1) attempts to minimize the error (his input) in compensatory tasks;
- (2) doesn't care about the sign of the error, at least when he possesses no knowledge of instruction about positive errors being worse than negative values;
- (3) tends to give larger errors more weight than smaller ones.

On this basis the application of the rms error minimization criterion to human operator results might possibly be reasonable. In this subsection, therefore, we shall outline the results of an rms minimization problem for a simple servo having approximately the same characteristics as Elkind's analytical model. The actual experimental results can then be compared with the analytical rms minimization model.

The analogous servo system will be as shown in Fig. 40. If the remnant, n_e , is not linearly coherent with the input, $i(t)$, then, by using the methods leading to Eq. (III-58), the error spectral density will be given by

$$\Phi_{ee} = \left| \frac{1}{1+Y} \right|^2 \Phi_{ii} + \left| \frac{Y}{1+Y} \right|^2 \Phi_{nn} = \left| \frac{H}{1+Y} \right|^2 \Phi_{ii} + |H|^2 \Phi_{nn} \quad (V-11)$$

As will be shown in the next subsection, a reasonable representation for the noise spectra will be (if referred to the operator's input and if only the lower four rectangular input spectra are considered) white noise with a magnitude $\Phi_{nn}(0)$. Also, for the rectangular spectra Φ_{ii} can be represented by a spectrum characterized by $\Phi_{ii}(0)$ extending to the cutoff frequency ω_{co} . Then, since the mean square error in general is given by

$$\bar{\epsilon}^2 = \frac{1}{2} \int_{-\infty}^{\infty} \Phi_{ee}(f) df = \frac{1}{4\pi} \int_{-\infty}^{\infty} \Phi_{ee}(\omega) d\omega = \frac{1}{2\pi} \int_0^{\infty} \Phi_{ee}(\omega) d\omega \quad (V-12)$$

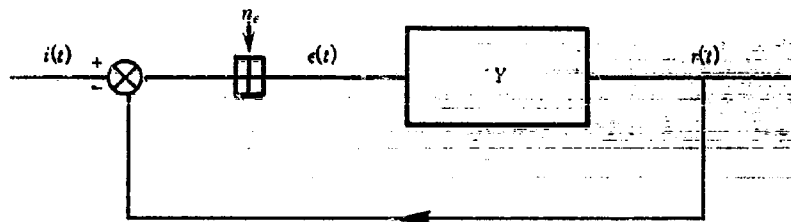


Figure 40. Analogous Servosystem to Elkind's Simple Tracker.

that for this particular case will be

$$\bar{\epsilon}^2 = \frac{\Phi_{ii}(0)}{2\pi} \int_0^{\omega_{co}} \frac{|H|^2 d\omega}{|Y|^2} + \frac{\Phi_{nn}(0)}{2\pi} \int_0^{\infty} |H|^2 d\omega \quad (V-13)$$

The approximate open loop transfer function, Y_p , for the lower four rectangular spectra is:

$$Y_p = \frac{K e^{-\tau_1 \omega}}{(T_0 j\omega + 1)(T_1 j\omega + 1)} \quad (V-14)$$

In the frequency range and for the quantities of interest this can be approximated by

$$Y_p = \frac{K e^{-\tau_1 \omega}}{T_0 j\omega + 1} = \frac{K(1 - r' j\omega)}{(1 + T_0 j\omega)(1 + r' j\omega)} \quad (V-15)$$

where $r' = \tau_1/2$. $|Y_p|^2$ then becomes

$$|Y_p|^2 = \frac{K^2}{1 + (T_0 \omega)^2} \quad (V-16)$$

The closed loop transfer function H will be

$$\begin{aligned} H &= \frac{Y}{1+Y} = \frac{K(1 - r' j\omega)}{(1 + T_0 j\omega)(1 + r' j\omega) + K(1 - r' j\omega)} \\ &= \frac{K}{1+K} \left(\frac{1 - r' j\omega}{1 + \left(\frac{T_0 + r'(1-K)}{K+1} \right) j\omega + \frac{T_0 r'}{K+1} (j\omega)^2} \right) \\ &= \frac{K}{1+K} \left(\frac{1 - r' j\omega}{1 + \frac{2\zeta j\omega}{\omega_n} - \left(\frac{\omega}{\omega_n} \right)^2} \right) \end{aligned} \quad (V-17)$$

where: $\omega_n^2 = \frac{K+1}{T_0 r'}$; $\zeta = \frac{T_0 + r'(1-K)}{2\sqrt{T_0 r'(K+1)}}$

The magnitude squared of the two transfer functions of interest, H and H/Y , will then be:

$$|H|^2 = \left(\frac{K}{1+K} \right)^2 \frac{1}{\left[1 - \left(\frac{\omega}{\omega_n} \right)^2 \right]^2 + \left(\frac{2\zeta \omega}{\omega_n} \right)^2} \quad (V-18)$$

$$|H_V|^2 = \frac{1 + (T_0 \omega)^2}{(1+K)^2 \left\{ \left[1 - \left(\frac{\omega}{\omega_n} \right)^2 \right]^2 + \left(\frac{2\zeta \omega}{\omega_n} \right)^2 \right\}} \quad (\text{V-19})$$

Using Equations (V-18) and (V-19) with (V-13) yields the following for the mean square error:

$$\bar{\epsilon}^2 = \frac{\Phi_{ii}(0)}{2\pi(1+K)^2} \int_0^{\omega_{co}} \frac{1 + (T_0 \omega)^2}{\left[1 - \left(\frac{\omega}{\omega_n} \right)^2 \right]^2 + \left(\frac{2\zeta \omega}{\omega_n} \right)^2} d\omega + \frac{K^2 \Phi_{nn}(0)}{4\pi(K+1)^2} \int_{-\infty}^{\infty} \frac{d\omega}{\left[1 - \left(\frac{\omega}{\omega_n} \right)^2 \right]^2 + \left(\frac{2\zeta \omega}{\omega_n} \right)^2} \quad (\text{V-20})$$

or

$$\bar{\epsilon}^2 = \frac{\Phi_{ii}(0)}{2\pi(1+K)^2} \mathfrak{I}(\omega_{co}) + \frac{K^2 \Phi_{nn}(0)}{2(K+1)^2} \mathfrak{I}_2 \quad (\text{V-21})$$

The first term, involving the integral $\mathfrak{I}(\omega_{co})$, is the mean square error in following the input; the second term with the integral \mathfrak{I}_2 is the mean square error due to the noise. The next step in the procedure is the evaluation of the two integrals, $\mathfrak{I}(\omega_{co})$ and \mathfrak{I}_2 . The integral \mathfrak{I}_2 is of the form

$$\mathfrak{I}_2 = \frac{1}{2\pi j} \int_{-\infty}^{\infty} \frac{d\omega}{\left[1 - \left(\frac{\omega}{\omega_n} \right)^2 \right]^2 + \left(\frac{2\zeta \omega}{\omega_n} \right)^2} = \frac{1}{2\pi j} \int_{-\infty}^{\infty} \frac{g_n(\omega) d\omega}{\mathfrak{D}_n(\omega) b_n(\omega)} \quad (\text{V-22})$$

where

$$b_n(\omega) = a_0 \omega^n + a_1 \omega^{n-1} + \dots + a_n$$

$$g_n(\omega) = b_0 \omega^{2n-2} + b_1 \omega^{2n-4} + \dots + b_{n-1}$$

Integrals of the type shown in Eq. (V-22) have been evaluated and are shown on page 369 of Reference 44. In this case, $n = 2$ and

$$\mathfrak{I}_2 = \frac{-b_0 + \frac{a_0 b_2}{a_1}}{2a_0 a_1} \quad (\text{V-23})$$

Since

$$b_n(\omega) = -\left(\frac{\omega}{\omega_n} \right)^2 + j \frac{2\zeta \omega}{\omega_n} + 1 \quad \text{and} \quad g_n(\omega) = 1$$

$$a_0 = -\frac{1}{\omega_n^2}, \quad a_1 = j \frac{2\zeta}{\omega_n}, \quad a_2 = 1$$

$$b_0 = 0, \quad b_1 = 1$$

then

$$\mathfrak{I}_2 = \frac{1}{2a_1} = \frac{\omega_n}{4j\zeta} \quad (\text{V-24})$$

Turning our attention now to the integral $\mathfrak{I}(\omega_{co})$, and letting $\alpha = \omega/\omega_n$, $\alpha_c = \omega_{co}/\omega_n$

$$\mathfrak{I}(\alpha_c) = \omega_n \int_0^{\alpha_c} \frac{1 + (T_0 \omega_n \alpha)^2}{(1 - \alpha^2)^2 + (2\zeta \alpha)^2} d\alpha \quad (\text{V-25})$$

This integral can be broken into partial fractions to obtain standard forms. After algebraic manipulation,

$$\frac{4j\zeta}{\omega_n} \mathfrak{I}(\alpha_c) = [1 + (T_0 \omega_n)^2] \int_0^{\alpha_c} \left(\frac{\alpha}{1 - 2j\zeta \alpha - \alpha^2} - \frac{\alpha}{1 + 2j\zeta \alpha - \alpha^2} \right) d\alpha + 2j\zeta \int_0^{\alpha_c} \left(\frac{1}{1 - 2j\zeta \alpha - \alpha^2} + \frac{1}{1 + 2j\zeta \alpha - \alpha^2} \right) d\alpha \quad (\text{V-26})$$

These integrals are both standard forms found in the integral tables (e.g., Pierce [68, 72]). After more grinding, the answer becomes:

$$\mathfrak{I}(a_c) = \frac{\omega_n}{4\zeta} [1 + (T_0\omega_n)^2] \tan^{-1} \frac{2\zeta a_c}{1 - a_c^2} + \frac{\omega_n}{4\sqrt{1 - \zeta^2}} [1 - (T_0\omega_n)^2] \tanh^{-1} \frac{2a_c\sqrt{1 - \zeta^2}}{1 + a_c^2} \quad (V-27)$$

The total expression for the rms error, made up of Equations (V-21), (V-24), and (V-27) is a fairly complex result. To simplify the expression, we can restrict the results to be applicable only to inputs R.16 through R.64.* Then:

$$(T_0\omega_n)^2 \gg 1; \quad K \gg 1; \quad \left(\frac{\omega_c}{\omega_n}\right)^4 \ll 1 \quad (\text{R.16 - R.64}) \quad (V-28)$$

so that

$$\omega_n^2 \doteq \frac{K+1}{T_0 r'} \doteq \frac{K}{T_0 r'} \quad \text{and} \quad \frac{2\zeta}{\omega_n} \doteq \frac{T_0 + r'(1-K)}{K+1} \doteq \frac{T_0 \cdot K r'}{K} \quad (V-29)$$

The much simplified expression for the mean square error then becomes, within these restrictions

$$\bar{\epsilon}^2 \doteq \frac{\Phi_{ii}(0)\omega_{co}^3}{2\pi} \left(\frac{T_0}{K}\right)^2 + \frac{\Phi_{nn_e}(0)}{4} \left(\frac{K}{T_0}\right) \left(\frac{1}{1 - r' \frac{K}{T_0}}\right) \quad (V-30)$$

or, letting $\lambda = K/T_0$

$$\bar{\epsilon}^2 \doteq \left(\frac{\Phi_{ii}(0)\omega_{co}^3}{2\pi}\right) \frac{1}{\lambda^2} + \frac{\Phi_{nn_e}(0)}{4} \left(\frac{\lambda}{1 - r'\lambda}\right) \quad (V-31)$$

At this point, the rms error can be differentiated with respect to λ and the result set equal to zero. This operation will give us the criterion to use in adjusting the analogous servo system so that $\bar{\epsilon}^2$ will be minimized.

$$\frac{d\bar{\epsilon}^2}{d\lambda} = 0 = -\frac{4\Phi_{ii}(0)\omega_{co}^3}{\pi\lambda^3} + \frac{\Phi_{nn_e}(0)}{(1 - r'\lambda)^2} \quad (V-32)$$

If a new parameter, β , is defined as $\beta = \frac{4\omega_{co}^3 \Phi_{ii}(0)}{\pi \Phi_{nn_e}(0)}$, Eq. (V-32) becomes

$$\lambda^3 - \beta r'^2 \lambda^2 + 2\beta r' \lambda - \beta = 0 \quad (V-33)$$

From the experimental data for the remnant term considered as noise at the input (see the next subsection), the approximate value of $\Phi_{nn_e}(0)$ for R.16 through R.64 is,

$$\Phi_{nn_e}(0) \doteq \frac{1}{\pi} \int_0^\infty \Phi_{ii} df \quad (V-34)$$

Also, for rectangular input spectra

$$\int_0^\infty \Phi_{ii} df = \int_0^{f_{co}} \Phi_{ii}(0) df = \Phi_{ii}(0) f_{co} \quad (V-35)$$

The parameter β then becomes

$$\beta = \frac{4\omega_{co}^3}{\pi} \frac{\Phi_{ii}(0)}{\Phi_{nn_e}(0)} \doteq 64\omega_{co}^2 \quad (V-36)$$

* This point is the first place where it was actually necessary to restrict the expressions to these cases for analytical simplicity, although we had already taken advantage of the impending simplification in considering the noise essentially white.

The actual roots for λ from Eq. (V-33) are therefore functions of ω_{c0} and r' . Investigating these roots for the values of ω_{c0} and r' corresponding to the first four rectangular spectra forcing functions reveals that an approximate root is given by the last term of Eq. (V-33) divided by the next to last, i.e.,

$$\lambda_1 \doteq \frac{\beta}{2\beta r'} = \frac{1}{2r'} = \frac{1}{r_1} \quad (V-37)$$

To the extent that r_1 is constant, this result is independent of the bandwidth of the forcing function. From the definition of λ [see Eq. (V-31)];

$$\lambda_1 = \frac{K}{T_0} = \frac{1}{r_1};$$

or, since $T_0 = 1/(2\pi f_0)$, and the average value of r_1 for the first four rectangular spectra inputs (.328 seconds)

$$K/f_0 = \frac{1}{2\pi r} \doteq \frac{1}{2\pi(.328)} \doteq 0.5 \quad (V-38)$$

If the Elkind data for R.16 through R.64 are used to establish a trend, the result is

$$K/f_0 \doteq 1.3 \quad (V-39)$$

The correspondence between the general forms of Equations (V-38) and (V-39) is quite startling — to the point of being misleading. The above results are based on simplifying assumptions in formulating the mean square error. It should be noted particularly that the measured mean square errors do not agree well with those computed by use of (V-31) for R.16 through R.64. The crux of the answers of Eq. (V-38) and (V-39) involves three relatively simple steps. These are:

- (1) The assertion that $\lambda_1 \doteq 1/(2r')$ is an approximate root of $\lambda^3 - \beta r'^2 \lambda^2 + 2\beta r' \lambda - \beta = 0$
- (2) The value used for r in the expression $K/f_0 = 1/(2\pi r)$
- (3) The experimental values for K/f_0 .

When one realizes that the methods of obtaining values of r for the first four rectangular spectra were relatively crude, and that the accuracy of the data of the next section yielding Φ_{me} , which is involved in β , is subject to some question, etc., the fairly close correspondence of Equations (V-38) and (V-39) tends to lose significance. However, even a difference of a large factor in the two results would still give one a considerable amount of insight into possible behavioral criteria and it is in this sense that the entire development is considered interesting. While it would be too much to say that the operator's criterion demands that he attempt to minimize the rms error, it is probably possible to state that the actual criterion used by the operator gives results which are similar to this one.

To put a pedagogic interpretation on the foregoing development, it may be considered to be a theoretical structure for evaluating subsequent tracking data. In this regard, first Phillips and Sobczyk [44] and then Walston and Warren [88] have applied mean square error techniques to the interpretation of tracking data in terms of transfer functions. In 1943, Phillips and Sobczyk made the assumption that $Y_p = K e^{-Ts} [(Ts + 1)/s]$ and then used the rms minimization concept and stability criteria to derive aided tracking ratios. Walston and Warren espoused an a priori linear plus noise model in which the describing function had the same form as used by Phillips and Sobczyk. Then by comparing theoretical with measured mean square errors as well as taking stability restrictions into account, they were able to determine fairly consistent values for the parameters of their model after an extensive and careful series of experiments.

2. Russell's Simple Tracker

Just as Elkind's experiments represent an impressive attempt to study the effects of forcing function characteristics upon a simple control loop with a human operator, the work of L. Russell is an elegant effort to

provide the experimental basis for determining the gross effects of controlled element variation on the operator's linearized transfer characteristics. While Russell [70] studied a wide variety of controlled element dynamics, the results presented in this subsection, in keeping with our general plan, are those obtained for a "simple tracker" with no controlled element dynamics save for the characteristics of the mechanical linkages through which tracking was effected.

Russell's experimental setup consisted of an oscilloscope display where the deflection of a vertical line from the center of the scope was proportional to a function of the system error. The input signal consisted of the sum of four sine waves selected to avoid harmonic relationships. The mechanism used for generating the input could be run at three different speeds, with the result of a speed change being a proportional increase or decrease of the frequency of each sinusoidal component while leaving the amplitude unchanged. Table 2 and Fig. 41 show the various components of the input, with the amplitudes of each sinusoidal component being given in terms of inches rms deflection on the oscilloscope at normal gains. These forcing function forms, while not as general as those used by Elkind, still resulted in a signal which was random appearing to a high degree. The error signal

Table 2. Characteristics of Russell's Forcing Function.

INPUT COMPONENT.....	F_1	F_2	F_3	F_4
AMPLITUDE (inches rms).....	0.78	0.52	0.29	0.20
FREQUENCIES				
Low Speed, cps.....	0.0442	0.118	0.192	0.287
rad/sec.....	.277	.741	1.21	1.80
Medium Speed, cps.....	0.105	0.268	0.457	0.679
rad/sec.....	.66	1.68	2.87	4.27
High Speed, cps.....	0.220	0.563	0.960	1.43
rad/sec.....	1.38	3.54	6.03	8.98

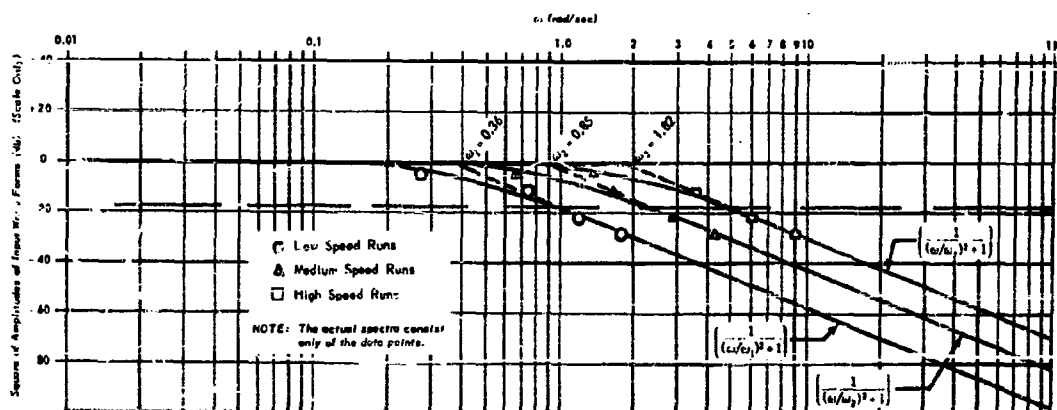


Figure 41. Russell's Power Spectra of Low, Medium, and High Speed Forcing Functions and Approximate White Noise Thru First Order Filter "Equivalents".



Figure 42. Russell's Tracking Apparatus.
(Page 29, Ref. 70)

was generated by subtracting a function of the operator's output displacement from the forcing function. Physically, the tracking control was like a conventional aircraft control "wheel", operated in a fashion similar to that used in controlling ailerons (Fig. 42).

The apparatus was set up so that both the system error and the operator's displacement signal could be operated upon by selected transfer functions. This arrangement, shown in schematic form in Fig. 43, allowed Russell to vary the controlled element dynamics in various ways.

The controlled element transfer function, Y_c , is the product of the transfer functions of the pre and post filters, so the difference between post and pre filter positions is not important in the closed loop stability sense as

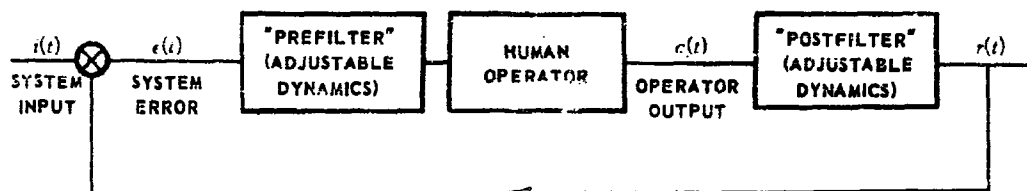


Figure 43. Block Diagram of Russell's Experimental Setup.

long as the operator behaves in a reasonably linear fashion. However, in terms of particular signal characteristics, such as the rms error, it is important to note the division of controlled element dynamics into the two filter elements.

In the simple tracker case neither of the filters had dynamics inserted. Russell presented his results in the form of Nyquist diagrams; these have been transcribed into the Bode diagram form both for convenience in curve fitting procedures as well as for consistency with the rest of this report.

Averaged data for four low speed (0.277-1.8 rad/sec) simple tracker runs are shown in Fig. 44, taken originally from Russell's Figures 15, 33, 35 and 36. Averaged medium speed (0.66-4.27 rad/sec) data from nine runs (originally Russell's Figures 11, 14, 26, 29, 30, 32, 34, 41 and 42) are shown in Fig. 45. Finally, a single high speed (1.38-8.98 rad/sec) run is given in Figure 46 from Russell's Fig. 20. All of these runs were between five and seven minutes in duration.

It will be noted on the figures that the data have all been fitted by transfer functions of the form

$$Y_p = \frac{Ke^{-T_d}(T_f s + 1)}{(T_f s + 1)} = \frac{Ke^{-T_d}(aT_f s + 1)}{(T_f s + 1)} \quad (V-40)$$

Unfortunately, the existence of but four data points for each input characteristic is a severe handicap to the analyst interested in finding analytical models which approximate the data. Of course, the selection of the simplest form of transfer function, consistent with all the data of the three runs, leads rather directly to the form given in

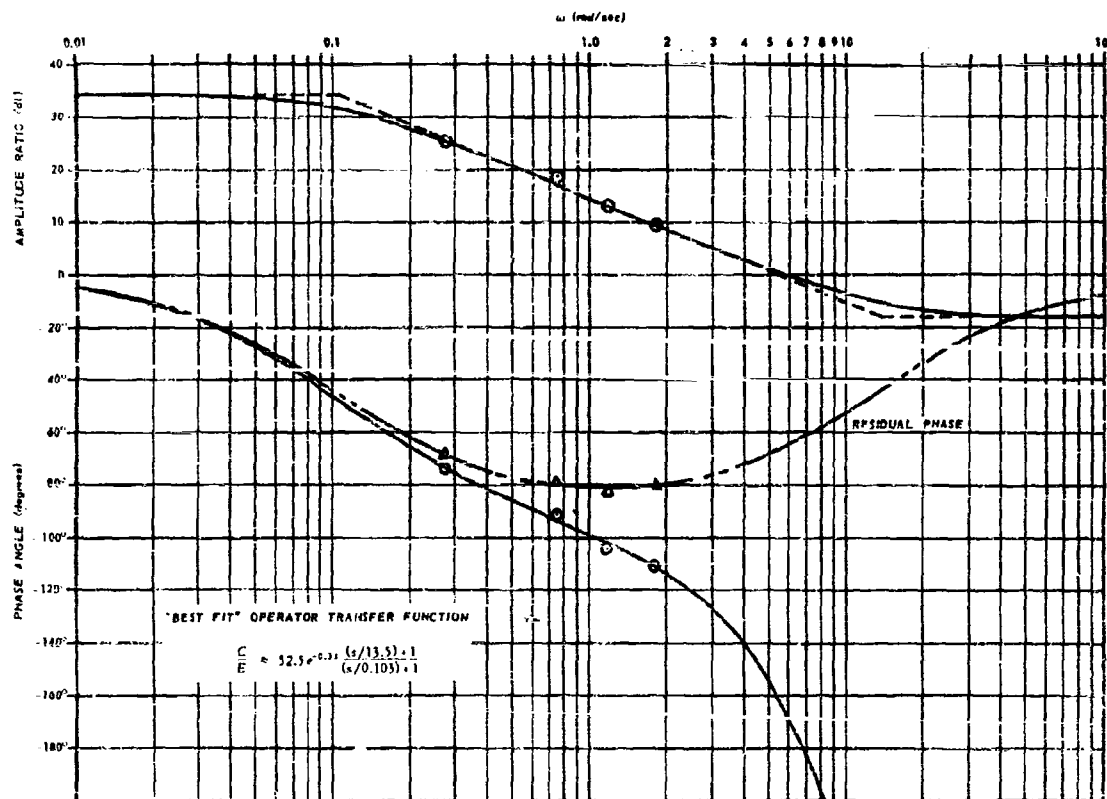


Figure 44. Russell Simple Tracker, Low Speed Forcing Function, Averaged Data.
(Source: Reference 70, Figures 15, 33, 35, 36)

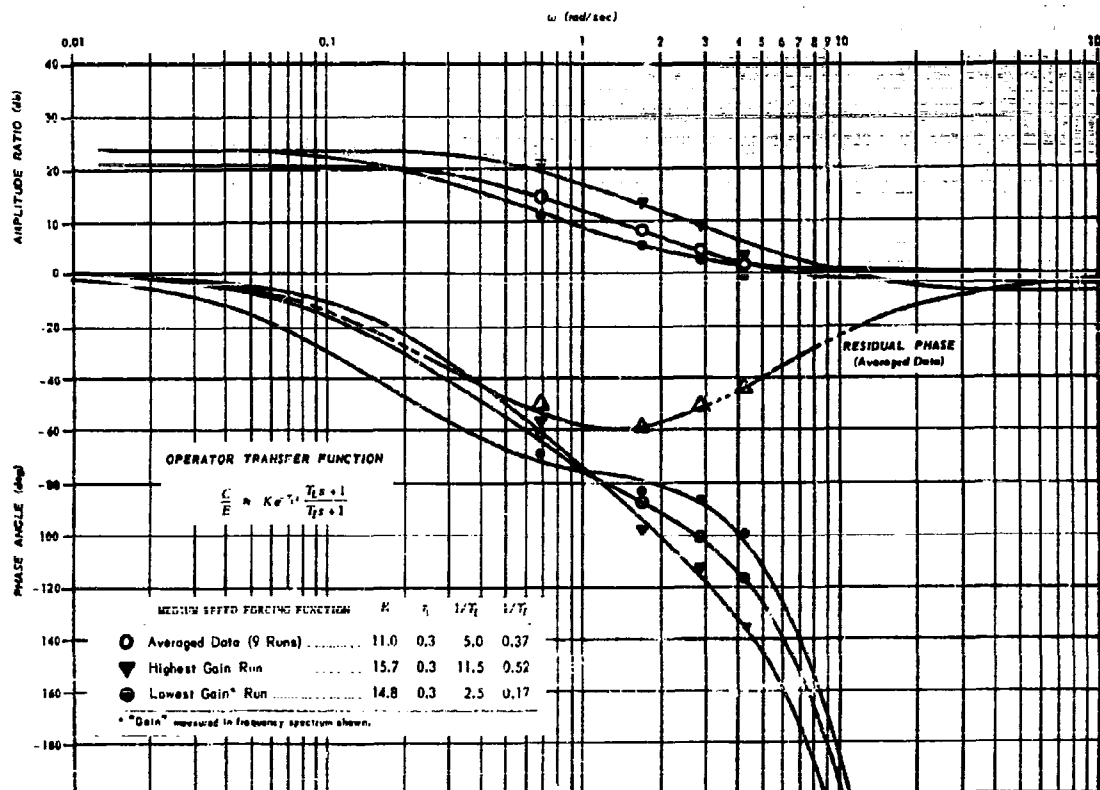


Figure 45. Russell Simple Tracker. Medium Speed Forcing Function, Averaged Data.
(Source: Reference 70, Figures 11, 14, 20, 27, 30, 33, 34, 41, 42)

Eq. (V-40).^{*} However, with the exception of the high speed data of Fig. 46, the amplitude ratio points do not define clearly the location of the break points. As a consequence of this shortcoming it becomes necessary to make some reasonable assumptions. Therefore, it was assumed that the values of τ_1 would be the same for all runs and that the closed loop transfer functions derived from the fitted models should be stable. Then, the superposition of the data for the three forcing function conditions on top of one another lead to the conclusions that (with the above restrictions)

$$K_{\text{LOW SPEED}} > K_{\text{MEDIUM SPEED}} > K_{\text{HIGH SPEED}}$$

$$\alpha_{\text{HIGH SPEED}} > \alpha_{\text{MEDIUM SPEED}} > \alpha_{\text{LOW SPEED}}$$

(V-41)

The observations of (V-41), together with the possible necessity of a lead term for the high speed run, are actually the most significant characteristics that can be obtained from these data.

With all of these items of information, the data points can be fitted quite well by transfer functions of the form given by Eq. (V-40). The value of τ_1 , however, can be varied over a fairly wide range without seriously

^{*} Only the single High Speed run demanded a lead term for a good fit. The other data were fitted equally well by a simple lag form similar to Elkind's. Transfer functions obtained using the simpler fit were: Low Speed, $56e^{-0.25s}/(s/0.105 + 1)$; Medium Speed, $10e^{-0.15s}/(s/0.55 + 1)$; High Speed, $2e^{-0.15s}/(s/1.0 + 1)$. This last fit was quite poor relative to that given in the body of the report.

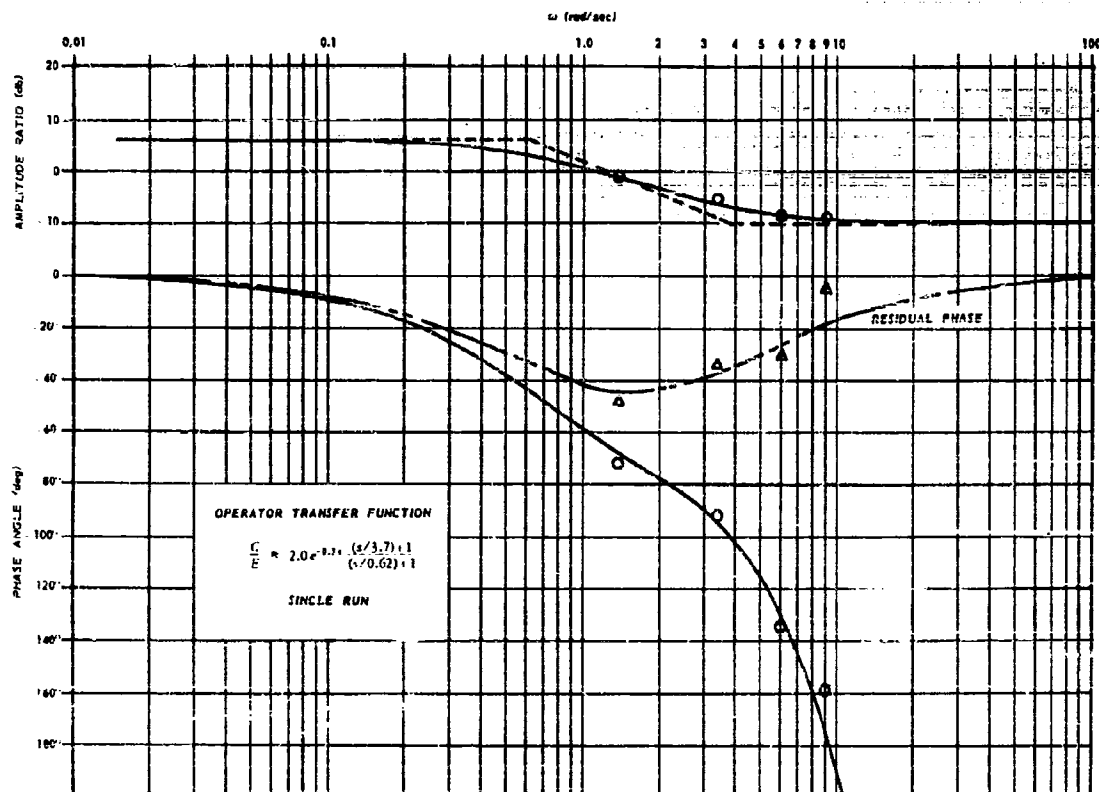


Figure 46. Russell Simple Tracker, High Speed Forcing Function, Averaged Data.
(Source: Reference 70, Figure 20.)

affecting the transfer function form, i.e., forcing one to complicate the transfer function with an additional lag or lead. Since we have no real basis, in Russell's case, for deciding which data points were more accurate than others, one should probably assume that all were about equally good. The single high speed forcing function run then had the most influence on the selection of the ranges of τ_1 ; i.e., a value of τ_1 was selected that would be consistent with a residual phase, which was derived from the form of the amplitude ratio alone, that did not go over zero degrees for any of the forcing function inputs. A τ_1 of about 0.3 seconds was consistent with these requirements.

With the value of τ_1 selected in this somewhat arbitrary fashion, "residual" phase points were found by subtracting the phase of $e^{-0.3j\omega}$ from the measured phase data. These residual phases are shown in Figures 44, 45, and 46. The residual phases were then fitted with the aid of a simple template for lag-lead transfer functions, giving values of α , $1/T_1$ and $1/T_L$. The amplitude ratios consistent with these parameters were then drawn in and the gain K determined. The general adequacy of the fits is apparent from examination of the figures. Table 3 lists the values of the fitted parameters. It should be noted again that this somewhat tautological fitting procedure is necessary because the measured amplitude response is not capable of defining a residual phase with sufficient precision so that τ_1 values may be determined from the slope of $\tau_1\omega$ versus ω as in the case of Elkind's data. This problem will recur when we examine the Franklin Institute data.

The reader should carefully note that the numerical values assigned to the transfer function models are only valid for τ_1 's of the order of 0.30, and the selection of this value was made upon nebulous, though internally consistent, grounds. If the single high frequency point of Fig. 46 is ignored, it is possible to obtain equally adequate

Table 3. Recapitulation of Analytical Transfer Function Characteristics Derived from Russell Data for $r = 0.30$ sec.

INPUT	$1/T_I$	$1/T_L$	a	K
Low Speed	0.103	13.5	0.0076	52.5
Medium Speed37	5.0	.074	11.0
High Speed62	3.7	.167	2.0

fits to those shown in the figure with a value of r of 0.30 second or below, without having to add terms to the transfer function of Eq. (V-40). This conclusion, and the relative order of a and K values, are really all that one should consider important from these fits to the data — the actual numbers in the analytical describing function, with the general structure described above, are subject to the whims of the analyst doing the fitting.

One final point should be noted — the above data would also be consistent with a transfer function form

$$Y_p = \frac{K e^{-Ts} (T_I s + 1)}{(T_I s + 1)(T_N s + 1)} \quad (V-42)$$

if $1/T_N > 20$ rad/sec (for the high speed input run) and $1/T_N > 7$ rad/sec for the other two; and in addition, $r + T_N = r_i \approx 0.30$. On this basis, the value of reaction time could be adjusted downward from 0.3 seconds to something between 0.15 and 0.25 seconds. Further reduction would not be too compatible with the data. The form shown in Eq. (V-42) is somewhat more desirable than that of Eq. (V-40) since Y_p goes to zero as s goes to infinity, as it should from physical considerations. Both forms are, of course, equally appropriate approximations over the frequency band of measurement.

3. The Franklin Institute Simple Tracker

The final set of simple tracker experiments were performed at the Franklin Institute as a prelude to their tests on the description of human pilots in the control of aircraft. The test apparatus was much more elaborate than that used by other investigators, consisting primarily of a cockpit mockup (Figures 47 and 48), an analog computer to generate controlled element dynamics, and sundry data reduction and forcing function gear [31].

The simulator cockpit contains a 5 inch oscilloscope which presented, for the simple tracker experiments, a display consisting of a fiduciary cross hairs and a pip representing the pilot's target. The operator's control was a conventional, spring-loaded, aircraft type control stick whose feel had been designed to simulate loads on an F-80A stick under the conditions of test described in Section VI-D. The static characteristics of this control are shown in Figure 49. These static characteristics are valid representations of the stick dynamics to a



Figure 47. Interior of Cockpit, Franklin Institute Simulator.



Figure 48. Cockpit and Computer Racks, Franklin Institute Simulator.

frequency of about 35 rad/sec in aileron and 90 rad/sec in elevator.

The forcing function was generated by a white noise source, feeding through a three section RC filter, giving a high frequency attenuation rate of 60 db/dec. The corner frequency of the filter was adjustable to values of 1, 2 and 4 rad/sec at continuously adjustable rms voltage levels. The system error was two dimensional, consisting of an azimuth and elevation error derived from subtracting functions of the aileron and elevator control positions from the forcing functions.

In the simple tracker experiments the simulator was instrumented as a stick controlled tracking device with a two dimensional display. No aircraft control dynamics were generated. Each of the three forcing function bandwidth conditions were used. The forcing functions had approximately equal statistics in both aileron and elevator, and each had an amplitude of 0.6 inch rms on the oscilloscope. The control parameters were 1.2 inches CRO deflection per inch azimuth stick movement (at the top of the stick), and 3.2 inches CRO deflection per stick inch in elevation. The stick hand grip position was about 28 inches from the pivot point and the subject was about 28 inches from the scope, so the above control ratios are numerically equal whether expressed in degrees or inches. The stick forces were as shown in Figure 49, i.e., 1.35 lb/degree aileron and 13.3 lb/degree elevator. Two experienced subjects tracked all forcing functions in the presentation order of 1, 4 and 2 rad/sec bandwidths, tracking

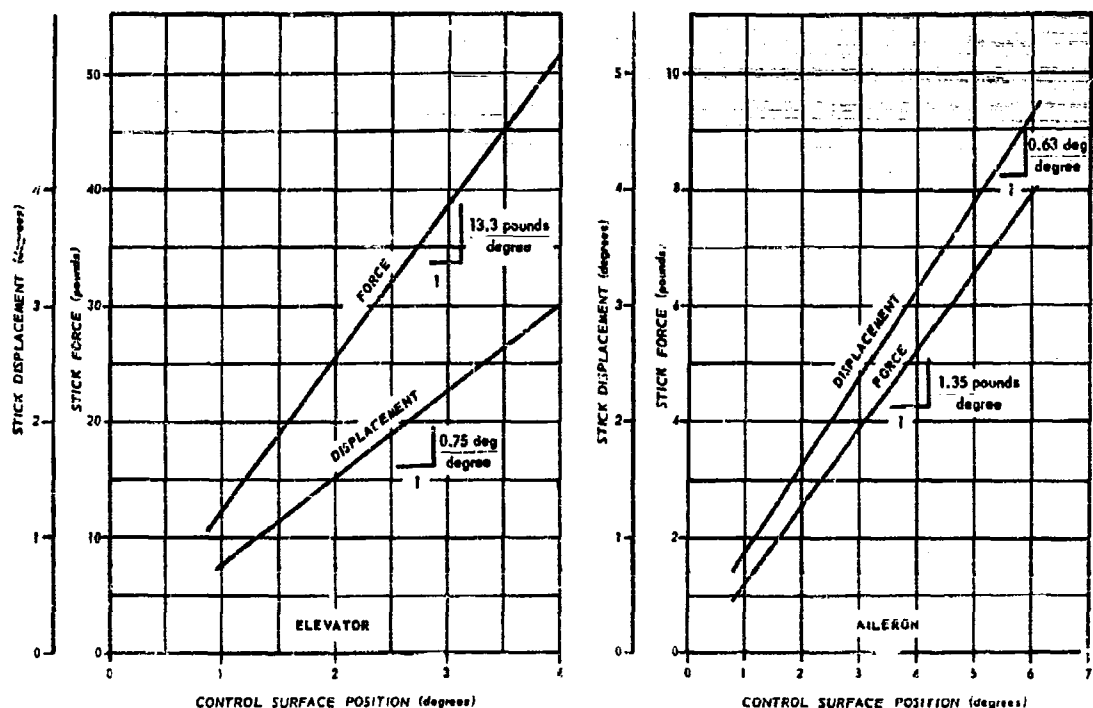


Figure 49. Franklin F-80A Simulator Characteristics.

in elevation and azimuth simultaneously. Each run lasted two minutes, with a three minute pause between runs.

While data from both control axes were available, only aileron control was analyzed, and of these one run had to be discarded due to data reduction difficulties. The remaining experimental data are presented in Fig. 50.

It will be noted on the amplitude ratio data that there is a well defined lead term within the bandwidth of measurement, and further that a high frequency lag outside the measurement bandwidth will be necessary for stable operation if the phase data is extrapolated in any reasonable way. Therefore, the simplest transfer function form consistent with stability and fitting the data will be

$$Y_p(s) = \frac{K e^{-\tau_2}(T_L s + 1)}{(T_I s + 1)(T_N s + 1)} = \frac{K e^{-\tau_2}(a T_I s + 1)}{(T_I s + 1)(T_N s + 1)} \quad (V-43)$$

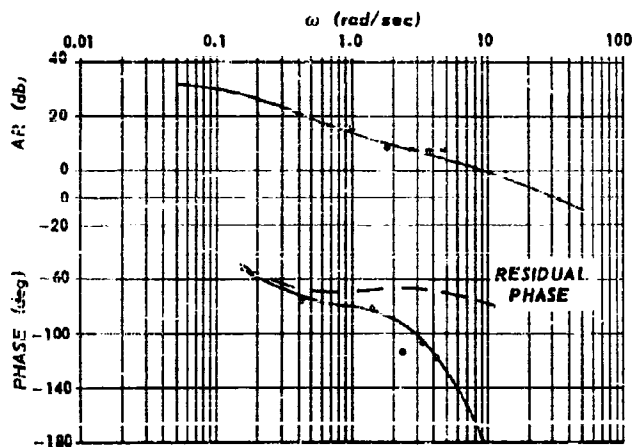
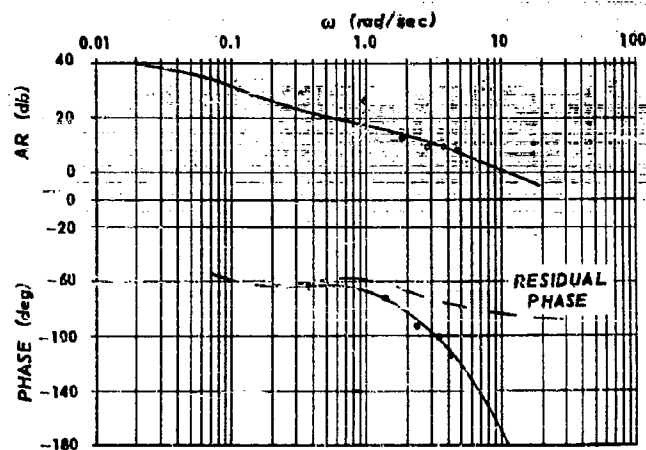
Following the general procedure noted previously in the discussion of the Russell data, the analytical values of the transfer function approximation were determined. These are summarized in Table 4.

a. 1 Rad/Sec Forcing Function Bandwidth.

• Franklin Data, 2 Subjects

"Best Fit" Pilot Transfer Function:

$$Y_p = \frac{100 e^{-0.15s} [(s/0.5) + 1]}{[(s/0.04) + 1] [(s/1.5) + 1]}$$



b. 2 Rad/Sec Forcing Function Bandwidth.

• Franklin Data, 1 Subject

"Best Fit" Pilot Transfer Function:

$$Y_p = \frac{40 e^{-0.2s} [(s/2) + 1]}{[(s/0.11) + 1] [(s/4.55) + 1]}$$

c. 4 Rad/Sec Forcing Function Bandwidth.

• Franklin Data, 2 Subjects

"Best Fit" Pilot Transfer Function:

$$Y_p = \frac{15 e^{-0.25s} [(s/3.0) + 1]}{[(s/0.2) + 1] [(s/11) + 1]}$$

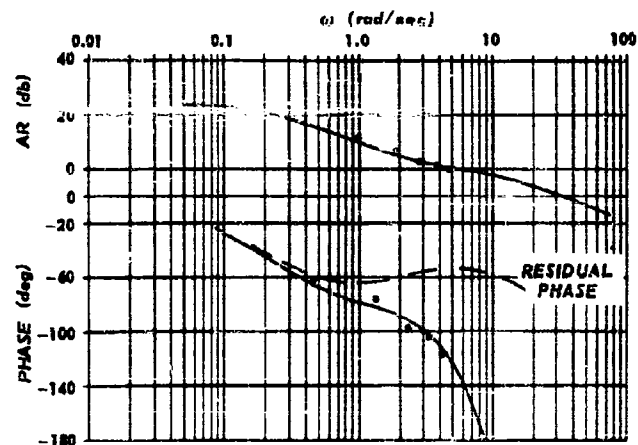


Figure 50. Franklin Simple Tracker.
(Ref. 53, Fig. 8)

Table 4. Recapitulation of Analytical Transfer Function Characteristics
Derived from Franklin Data.

CORNER FREQUENCY OF FORCING FUNCTION SPECTRA	$1/T_I$	$1/T_H$	$1/T_L$	ζ	K	a
1 Rad/sec	0.04	1.5	0.5	0.15	100	0.08
2 Rad/sec	.11	4.55	2.0	.20	40	.055
4 Rad/sec	.2	11.0	3.0	.25	15	.067

C. HUMAN OPERATOR REMNANT CHARACTERISTICS IN COMPENSATORY SYSTEMS WITH NO CONTROLLED ELEMENT DYNAMICS

1. Linear Correlations

Since the concept of a describing function is so similar to common transfer function usage, the reader probably has accepted this notion readily. On the other hand the remnant, which is by no means as familiar a "property" of system elements as the describing function, although quite as important, may require additional discussion. This lack of familiarity arises from the natural translation of ideas about linear systems, where the remnant is zero, to quasi-linear systems where the remnant is not zero. To help overcome this deficiency we have devoted a portion of Section III of this report to the definition of terms and to a discussion of the physical meaning of the remnant. Remnant description is extremely important for the full understanding of human operator behavior in operator description, for if the remnant is large it must be taken into account and the linear correlation theories are not complete.

It will be recalled from Section III that the linear correlation was a simple and meaningful measure of the ratio of linearly correlated output to actual output. In terms of closed loop characteristics, the operator output power density spectrum was given by

$$\Phi_{cc} = |H|^2 \Phi_{ii} + \Phi_{nn} \quad (V-44)$$

where the closed loop describing function, H , for a simple tracker is just $Y/(1+Y)$. The linear correlation squared was given by

$$\rho^2 = \frac{|H|^2 \Phi_{ii}}{\Phi_{cc}} = 1 - \frac{\Phi_{nn}}{\Phi_{cc}} \quad (V-45)$$

or in terms of cross-spectra as

$$\rho^2 = \frac{|\Phi_{ic}|^2}{\Phi_{ii} \Phi_{cc}} \quad (V-46)$$

Physically ρ^2 is the ratio of the output power density which is linearly coherent with the input, to the total output power density.

It will also be recalled that the total remnant due to all sources was lumped into the term Φ_{nn} . Φ_{nn} physically is the power spectral density of all of the operator output which cannot be explained as the result of a deterministic linear operation on the system forcing function. The chief interests then, in the discussion of the remnant term, will be the linear correlations and the Φ_{nn} term.

Unfortunately, the Franklin and Russell simple tracking experiments did not include a thorough measurement of the remnant. It is possible, however, to note from the data for an isolated point or so, and from

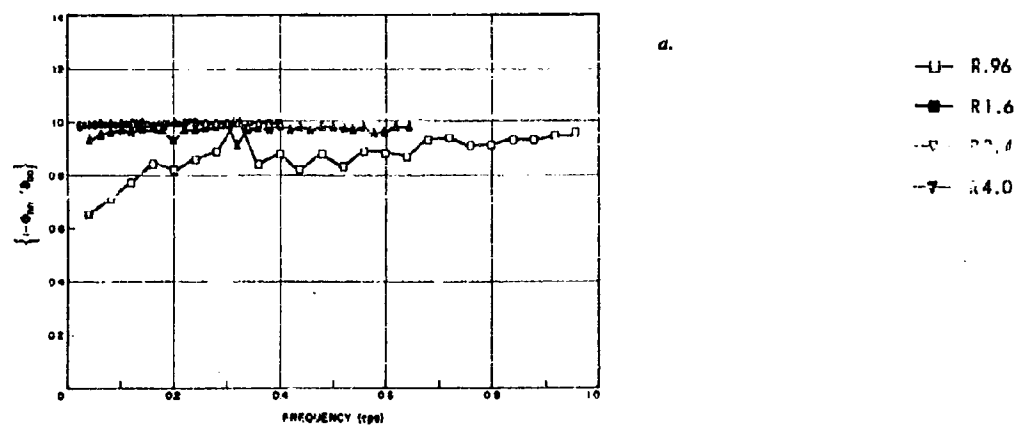
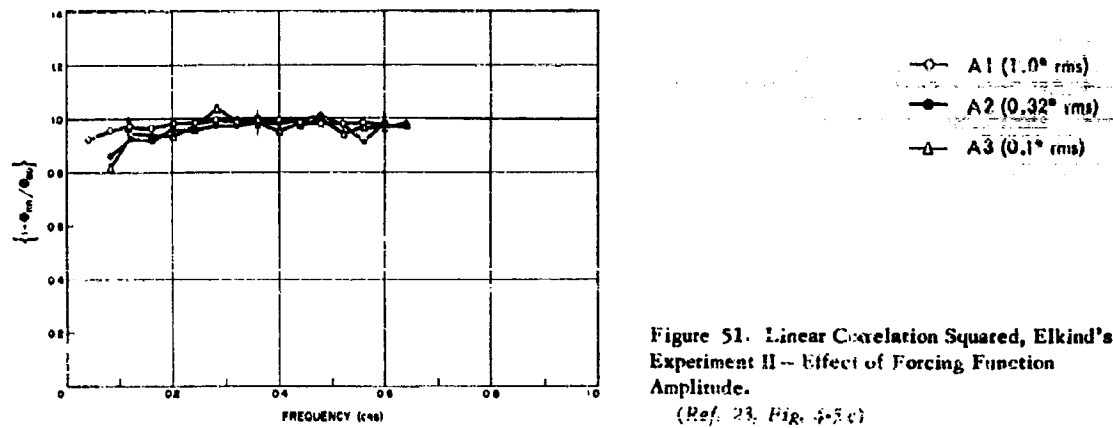
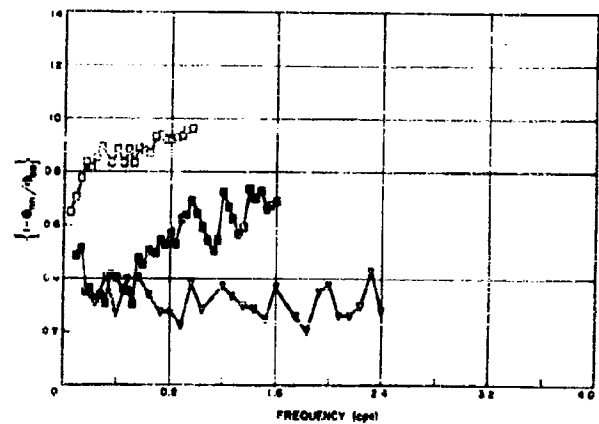


Figure 52. Linear Correlation Squared, Elkind's Experiment III - Effect of Forcing Bandwidth.
(Ref. 23, Figures 4-7c & 4-8c)



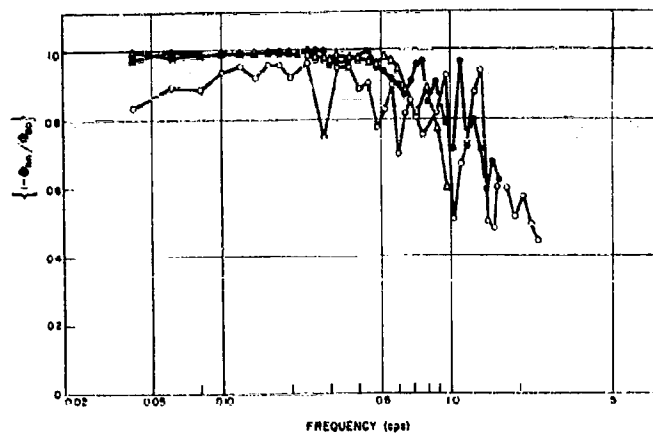
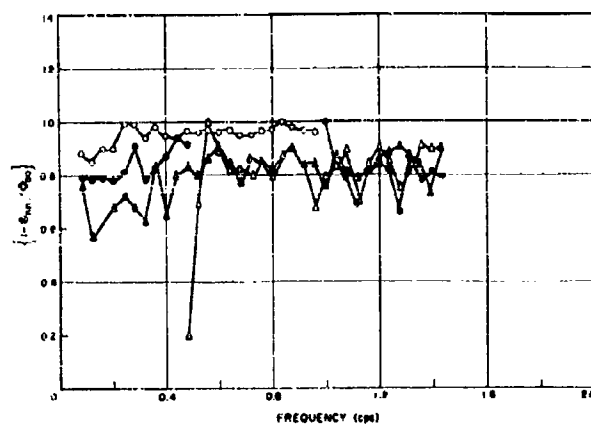


Figure 53. Linear Correlation Squared, Elkind's Experiment IV - Effect of Shape (RC Filtered Forcing Functions). (Ref. 23, Fig. 4-13c)



a.

- B1
- B2
- △ B3
- ▲ B4
- B5
- B6
- ▽ B7

b.

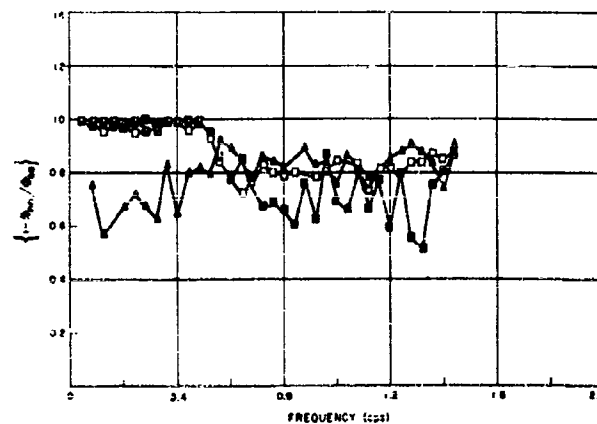
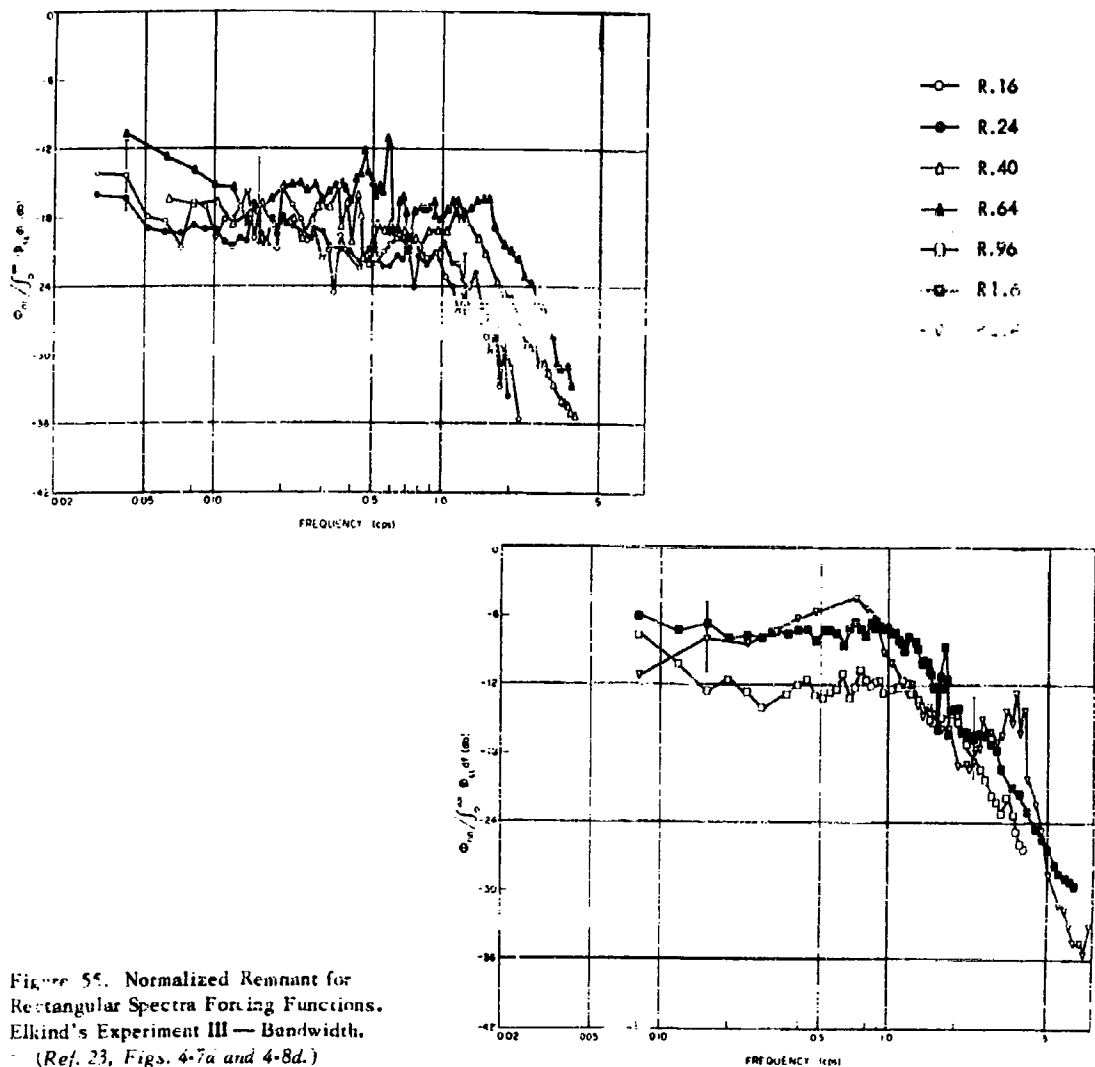


Figure 54. Linear Correlation Squared, Elkind's Experiment IV - Effect of Shape (Selected Band Forcing Functions). (Ref. 23, Figures 4-17c & 4-18c)

2. Remnant Data and Attempted Explanations

One would feel confident in applying a linear analysis to data for which ρ was about 0.95, but even so we must remember that ρ is not the sole criterion for determining linear behavior. This is to say, low ρ 's indicate that the transfer function may be nonlinear, but the actual test is whether or not the measured transfer characteristic is dependent on the input amplitude. Little would be gained from an attempt to explain the reasons for slight departures of ρ from unity without a very thorough and extensive investigation into the data gathering, reduction, and processing errors. On the other hand, data with lower linear correlations should have some reasonable explanation if they are to be considered indicative of linear behavior. Our major attempt, therefore, will be to provide possible explanations of these types of data. Our attention will be confined to Elkind's rectangular forcing function spectra since they present the simplest overall picture and will be easiest to deal with. Elkind's results for the total closed loop remnant, $\Phi_{nn}/\int_0^\infty \Phi_{11} d\omega$ for these data are illustrated in Figure 55.



Elkind notes that these data can be fitted very approximately by the relation*

$$\frac{\Phi_{nn}(f)}{\int_0^\infty \Phi_{nn} df} = \frac{\sigma_n^2}{\left[\left(\frac{f}{f_n} \right)^2 + 2\zeta \frac{f}{f_n} + 1 \right]^2} \quad (V-50)$$

where the parameter ζ is of the order of 0.8-1.0, and f_n is about 1 or 2 cps. He further notes that:

- (1) None of the Φ_{nn} spectra exhibit resonant peaks of significant magnitude either in the data presented or in those obtained from single runs with any of the subjects.
- (2) The bandwidth of the closed loop remnant does not increase in any significant proportionate way with that of the forcing function, i.e., the remnant bandwidth, given by f_n , goes from about 1.0 to 1.5 cps as f_{co} increases from 0.16 to 0.96 cps, and then stays at about this same value as the forcing function bandwidth increases to 2.4 cps.
- (3) Oscillograms of response and direct observation indicate that the human operator's responses become more erratic and variable as the forcing function bandwidth increases.

While these comments are not solutions to the problem of remnant description, they do offer valuable clues for analytical follow-up.

In Section III we noted that components of the remnant could result from four possible sources. In the present instance it appears reasonable to reject the possibility of the operator responding to other than the supposed system input as being highly unlikely. Although a nonlinear operation on the forcing function is a possible explanation for some of the noise power, the results of Elkind's Experiment II fortunately indicate that series nonlinearity is a minor factor at an f_{co} of 0.24 cps. Furthermore it would be desirable to save as much of the usefulness of quasi-linear description as possible, therefore alternate explanations of the remnant will be thoroughly examined for their applicability in the hope that we will not have to consider series nonlinear effects. This leaves us with the following remnant sources to investigate further:

- (1) Injection of noise which is not correlated with the forcing function into the loop, i.e., is unexplained by any linear or nonlinear correlation.
- (2) Nonsteady behavior of the operator, i.e., essentially random variation of operator characteristics during a measurement run.

The general analytical background for both of these possibilities was developed in Section III. Since we have no way of knowing which source, if either, is dominant, our only recourse is to look at each separately and assume that all of the remnant is due solely to that particular source. We are not in any way implying that an all or none explanation necessarily prevails, but we use this approach since any theory based on a mixture of effects leads to hypotheses for which we may have no experimental check.

a. Noise Models

If a portion or all of the remnant term were due to uncorrelated noise injected into the loop, the point of injection of this extraneous signal could be almost anywhere within the human operator block in the block diagram. From the standpoint of the measurements, the operator is considered to have only an input and output terminal, and the experimenter can measure only the effects occurring at the output. The exact source within the operator block and the spectral form of the components that would make up the overall signal are therefore impossible to determine by experimental techniques based only upon a two terminal model.

* Later, when we desire a fit suitable for simpler interpretation and expression both as spectral density and autocorrelation we shall use a form $\left(\frac{\sin \frac{1}{2}\omega T}{\frac{1}{2}\omega T} \right)^2$. With T allowed to vary with forcing function conditions, this latter form provides just as close a fit as that given in Eq. (V-50).

On the other hand, it may be possible, by the following process, for us to derive some equivalent model for noises inserted at various places.

- (1) Converting the closed loop remnant term into equivalent open loop spectra injected at various points.
- (2) Attempting to develop, from other data and reasonable assumptions, a suitable a priori model having similar spectral characteristics.

The first step of the process is simple enough, and is independent of the second in that it gives answers to the question "If noise were injected by the operator at a particular form would it take?" The second step, no matter how successful a model is derived, must be considered only an "equivalent" hypothetical model at best. Such a model, however, is much better than nothing and may be as realistic in describing some of the operator's actions as the describing function is for a system.

To obtain an idea of the possible forms that might be taken by an injected noise, the remnant term is first converted to an open loop form. The two simple cases to find are those corresponding to the cases where

- (1) All of the closed loop remnant is assumed to be due to noise injected by the operator at his output. The power spectral density of this open loop output will then be

$$\Phi_{nn_e} = |1 + Y|^2 \Phi_{nn} \quad (V-51)$$

- (2) All of the closed loop remnant is assumed to come from noise injected by the operator at his input. The power spectral density of this open loop input noise will be

$$\Phi_{nn_e} = \frac{\Phi_{nn}}{|H|^2} \quad (V-52)$$

The values of $\Phi_{nn_e}/\int_0^\infty \Phi_{nn} df$ and $\Phi_{nn_e}/\int_0^\infty \Phi_{nn} df$ for Elkind's rectangular spectra have been computed using his experimentally determined values of $\Phi_{nn}/\int_0^\infty \Phi_{nn} df$ (Fig. 29); Y (Fig. 29); and H [23]. These are shown in Figures 56-62.

Examining the form of these plots, it is immediately apparent that no one simple spectral form, even with adjustable parameters, will fit all of the data well.

The Φ_{nn_e} curves for R.16 to R.64, viewed as a whole, appear to be fitted best by a horizontal straight line at about -18 db. If the Φ_{nn} values for these input bandwidths have any experimental significance (it is certainly possible that they do not have much significance, for Φ_{nn} in these cases corresponds to about 5% or less of the output power and the experimental inaccuracies are not well known), then Φ_{nn_e} for these cases appears to be approximately white over the frequency range of the forcing function and has a dc value of about

$$\Phi_{nn_e}(0) \Big|_{R.16-R.64} = \frac{1}{2} \int_0^\infty \Phi_{nn} df \quad (V-53)$$

For the rectangular input spectra, the low frequency level of Φ_{nn_e} increases, with the higher frequency behavior tending to increase slightly toward the form where $\Phi_{nn_e} \Big|_{R.24}$ might even be fitted with the form $[1 + (T\omega)^2]^{-2}$.

The Φ_{nn_e} data are somewhat more complex than those for Φ_{nn} , but not to the point that they are easily susceptible to a fitting by a single simple analytical form. It will be noted that the general behavior of the Φ_{nn_e} data indicates a decrease in the low frequency magnitude and an increase in the bandwidth as f_{co} increases.

After trying a wide variety of analytical forms to attempt to fit all of the Φ_{nn_e} data with a similar quantity, it was concluded that the form $[(\sin \omega T_c) / (\omega T_c)]^2 + 1$ is the most generally appropriate approximation. The data of Figures 56 through 62 show the results of this fit and Table 6 summarizes the fitted parameters. The accuracy of the approximation is variable, but is fairly good for the higher bandwidth forcing functions which are our main concern. Figure 63 shows the interesting and simple variation of $1/T_c$ versus f_{co} for this model, i.e.,

$$\frac{\Phi_{mc}}{\int_0^\infty \Phi_{ii} df} = \frac{\Phi_{nn}}{\int_0^\infty \Phi_{ii} df} \frac{|Y|^2}{|H|^2}$$

$$\frac{\Phi_{nn}}{\int_0^\infty \Phi_{ii} df}$$

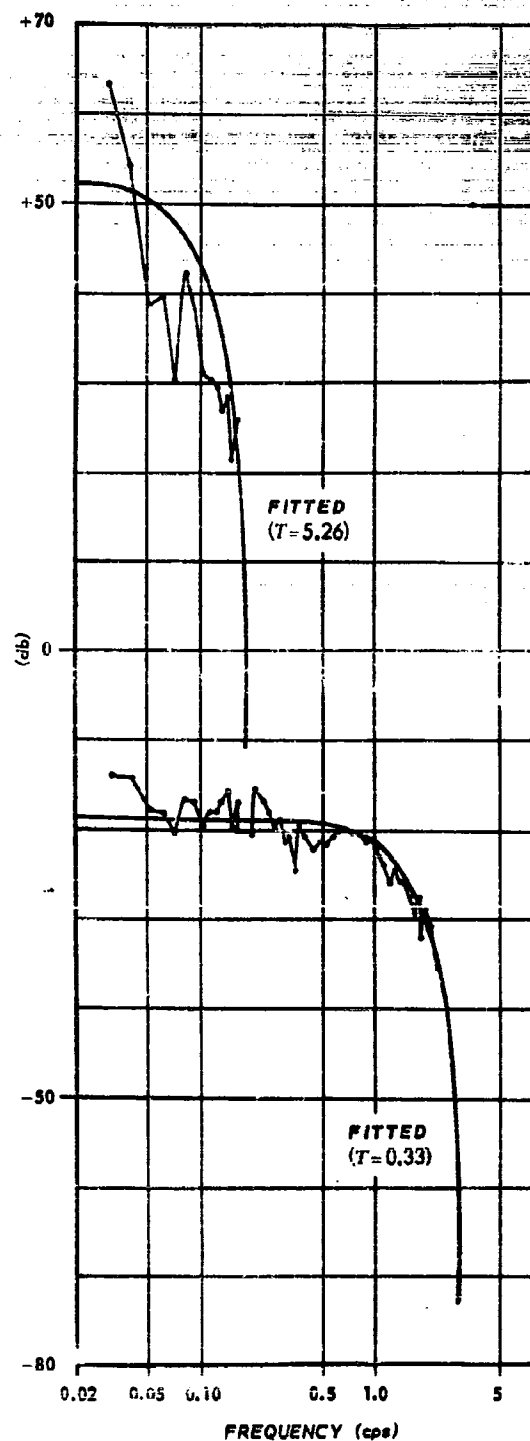


Figure 56. Remnant Characteristics of the Elkind Compensatory Experiment R.16. Rectangular Forcing Function Spectra: rms amplitude = 1 inch and $f_{co} = 0.16$ cps. Fitted: $[(\sin \frac{1}{2}\omega T)/(\frac{1}{2}\omega T)]^2$.

(Reference 23, Figures 4-7, 4-11.)

$$\frac{\Phi_{mc}}{\int_0^\infty \Phi_{ii} df} = \frac{\Phi_{mi}}{\int_0^\infty \Phi_{ii} df} \frac{|Y|^2}{|H|^2}$$

$$\frac{\Phi_{mi}}{\int_0^\infty \Phi_{ii} df}$$

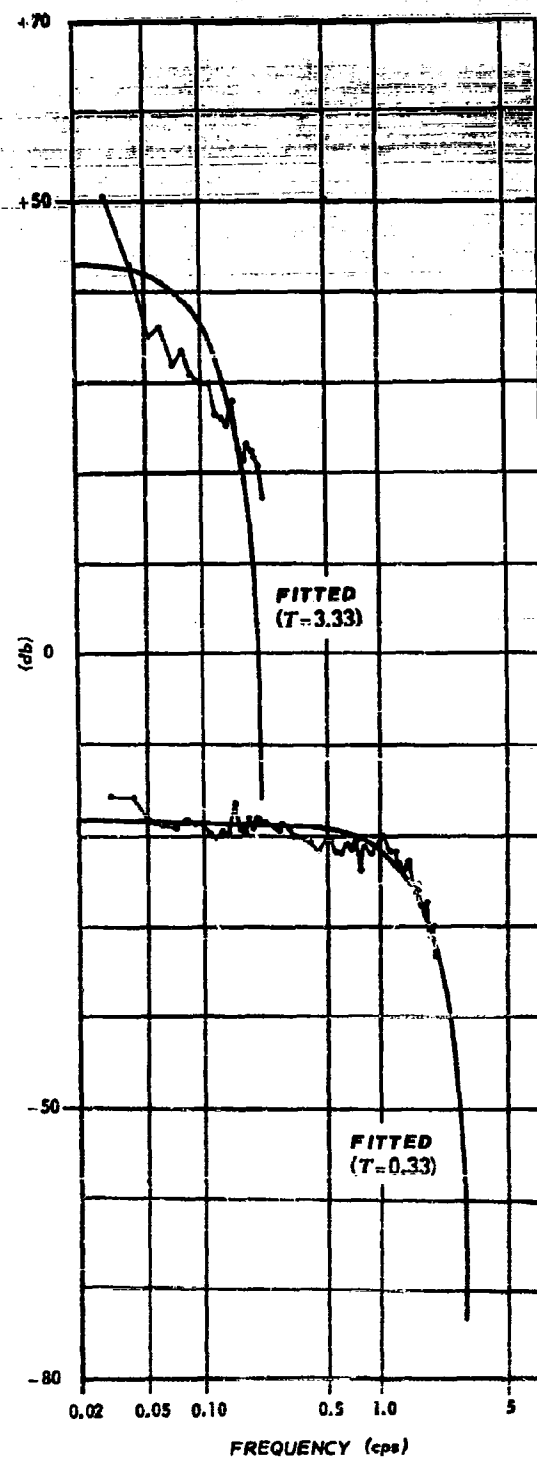


Figure 57. Remnant Characteristics of the Elkind Compensatory Experiment R.24. Rectangular Forcing Function Spectra: rms amplitude = 1 inch and $f_{co} = 0.24$ cps. Fitted: $[(\sin \frac{1}{2}\omega T)/(\frac{1}{2}\omega T)]_T^2$.
(Reference 23, Figures 4-7, 4-11.)

$$\frac{\Phi_{nne}}{\int_0^\infty \Phi_{ii} df} = \frac{\Phi_{nn}}{\int_0^\infty \Phi_{ii} df |H|^2}$$

$$\frac{\Phi_{nne}}{\int_0^\infty \Phi_{ii} df} = \frac{\Phi_{nn}}{\int_0^\infty \Phi_{ii} df |H|^2}$$

$$\frac{\Phi_{nn}}{\int_0^\infty \Phi_{ii} df}$$

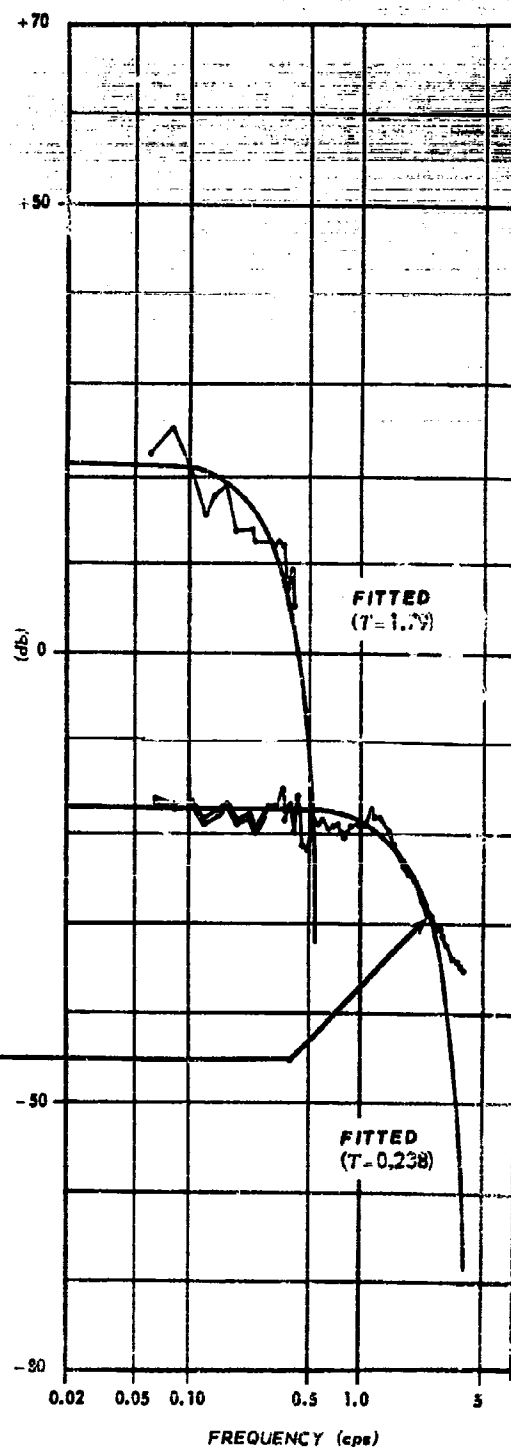


Figure 58. Remnant Characteristics of the Elkind Compensatory Experiment R.40. Rectangular Forcing Function Spectra: rms amplitude = 1 inch and $f_{co} = 0.4$ cps. Fitted: $[(\sin \frac{1}{2}\omega T)/(\frac{1}{2}\omega T)]_T^2$.

(Reference 23, Figures 4-7, 4-11.)

$$\frac{\Phi_{nn_c}}{\int_0^\infty \Phi_{ii} df} = \frac{\Phi_{nn}}{\int_0^\infty \Phi_{ii} df |H|^2}$$

$$\frac{\Phi_{nn_c}}{\int_0^\infty \Phi_{ii} df} = \frac{\Phi_{nn}}{\int_0^\infty \Phi_{ii} df |H|^2}$$

$$\frac{\Phi_{nn}}{\int_0^\infty \Phi_{ii} df}$$

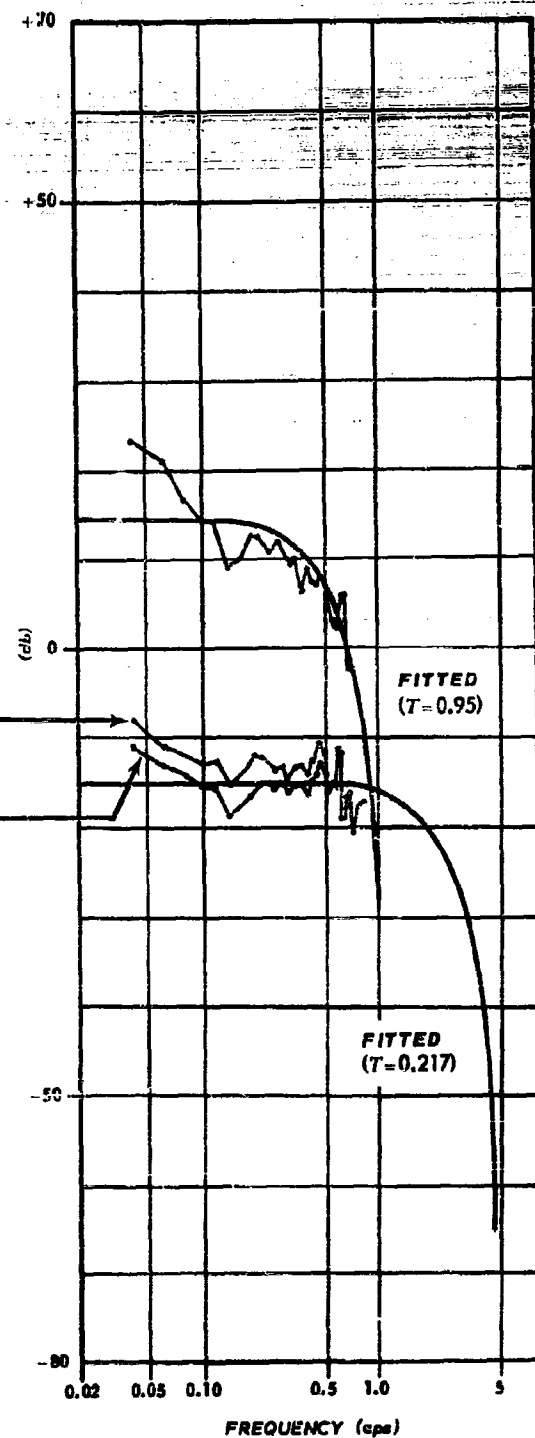


Figure 59. Remnant Characteristics of the Elkind Compensatory Experiment R.64. Rectangular Forcing Function Spectra: rms amplitude = 1 inch and $f_{co} = 0.64$ cps. Fitted: $[(\sin \frac{1}{2}\omega T)/(\frac{1}{2}\omega T)]_T^2$.

(Reference 23, Figures 4-7, 4-11.)

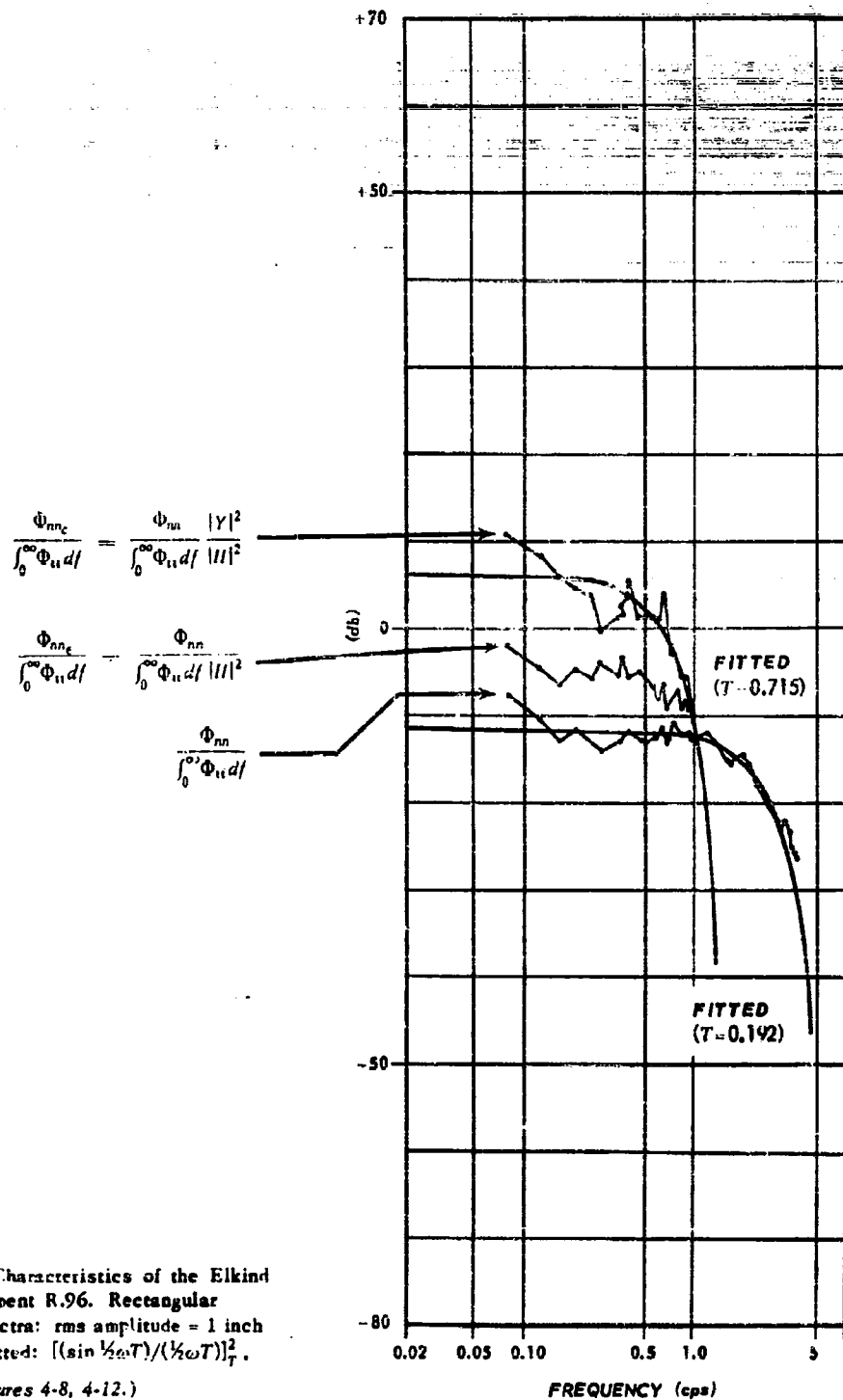


Figure 60. Remnant Characteristics of the Elkind Compensatory Experiment R.96. Rectangular Forcing Function Spectra: rms amplitude = 1 inch and $f_{co} = 0.96$ cps. Fitted: $[(\sin \frac{1}{2}\omega T)/(\frac{1}{2}\omega T)]^2_T$.

(Reference 23, Figures 4-8, 4-12.)

$$\frac{\Phi_{nn_c}}{\int_0^\infty \Phi_{ii} df} = \frac{\Phi_{nn}}{\int_0^\infty \Phi_{ii} df} \frac{|Y|^2}{|H|^2}$$

$$\frac{\Phi_{ii_e}}{\int_0^\infty \Phi_{ii} df} = \frac{\Phi_{nn}}{\int_0^\infty \Phi_{ii} df} \frac{|H|^2}{|Y|^2}$$

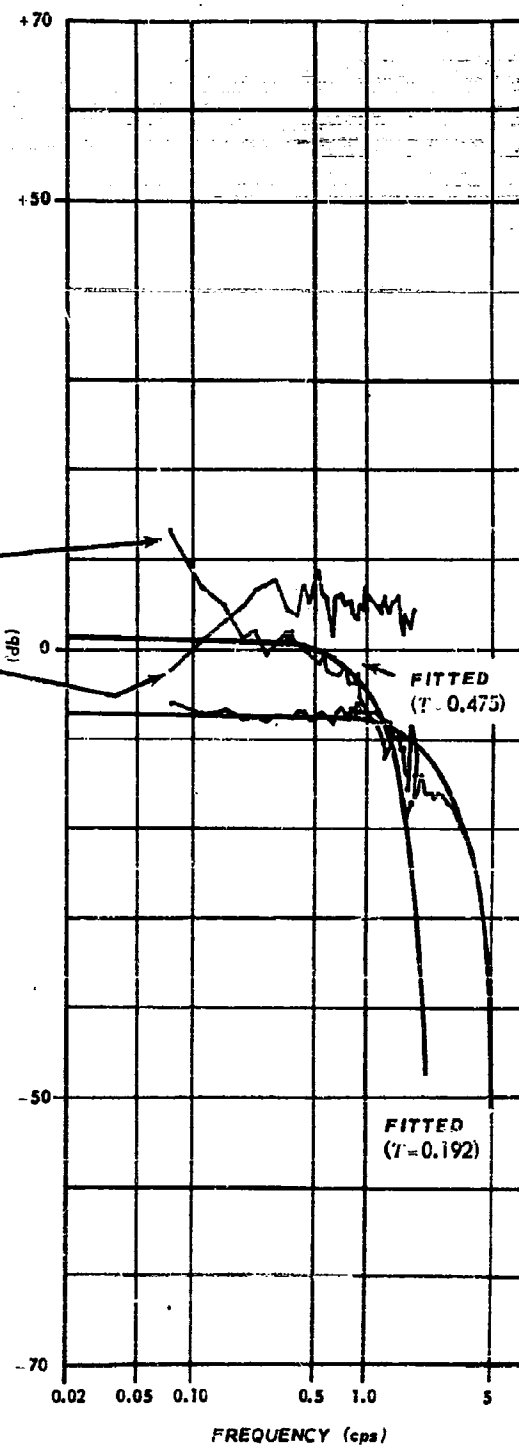


Figure 61. Remnant Characteristics of the Elkind Compensatory Experiment R1.6. Rectangular Forcing Function Spectra: rms amplitude = 1 inch and $f_{co} = 1.6$ cps. Fitted: $[(\sin \frac{1}{2}\omega T)/(\frac{1}{2}\omega T)]_T^2$.

(Reference 23, Figures 4-8, 4-12.)

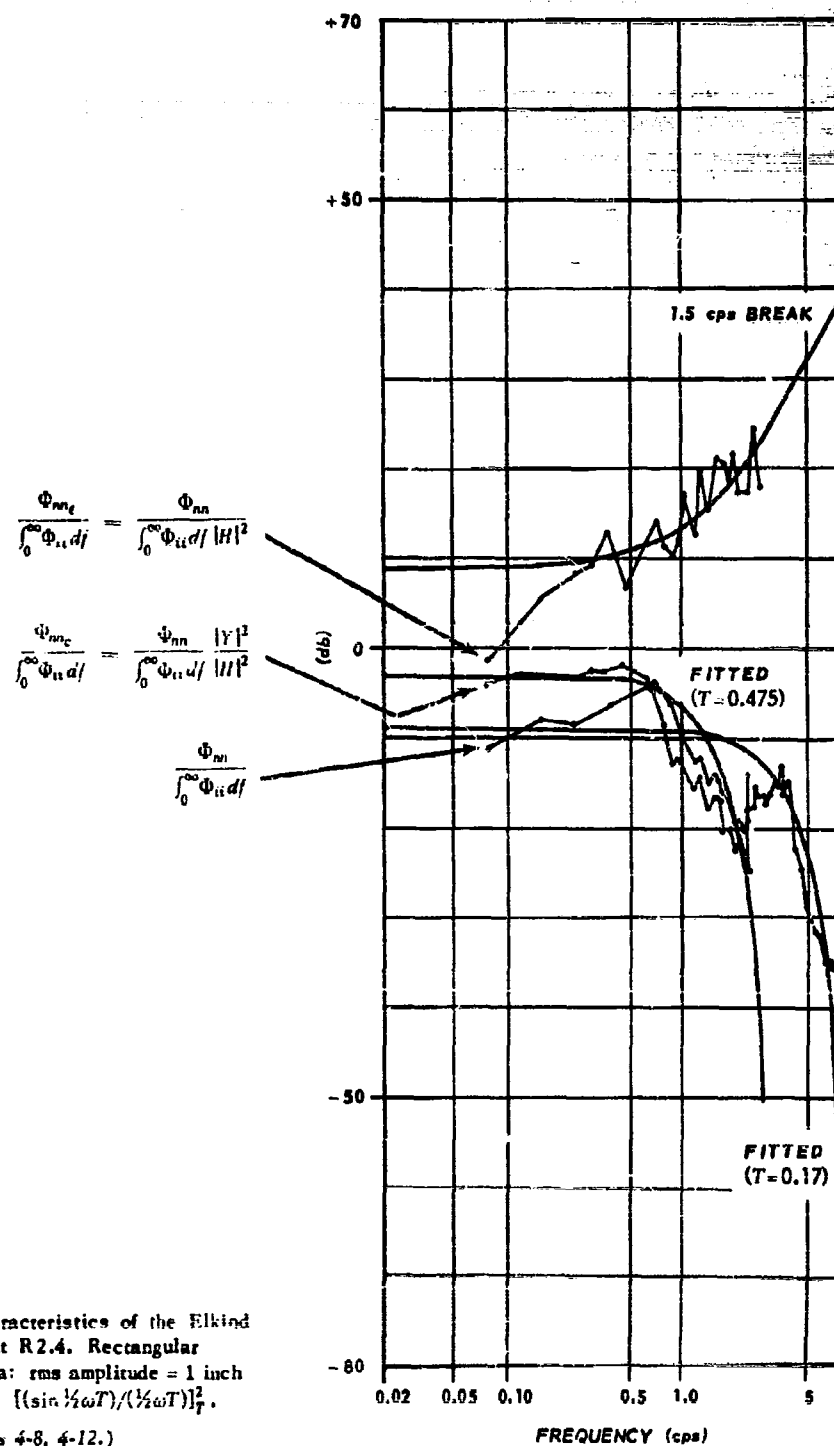


Figure 62. Remnant Characteristics of the Elkind Compensatory Experiment R2.4. Rectangular Forcing Function Spectra: rms amplitude = 1 inch and $f_{co} = 2.4$ cps. Fitted: $[(\sin \frac{1}{2}\omega T) / (\frac{1}{2}\omega T)]^2$.
 (Reference 23, Figures 4-8, 4-12.)

Table 6. Output Noise Parameters Obtained by Fitting Φ_{nn_c} with $2T_c\sigma_c^2 \left(\frac{\sin \frac{1}{2}\omega T_c}{\frac{1}{2}\omega T_c} \right)^2$

ITEM	$2(T_c\sigma_c^2)/\int_0^\infty \Phi_{ii} df$		FREQUENCY OF FIRST ZERO†		$\frac{\sigma_c^2}{\int_0^\infty \Phi_{ii} df}$
	DC VALUE† (db)	DC VALUE (linear)	(f)	(1/f)	
R.16	52.5	420	0.19	5.26	40.0
R.24	42.5	133	.30	3.33	20.0
R.40	22	12.5	.56	1.79	3.5
R.64	+14.6	5.40	1.05	.95	2.83
R.96	+6.5	2.13	1.40	.715	1.49
R1.6	+1.5	1.20	2.1	.475	1.26
R2.4	-3.0	.74	2.9	.345	1.08

† Actual data derived from curves of: $|Y|^2/|H|^2$. $\Phi_{nn}/\int_0^\infty \Phi_{ii} df = \Phi_{nn_c}$.

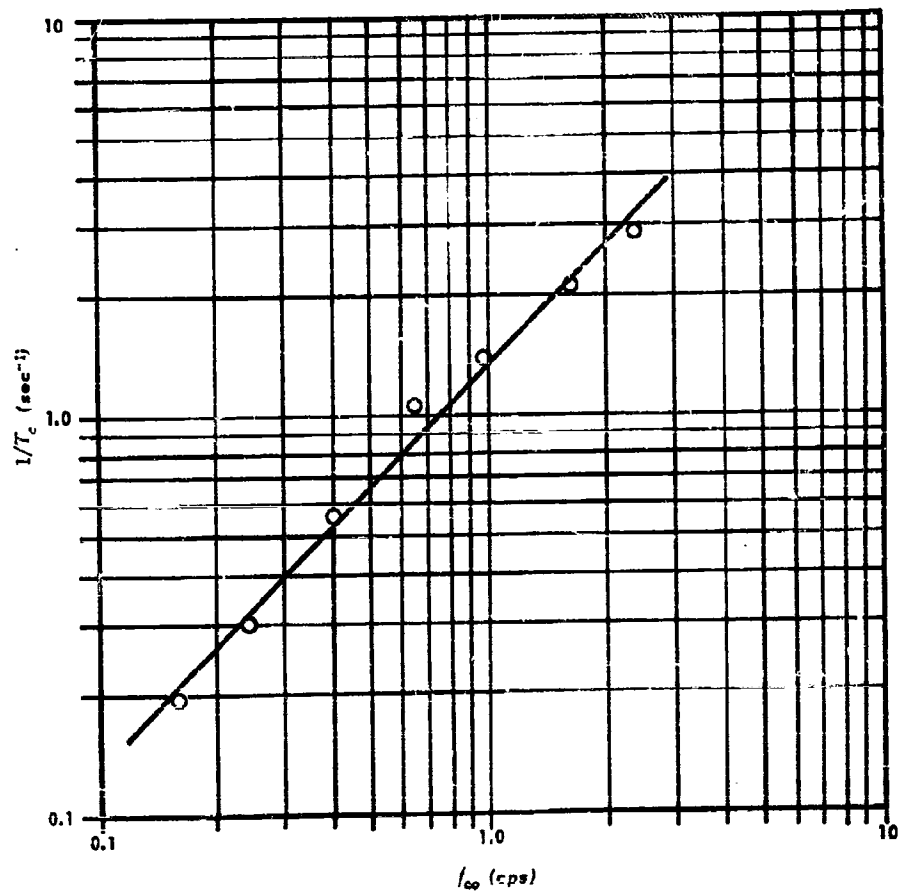


Figure 63. Variation of Frequency of First Zero with Cutoff Frequency for Elkind Rectangular Forcing Functions.

$$T_c = \frac{0.75}{f_{\infty}}$$

(V-54)

Since the assumed $[(\sin \frac{1}{2}\omega T_c)/(\frac{1}{2}\omega T_c)]^2$ form appears to yield a fairly reasonable fit, it is desirable to see whether something equivalent can be derived on an a priori basis. To do this we shall assume that:

- (1) The human's output response, $c(t)$, can be approximated by a series of discrete steps spaced T_c seconds apart. Each step is assumed to consist of two components
 - (a) A part, $\Delta e_0(t)$, linearly related to the forcing function.
 - (b) A part, $n(t)$, representing random error or noise in the discrete step which is not linearly related, in a deterministic fashion, to the forcing function.
- (2) The noise component of each step is independent of all other steps.
- (3) A sort of Weber's law type of variation applies to the overall behavior. That is, the mean square error in the discrete step is assumed to be proportional to the mean square value of Δe_0 , the linear component of this step, or

$$\overline{n(t)^2} = \sigma_n^2 \sim \overline{\Delta e_0(t)^2}$$

A time function having the above sort of characteristics is shown in Figure 64. From the form of the time function and the assumptions given above, the autocorrelation function can be derived. Fairly obviously, the

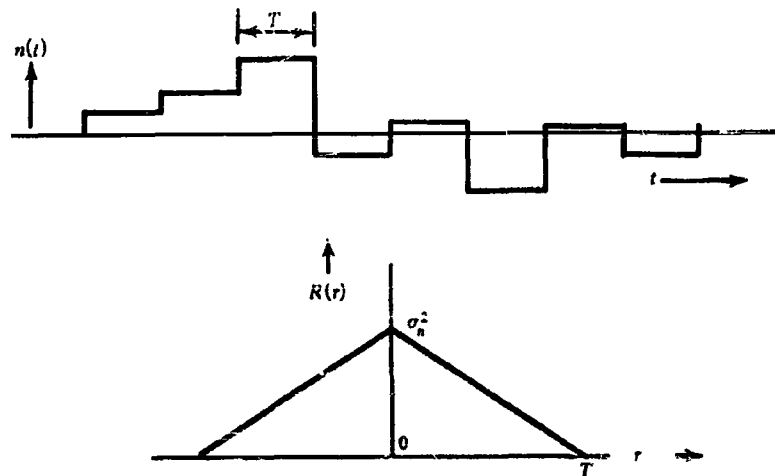


Figure 64. Typical Time Variation of Noise and Autocorrelation Function.

autocorrelation of $n(t)$ will be of the form shown in the second figure. The autocorrelation will depend only upon σ_n and T , and will be independent of the amplitude distribution of the steps composing $n(t)$. Both of these facts can be shown as follows:

* The assumptions and part of this development are similar to a discussion appearing in Reference 23. It differs in detail, however, in several important respects.

If a_n is the magnitude of a particular step of $n(t)$, then

$$n(t) = a_n \quad \text{from } t = mT \text{ to } t = (m+1)T$$

The magnitude of these steps has some probability distribution $p(x)$. The probability that a_n lies between x and $x + dx$ is then

$$P(x < a_n < x + dx) = p(x) dx$$

In terms of the second probability distribution the autocorrelation is

$$R(\tau) = \int_{-\infty}^{\infty} \int_{-\infty}^{\infty} x_1 x_2 p_2(x_1, t_1; x_2, t_2) dx_1 dx_2$$

where $p_2(x_1, t_1; x_2, t_2) dx_1 dx_2$ is the probability that:

(a) $n(t)$ lies between x_1 and $x_1 + dx_1$ at time t_1

and further that:

(b) $n(t)$ lies between x_2 and $x_2 + dx_2$ at time t_2 (or τ seconds after t_1)

The first problem is then to compute the second probability distribution. This can be done by considering the following:

- (1) The probability that $n(t)$ lies between x_1 and $x_1 + dx_1$ at any time t is simply $p(x_1) dx_1$
- (2) The probability that $n(t)$ has the same value at time t_2 as at time t_1 is the probability that t_1 and t_2 (or $t_1 + \tau$) lie in the same time interval [between say mT and $(m+1)T$]. This probability will be

$$\begin{aligned} 1 - |\tau|/T & \quad \text{if } |\tau| \leq T \\ 0 & \quad \text{if } |\tau| > T \end{aligned}$$

- (3) Also, for $|\tau| > T$, $n(t_2)$ is completely independent of $n(t_1)$, from assumption (2) above. So for this case, the second probability distribution is simply the product of the first distribution by itself, i.e., $p_2(x_1, t_1; x_2, t_2) = p(x_1, t_1)p(x_2, t_2)$. The portion of the autocorrelation due to these terms, i.e., for $|\tau| > T$, is then

$$\begin{aligned} R(\tau)_{|\tau| > T} &= \iint x_1 x_2 p(x_1, t_1) p(x_2, t_2) dx_1 dx_2 = [\int x_1 p(x_1, t_1) dx_1] [\int x_2 p(x_2, t_2) dx_2] \\ &= \bar{x} \cdot \bar{x} = 0 \end{aligned}$$

since the mean value of $n(t)$ is zero by definition.

Then, from these considerations the second probability distribution becomes:

$$\begin{aligned} p_2 dx_1 dx_2 &= \left(1 - \frac{|\tau|}{T}\right) p(x) dx, \quad |\tau| \leq T \\ &= p(x_1) p(x_2) dx_1 dx_2, \quad |\tau| > T \end{aligned}$$

The part of the autocorrelation for $|\tau| > T$ has already been shown to be zero, so the entire autocorrelation function is

$$\begin{aligned} R(\tau) &= \int_{-\infty}^{\infty} x^2 p(x) \left(1 - \frac{|\tau|}{T}\right) dx \quad \text{for } |\tau| \leq T \\ &= 0 \quad \text{for } |\tau| > T \end{aligned}$$

Since the integration is over x ,

$$\begin{aligned} R(\tau) &= \left(1 - \frac{|\tau|}{T}\right) \int_{-\infty}^{\infty} x^2 p(x) dx, \quad |\tau| \leq T \\ &= 0 \quad |\tau| > T \end{aligned}$$

Finally, the quantity $\int_{-\infty}^{\infty} x^2 p(x) dx$ is just the mean-squared value of $n(t)$, or σ_n^2 . That is

$$\overline{n(t)^2} = \sigma_n^2 = \int_{-\infty}^{\infty} x^2 p(x) dx$$

Therefore the autocorrelation is

$$R_{nn_c}(r) = \sigma_n^2 \left(1 - \frac{|r|}{T}\right); \quad |r| \leq T$$

$$= 0 \quad |r| > T \quad (V-55)$$

and is independent of the probability distribution of the individual amplitudes of $n(t)$, being dependent only upon their mean-squared value, and their spacing in time.

The spectral density is, of course, the Fourier cosine transform of the autocorrelation, or

$$\Phi_{nn_c} = 4 \int_0^\infty R_{nn_c}(r) \cos \omega r dr = 4 \int_0^T \sigma_n^2 \left(1 - \frac{r}{T}\right) \cos \omega r dr$$

$$= 2(T\sigma_n^2) \left[\frac{\sin \frac{\omega T}{2}}{\frac{\omega T}{2}} \right]^2 \quad (V-56)$$

This is the interesting and well known spectrum given in Figure 65. $\frac{\sin^2 x}{x^2}$ has its first zero at $x = \pi$, or $\frac{\omega_1 T}{2} = \pi$; so $T = \frac{2\pi}{\omega_1} = \frac{1}{f_1}$. This spectral form is encouraging since we have already concluded that a $[(\sin x)/x]^2$

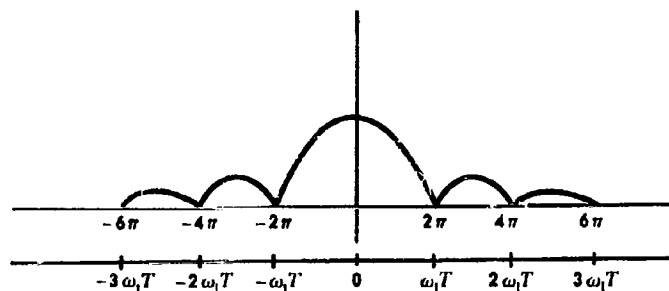


Figure 65. Spectrum of $2(T\sigma_n^2)[(\sin \frac{1}{2}\omega T)/(\frac{1}{2}\omega T)]^2$.

form was the most generally appropriate simple approximation to the Φ_{nn_c} data. The values of f_1 have already been determined from the empirical data (Table 6 and Fig. 63). The mean-square value, $\sigma_{n_c}^2$, of the assumed output noise can also be determined from the curve fits, and values are tabulated in Table 6. A very approximate relationship between σ_{n_c} and forcing function characteristics for the R.40 through R2.40 spectra is given by

$$\frac{\sigma_{n_c}^2}{\int_0^\infty \Phi_{11} df} = \frac{1.75}{\sqrt{f_{co}}} \quad (V-57)$$

This equation, together with Equations (V-54) and (V-55) can be considered to be an equivalent model for remnant "explanation" on the hypothesis that all the remnant is due to noise injected by the operator at his output. To the extent that the data fits represent the actual results, we can say that the human output contains an error component which consists of a series of discrete steps spaced an average of T_c seconds apart. Also, that the rms value of these random steps is an inverse square root function of forcing function cutoff frequency and the time between steps is an inverse function of forcing function frequency.

With this crude model of the data established, we can now continue with the development of the a priori model. The next part of the problem is to derive an approximate relationship for σ_n^2 . If v_i is the velocity of the input and $H = Y/(1+Y)$ the closed loop describing function, then the velocity of the linearly correlated part of the output,

previously defined as Δe_0 , will be $v_i H$. If we assume that the velocity $v_i H$ is approximately constant within the interval T , then $v_i H T$ is approximately equal to the incremental amplitude of the linearly correlated output, Δe_0 , i.e.,

$$\Delta e_0 \doteq v_i H T$$

so that

$$\overline{\Delta e_0^2} \doteq (\overline{v_i H T})^2$$

T has been assumed constant previously, and H , which is fairly constant over the bandwidth of interest, can be replaced by an average value, H_a . These crude assumptions and approximations allow us to evaluate $\overline{\Delta e_0^2}$ easily without having to integrate all the terms represented by $\langle v_i H T \rangle$, since Δe_0^2 then becomes

$$\overline{\Delta e_0^2} \doteq (H_a T)^2 (\overline{v_i})^2$$

The mean-square velocity of the input is simply

$$(\overline{v_i})^2 = (2\pi)^2 \int_{-\infty}^{\infty} f^2 \Phi_{ii} df$$

so that

$$\overline{\Delta e_0^2} \doteq (2\pi)^2 (H_a T)^2 \int_{-\infty}^{\infty} f^2 \Phi_{ii} df$$

Since we assumed a kind of Weber law type of variation, i.e., $a_n^2 = \overline{n(t)^2} \propto (\overline{\Delta e_0})^2$, and $f^2 \Phi_{ii}$ is even, then

$$\sigma_n^2 \propto (H_a T)^2 \int_0^{\infty} f^2 \Phi_{ii} df \quad (V-58)$$

If all the above assumptions are correct, we would expect the open loop output noise spectra to be proportional to:

$$\frac{\Phi_{nn_c}(\omega)}{\int_0^{\infty} \Phi_{ii} df} \propto \frac{H_a^2 T^3 \left(\int_0^{\infty} f^2 \Phi_{ii} df \right) \left(\frac{\sin \frac{1}{2} \omega T}{\frac{1}{2} \omega T} \right)}{\int_0^{\infty} \Phi_{ii} df} \quad (V-59)$$

For the rectangular forcing function spectra, the ratio of the integrals involving Φ_{ii} will be

$$\frac{\int_0^{\infty} f^2 \Phi_{ii} df}{\int_0^{\infty} \Phi_{ii} df} = \frac{\Phi_{ii}(0) f_{co}^3}{3 \Phi_{ii}(0) f_{co}} = \frac{f_{co}^2}{3}$$

For rectangular forcing function spectra, then, the open loop output noise spectra should be of the form

$$\frac{\Phi_{nn_c}}{\int_0^{\infty} \Phi_{ii} df} \propto |H_a|^2 T^3 / f_{co}^2 \left(\frac{\sin \frac{1}{2} \omega T}{\frac{1}{2} \omega T} \right)^2 \quad (V-60)$$

If the experimentally determined value of $T = 0.75 / f_{co}$ is used, the low frequency value of Φ_{nn_c} should be

$$\frac{\Phi_{nn_c}(0)}{\int_0^{\infty} \Phi_{ii} df} \propto \frac{|H_a|^2}{f_{co}} \quad (V-61)$$

The actual data to check this possibility are summarized in Table 7. While the general trend of these data is in the proper direction, the higher input bandwidth information is much closer to a variation of $\Phi_{nn_c}(0)$ with the square root of $|H_a|^2 / f_{co}$ than with the quantity itself. If the lower input bandwidth data are admitted, the overall trend becomes more closely proportional. All in all, the overall model is not too bad an approximate "explanation" of the remnant.

Table 7. Data to Check the Possible

Proportionality of $\frac{\Phi_{nn}(0)}{\int_0^\infty \Phi_{ii} df}$ and $\frac{ H_o ^2}{f_{co}}$			
INPUT	MEASURED		
	$\frac{\Phi_{nn}(0)}{\int_0^\infty \Phi_{ii} df}$	$ H_o ^2$	$\frac{ H_o ^2}{f_{co}}$
0.16	420	1.0	6.25
.24	130	0.98	4.10
.40	12.5	0.93	2.30
.64	5.4	0.827	1.30
.96	2.1	0.532	0.55
1.6	1.2	0.250	0.16
2.4	0.74	0.075	0.03

If the above type of model is considered adequate, its consequences would require:

- (1) The operator's output would tend to be a jerky, step-like motion which is more or less the result of a linear operation on the forcing function and which contains a random "error" whose rms value is roughly proportional to the linear portion of his output.
- (2) The average time interval between these step-like motions should be directly proportional to the input bandwidth.

Presumed and observed operator behavior which is similar to both of these characteristics has long had its proponents among engineering psychologists, so the output noise model also has a certain amount of soul satisfying and intuitive merit. At the present time, however, it must be considered only as a hypothesis which is reasonably consistent with the available experimental evidence.

b. Model Based Upon Nonsteady Operator Behavior

The second origin of the remnant to be considered is the possibility of nonsteady operator behavior. Our only recourse, as before, is to assume that the major portion of the remnant may be described by a nonsteady operator phenomenon, and then to develop the consequences of such an assumption. In this case, the spectral density due to nonsteady operator behavior, $\Phi_{nn}(\omega)$, will be approximately equal to the total remnant, i.e.,

$$\Phi_{nn}(\omega) \approx \Phi_{\Delta H}(\omega) \quad (V-62)$$

Under these circumstances, the analysis of Section III reveals that the autocorrelation of the uncorrelated stochastic variation in the closed loop transfer function, $\Delta H(t)$ will be given by

$$R_{\Delta H \Delta H}(r) = \frac{R_{nn}(r)}{K_{ii}(r)} \quad (V-63)$$

To determine the type of $R_{\Delta H \Delta H}(r)$ which would have to exist if nonsteady behavior were the sole explanation for the remnant, we can compute $R_{nn}(r)$ and $R_{ii}(r)$, and then use Equation (V-63). This process is shown in the following paragraphs for the Elkind rectangular spectra data.

The power spectral density of the normalized closed loop remnant can be approximated quite closely by

$$\frac{\Phi_{nn}(\omega)}{\int_0^\infty \Phi_{ii} df} = c_n^2 \left(\frac{\sin \frac{1}{2} \omega T_1}{\frac{1}{2} \omega T_1} \right)^2 \quad (V-64)$$

Table 8 summarizes the constants of these approximate fits.

For the rectangular spectra, then the spectral density of the remnant is approximately

$$\Phi_{nn}(\omega) = c_n^2 \sigma_i^2 \left(\frac{\sin \frac{1}{2} \omega T_1}{\frac{1}{2} \omega T_1} \right)^2 \quad (V-65)$$

The autocorrelation function corresponding to Eq. (V-65) is

$$R_{nn}(r) = \sigma_n^2 \left(1 - \frac{|r|}{T_1}\right) \quad (V-66)$$

where σ_n^2 is the mean square value of the remnant. Since the spectrum corresponding to Eq. (V-66) is $2T_1 \sigma_n^2 \left(\frac{\sin \frac{1}{2} \omega T_1}{\frac{1}{2} \omega T_1}\right)^2$ the value of σ_n^2 in terms of the measurements for the fitted curves will be

$$\sigma_n^2 = \frac{c_n^2 \sigma_i^2}{2T_1} = \frac{c_n^2 \sigma_i^2 f_1}{2} \quad (V-67)$$

The autocorrelation of the forcing function will be

$$\begin{aligned} R_{ii}(r) &= \int_0^\infty \Phi_{ii}(f) \cos 2\pi f r df = \frac{\sigma_i^2}{f_{co}} \int_0^{f_{co}} \cos 2\pi f r df \\ &= \sigma_i^2 \left(\frac{\sin 2\pi f_{co} r}{2\pi f_{co} r} \right) \end{aligned} \quad (V-68)$$

The required autocorrelation for $\Delta H(t)$ which would account for the remnant would then be

$$R_{\Delta H \Delta H}(r) = \frac{R_{nn}(r)}{R_{ii}(r)} = \frac{c_n^2 \omega_{co}}{2T_1} \left(1 - \frac{|r|}{T_1}\right) r \quad (V-69)$$

The mean-square or expected value of $\Delta H(t)$ will be

$$\overline{\Delta H(t)^2} = \sigma_{\Delta H}^2 = R_{\Delta H \Delta H}(0) = \frac{R_{nn}(0)}{R_{ii}(0)} = \frac{c_n^2}{2T_1} = \frac{c_n^2 f_1}{2} \quad (V-70)$$

The required mean-square values of the closed loop transfer function variation, $\sigma_{\Delta H}^2$, based upon the fitted data are given in Table 8 and plotted as a function of forcing function bandwidth in Fig. 66. The data fall reasonably well

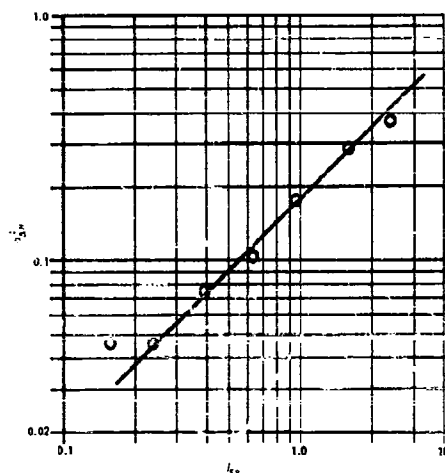


Figure 66. Expected Value of $\sigma_{\Delta H}^2 = \overline{\Delta H(t)^2}$ vs. Forcing Function Bandwidth, f_{co} .

Table 8.† Derived Data for $\frac{\Phi_{nn}}{\int_0^\infty \Phi_{ii} df}$
Fitted by $c_n^2 \left(\frac{\sin \frac{1}{2} \omega T_1}{\frac{1}{2} \omega T_1}\right)^2$.

INPUT	c_n^2 (db)	c_n^2 (linear)	$\frac{1}{T_1} = f_1$	$\sigma_{\Delta H}^2 = \frac{c_n^2 f_1}{2}$
R .16	-18.5	0.122	3.0	0.183
R .24	-18.6	.120	3.0	.181
R .40	-17.0	.142	4.2	.298
R .64	-15.0	.180	4.6	.414
R .96	-11.7	.265	5.2	.690
R1.6	-7.1	.441	5.2	1.145
R2.4	-8.7	.373	8.0 (Poor)	1.48

† See Figures 56 to 62.

on a straight line of unit slope, with the exception of the point for R2.4, where $[(\sin x)/x]^2$ is a rather poor fit for $\Phi_{HH}/\int_0^\infty \Phi_{HH} df$. The approximate equation is

$$\sigma_{\Delta H}^2 \approx 0.7/f_{co} \quad (V-71)$$

From this result, it appears that the nonsteady operator behavior, as measured by the computed value $\sigma_{\Delta H}^2$, must increase approximately linearly with forcing function cutoff frequency. Since the value of f_{co} is the primary measure of task difficulty for Elkind's rectangular spectra experiments, this would imply that the more difficult the task, the larger the nonsteady operator behavior. This logical conclusion from the results of the nonsteady assumption appears reasonable, and in a qualitative way checks well with general observations of recorded operator responses.

Since the $\sigma_{\Delta H}^2$ required to explain the remnant in nonsteady terms looks fairly reasonable, it is desirable to proceed further in an attempt to derive other consequences resulting from the assumption of nonsteady behavior and its imposition upon the data. We shall therefore consider both the T_1 and the normalized autocorrelation function, $R_{\Delta H \Delta H}(r)/\sigma_{\Delta H}^2$, required to match the data.

The values of T_1 determined from the fitted data (see Table 8) vary from 0.33 to 0.19 seconds in a fairly orderly fashion. In a very approximate way $T_1 \approx 0.5/(\omega_{co})^{1/3}$, though perhaps an average value for T of about 0.25 seconds is just as appropriate.

To get a better feeling for the major variation in the autocorrelation, the normalized autocorrelation, $R_{\Delta H \Delta H}(r)/\sigma_{\Delta H}^2$ for the R.96 data is shown in Figure 67. As can be seen from the figure, a very good approximation is just the simple form $(1 - |r|/T_1)$. This is also the case for the lower f_{co} 's. For the R1.6 and R2.4 data the approximation is not so good, and the form $(1 - |r|/T_1)[1 + (\omega_{co}r)^2/6]$ is superior. To the extent that the simple form is a

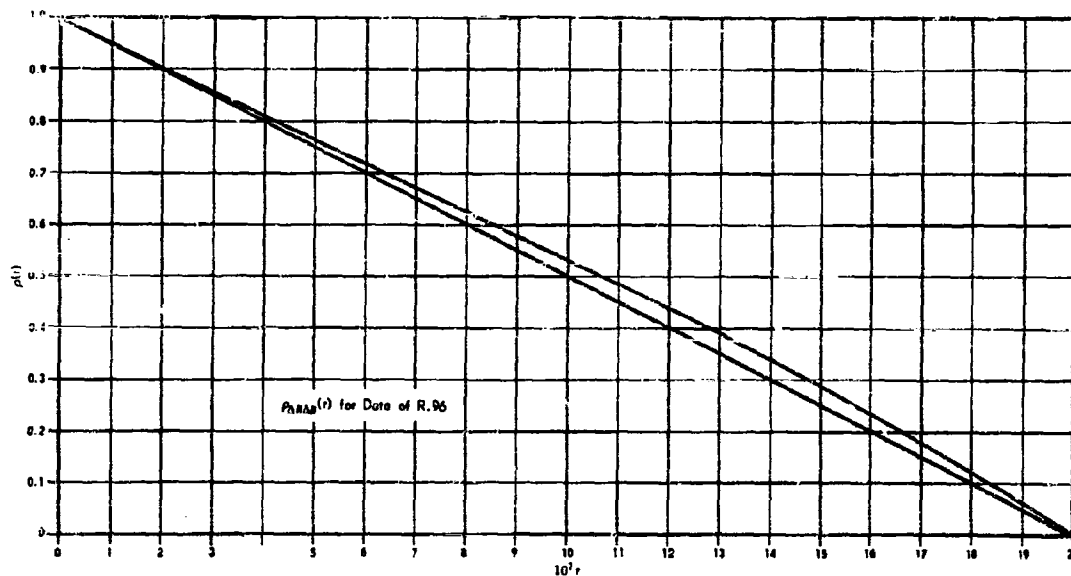


Figure 67. Sample Variation of the Normalized Autocorrelation.

good approximation, $\Delta H(t)$ would have to consist of a time function similar (in its boxcar-like structure and average time intervals) to that shown previously in Fig. 64. In other words, a random time variation in the closed loop transfer function having axis crossings on an average of about 0.2-0.33 seconds or so would be required to explain the remnant term on a nonsteady basis.

Perhaps the most profound consequence of the above results is the tentative assertion that a linear, though time varying, model is suitable to describe the data presented thus far. That is, the total action of the human in Elkind's task can be closely approximated by using a time-varying transfer function $H(j\omega; t)$. On this basis, the linear correlation, ρ , becomes a measure of the non-steadiness of the operator. Likewise, the remnant would not be the result of a nonlinear operation, but rather the consequence of an uncorrelated time-varying portion of the transfer function. It is also desirable to note again that the nonsteady behavior is a strong function of task difficulty. Therefore, if the nonsteady model is used as a remnant explanation, ρ becomes a reasonable definition of task difficulty (which it really is in general anyway) and $\sigma_{\Delta H}^2$ is a good particular definition. Whether such a definition of task difficulty in terms of ρ will obtain with controlled element dynamics in the loop remains to be seen. Actually, if the operator is generating a Y_p to equalize Y_c his repertory of possible Y_p 's may become severely restricted as the task becomes more difficult. Hence, if ρ is due to nonsteady behavior, our conclusions may not carry over to this case.

The level of values of $\sigma_{\Delta H}^2$ shown in Fig. 66 and the results of the above discussion appear quite reasonable, so it appears that nonsteady behavior is a distinct possibility for explanation of the remnant. It is therefore desirable to carry the analysis further to explore the required open loop characteristics. Unfortunately, the open loop variations required to give the required closed loop ΔH^2 are difficult to assess. This can be shown if we assume that the open loop transfer function is given by $Y(j\omega; t) = Y_0(j\omega) + \Delta Y(t)$, for then

$$H(j\omega; t) = H_0(j\omega) + \Delta H(t) = \frac{Y(j\omega; t)}{1 + Y(j\omega; t)} = \frac{Y_0(j\omega) + \Delta Y(t)}{1 + Y_0(j\omega) + \Delta Y(t)} \quad (V-72)$$

As can be seen by Eq. (V-72), the solution for $\Delta Y(t)$ in terms of $\Delta H(t)$ presents a touchy problem. However, if $\Delta Y(t)$ is much less than $1 + Y_0(j\omega)$, then

$$H_0(j\omega) + \Delta H(t) \approx \frac{Y_0(j\omega)}{1 + Y_0(j\omega)} + \frac{\Delta Y(t)}{1 + Y_0(j\omega)} \quad (V-73)$$

or

$$\Delta H(t) \approx \frac{\Delta Y(t)}{1 + Y_0(j\omega)} = \Delta Y(t) \frac{H_0(j\omega)}{Y_0(j\omega)} \quad (V-74)$$

Under the special restrictions leading to (V-74), the approximate open loop transfer function time variation will generally be larger than the closed loop. It will tend to approach the closed loop value as $H_0(j\omega)/Y_0(j\omega)$ approaches unity. This latter condition becomes approximately the case when the tasks are particularly difficult, i.e., as f_{co} becomes large in Elkind's examples where $Y_c = 1$.

From the general variation of $Y_0(j\omega)$ and $R_{\Delta H \Delta H}(r)$ with forcing function conditions, a fairly constant $R_{\Delta Y \Delta Y}(r)$ would almost suffice to describe the remnant behavior. This observation leads to the conjecture that the operator's bandwidth limitations and optimizing behavior, coupled with a small amount of nonsteadiness, inevitably leads to large remnants for broad forcing function bandwidths. The operator could then get around this to some extent by not optimizing as much as was done on these runs, i.e., attempt to follow only the lower frequencies in the forcing function. This would keep $Y_0(j\omega)$ large, tending to reduce the value of $\sigma_{\Delta H}$ and hence the remnant and system error. This tactic, of course, would only be valid for the higher f_{co} tasks (above f_{co} of 0.96 or so), where nonsteady behavior may be an important factor in the remnant.

With the assumption of nonsteady behavior giving the generally reasonable results above, we have another consistent possibility for the explanation of the remnant term. Here again, we must not allow the results presented to be considered an answer, but merely as a possible source. One would suspect that both noise injection and nonsteady possibilities are involved together in the remnant, possibly in conjunction with some nonlinear transfer behavior. The general reasonableness of the analyses given above do give valuable leads, and are fairly suitable as equivalent models partially describing the remnant.

c. Comparison of the Simple Tracker Data From The Three Sources

In general the Franklin and Russell's simple trackers and the Elkind pip-trapper experiments yielded results which were fairly similar and consistent. Since the forcing function spectra were different in all three cases

it is difficult to arrive at an exact comparison. The closest comparable runs were Elkind's R.16 and R.64 and the Franklin simple tracker 1 and 4 rad/sec corner frequency runs. Elkind's F3, and 18 db/oct filter-breaking at 1.5 rad/sec is fairly close to the Franklin 2 rad/sec forcing function bandwidth in form.

Unfortunately we can only compare describing function data, since the Franklin remnant data are so sparse. For the describing functions, and within Elkind's measurement bandwidth, the R.16 and R.64 data points are fairly close to those for the two equivalent Franklin cases, being almost within the limits of the individual runs for either case. All of the comparable cases are shown in Figures 68 through 70, which tend to show that the data are reasonably consistent.

The lead term in the Franklin data shows up beyond the bandwidth of measurement of the Elkind data. On the other hand the Elkind data have measured values back to about 0.02-0.03 cps, while the lowest frequency Franklin data is at 0.4 rad/sec. The presence of a lead term outside the bandwidth of measurement for Elkind's data is a possibility, and such a lead would tend to increase the low values of r presently used in the transfer function curve fits for the Elkind data. It should be noted in this connection, however, that the Elkind F-3 RC filtered spectra shows no evidence of a lead out to a frequency of 0.9 cps.

From all of the above comments, it appears reasonable to state that:

- (1) The describing function data points are roughly comparable.
- (2) The differences between the Elkind and Franklin describing function data, if any, are largely in the possibility of a lead outside Elkind's bandwidth of measurement. While possible, this does not appear likely because Elkind's F-3 runs do not indicate the presence of a lead with 0.9 cps.

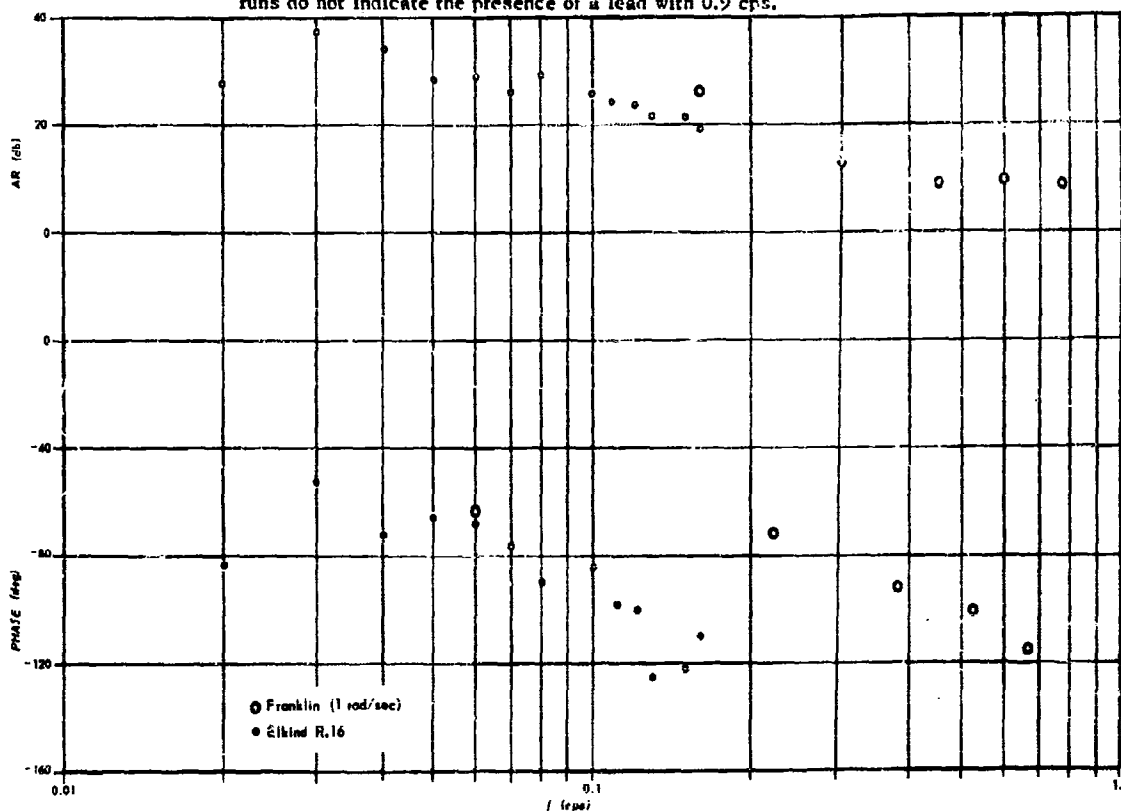


Figure 68. Comparison of Simple Tracker Data (Franklin and Elkind).
(References 23, 53.)

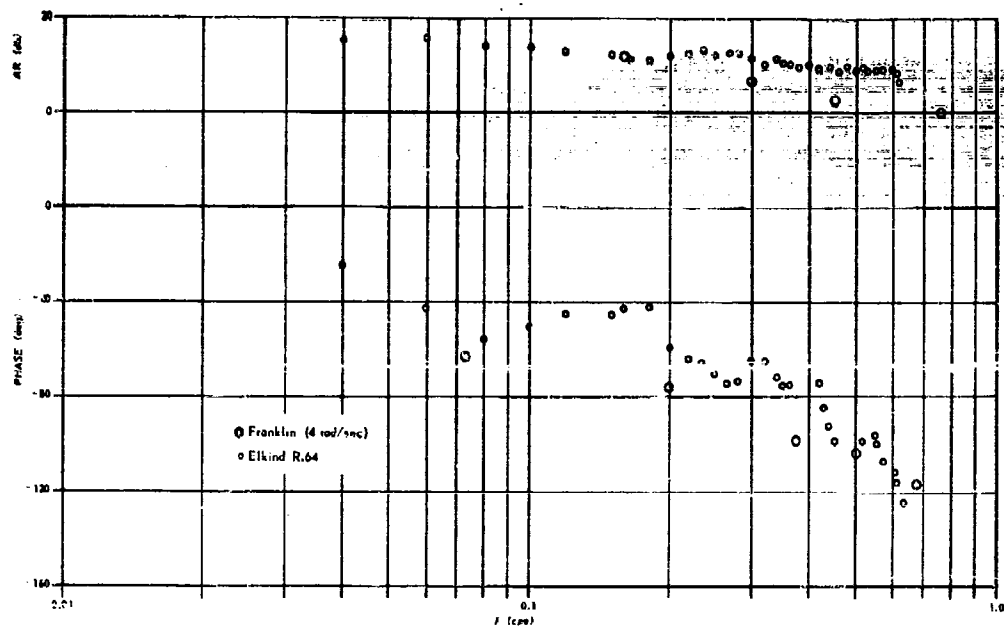


Figure 69. Comparison of Simple Tracker Data (Franklin and Elkind).
(References 23, 53.)

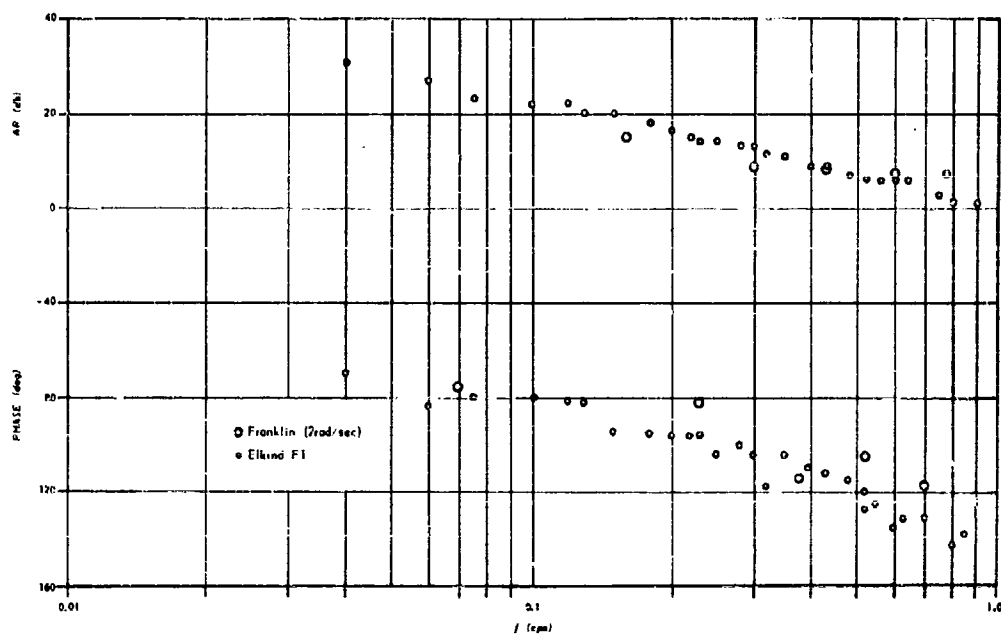


Figure 70. Comparison of Simple Tracker Data (Franklin and Elkind).
(References 23, 53.)

While it is problematical whether any real differences exist in the Elkind and Franklin data, it should be noted again that Elkind's tracking control was considerably simpler than the spring restrained stick used by Franklin. This difference in controllers could conceivably be responsible for the minor data differences, but the present overall picture is probably too vague to be definitive.

Section VI

LINEARIZED OPERATOR RESPONSE TO RANDOM APPEARING VISUAL FORCING FUNCTIONS IN COMPENSATORY TASKS WITH CONTROLLED ELEMENT DYNAMICS

A. INTRODUCTION

This section is a companion and extension to Section V, covering linearized operator behavior in situations having controlled element dynamics other than unity. The simple tracker cases discussed in Section V were well covered experimentally for a wide variety of conditions, and it would be very nice if this section could be composed of a series of operator describing functions and remnants for increasingly complex situations in terms of controlled element dynamics, together with a full coverage of forcing function conditions. Unfortunately the experimental basis for such a presentation does not yet exist.

The primary experimental work with controlled elements has been done by Tustin [85], Russell [70], and the Franklin Institute. Tustin's study was a pioneering effort, but was quite short and limited in scope. While three different controlled elements were used, they had very similar dynamics in the frequency range of interest. Typical information on the remnant was presented in Ref. 85, but the total remnant picture was relatively incomplete. Russell's study considered a logical progression of more and more complex controlled element characteristics, with the primary emphasis of the experimental work being placed upon the operator's describing function. Remnant characteristics, in a spectral form, were not thoroughly explored but their effects were revealed to some extent in some cases by total remnant power and error power data. The Franklin Institute F-80 simulator studies are documented in terms of both describing function and remnant characteristics. Here the controlled element dynamics were those of an F-80 aircraft in a constant range tracking task—by far the most complex situation studied in detail to date.

From this general summary we can conclude that the delineation of describing function characteristics as a function of controlled element dynamics can be fairly well defined, but that thorough remnant data exist only for the most simple controlled element situation (Elkind), and the most complex (Franklin). As previously noted in Section V, the remnant becomes very important as the control task increases in difficulty, so it is unfortunate that remnant data are so sparse for the succession of increasingly difficult tasks.*

* At the time of writing an additional source of variable controlled element data is in the experimental stage. This project is being performed by Ian A. M. Hall at Princeton University as part of the overall USAF coordinated effort. The study utilizes a Navion simulator with both lateral and longitudinal control to forcing functions having spectra flat to a 1 rad/sec corner frequency and an 18 db/oct high frequency asymptote. The lateral controlled element dynamics are fixed, being those of a typical Navion flight condition. The longitudinal controlled elements are varied, with the following forms presently being considered for study:

Simple Forms:

$$Y_c = K; (K = 5, 10 \text{ and } 15 \text{ deg/deg})$$

$$Y_c = \frac{K}{s}; (K = 1, 5 \text{ and } 15 \text{ deg/deg})$$

$$Y_c = \frac{K}{Ts+1}; K = 15; (T = 1.5, 5 \text{ and } 10 \text{ sec})$$

$$Y_c = \frac{K(Ts+1)}{s(T_g s+1)}; K = 5, T_g = 5 \text{ sec}; (T = 0.6, 2, 5 \text{ and } 10 \text{ sec})$$

Short Period Approximation Form:

$$Y_c = \frac{K(Ts+1)}{s \left[\left(\frac{s}{\omega_n} \right)^2 + \frac{2\zeta s}{\omega_n} + 1 \right]}; K = 5, T = 0.6$$

A complete survey will be run for $0.2 \leq \zeta \leq 1$ and $0.1 \leq \frac{\omega_n}{2\pi} \leq 1$ cps.

It is anticipated that the results of this study will fill in many of the presently existing gaps in controlled element forms as well as providing more adequate low frequency remnant data.

In the discussion that follows, the Russell data will be summarized first, the Tustin experiments second, and the Franklin Institute F-80 simulator data third. In all of these cases the transfer characteristics of the operator have been derived by the authors and their associates from the original data. Both Russell and Tustin fitted some of their data with transfer function forms, but based their efforts upon the use of Nyquist diagrams and other types of linear plots. In our curve fits the Bode diagram form has been used, sometimes in conjunction with linear phase vs. frequency plots, as being more consistent with simplicity and accuracy in the fitting process. In general the Tustin and Russell data were fitted using criteria and methods outlined below:

- (1) The linearized operator response data, which appeared in the original data as vector diagrams, were first placed in the form of Bode diagrams.
- (2) The data were then carefully examined to determine the simplest describing function form consistent with the general trends. In almost all cases this came out to be either

$$Y_p(s) = \frac{Ke^{-\tau s}(T_L s + 1)}{T_I s + 1} = \frac{Ke^{-\tau s}(a T_I s + 1)}{T_I s + 1} \quad (VI-1)$$

$$Y_p(s) = \frac{Ke^{-\tau s}(T_L s + 1)}{(T_I s + 1)(T_N s + 1)} = \frac{Ke^{-\tau s}(a T_I s + 1)}{(T_I s + 1)(T_N s + 1)} \quad (VI-2)$$

The form shown in Eq. (VI-2) is generally preferred, since $|Y(s)| \rightarrow 0$ as $s \rightarrow \infty$ which is necessary physically. In most cases, however, the data available were such that the T_N term could not be determined, and hence the form shown in Eq. (VI-1) was used. When this is the case, the reader should recognize that higher frequency describing function factors are actually present, and their low frequency effect is lumped with the τ of the reaction time delay term.

- (3) In the fitting of the data, any amplitude information indicating a lead or lag break point was used to define T_I or T_L respectively. For example, in the Tustin data, fitted initially with Eq. (VI-1), the value of T_L was indicated by the amplitude ratio.
- (4) Further constants in the rational transfer function terms, e.g., T_I in the above example, were adjusted so that the phase lag attributable to the reaction time delay, τ [that is the measured phase minus the phase due to the contribution of the rational terms, $(T_L s + 1)/(T_I s + 1)$], would show a linear variation with frequency.
- (5) The initial value of τ , which will include, of course, possible high frequency leads and lags as well as reaction time delay, was then taken as the slope of the best fit line passing through the origin of this linear plot of phase versus frequency.
- (6) The total open loop transfer function, i.e., operator plus controlled element, was then checked for stability. In most cases with forcing functions containing low frequencies, the fitted operator form plus the controlled element transfer function would predict an unstable closed loop system. Therefore an additional lag, i.e., T_N in Eq. (VI-2), was often required as a minimum addition to obtain stability of the fitted transfer function form. This additional lag was almost always beyond the bandwidth of measurement, and the frequencies in the forcing function were usually low, so the value of T_N was adjusted in these cases to provide just marginal stability of the overall closed loop system. This latter procedure, while not yielding a unique transfer function form, is consistent with that adopted previously in Section V.
- (7) The final value of reaction time delay τ was then found by subtracting T_N from the initial τ value determined in (5) above.

Most of the fundamental basis for the evolution of this detailed procedure was discussed in Section V. The F-80 Simulator data, being somewhat more adequate in terms of the number of frequency points available, was fitted by a more detailed procedure than that above; this is outlined in the subsection on those data. As a final point on data fitting, we must emphasize again that the fitted forms are only a convenient "model", and only the actual data points have a physical basis.

B. THE RUSSELL DATA

The experimental setup used by Russell has already been discussed in Section V and needs no further comment except to say that the post and pre-filters now consist of various inserted transfer function forms, and that most of Russell's tests with various controlled elements were short studies, using one or two subjects and a small number of runs, some undocumented. Therefore, while we shall devote some of our attention in the following to the data, a very important part of the discussion is a recapitulation of Russell's comments and observations on the individual tests.

1. Effect of Gain Changes in Controlled Element: $Y_c = K_c$

The effect of gain changes in the scope or the control, either during a run or from run to run, is almost entirely compensated for by the operator, who tends to set his gain in such a way as to hold the overall loop gain at some given value. Slight changes in overall loop gain can be effected by changes in the scope gain, but nowhere near the amount that would occur if the operator held his gain constant. Besides this point, Russell also shows that an increase in loop gain can be the result of instructions to "put more into it" or "try harder". In both cases the describing function is, of course, that of the simple tracker discussed in Section V.

2. Effects of Insertion of a Simple Lag: $Y_c = 1/(Ts + 1)$

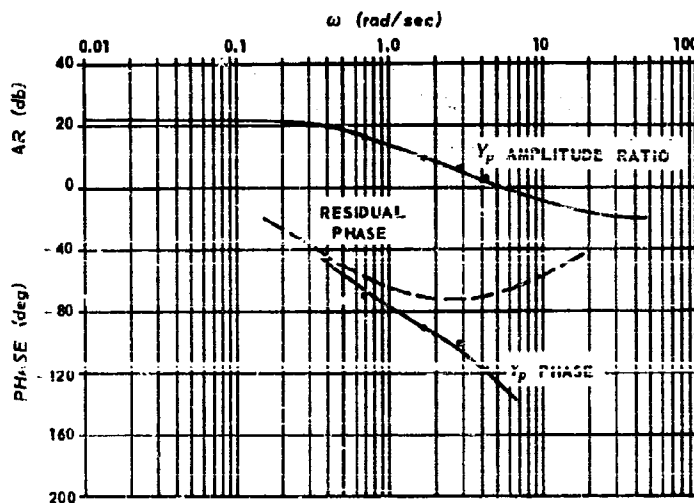
When simple lags were placed into the control loop the operator's transfer characteristics changed to a marked degree. This is exemplified in Figures 71, 72, and 73 where describing function data are presented for before and after conditions, i.e., $T = 0$ (no lag) for each case, and then $T = 1.0, 0.5$ and 5.0 seconds respectively. In all cases it is noticed that the major effects are the operator's use of his lead term in a fashion tending to compensate for the introduced lag, a reduction in gain, and probably a change in the first lag time constant. For an inserted lag time constant of 0.5 and 1.0 seconds, the operator's first lag time constant appears to increase over that with no dynamics; a reverse tendency is noted in the case where the inserted controlled element lag was 5.0 seconds.

In addition to the data given in these figures, Russell also notes the following:

- (a) When the lag time constant was smaller than about 0.05 seconds, the inserted lag had no effect on the describing function. In addition, the operator could scarcely notice the effect of the inserted lag on his stimulus.
- (b) As the controlled element time constant was increased above 0.05 , the operator could detect a distinct sluggishness in the system. This became more and more prominent until values of controlled element lag time constant, T , of 2 seconds or larger were used, when the controlled element appeared to the operator to take on the characteristics of a pure integrator.
- (c) When the lag was initially inserted into the loop (usually in the postfilter position), the operator tended to overshoot somewhat, occasionally to the point of system instability, until he had acquired some practice. After practice for a minute or so, he adapted his characteristics to suitable values for stability.
- (d) The reduction in loop gain when the lag was inserted was larger than required to maintain stability.
- (e) The mean square noise power and the noise component of the error were about twenty percent higher with the controlled element lag than without it.

3. Effect of Insertion of Pure Integration: $Y_c = 1/s$

With a controlled element consisting of a simple pure integrator the operator lowered his gain and introduced a considerable amount of lead, as shown in Fig. 74. In one case this was as much as $T_L = 5$ seconds. These changes allowed the overall system to be stable, but were also in the direction to increase the mean square tracking error over that with no controlled element dynamics. The low frequency response, however, is improved because of the higher overall system amplitude ratio at low frequencies due to the $Y_c = 1/s$ term.



a. Russell Experimental Characteristics Before Inserting Controlled Element.

○ Russell Data

$$Y_c = 1$$

"Best Fit" Operator Transfer Function:

$$Y_p = \frac{C}{E} = \frac{12.5 e^{-0.2s} (s/17.5 + 1)}{s/0.42 + 1}$$

b. Russell Experimental Characteristics After Inserting Controlled Element.

○ Russell Data, $Y_c Y_p$

□ Controlled Element Removed

$$Y_r = \frac{1}{s+1}$$

"Best Fit" Operator Transfer Function:

$$Y_p = \frac{C}{E} = \frac{17.7 e^{-0.16s} (s/0.68 + 1)}{s/0.1 + 1}$$

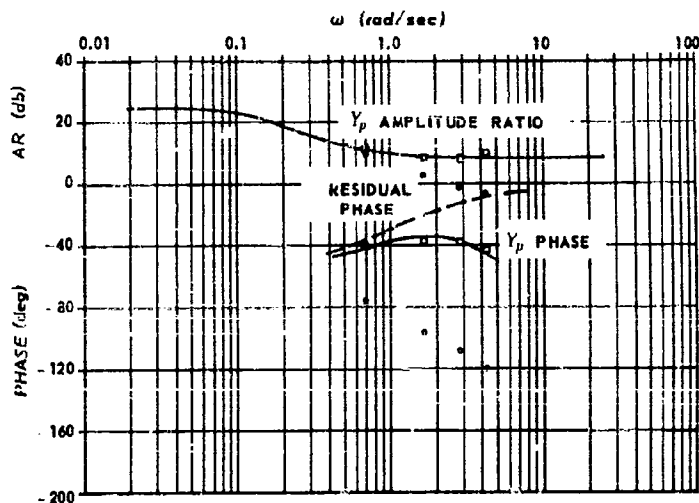
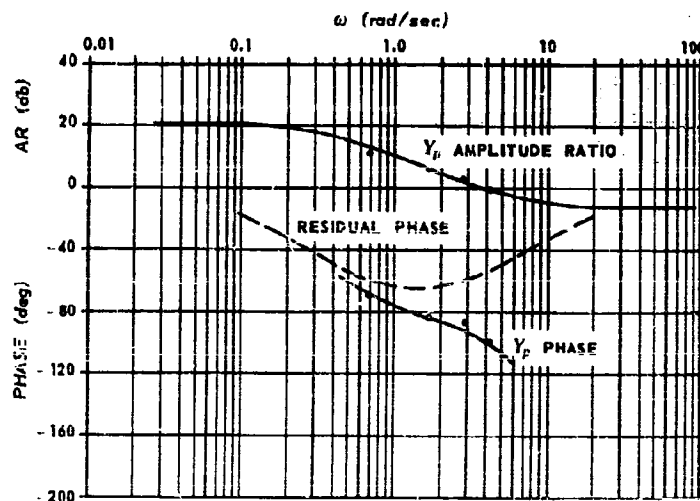


Figure 71.
(Reference 70, Figure 29.)



a. Russell Experimental Characteristics Before Inserting Controlled Element.

o Russell Data

$$Y_c = 1$$

"Best Fit" Operator Transfer Function:

$$Y_p = \frac{C}{E} = \frac{11.2 e^{-0.2s} (s/6.8 + 1)}{s/0.3 + 1}$$

b. Russell Experimental Characteristics After Inserting Controlled Element.

o Russell Data, $Y_c Y_p$

□ Controlled Element Removed

$$Y_c = \frac{1}{s/2 + 1}$$

"Best Fit" Operator Transfer Function:

$$Y_p = \frac{C}{E} = \frac{7.55 e^{-0.1s} (s/0.9 + 1)}{(s/0.13 + 1)(s/25 + 1)}$$

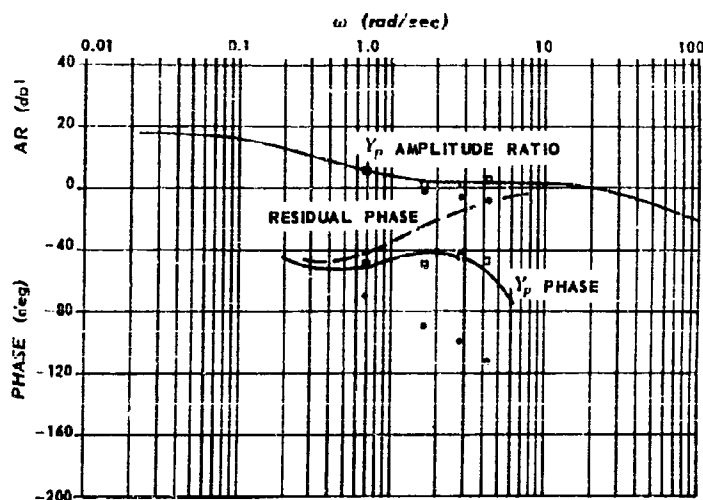
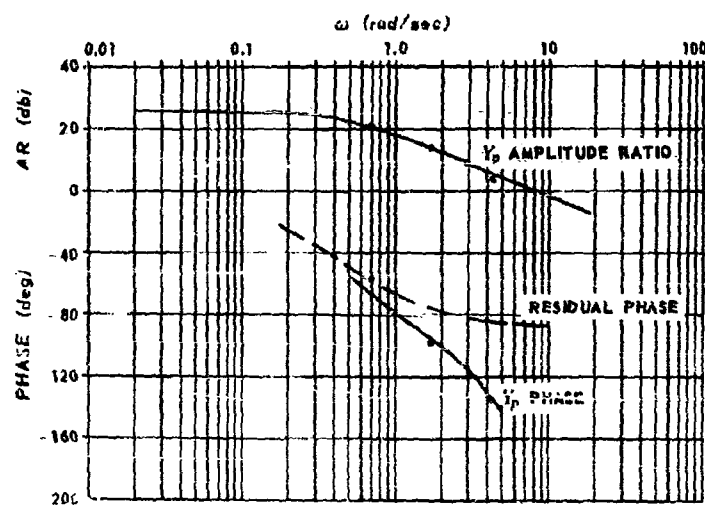


Figure 72.
(Reference 70, Figure 30.)



a. Russell Experimental Characteristics Before Inserting Controlled Element.

○ Russell Data

$$Y_c = 1$$

"Best Fit" Operator Transfer Function:

$$Y_p = \frac{C}{E} = \frac{19.7e^{-0.2s}}{s/0.44 + 1}$$

b. Russell Experimental Characteristics After Inserting Controlled Element.

- Russell Data, $Y_c Y_p$
- Controlled Element Removed

$$Y_c = \frac{1}{s/0.2 + 1}$$

"Best Fit" Operator Transfer Function:

$$Y_p = \frac{C}{E} = \frac{10e^{-0.15s}(s/2 + 1)}{(s/3 + 1)(s/14 + 1)}$$

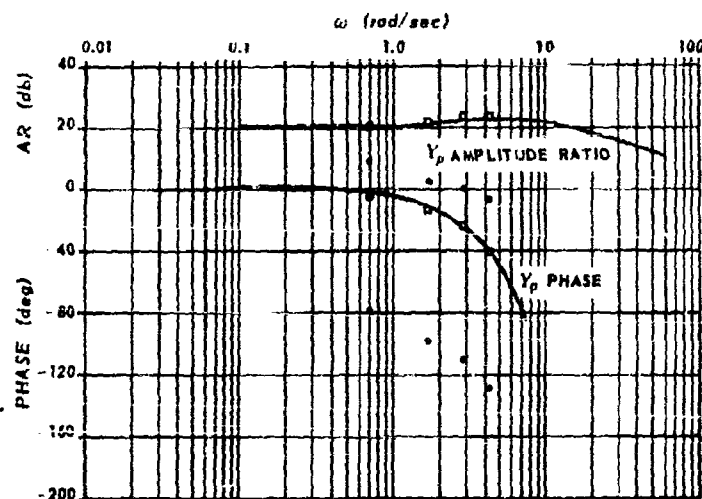
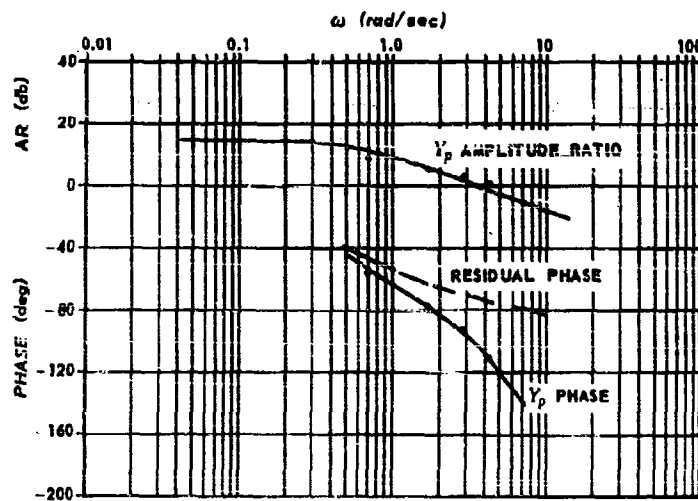


Figure 73.
(Reference 70, Figure 32.)



a. Russell Experimental Characteristics Before Inserting Controlled Element.

○ Russell Data

$$Y_c = 1$$

"Best Fit" Operator Transfer Function:

$$Y_p = \frac{C}{E} = \frac{5.6 e^{-0.15s} (s/1.76 + 1)}{(s/0.5 + 1)(s/2.6 + 1)}$$

b. Russell Experimental Characteristics After Inserting Controlled Element.

○ Russell Data, $Y_c Y_p$

□ Controlled Element Removed

$$Y_c = 1/s$$

"Best Fit" Operator Transfer Function:

$$Y_p = \frac{C}{E} = \frac{14 e^{-0.123s} (s/0.19 + 1)}{s/\omega_{small} + 1}$$

$$\omega_{small} \leq 0.015 \text{ rps}$$

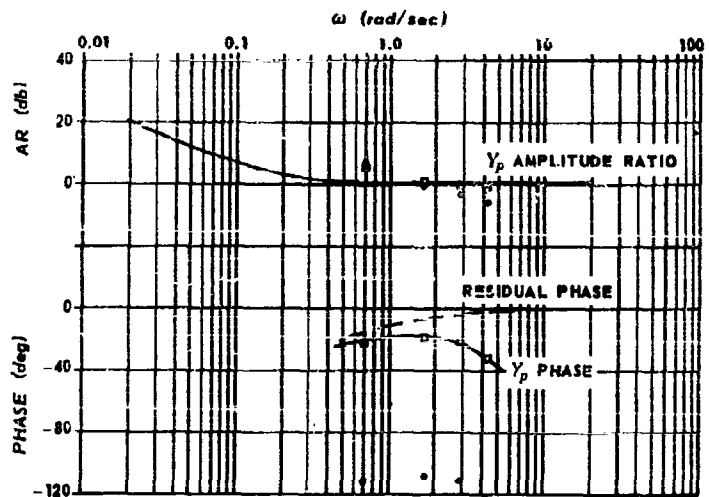


Figure 74.
(Reference 70, Figure 34.)

4. Effect of Insertion of Lead — Pure lag: $Y_c = (Ts + 1)/s$

A brief examination of the effects of a controlled element with lead-pure lag form, with $T = 0.5$ and 1.0 seconds, gave the results shown in Figure 75. It will be noted that the operator still introduced some lead for these values. Russell also observed that:

- (a) When $T \geq 2.5$ seconds, the operator does not appear to change his describing function appreciably from that with no controlled element dynamics.
- (b) When $T \leq 2.5$ seconds, the operator develops lead over and above that used in normal control with no controlled element dynamics.
- (c) The location of the dynamics making up Y_c in post or pre-filter position made no essential difference on the overall operation of the loop.
- (d) The output noise power was generally higher than the case with $Y_c = 1$.

5. Effect of Insertion of Lag-Lead: $Y_c = [a(Ts + 1)]/(aTs + 1)$

Russell studied the effects of a lag-lead control for $a = 10$ and T equal to 0.165, 0.5 and 2.0 seconds. The operator transfer functions for the last two of these conditions are shown in Figure 76. Russell also tabulated the mean square tracking error, with the dynamics of Y_c in the *pre-filter* position, for the two larger time constants.

T	Mean Square Error (in ²)	Error Due to Remnant (%)
0	0.045	32
0.5	0.34	56
2.0	0.041	24

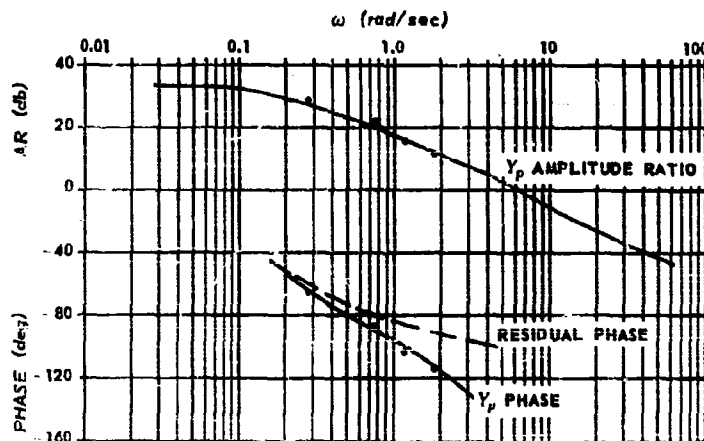
In another test, the $T = 0.165$ seconds value was used, with the results shown below.

T	Total Error Power (in ²)	Error Due to Remnant (%)
0	0.195	22
0.165	0.190	38.5

These data indicate that the noise power in the error signal decreases as the time constant, T , is increased to the order of 2.0 seconds or so, where the system, in terms of mean square tracking error, is just as good or better than a simple tracker.

6. Effect of $1/(Ts+1)$ in Postfilter and $(Ts+1)/(Ts+10)$ in Prefilter Positions

From the results of item 6, Russell found an effective way to remove some of the remnant without introducing adverse affects. A filter having a transfer function $1/(Ts + 1)$ was inserted in the postfilter location to smooth the higher frequency remnant power (which in Russell's case appeared to have a peak near $\omega = 8$ rad/sec), and then a lead-lag $(Ts+1)/(Ts+10)$ in the prefilter position to cancel out the lag introduced. Setting T at 0.5 seconds results in an effective controlled element transfer function of $Y_c = 1/(0.05s+1)$, which was noted in item 2 above to have negligible effect, i.e., the operator responded in the same fashion as that for a simple tracker. With the equalization inserted two tests were made with the following results:



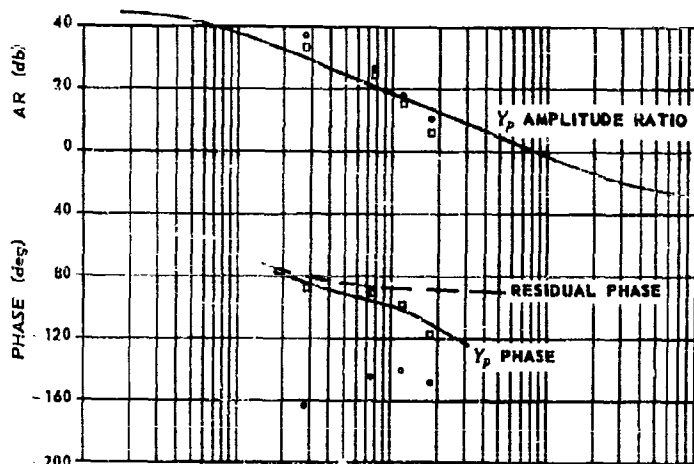
a. Russell Experimental Characteristics Before Inserting Controlled Element.

○ Russell Data

$$Y_c = 1$$

"Best Fit" Operator Transfer Function:

$$Y_p = \frac{C}{E} = \frac{46e^{-0.2s}(s/12+1)}{(s/0.16+1)(s/7+1)}$$



b. Russell Experimental Characteristics After Inserting Controlled Element.

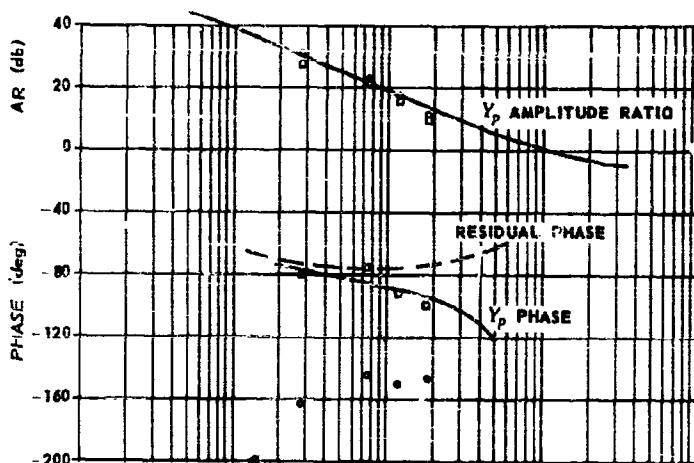
○ Russell Data, $Y_c Y_p$

□ Controlled Element Removed

$$Y_c = \frac{s+1}{s}$$

"Best Fit" Operator Transfer Function:

$$Y_p = \frac{C}{E} = \frac{118e^{-0.2s}(s/45+1)}{s/0.048+1}$$



c. Russell Experimental Characteristics After Inserting Controlled Element.

○ Russell Data, $Y_c Y_p$

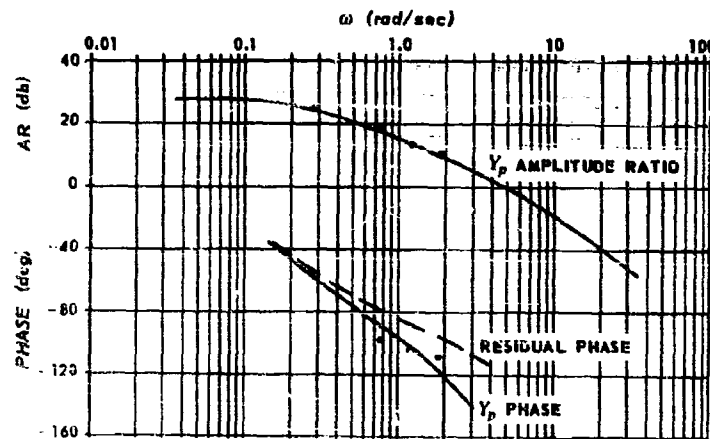
□ Controlled Element Removed

$$Y_c = \frac{s/2+1}{s}$$

"Best Fit" Operator Transfer Function:

$$Y_p = \frac{C}{E} = \frac{250e^{-0.2s}(s/17+1)}{s/0.03+1}$$

Figure 75.
(Reference 70, Figure 35.)



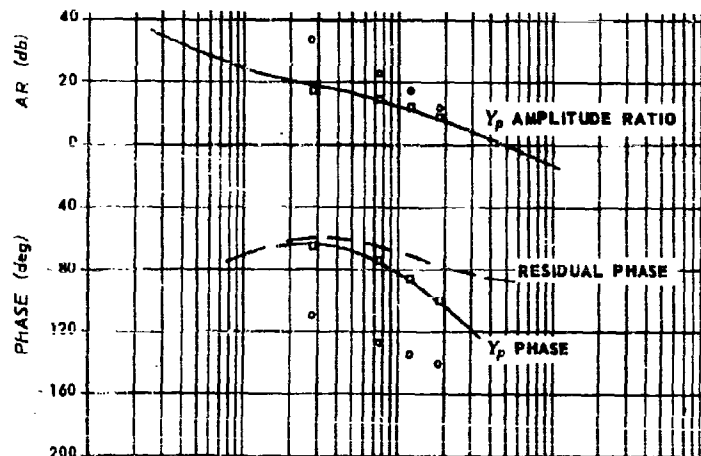
a. Russell Experimental Characteristics Before Inserting Controlled Element.

○ Russell Data

$$Y_c = 1$$

"Best Fit" Operator Transfer Function:

$$Y_p = \frac{C}{E} = \frac{25e^{-0.2s}}{(s/0.22 + 1)(s/8 + 1)}$$



b. Russell Experimental Characteristics After Inserting Controlled Element.

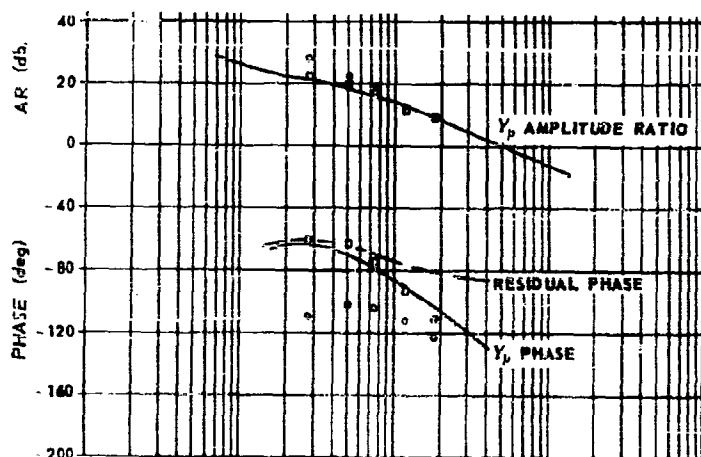
○ Russell Data, $Y_c Y_p$

□ Controlled Element Removed

$$Y_c = \frac{10\tau s + 10}{10\tau s + 1} \bigg|_{\tau = 0.5}$$

"Best Fit" Operator Transfer Function:

$$Y_p = \frac{C}{E} = \frac{K_{high} e^{-0.2s} (s/0.2 + 1)}{(s/\omega_{small} + 1)(s/0.6 + 1)}$$



c. Russell Experimental Characteristics After Inserting Controlled Element.

○ Russell Data, $Y_c Y_p$

□ Controlled Element Removed

$$Y_c = \frac{10\tau s + 10}{10\tau s + 1} \bigg|_{\tau = 2.6}$$

"Best Fit" Operator Transfer Function:

$$Y_p = \frac{C}{E} = \frac{K_{high} e^{-0.2s} (s/0.15 + 1)}{(s/\omega_{small} + 1)(s/0.45 + 1)}$$

Figure 76.
(Reference 70, Figure 36.)

	TEST I		TEST II	
	Remnant	Total	Remnant	Total
	Power	Error	Power	Error
	(in ²)	Power	(in ²)	Power
	(in ²)	(in ²)	(in ²)	(in ²)
No Equalization ($Y_c = 1$).....	0.013	0.043	0.029	0.042
With Equalization	0.0019	0.025	0.004	0.017

It is noted that a general improvement, of the order of a factor of two, in mean square error is obtained with this scheme.

7. Effect of a Quadratic Controlled Element: $Y_c = K_c / [(s/\omega_n)^2 + (2\zeta s/\omega_n) + 1]$

With a quadratic controlled element transfer characteristic, the operator describing functions obtained are shown in Figures 77. It will be noted from these figures that the insertion of the rather difficult controlled element dynamics with $\omega_n = 7.8$ rad/sec in the postfilter position resulted in a general deterioration of system performance. This is due largely to the reduction in the operator's gain. With ω_n increased an octave, to 16 rad/sec, the operator's characteristics returned to essentially those of a simple tracker. For another run with $\omega_n = 7.8$ rad/sec, the error components were as shown below:

Frequency Component	Error Power (in ²)
F_1 (0.105 cps).....	0.005
F_2 (0.268 cps).....	0.015
F_3 (0.457 cps).....	0.018
F_4 (0.679 cps).....	0.027
Remnant	0.045
Total Error	0.110

The approximate average linear correlation derived from signal to noise considerations was about 0.76 in this particular case, or the lowest achieved on any of the Russell data.

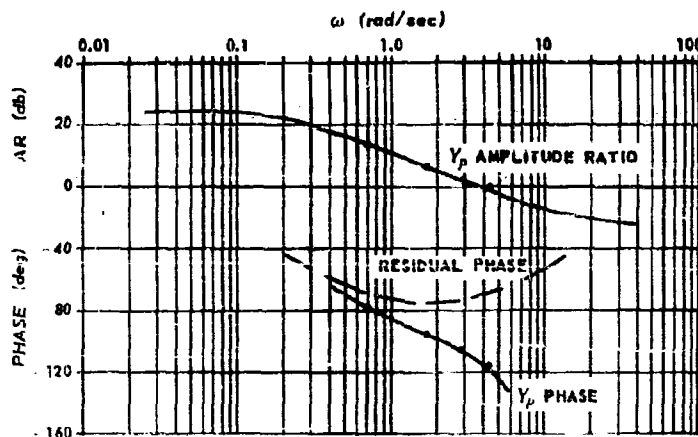
C. THE TUSTIN DATA

In Tustin's experiments [85], the general situation was set up to simulate a tank turret fire control problem. The operator and a sight were mounted on a motor driven turntable controlled by a twistable, spring-centered, spade grip handle. The target moved back and forth in different combinations of three simple harmonic components sufficiently mixed to eliminate any sense of regularity. Equivalent transfer function data were obtained from the harmonic components of the traces that were of the same frequencies as those contained in the target displacement. These data were then presented in the form of vector diagrams of the ratio of handle speed/error.

Three basic variations in the controlled element (turntable) dynamics were investigated with a variety of operators and target inputs.

The linearized transfer characteristics for each of these controlled elements are presented as solid lines in the Bode plots of Figure 78. The plotted data points shown correspond to those measured from the vector diagrams appearing in the original paper. The operator response data were reduced in terms of target inputs having harmonic components with a spread from 0.113 to 1.3 rad/sec; hence it is obvious from Figure 78 that, for this range of frequencies, there is very little difference in controlled element dynamics between the displacement speed control and the "second-differential" control. This similarity was apparent during the course of the tests and very few data points were obtained for the latter type of control, which has therefore been deleted from further consideration. The static characteristics of the control are shown in Figure 79.

The linearized operator response data which, as mentioned, appeared in the original data as vector diagrams, have been assembled in Figures 80 and 81 in the form of Bode plots. It will be noted that, for the first and only time in this report, we have combined the data points for two different forcing function "bandwidths" on one



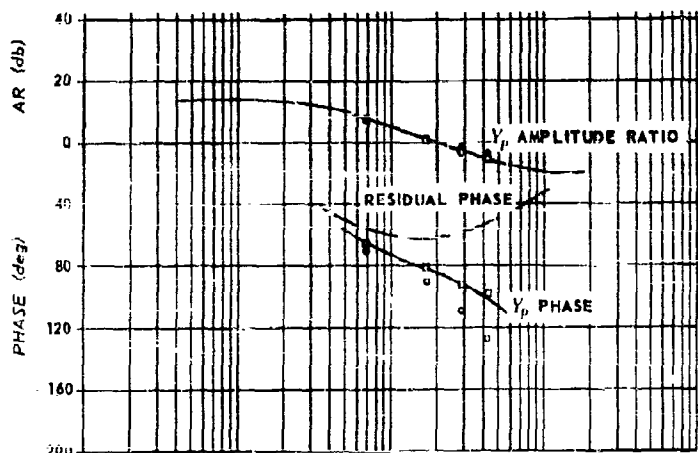
a. Russell Experimental Characteristics Before Inserting Controlled Element.

○ Russell Data

$$Y_c = 1$$

"Best Fit" Operator Transfer Function:

$$Y_p = \frac{C}{E} = \frac{16.7 e^{-0.2s} (s/14 + 1)}{s/0.215 + 1}$$



b. Russell Experimental Characteristics After Inserting Controlled Element.

○ Russell Data, $Y_c Y_p$

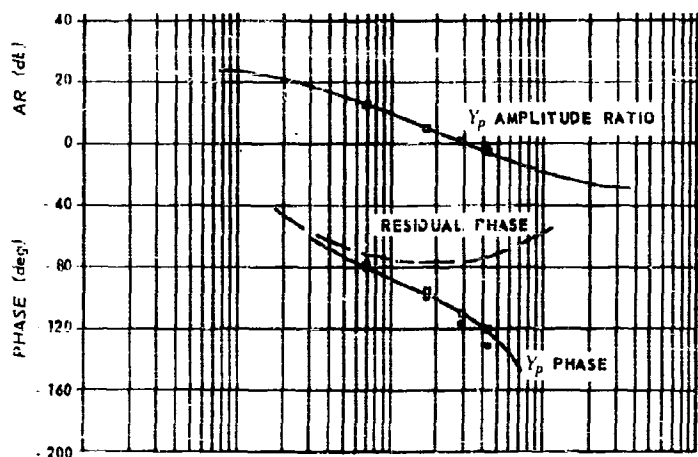
□ Controlled Element Removed

$$Y_c = \frac{K_c}{(s/\omega_n)^2 + (2\zeta s)/\omega_n + 1}$$

$$\omega_n = 7.8; \zeta = 0.371$$

"Best Fit" Operator Transfer Function:

$$Y_p = \frac{C}{E} = \frac{5.3 e^{-0.2s} (s/6.8 + 1)}{s/0.38 + 1}$$



c. Russell Experimental Characteristics After Inserting Controlled Element.

○ Russell Data, $Y_c Y_p$

□ Controlled Element Removed

$$Y_c = \frac{K_c}{(s/\omega_n)^2 + (2\zeta s)/\omega_n + 1}$$

$$\omega_n = 16; \zeta = 0.371$$

"Best Fit" Operator Transfer Function:

$$Y_p = \frac{C}{E} = \frac{16 e^{-0.2s} (s/17 + 1)}{s/0.195 + 1}$$

Figure 77.
(Reference 76, Figure 41.)

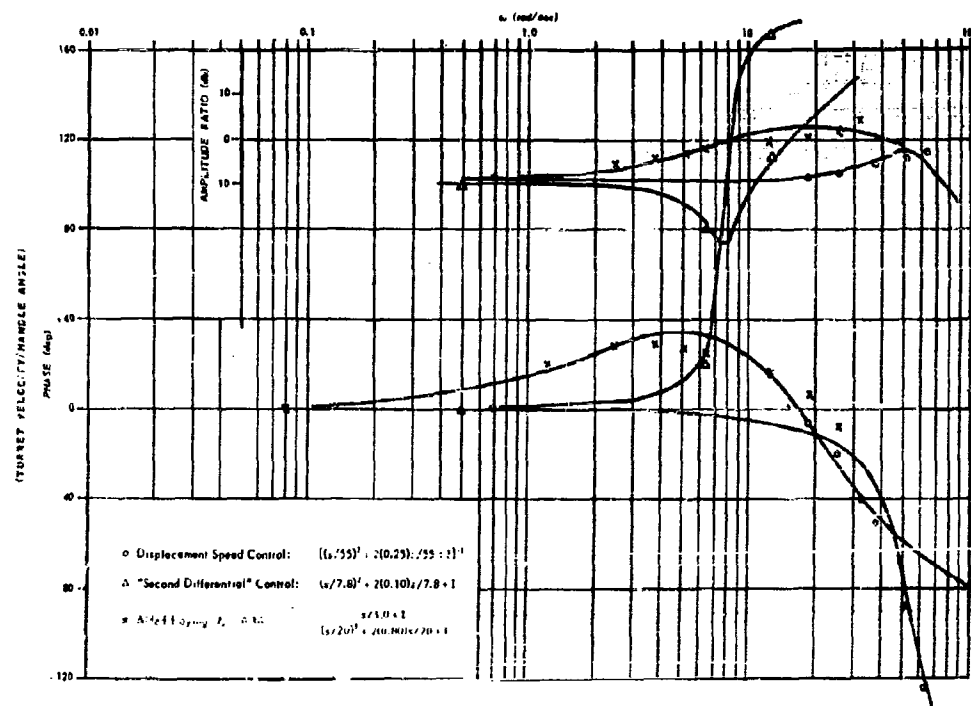


Figure 78. Tustin Experiments, Controlled Element Dynamics.

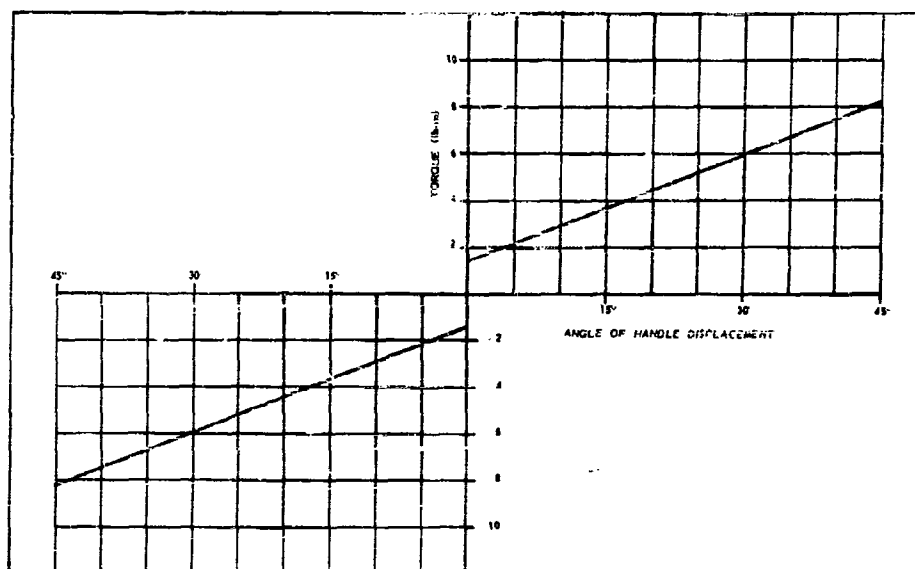
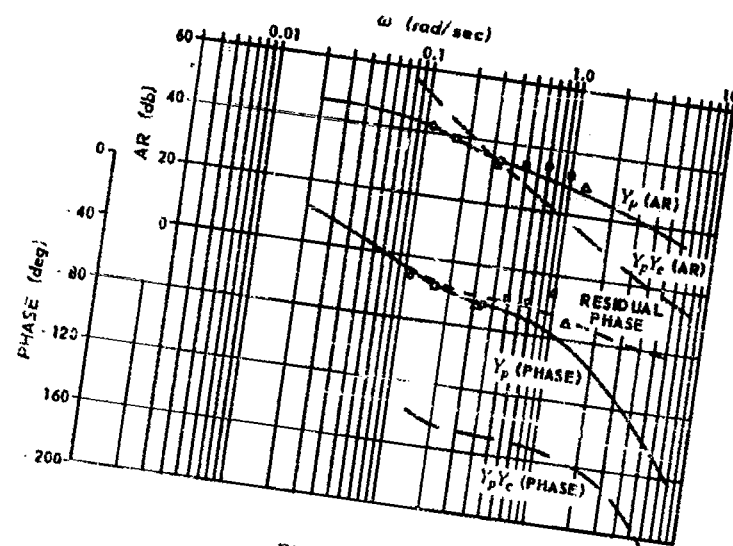


Figure 79. Handle Force-Displacement Characteristics for Tustin Data.



NOTE: Points shown are with controlled element removed:

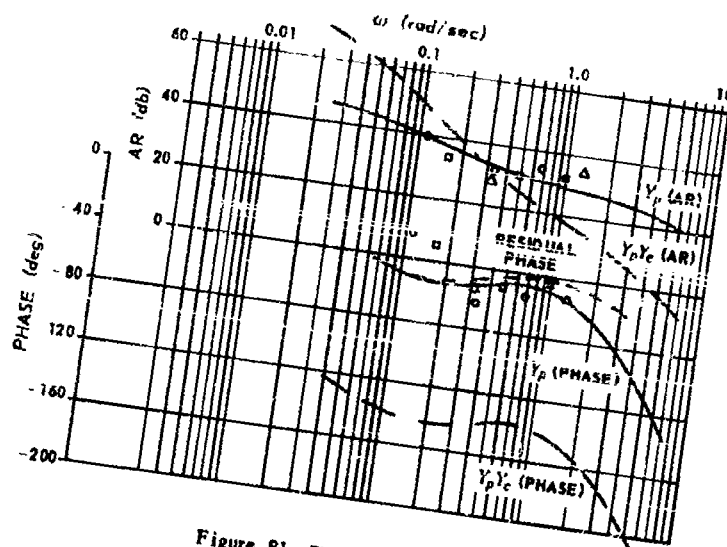
- Cam No. 1 at 1 rpm, 4 test average
- Cam No. 1 at 1.5 rpm, 4 test average
- △ Cam No. 2 at 1 rpm, 6 test average, with 0.36 sec time constant included

"Best Fit"

Net Operator Transfer Function:

$$Y_p = \frac{200 e^{-0.2s} (s/0.40 + 1)}{(s/0.07 + 1)(s/1.0 + 1)}$$

Figure 80. Tustin "Autoleveling" Characteristics.
(Reference 85, Figure 6.)



NOTE: Points shown are with controlled element removed:

- Cam No. 1 at 1 rpm, 5 tests, 3 operators
- Cam No. 1 at 1.5 rpm, 6 tests, various operators
- △ Cam No. 2 at 1 rpm, 5 tests, unspecified operators

"Best Fit"

Net Operator Transfer Function:

$$Y_p = \frac{220 e^{-0.15s} (s/0.4 + 1)}{(s/0.05 + 1)(s/2.5 + 1)}$$

Figure 81. Tustin Characteristics, "Displacement Speed Control".
(Reference 85, Figure 6.)

plot. The primary justification for this step is the extremely low frequency content of the forcing functions and the overlap of the data. The number of subjects and trials were variable. Therefore, they are noted on the diagram for the various data points. Most of the data are similar to those previously discussed in detail and need no further explanation. One interesting point is worth further comment, however. This is the rather drastic departure of the

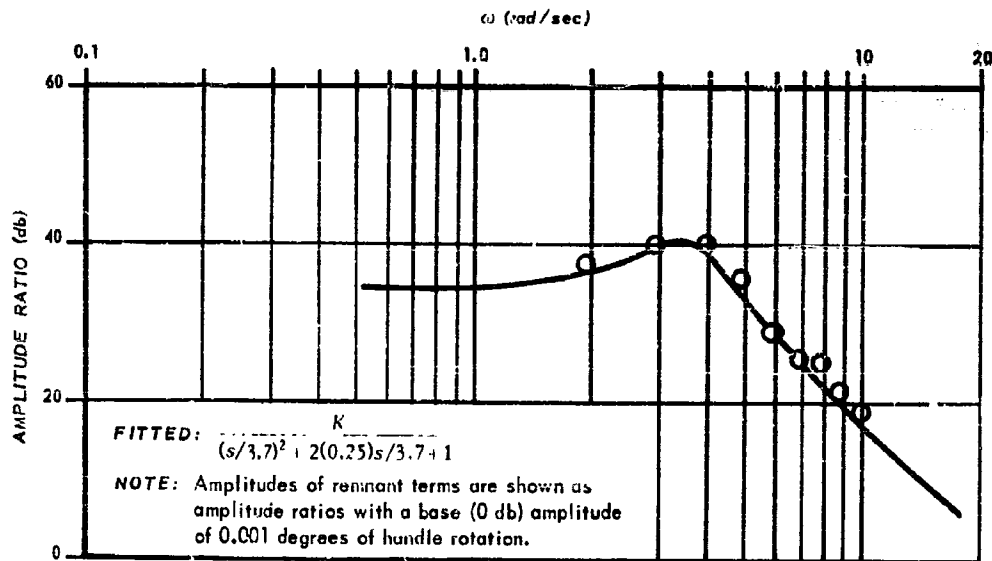


Figure 82. Tustin Residual Data.

two low frequency phase points from the general phase trend of Figure 81. These two points are the lowest frequency, largest forcing function amplitude data for two separate runs. In these cases it is quite probable that the operator was acting in either a pursuit or even a synchronous mode for the lowest frequency.

Tustin made a harmonic analysis of all the frequencies appearing in the pilot's output, associating those terms containing input frequencies with the complex input to derive the transfer function data which was presented above. The result of the harmonic analysis of the residual signal or remnant is shown in Figure 82.

The original paper did not present data on linear correlations, but an estimated value of about 0.94 for ρ is possible on the basis of a "typical" tracking record shown therein.

L. THE FRANKLIN INSTITUTE F-80A SIMULATOR DATA

1. The F-80A Simulator

The general experimental set-up used in the F-80A simulator tests was similar to that discussed in the simple tracker description of Section V. The essential difference is that now the controlled element dynamics were those of an F-89A aircraft engaged in a tail chase. In addition, the display was elaborated by an artificial horizon consisting of a line which was rotated and displaced vertically in the same fashion as the true horizon would be were it viewed through the wind screen under contact flying conditions. In order to minimize orientation difficulties on the part of the subjects, a pair of wings was drawn on the stationary cross-hairs so as to clearly associate the cross-hairs with the subject's aircraft, and the pip with the target aircraft. See Figure 83 for an abstracted sketch of the display. Figure 47 is an actual view of the interior of the cockpit, and Figure 48 is an overall view of the simulator and the associated computing equipment. It should be noted that the actual cockpit, which was modified for the purposes of this experiment, was obtained from an F-51. The cockpit instruments, none of which were functioning and whose sole purpose was to provide a certain amount of face validity, were obtained from an F-80A aircraft. The stick was loaded so as to simulate, without nonlinearities, the forces a pilot would encounter at Mach 0.7 at an altitude of 20,000 feet. Although rudder pedals were present in the simulator, they were impotent in controlling the F-80A aircraft simulator. As was indicated in an earlier experiment [52], jet pilots used only stick control at the simulated speed and altitude. It was therefore decided to describe the pilot's

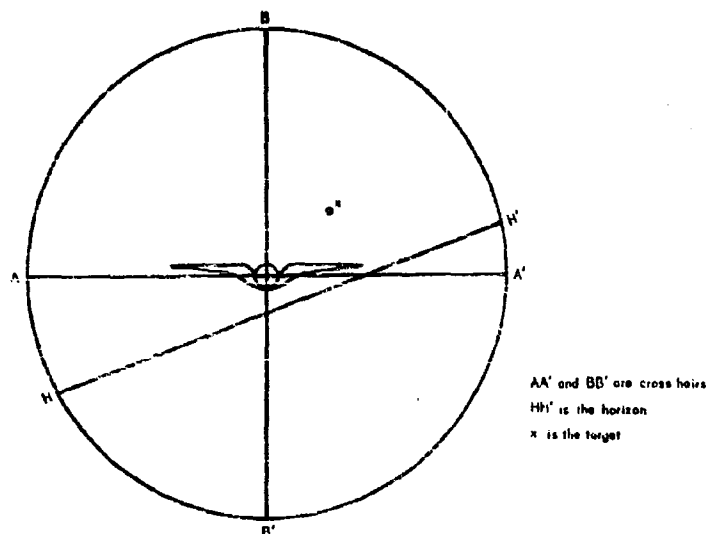


Figure 83. The F-80A Simulator Display.

behavior in terms of stick control only, i.e., aileron control governing the lateral response and elevator control governing longitudinal responses.

The controlled element dynamics included both the aircraft equations of motion, in five degrees of freedom, forward speed assumed constant, and the geometrical relationships between the target and the tracking aircraft. The target angles were given by:

$$\dot{\theta}_A = r - p r_E - \frac{V_A}{X_T} + \frac{U_0 \beta}{X_T} \quad (\text{VI-3})$$

$$\dot{\theta}_E = q + p r_A + \frac{V_E}{X_T} - \frac{U_0 \alpha}{X_T} \quad (\text{VI-4})$$

where $(\theta)_A \sim$ azimuth; $(\theta)_E \sim$ elevation

$$\dot{V}_A = -U_0 r + p V_E$$

$$\dot{V}_E = U_0 q - p V_A$$

r = target angle

X_T = distance from target = 3000 ft constant

p, q, r = angular velocities in roll, pitch, yaw

α, β = angles of attack and sideslip

V = velocity of target in plane perpendicular to x axis of interceptor

δ_a, δ_e = aileron and elevator deflections

Since the lateral-longitudinal cross coupling terms are fairly small for the case of interest, it can be assumed that the pertinent error angle observed by the pilot would be given by the above expressions with $p = 0$ for the elevation error and $r_E = V_E = 0$ for the azimuth error. Accordingly the equations simplify to:

$$\dot{\theta}_A = r + \frac{U_0}{X_T}(\psi + \beta) \quad (\text{VI-5})$$

$$\dot{\theta}_E = q + \frac{U_0}{X_T}(\theta - \alpha) \quad (\text{VI-6})$$

and the transfer functions of interest become

$$\frac{r_A}{\delta_A}(s) = \frac{1}{s} \left[\frac{r}{\delta_A}(s) + \frac{U_0}{X_T} \left(\frac{1}{s} \frac{r}{\delta_A}(s) + \frac{\beta}{\delta_A}(s) \right) \right] \quad (\text{VI-7})$$

$$\frac{r_E}{\delta_E}(s) = \frac{1}{s} \left[\frac{q}{\delta_E}(s) + \frac{U_0}{X_T} \left(\frac{1}{s} \frac{q}{\delta_E}(s) - \frac{\alpha}{\delta_E}(s) \right) \right] \quad (\text{VI-8})$$

The various longitudinal and lateral airframe transfer functions making up the above expressions were evaluated for the following airplane parameters as set in the simulator:

$L_\beta = -22.4$	$M_\alpha = -12.7$	$N_\beta = 14.8$	$g/U_0 = 0.044$
$L_p = -5.62$	$M_{\dot{\alpha}} = -.908$	$N_p = -.026$	$\dot{Y}_v = -.185$
$L_r = +.525$	$M_{\dot{\alpha}} = -1.66$	$N_r = -.493$	$Z_w = -1.87$
$L_{\delta_A} = -49.1$	$M_{\delta_E} = -31.1$	$N_{\delta_A} = .318$	

Collecting the numerator terms and factoring both numerator and denominator, the final controlled element transfer functions may be expressed as:

$$\frac{r_A}{\delta_A}(s) = \frac{-53.5 \left(\frac{s}{2.42} + 1 \right) \left(\frac{s}{-2.92} + 1 \right) \left(\frac{s}{4.11} + 1 \right) \left(\frac{s}{8.32} + 1 \right)}{s^2 \left(\frac{s}{0.0017} + 1 \right) \left(\frac{s}{5.65} + 1 \right) \left(\frac{s^2}{(3.88)^2} + \frac{2(0.084)s}{3.88} + 1 \right)} \quad (\text{VI-9})$$

$$\frac{r_E}{\delta_E}(s) = \frac{-0.89 \left(\frac{s}{0.28} + 1 \right) \left(\frac{s}{1.58} + 1 \right)}{s^2 \left(\frac{s}{3.98} \right)^2 + \frac{2(0.56)s}{3.98} + 1} \quad (\text{VI-10})$$

Bode plots of the above functions are shown in Figures 84 and 85.

A forcing function was generated independently in azimuth and elevation by passing white noise through a third order RC filter with a single corner frequency. Three forcing function bandwidths were used, with corner frequencies of 1, 2, and 4 radians/second. The rms value of the forcing function was continuously adjustable, although the primary values used were nominally 0.3, 0.8 and 1.1 rms inches at the display for azimuth control, and 0.2, 0.5, and 0.8 for elevation control. The basic reason for using a random input for the forcing function to the pilot-airframe system has been discussed in Section III. The choice of the particular rms amplitudes and bandwidths was governed by the desire to present a signal that was within the limits of the pilot's ability to track as well as realistic. These target disturbances simulated atmospheric turbulence of various degrees of severity. The Air Force pilots who served as subjects generally felt that the 1 and 2 radians/second bandwidths provided turbulence conditions that they had commonly experienced, whereas the 4 radians/second input represented unusual conditions. An unsolicited comment from one of the pilots about the 4 radians/second input was, "I wouldn't fire in air *that* turbulent!" During the pretrial briefing the subjects were told that they were flying a simulated firing run tail chase at a target distance of 1000 yards. This task orientation was readily accepted by the pilots despite the unusually long run length (two minutes) and the difficult tracking conditions which prevailed.

It is of interest to examine a pilot's comments and reactions during his pre-test familiarization runs. From these data it is possible to get insights as to the development of an acceptance of the simulator by the pilot. The first 6 comments in what follows were selected from a series of remarks made during the first hour, by a pilot with considerable experience in crystallizing his opinions on aircraft control systems. The same pilot made the subsequent comments during the course of a two day experimental session.

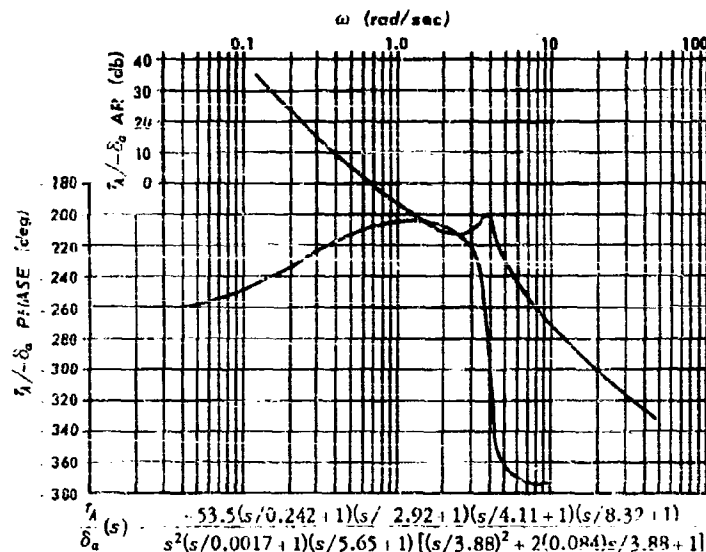


Figure 84. Franklin F-80A Simulator Response in Azimuth.

1. "In an aircraft, control is more positive. Here I find myself constantly jiggling the stick. An actual aircraft would have more slop at the zero point, however, I think it's a good idea for a simulator to have tight control."
2. "Longitudinal control seems slightly unstable--in other words the response of the simulator to control motion seems to produce an overshoot. This effect may be present in lateral control as well."

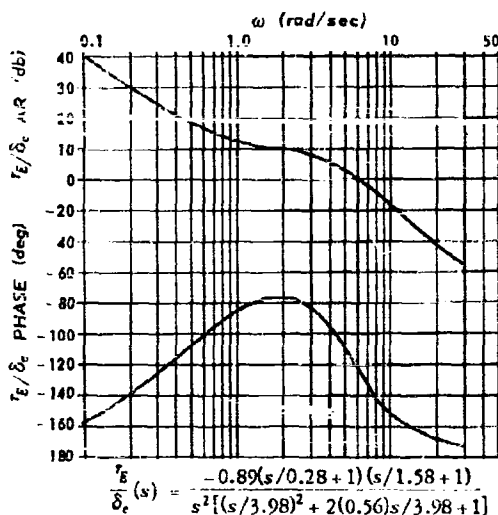


Figure 85. Franklin F-80A Simulator Response in Elevation.

3. "The response time for longitudinal and lateral control appears to be about equal. I expected the lateral control to be faster. Simulators never seem to have the dynamics of aircraft in flight; they always miss some aspect of the 'feel'."

4. "My flying technique consisting of smooth easy corrections which I use in an actual F-80A is inappropriate here. I am forced to use jerky corrective motions."

5. "I believe that four radians is unreasonable as an input for this control system. It may be possible in elevator, but just barely so."

6. "This control system seems to cause pilot to overcontrol."

Following the pre-trial period, the pilot then proceeded to track twenty runs which were recorded. In these runs forcing functions of 1 and 2 radians/second bandwidths and 0.3 and 0.9 inches rms in lateral control and 0.2 and 0.5 inches rms in longitudinal control were used. During these runs his commenting continued.

7. "Run No. 4 started out well. I'd rate the runs as 1, 4, 2, 3. I seem to pace myself against time. I think that the first minute is always the best. I'm convinced that the 'smooth' mode is superior to the 'frantic' mode; i.e., fly the simulator like an airplane, graceful and easy.

NOTE: The pilot had introspected aloud on the best control philosophy to use in the simulator. One style of control, the so-called "frantic" mode was characterized by abrupt sudden corrections in an attempt to maximize zero crossings. The alternative style of control the so-called "smooth" mode required the pilot to execute his control responses slowly and gracefully. From the viewpoint of the observer, the "frantic" mode appeared like an intermittent relay type control; whereas the "smooth" mode was much like smooth linear control.

8. "The 'frantic' mode isn't any good. I work harder but get no results. I'm always bracketing the target. More zero crossings, but not useful for gunnery. Unlike the 'smooth' mode where my error increases with time, I believe that my error is relatively constant in the 'frantic' mode."

9. At run No. 16 the subject said the following: "This simulator has good 'positive' control in elevator. The aileron feel is more spongy than it should be; it should be more mechanical. There is too much overshoot. Generally, however, the control system is not bad at all. Elevator control is excellent."

10. Toward the end of the first day's tests, the subject experienced several test runs of ten minutes duration. The following comments arose after these runs.

"Momentarily I got vertigo. I think that my performance deteriorated in time, but not as badly as it might have."

After the last run of the day he said "I actually thought that the fuselage moved. I find myself preferring the four radians/second input at the lower rms amplitude. Since I no longer make reversals, I find the quick responses required by the fast noise to be desirable."

On the second day of the tests, this subject made the following remarks:

11. "The four radians/second input is not unreasonable. In fact, I'm still flying in the 'smooth' mode. I like the fast recovery rate, and I'm positive of my control."

12. "There is still lag in the pip presentation laterally. I think it's due to rolling to change heading. I'd like to see faster response. Longitudinally the control is good."

13. "It's a good, representative aircraft system."

Although all of the foregoing remarks were generated by one pilot, they are representative of both solicited and unsolicited comments made by the other subjects during both their familiarization and test runs. The major conclusion which one can draw from the series of remarks is that after an initial period of warily testing the simulator, the pilot accepts the simulation as an adequate ground representation of the aircraft.

2. Experimental Procedures

The experimental procedures used in obtaining the data which are presented in this section were essentially the same as those reported in a previous report [53]. A brief recapitulation of the general approach and experimental design will be presented here for convenience.

The major problems which the experimental program sought to answer were: the extent to which the subject behaved in a linear fashion, the manner in which his response was frequency dependent, the extent to which his describing function was time dependent,* and the variability in describing functions among subjects. An extremely important question which the experiments left untouched was the effect of changes in the controlled element dynamics. The data reduction was so laborious that rather early in the program the decision was made to concentrate on a human response study for which only one aircraft's dynamics would be simulated rather than to risk diluting the effort by considering aircraft dynamics as still another experimental variable. Despite this effort to

* For long time intervals, of the order of minutes, only. Detection of short time variations (of the order of seconds) is not practical by the techniques used here.

concentrate on pilot centered variables, the experimental program's reach exceeded its grasp. The accuracy and resolution of the analytical tools were not adequate for discriminating many of the variables which were considered to be important in the experimental design.

Each of the six subjects, five highly trained jet pilots furnished by the USAF for a period of two days, and one highly trained civilian jet pilot, participated in preparatory and recorded trials under the following experimental conditions. After being briefed on the purposes of the experiment, the subject "flew" the simulator with no forcing function input for a period of about ten minutes. The purpose of this was to familiarize the subjects with the feel of the controls. A second phase in the pre-trial familiarization consisted of a total period varying from half an hour to an hour of simulator time during which the subject practiced tracking the various stimuli which would later be presented to him. The predominant stimulus in this familiarization period was of 2 radians/second bandwidth and 0.3 rms inches in amplitude for azimuth control and 0.2 rms inches for elevation control. These inputs were produced by passing broadband noise through a low pass filter whose corner frequency was 2 radians/second and which attenuated at 18db/octave thereafter. The subject's practice runs were approximately two minutes in duration and separated by intervals ranging from two to ten minutes. Since in general, the pilots arrived in groups of two, they alternated with one another in these practice runs.

It is rather difficult to assess the amount of familiarization necessary to produce stable and representative response behavior on the part of pilots in the simulator. If the data are to be meaningfully related to the airborne problem our subjects must be responding in the ground simulator with habit patterns which are like the habit patterns employed in the air. It is possible that a protracted familiarization period in the ground simulator might result in lessening the effective transfer to our test situations of these airborne habit patterns in which we are basically interested, and the corresponding strengthening of response patterns generated in, and peculiar to, ground simulation. These response patterns which might develop from experience in the ground simulator would tend to make the subject "play a game" rather than fly an aircraft. The ideal situation would be for a pilot to be convinced rather rapidly that the ground simulator provided an adequate representation of flight conditions, and then to transfer his airborne response patterns to the ground environment without attempting to analyze the ground system too critically. This thinking dictated the type of familiarization procedures used. Since the pilots were presumed to be at a stable plateau of flying performance, our problem was essentially to arrange matters so that our measuring device, the ground simulator, was actually sampling their flying performance at this presumed plateau.

Following the familiarization period, each group of two pilots (pilot A and pilot B) tracked the following program for ten two-minute trials each.

Pilot	Bandwidth (rad/sec)	Amplitude rms inches	
		Azimuth	Elevation
A	1	0.3	0.2
B	2	0.3	0.2
A	1	0.8	0.5
B	2	0.8	0.5

The pattern illustrated was repeated five times. The separation between trials was about 2.5 minutes. After a rest period of half an hour to an hour a second similar series of ten runs per pilot was recorded. This second series differed from the first only in that pilot A now experienced the 2 radian/second input and pilot B the 1 radian/second input. The purpose of these trials was to see what effects in the measured describing functions could be attributed to an increase in experience during the time intervals studied. The remainder of the several bandwidths and rms amplitude levels used, and to studies of tracking continuously for ten minute intervals. As will be seen when the data are examined, much of the fine detail which the experimental design was intended to reveal was obliterated due to the statistical spread of the data. Consequently there is little point in dwelling further on the experimental design at this point.

3. The Accuracy of Spectral Estimates

The manner in which the data were analyzed, the statistical significance of these data, and the experimental design are all intimately related. In fact, certain of the questions which the experimental program attempted to answer were directed toward validating some of the assumptions of our analytical techniques.

Since the data from the F-80A simulator experiments in this section are being presented for the first time, it may be helpful to discuss the statistics and the analysis procedures. This discussion, derived from Tukey [8, 80, 81], applies equally well when evaluating data from the other experimenters referenced in this report who have used the spectral analysis of time series as their basic measurement technique. The following material is an effort to provide an intuitively satisfying summary of material which the interested reader is urged to pursue in the primary sources [4, 8, 37, 38, 65, 75, 80, 81]. In their text [38] Grenander and Rosenblatt present the most refined readily available treatment of the statistical estimation problems arising in measuring the spectra of time series, whereas in their referenced paper [37] they present a heuristic derivation of their main sampling theorem together with an expository problem and limiting distribution functions relevant to their theory. The estimates Grenander and Rosenblatt developed are stated in terms of the spectral distribution function, which is the integral of the power spectral density function. They also present the variances and biases associated with spectral density estimates derived from different smoothing techniques, and leave the selection of the smoothing technique to be determined by the reader for his particular problem.

As has been stated in Section III of this report spectral densities and cross-spectral densities can be defined in the following form:

$$\begin{aligned}\Phi_{ii}(\omega) &= \lim_{T \rightarrow \infty} \frac{1}{T} [I^*(j\omega) I(j\omega)] = \lim_{T \rightarrow \infty} |I(j\omega)|^2, \\ \Phi_{ii}(\omega) &= \lim_{T \rightarrow \infty} \frac{1}{T} [I^*(j\omega) R(j\omega)]\end{aligned}\quad (VI-11)$$

The fact that the definition of these spectra depends on a limiting process implies that all realizable measurements are approximations to a lesser or greater extent. This necessary truncation of the time series record is the source of the sampling errors, $\Delta\Phi$, associated with spectral measurements. For the case of a Gaussian input spectrum which is essentially constant over the interval of estimation one can determine the standard deviation of the spectral estimate over the interval $\omega_2 - \omega_1$ as:

$$\sigma_{\Delta\Phi} = \frac{\langle \Delta\Phi \rangle}{\left(\frac{T(\omega_2 - \omega_1)}{2\pi} \right)^{1/2}} \quad (VI-12)$$

where $\Delta\Phi$ can be estimated by $\Delta\Phi = \int_{\omega_1}^{\omega_2} \Phi(\omega) d\omega$. In the above, T is the length of the record and $(\omega_2 - \omega_1)$ measures the resolution of the filter with which the spectrum is scanned.

One can see, therefore, that for a given length of record, the resolution and the accuracy of the spectral estimates are mutually exclusive desiderata. This reciprocal relationship provides a challenge to the experimenter to make a reasonable advance judgment which will provide the best compromise between record length and resolution. The design of the filter whose width is approximated by $(\omega_2 - \omega_1)$ poses certain problems whether the filter be numerical, as in digital procedures, or an electrical device as in analog techniques. Ideally, we would like to have a filter whose scanning window in the frequency domain is rectangular in shape, but this is impossible to achieve. The effect of measuring the spectrum in frequency bands defined by the resolution of the scanning filter is equivalent to considering the measured spectrum, $\Phi_n(\omega)$, to be the result of convolving the true spectrum, $\Phi_t(\omega)$, with a band pass filter of transfer function $Y_f(\omega)$.

$$\Phi_n(\omega) = \int_{-\infty}^{\infty} \Phi_t(\omega) Y_f(\omega - \omega_1) d\omega_1 \quad (VI-13)$$

Since $Y_f(\omega)$ passes a small amount of energy at all frequencies, we have a distortion of the true spectrum due to a diffusion of power from more or less distant frequencies. Minimizing the effects of wide filter skirts is often

a cut and try procedure in an effort to approximate the ideal rectangular shape for the filter's window. These procedures are all based in practice on assumptions of smoothness and Gaussian amplitude distributions for the measured spectrum.

The foregoing has referred to the measurement of power spectra mainly from the viewpoint of one who is using analog techniques. In using an analog device as a spectrum analyzer, the bandwidth of the spectrum analyzer must be selected so as to cover adequately the frequency range expected in the measured quantity. This remark is less obvious when digital techniques are employed, for in this case the experimenter must select his sampling interval, Δt so that $\Delta t = \pi/\omega_{ny}$ where ω_{ny} , the Nyquist or folding frequency, is the highest frequency expected in the data. If this is not done there will be an aliasing of frequency components such that one cannot distinguish sinusoids of frequency $2n\omega_{ny} \pm \omega$ where $n = 1, 2, 3, \dots$, and $0 \leq \omega \leq \omega_{ny}$.

Central to this discussion of the measurement problem is the assumption that the time series whose spectrum we desire is both stationary and Gaussian. In some instances, if the physics underlying the process by which the time series was generated is known, it is possible to state whether the series is stationary on an a priori basis. Otherwise, it is necessary to study the process itself in order to determine if observed variations among samples of the process are greater than sampling errors would predict. In this empirical examination of the process the experimenter must make a preliminary estimate of the maximum sample duration over which he can reasonably expect stationarity; and similarly estimate the minimum duration (for a selected resolution) which will yield adequate accuracy. The goodness of the Gaussian hypothesis can be tested by examining the first probability densities of the amplitude distributions of the random functions in question. In the experiments which were conducted with the F-80A simulator the best compromise between these two durations was thought to be two minutes. For this duration, and the spectrum analyzer used, $[T(\omega_2 - \omega_1)]/(2\pi)$, which Tukey has called degrees of freedom, is about 22.5. The degrees of freedom will be recognized as the square of the denominator of (VI-12).

Actually, Tukey has discussed the variability of spectral density estimates in more detail by noting that the ratio of the mean square of a spectral component to the variance of this spectral component is distributed as $\chi^2/\text{degrees of freedom}$. In other words, if we use the conventional notation $\hat{\Phi}$ to denote the true population of Φ , and f is degrees of freedom then $f\hat{\Phi}/\Phi$ is distributed as χ^2 with f degrees of freedom. He is then able to state confidence limits with considerable precision in terms of a readily available limiting distribution.

The measurement of cross spectra from paired phenomena which have a transport type delay; such as the human operator's reaction time, introduces another consideration in sampling. If the transport type delay is r seconds one must provide an analog computer of bandwidths equal to π/r to prevent a contamination of our measurements. If a digital computing technique is used the sampling interval, Δt , preferably should be less than r and at worst equal to r . The precise size of Δt depends on the desired resolution in the measurement of r .

Very little has been said about the confidence limits on cross-spectra. One can reasonably expect that computations of Y_p based on Equation (III-54), in which we compute the ratio of two cross-spectra computed from the same record, will be reasonably accurate even though the sampling variability of the individual cross-spectra may be large. This expectation is based on the assumption that the fluctuations in these two related cross-spectra are not independent. The problem of assigning sampling confidence limits to the phase and the amplitude ratio parts of Y_p , determined by (III-54), has not as yet been solved in rigorous form, although a heuristic development has been attempted and will be presented here.

Referring to the steps leading up to Equation (III-54), one can write:

$$Y_p = \frac{\Phi_{ic}}{\Phi_{ie}} = \frac{\lim_{T \rightarrow \infty} \frac{1}{T} (I^* N_c) + Y_{pt} \lim_{T \rightarrow \infty} \frac{1}{T} (I^* I)}{\lim_{T \rightarrow \infty} \frac{1}{T} (I^* I) - Y_c \lim_{T \rightarrow \infty} \frac{1}{T} (I^* N_c)} \quad (\text{VI-14})$$

Y_{pt} is the true value, and Y_p is the calculated value for the open loop pilot's transfer function.

Using the usual symbol, $\langle \rangle$, for ensemble average to denote the true values for above averages, one can write the calculated time averages as true averages plus small errors.

$$\lim_{T \rightarrow \infty} \frac{1}{T} (I^* I) = \langle I^* I \rangle + \epsilon_{ii} = \Phi_{ii} + \epsilon_{ii} \quad (\text{VI-15})$$

$$\lim_{T \rightarrow \infty} \frac{1}{T} (I^* N_c) = \langle I^* N_c \rangle + e^{j\phi_1} \epsilon_{in_c} = 0 + e^{j\phi_1} \epsilon_{in_c} \quad (VI-16)$$

In the above, ϵ_{ii} is a real quantity, but the errors associated with the complex cross-spectral estimates have imaginary components. Substituting Equations (VI-15), (VI-16) in Equation (VI-14), and estimating Y_{pt} by Y_p we obtain

$$Y_p = \frac{e^{j\phi_1} \epsilon_{in_c} + Y_{pt}(\Phi_{ii} + \epsilon_{ii})}{\Phi_{ii} + \epsilon_{ii} - Y_c e^{j\phi_1} \epsilon_{in_c}} = \frac{Y_{pt} \left(1 + \frac{\epsilon_{ii}}{\Phi_{ii}} + \frac{e^{j\phi_1} \epsilon_{in_c}}{Y_{pt} \Phi_{ii}} \right)}{1 - \frac{Y_c}{\Phi_{ii}} e^{j\phi_1} \epsilon_{in_c} + \frac{\epsilon_{ii}}{\Phi_{ii}}} \quad (VI-17)$$

Using the first order approximation for small errors

$$\frac{1 + \Delta X}{1 + \Delta Y} \approx 1 + \Delta X - \Delta Y$$

one obtains after cancellations:

$$Y_p = Y_{pt} \left(1 + \frac{\frac{1}{Y_{pt}} + Y_c}{\Phi_{ii}} e^{j\phi_1} \epsilon_{in_c} \right) \quad (VI-18)$$

One can demonstrate that if X and Y be complex random variables:

$$\lim_{T \rightarrow \infty} \frac{1}{T} (XY^*) = 0 + \epsilon_R + j\epsilon_I$$

where

$$\sigma_R = \sigma_I = \frac{1}{\sqrt{2n}}$$

and n is the number of degrees of freedom in the estimate. Arguing by analogy with Equation (VI-12) in which the denominator is the square root of the degrees of freedom of the spectral estimate, one can write

$$\sigma_{in_c} = \frac{(\Phi_{nn_c} \Phi_{ii})^{1/2}}{\left[T \left(\frac{\Delta \omega}{2\pi} \right) \right]^{1/2}} \quad (VI-19)$$

One can therefore rewrite Equation (VI-18) as

$$Y_p = Y_{pt} \left[1 + \frac{\left(\frac{1}{Y_{pt}} + Y_c \right) \sqrt{\Phi_{nn_c} \Phi_{ii}}}{\Phi_{ii} \left[T \left(\frac{\Delta \omega}{2\pi} \right) \right]^{1/2}} \right] \frac{\epsilon_R}{\sqrt{2}} + j \frac{\epsilon_I}{\sqrt{2}} \quad (VI-20)$$

The ϵ 's are random variables for which $\bar{\epsilon} = 0$, $\bar{\epsilon^2} = 1$, so that $\epsilon_R + j\epsilon_I$ is distributed circularly on the Y_p plane.

In order to obtain phase and amplitude standard deviations, rewrite Equation (VI-20) in a simpler form so that

$$Y_p = Y_{pt} (1 + k_1 + jk_2)$$

where k_1 and k_2 are small. One can then write, since the small change in magnitude of Y_{pt} orthogonal to its length is negligible:

$$|Y_p| e^{j\angle Y_p} = |Y_{pt}| e^{j\angle Y_{pt}} [1 + k_1 + jk_2] \approx |Y_{pt}| e^{j\angle Y_{pt}} [1 + k_1] e^{jk_2}. \quad (VI-21)$$

Similarly one can equate real and imaginary parts in (VI-21) and obtain:

$$\angle Y_p = \angle Y_{pt} + k_2. \quad (VI-22)$$

Hence k_1 is the error in magnitude and k_2 the error in phase. The net result is that the sampling standard deviation in AR is:

$$\sigma_{AR} = |1 + Y_c Y_{pt}| \sqrt{\frac{\Phi_{nn_c}}{\Phi_{ii}}} \frac{1}{\left(T \frac{\omega}{n}\right)^{\frac{1}{2}}}, \quad (VI-23)$$

and the sampling standard deviation for phase is:

$$\sigma_\phi = \left| \frac{1}{Y_{pt}} + Y_c \right| \sqrt{\frac{\Phi_{nn_c}}{\Phi_{ii}}} \frac{1}{\left(T \frac{\omega}{n}\right)^{\frac{1}{2}}}. \quad (VI-24)$$

In order to compute the total standard deviation in phase and AR one must combine the variances due to instrumentation and computer errors, σ_i^2 , and sampling errors, σ_s^2 , so that:

$$\sigma_z^2 = \sigma_i^2 + \sigma_s^2 \quad (VI-25)$$

In general, it will be easier to measure the quantity σ_z^2 from known inputs rather than to attempt to estimate the effects of the various measurement errors on the total standard deviation. It is advantageous to be able to compute (VI-25) so that a priori statements can be made about the possibilities of resolving desired differences in Y_p with a given experimental design. Unfortunately, we must have information about the form of Φ_{nn_c} , which is difficult to estimate prior to an experiment. As a practical matter, an a posteriori computation of σ_z^2 from the collected data is the most convenient method for assessing the significance of findings for which adequate number of measurements of Y_p exist.

If, however, we are comparing a small number, or perhaps unique measurements of Y_p , with one another, and we would like to be able to discuss the statistical significance of these comparisons, then an effort to compute (VI-25) is necessary.

Equations (VI-23) and (VI-24) enable us to make quantitative judgment about the accuracy of phase and AR estimates which are extended beyond the nominal bandwidth of the input $i(t)$. Since Φ_{ii} is 9 db down at the corner frequency, which defines the nominal bandwidth, and attenuates at 18 db/octave thereafter, one can see from Equations (VI-23) and (VI-24), that if Φ_{nn_c} is either flat or attenuates at a moderate rate, the confidence bands about our data will spread as ω approaches and exceeds the cut-off frequency of the input $i(t)$. Equation (III-36), which relates Φ_{nn_c} to Φ_{cc} , indicates that Φ_{cc} , which could hardly be expected to attenuate as rapidly as Φ_{ii} , might very well influence Φ_{nn_c} so as to create an approximately flat spectrum. Further on in this report (Figure 107) we will see that this is actually the case for azimuth or lateral control although not quite the case for elevation or longitudinal control.

A further characteristic of the measuring process, which tends to deteriorate the quality of the data, involves a paradox of sorts. If the input forcing function and the controlled element dynamics are such that the tracking task is simple; i.e., the rms tracking error is very small, then our measurement of Y_p , the open loop transfer function, is subject to rather large errors. This condition arises from the fact that we measure the open loop transfer function as follows: $Y_p = \Phi_{ic}/\Phi_{ii}$. As a consequence if $\epsilon(t)$ be small and of the same order of magnitude as instrumentation and computer errors, measurements will be confounded by noise. The closed loop measure of the pilot's transfer function Φ_{ic}/Φ_{ii} computation is not affected by small values of $\epsilon(t)$, since we only need to measure the cross spectrum, Φ_{ic} , and the input spectrum Φ_{ii} . In the F-80A simulator tracking problem, one cannot blithely

assume that, by dint of the foregoing argument, the more difficult the task the better the measure of Y_p . In the more difficult tasks, which are characterized by high input amplitudes and bandwidths, not only does the linear model on which Y_p is based become less pertinent to tracking behavior but the task may begin to lose verisimilitude, and the pilot begins to play a game rather than accept our innocent deception. In such a case, we would expect greater variability among pilots since we would no longer be comparing the pilots with regard to their ability to fly jet aircraft which is the common characteristic making pilots a stratified sample. The foregoing intuitive reasoning yields the conclusion that our best data are those obtained for an Φ_{ii} bandwidth of 2 radians/second and an rms input amplitude of 0.2 to 0.8 inches. Indeed, it has been the case that the bulk of our usable data was measured with these inputs.

4. The Data Reduction Equipment

The earliest data obtained from the F-80A simulator and previously reported [2] were analyzed on a device designed following a principle suggested by J. W. Tukey. The present data were analyzed on a device whose design derives from the procedure used by J. I. Elkind, and independently developed by F. B. Smith and others at NACA, Langley. [3, 23, 74]

The general analog procedure for computing cross-spectra from cross-correlations is first to multiply the two input functions at various time lags. The average product at each lag, which is the cross-correlation, is then passed through a narrow band filter to find each point on its Fourier transform.

By properly changing the order of these procedures the cross-spectrum will still be computed, but without the necessity for intermediate storage of the cross-correlation. The following describes the computer to analyze the F-80A simulation data [3]. First the narrow band filter was used on the input functions, the resulting narrow band functions were multiplied, and the average product over the length of the input record was then determined. To follow this description exactly, we should have the narrow band functions in complex form and average both the real and imaginary parts of the product to find the real and imaginary parts of the cross-spectrum. In practice one filtered function was shifted in frequency, so that the real and imaginary parts occurred as in-phase and quadrature components about some suppressed carrier. These were phase-sensitive detected before being put into a low-pass filter for averaging. In the NACA analyzer the same result was obtained by phase shifting the narrow band function outputs of the filter before multiplying. One multiplier output was then averaged to give the real part, and another multiplier was used for the imaginary part of the cross-spectrum where the zero-beat part of the multiplier output corresponds to the detector output in the Franklin Institute analyzer.

The narrow band filters used were identical and fixed. The frequency of the signal component passing through the filter was varied by a heterodyne scheme. One of the filter outputs was further heterodyned with a fixed oscillator. The carrier was completely suppressed in the second mixer. The output of this second mixer was multiplied with the output of the other filter to give an output whose frequency is that of the fixed oscillator, and whose in-phase and quadrature amplitudes are very short time estimates of the cross-spectrum. We now computed the average values of the in-phase and quadrature components of the multiplier output. In order to average conveniently, using d-c amplifiers, these two components of the multiplier output were converted to low frequency signals by two phase-sensitive detectors which are driven by the fixed oscillator. The d-c levels of these two signals, averaged over the run length of two minutes in real time, were the desired outputs. They represent the real and imaginary parts of the cross-spectrum. A block diagram of this scheme is shown in Figure 86, and a photograph of the equipment is shown in Figure 87.

The inputs to this cross-spectrum analyzer were frequency modulated signals recorded by means of a modified Ampex 306 on $\frac{1}{2}$ inch magnetic tape at $1\frac{1}{4}$ inches per second and played into the analyzer at 60 inches per second in the F-80A studies. The maximum speed-up ratio obtainable with the record and playback equipment was 32:1, and this speed up ratio was used for F-80A data, but 16:1 and 8:1 ratios have been used for other purposes. In analyzer time, the system's bandwidth is 600 cycles, and the width of the narrow band scanning filter is 6 cycles. In order to validate the performance of the analyzer under conditions as closely analogous to the conditions under which Y_p was measured, the following circuit was used.

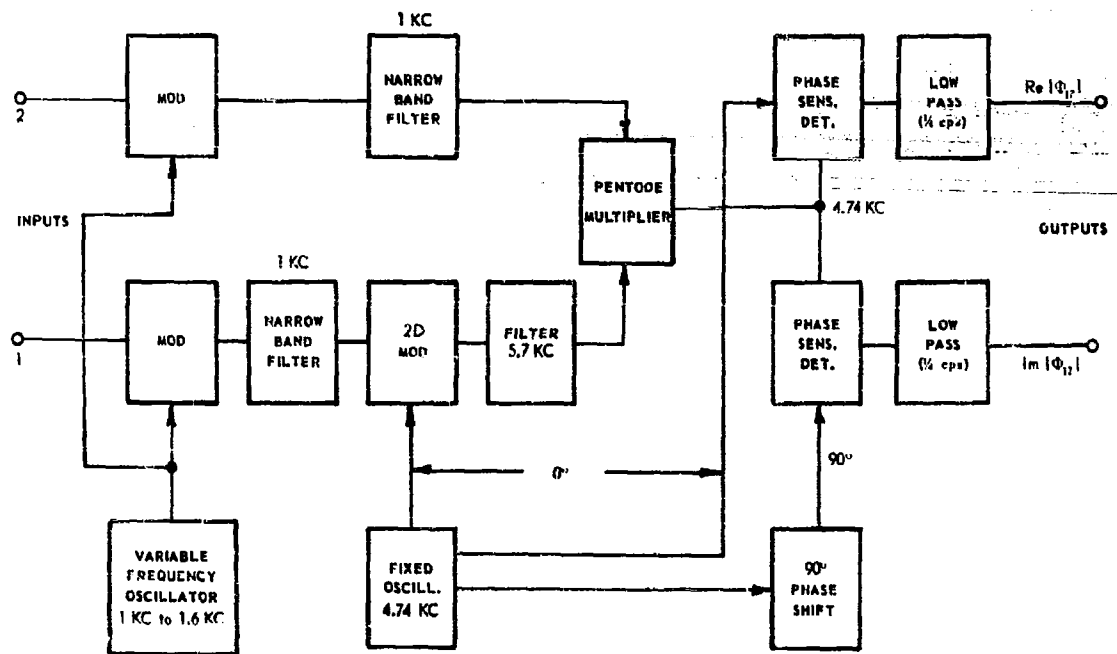


Figure 86. Block Diagram of the Cross-Spectrum Analyzer.

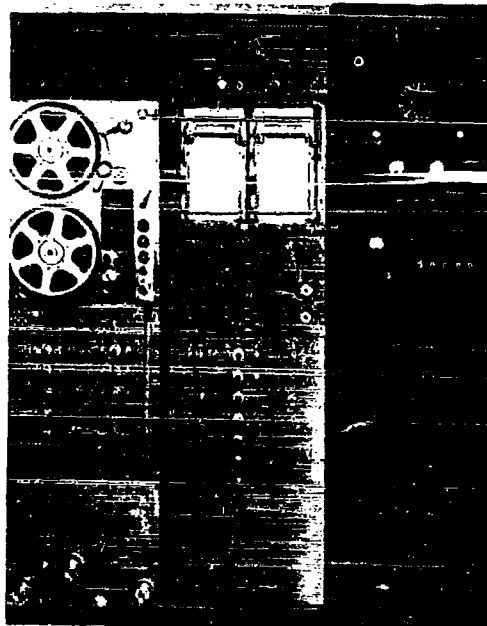
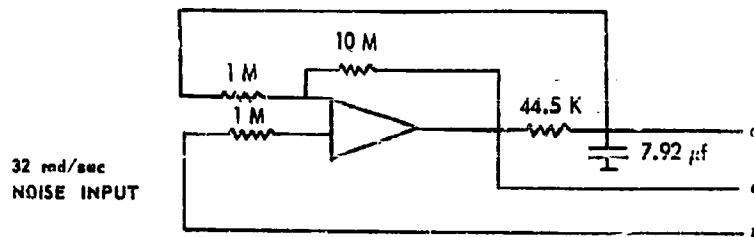


Figure 87. Cross Spectrum Analyzer.



The calculated magnitude and phase of the filter Y_F are plotted on Figure 88 and given by

$$Y_F = 0.46 \left(\frac{1}{1 + \frac{j\omega}{6.6}} \right)$$

A measure of $Y_p = \Phi_{ic}/\Phi_{ie}$ which is analogous to the open loop pilot transfer function, Y_p , was obtained from the cross-spectrum analyzer by using a 32 radian/second noise source input directly, and by-passing the record and playback speed-up system. The measured points are to be found on Figure 89.

In addition, a large number of measurements of $H = \frac{Y_F}{1 + Y_F} = \frac{\Phi_{ic}}{\Phi_{ii}}$, which are analogous to measurements of the closed loop transfer function H have been made using the tape recorder speed-up system, and their accuracy is the same as Figure 88 indicates for the open loop measurements. These results were very stable for many repetitions made over a period of six months.*

One additional test was made of the cross spectrum analyzer's performance. A simple handwheel tracker, which had a small amount of mechanical inertia, was used to track an input of 4 radians/second bandwidth. The controlled element transfer function was approximately $Y_c = 1$. The closed loop transfer function, $H = Y_c/(1 + Y_c)$, since $Y_c = 1$, was measured by Φ_{ic}/Φ_{ii} . A tracking record for $i(t)$ and $c(t)$ of two minutes duration was produced by a highly experienced operator, and was recorded simultaneously both on magnetic tape and in digital form. The digital data were accurate to three significant decimal digits and were produced at a sampling rate of 2 samples/sec. The data on magnetic tape were reduced with the Franklin Institute cross spectrum analyzer to obtain Φ_{ic}/Φ_{ii} . The digital data were used to compute Φ_{ic}/Φ_{ii} on a desk calculator using eight lags. The raw spectral estimates were smoothed by Tukey's running weighted average of weights 0.23, 0.54, and 0.23 [80]. Figure 89 shows the digital computations of phase and amplitude ratio as solid lines with the analog determinations as unconnected points. The spectral densities were not computed at identical frequencies, which explains the frequency displacements between analog and digital determinations on Figure 89. Figure 89 illustrates that the cross spectrum analyzer errors are fairly random, and that the device produces acceptable linear transfer functions.

5. Measured Describing Functions

We shall present the results of the previously described experiments in the following manner. Experimental parameters will be removed by averaging in a successive fashion until smooth Bode plots for Y_p , characterizing the three input bandwidths, remain. These grand average curves will then be fitted by following a stated procedure, and analytic approximations to Y_p obtained.

The first set of data is found on Figures 90 through 95, and presents Bode plots for elevation and azimuth control for pilots P-1, P-2, P-3, P-4, P-5, and P-6.

* While these results indicate that the accuracy of transfer function measurements with the equipment is quite good, we should also note that these same measurements revealed possible bias errors in the ρ values. These were on the low side, i.e., measured ρ is less than the actual. Therefore one should not place too much confidence in the values of ρ and derived remnant quantities shown later.

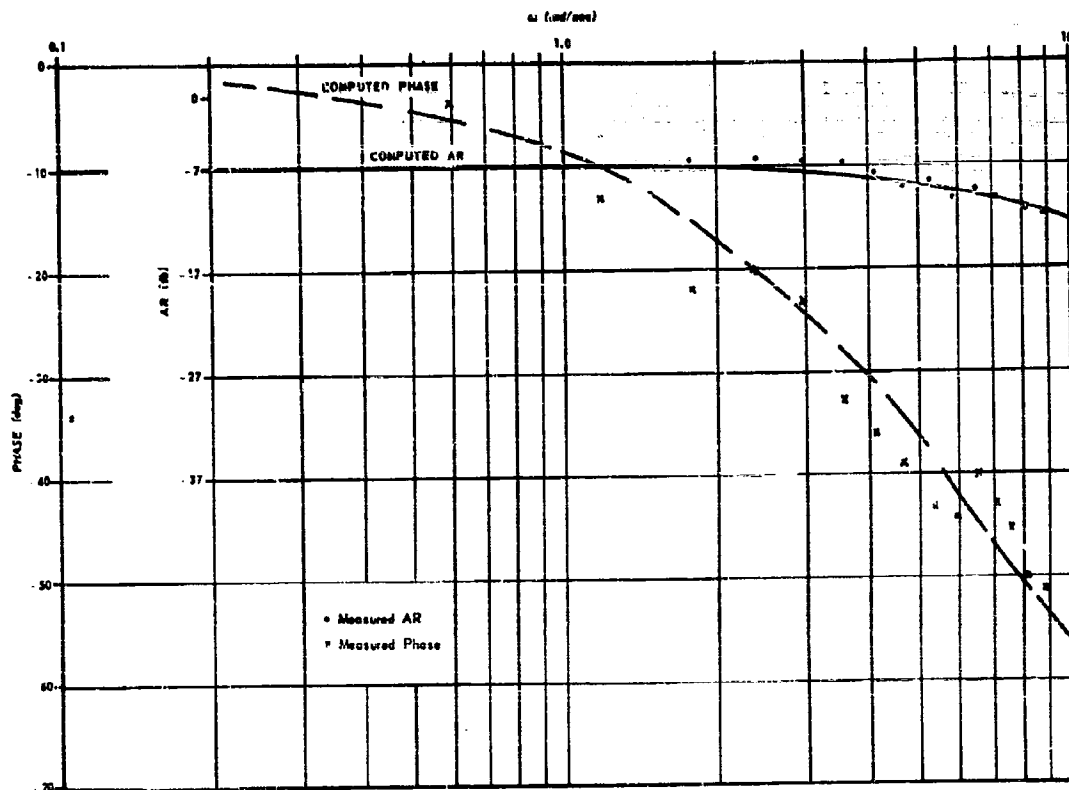


Figure 88. Comparison of H Computed with H Measured by the Cross Spectrum Analyzer.

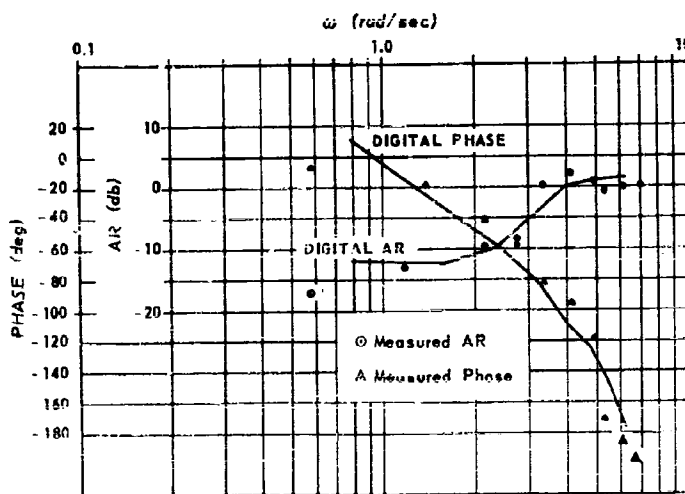


Figure 89. A Comparison of H for a Human Operator Measured by Digital and Analog Methods.

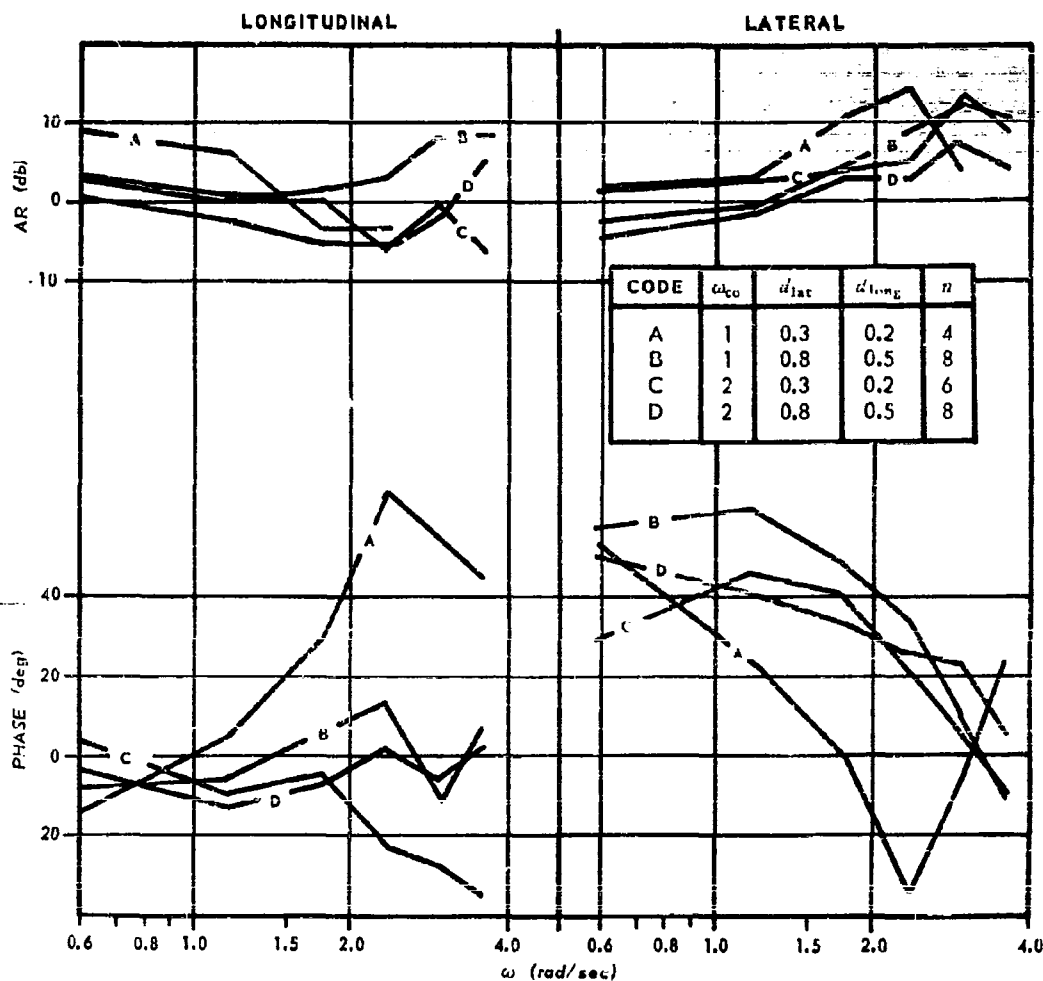


Figure 90. F-80A Simulator Open Loop Describing Function for Pilot P-1.

In the legend for these and all subsequent figures the forcing function bandwidth, or corner frequency, is ω_{co} in radians/second, the rms amplitude of the forcing functions is d in inches, and the number of runs contributing to each average is n . In averaging these curves the various experimental effects such as might arise from satiation, habituation, and any possible time or order effects were ignored since these effects did not manifest themselves in a discriminable fashion in the Bode plots obtained from individual two minute records. These first data are the most highly differentiated descriptions of pilot performance which we will present. An examination of Figures 90 through 95 reveals the following:

- (a) both the controlled element and the input signal bandwidth are strong influences on the form of Y_p ;
- (b) the input amplitude, as it was varied in our procedure, is a relatively weak influence on Y_p .

The straightforward procedure for examining the effects of forcing function input characteristics, controlled element, and subjects, on the describing function would be to perform an analysis of variance. Such an analysis involves the computation of variances from various experimentally defined groupings of samples which

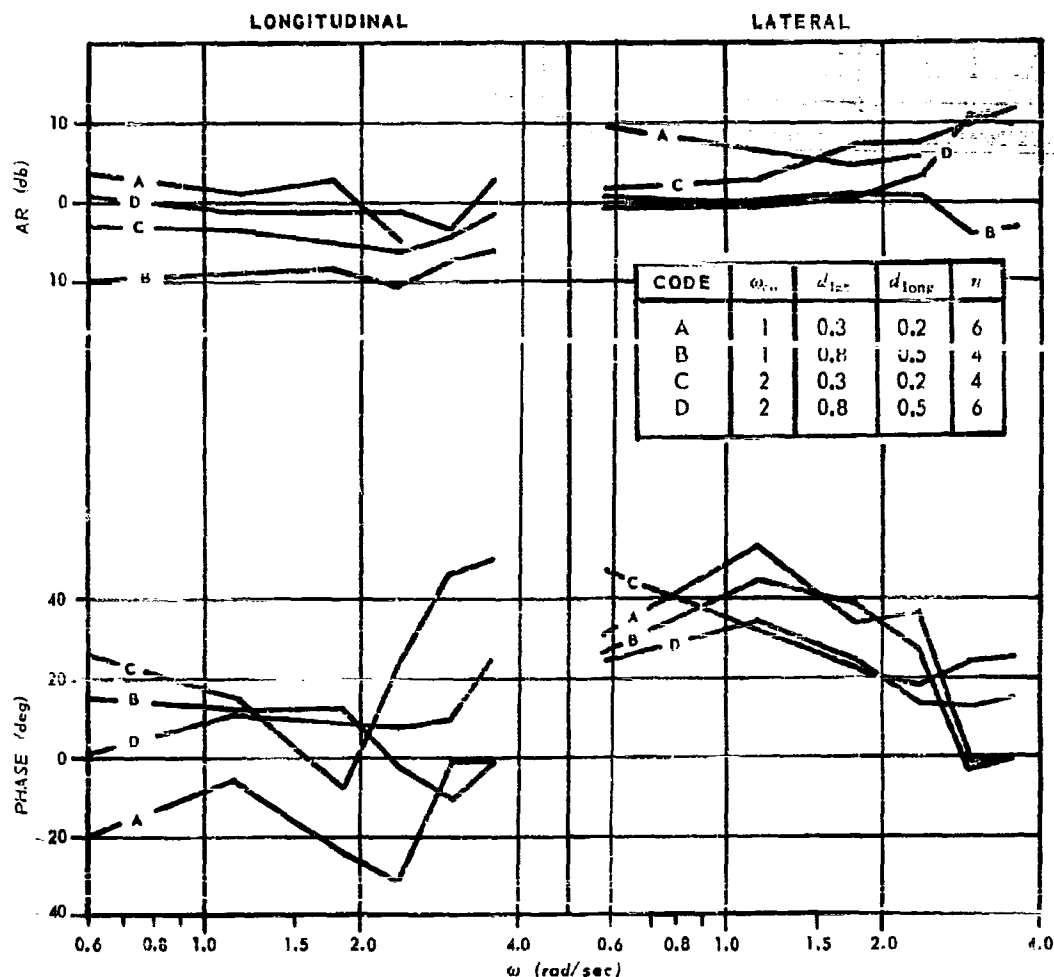


Figure 91. F-80A Simulator Open Loop Describing Function for Pilot P-2.

are characterized as follows:

- (a) They are drawn at random from normal populations.
- (b) These normal populations all have the same variance.

Although condition (a) was fulfilled for the Franklin F-80 data, an F test demonstrated that condition (b) was not met. Consequently the following types of statistical tests were implied.

Trends were examined by " t " tests to determine whether means were progressively decreasing or increasing as a function of some independent variable. Since hypothesized inequalities were often examined, one sided " t " tests were appropriate in general. Due to the occasional small samples, and the inequality of variances, special forms of " t " test were indicated. In order to obtain even small samples of describing function estimates it was necessary to average together data from experimental runs obtained under different conditions. In fact, since the rms amplitude of the forcing function input appeared to be a weak influence on Y_p as indicated by Figures 90 through 95, significance tests were made on the differences of the means for $|Y_p|$ and ϕ for 0.3 and 0.8 and

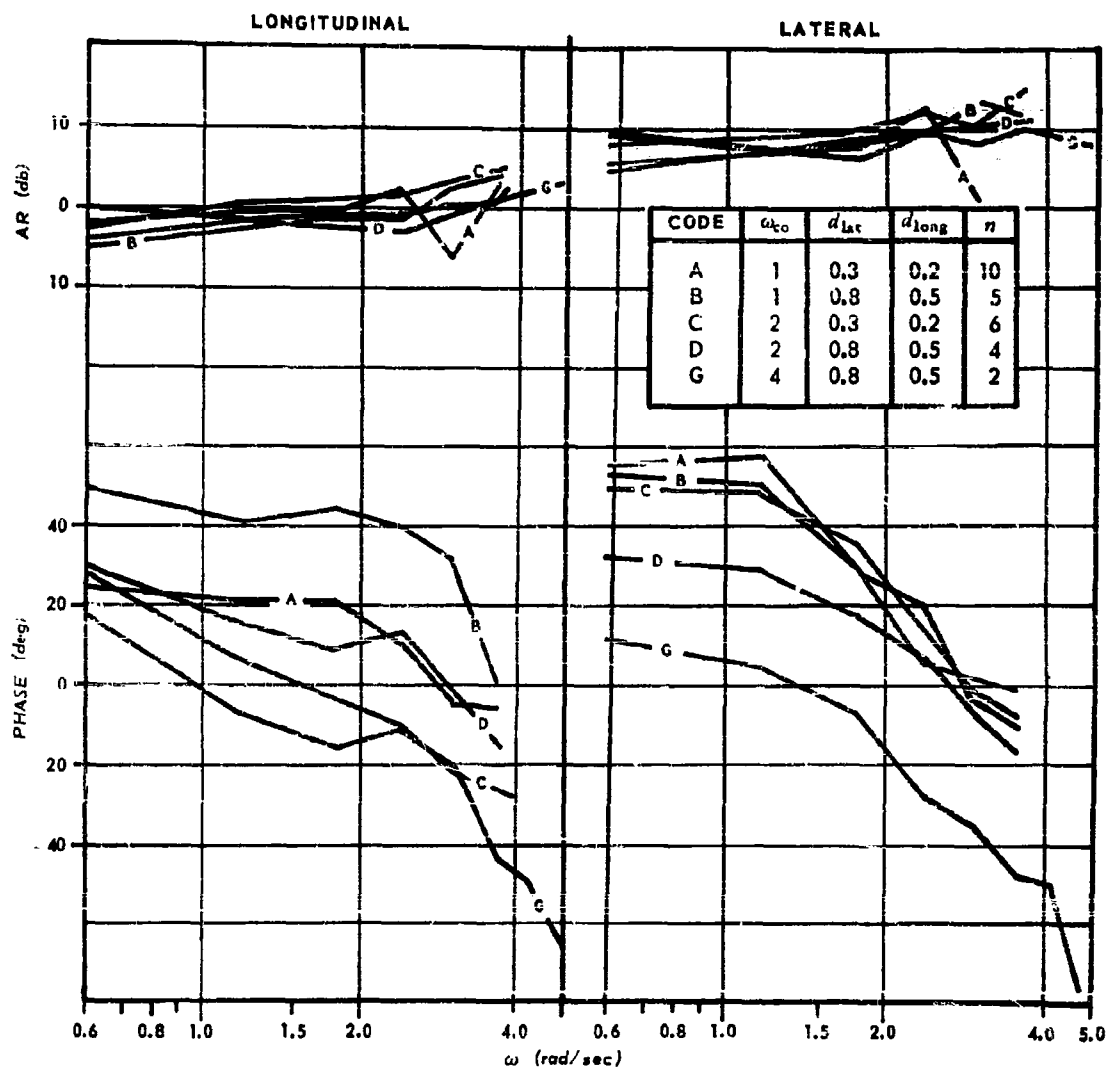


Figure 92. F-80A Simulator Open Loop Describing Function for Pilot P-3.

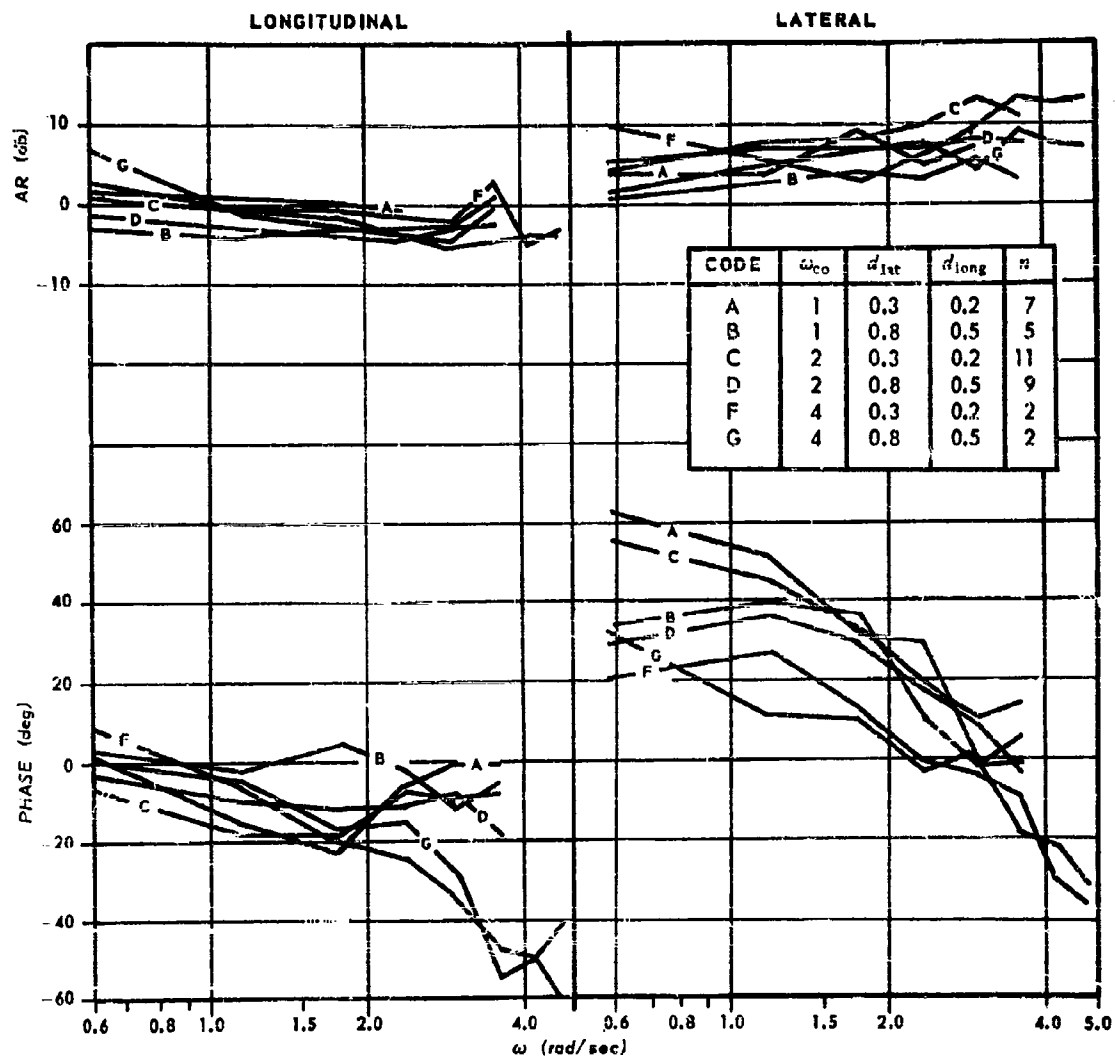


Figure 93. F-80A Simulator Open Loop Describing Function for Pilot P-4.

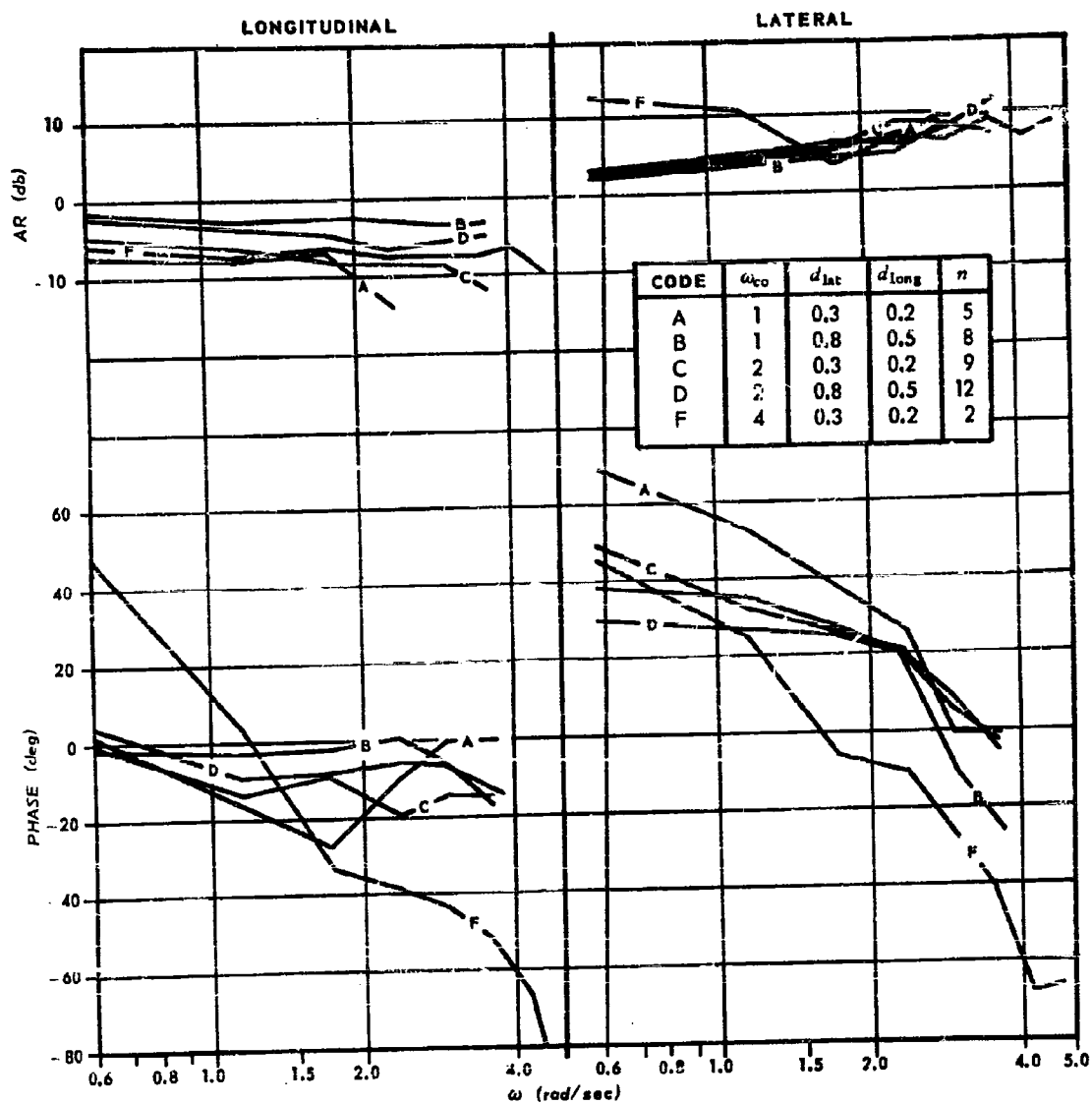


Figure 94. F-80A Simulator Open Loop Describing Function for Pilot P-5.

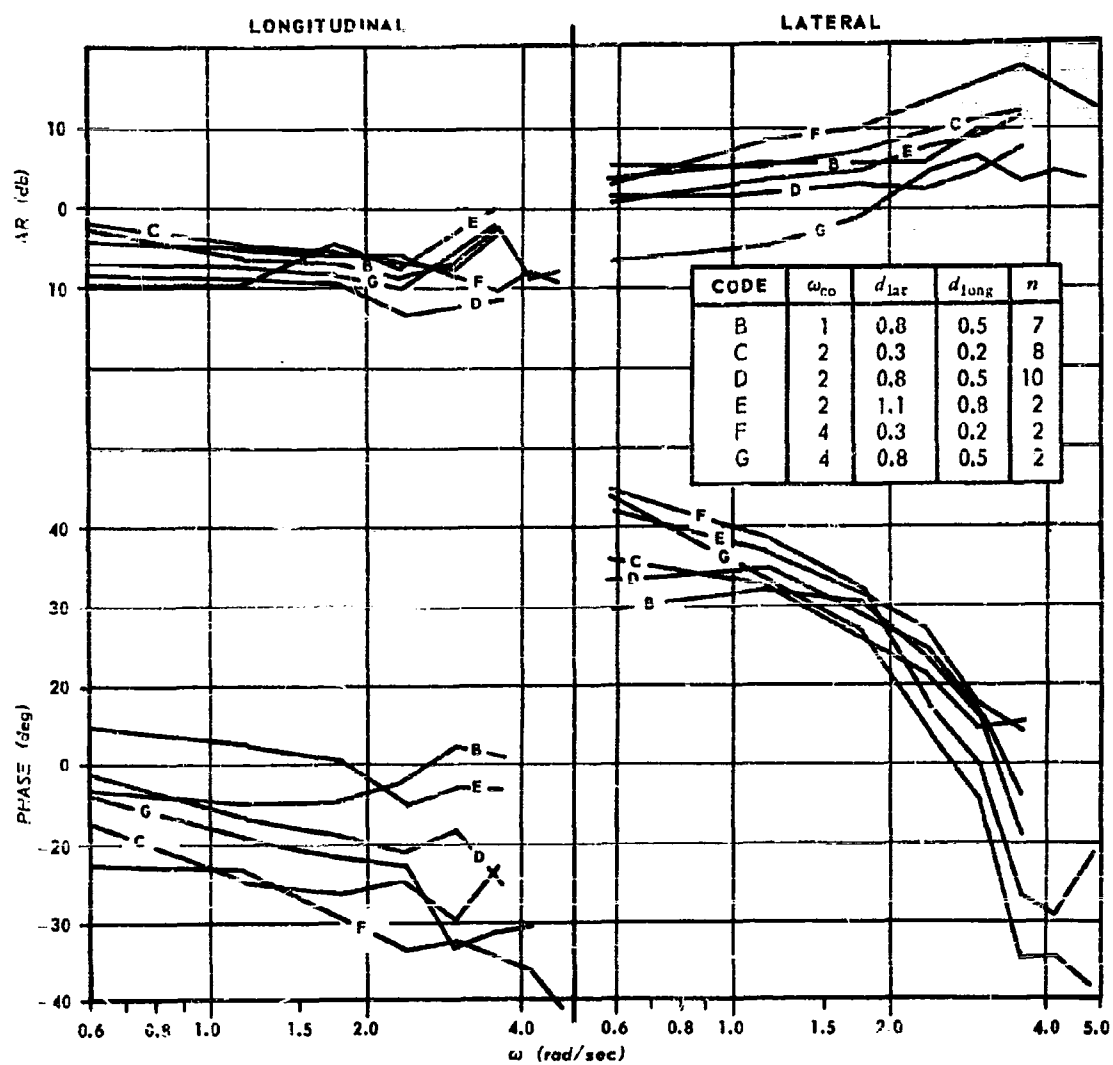


Figure 95. F-80A Simulator Open Loop Describing Function for Pilot P-6.

0.2 and 0.5 inches rms amplitudes in lateral and longitudinal control respectively. Although there were clusterings of significant differences for individual pilots in ϕ or $|Y_p|$, these were about what would be expected by chance at the 0.1 level when the population of pilots was considered as a whole.

As a result of this test, Figures 96 through 99, which present the results of averaging input amplitudes are presented. There were so few $\omega_{co} = 4$ rad/sec runs that they are not presented in these figures. Although the foregoing procedure has the advantage of simplifying the data presentation considerably, it has the unavoidable effect of increasing the total variance in the various estimates for Y_p . This increase in variance serves to obliterate many details which the experiments had been designed to resolve. However, such clear and striking effects as the pilots adaptation to Y_c were significant and manifest despite increases in variance.

Some idea of the differences between pilots can be obtained from Figures 96 through 99 by noting the 2σ confidence bands. An effort to quantify the differences in averaged describing function Bode plots for individual pilots was made by comparing highly similar and highly dissimilar Bode plots for $\omega_{co} = 1$ rad/sec. Comparing pilots P 4, P 5, and P 6 there were no significant differences at the 0.10 level for $|Y_p|$ in lateral and longitudinal control. For pilots 3 and 6, who generated markedly different Bode plots, there were 3 differences out of a possible 6 which were significant at the 0.02 level for $|Y_p|$ in lateral control and two differences out of a possible 6 which were significant at the 0.1 level in ϕ for lateral control. Pilots 1 and 3 demonstrated 5 out of 6 possible differences to be significant for $|Y_p|$ in longitudinal control at the 0.02 level, and 3 out of 6 possible differences were significant at the 0.02 level for ϕ in lateral control. This analysis was too cumbersome to carry out much further and the large variances associated with our small sample measurements made detailed statistical analyses inappropriate.

In Figures 100 and 101 we present grand averages with 2σ bands about these averages for all six pilots for each of the three input bandwidths and two controlled elements. Azimuth, or lateral, control is presented in Figure 100, and elevation, or longitudinal, control in Figure 101.

In order to determine the significance of the trend in Figures 100 and 101 for ϕ to decrease for any given measurement frequency, ω , as the input forcing function bandwidth, ω_{co} , increases a series of "t" tests was performed. Tests were made for the significance level of the inequalities $\bar{\phi}_1 > \bar{\phi}_2$, $\bar{\phi}_1 > \bar{\phi}_4$ and $\bar{\phi}_2 > \bar{\phi}_4$, where the subscripts refer to the values of ω_{co} . Table 9 presents the results of these tests. The fact that Table 9 confirms the visually apparent trend is all the more convincing in view of the high variances associated with these phase averages. A similar analysis was performed on $|Y_p|$ but the results showed only five differences, two of which were in the predicted direction. This is what one would expect by chance alone on a two tailed "t" test at the 0.1 level. The conclusion shown was that $|Y_p|$ was not a function of ω_{co} .

The averages in Figures 100 and 101 are the basis of the curves fitted to the describing function data for the purpose of getting analytic approximations to Y_p .

The actual fitting procedures were based on the following considerations:

- (a) The pilot-airframe (simulator) system was stable.
- (b) The controlled element characteristics (airframe transfer function) required the operator to develop lead in certain specific frequency ranges, either for stability or for low frequency performance reasons.
- (c) The simplest fit consistent with the data should be used, though an e^{-Ts} would always be required.
- (d) The value of T should not be restricted or assumed, though it should be greater than 0.1 seconds. Since the subject and general situation was the same for all of an individual's runs, and the subject was presumably not exposed to preconditioning of any sort other than general instructions, one should be safe in assuming that the value of T obtained should not be an extreme function of bandwidth. This latter point was not taken for granted, however, being subject to a check of sorts.

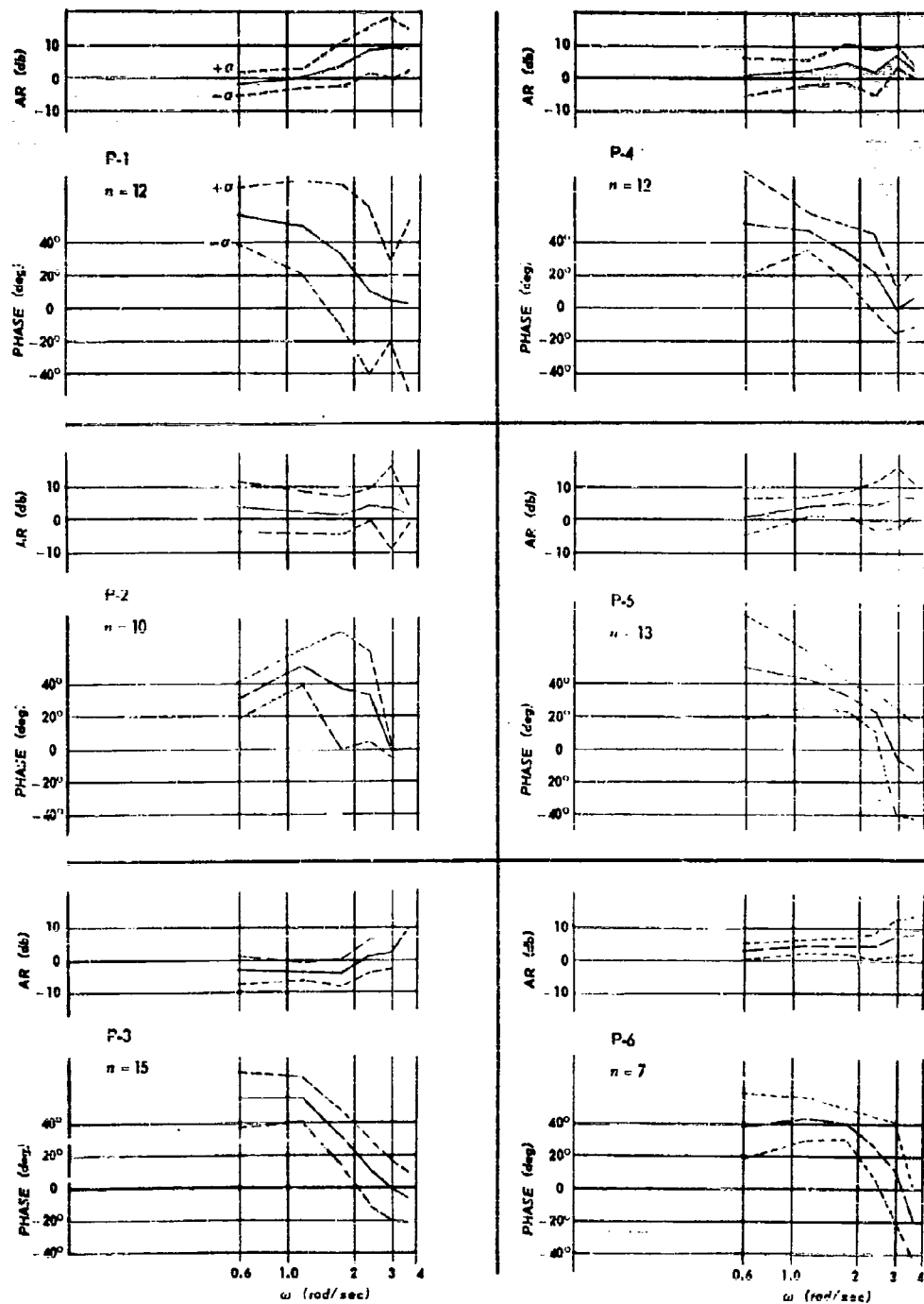


Figure 96. F-80A Simulator Y_p with $\pm\sigma$ Confidence Bands (Lateral; $\omega_{co} = 1$ rad/sec).

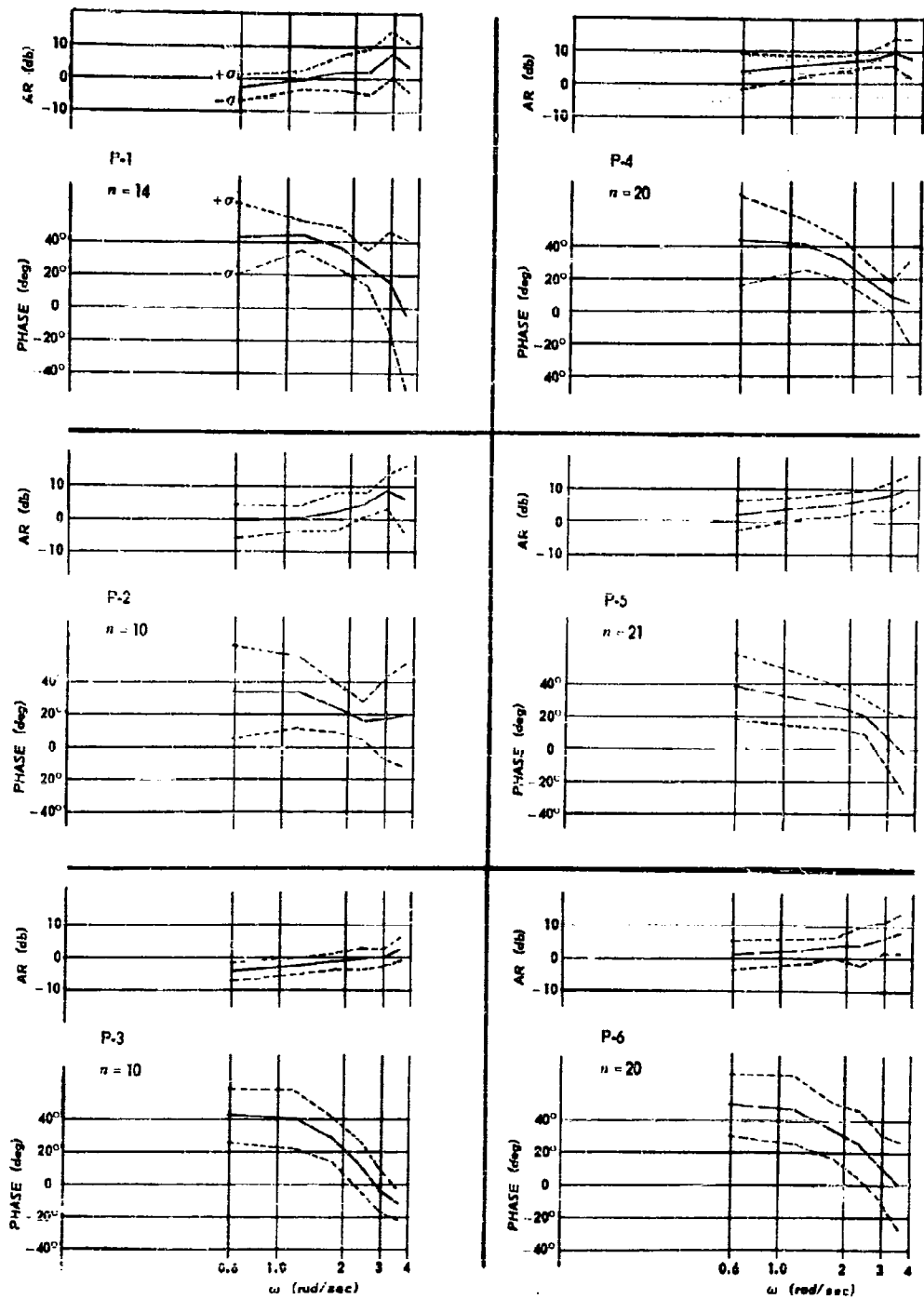


Figure 97. F-80A Simulator Y_p with 1σ Confidence Bands (Lateral; $\omega_{td} = 2$ rad/sec).

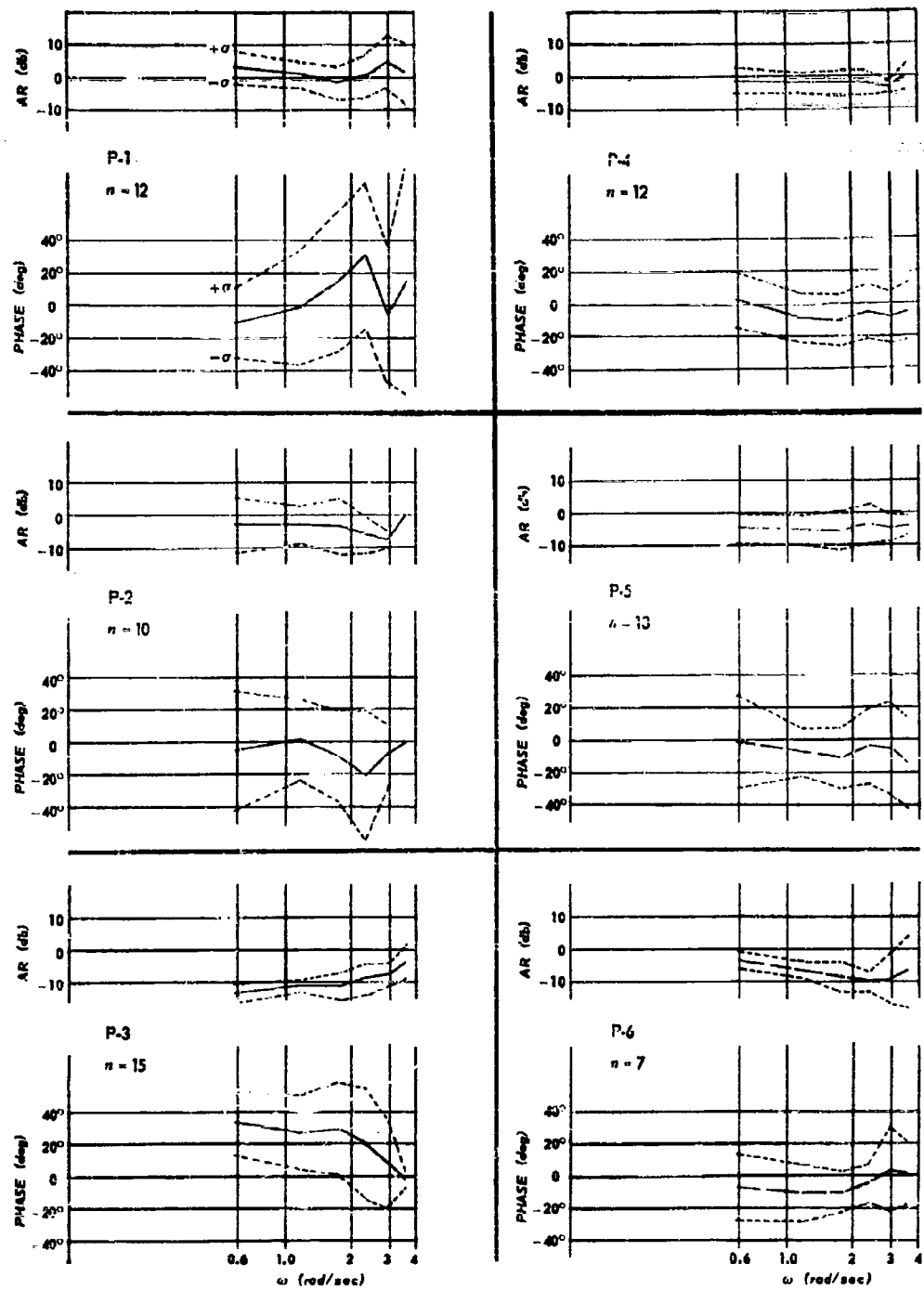


Figure 98. F80-A Simulator Y_p with 2σ Confidence Bands (Longitudinal; $\omega_{k0} = 1$ rad/sec).

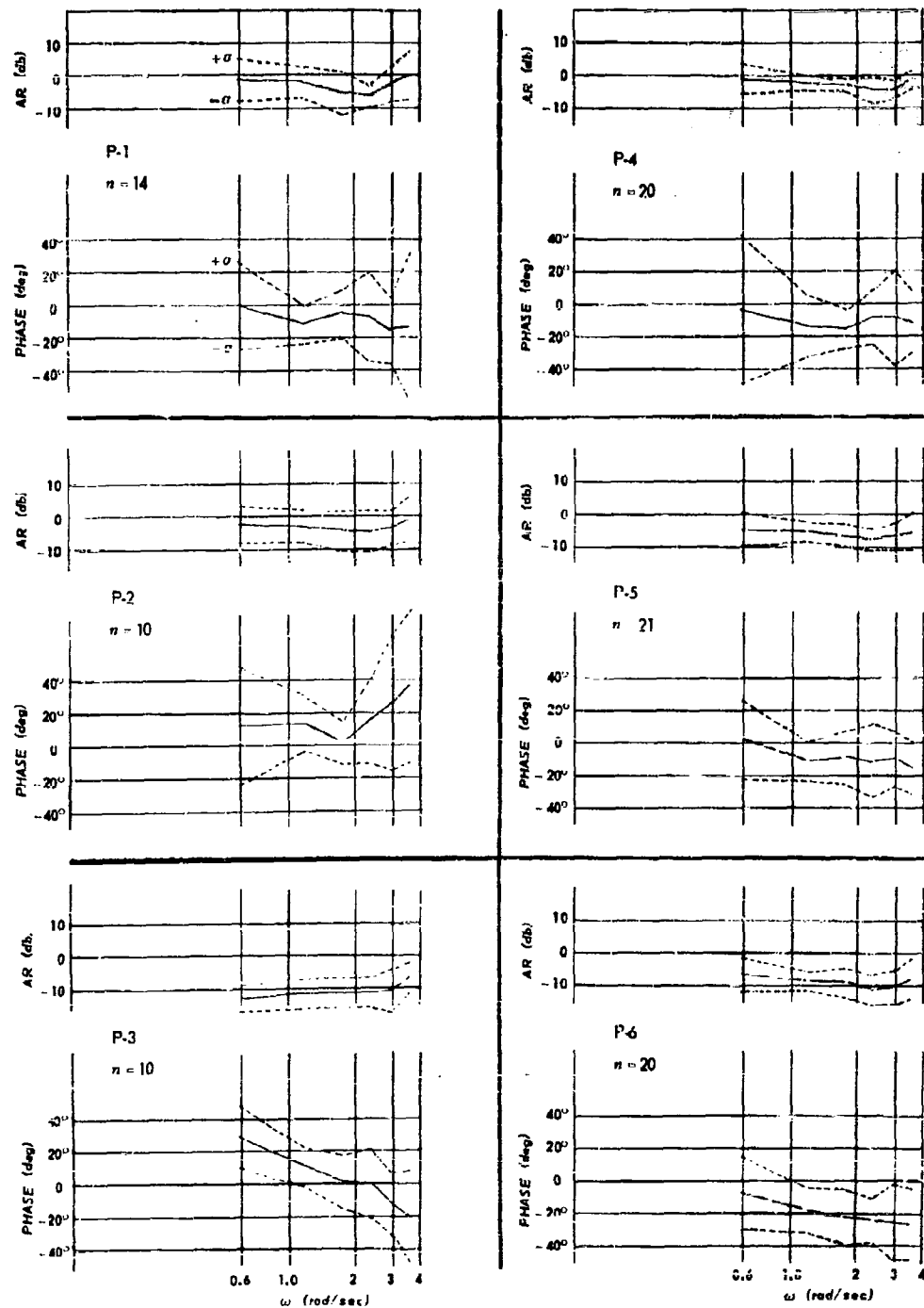


Figure 99. F80-A Simulator Y_p with 1σ Confidence Bands (Longitudinal; $\omega_{co} = 2$ rad/sec).

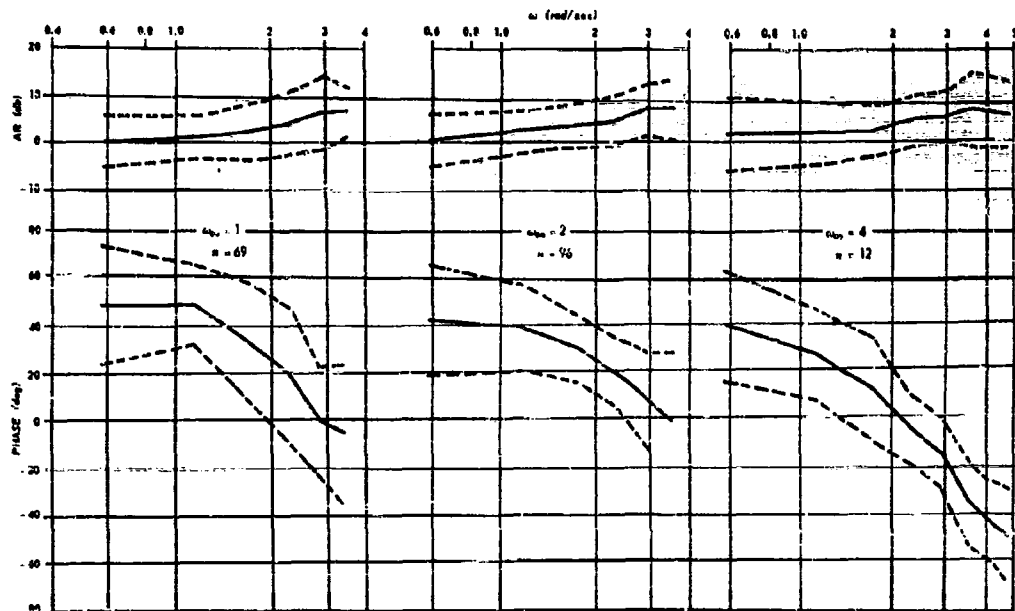


Figure 100. F-80A Simulator Grand Averages for Y_p in Azimuth Control.

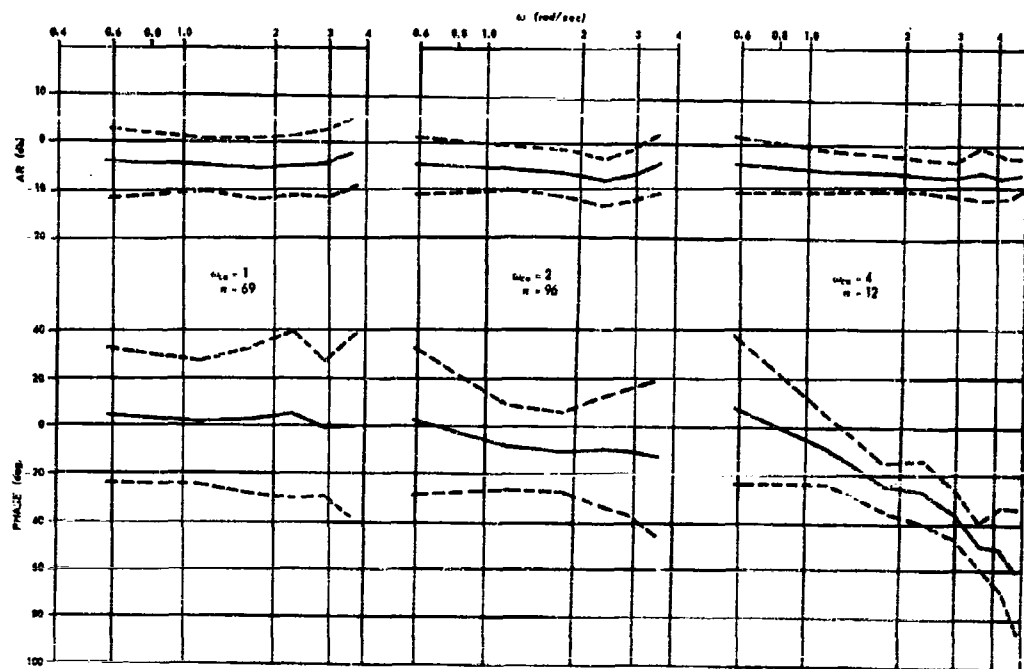


Figure 101. F-80A Simulator Grand Averages for Y_p in Elevation Control.

Table 9. Significance Levels for Three $\bar{\phi}$ Inequalities.

CODE: $\bar{\phi} = \angle Y_p$; $\phi_A = \phi_{\omega_{co}} = A$

ω rad/sec	LATERAL CONTROL MODE			LONGITUDINAL CONTROL MODE		
	$\bar{\phi}_1 > \bar{\phi}_2$	$\bar{\phi}_1 > \bar{\phi}_4$	$\bar{\phi}_2 > \bar{\phi}_4$	$\bar{\phi}_1 > \bar{\phi}_2$	$\bar{\phi}_1 > \bar{\phi}_4$	$\bar{\phi}_2 > \bar{\phi}_4$
0.6	n. s.	n. s.	n. s.	n. s.	n. s.	n. s.
1.2	.01	.01	.025	.01	n. s.	n. s.
1.8	n. s.	.01	.01	.01	.01	.01
2.4	n. s.	.01	.01	.01	.01	.01
3.0	†(.01)	.05	.01	.025	.01	.01
3.6	n. s.	.01	.01	.05	.01	.01

† Denotes a significant inequality in an opposite sense from the column heading.

The initial step of the detailed fitting procedure, since an e^{-Ts} was necessary from a general consideration of the amplitude ratio and phase curves, was the construction of a series of families $\phi_{p,i,r} = r\omega$ for various values of r . This was done to determine an allowable range of values for simple fits, and the general type of fit required. From this step it was determined that

- (1) The simplest possible form of transfer function consistent with all the F-80A simulator data was

$$Y_p(s) = \frac{K_p e^{-Ts} (aTs + 1)}{Ts + 1} \quad (\text{VI-26})$$

As has been pointed out previously the above form has the disadvantage of not approaching zero as s becomes infinitely large. Should we assume that the describing function is of the form shown in Equation (V-24), $Y_p(j\omega)$ approaches 0 as $j\omega \rightarrow \infty$. It should be understood, however, that our fits are not meant to be naively extended beyond the range defined by the measured points nor should one lose sight of the fact that the measured points are the basic data. In addition, since an appropriate selection of the four constants in Equation (VI-26) in accordance with the following considerations results in a stable pilot aircraft system, a principle of parsimonious description would argue against adding a high frequency lag of Equation (V-42) to Equation (VI-26). If, on the other hand, it is desirable to follow a principle of consistency with a larger body of data and theory, then following the Eq. (V-42) form is indicated. Although the present development presupposes the form of Equation (VI-26), the utility of the Equation (V-42) form is examined later on.

- (2) With all three input bandwidths considered, the value of r must be larger than 0.20 seconds and equal to or less than 0.30 seconds if the form of Equation (VI-26) is accepted.

Data for amplitude ratio and phase were then examined in detail. This examination revealed that:

- (1) The dc gain K_p is essentially the same for all three bandwidth conditions.
- (2) The values of a are in the sequence $a_1 > a_2 > a_4$ (rad/sec).
- (3) In general, the amplitude ratio of the pilot data indicated that the lead break $(1/aT)$ should occur in the region of $1 < (1/a)T < 2.5$ rad/sec for elevation control and in the region $2 < (1/a)T < 5$ rad/sec for azimuth control. This conclusion checked nicely with intuitive notions about "requirements" imposed upon the operator by the airframe transfer function.

The conclusions of the foregoing were then rechecked with the residual phases of the $\phi_{pilot} + r\omega$ plots. This resulted in the selection of a $r = 0.25$ seconds as an excellent value consistent with all of the above work for all three cases. With r selected, and the above points kept in mind, the final fits were made.

The fitted forms obtained above, and the original data points were then added to a Bode plot of the airframe transfer function to make certain that the overall system was stable.

The results of the foregoing fitting procedure are shown on Figures 102 and 103. When the fitted analytic forms are added to Figure 85 we have nearly neutral stability in the region of the aircraft's resonant frequency in lateral response of 3.8 radians/second. When the measured values of Y_p for lateral response are plotted on Figure 85, we have good stability over the entire measured range. One can see from Figure 86, however, that stability is not an important criterion in longitudinal control. It is comforting to find that, after boiling the data down to just three Bode plots for lateral and for longitudinal control, these averaged data are consistent with the demands the controlled element imposes on the pilot. In a sense, this consistency, which implies an equalizing function on the pilot's part, justifies many of the debatable manipulations to which the data were subjected enroute to this point.

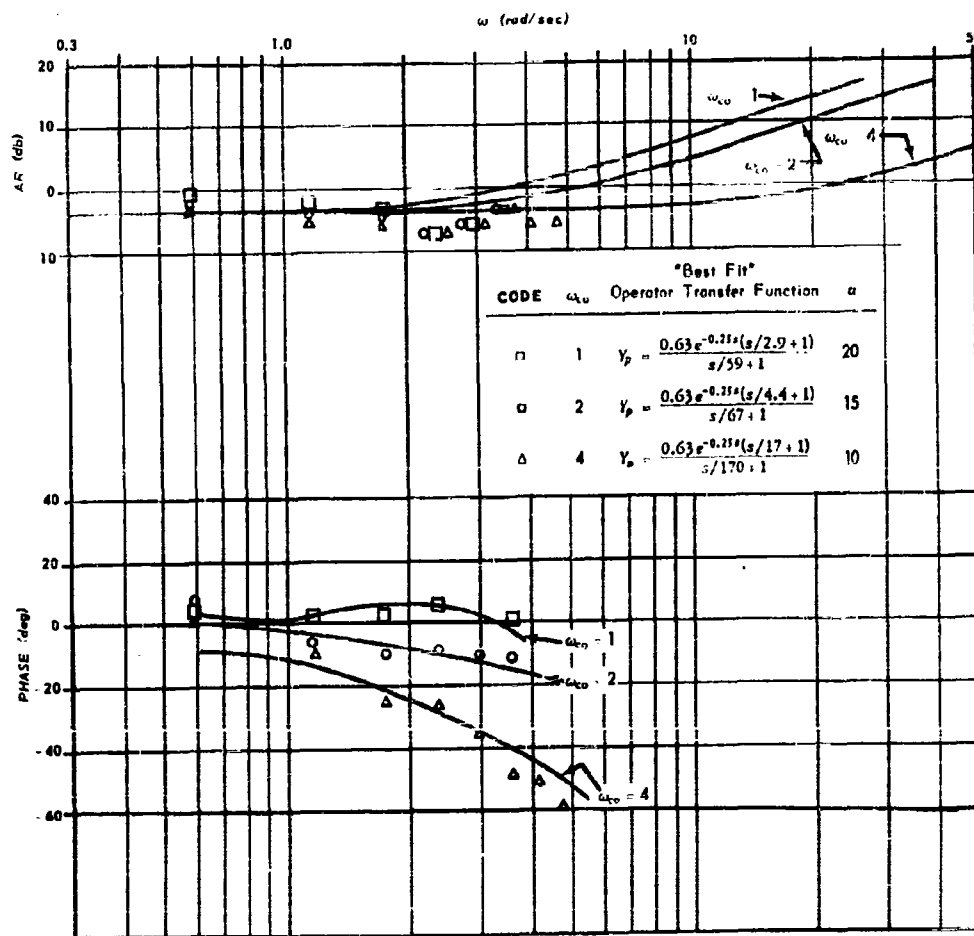


Figure 102. F-80A Simulator Closed Form Approximations to Y_p for Longitudinal Control.

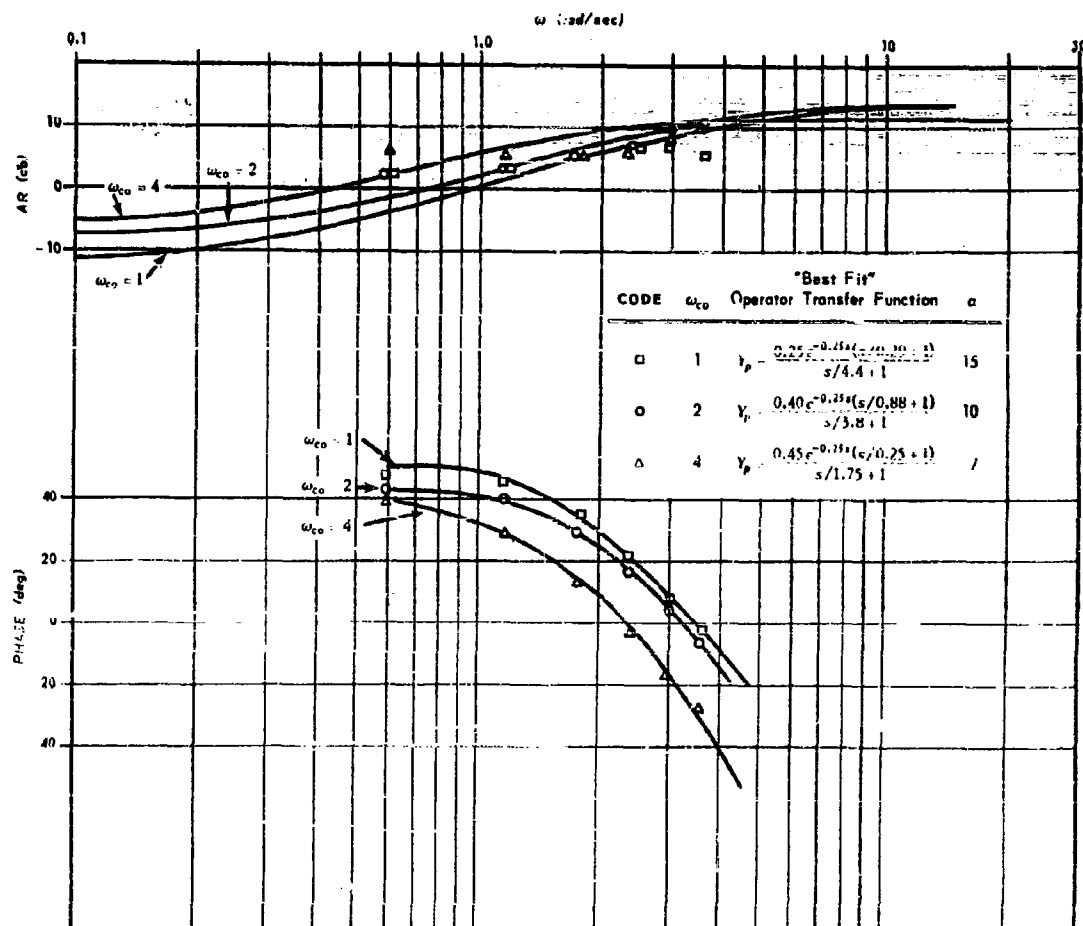


Figure 103. F-80A Simulator Closed Form Approximations to Y_p for Lateral Control.

The analytic approximations presented in Figures 102 and 103 can be complemented by the following equally good fits according to Equation (V-42) to the data for aileron control.

ω_{co}	Analytic Form for Y_p	a
1	$\frac{0.20 e^{-0.15s} (s/0.18 + 1)}{(s/7.5 + 1)(s/10 + 1)}$	14
2	$\frac{0.28 e^{-0.16s} (s/0.31 + 1)}{(s/3.1 + 1)(s/10 + 1)}$	10
4	$\frac{0.50 e^{-0.15s} (s/0.19 + 1)}{(s/1.3 + 1)(s/10 + 1)}$	7

In elevation control we have the following comparable array:

ω_{co}	Analytic Form for Y_p	a
1	$\frac{0.63 e^{-0.15s} (s/4 + 1)}{(s/40 + 1) (s/10 + 1)}$	10
2	$\frac{0.63 e^{-0.15s} (s/6 + 1)}{(s/20 + 1) (s/10 + 1)}$	5
4	No reasonable fit was achieved	

The observed rather poor fit for $\omega_{co} = 4$ in Figure 103 was considerably worsened when the effort was made to shift r down to 0.15 seconds and compensate with a time constant of 0.1 seconds in the so-called neuromuscular lag term. An improvement over either of these approximations to $\omega_{co} = 4$ for elevation control could have been effected by relaxing our condition that r 's be equal over all bandwidths. A r of 0.3 to 0.4 seconds improves matters considerably, if we do not relax our conditions on the desired amplitude response form of Equation (VI-26).

An examination of Figures 100 or 103, where the grand average data for elevation control are presented, reveals that both Equations (V-42) and (VI-26) are forced fits to the data. A more attractive explanation of these data will be found in Figure 146c of this report. Here we have hypothesized a linear describing function with an anticipation or sgn function in parallel. This model would predict that for low linear correlations Eq. (III-68), the sgn function would dominate and the overall describing function of the human operator would approach a pure gain with zero phase lag. This is precisely what we find for elevation control for input forcing function bandwidths of one and two radians/second. The averaged describing function for the 4 radians/second forcing function input has the form of a sgn function in parallel with a pure delay time phase lag of $e^{-0.25s}$. It is of interest to note in Fig. 108 that the trend for measured linear correlations is to increase with increasing forcing function bandwidth. Consequently, and consistent with our observations, the sgn function is most influential for these lower bandwidths.

6. The Remnant and Tracking Errors

An experimental measure of equal importance with Y_p , the open loop describing function, is ρ , the linear correlation, which we discussed initially in paragraph 4 of Section III of this report. In the assessment of the adequacy of our describing functions, an important criterion is: how much of the total output of the man is derivable from the describing functions we have extracted. This is precisely what ρ measures, for referring to Equation (III-64), we find the ratio of remnant power to the total power output:

$$\frac{\Phi_{nn}}{\Phi_{cc}} = 1 - \rho^2,$$

or if we desire we can express the output signal to noise power ratio as in Equation (III-65)

$$\frac{|H^2| \Phi_{ii}}{\Phi_{nn}} = \frac{\rho^2}{1 - \rho^2}$$

We can compute these and other characteristics of the remnant from ρ which is [cf. Equation (III-68)]:

$$\rho = \frac{|\Phi_{ic}|}{\sqrt{\Phi_{ii} \Phi_{cc}}}$$

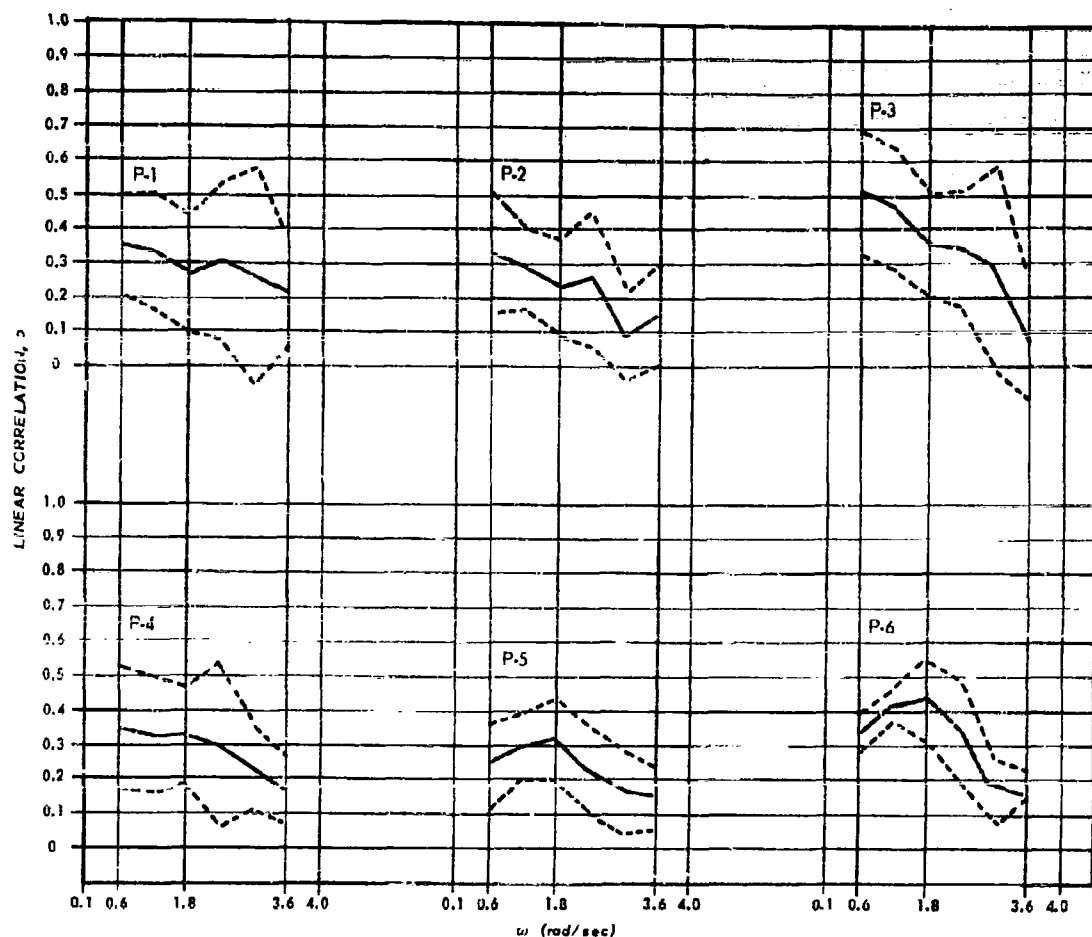


Figure 104. Linear Correlations for 6 Pilots with 4σ Confidence Bands (Lateral; $\omega_{co} = 1$ rad/sec).

Although ρ was determined for each of the several conditions for which Y_p values were measured, we will only present certain representative determinations of ρ at this time. Some general statements can be made about the bulk of these data. Although the shape of a given ρ plot as a function of frequency is characteristic of individual pilots, there seems to be a consistent increase in the average value of ρ as a function of the bandwidth of the system forcing function, which is demonstrated by all pilots.

In Figures 104 through 107 we present the ρ measurements for 6 pilots averaged over input amplitudes, together with the 2σ confidence bands, for both longitudinal and lateral control of the F-80A simulator.

In order to get some notion of the range of significant differences in the ρ plots of individual pilots, a comparison was made between the most and the least similar ρ plots on Figures 104 and 106. Similarity and dissimilarity were defined subjectively. A comparison on Figure 104 between P-1 and P-4 showed no significant differences; whereas P-3 and P-5 showed 3 out of a possible 6 differences to be significant at the 0.02 level. On Figure 106; P-1 and P-3 showed no significant differences; whereas P-2 and P-6 had 2 out of 6 possible differences

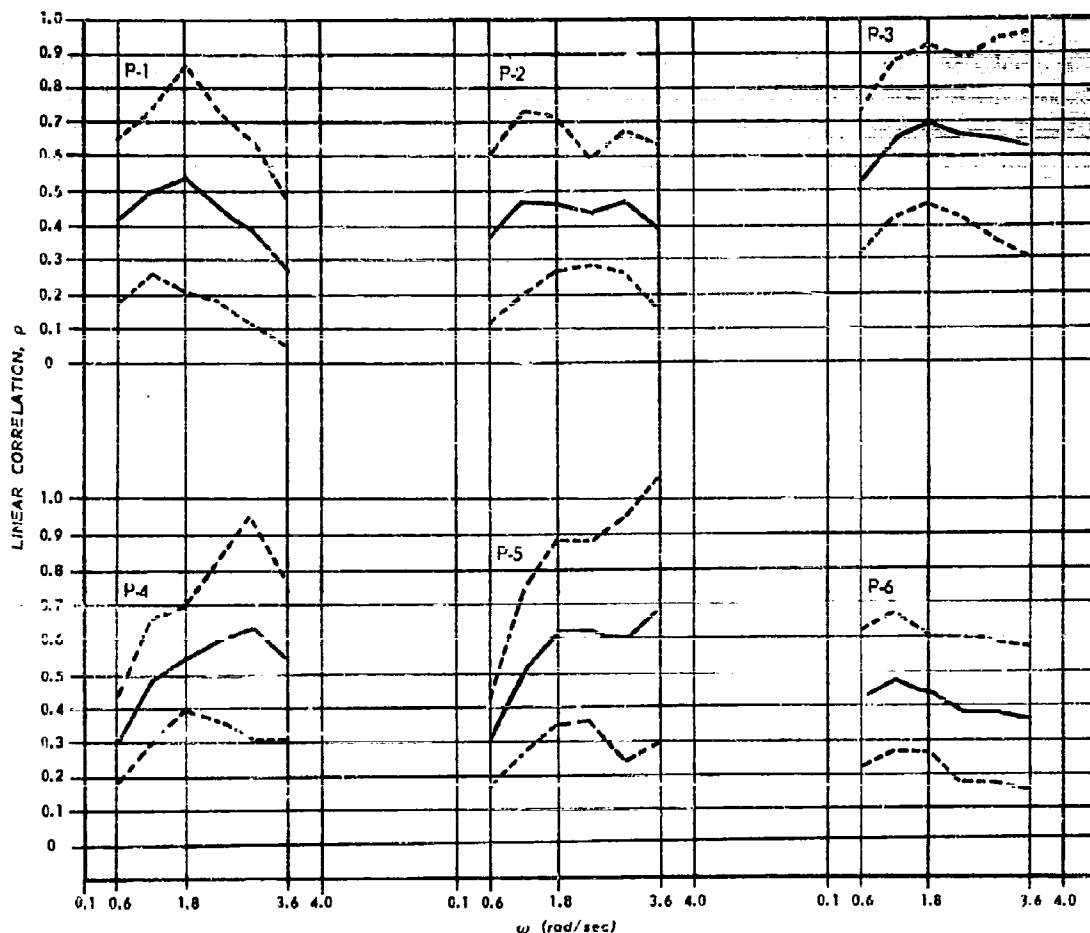


Figure 105. Linear Correlations for 6 Pilots with $\pm\sigma$ Confidence Bands (Lateral; $\omega_0 = 2$ rad/sec).

significant at the 0.05 level. This crude assessment was too awkward to apply to other pairs of ρ curves, but it should serve the reader in making casual judgments about variability between pilots in average ρ .

In Figure 108, we have ρ versus ω for $\omega_0 = 1, 2$, and 4, radians/second averaged over pilots.

Since an analysis of variance could not be performed due to the lack of variance equality for the populations of $\bar{\rho}$ -values sampled, a "t" test was performed to check the visually observed trend for average ρ to increase with ω_0 . In Table 10 we present the results of a test of this observed trend. As with our data for Y_p , the high variances about $\bar{\rho}$ make Table 9 all the more convincing.

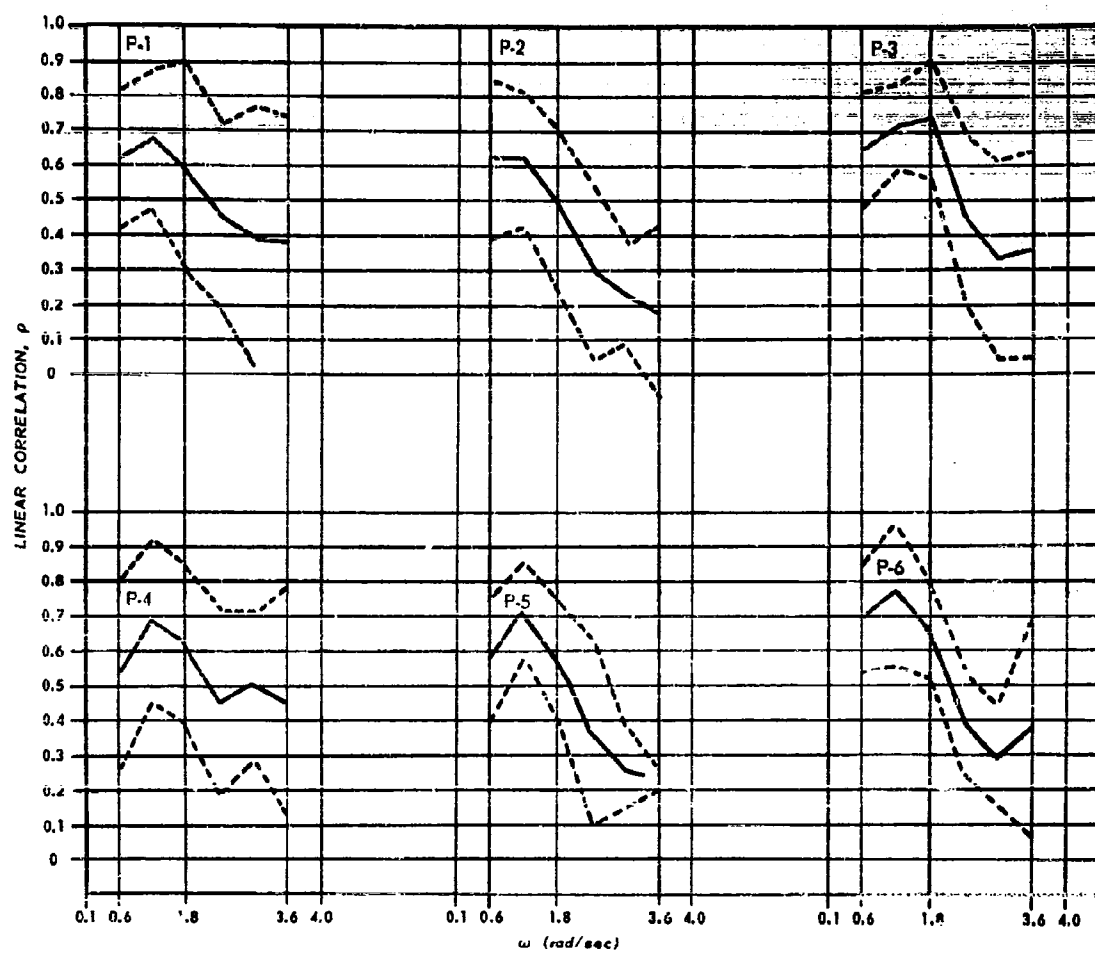


Figure 106. Linear Correlations for 6 Pilots with $\pm\sigma$ Confidence Bands (Longitudinal; $\omega_{co} = 1$ rad/sec).

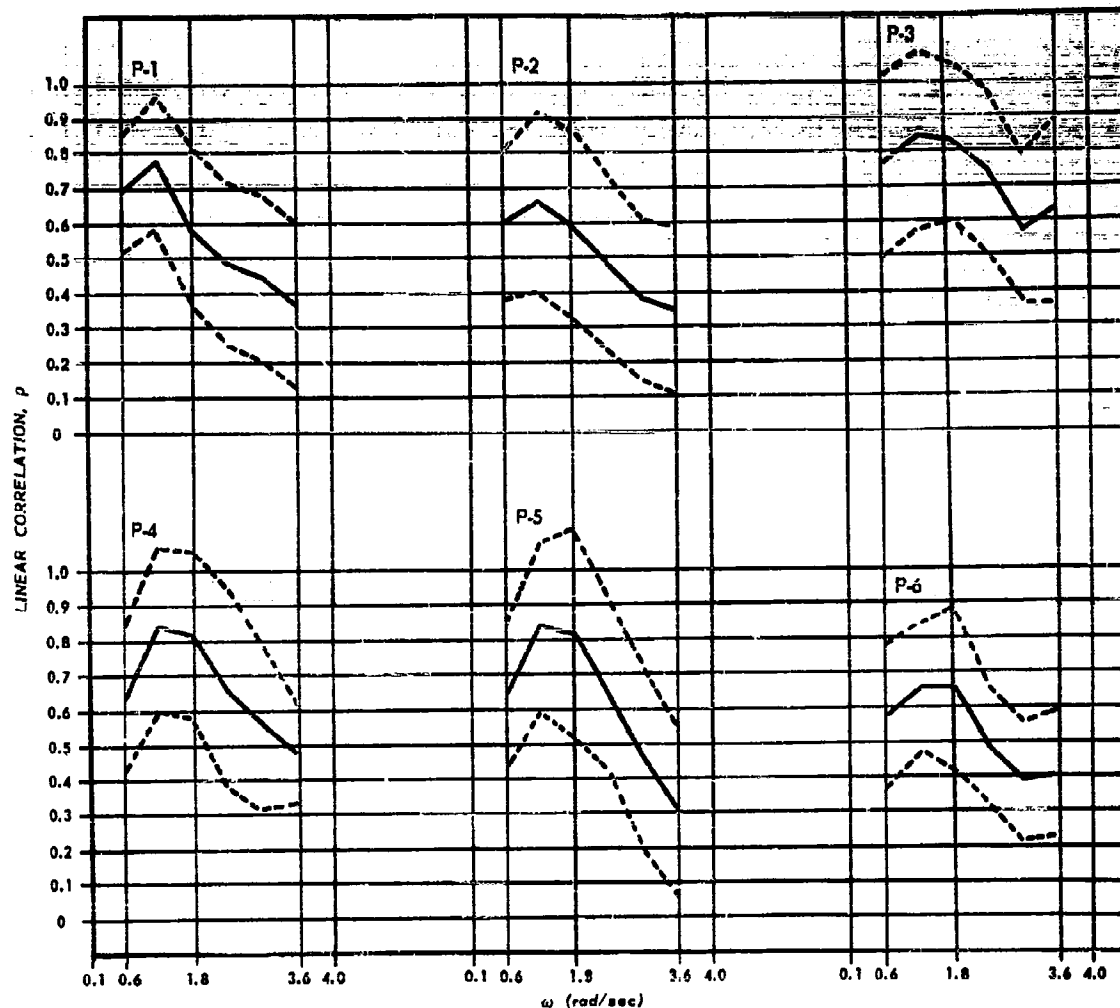


Figure 107. Linear Correlations for 6 Pilots with $\pm\sigma$ Confidence Bands (Longitudinal; $\omega_{co} = 2$ rad/sec).

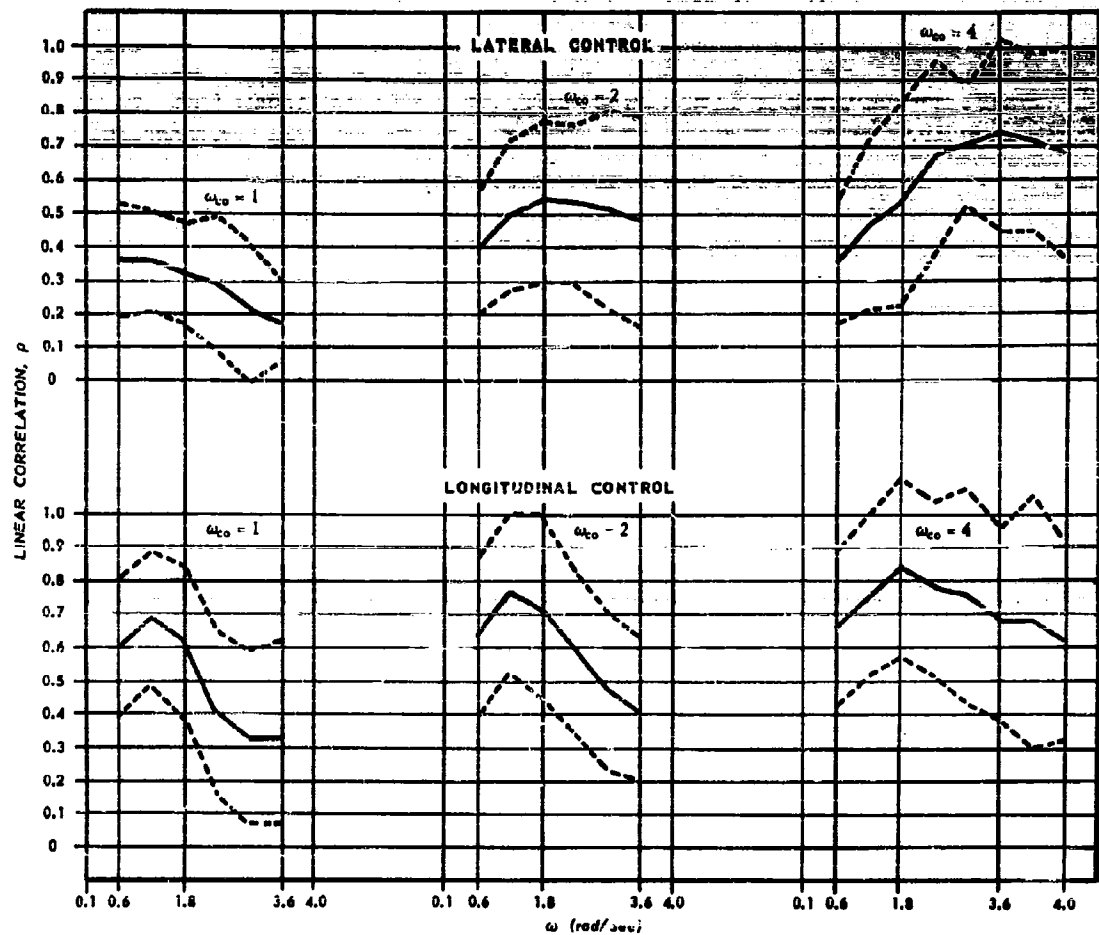


Figure 108. Averaged Linear Correlation for All Pilots with $\pm\sigma$ Confidence Bands.

Table 10. Significance Levels for Three \bar{p} Inequalities.

CODE: $\bar{p}_A = \bar{p}_{\text{acc}} = A$

ω rad/sec	LATERAL CONTROL MODE			LONGITUDINAL CONTROL MODE		
	$\bar{p}_2 > \bar{p}_1$	$\bar{p}_4 > \bar{p}_1$	$\bar{p}_4 > \bar{p}_2$	$\bar{p}_2 > \bar{p}_1$	$\bar{p}_4 > \bar{p}_1$	$\bar{p}_4 > \bar{p}_2$
0.6	n. s.	n. s.	n. s.	.10	.10	n. s.
1.2	.01	.01	n. s.	.01	.05	n. s.
1.8	.01	.01	n. s.	.01	.01	.01
2.4	.01	.01	.01	.01	.01	.01
3.0	.01	.01	.01	.01	.01	.01
3.6	.01	.01	.01	.01	.01	.01

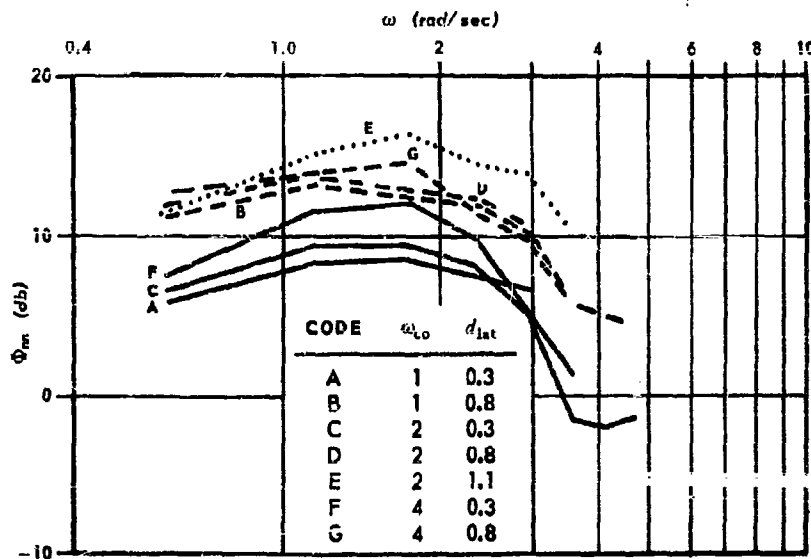


Figure 109. F-80A Closed Loop Remnant, Lateral Control.

When we compute the remnant from ρ , we cannot average out forcing function amplitudes as we have done in our plots of ρ since Φ_{cc} is obviously a strong function of the input amplitude; Equation (III-64). In Fig. 109 and 110, Φ_m is measured in db, where db conversion is from units of inches²/radian/second, measured on the oscilloscope. Since the flight problem is calibrated so that $\frac{1}{2}$ inch deflection on the scope corresponds to one degree of displacement for the target at 1000 yards range, these data can be converted to degrees, mils, or whatever unit is appropriate for the reader's purpose.

In Figure 111 we have presented relative measures of the open loop output noise, Φ_{m_e} , based on the assumption that Φ_m is all due to noise injected by the operator at his output.

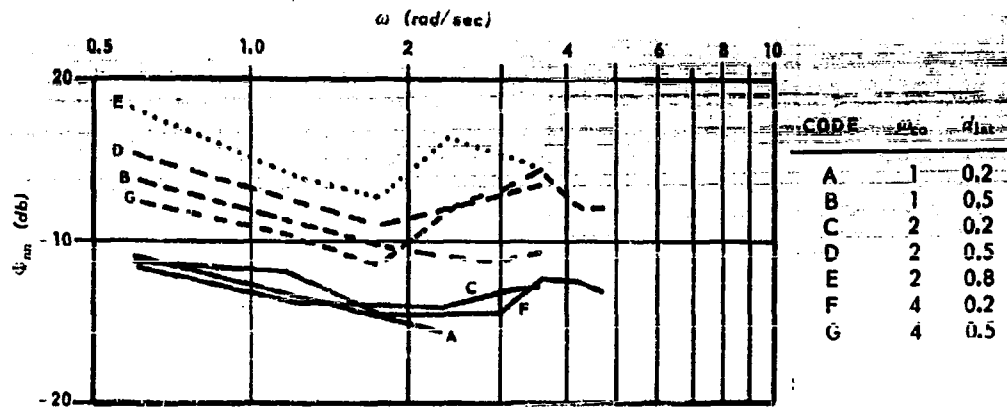


Figure 110. F-80A Closed Loop Remnant, Longitudinal Control.

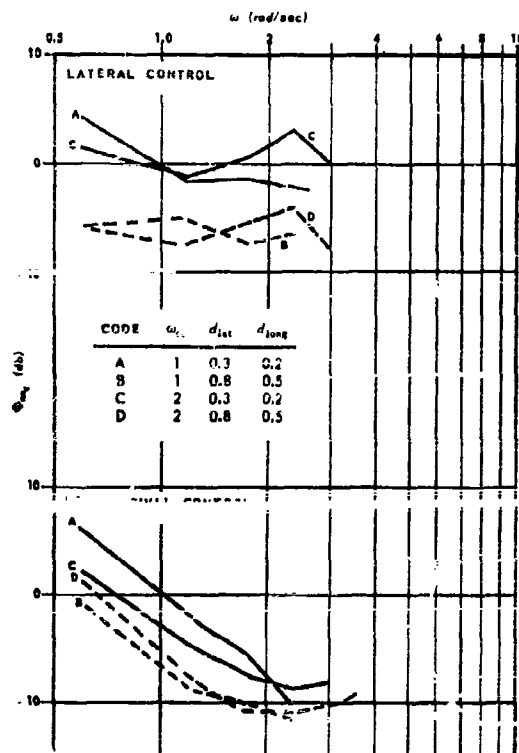


Figure 111. F-80A Remnant Due to Noise Injected at Operator's Output.

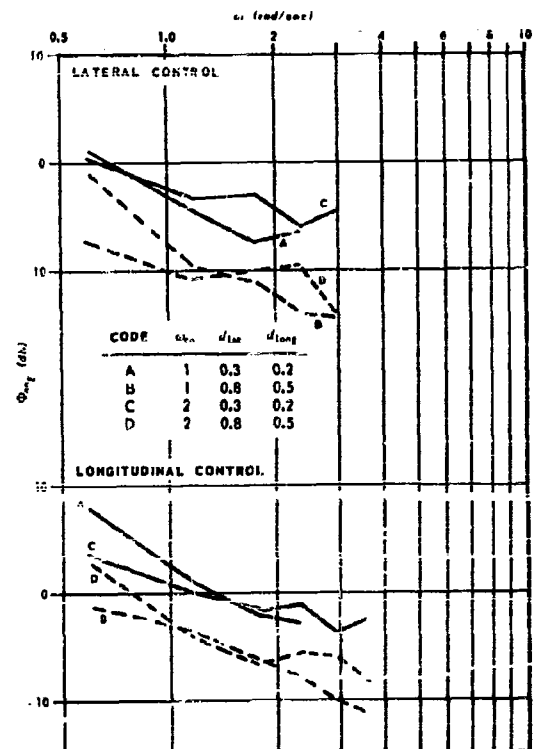


Figure 112. F-80A Remnant Due to Noise Injected at Operator's Input.

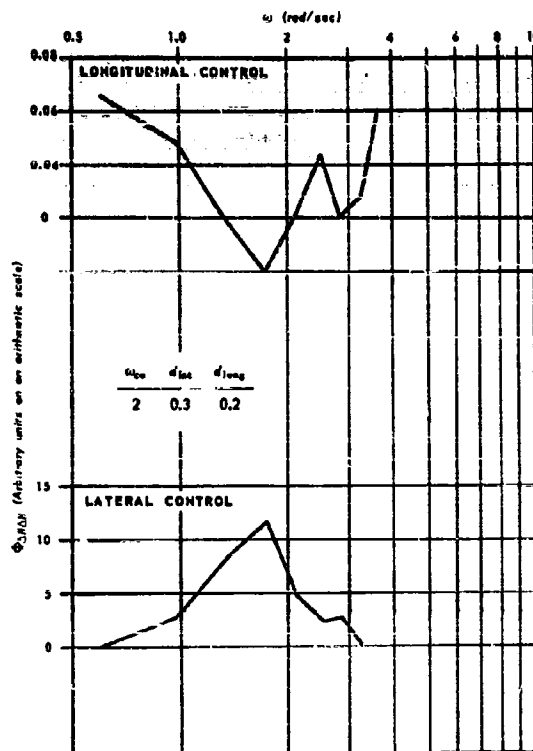


Figure 113. F-80A Remnant Due to Non-Steady Describing Function.

Since the hand computations involved in transforming the spectral densities $\Phi_{nn}(\omega)$ and $\Phi_{uu}(\omega)$ to the corresponding autocorrelations, and then obtaining the Fourier transform of the ratio, $R_{\Delta H \Delta H}(r)$ to obtain $\Phi_{\Delta H \Delta H}(\omega)$ were long and tedious only one sample computation for $\Phi_{\Delta H \Delta H}(\omega)$ was made. Figure 113 is $\Phi_{\Delta H \Delta H}(\omega)$ which represents an average for all pilots for $\omega_{co} = 2$ rads/sec, and for $d = 0.3$ inches rms for lateral control and $d = 0.2$ inches rms for longitudinal control. The units of the spectral density are arbitrary, and the scale is arithmetic rather than in db since zeros occur in the spectral density values. Figure 113 presents a general shape which is typical of the other input conditions as can be inferred by examining the form of the curves on Figures 109, 110, 116, and 117. The scale units of Figure 113 are arbitrary, although consistent for longitudinal versus lateral comparisons. The significant feature of 113, however, is the curve shape rather than the magnitudes of spectral density values.

With the remnant data presented in the various forms previously found useful in analyzing other results, it is appropriate to comment upon the application of the various remnant models to the F-80A data. In most cases this is difficult because the limited frequency range of our measurements unfortunately does not coincide with frequency ranges in which the remnant forms are varying in any exciting ways. In addition the ρ values upon which the remnant values are based are suspect, and the averaging process has obliterated much of the fine detail in the data. Some of the rapid fluctuations in individual measurements may have meaning, but the variability is so great that it is impossible to determine other than grossly smoothed trends. Most important of all, the effects of the extreme controlled element characteristics tends to override most others, such as the influence of forcing function amplitude and bandwidth. Since we are hemmed in by these factors, about all that can be done is to search for trends that may either be consistent or inconsistent with the other data sources. The net result of such an examination, considering the application of both the previously considered "nonsteady operator" and "output noise"

Thus following (III-74):

$$\Phi_{nn_e} = |1 + Y_p Y_c|^2 \Phi_{nn} = \frac{|Y_p|^2}{|H|^2} \Phi_{nn}$$

The data shown were normalized by dividing by the integrated spectrum;

$$\frac{1}{2\pi} \int_0^\infty \Phi_{nn}(\omega) d\omega$$

In Figure 112 we present similar curves based on assumption that the noise was injected at the operator's input; i.e., Φ_{nn_e} . Thus following (III-75):

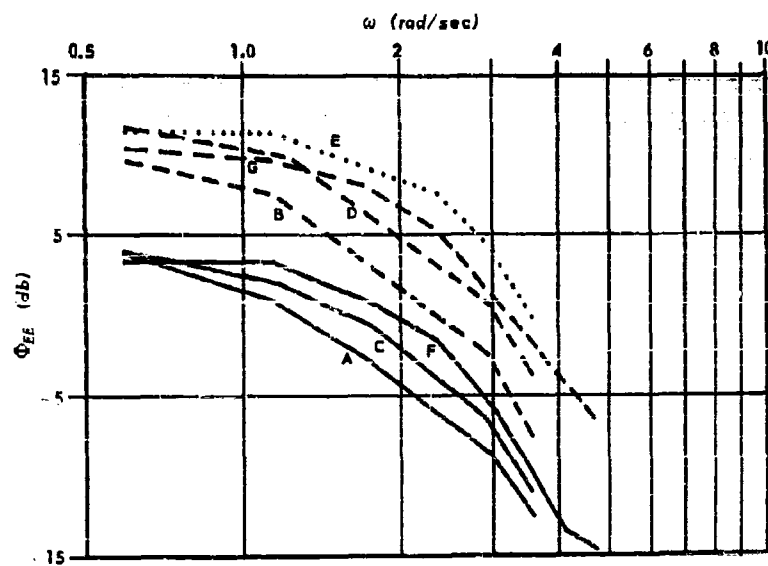
$$\Phi_{nn_e} = \left| \frac{1 + Y_p Y_c}{Y_p} \right|^2 \Phi_{nn} = \frac{\Phi_{nn}}{|H|^2}$$

Where the data were normalized as before by

$$\frac{1}{2\pi} \int_0^\infty \Phi_{nn}(\omega) d\omega$$

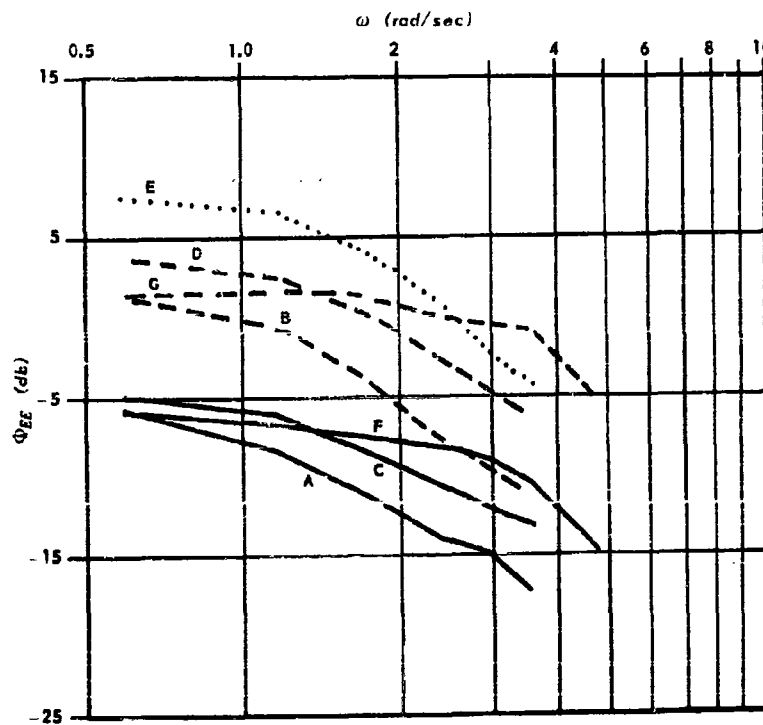
It is also possible to plot the spectrum of the remnant assuming that all of the remnant is due to non-steady behavior as discussed in Section III, subsection 5-d of this report by using Equation (III-92) which defines the non-steady remnant autocorrelation as follows:

$$R_{\Delta H \Delta H}(r) = \frac{R_{nn}(r)}{R_{uu}(r)}$$



CODE	ω_{co}	d_{lat}	n
A	1	0.3	32
B	1	0.8	37
C	2	0.3	44
D	2	0.8	49
E	2	1.1	2
F	4	0.3	6
G	4	0.8	6

Figure 114. Averaged Error Spectra, Lateral Control.



CODE	ω_{co}	d_{long}	n
A	1	0.2	32
B	1	0.5	37
C	2	0.2	44
D	2	0.5	49
E	2	0.8	2
F	4	0.2	6
G	4	0.5	6

Figure 115. Averaged Error Spectra, Longitudinal Control.

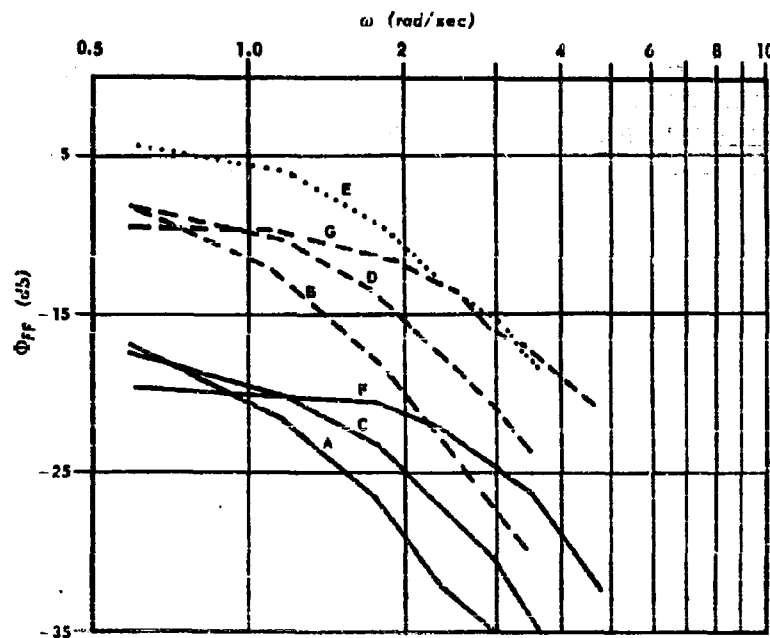


Figure 116. Averaged Forcing Function Spectra, Lateral Control.

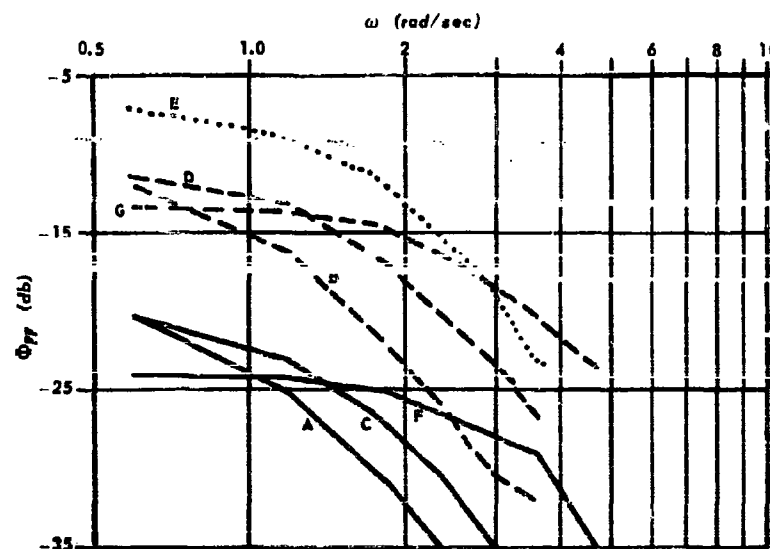


Figure 117. Averaged Forcing Function Spectra, Longitudinal Control.

models, can be summed up in the negative statement that the F-80A data is not inconsistent with these remnant "explanations". The possibility of a simple "input noise" injection model similar to the white noise approximation which had some limited value for Elkind's data, is largely ruled out for F-80A data.

A straightforward method for evaluating a tracking system is to compute the rms error of the error spectrum. Our measurements of the describing functions have enabled us to tell how the pilot has been controlling his aircraft, but they do not tell us how well, in an rms error sense, the pilot is tracking. To compute such a measure we need both the describing function data, the input forcing function and the closed loop noise, Φ_{nn} . We can, however, measure the error spectral density directly, and this has been done and averaged over all pilots. In Figures 114 and 115 we present the error spectra for azimuth and elevation control. The ordinates are db converted from Φ_{ee} expressed in units of inches²/rad/sec, measured on the pilot's oscilloscope. It is difficult to obtain rms errors for these data since we cannot be sure how the curves extrapolate to zero. It is instructive to compare these spectra with the averaged input spectra shown on Figures 115 and 116. As before, the underlying units of the ordinate scale are inches²/rad/sec. Since the filters used to shape Φ_{ii} were known, the zero frequency asymptotes are known, hence the Figures, 115 and 116 were used to obtain rms values for the forcing function input using the relation:

$$\sqrt{i^2} = \left(\frac{1}{2\pi} \int_0^\infty \Phi_{ii}(\omega) d\omega \right)^{1/2}.$$

The rms magnitudes are approximately equal over input bandwidths, and the derived values in inches rms for the low, medium and high magnitudes in azimuth, or longitudinal control, and elevation, or lateral control, are:

	Low	Medium	High
Aileron	0.25	0.81	1.0
Elevation.....	0.18	0.48	0.80

It can be noted from Figures 113 through 116 that the error spectrum is not proportional to the input spectrum since the spread between low, medium, and high input magnitudes is compressed considerably in the error spectrum. A second obvious point is that the error spectrum is always higher than the corresponding input spectrum. This state of affairs might prompt the remark that the airplane would do better without the pilot attempting to fly it! This remark, of course, ignores the fact that the pilot is stabilizing and directing; that is, flying the aircraft, and the error spectrum results from this process.

Section VII

THE VARIABILITY OF DESCRIBING FUNCTION DATA

A. INTRODUCTION

One of the first questions that arises in an attempt to apply measured describing functions for human operators is the extent to which a specified function applies to the problem at hand. In Sections V and VI we indicated how the dynamic response of the human operator adapted itself to the demands of the forcing function input to the control system as well as to the constraints imposed by the dynamics of the controlled element. In addition, we presented a brief discussion of the sampling variability to be expected in describing function estimates together with illustrations of measurement variability for individual subjects tracking with a controlled element (Figures 96 through 99). There are many additional influences which might be expected to increase the variability of our estimates, and we will attempt to discuss some of them in this section. Several of the influences which immediately come to mind are:

- (a) Variations in the describing function over time intervals which are long with respect to run length
 - i. changes due to fatigue or satiation
 - ii. changes due to practice
 - iii. changes due to motivational factors
 - iv. length of time interval over which data were examined
 - v. "set" to respond and instructions
- (b) Variations in the describing function due to differences among subjects
 - i. level of skill attained by the subject as limited by physiological factors
 - ii. see a-i, a-ii, and a-iii.
 - iii. changes in physiological state due to drugs
- (c) Variations in the describing function due to a dilution of the operator's best efforts
 - i. conflicting demands competing for either visual or manual attention
 - ii. manual encumbrances such as pressure suits.

The foregoing listing could easily be extended and expanded, but since we will only be able to present empirical evidence for a few of the possibilities outlined, further conjectural detail is not valuable at the moment.

B. VARIABILITY IN SIMPLE MAN GENERATED TIME SERIES

Since the describing functions in which we are interested derive from spectral density and cross-spectral density measures of time series generated by human operators in closed loop eye-hand control tasks, it is of interest to determine whether there exist measures of the variability of either the visual sensor or of the manual effector considered either separately or in tasks peripherally related to tracking problems. It would be unrealistic at this stage to expect a simple relationship such that, for example, certain types of variability could be specifically associated with end organ, central processes, or the neuro-muscular system of the tracker. (In a sense, we are implying the possibility of measuring and assigning variability to the various internal human operator components, much as we attempted to analyze dead time in human control behavior in Section IV.) We can, though perhaps naively, hope for the attractive possibility of such an eventual development. We shall present two examples of experimentation in this direction. First we will discuss measurements made in brain wave time series.

As part of a general investigation of the electroencephalographic correlates of "state of consciousness" carried out at the Franklin Institute [54], spectral densities were computed from the voltages generated in the visual cortex for six subjects. In addition, cross-spectral densities were computed of the so-called visual forcing function (created by a strobe lamp of duty cycle varying from 2 to 22 cycles per second depending on the experiment) and the evoked or driven electroencephalographic voltages measured on the scalp area above the visual cortex. The spectra, measured from two to three minute runs, were characterized by approximately 100 degrees of freedom in the Tukey sense, and consequently it was possible to make significant discriminations of measured effects. Findings peripherally related to tracking can be summarized as follows:

(a) The visual process measured by the spectra computed from visual cortex voltages was significantly different from individual to individual.

(b) Drugs such as epinephrine and metrazol, and trial order and possible fatigue in the experimental situation, had significantly different effects from subject to subject.

(c) Cross-spectral density measures between visual input and evoked response indicated that the time lag between the fundamental of the visual forcing function and the fundamental of response evoked in the visual cortex was generally within the range of .035 to .07 seconds which was stated to be the latency of the visual process in Section IV. The time lag measured from the cross-spectra decreased as the visual input frequency increased. This effect is consistent with our remarks in Section IV since the higher flash rates may be considered to produce stimulus of higher energy content by dint of the integrative action of the visual process.

The foregoing findings are not capable of extensive generalization because of both the casual experimental design employed, and the small number of subjects studied. The data are stimulating, however, and we present them in this light.

It is difficult to find data pertinent to the variability of time series associated with the various internal components of the human tracking mechanism. The next step in complexity, as we approach studies devoted to closed loop tracking tasks, is provided by Abelson's study of individual differences in the performance of routine repetitive tasks [1]. Abelson refers to some conversational remarks by Dr. Shewhart to the effect that from his own observations it is virtually impossible to find a series of repetitive human performances which is "in control". By "in control" is meant that measurements on successive outputs are independent, and that these individual measurements are normally distributed with a fixed predetermined variance. In other words "in control" refers to a stationary time series for which the spectrum is flat out to some limiting measurement. Various human decision and judgment processes, which have been shown to be describable by a Markoff process, would thus be "out of control", and would corroborate Shewhart's position [90]. Abelson's study was directed toward specifying this unusual "out of control" behavior, and attempting to relate individual differences to this behavior.

The sample of behavior examined was the task of jabbing a stylus at a target, a sort of open loop discrete tracking problem. This choice of task was made for the following reasons, among others:

(a) It is desirable to minimize learning and fatigue factors since they tend to make the time series non-stationary.

(b) The observations should be easily measured and the task production rate should be high.

(c) The goal of the perceptual-motor task should be kept constant, for otherwise the results may be dependent on the manner in which the goal changes. The task should not, however, be so simple that performance variability is negligible.

In the experimental procedure the subject stood alongside a table on which a box was placed. A square of paper on the box served as a target area, and the extent to which this target was defined was one of the experimental variables. Under the target, a typewriter ribbon backed metal sheet served to record the subjects jabs on a tape which moved at a constant rate across the length of the box. To minimize the effect of the subject being influenced by the knowledge of where his previous jabs had landed, the target papers were covered with a large number of indentations prior to the experiment. The stylus was held so that the top touched a backstop placed fifteen inches above the target area. When in this position the point of the stylus was eight inches from the target area. The subject set his own jabbing rate, lifting the stylus so that it made contact with the backstop after each jab, and continuing until he had produced 100 jabs for each of five task variations. The task variations, which were minor redefinitions of the target area, are of little interest for our purposes. Thirty-three subjects were used and fifteen of them were retested on the same tasks one month later.

The time series so generated were converted to spectra, Φ_p , after appropriate smoothing, and for each subject, each task, and lag values of $p = 0, 1, 2, 3, 4, 7, 12, 17$ jabs the ratios of the spectra

$$\frac{\Phi_{p_{\text{retest}}}}{\Phi_{p_{\text{test}}}}$$

were computed. According to Tukey [81], if the true population value of Φ is $\hat{\Phi}$ then

$$\frac{\Phi}{\hat{\Phi}}$$

is distributed as χ^2 with f degrees of freedom where:

$$f = \frac{2(\text{NUMBER OF OBSERVATIONS IN THE TIME SERIES})}{\text{NUMBER OF LAG COVARIANCES COMPUTED}} = \frac{2N}{m}$$

for a reasonably flat spectrum. There is a loss in degrees of freedom as the spectrum departs from flatness.

Under a null hypothesis of no difference between test and retest and with a selected significance level of 20% (χ^2/f is approximately distributed as F , where $f = n_1$ and n_2 is very large, and a two tailed F list with 10% on each tail was used), 33% of the ratios were significant. This is considerably higher than the expected 20%. An analysis of variance further demonstrated that the task and subject task interaction variances were not significant. Thus individual differences were the major causes of significant difference. It turned out that the variance, σ^2 , the proportion of low frequency components in the spectrum, and job speed, were particularly good indices of individual differences. Job rate, of course, is not a measure derived from the spectra.

In an effort to relate these patterns of individual difference to personality variables a correlation of sorts was obtained with the following factors:

- (a) Degree of persistence of perceptual focus (i.e., power of attention).
- (b) Manual dexterity.
- (c) Degree of emotional commitment to task situation.

These personality factors are pertinent to closed loop tracking as well, and it can be seen that they reflect some of our a priori notions of sources of individual variability.

The only summary statements that we can make about the two foregoing studies are that:

- (a) They leave much to be desired in our unrealistic hope of being able to apply a "system reliability" approach to a human control system.
- (b) Both tasks demonstrated relatively high differences between the performances of individuals.

It is of interest to wonder whether the preceding studies did not favor high individual differences by dint of their free structures, since behavior was neither constrained by a mechanism nor oriented by a rigid task goal. The fact that this freedom of action resulted in individual differences is something which we could have expected with all the wisdom inherent in hindsight.

C. VARIABILITY IN TRACKING TASKS WITHOUT DYNAMICS

In the introduction to this section we mentioned several of the possible sources of contaminating variability in describing function measurements. As implied in our treatment of the previous subsection, the variability of describing functions has the same origin as variability associated with other time series measurements of human performance without regard to subsequent manipulations which may formally restructure such time series measurements into describing functions or other useful functions. The argument that these variabilities are related does not, of course, make any provision for predicting how variability will manifest itself in describing function data. Therefore, wherever possible, we prefer to examine describing function data directly. Much of the early and peripheral research, however, was presented in terms of power spectra or magnitudes only of describing functions, and we will present some of these more primitive data in order to make our development more comprehensive.

Although all of the early experimenters who used spectral analysis techniques to characterize human operators in tracking tasks were aware of the basic assumption (i.e., that the time series generated by the tracker were stationary), very few attempts were made to study this assumption in any detail. In general, the experimenter made a small number of measurements which satisfied him that the process was time stationary, and he then proceeded to examine the effects of other variables. As a rule a run duration of from half-a-minute to four minutes was

selected as providing a stationary sample of behavior. There is, however, a reference to work performed at the University of Indiana [5], by Benepe, Narasimhan and Ellison, which is a rather complete study of run-to-run variability in human tracking performance. The Indiana experiments examined the spectral density of tracking error in a one dimensional pursuit tracking situation.* The visual display consisted of a 1 inch to 6 inch opening in a large gray panel. The background of the opening was an evenly illuminated white to permit easy observation of two black pointers. The upper pointer was driven by a target generator which was used to produce two forcing functions of interest to us: $i_1(t) = 2 \sin(\frac{2\pi}{3}t)$, the simple input, and $i_2(t) = \frac{4}{3} \sin(\frac{2\pi}{3}t) + \sin(\frac{4\pi}{3}t)$, the complex input, both in inches. The maximum horizontal excursion was set at 4 in. for both inputs, and the maximum horizontal excursion of the subject's control pointer was six inches. The difference between the control and forcing function signals was fed to a Brush recorder. Spectral densities of Φ_{EE} were obtained by sampling the recorded error function twelve times a second for a total of 450 samples, computing autocorrelations for 60 lags, and then computing the Fourier transforms of these autocorrelations. Since no mention is made of any smoothing either on the autocorrelation or the spectral density, we must assume none was done. As Wiener points out [Ref. 93, pp. 36-43] the smoothness of the spectral density $\Phi(\omega)$ is related to the value of the autocorrelation $\phi(\tau)$ for high values of τ , thus one can see that formal transformation of an autocorrelation of 60 lags may produce spurious spectral density detail due to possible computation noise and other inaccuracies at the high values of τ . Secondly, raw spectral estimates, as Tukey points out, are not as accurate estimates of the process under measurement as properly smoothed estimates. As a consequence we have smoothed the Indiana spectra in an effort to obtain better estimates than those presented in Ref. 5. The smoothing formula used was:

$$\Phi_{EE}(\omega) = 0.54\Phi_{EE_R}(\omega_2) + 0.23[\Phi_{EE_R}(\omega_1) + \Phi_{EE_R}(\omega_3)]$$

where Φ_{EE_R} are raw, or unsmoothed, spectra and Φ_{EE} is a smoothed spectrum.

The first data we will discuss were generated by 16 subjects after nine practice trials using the simple forcing function input. Two adjacent 450 point, (37.5 second) samples were taken from each record and the computed spectra were presented in Ref. 5. In order to determine whether the test-retest comparisons for the subjects were significant, we smoothed the spectra and computed the ratios of Φ_{EE} test to Φ_{EE} retest for the first seven points on the spectrum, which covered an 8 rad/sec bandwidth. The data presented actually extended to 34 radians, but there was clearly no need to examine the data beyond the bandwidth we selected. The number of degrees of freedom were:

$$\frac{2N}{m} = \frac{2 \times 450}{60} = 15.$$

Each ratio was distributed as $\chi^2/15$ and it was thus possible to make a test of the significance of the test-retest comparison for each of the seven spectral components and sixteen subjects. Using a significance level of 10%, i.e., a two tailed χ^2 of 5% on each tail, 10 of the 112 ratios were significant. This is, of course, what would be expected on the basis of chance and indicates that there is no reason to believe from the data available that the individual trackers were not behaving in a stationary fashion, or that there were differences between subjects in their "degree of stationarity".

A similar experiment was conducted using the complex forcing function input. Again, we smoothed the raw test and retest spectra, and examined the test-retest ratios for significance. A bandwidth of 9.2 radians/second including 8 points per subject was examined. Again, examining ratios at the 10% level of significance, 27 out of 128 ratios were significant. However, 14 of these significant differences were contributed by subjects 10 and 15, so we have a clear individual difference effect. We can then conclude that the human operator is time stationary over the 37.5 second samples, and that individual differences are more important as the task increases in difficulty. In Figure 118 we have plotted test and retest spectra averaged over the sixteen subjects for the simple complex inputs. The line spectra represent the difference between the two inputs on an arbitrary dB scale.

* As a rule, in this report we have discussed compensatory tracking separately from pursuit tracking. Further along in Section XI we will discuss pursuit tracking in detail. It was felt, however, that the Indiana data were primarily of interest because of the variability they studied rather than as examples of pursuit tracking, and therefore they are presented in this section.

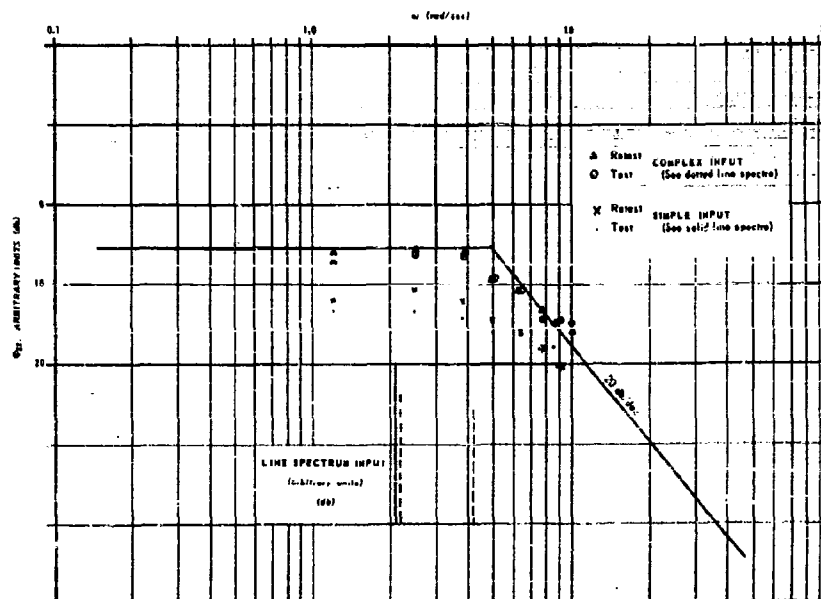


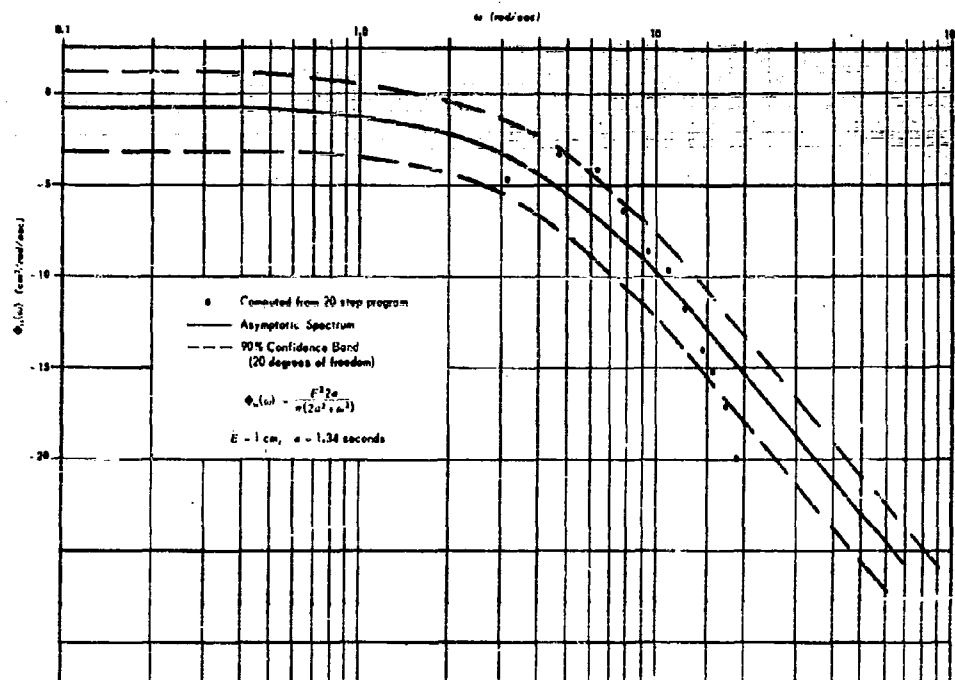
Figure 11A. Smoothed Error Spectra From Indiana Data.
(Reference 5, Tables V, VI, XIII, XIV)

A "t" test was used to determine those differences for both simple and complex inputs between test and retest averages for Φ_{EE} which were significant at the 0.1 level. The number of significant differences, which was one for the simple and one for the complex input, did not exceed the number to be expected by chance alone. The foregoing, together with the fact that the ratio $\sigma_{\Phi_{EE}}/\Phi_{EE}$ for the Φ_{EE} values averaged over subjects for each measurement frequency was usually $\frac{1}{2}$ or greater, indicates that a large residual variance due to differences between subjects made our measurements incapable of resolving any detailed differences between means over subjects.

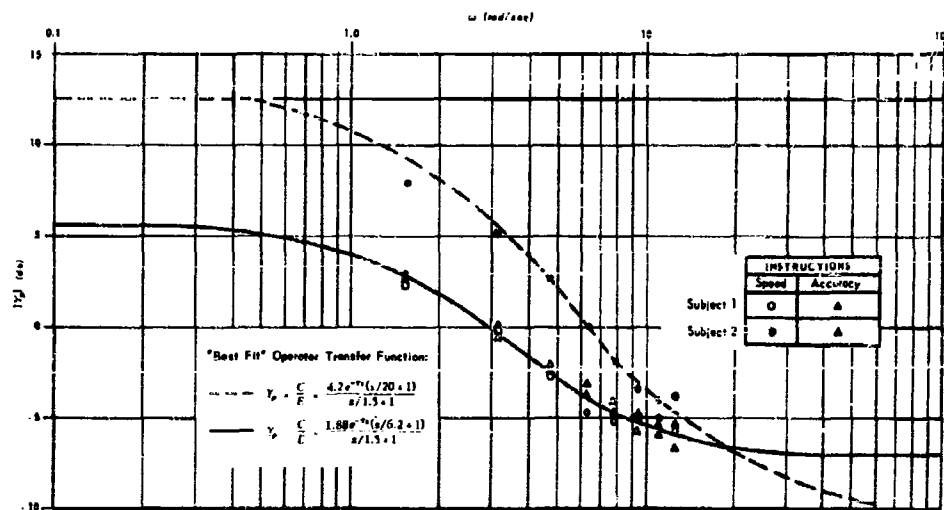
It is of further interest to note that the comparison of the averaged error spectra between simple and complex inputs indicates that the only difference between them is a constant increase of 2 or 3 db in error power. There is no manifestation in the error spectrum of the different spectral content of the two input signals. In order to determine whether variability increased with task complexity, an F test was performed on the variances about Φ_{EE} for simple and for complex inputs. For the test: $\sigma_{\Phi_{EE, \text{complex}}}^2 > \sigma_{\Phi_{EE, \text{simple}}}^2$ at the 0.05 level one would expect about one chance inequality out of our 14 comparisons. Actually, 5 out of 14 inequalities were significant at the 0.05 level in the predicted direction. All the other variance comparisons were not significant. This finding indicates an interaction between task complexity and variability between subjects.

The foregoing interpretation of the Indiana data is not the same as that expressed in Reference 5.

In a series of small scale experiments at the Franklin Institute [49, 50, 51] efforts were made to examine certain aspects of the causes of variability in the spectra of tracking time series. A one dimensional compensatory tracker was used for which the display was a cathode ray oscilloscope mounted 28" from the subjects eyes. A pip on the CRO executed discrete left and right steps in a fixed horizontal line on the CRO face. The subjects task was to center this spot on a vertical fiducial line using a spring restrained joy stick which had essentially no dynamic influence in the region of the operator's bandwidth. The programming apparatus for the forcing function was designed to produce square pulses of durations which could vary in eight discrete steps from 0.25 to 1.91 seconds. A program was devised so that a total of 20 pulse durations were selected from a Poisson distribution of zero crossings such that the average pulse duration was 0.75 seconds, whereas the pulse amplitudes were selected from a Gaussian distribution of mean amplitude of one centimeter and standard deviation 0.25 cm. The pulses were presented alternately left and right. The measured spectrum for this forcing function is presented in Figure 119a



a. Input Spectrum For Franklin Step Tracker.
 (Ref. 49, p. 9; Ref. 50, p. 4)



b. Franklin Step Input Tracker; The Effect of Instructions.
 (Ref. 50, Figures 10, 13)

Figure 113.

together with a plot of the asymptotic value of this input spectrum. The experiment in which we are interested attempted to determine the effect of instructions on the describing function of the human tracker. Unfortunately only the magnitudes $|Y_p| = |C|/|E|$ were computed.

Two male subjects S1 and S2 were used; S1 was a retired military man who had at least thirty years of flying experience, and S2 was a male non-pilot in his early twenties. The same program of square pulses was presented to each subject, and each subject was given intensive training in the tracking problem. On the first day of the experiment S1 was instructed as follows: "It is of crucial importance to this study that you pay careful attention to these instructions. Return the pip to the vertical line as accurately as you can." On the same day S2 was given instructions which differed from the foregoing only in that the word "rapidly" was substituted for the word "accurately". Prior to recording the three time functions, $i(t)$, $c(t)$, $e(t)$ for each subject, the subjects received a familiarization training of a few minutes with the tracker. Following this session, the subjects underwent four training sessions of five minutes each, separated by intervals of about one hour. During these sessions each subject repeatedly tracked the same program under his particular instructions, which were repeated at the onset of each training period. An hour after the last training session the subject was once again given the appropriate instructions and presented a succession of five 20-step programs each of which was about 15 seconds long. The signals $i(t)$, $c(t)$, $e(t)$ were recorded for the last two of these programs, and these recorded signals were considered to be representative of a trained subject.

On the second day of the experiment the same procedure was adhered to except that S1 was instructed to track for speed and S2 was instructed to track for accuracy.

The results of this experiment are shown on Figure 119b. The two accuracy runs and the speed run for S1 provide describing function magnitudes, the differences between which are not detectable, but the speed run for S2 was significantly different from the other three runs. Efforts were made to fit the data on Figure 119b using the conventional form of Equation (VI-26):

$$Y_p = \frac{Kc^{-1}(T_L s + 1)}{T_I s + 1}.$$

Of course, we can't put much faith in such a construction of Y_p based on the amplitude response alone. It was possible to estimate τ from time records of previous data in this experiment as 0.25 to 0.3 seconds. It is interesting to examine the fits for insights into the meaning of "speed" and "accuracy." For S2 "speed" meant:

- a. higher dc gain
- b. a shorter integration time for his smoothing action implied in the lag term in Y_p .

On the other hand "accuracy" meant:

- a. lower dc gain
- b. a smoothing time constant triple what it was for speed tracking
- c. the same lead time constant.

This is an eminently reasonable interpretation of the instructions! S1, however, provides a problem since his "speed" and "accuracy" runs are not different. We are confronted with both individual differences in performance, which may be based on the order of performing the task, on the interpretation of the instruction, or perhaps a difference in performance capabilities. The main point of this little experiment is that a subject can change his manner of response due to instructions. It is of added interest to note the lack of individual differences when both subjects interpreted "accurately" the same way.

Russell was the first experimenter to study sources of variability in their effect on the complex describing function. We will discuss only his examination of the effects of instruction and of physiological changes in the tracker. Using the apparatus we described in Section V in a task for which $V_c = 1$, Russell asked a subject to try harder and then to try very hard, after obtaining his describing function for normal effort. On Figure 120 we present Bode plots of these data, together with simple fits to these plots. There is little difference between "harder" and "very hard," and it appears that asking for increased effort was interpreted by this particular subject as meaning

- a. increase dc gain
- b. decrease lead
- c. maintain about the same smoothing time constant.

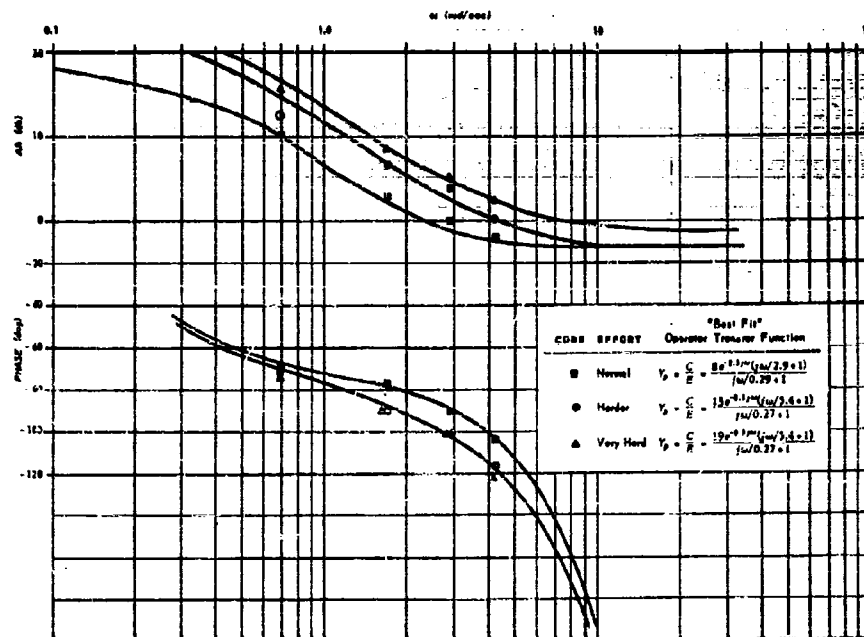


Figure 120. Russell Simple Tracker; The Effect of Instructions.
(Reference 70, Figure 25)

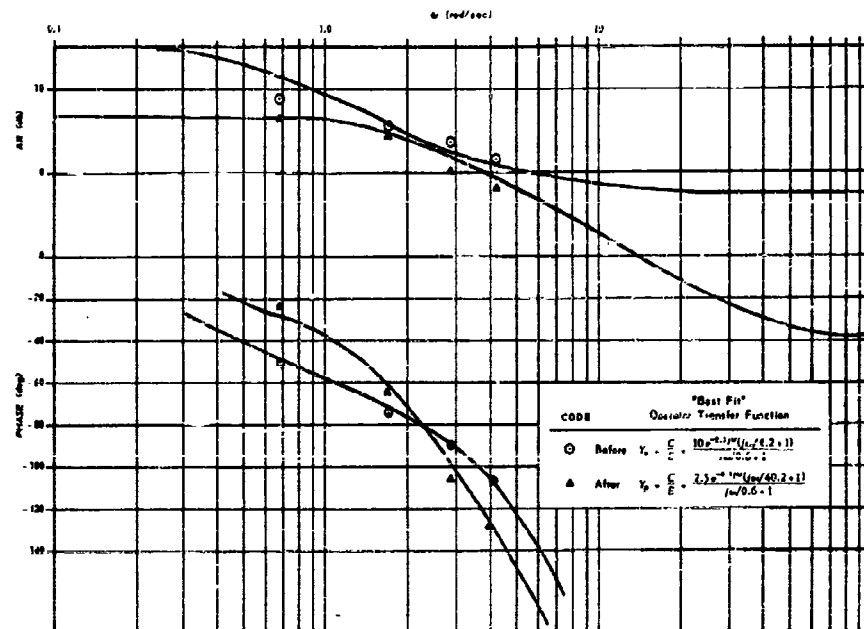


Figure 121. A Physiological Cause of Variability.
(Reference 70, Figure 26)

There are other means of changing the describing function the tracker selects for a given problem besides changes in his instructions. His physiological characteristics could be changed by stimulants or depressants. Russell chose to examine the effects of a depressant ingested in two ounce, 90 proof, units. The subject made a series of five, 4-minute tracking runs over a two hour period, starting sober, and consuming two ounces of 90-proof whiskey after each run. At the end of this period the subject could walk satisfactorily, but was in a condition where it would have been inadvisable to drive a car. On Figure 121 we see the before and after results of this noble experiment. We note that the subject's gain decreases and that his ability to generate lead deteriorates ten-fold. The implications for future research are clear. It should be possible to design automobiles so that their effective controlled element could compensate for the drunken driver's deficiencies. Thus a sensor on the dashboard operating on the alcoholic concentration of the air could adjust the gain and phase of Y_c so that good system performance might be maintained despite the deterioration of Y_p . Before such a venture could be considered seriously, a large scale measurement of the describing functions of the population of motorists would be needed. The prospects are intoxicating.

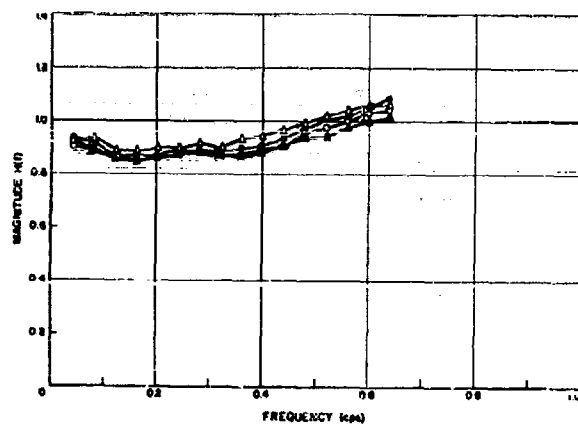
Elkind made a thorough study of both individual differences and time effects on describing functions in the following experiment performed with his apparatus previously described in Section V.

As described in [23]:

Three subjects tracked in a compensatory system four identical groups of input signals, each group containing three members. These subjects had previously trained by tracking thirty 4 minute runs over a period of a week. The time that elapsed between presentations of the groups was the chief variable, being one hour, 4 hours and 4 days. The interval between presentations of the individual of a group was only a few minutes. This procedure made it possible to examine both long-time and short-time variations in the operator's characteristics. The input had a rectangular spectrum with cutoff frequency of 0.64 cps and 1 inch root-mean-square amplitude. The three input signals of a group were identical in all respects.

Figures 122 and 123 present part of the results of this experiment. Figure 122 was obtained by averaging over subjects and over the three replications in each group. Therefore each point represents, save for one minor exception, the average of 9 quantities. The long-time variations in subject performance are given by the differences in the group means in Figure 122. In Figure 123 the averages are over replications and groups and the differences are due to variations among subject means. The standard deviations from the magnitude and phase are shown on Figures 122 and 123 about the means for the quantity at the following frequencies 0.08, 0.32, and 0.60 cycles/second. Inspection of the Figures 122 and 123 indicates that the differences between the averages are small. The standard deviation in magnitude is about 3 percent of the mean, and the standard deviation in phase is about 3° . Analyses of variance were performed on the real and imaginary parts of the closed loop describing function $H(f)$, and at the three frequencies for which the standard deviations were shown. There were no significant differences at the 0.01 level for the compensatory runs. At the 0.05 level of significance the differences among subjects at 0.08 cps and 0.32 cps for the imaginary part of H were significant, and three subjects and group interactions were significant. The interactions of subjects and groups could be an artefact due to equipment inaccuracies since each group of runs was performed as a unit. Assuming such inaccuracies were random, they could cause the 3 significant interactions found between subjects and groups. The two significant subject mean differences would be expected by chance for 54 F ratios at a significance level of 0.05. It is important to note that the lack of significant differences does not result from a large residual variance attributable to experimental variables which could obscure large variations in operator characteristics. The fact that the individual standard deviations in Figures 122 to 123 are small indicates that the residuals are small. Thus Elkind's data provide the final argument against the importance of either time variation between runs or differences among trained subjects for simple tracking tasks.

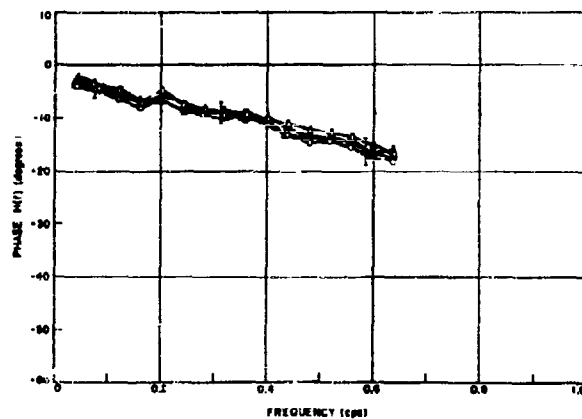
As an interesting aside to the main line of his study, Elkind demonstrated the human operator's ability to vary his tracking parameters as a function of instructions or set to respond. One subject, in a different series of tests from the one just described, believed that he could improve his pursuit tracking of input F-1 (see Fig. 27) if he were to consciously attempt to smooth out his high frequency output. Input F-1 is phenomenally a low frequency random signal with a superimposed high frequency noise. This subject tracked F-1 using two different tactics: his normal mode in which he attempted to follow all the input fluctuating, and a filtered mode in which he concentrated on the low frequency components and attempted to suppress the highs. Closed loop describing functions were computed and these showed a very slight increase in low frequency gain at the expense of a phase retardation of about 40° beyond the input signal's bandwidth. The mean square errors for both tactics were essentially equal, but were



a.

- Group I
- Group II
- △ Group III
- ▲ Group IV

b.



c.

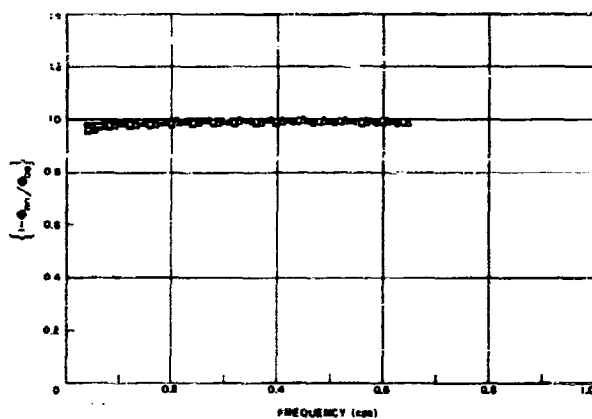
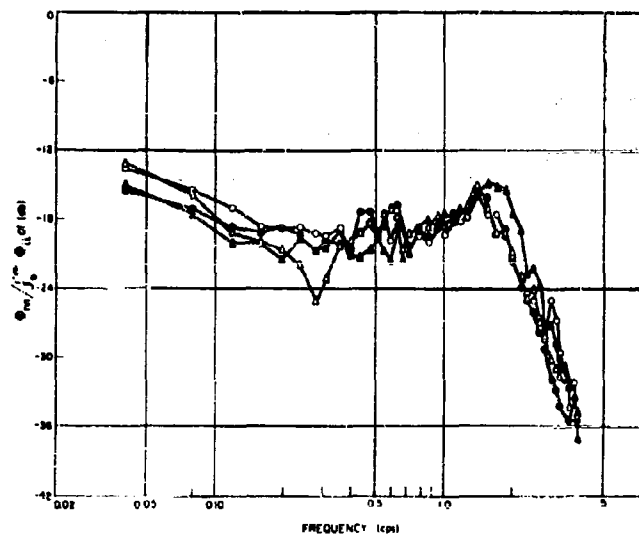


Figure 122. Elkind's Long Time Variations.
(Reference 23, Figure 4-1)



d.

- Group I
- Group II
- △ Group III
- ▲ Group IV

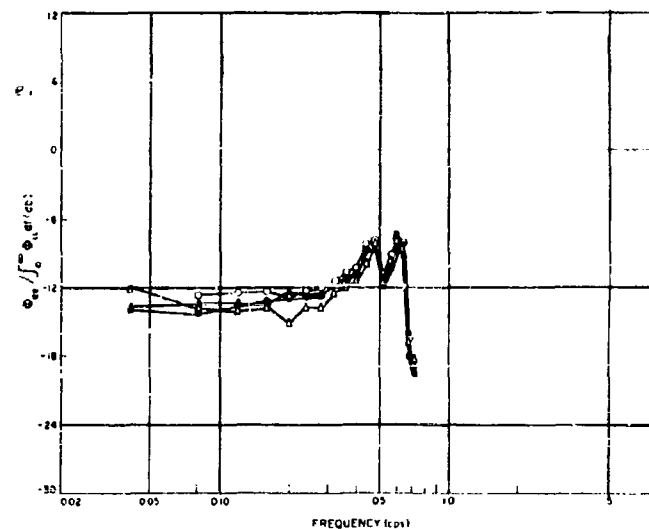


Figure 122 (Continued).

$Y_c \neq 1$ this situation might not have obtained. The comparison provides added evidence that the operator's set to respond or interpretation of instructions provides a source of variability since the operator has some control over his time constants.

The studies in this sub-section have demonstrated that variability, in tracking tasks without controlled element dynamics, is dependent on both the task and the degree of subject training. Both the Elkind and Indiana data point this up. However, in both cases, the imposition of a well defined task goal appears to diminish the variability among subjects as compared with a simple tapping task. For example, compare the chance level of significant individuals test to retest ratios of spectra for the Indiana data with the well above chance level for the Abelson test-retest ratios for individuals. There does not appear to be any significant amount of variability assignable to time effects in simple tracking tasks. The parameters of the human describing function are functions of instructions and the physiological condition of the tracker.

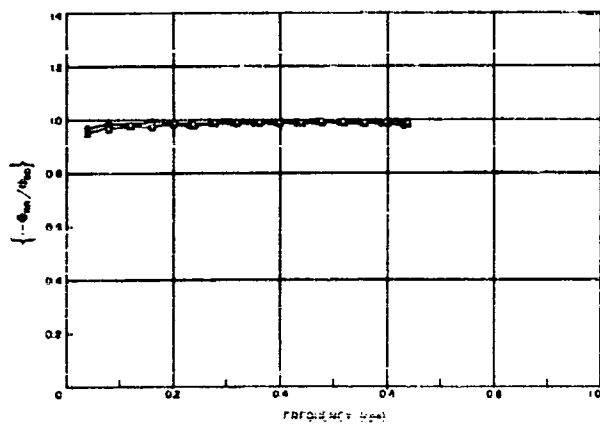
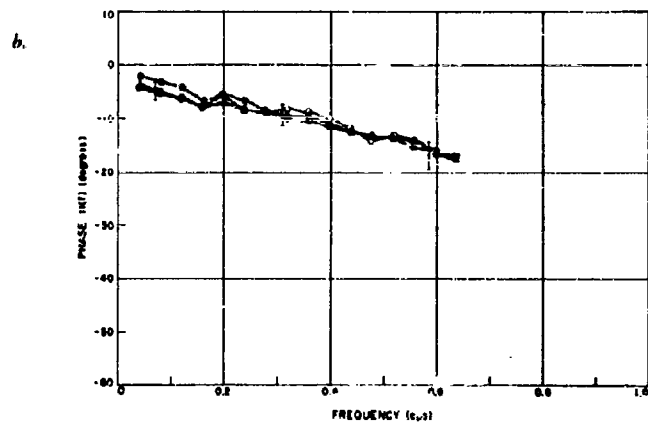
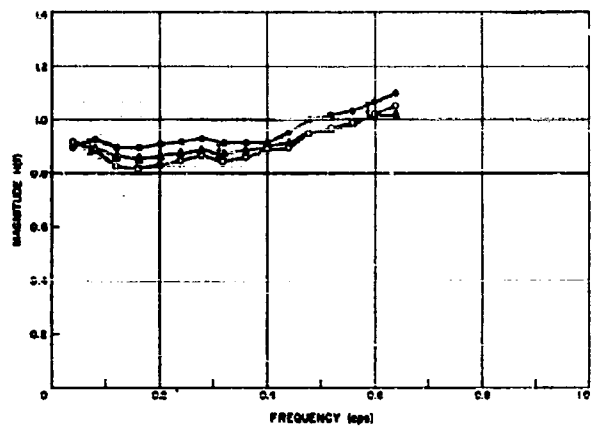
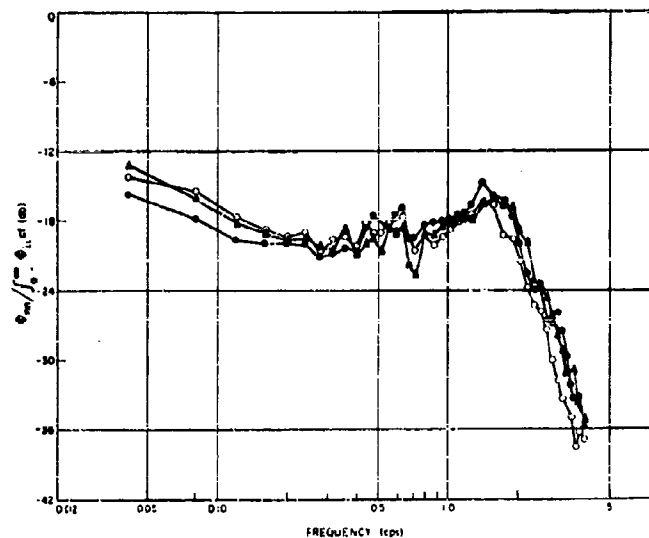


Figure 123. Elkind's Among Subjects Variations.
(Reference 23, Figure 4-2)



d.

—●— Subject A
—○— Subject B
—●— Subject C

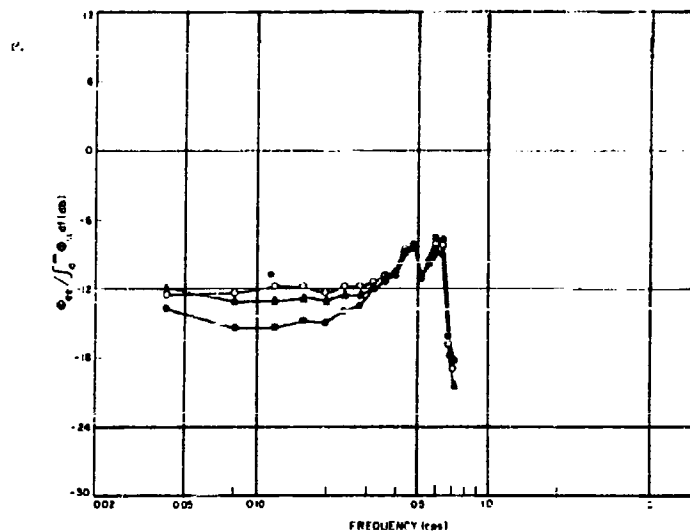


Figure 123 (Continued).

D. VARIABILITY IN COMPENSATORY TRACKING SYSTEMS WITH DYNAMICS

The data on variability in control systems with dynamics are not as well defined as the Elkind data presented in the preceding sub-section. This unfortunate circumstance is due to the large amount of residual variability associated with the presently available measurements. In Section VI, Figures 96 to 99 and 104 to 107, we have previously presented data which indicate the extent of variability both within and among subjects. However, as we cautioned at the time, there were many confounding effects associated with the averages such as, amplitude, time order effects and measurement fallibility. We are, therefore, reluctant to attempt to draw any strong conclusions from these data.

It is, however, of some interest to present some data taken from one subject in an experiment which attempted to determine the effects of "tracking fatigue". The procedure was as follows. The subject, a trained

Air Force jet pilot, had tracked 50 or 60 runs in the Franklin F-80 simulator over a period of six hours with various forcing function band widths and rms amplitudes. The experimental problem was to track continuously for ten minutes for each of several input forcing functions. Adequate rest periods were used between these ten minute bouts. During the course of this continuous tracking two minute samples of the pilot's describing function data were recorded. We have reproduced the results of the first and last two minute intervals for a forcing function cutoff frequency of 2 radians. Figures 124a, b, c, d are for an rms forcing function amplitude of 0.3 inches on the CRO face, and Figures 125a, b, c, and d are for an rms amplitude of 0.8 inches. Although this experiment was performed on other subjects, much data had to be discarded due to computation difficulties, so too few first and last run pairs were available to make averaging over subjects meaningful. In as far as subject P-6's describing functions and ρ measures are typical of the sample of pilots studied, Figures 124 and 125 are representatives of "tracking fatigue" effects on Y_p and on relative Φ_{NN} and Φ_{EE} .

It will be noted that there was no attempt made to fit Y_p for longitudinal control in either Figures 124b or 125b. The reason for this is not that we didn't try; we just weren't successful with any simple fit to the data. Furthermore, although the data points are presented up to 4.8 radian/second, the reader should not put much weight on data beyond 4 radian/second. Except for the differences in error spectra between first and last runs for the 0.3 inch rms amplitude forcing function, which are barely significant for a few frequency bands at the 0.1 level, and a few differences in Y_p , there is no strong effect due to "tracking fatigue". The two different fits to the Y_p data in Figure 125a are not based on firm statistical ground, and their weak reason for being is a search for trends. The conclusion to be drawn from these data is that our measures were not sufficiently sensitive to discriminate "tracking fatigue", or that such an effect does not occur for the conditions we studied.

It is of interest to examine the data summarized in Figures 96 through 99, and Figures 104 through 107. One can compute the variances associated with the computed quantities $|Y_p|$, $\angle Y_p$, and ρ for each of the six pilots, and then determine whether the demands of the tracking task, as indicated by ω_{co} and the mode of control, influences the size of the variance for the various quantities. One might expect that, as the task becomes more demanding, the range of possible Y_p 's available to the pilot would become more restricted since failure to generate the proper Y_p 's means the pilot-aircraft combination is effectively "dead". Consequently, a decrease in Y_p variance might be expected as ω_{co} successively assumes the values 1, 2, and 4 radians/second. Since lateral control is more demanding than longitudinal control, one would further expect that this hypothesized trend would be more pronounced in lateral control. There is, however, no such influence toward greater uniformity operating on ρ . In fact, one might argue that as the task became more demanding ρ , which is characteristic of individual behavior unrestricted by controlled element constraints, might show increased dispersion.

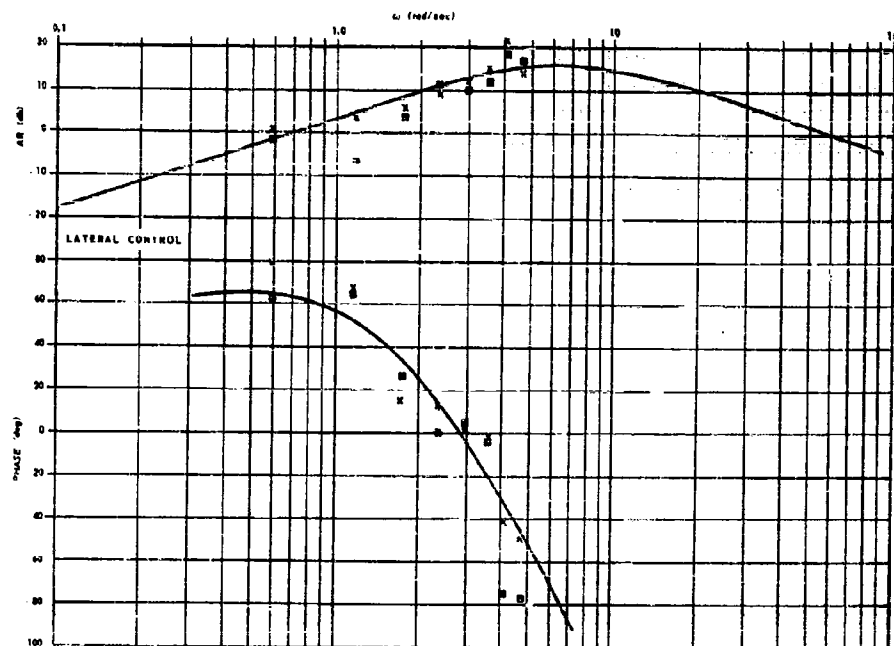
For each of six pilots, the variances for $|Y_p|$, $\angle Y_p$, and ρ for longitudinal and lateral control and for each of the 6 measured frequency bands were computed for $\omega_{co} = 1$ and 2. An F test was applied to variance ratios which differed only with respect to the forcing function input bandwidth. Table 11 presents results of a two sided F test at the 0.10 level of significance for $|Y_p|$, $\angle Y_p$, and ρ for variance ratios not equal to unity. Thus the "inequality" hypothesis, in either direction, is significant at the 0.05 level.

In Table 11 the notation $2 > 1$ means $\sigma_{\omega_{co}=2}^2 > \sigma_{\omega_{co}=1}^2$ at the 0.05 level. We can make the following inferences from Table 11, which describes Y_p variances.

- There are strong individual difference trends which are not common to $|Y_p|$ and $\angle Y_p$.
- The fraction of $|Y_p|$ table entries for which $2 > 1$ is 0.055, and for $1 > 2$ this fraction is 0.155. A value of 0.05 would be expected by chance for each individual fraction.
- The fraction of $\angle Y_p$ table entries for which $2 > 1$ is 0.083, and for $1 > 2$ this fraction is 0.22. As before 0.05 would be expected by chance for each individual fraction.
- The control mode does not appear to have much effect.

In Table 11 we also present the significant variance inequalities for ρ . Here we note:

- There are strong individual differences.
- There is no strong effect due to control mode.



a. Y_p Measured in a Ten Minute Tracking Fatigue Test; Lateral Control ($d = 0.3$ in. rms).

"Best Fit"
Operator Transfer Function:

$$Y_p = \frac{0.1 e^{-0.25s} (s/0.08 + 1)}{(s/1 + 1)(s/10 + 1)}$$

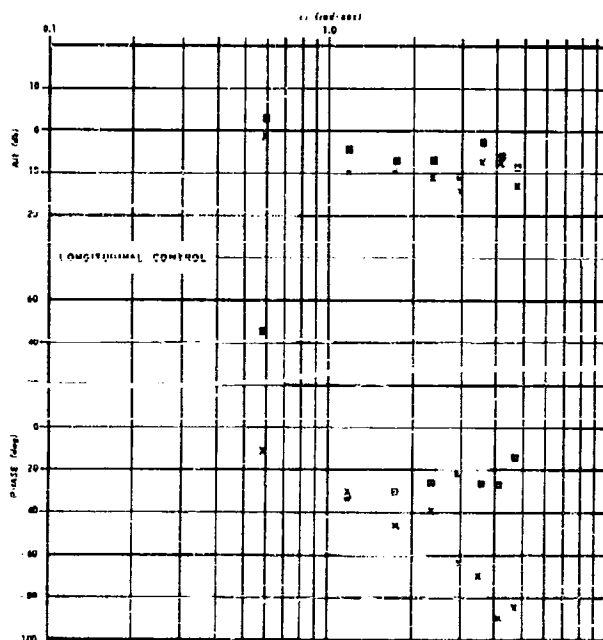
Subject P-6

x First Two Minutes

□ Last Two minutes

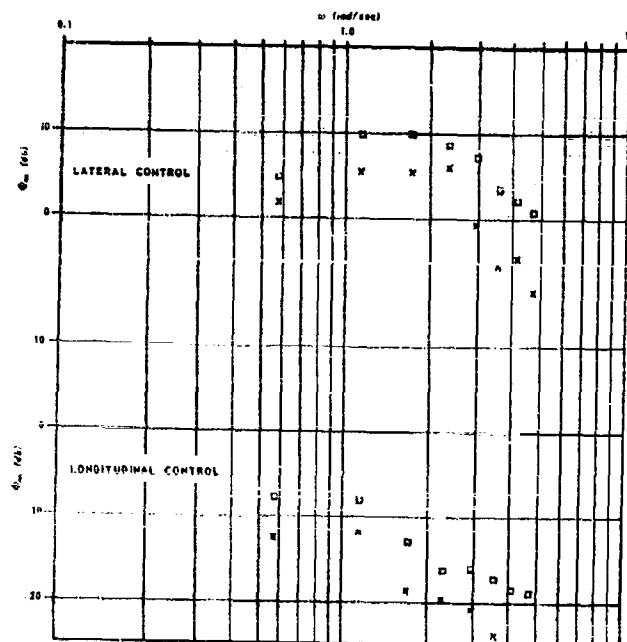
$\omega_{co} = 2$ rad/sec

$d = 0.3$ in. rms



b. Y_p Measured in a Ten Minute Tracking Fatigue Test; Longitudinal Control ($d = 0.3$ in. rms).

Figure 124.



Subject P-6

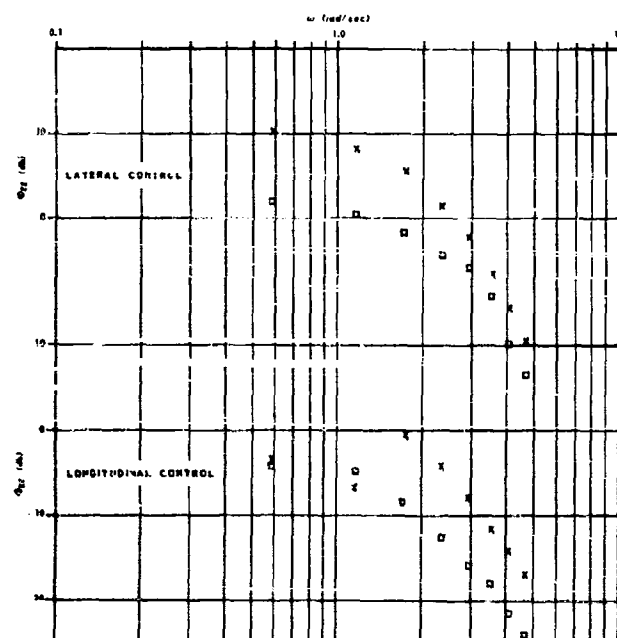
x First Two Minutes

□ Last Two Minutes

$\omega_{co} = 2$ rad/sec

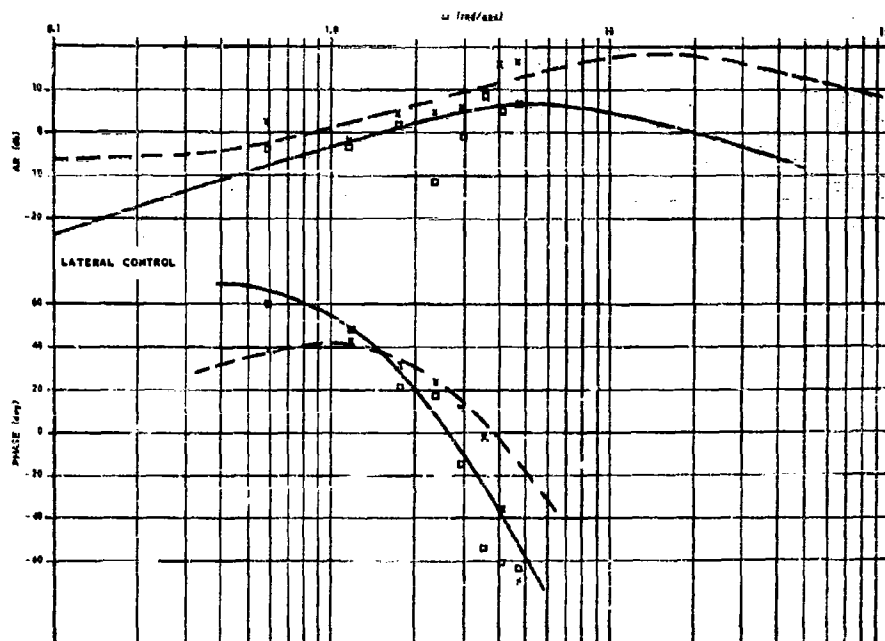
$d = 0.3$ in. rms

c. Relative Closed Loop Remnant, Φ_{RL} , Measured in a Ten Minute Tracking Fatigue Test ($d = 0.3$ in. rms).



d. Error Spectrum, Φ_{EG} , Measured in a Ten Minute Tracking Fatigue Test ($d = 0.3$ in. rms).

Figure 124 (Continued).



a. Y_p Measured in a Ten Minute Tracking Fatigue Test; Lateral Control ($d = 0.8$ in. rms).

"Best Fit" Operator Transfer Function:

$$Y_p = \frac{0.5e^{-0.25s}(s/0.5 + 1)}{(s/25 + 1)(s/10 + 1)}$$

$$Y_v = \frac{0.04e^{-0.25s}(s/0.06 + 1)}{(s/3 + 1)(s/10 + 1)}$$

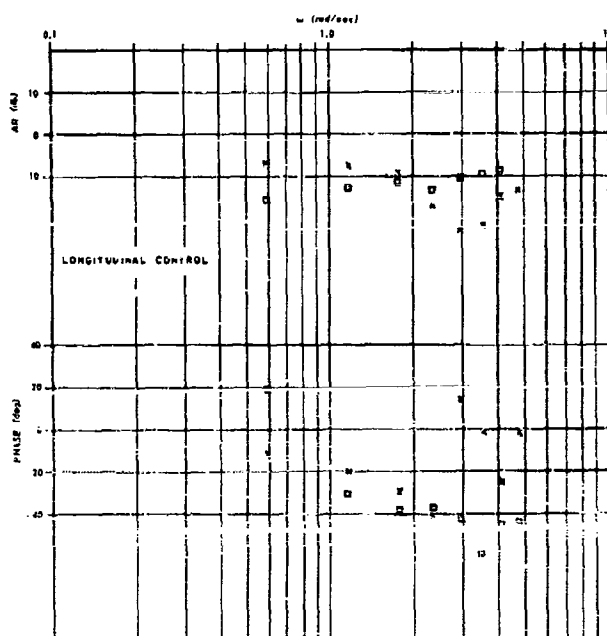
Subject F-6

x First Two Minutes

□ Last Two Minutes

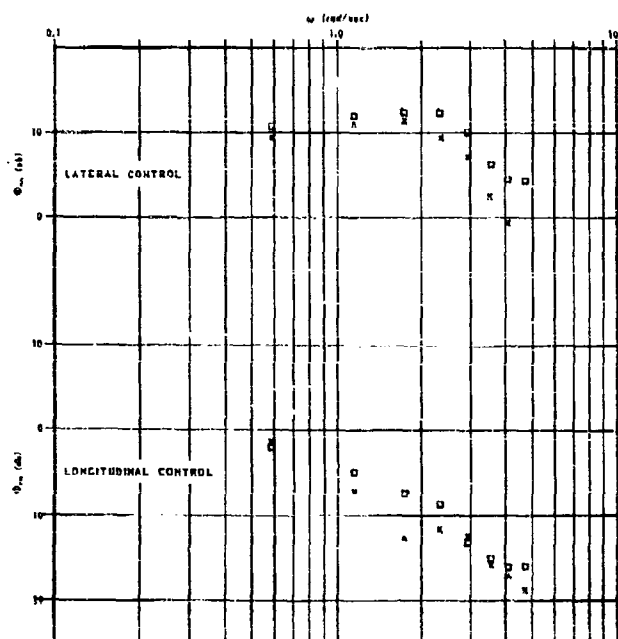
$\omega_{co} = 2$ rad/sec

$d = 0.8$ in. rms



b. Y_p Measured in a Ten Minute Tracking Fatigue Test; Longitudinal Control ($d = 0.8$ in. rms).

Figure 125.



Subject P-6

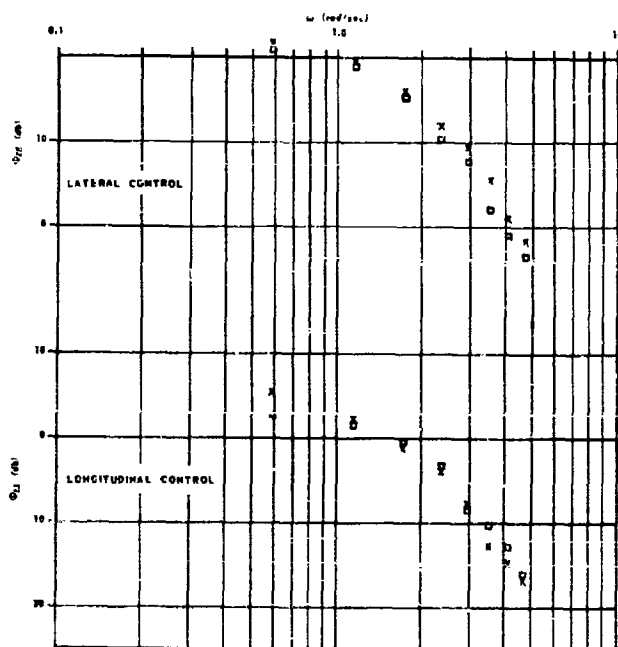
x First Two Minutes

o Last Two Minutes

$\omega_{co} = 2$ rad/sec

$d = 0.8$ in. rms

c. Relative Closed Loop Remnant, Φ_m ,
Measured in a Ten Minute Tracking Fatigue
Test ($d = 0.8$ in. rms).



d. Error Spectrum, Φ_{EE} , Measured in a Ten
Minute Tracking Fatigue Test ($d = 0.8$ in.
rms).

Figure 145 (Continued).

Table 11. Significant Variance Inequalities for Six Pilots.

PILOT	CONTROL MODE	$ Y_p $						$\angle Y_p$						p					
		ω (rad/sec)						ω (rad/sec)						ω (rad/sec)					
		0.6	1.2	1.8	2.4	3.0	3.6	0.6	1.2	1.8	2.4	3.0	3.6	0.6	1.2	1.8	2.4	3.0	3.6
P-1	LONGITUDINAL	1>2	1>2	1>2	1>2	1>2
	LATERAL	1>2	1>2	1>2	2>1	...	2>1
P-2	LONGITUDINAL	1>2	...	2>1
	LATERAL	1>2	2>1	2>1	2>1	1>2	1>2	2>1	2>1
P-3	LONGITUDINAL	...	2>1	1>2	2>1	...	2>1
	LATERAL	1>2
P-4	LONGITUDINAL	1>2	2>1	1>2
	LATERAL	1>2	1>2	...	2>1	1>2	1>2	2>1	2>1
P-5	LONGITUDINAL	1>2	1>2	1>2	1>2	...	2>1	2>1	...	2>1	2>1
	LATERAL	1>2	1>2	...	1>2	1>2	2>1	2>1	2>1	2>1	2>1
P-6	LONGITUDINAL	1>2	1>2
	LATERAL	...	2>1	2>1	2>1	2>1	2>1

Table 12. Significant Variance Inequalities for Pilot Averages.

COMPUTED VARIABLE	CONTROL MODE	ω (rad/sec)					
		0.6	1.2	1.8	2.4	3.0	3.6
$ Y_p $	LONGITUDINAL	1>2, 1>4	1>2, 1>4	1>4, 1>2	...
	LATERAL	4>1, 4>2	4>1, 4>2	1>2	1>2	1>2	4>1
$\angle Y_p$	LONGITUDINAL	...	1>4, 1>2	1>2>4	1>2>4	1>4, 2>4	1>4, 2>4
	LATERAL	1>2, 4>2	1>2, 1>4	...	1>4, 2>4
p	LONGITUDINAL	...	2>1
	LATERAL	...	4>1, 2>1	4>1, 2>1	4>1, 2>1	2>1, 2>4	4>1, 2>1

(c) The fraction of p table entries for which 1>2 is 0.041 and for 2>1 this fraction is 0.26. As before 0.05 would be expected by chance for each fraction.

Thus the direction of trends is what we would have expected from our rather vague hypothesis.

In Table 12 we present significant variance inequalities, at the 0.05 level as before, for over-all averages for pilots. In averaging over pilots we can include $\omega_{t0} = 4$ runs, so that inequalities related to $\omega_{t0} = 4$ can be presented in Table 12. From Table 12 we note that the trends of Table 11 are maintained by the inclusion of $\omega_{t0} = 4$. Seven of the variance inequalities shown are in a different direction from what our hypothesis on the effects of ω_{t0} on variability would predict, but five of these inequalities would be expected on the basis of chance alone.

We can make the following conclusions on the variability exhibited by human operators in compensatory tracking tasks with dynamics:

- (a) Time effects, be they over long or short intervals, are of relatively little importance.
- (b) There are strong individual differences in the variance inequalities for different forcing function bandwidths.
- (c) The variability of the describing function, Y_p , appears to be inversely proportional to "task demands".
- (d) The variability of the linear correlation, ρ , appears to be directly proportional to "task demands".

Section VIII

NONLINEAR MODELS OF HUMAN OPERATORS IN COMPENSATORY TASKS

A. INTRODUCTION

From the preceding sections the bases of a fairly reasonable linear theory of the human operator can be hypothesized from the limited data of various restricted experiments. As pointed out in Sections V and VI, the operator in simple continuous control tasks with visual inputs, and motion or force outputs, will act like a servo element having an input-output relationship of the form

$$C(j\omega) = Y(j\omega; t)E(j\omega) + N_c(j\omega) \quad (\text{VIII-1})$$

where $N_c(j\omega)$ is a small remnant which does not include any time-varying or other "linear" phenomena. An alternate representation can be used where the remnant, now denoted $N_e(j\omega)$, is considered to contain all the operator power which is not linearly coherent with the forcing function, i.e.,

$$C(j\omega) = Y(j\omega)E(j\omega) + N_e(j\omega) \quad (\text{VIII-2})$$

Y may be considered to be a describing function of an adaptive, optimizing servo of relatively restricted form. The word "adaptive" refers to the operator's ability to adjust the form of his describing function (within fairly well defined limits and as a function of input predictability) to one required for good low frequency response and marginal high frequency stability of the operator-controlled element system. The word "optimizing" refers to his ability to adjust some of his describing function "constants", as functions of the forcing function and controlled element, to values tending to optimize the system response.

The remnant term has been fairly well "explained" in previous sections as the result of either noise injected by the operator at his output, or his nonsteady behavior. These explanations have largely ignored the slight nonlinearities shown to be present by the data, and further, have stressed a model which is correct in the statistical sense rather than one deliberately designed to give a point-by-point match of actual human and model output data. It should also be emphasized that both models have really been derived in an attempt to match data rather than on a completely a priori basis.

While the overall linear models are reasonably satisfying and usable, particularly for stability and overall performance studies, an equivalent nonlinear model would be of great value for detailed system response predictions and for studies including the effects of nonlinear controls. Such a model should be consistent with the linear models, should help explain the remnant term, and should assist in better visualization of the mechanisms involved in human response. Just such nonlinear studies have been carried out by Mayne and Mead and their associates at Goodyear Aircraft with very interesting and instructive results.

The basic approach in all of the Goodyear studies involved the use of analog computer elements to simulate a pilot, actual pilots in various mockups, and an analog computer representation of the longitudinal or lateral dynamics of an airframe. Either the pilot or the "analog pilot" could be placed in control of the simulated airframe at the option of the investigator. The "analog pilot" elements were varied until the airframe-"analog pilot" responses to known complex inputs were very similar to those of the airframe-pilot combination. In many instances the analog pilot was such a good simulation that control by the actual and analog pilots could be interchanged for fairly extended periods (30 sec or so) without the actual pilot's knowledge.

The Goodyear studies utilized this fundamental approach in several types of experimental setups, encompassing such variations as stationary and moving (pitching or rolling) mockups, different forcing functions, and different artificial feel forces for the pilot. These studies shall be summarized in chronological order below.

B. GOODYEAR STATIONARY MOCKUP STUDY

In the first study, (Ref. 33) the pilot was seated in a stationary chair and operated a control stick provided with a simple spring feel. An oscilloscope resembling an artificial horizon was used to present an error signal

to the pilot. This error signal was formed by subtracting the pitch angle due to the pilots' elevator deflection from a forcing function. The forcing function, $i(t)$, was made up of four complex waves as shown in Figure 126.

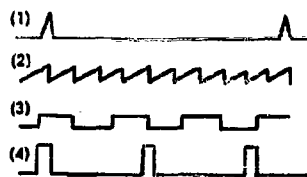


Figure 126. Forcing Function Used in First Goodyear Study.

The autocorrelation function corresponding approximately to this forcing function is

$$R_{ii}(\tau) = e^{-0.15\tau} \cos(0.35\pi\tau) = e^{-a\tau} \cos(\omega_n\tau) \quad (\text{VIII-3})$$

which is equivalent to a spectral density of

$$\Phi_{ii}(\omega) = 4 \int_0^\infty R(\tau) \cos(\omega\tau) d\tau = 2 \left[\frac{a[a^2 + (\omega_n + \omega)^2] + (\omega - \omega_n)[a^2 + (\omega_n - \omega)^2]}{[a^2 + (\omega_n + \omega)^2][a^2 + (\omega_n - \omega)^2]} \right] \quad (\text{VIII-4})$$

Very roughly this is similar to that forcing function used in the Franklin Institute studies having a bandpass of about two rad/sec.

The simulated airframe portion of the controlled element transfer function used was equivalent to that of a very well damped airframe pitching oscillation at a constant forward speed, with a pitch angle/elevator transfer function* of

$$\frac{\theta}{\delta_e} = \frac{2.0(0.73s + 1)}{s(0.24s^2 + s + 1)} = \frac{2.0(0.73s + 1)}{s(0.6s + 1)(0.4s + 1)} = \frac{2.0 \left[\frac{s}{1.37} + 1 \right]}{s \left[\frac{s}{1.67} + 1 \right] \left[\frac{s}{2.5} + 1 \right]} \quad (\text{VIII-5})$$

An additional portion of the controlled element was a 30 inch simulated aircraft control stick with travel limits of ± 18 degrees. Control feel was simulated by spring loading the stick to produce a spring gradient of 1.67 pounds/degree. The dynamics of the stick system were presumably negligible relative to those of the airframe at the low frequencies of interest.

The subjects for most of the tests considered here were drawn from a group of six military reservist pilots. While all had fighter aircraft training, the piloting experience level included little jet aircraft time and that was confined to the T-33 trainer.

All of the subjects were allowed to practice for a time sufficient to develop a uniform and effective response motion. This required just a few minutes for the pilot subjects. (One non-pilot was also tested thoroughly, requiring about 20 hours of mockup practice before achieving a level of proficiency comparable to that of the pilots.) The actual runs on individual pilots during which data were taken lasted for 30 minutes.

In the portions of the study directly applicable to the process of obtaining a pilot analog, Goodyear servo engineers started by examining pilot input and output data as recorded on an oscillograph. Then, taking into account what was known or suspected about the physiological makeup of the human controller, an analog computer circuit was constructed which could yield output results similar to those obtained with actual operators in the same situation. The differences between human and analog outputs for identical forcing functions were then used as clues for refinement of the analog. The refinement process was carried on to the point where the pilot could not detect the substitution, into the control loop, of the analog for himself for fairly long time periods of the order of a minute.

As a result of preliminary tests with human operators, it was decided that the analog pilot should include the following characteristics:

- (1) **Rate Judgment** — To control adequately the longitudinal motions the pilot should utilize the pitch error and generate a lead; or alternately, should utilize signals proportional to both the pitch error and the rate of change of pitch error. Viewed externally these two possibilities amount to the same

* In another part of the referenced report a transfer function for the airframe of $\frac{\theta}{\delta_e} = \frac{1.97}{s} \frac{(0.73s + 1)}{[(0.24s)^2 + 0.24s + 1]}$ was cited. The one given above, however, was that set up for the operator studies.

thing. From a psychological standpoint, however, they are drastically different. The first (lead generation) implies that the operator perceives only the position of the dot on the scope and generates the lead equalization in the central nervous system. The second, for which there is more evidence, implies the visual perception of both the dot position and the dot velocity, with subsequent summing of quantities proportional to each signal. The precise nature of the human's mechanization of the lead function is beyond the scope of this report, and either possibility is considered here to fall into the general category of "equalizing behavior."

- (2) **Reaction Time Delay** — Since the forcing function is random-appearing a reaction time delay should always be present.
- (3) **Rate Threshold** — It was noted that pitch rate errors greatly in excess of the threshold of perception for visual motion were deliberately neglected by the pilot. This can be considered to be a *threshold of indifference*.
- (4) **Clamping** — Once a correction was made the pilots tended to "clamp" to this deflection until the pitch error approached zero.
- (5) **Neuromuscular Lag** — This lag is essentially an approximation to that contained in the transfer function for the dynamic portion of the response to a step input.

After approximating these quantities in the "pilot analog", and suitably adjusting the parameters, it was found that close agreement was obtained between analog pilot response and actual pilot response, e.g., Figure 127.

The computer schematic containing the "pilot analog" is shown in Figure 128. It should be noted that some liberties have been taken for expediency in the setup, e.g., the "clamp" is replaced by a simple limiter (since the operators tended to clamp at about the same value of stick deflection), and the reaction time delay is approximated as is the neuromuscular lag. Insufficient information is given in Reference 33 to enable computation of the values of the nonlinearities from the computer setup. Some misprints are present in the referenced report, so the schematic given in Figure 128 reflects a few additions and interpretations by the authors. These are starred on the computer diagram shown.

The nonlinear transfer characteristic simulated can be expressed symbolically (taking liberties with the describing function concept) by

$$\left\{ \frac{1 - 0.52s + 0.0022s^2}{1 + 0.52s + 0.0022s^2} \right\} \left\{ K_d + \frac{K_{\theta}s}{T_Ns + 1} \right\} \left[\text{Th} \left(\frac{a_r}{e_1} \right) \right] \left[\text{Li} \left(\frac{a_l}{e_2} \right) \right] \quad (\text{VIII-6})$$

REACTION TIME DELAY APPROXIMATION	PILOT DISPLACEMENT SIGNAL	RATE JUDGMENT AND NEUROMUSCULAR LAG	RATE INDIFFERENCE THRESHOLD	LIMITING
---	---------------------------------	--	-----------------------------------	----------

A close linear equivalent to this characteristic would be (with typical values obtained from analysis of the computer wiring diagram)

$$Y_p = \frac{K e^{-rs} (T_L s + 1)}{(T_N s + 1)} \quad (\text{VIII-7})$$

where typically $K = 0.425$

$$r = .25$$

$$T_N = .1877$$

$$T_L = 3.53$$

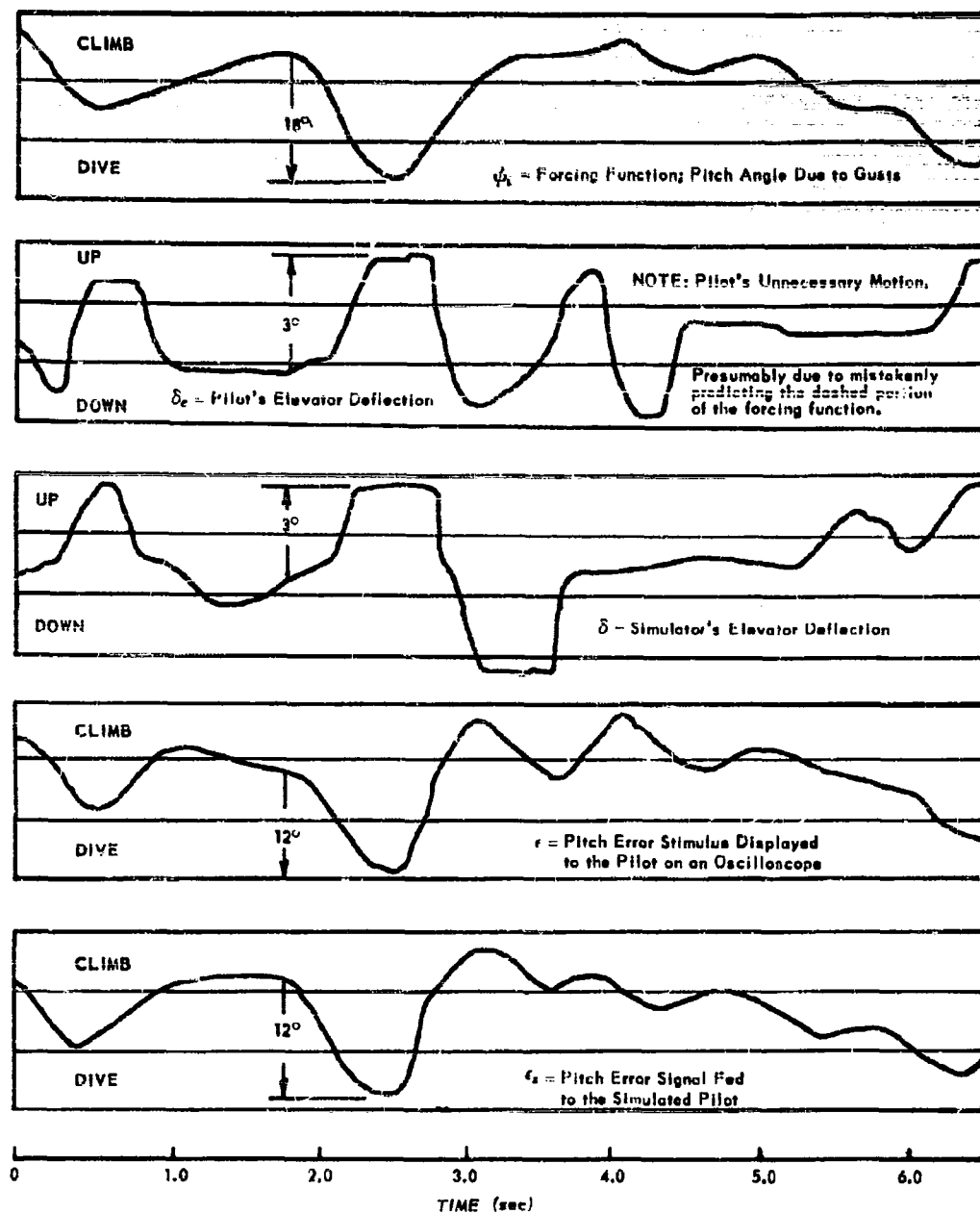
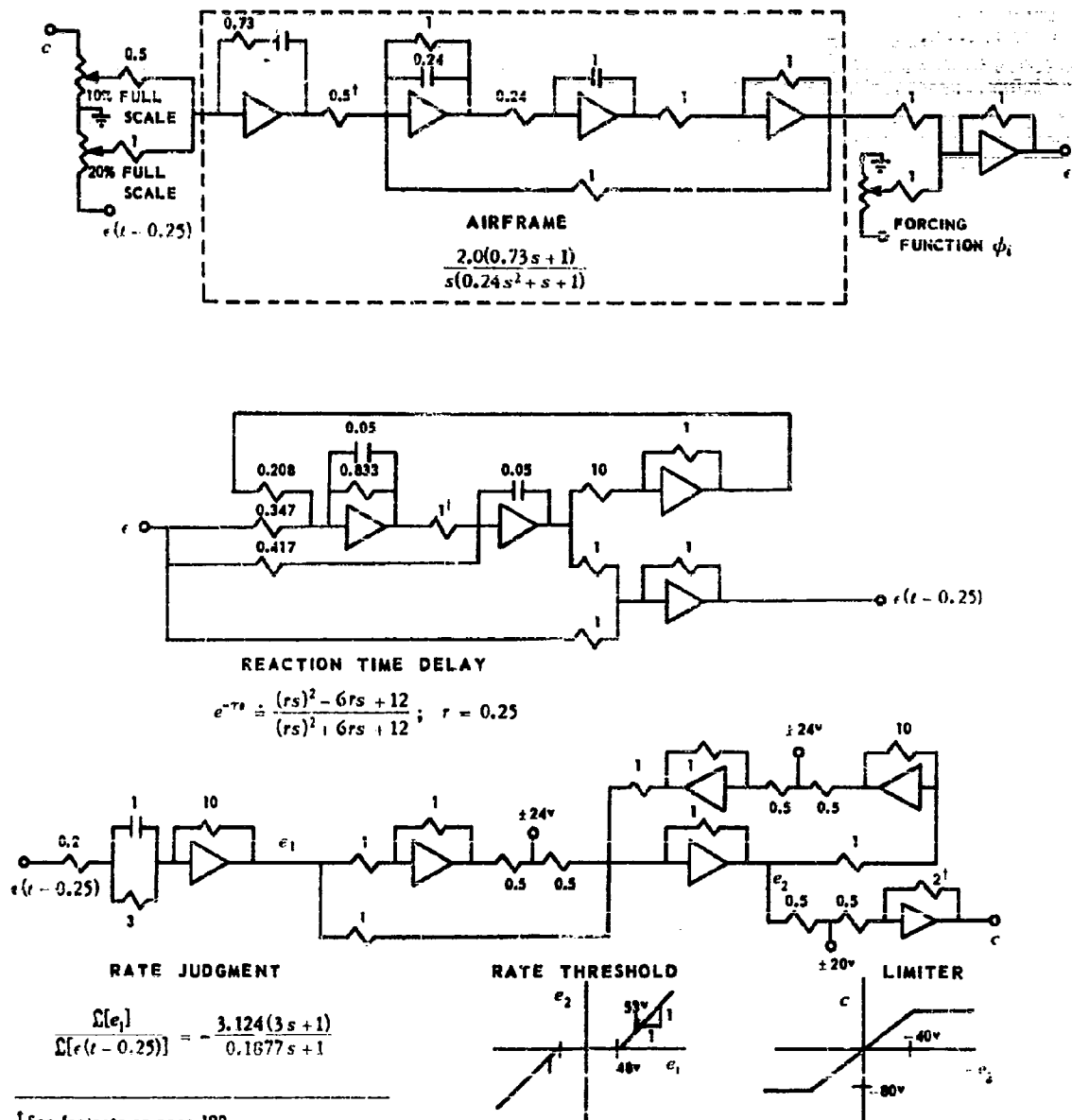


Figure 127. Record of Forcing Function and Responses from Both a Pilot and the Analog Pilot of Figure 128. (Reference 33)



[†] See footnote on page 190.

Figure 128. Goodyear "Stationary Mockup" Study, Computer Representation of Human Operator and Controlled Element.

From the form of Eq. (VIII-7) it is apparent that a great deal of similarity exists between this linear approximation and the linear models advanced in Section VI for similar tasks. This linearized approximation is plotted, in conjunction with the controlled element transfer function, on Fig. 129. The complete open-loop Bode plot exhibits the same low phase margin conditions (close to zero), previously noted for some of the linearized operator data of Elkind, Tustin, Franklin and Russell.

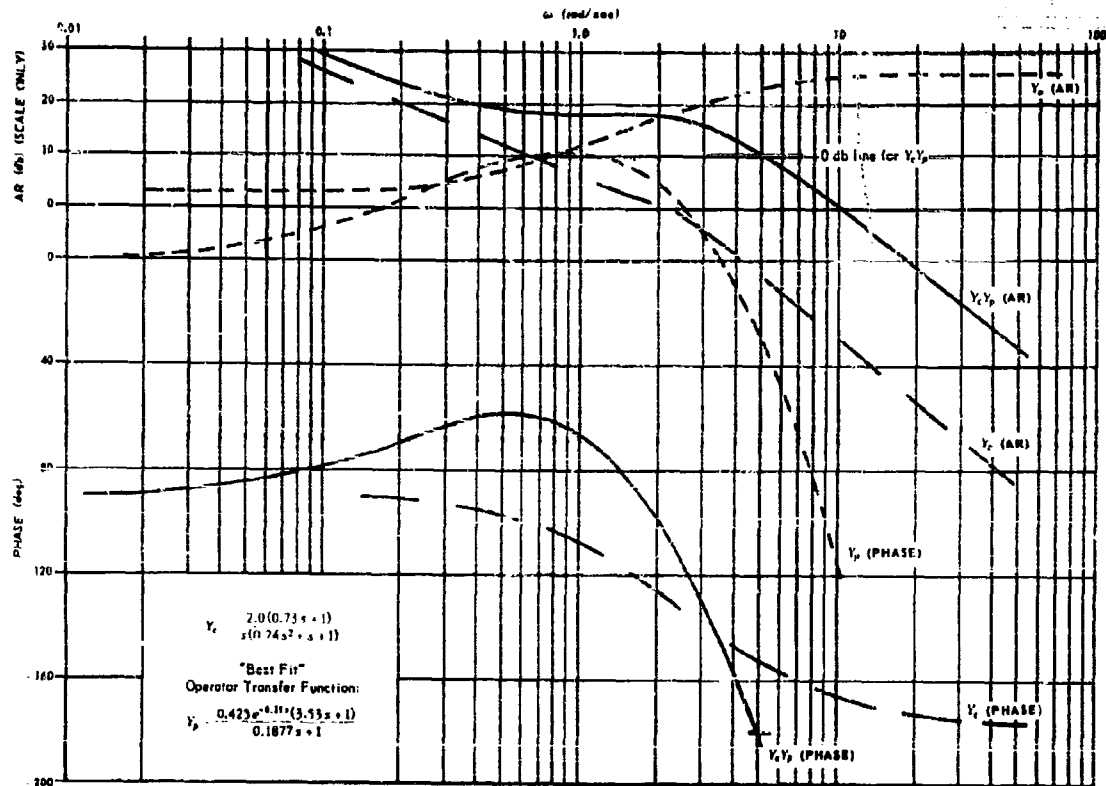


Figure 129. Equivalent Open Loop Bode Plot of Goodyear Computer Set-up, for the Stationary Mockup.

An interesting point is the absence of a low frequency lag term in Eq. (VIII-7). (It will be recalled that Tustin's data, with a similar controlled element but different forcing function bandwidth, showed a low frequency lag term.) If gain crossover had occurred at a lower frequency (reduced open loop gain) the low frequency lag term would have been admissible without instability, and the low frequency system response would have been improved. The reduced loop gain would, of course, cause a deterioration of the high frequency response.

In many ways these Goodyear data are directly comparable with the Franklin elevator tests. The effective forcing function bandwidth was of the order of 2 rad/sec, and the controlled element characteristics were similar. The operator transfer function forms are identical, and the numerical value of τ is essentially the same in both cases. The T_L values are, of course, different because of the detailed controlled element differences.

All of this strengthens the previously observed fact that the presence of the low frequency lag term is a function of controlled element and forcing function characteristics. It is also a further indication that the operator adjusts his transfer function in much the same way as a servo designer would adjust a similar fixed-form equalizer for a given system task.

Another interesting subject raised by the non-linear simulator representation of the pilot is the possible insight into the causes and form of the remnant term of the linear mode. With the operator analog, as constructed, the only sources of the remnant term considered are the nonlinear transfer characteristics. Both nonsteady behavior and pilot injected noise have been eliminated from the outset. Because of the relatively low (.5-.7) linear correlations obtained by Franklin on a similar task (elevator with 2 rad/sec forcing function), one would be inclined to think that an important discrepancy in results was present. The inclination is strengthened when it is realized that the nonlinearities of the Goodyear analog could hardly account for 30% or more of the output power. While it is difficult to resolve this problem because of the limited amount of data presented by Goodyear in their first study (Fig. 127 contains the only traces in Ref. 33), it should be noted that

- (1) The analog of Reference 33 required a considerable number of changes in later work to match trained jet pilots.
- (2) The time intervals during which a particular analog configuration matched the actual operator's output were probably fairly short, e.g., only 6 seconds of data are shown in Fig. 127.

Since the more extensive modified analog data presented later compares more favorably with the data from linearized measurements, it is probably not reasonable to say that the data from this first Goodyear study and the Franklin data are inconsistent on this point. Goodyear's ability to achieve a fairly reasonable and adequate pilot simulation for short time intervals using only transfer elements and a mild nonlinearity is, however, a point in support of the nonsteady behavior model over that of noise injection. Indeed, probably the best way to check experimentally the nonsteady versus noise injection hypothesis is a real-time simulation of this sort. If a good point by point data match was obtained for short periods of time, using only transfer elements, then the nonsteady explanation would be preferred, since the injected noise version would not allow such a match and would be relatively independent of the run lengths.

Probably the most important facet of the first Goodyear study in the light of the other data cited in this report, is the insight given regarding the nonlinear behavior of the operator. It will be recalled that Elkind's Experiment II (Effect of Amplitude) data indicated that the open-loop operator gain was a slightly increasing function of rms forcing amplitude. This effect is consistent with Goodyear's use of a threshold transfer characteristic. The limiting, or clamp, effect is also apparent on many tracking responses other than those obtained by Goodyear. Therefore, both the "indifference threshold" and "clamp" concepts are important additions to our knowledge of operator dynamics.

C. THE SECOND GOODYEAR STUDY — MOVING SIMULATOR WITH PISTON ENGINE FIGHTER PILOT SUBJECTS

The second Goodyear study [34] was concerned largely with the construction and use of a movable mockup capable of providing realistic simulation of aircraft movements in addition to the usual visual display. The study was relatively short, and, in essence, constitutes only a necessary connecting link between the first and third Goodyear efforts summarized herein.

The basic equipment used for the experimental work was similar to that of the first study, with the addition of a single degree of freedom dynamic cockpit mockup capable of simulating aircraft angular motions (see Figures 130 and 131). The pilot's visual input consisted of either sinusoids or filtered random noise added to the pitch (or roll) angles generated by the aerodynamic simulation. The mockup room could be darkened to eliminate spatial cues. The "cockpit" motion was set up to be equivalent to the airframe pitch (or roll) angle. Subjects were again pilots having largely piston engine fighter experience.



Figure 130. Dynamic Cockpit Mockup Showing Pilot in Position for Roll Studies.
(Ref. 34, Fig. 4)

The actual work of this study was largely exploratory, so the reports issued did not include detailed documentation of the specific computer setups and controlled element characteristics used. In the pitch case they were presumably similar to those previously described in the first study, with the addition of the cockpit motion to simulate pitch angle. One set of aileron test results were presented as an example and are repeated here as Fig. 132. In this particular run the pilot was controlling the lateral axis of a simulated T-33 aircraft. An aileron-rudder crossfeed circuit of $\delta_r/\delta_a = 0.8/(s + 4)$ was inserted to assist turn coordination since the operator had no rudder pedals. For the instance shown, the pilot kept flying for over a minute after control had been transferred to the analog, unaware of the transfer. Other pilots, who moved more cautiously, had motions which did not resemble that of the analog as well. These subjects took only a few seconds to recognize the transfer.

In addition to these data, Reference 34 makes some general observations which are quoted below:

- (1) "With the given random-motion input, there is no distinct difference between errors with visual input, motion input, or both. Reaction time and motion characteristics found previously still hold under the conditions of this study. No information was found to prove that vestibular-motion stimuli

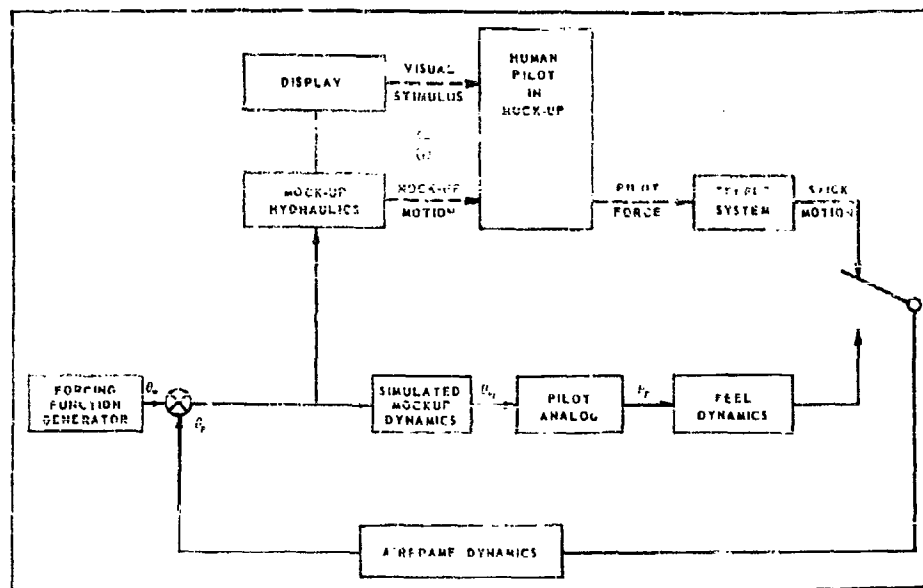


Figure 131. Goodyear Pilot Analog, Dynamic Substitution Test Schematic.
(Ref. 35, Fig. 13)

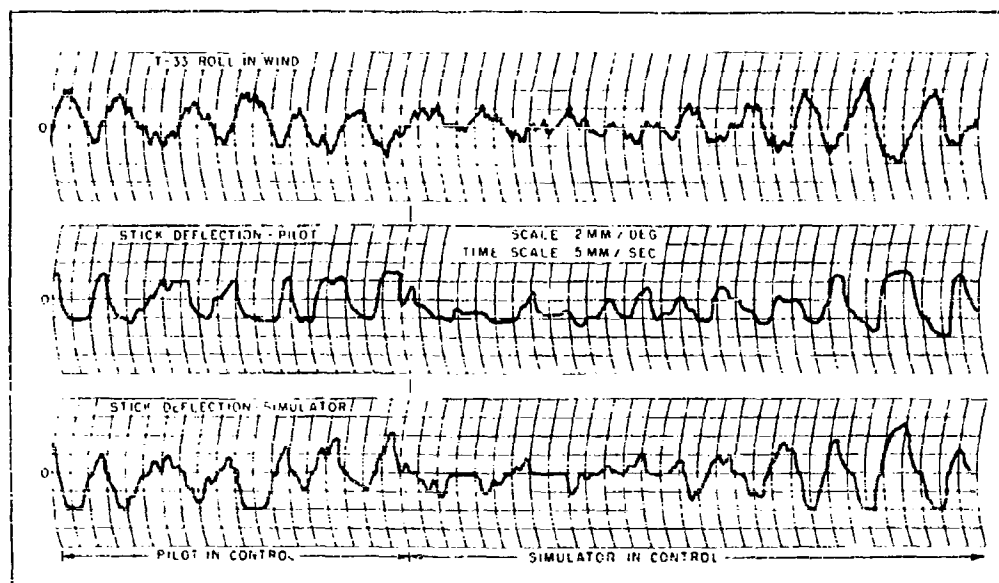


Figure 132. Goodyear Experimental Results for Pilot and Simulator in Parallel.
(Ref. 34, Fig. 7)

do not lead to drift and give faster transient response. However, it was found that the difference in results for a pilot with his eyes open and shut was much less than the variation between different pilots."

(2) "There is a great decrease in tracking effectiveness at frequencies above the natural frequency of the pilot-aircraft system. This was evident in both sinusoidal and random tracking."

(3) "Pilots show a tendency to phase in with frequencies below 0.5 cps and to drop out of phase for higher frequencies when they are tracking sinusoidal inputs. At or near 0.5 cps a pilot tends to phase in for periods as long as 30 seconds, but ultimately he executes a control reversal requiring several seconds to lock in again."

(4) "The results indicate that a general-purpose simulator representing the human pilot in closed-loop studies should have a linear transfer function as follows:

$$K \left(\frac{r^2 s^2 + 6rs + 12}{r^2 s^2 + 6rs + 12} \right) \left(\frac{1}{0.125s + 1} \right) (0.2s + 1)$$

where $r = 0.25$ second for the simple reaction-time delay and K is adjusted to represent a given pilot. The first bracketed factor is the approximation for pure delay of form e^{-Ts} . The second factor is a filter for smoothing the response of the first and also approximates the neuromuscular lag, and the third factor accounts for the pilot's use of the first derivative of input. A dead-zone type of nonlinearity should follow the above linear operation." [This entire statement only applies, of course, to the particular controlled element and forcing function conditions used in the Goodyear tests.]

The work of the second study appears to add some generality to the results of the first (as well as to the new results of Section VI which correlate with the first study). This generalization is specifically along the lines of forcing function type, and is given in comment (1) above. Here it is pointed out that, for the subjects of this study at least, the same transfer characteristic appears to be suitable for motion inputs *alone*, for visual inputs *alone*, and for a combination of both.

THE THIRD GOODYEAR STUDY — MOVING SIMULATOR WITH JET FIGHTER PILOT SUBJECTS

The third Goodyear study (Ref. 35) utilized four Navy jet interceptor pilots as subjects in the moving cockpit partially described previously. Part of this study was devoted to an evaluation of changes in rms error as functions of controlled element parameter changes, and the other part to the determination of a pilot analog. Only his latter work will be reviewed here.

The controlled element dynamics were those of the short-period pitching motion of an aircraft in conjunction with a variable artificial feel system consisting of a simulated aircraft control stick loaded with adjustable inertial, spring and viscous damping forces. For most of the analog runs the parameters of the controlled elements were set to "standard" values. For these cases the airframe dynamics set into the computer were represented by the transfer function,

$$\frac{\theta_p}{\delta_e} = \frac{1.97(0.73s + 1)}{s[(0.24s)^2 + 0.251s + 1]} = \frac{1.97(0.73s + 1)}{s \left[\left(\frac{s}{4.17} \right)^2 + \frac{2(0.523)s}{4.17} + 1 \right]} \quad (\text{VIII-8})$$

where θ_p is the simulated airframe pitch angle due to the elevator deflection δ_e . The "standard" feel system dynamics were

$$\frac{\delta_e}{F_p} = \frac{K_f}{0.015s^2 + 0.44s + 1} = \frac{K_f}{\left[\frac{s}{29.1} + 1 \right] \left[\frac{s}{2.4} + 1 \right]} = \frac{K_f}{\left[\left(\frac{s}{8.16} \right)^2 + \frac{2(1.8)s}{8.16} + 1 \right]} \quad (\text{VIII-9})$$

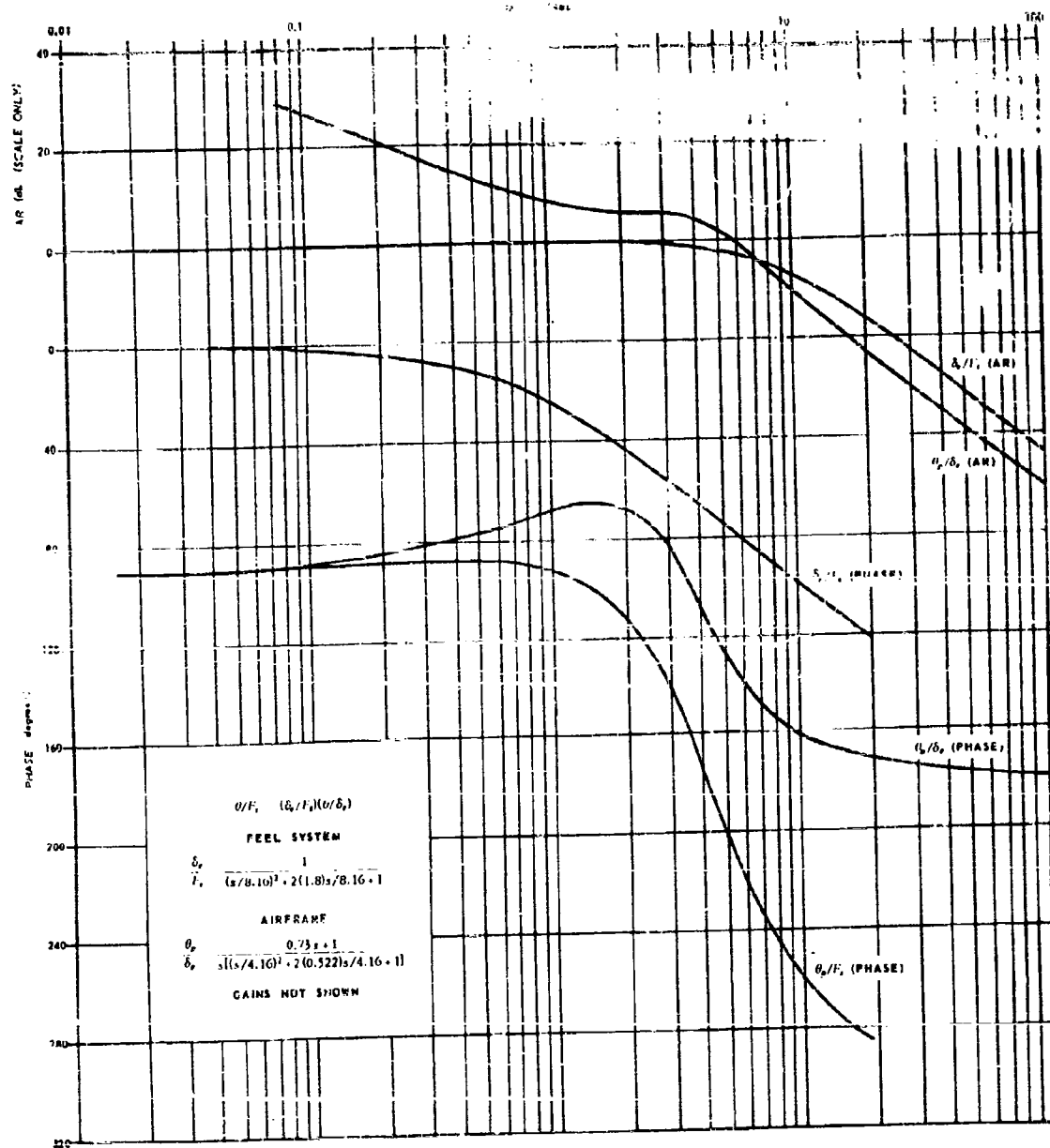


Figure 133. Goodyear Moving Mockup Controlled Element.

of the feel spring constant was 3.1 lb/in. The nominal overshift was 148 rad/sec/lb which was equivalent to a stick-force/g value of 0.00148. The stick force was adjusted for each subject during the analog runs, so the stick force was 0.148 lb for a 100 g acceleration.

$$\frac{K_{\text{ext}}}{\theta_{\text{xi}}} = \left[\frac{s}{14.9} + 1 \right] \quad (9)$$

Graph showing the magnitude response R (dB) versus frequency ω (rad/sec) for a second-order system. The y-axis is R (dB) (SCALE 0.1) and the x-axis is ω (rad/sec) on a logarithmic scale.

The curve shows a resonance peak at $\omega = 1$ rad/sec, where R reaches approximately 10 dB. The magnitude decreases as frequency increases beyond the resonance peak.

The asymptotic approximation is shown as a dashed line, which is 0 dB for $\omega < 1$ rad/sec and decreases at -40 dB/decade for $\omega > 1$ rad/sec.

Equation for the magnitude response:

$$R_{11} = \frac{4\sigma^2}{\beta[(\omega/\omega_p)^2 + 1][(\omega/\beta)^2 + 1]}$$

Parameters: $\omega_p = 1/2$, $\beta = 4$

The analog studies were based upon four Navy jet interceptor pilots and several other subjects with experience ranging from piston engine fighters to light planes. One subject had no piloting experience at all. The analog was constructed in the same general fashion as discussed previously, and tested by both visual comparison of pilot and analog output records and the process of changeover from actual pilot to analog control of the mockup. When an analog setup had been reached which showed good visual comparison and was capable of avoiding detection

by the mockup for periods (10 sec.) or more. When substituted for him in the loop, the analog system was used.

The initial analog design was modified that for the stationary mockup test. With some functions added as a result of additional exploratory testing and experience, the most important changes added to the analog, which is shown in block diagram form in Fig. 135, were:

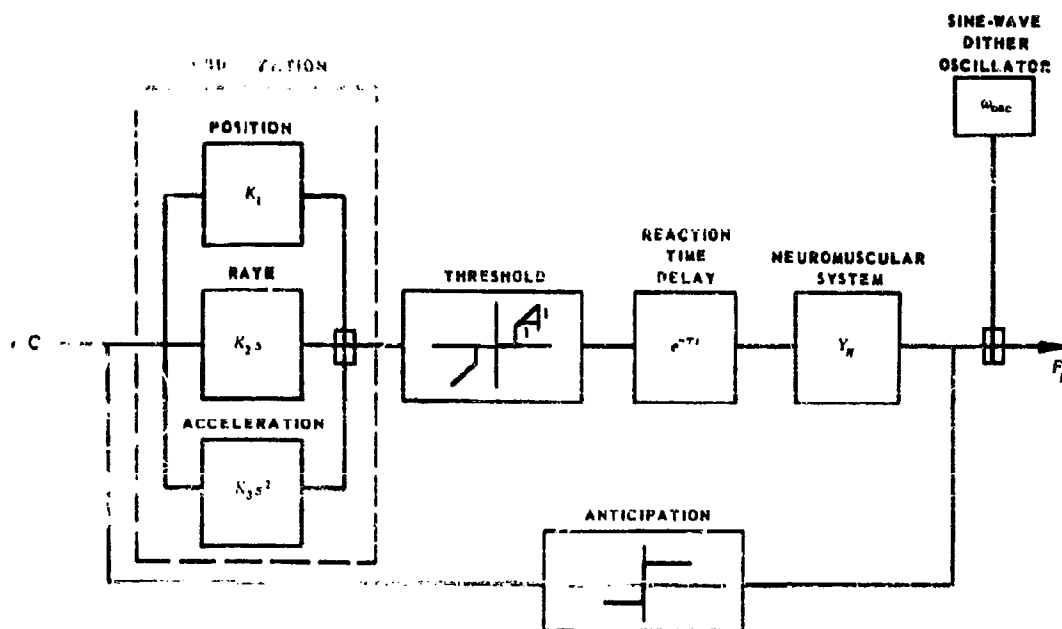
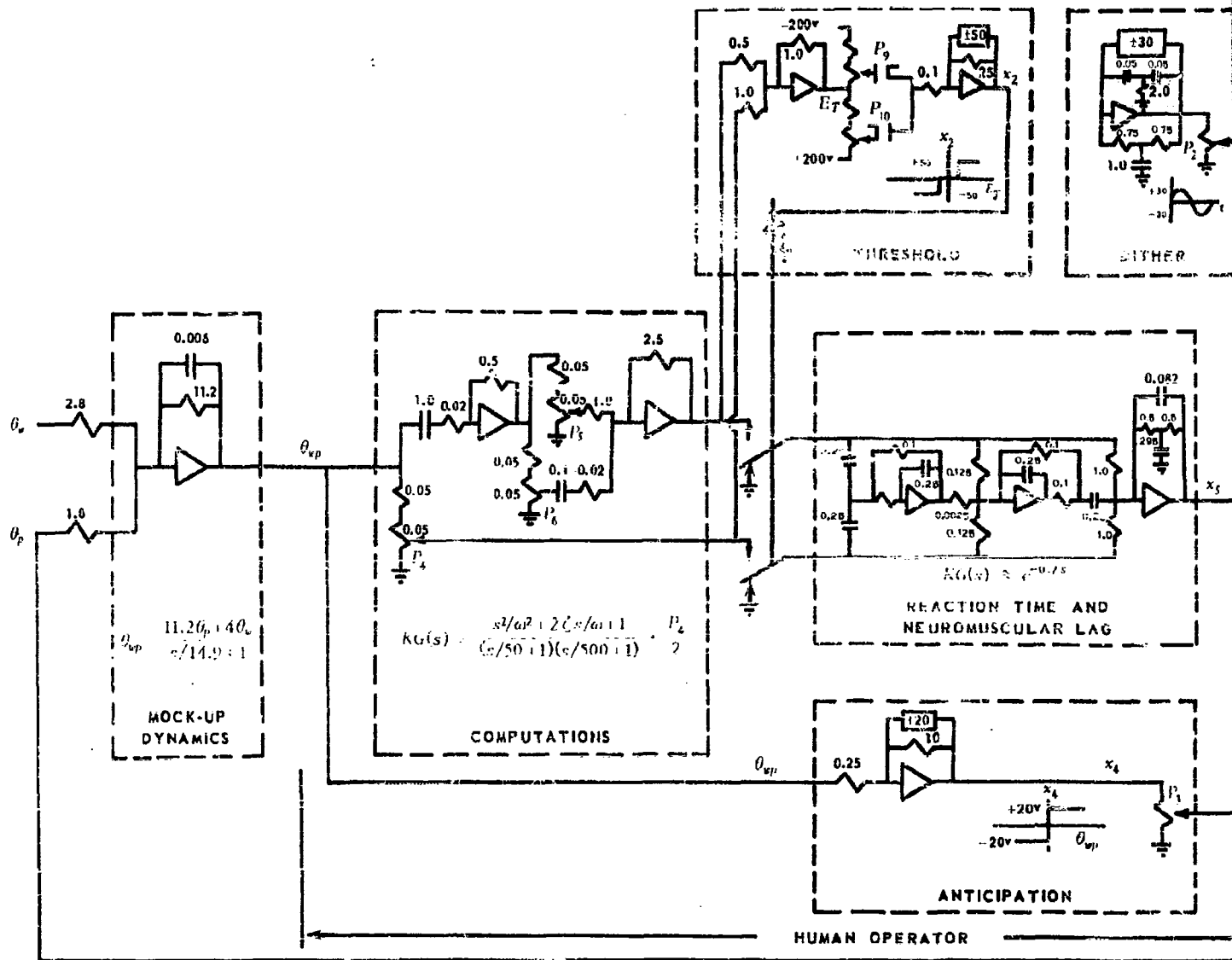


Figure 135. Block Diagram of Goodyear Hypothetical Jet Pilot Analog System with Moving Simulator. (Ref. 35, Fig. 9)

- (1) The addition of a higher derivative in the equalization term, i.e., a higher order lead. The total equalization may then take the form of either a quadratic or of two first order terms. The additional lead was based upon the observation that the moving mockup allowed distinctly higher derivative sensitivity of the pilot than that of the stationary mockup.
- (2) The addition of a relay-type characteristic operating directly off the presented error. This type of action was based upon the observation that the pilot initiates a portion of his motion whenever the sign of the error changes instead of after one reaction time interval. This part of the total motion is essentially a square wave with axis crossings corresponding to the zero values of the error signal. The phenomenon has been variously called "Alertness", "Zero Anticipation", and "Anticipation".
- (3) The superposition of a steady, essentially sinusoidal, hand oscillation upon the output. This "dither" phenomenon was observed only in the four Navy pilots and showed steady day-to-day variations which suggested that it was a learned technique. To a first approximation the dither signal can be simulated by a fixed amplitude oscillator generating a 1.4 cps sine wave.

In addition to these major modifications, the reaction time delay value was changed from 0.25 to 0.2 seconds.

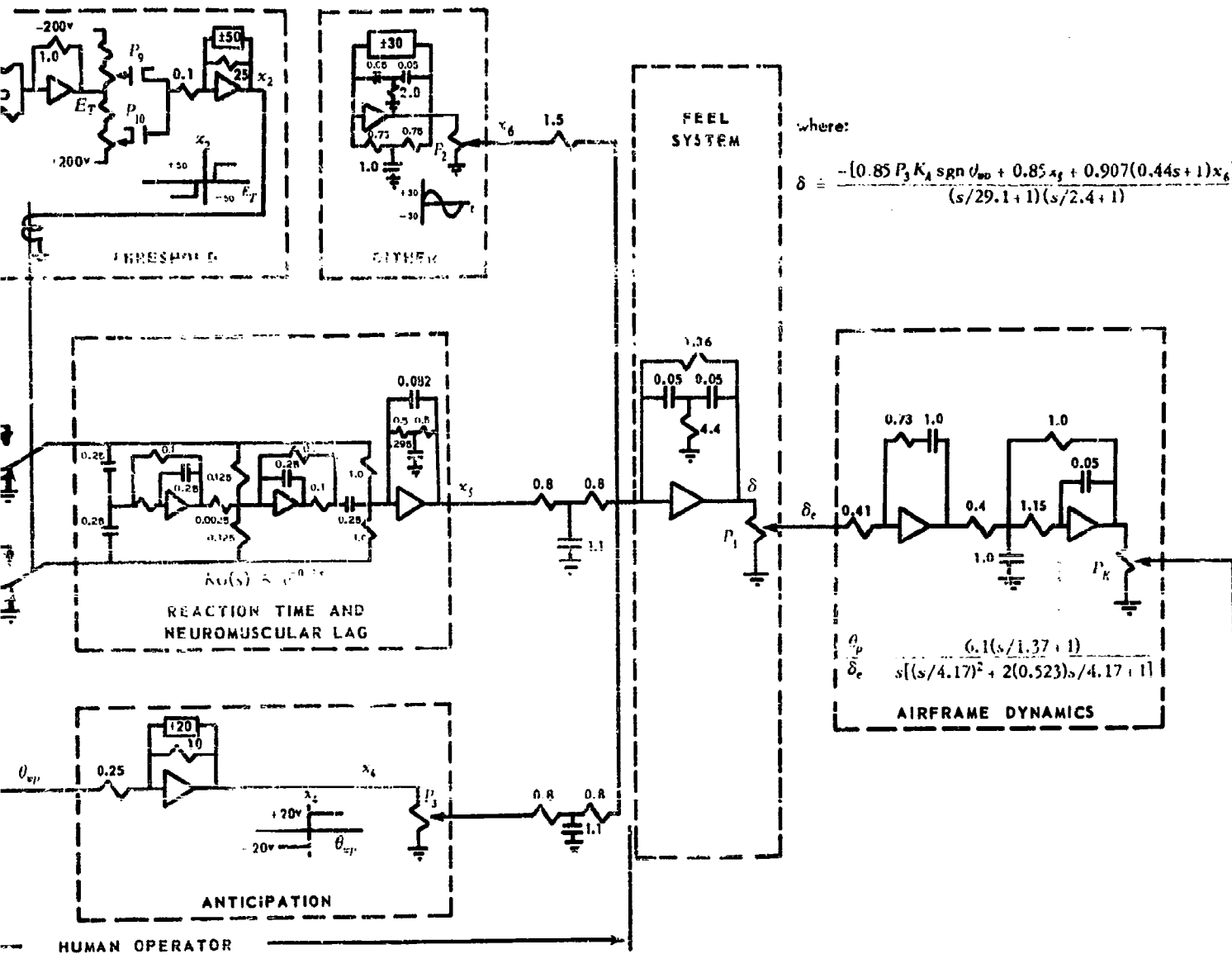
The detailed computer circuit diagram is presented as Fig. 136. It will be noted that the mechanization for comparable functions is changed considerably from that of Fig. 128, but these changes are indicative of taste



1

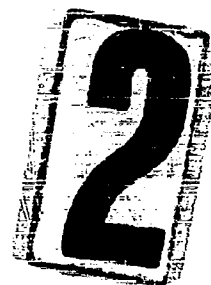
POTENTIOMETER	P ₁	P ₂	P ₃	P ₄	P ₅	ACCE
PILOT	DEFLECTION SENSITIVITY	DITHER LEVEL	ANTICIPATION SENSITIVITY	POSITION GAIN	RATE GAIN	
V. O.	0.100	0.025	0.200	0.53	0.30	
H. H.	0.080	--	0.400	0.60	0.60	
J. B.	0.080	--	0.300	0.05	0.60	
M. C.	0.075	0.100	0.500	0.50	0.60	

Figure 136. Goodyear "Moving Mockup" Study Computer Representation of the Human Operator



	P_3 ANTICIPATION SENSITIVITY	P_4 POSITION GAIN	P_5 RATE GAIN	P_6 ACCELERATION GAIN	P_9, P_{10} THRESHOLD LEVEL	ω_n	ζ
	0.200	0.53	0.30	0.30	0.75	0.821	0.298
	0.400	0.60	0.60	0.60	0.075	0.616	0.391
	0.360	0.05	0.60	0.40	0.040	0.18	1.350
	0.500	0.60	0.60	0.60	0.075	0.53	0.336

Meckup" Study Computer Representation of the Human Operator and Controlled Element.



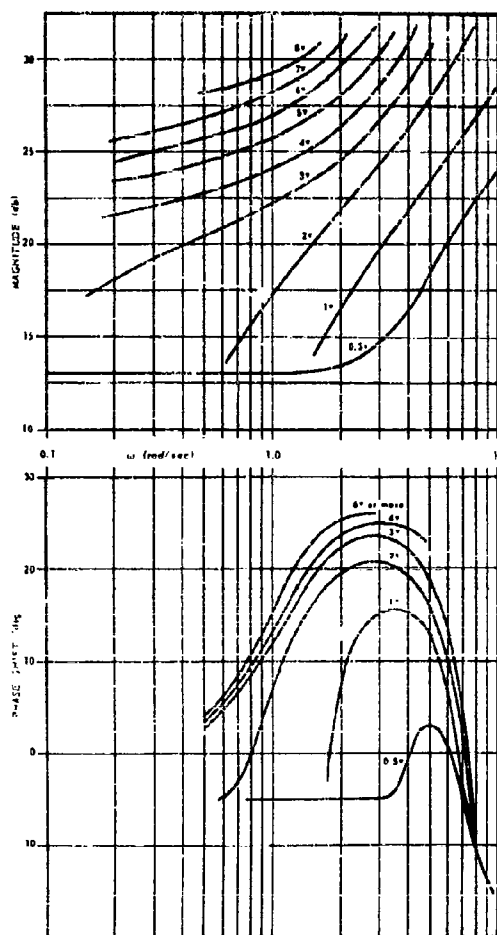


Figure 137. Phase Shift and Attenuation Characteristics for Pilot Analog Circuit.
(Ref. 35, Fig. 19)

duction in aircraft sensitivity, Fig. 142, the pilot's gain increased about a factor of two to compensate for the reduction, but otherwise the results were similar to those with "standard" settings (Fig. 140).

and method rather than fundamental. Only the additions summarized above are major modifications. The values for the nonlinearity magnitudes are not derivable from the computer setup because the per unit scale factors were not given in Ref. 35, but the transfer functions mechanized were computed and are shown on the schematic. A sinusoidal describing function for the settings of pilot V.O. is also shown as Fig. 137. This sinusoidal describing function indicates that the predominant characteristics of V.O.'s analog circuit are a first order lead (rate sensitivity), threshold effect, and reaction time delay. We must note at this point, however, that V.O.'s analog is not typical of those of the four Navy jet pilots. In general, these jet pilots generated a substantial amount of second order lead (acceleration sensitivity) and had less first order lead (rate sensitivity) than the non-jet pilots.

Reference 35 included five recordings of various actual pilot-pilot analog runs as examples of some eighty hours of similar recordings. Figures 138 through 140 illustrate the correspondence between these pilots and their analogs for the previously defined "standard" conditions. Pilot V.O., Fig. 138, is cited as a typical example of a light plane pilot with no experience in jet aircraft. The "dither" characteristic is nil, and the maximum pitch angles recorded are generally higher than those for the subjects with jet aircraft experience. Pilot G. C., Fig. 139 exhibited the most dither of the four Navy pilots, though the dither is scarcely discernable in the mockup motion record.

Pilot J. B., Fig. 140, is noted in Ref. 35 as "the least consistent of the four Navy pilots". His dither level in Fig. 140 is not nearly as high as that of G. C.

Additional data is given in Ref. 35 on the effects of controlled element changes, using J.B. as an example. Figure 140 is, of course, set up for the "standard" controlled element. For the data of Fig. 141, the damping ratio of the airframe short period motion was reduced to 0.2. Here the airframe-pilot system is tending toward instability. For the case with a fifty percent re-

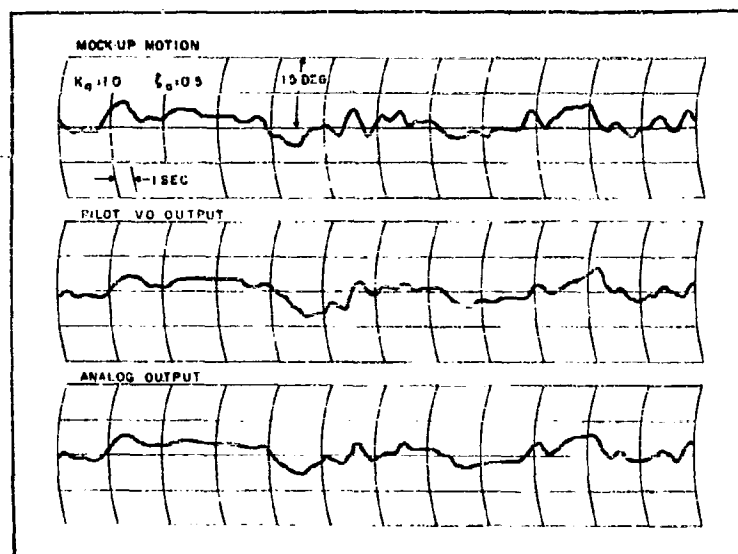


Figure 138. Goodyear Experimental Characteristics,
Light Plane Pilot with Mockup Pitch.
(Ref. 35, Fig. 14)

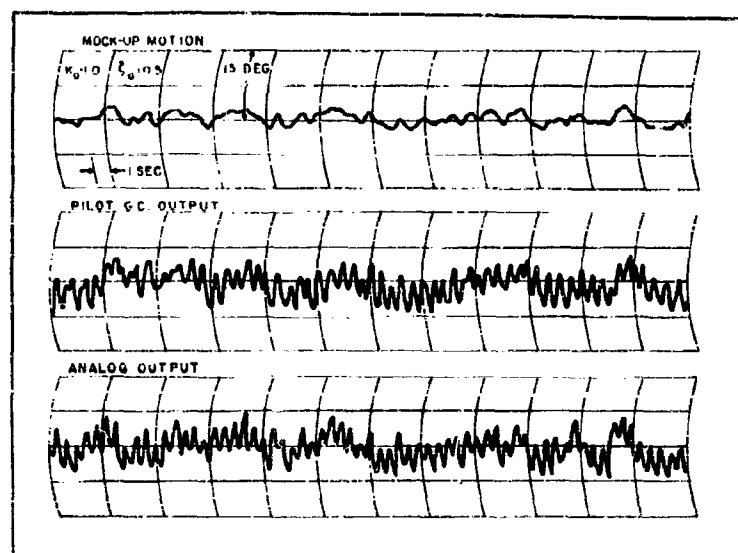


Figure 139. Goodyear Experimental Characteristics, Proficient
Jet Pilot Including Mockup Pitch.
(Ref. 35, Fig. 15)

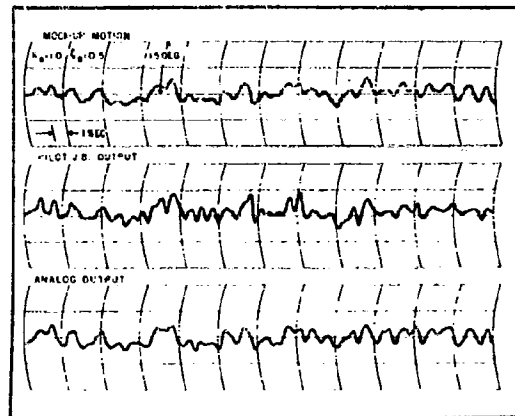


Figure 140. Goodyear Experimental Characteristics, Less Proficient Jet Pilot Including Mockup Pitch.
(Ref. 35, Fig. 16)

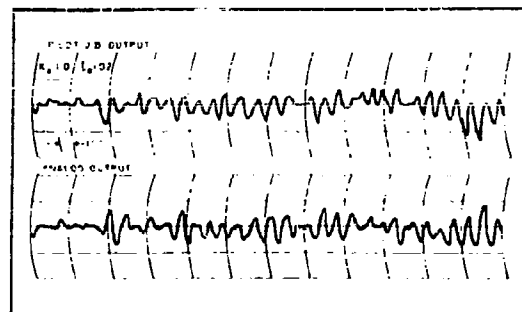


Figure 141. Goodyear Experimental Characteristics, Less Proficient Jet Pilot with Reduced Aerodynamic Damping.
(Ref. 35, Fig. 17)

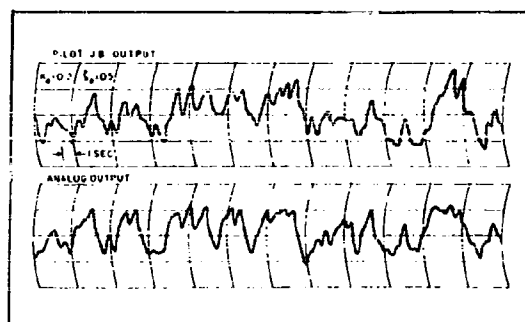


Figure 142. Goodyear Experimental Characteristics, Less Proficient Jet Pilot with Reduced Aircraft Sensitivity.
(Ref. 35, Fig. 18)

E. COMPARISON OF NONLINEAR AND QUASI-LINEAR MODELS OF HUMAN OPERATORS IN COMPENSATORY TASKS

In Part B of this section we have already compared the results of the first Goodyear analog (for the stationary mockup) with those of Sections V and VI. It will be recalled that the two types of results were generally consistent as far as transfer function forms were concerned. The Goodyear model's indifference threshold effect, reaction time delay values, and equalization parameters all appear to be compatible with the more extensive data from the quasi-linear models. A source of possible conflict was present in the remnant data, but there was insufficient analog data available to derive any definitive conclusions so the subject was deferred until this point.

Now that the Goodyear moving simulator program has been summarized, we are in a position to compare these results with those previously presented for the quasi-linear case. In this subsection, therefore, we shall attempt to compare the consequences of the two quite different experimental approaches by reconciling the Goodyear analog results with the quasi-linear data.

Perhaps the best way to approach this problem is to compute the approximate describing function and remnant of the Goodyear moving simulator analog. As the first step in this process we require the statistical input describing functions of the threshold and anticipation circuits. These will be derived below and then combined with the linear portion of the analog to find the total describing function. An approximation to the remnant will be derived, giving us a total approximation to the quasi-linearization of the Goodyear analog. This result can then be compared with the other linearized data and conclusions made.

1. Describing Function of Goodyear Analog Pilot for Moving Simulator Case

The development of a describing function for the analog computer circuitry is straightforward if the quantities throughout the overall loop have amplitude distributions which are approximately Gaussian. Assuming that this is the case, the describing functions, when an amplitude dependent pure gain can serve to approximate the non-linearity, can be obtained directly from Eq. (III-42), which is repeated below as Eq. (VII-11).

$$K_{\text{equivalent}} = \frac{\int_{-\infty}^{\infty} x f(x) p(x) dx}{\int_{-\infty}^{\infty} x^2 p(x) dx} = \frac{\int_{-\infty}^{\infty} x f(x) e^{-\frac{x^2}{2\sigma^2}} dx}{\sqrt{2\pi} \sigma^3} \quad (\text{VII-11})$$

For the anticipation, or sgn function, shown in Fig. 143, the switching level is set at a value a_A . Then,

$$\begin{aligned} f(x) &= +a_A, \quad x > 0 \\ &= -a_A, \quad x < 0 \end{aligned} \quad (\text{VII-12})$$

Denoting the rms value of the error signal, e , as σ_e , the Gaussian input describing function is

$$\begin{aligned} K_A &= \frac{-\int_{-\infty}^0 a_A x p(x) dx + \int_0^{\infty} a_A x p(x) dx}{\sigma_e^2} = \frac{2a_A \int_0^{\infty} x p(x) dx}{\sigma_e^2} \\ &= \frac{2a_A \int_0^{\infty} \frac{1}{\sqrt{2\pi}} e^{-\frac{x^2}{2\sigma_e^2}} \frac{x dx}{\sigma_e^2}}{\sigma_e^2} = \sqrt{\frac{2}{\pi}} \frac{a_A}{\sigma_e} \int_0^{\infty} e^{-u} du = \sqrt{\frac{2}{\pi}} \frac{a_A}{\sigma_e} \end{aligned} \quad (\text{VIII-13})$$

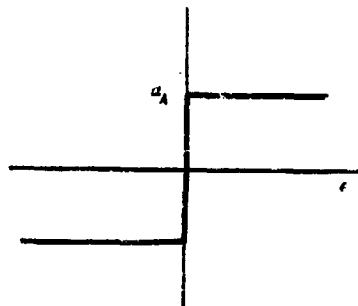


Figure 143. Anticipation or Sgn Function Transfer Characteristic.

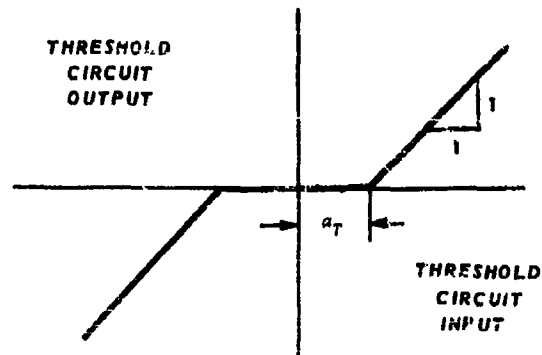


Figure 144. Threshold Transfer Characteristic.

We shall approximate the actual threshold characteristic used by that shown in Fig. 144. Here the threshold is a_T and the rms value of the signal presented to the threshold characteristic is σ_T . Then

$$\begin{aligned} f(x) &= x; \quad x > a_T \quad \text{or} \quad x < -a_T \\ &= 0; \quad -a_T \leq x < a_T \end{aligned} \quad (\text{VIII-14})$$

The integral involving $x f(x) p(x)$ will become

$$\int_{-\infty}^{\infty} x f(x) p(x) dx = \int_{-\infty}^{-a_T} x^2 p(x) dx + \int_{a_T}^{\infty} x^2 p(x) dx = \sigma_T^2 \left[1 - \Phi\left(\frac{a_T}{\sqrt{2}\sigma_T}\right) + \sqrt{\frac{2}{\pi}} \frac{a_T}{\sigma_T} e^{-\left(\frac{a_T}{\sqrt{2}\sigma_T}\right)^2} \right] \quad (\text{VIII-15})$$

where $\Phi[a_T/(\sqrt{2}\sigma_T)]$ is the error function. The threshold describing function will then be given by

$$K_T = 1 - \Phi\left(\frac{a_T}{\sqrt{2}\sigma_T}\right) + \sqrt{\frac{2}{\pi}} \frac{a_T}{\sigma_T} e^{-\left(\frac{a_T}{\sqrt{2}\sigma_T}\right)^2} \quad (\text{VIII-16})$$

The overall Gaussian input describing function of the Goodyear pilot analog in the frequency region of interest will then be approximately

$$Y_p \doteq K_p e^{-\tau s} \left[K_T \left(\frac{\sigma_T}{\sigma_e} \right) \left(\left(\frac{s}{\omega_n} \right)^2 + \frac{2\zeta\omega_n}{s} + 1 \right) Y_N + K_A \left(\frac{a_A}{\sigma_e} \right) \right] \quad (\text{VIII-17})$$

Having Eq. (VIII-17) we can compare directly the Goodyear and other describing function results. The gain, K_p , reaction time delay, τ (taken by Goodyear as 0.2 sec), and neuromuscular transfer function, Y_N , are completely consistent with the quasi-linear data in form. The equalization characteristic is quadratic rather than the first order lead obtained in the quasi-linear measurements taken in situations with comparable controlled element characteristics. This, however, is cited by Goodyear as a significant difference between their moving and non-moving mockup experiments as well as being most dominant in their highly trained subjects. The second order lead, therefore, does not enter into our comparison per se, but rather is evidence of a skilled pilot's ability to generate higher order leads due to the additional motion input information. On this basis, all of the linear terms can be said to compare favorably with those from other data.

This leaves us with the linearized portions of the nonlinear threshold and anticipation terms. While we have no exact data on the a_A/σ_e ratio which defines the anticipation term, the output data plots presented by Goodyear and the assumption of a reasonable computer scaling make it evident that the ratio is fairly small, relative to the other terms in Y_p , for this forcing function-controlled element situation. Since the effect of the anticipation terms in the linearized open loop describing function is negligible, one can reasonably expect that the major change in

Y_p will be due to the addition of a linearized description of the non-linear "indifference threshold" represented by $K_T(a_T/\sigma_T)$. Since the existence of such a threshold is compatible with Elkind's data on the effects of forcing function amplitude variation, and is consistent with the F-80A data, we can conclude that the Goodyear analog is consistent with other measurements of quasi-linear describing functions.

2. Remnant for Goodyear Analog Pilot for Moving Simulator Case

The problem now at hand is to find the approximate power spectrum of the Goodyear analog remnant. The remnant in this model must come from the threshold, anticipation and dither effects. Since the linearized portion of the "indifference threshold" $K_T(a_T/\sigma_T)$ accounts for its effects fairly completely, the contribution of the threshold to the non-coherent output power can be neglected. This leaves us with the anticipation circuit and dither as prime remnant sources.

The dither characteristic was approximated in the Goodyear study by a sine wave of amplitude A_d and frequency ω_d . The power spectra of a sinusoid is a delta function, so the output power spectra due to the dither will be

$$\Phi_{nnc,dither} = \pi A_d^2 [\delta(\omega_d + \omega) + \delta(\omega_d - \omega)] \quad (\text{VIII-18})$$

It was stated above that the linearized effect of the anticipation circuit on the describing function was probably small compared to that of the other describing function terms. Consequently its effects will be found in the remnant. In fact, we shall assume in the following that all of the power from the anticipation circuit will be in the remnant.

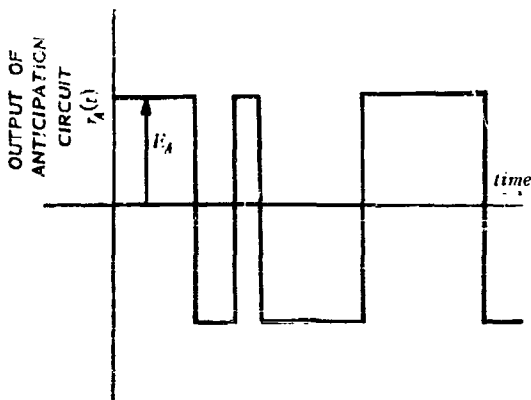


Figure 145. General Form of Anticipation Circuit Output.

The action of the anticipation circuit is essentially that of a perfect relay with no threshold. The circuit output will be a square wave symmetrical in amplitude about zero and having axis crossings coincident with those of the error signal. Its general form will be as shown in Fig. 145. Our current problem is to compute an approximate spectral density or autocorrelation of $r_A(t)$. These, unfortunately, will depend upon the probability distribution of the axis crossings of $r_A(t)$ or the equivalent quantity for the crossings of the error. Finding the axis crossings can be very difficult. However, even though the exact distribution of the zeros is difficult to obtain, we can make an estimate of the average number of axis crossings of the error, $e(t)$, if its amplitude distribution is assumed to be Gaussian. Then, if we assume further that the distribution of the axis crossings is known, having this average rate, we can estimate the autocorrelation of $r_A(t)$. This will be our procedure in the following.

First, the average number of axis crossings per second of a random function with a Gaussian distribution is*

$$\beta_t = \frac{1}{\pi} \left(-\frac{R''_e(t)}{\sigma_e^2} \right)^{1/2} \quad (\text{VIII-19})$$

* See Reference 68.

where $[R_{\epsilon\epsilon}''(r)]/\sigma_\epsilon^2$ is the second derivative of the normalized autocorrelation of the function, and $R'(0)$ is zero. To obtain an estimate of the normalized error autocorrelation near zero values of r , one can recognize that only the higher frequency components of the error spectrum, $\Phi_{\epsilon\epsilon}$, need be involved. At high frequencies, the error spectrum will approach

$$\Phi_{\epsilon\epsilon} \rightarrow \Phi_{11} = |Y_f|^2 \Phi_{\text{noise source}} \quad (\text{VIII-20})$$

where Y_f is the transfer function of the filter used to obtain the forcing function spectrum from the noise generator. While Eq. (VIII-20) is only a high frequency approximation to the error spectrum it is all we require for an estimate of $\rho_\epsilon(r)$ as r approaches zero.

The form of Φ_{11} was given previously in Fig. 134. The normalized autocorrelation can be obtained by transforming the equation shown there, and is

$$\frac{R_{\epsilon\epsilon}(r)}{\sigma_\epsilon^2} = \frac{\omega_f e^{-\beta_1 |r|}}{\omega_f - \beta_1} - \frac{\beta_1 e^{-\omega_f |r|}}{\omega_f - \beta_1} \quad (\text{VIII-21})$$

The second derivative of Eq. (VIII-21), evaluated at $r = 0$, is

$$\frac{R_{\epsilon\epsilon}''(0)}{\sigma_\epsilon^2} = -\omega_f \beta_1 \quad (\text{VIII-22})$$

Since $\omega_f = 1/2$ rad/sec and β_1 is somewhat greater than 4 rad/sec, the average number of error signal axis crossings per second will be of the order of 0.37. The average time, T_A , between crossings will then be approximately 2.7 seconds.

If we now assume that the probability, $Q(r)$, that t and $t+r$ lie in the same interval is known, then the autocorrelation of the sgn function output is:

$$R_A(r) = \left(\frac{E_A}{2} \right)^2 Q(r) \quad (\text{VIII-23})$$

If $H(\lambda)$ is the probability that an axis crossing occurs between time λ and time $\lambda + d\lambda$, then the average time between axis crossings is

$$T_A = \int_0^\infty \lambda H(\lambda) d\lambda \quad (\text{VIII-24})$$

and $Q(r)$ is given by

$$Q(r) = \frac{1}{T_A} \int_{|r|}^\infty (\lambda - |r|) H(\lambda) d\lambda \quad (\text{VIII-25})$$

so that $Q(r)$, and hence the autocorrelation of the sgn function output $R_A(r)$, is known if we know $H(\lambda)$.

Unfortunately, the distribution of axis crossings is not known. It is instructive, however, to consider some examples which give insight into the problem. For example, if the axis crossings obey a Poisson distribution, then

$$H(\lambda) = T_A^{-1} e^{-\lambda/T_A} \quad (\text{VIII-26})$$

so $Q(r) = e^{-|r|/T_A}$ and the autocorrelation is

$$R(r) = \left(\frac{E_A}{2} \right)^2 e^{-|r|/T_A} \quad (\text{VIII-27})$$

As a second example, consider that the axis crossings are purely random in a given interval $2T_A$; i.e., λ can have any value between zero and $2T_A$ with equal likelihood although the average time between axis crossings is T_A . Then $Q(r) = 1/(2T_A)^2 (2T_A - |r|)^2$; $|r| \leq 2T_A$, and zero elsewhere. The autocorrelation, $R_A(r)$, is, for this case,

$$R_A(r) = \left(\frac{E_A}{2}\right)^2 \left(1 - \frac{|r|}{T_A} + \frac{|r|^2}{(2T_A)^2}\right) \quad (\text{VIII-28})$$

It will be noted that the first approximation to the autocorrelation $R_A(r)$ based upon both these widely different axis crossing distributions will be

$$R_A(r) \doteq \left(\frac{E_A}{2}\right)^2 \left(1 - \frac{|r|}{T_A}\right); \quad \frac{|r|}{T_A} \ll 1 \quad (\text{VIII-29})$$

By this time, the diligent reader will look upon this autocorrelation as an old and valued friend, for it has appeared in all of the attempted remnant "explanations" (i.e., Weber law type output noise, nonsteady operator behavior, etc.). The power spectral density is, as before,

$$\Phi_{nnc, \text{anticipation circuit}}(\omega) = 2T_A \left(\frac{E_A}{2}\right)^2 \left(\frac{\sin \frac{\omega T_A}{2}}{\frac{\omega T_A}{2}}\right)^2 \quad (\text{VIII-30})$$

The total open loop remnant, referred to the operator's output, of the Goodyear analog is then, approximately,

$$\Phi_{nnc}(\omega) = 2T_A \left(\frac{E_A}{2}\right)^2 \left(\frac{\sin \frac{\omega T_A}{2}}{\frac{\omega T_A}{2}}\right)^2 + \pi A_d^2 [\delta(\omega_d + \omega) + \delta(\omega_d - \omega)] \quad (\text{VIII-31})$$

Both of these terms have distinct parallels in the quasi-linear data. The $[(\sin x)/x]^2$ form is a good approximation to Elkind's remnant and is not inconsistent with the Franklin data. It even has values of T_A which are comparable to those obtained from Elkind's data. The dither, giving a delta function peak at about 1.4 cps, is consistent with a similar measurement made by Russell. We can therefore say that there are no striking inconsistencies between the analog and quasi-linear data.

The apparent correlation between the remnant due to the anticipation circuit and that found from Elkind's measurements leads to the conjecture that the principal remnant cause is the "perfect relay" action of anticipation in parallel with an almost linear transfer function. If this action is indeed the primary remnant cause, it would have to increase in importance relative to the linear transfer function term as the task became more difficult. This would imply that the human has three different behavioral modes when tracking random appearing forcing functions, i.e.,

- a. For tasks presenting slight demands, e.g., simple controlled element dynamics and low bandwidth forcing functions, the linear correlation will approach unity and the operator will generate a linear transfer function.
- b. For very demanding tasks the linear correlation will be very small, the open loop operator describing function will approach $K_A(a_A/A)$, and the human transfer characteristic will be that of a perfect relay (or sgn function).
- c. For tasks where the demands are between these two extremes the operator will operate both modes in parallel.

The above remnant "explanation" is probably the most physically suitable of any developed in the report. Its consequences match most of the quasi-linear data in a qualitative way, and is further corroborated by observation of the operator and tracking records.

The dither phenomenon observed in the Goodyear tests must also be considered to be a possible human output under certain conditions. It does, however, appear to be an individual tactic which is consciously used depending upon the operator temperament and task. The dither action is analogous to that used in servo systems as a general linearizing technique, e.g., to reduce the effects of coulomb friction. Besides the Goodyear tests it has also been observed in human dynamics experiments where such a technique appeared to the operator to be an applicable tactic. In this regard,

- a. No dither was present in Elkind's tasks, probably because there were no restraints whatsoever upon the control. Possibly its general desirability had been rejected by the subjects during their training period as a technique which wasn't particularly helpful in that task.
- b. Dither was probably present in some of Russell's runs since a sharp peak at 1.23 cps was found on the only remnant spectrum measured. Russell's control bar was attached directly to a Variac type instrument, which has a fairly high coulomb friction level. Dither would therefore be generally desirable.
- c. In the Franklin Institute test series several of the subjects tried out the use of a dither signal during their training periods but abandoned it before their record runs were taken. This was done not because dither introduction was an unsuitable technique for operating the simulator, but because these pilots did not consider it to be part of their normal piloting style. A typical comment was, "I think that I can control the *simulator* best by using the frantic mode, (which included dither), but I would not use it in an *airplane*."

Section IX

HYPOTHETICAL MODEL OF THE HUMAN OPERATOR IN COMPENSATORY TASKS

A. SUMMARY OF MODELS

In the previous sections, past experimental data have been reviewed in detail and grouped into various classes depending on forcing function type and controlled-element characteristics. Simple analytical describing function forms and approximate linear correlations were determined for those instances where they were available, redetermined in some cases and accepted outright from the original sources in others. The net result of this effort is summarized in Tables 13 and 14.

While the controlled element transfer functions shown are correct over a wide frequency band, the human operator describing functions are not, since either particular frequencies or a narrow band of frequencies were used in their determination. To present the measurements in a more precise context, Tables 13 and 14 also show the controlled element approximate characteristics in the frequency region covered by the human response data.

The remnant data are not nearly as extensive as the describing function characteristics, though they are still extremely important to the description of an analytical operator model. Such data as are available on remnant models are summarized in Table 15. It will be recalled that, while there was a forcing function amplitude effect on the Elkind and Franklin describing function data, the overall dependence upon forcing function was relatively small over a wide range of forcing function rms amplitudes. One can conclude from this that the remnant power due to operator nonlinear transfer characteristics in series with the describing function was relatively small for the conditions tested. This implies that a large portion of the remnant must be due to other phenomena. In the previous discussions of the quasi linear data the major possibilities for the particular data were narrowed down to nonsteady operator behavior and operator injected noise. These two sources were not separable from the data available, so models were derived assuming each phenomena was to account for the entire picture. In the discussion of nonlinear models it was pointed out that a third remnant source was also a possibility. This was the action of a nonlinear transfer characteristic essentially in parallel with a describing function. When the linearized portion of the parallel nonlinear transfer characteristic is small relative to the describing function amplitude, the parallel nonlinear channel will have relatively little effect on the overall open loop describing function. The action of the parallel nonlinear element will, however, have a substantial effect upon the remnant. The summary in Table 15 reflects the consequences of these various possible models.

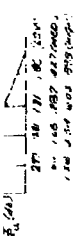
From the data presented in Tables 13 through 15 we shall endeavor in this section to hypothesize a reasonable model of the operator for the case of random appearing visual inputs and motion outputs. In constructing the hypothetical model, the transfer characteristics will be considered first, on a term by term basis.

B. HYPOTHETICAL TRANSFER OR DESCRIBING FUNCTION MODEL

1. Reaction Time Delay

The reaction time delay, represented by the e^{-Ts} term, appears in all transfer functions for forcing functions having a degree of unpredictability. Also, while it has not been thoroughly investigated to date, it is probable that an e^{-Ts} term is present in all tracking tasks in which the operator's input is random appearing. The line of demarcation, however, between random appearing and predictable inputs is not well defined at present. For instance the use of a perfectly predictable sine wave forcing function on a system with an operator plus complex controlled element dynamics, resulting in a complex, nonsinusoidal error signal (operator input), probably falls into the random appearing input class. In the same case, reduction of the controlled element dynamics to some simpler (but presently unknown) form would tend to preserve the predictable sinusoidal wave form, and the operator input would then fall into the predictable class.

When the simplest of the fitted transfer function forms is used to derive a value for τ , a considerable variation in this initially determined pure time delay is apparent. Then, when a stability requirement is asserted, and stability of the fitted form is obtained by the introduction of a high frequency lag beyond the bandwidth of measurement, the resultant τ values appear to lie within a relatively small grouping, with a central value of about 0.15

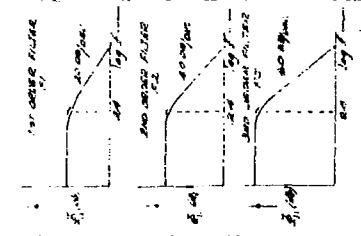


6) RANDOM ADDRESSING
FUNCTION MADE UP
OF 40-100 SHARDON
GIVING ANY DESIRABLE
SHAPE TO THE SIGNAL
IN THE ADDRESSING
CIRCUIT

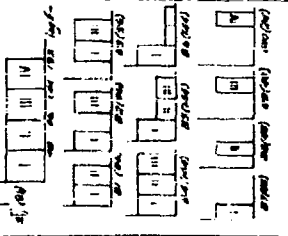


7) RANDOM ADDRESSING
FUNCTION MADE UP
OF 40-100 SHARDON
GIVING ANY DESIRABLE
SHAPE TO THE SIGNAL
IN THE ADDRESSING
CIRCUIT

8) RANDOM ADDRESSING
FUNCTION MADE UP
OF 40-100 SHARDON
GIVING ANY DESIRABLE
SHAPE TO THE SIGNAL
IN THE ADDRESSING
CIRCUIT



9) RANDOM ADDRESSING
FUNCTION MADE UP
OF 40-100 SHARDON
GIVING ANY DESIRABLE
SHAPE TO THE SIGNAL
IN THE ADDRESSING
CIRCUIT



LOW FREQ	HIGH FREQ
37 1.0 1.5	42 1.5 2.0

10) RANDOM ADDRESSING
FUNCTION MADE UP
OF 40-100 SHARDON
GIVING ANY DESIRABLE
SHAPE TO THE SIGNAL
IN THE ADDRESSING
CIRCUIT

LOW FREQ	HIGH FREQ
37 1.0 1.5	42 1.5 2.0

11) RANDOM ADDRESSING
FUNCTION MADE UP
OF 40-100 SHARDON
GIVING ANY DESIRABLE
SHAPE TO THE SIGNAL
IN THE ADDRESSING
CIRCUIT

LOW FREQ	HIGH FREQ
37 1.0 1.5	42 1.5 2.0

12) RANDOM ADDRESSING
FUNCTION MADE UP
OF 40-100 SHARDON
GIVING ANY DESIRABLE
SHAPE TO THE SIGNAL
IN THE ADDRESSING
CIRCUIT

LOW FREQ	HIGH FREQ
37 1.0 1.5	42 1.5 2.0

LOW FREQ	HIGH FREQ
37 1.0 1.5	42 1.5 2.0

13) RANDOM ADDRESSING
FUNCTION MADE UP
OF 40-100 SHARDON
GIVING ANY DESIRABLE
SHAPE TO THE SIGNAL
IN THE ADDRESSING
CIRCUIT

LOW FREQ	HIGH FREQ
37 1.0 1.5	42 1.5 2.0

14) RANDOM ADDRESSING
FUNCTION MADE UP
OF 40-100 SHARDON
GIVING ANY DESIRABLE
SHAPE TO THE SIGNAL
IN THE ADDRESSING
CIRCUIT

LOW FREQ	HIGH FREQ
37 1.0 1.5	42 1.5 2.0


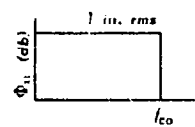
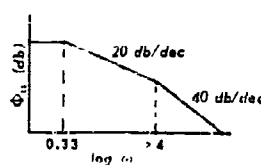
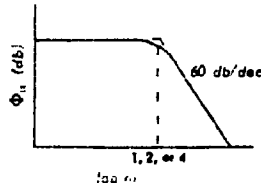
15) RANDOM ADDRESSING
FUNCTION MADE UP
OF 40-100 SHARDON
GIVING ANY DESIRABLE
SHAPE TO THE SIGNAL
IN THE ADDRESSING
CIRCUIT

LOW FREQ	HIGH FREQ
37 1.0 1.5	42 1.5 2.0

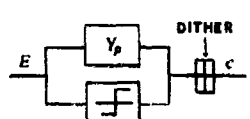
Table 14. Summary of Operator Describing Functions in Compensatory Tasks with Various Controlled Elements.

TYPE OF FORCING FUNCTION	GENERAL CONTROL TASK	CONTROLLED ELEMENT TRANSFER FUNCTION (G(s) NOT SHOWN)	"EASY" FIT TO HUMAN OPERATOR TRANSFER FUNCTION	FREQUENCY RANGE OF HUMAN OPERATOR MEASUREMENTS	AVERAGE LINEAR CORRELATION	INVESTIGATORS AND REFERENCES																																				
③ RANDOM ARBITRARY SUPERPOSITION OF 4 SINUSOIDS	HANDWHEEL TYPE CONTROL WITH NO RESTRAINTS	$\frac{1}{(s+1)}$ $\frac{1}{(s+1)}$ $\frac{1}{(s+1)}$	$\frac{K \cdot \frac{1}{s} \cdot \frac{1}{(s+1)}}{(\frac{1}{s+1})^2 (\frac{1}{s+1})}$ <table><tr><th>FORCED FREQUENCY</th><th>1/2</th><th>1/10</th><th>1/100</th><th>1/1000</th><th>1/10000</th></tr><tr><td>1/2</td><td>0.9</td><td>0.8</td><td>0.7</td><td>0.6</td><td>0.5</td></tr><tr><td>1/10</td><td>0.8</td><td>0.7</td><td>0.6</td><td>0.5</td><td>0.4</td></tr><tr><td>1/100</td><td>0.7</td><td>0.6</td><td>0.5</td><td>0.4</td><td>0.3</td></tr><tr><td>1/1000</td><td>0.6</td><td>0.5</td><td>0.4</td><td>0.3</td><td>0.2</td></tr><tr><td>1/10000</td><td>0.5</td><td>0.4</td><td>0.3</td><td>0.2</td><td>0.1</td></tr></table> where $\tau = 1.5$	FORCED FREQUENCY	1/2	1/10	1/100	1/1000	1/10000	1/2	0.9	0.8	0.7	0.6	0.5	1/10	0.8	0.7	0.6	0.5	0.4	1/100	0.7	0.6	0.5	0.4	0.3	1/1000	0.6	0.5	0.4	0.3	0.2	1/10000	0.5	0.4	0.3	0.2	0.1	SAME FREQUENCIES AS SHOWN IN FORCING FUNCTION	0.94	RUSSELL [70]
FORCED FREQUENCY	1/2	1/10	1/100	1/1000	1/10000																																					
1/2	0.9	0.8	0.7	0.6	0.5																																					
1/10	0.8	0.7	0.6	0.5	0.4																																					
1/100	0.7	0.6	0.5	0.4	0.3																																					
1/1000	0.6	0.5	0.4	0.3	0.2																																					
1/10000	0.5	0.4	0.3	0.2	0.1																																					
④ RANDOM ARBITRARY SUPERPOSITION OF 4 SINUSOIDS	HANDWHEEL TYPE CONTROL WITH NO RESTRAINTS	$\frac{1}{s}$	$\frac{K \cdot \frac{1}{s} \cdot \frac{1}{(s+1)}}{(\frac{1}{s+1})^2 (\frac{1}{s+1})}$ <table><tr><th>FORCED FREQUENCY</th><th>1/2</th><th>1/10</th><th>1/100</th><th>1/1000</th><th>1/10000</th></tr><tr><td>1/2</td><td>0.9</td><td>0.8</td><td>0.7</td><td>0.6</td><td>0.5</td></tr><tr><td>1/10</td><td>0.8</td><td>0.7</td><td>0.6</td><td>0.5</td><td>0.4</td></tr><tr><td>1/100</td><td>0.7</td><td>0.6</td><td>0.5</td><td>0.4</td><td>0.3</td></tr><tr><td>1/1000</td><td>0.6</td><td>0.5</td><td>0.4</td><td>0.3</td><td>0.2</td></tr><tr><td>1/10000</td><td>0.5</td><td>0.4</td><td>0.3</td><td>0.2</td><td>0.1</td></tr></table>	FORCED FREQUENCY	1/2	1/10	1/100	1/1000	1/10000	1/2	0.9	0.8	0.7	0.6	0.5	1/10	0.8	0.7	0.6	0.5	0.4	1/100	0.7	0.6	0.5	0.4	0.3	1/1000	0.6	0.5	0.4	0.3	0.2	1/10000	0.5	0.4	0.3	0.2	0.1	SAME FREQUENCIES AS SHOWN IN FORCING FUNCTION	0.94	RUSSELL [70]
FORCED FREQUENCY	1/2	1/10	1/100	1/1000	1/10000																																					
1/2	0.9	0.8	0.7	0.6	0.5																																					
1/10	0.8	0.7	0.6	0.5	0.4																																					
1/100	0.7	0.6	0.5	0.4	0.3																																					
1/1000	0.6	0.5	0.4	0.3	0.2																																					
1/10000	0.5	0.4	0.3	0.2	0.1																																					
⑤ RANDOM ARBITRARY SUPERPOSITION OF 3 SINUSOIDS	SIMULATED TANK TARGET TRACKING WITH SIGHT GRID HANDBEEL	$\frac{s \left(\frac{1}{s} \right)^2 \cdot \frac{1}{(s+1)}}{s \cdot \frac{1}{s} \cdot \frac{1}{(s+1)}}$ <p>THIS IS A 1/2 ORDER RANGE OF MEASUREMENT</p>	$\frac{K \cdot \frac{1}{s} \cdot \frac{1}{(s+1)}}{(\frac{1}{s+1})^2 (\frac{1}{s+1})}$ <table><tr><th>FORCED FREQUENCY</th><th>1/2</th><th>1/10</th><th>1/100</th><th>1/1000</th><th>1/10000</th></tr><tr><td>1/2</td><td>0.9</td><td>0.8</td><td>0.7</td><td>0.6</td><td>0.5</td></tr><tr><td>1/10</td><td>0.8</td><td>0.7</td><td>0.6</td><td>0.5</td><td>0.4</td></tr><tr><td>1/100</td><td>0.7</td><td>0.6</td><td>0.5</td><td>0.4</td><td>0.3</td></tr><tr><td>1/1000</td><td>0.6</td><td>0.5</td><td>0.4</td><td>0.3</td><td>0.2</td></tr><tr><td>1/10000</td><td>0.5</td><td>0.4</td><td>0.3</td><td>0.2</td><td>0.1</td></tr></table>	FORCED FREQUENCY	1/2	1/10	1/100	1/1000	1/10000	1/2	0.9	0.8	0.7	0.6	0.5	1/10	0.8	0.7	0.6	0.5	0.4	1/100	0.7	0.6	0.5	0.4	0.3	1/1000	0.6	0.5	0.4	0.3	0.2	1/10000	0.5	0.4	0.3	0.2	0.1	SAME FREQUENCIES AS SHOWN IN FORCING FUNCTION	0.94	TUSTIN [85]; INDICATED TRANSFER FUNCTION DOES NOT AGREE EXACTLY WITH THAT GIVEN BY TUSTIN
FORCED FREQUENCY	1/2	1/10	1/100	1/1000	1/10000																																					
1/2	0.9	0.8	0.7	0.6	0.5																																					
1/10	0.8	0.7	0.6	0.5	0.4																																					
1/100	0.7	0.6	0.5	0.4	0.3																																					
1/1000	0.6	0.5	0.4	0.3	0.2																																					
1/10000	0.5	0.4	0.3	0.2	0.1																																					
⑥ RANDOM ARBITRARY SUPERPOSITION OF 3 SINUSOIDS	SIMULATED TANK TARGET TRACKING WITH SIGHT GRID HANDBEEL	$\frac{s \left(\frac{1}{s} \right)^2 \cdot \frac{1}{(s+1)}}{s \cdot \frac{1}{s} \cdot \frac{1}{(s+1)}}$ <p>THIS IS A 1/2 ORDER RANGE OF MEASUREMENT</p>	$\frac{K \cdot \frac{1}{s} \cdot \frac{1}{(s+1)}}{(\frac{1}{s+1})^2 (\frac{1}{s+1})}$ <table><tr><th>FORCED FREQUENCY</th><th>1/2</th><th>1/10</th><th>1/100</th><th>1/1000</th><th>1/10000</th></tr><tr><td>1/2</td><td>0.9</td><td>0.8</td><td>0.7</td><td>0.6</td><td>0.5</td></tr><tr><td>1/10</td><td>0.8</td><td>0.7</td><td>0.6</td><td>0.5</td><td>0.4</td></tr><tr><td>1/100</td><td>0.7</td><td>0.6</td><td>0.5</td><td>0.4</td><td>0.3</td></tr><tr><td>1/1000</td><td>0.6</td><td>0.5</td><td>0.4</td><td>0.3</td><td>0.2</td></tr><tr><td>1/10000</td><td>0.5</td><td>0.4</td><td>0.3</td><td>0.2</td><td>0.1</td></tr></table>	FORCED FREQUENCY	1/2	1/10	1/100	1/1000	1/10000	1/2	0.9	0.8	0.7	0.6	0.5	1/10	0.8	0.7	0.6	0.5	0.4	1/100	0.7	0.6	0.5	0.4	0.3	1/1000	0.6	0.5	0.4	0.3	0.2	1/10000	0.5	0.4	0.3	0.2	0.1	SAME FREQUENCIES AS SHOWN IN FORCING FUNCTION	0.94	TUSTIN [85]; INDICATED TRANSFER FUNCTION DOES NOT AGREE EXACTLY WITH THAT GIVEN BY TUSTIN
FORCED FREQUENCY	1/2	1/10	1/100	1/1000	1/10000																																					
1/2	0.9	0.8	0.7	0.6	0.5																																					
1/10	0.8	0.7	0.6	0.5	0.4																																					
1/100	0.7	0.6	0.5	0.4	0.3																																					
1/1000	0.6	0.5	0.4	0.3	0.2																																					
1/10000	0.5	0.4	0.3	0.2	0.1																																					
⑦ RANDOM ARBITRARY SUPERPOSITION OF 4 SINUSOIDS	HANDWHEEL TYPE CONTROL WITH NO RESTRAINTS	$\frac{1}{(s+1)}$ $\frac{1}{(s+1)}$ $\frac{1}{(s+1)}$	$\frac{K \cdot \frac{1}{s} \cdot \frac{1}{(s+1)}}{(\frac{1}{s+1})^2 (\frac{1}{s+1})}$ <table><tr><th>FORCED FREQUENCY</th><th>1/2</th><th>1/10</th><th>1/100</th><th>1/1000</th><th>1/10000</th></tr><tr><td>1/2</td><td>0.9</td><td>0.8</td><td>0.7</td><td>0.6</td><td>0.5</td></tr><tr><td>1/10</td><td>0.8</td><td>0.7</td><td>0.6</td><td>0.5</td><td>0.4</td></tr><tr><td>1/100</td><td>0.7</td><td>0.6</td><td>0.5</td><td>0.4</td><td>0.3</td></tr><tr><td>1/1000</td><td>0.6</td><td>0.5</td><td>0.4</td><td>0.3</td><td>0.2</td></tr><tr><td>1/10000</td><td>0.5</td><td>0.4</td><td>0.3</td><td>0.2</td><td>0.1</td></tr></table>	FORCED FREQUENCY	1/2	1/10	1/100	1/1000	1/10000	1/2	0.9	0.8	0.7	0.6	0.5	1/10	0.8	0.7	0.6	0.5	0.4	1/100	0.7	0.6	0.5	0.4	0.3	1/1000	0.6	0.5	0.4	0.3	0.2	1/10000	0.5	0.4	0.3	0.2	0.1	SAME FREQUENCIES AS SHOWN IN FORCING FUNCTION	0.94	RUSSELL [70]
FORCED FREQUENCY	1/2	1/10	1/100	1/1000	1/10000																																					
1/2	0.9	0.8	0.7	0.6	0.5																																					
1/10	0.8	0.7	0.6	0.5	0.4																																					
1/100	0.7	0.6	0.5	0.4	0.3																																					
1/1000	0.6	0.5	0.4	0.3	0.2																																					
1/10000	0.5	0.4	0.3	0.2	0.1																																					
⑧ RANDOM ARBITRARY SUPERPOSITION OF 4 SINUSOIDS	HANDWHEEL TYPE CONTROL WITH NO RESTRAINTS	$\frac{10(s+10)}{10(s+1) \cdot \frac{1}{s+1}}$ $\frac{10(s+10)}{10(s+1) \cdot \frac{1}{s+1}}$ $\frac{10(s+10)}{10(s+1) \cdot \frac{1}{s+1}}$	$\frac{K \cdot \frac{1}{s} \cdot \frac{1}{(s+1)}}{(\frac{1}{s+1})^2 (\frac{1}{s+1})}$ <table><tr><th>FORCED FREQUENCY</th><th>1/2</th><th>1/10</th><th>1/100</th><th>1/1000</th><th>1/10000</th></tr><tr><td>1/2</td><td>0.9</td><td>0.8</td><td>0.7</td><td>0.6</td><td>0.5</td></tr><tr><td>1/10</td><td>0.8</td><td>0.7</td><td>0.6</td><td>0.5</td><td>0.4</td></tr><tr><td>1/100</td><td>0.7</td><td>0.6</td><td>0.5</td><td>0.4</td><td>0.3</td></tr><tr><td>1/1000</td><td>0.6</td><td>0.5</td><td>0.4</td><td>0.3</td><td>0.2</td></tr><tr><td>1/10000</td><td>0.5</td><td>0.4</td><td>0.3</td><td>0.2</td><td>0.1</td></tr></table>	FORCED FREQUENCY	1/2	1/10	1/100	1/1000	1/10000	1/2	0.9	0.8	0.7	0.6	0.5	1/10	0.8	0.7	0.6	0.5	0.4	1/100	0.7	0.6	0.5	0.4	0.3	1/1000	0.6	0.5	0.4	0.3	0.2	1/10000	0.5	0.4	0.3	0.2	0.1	SAME FREQUENCIES AS SHOWN IN FORCING FUNCTION	0.94	RUSSELL [70]
FORCED FREQUENCY	1/2	1/10	1/100	1/1000	1/10000																																					
1/2	0.9	0.8	0.7	0.6	0.5																																					
1/10	0.8	0.7	0.6	0.5	0.4																																					
1/100	0.7	0.6	0.5	0.4	0.3																																					
1/1000	0.6	0.5	0.4	0.3	0.2																																					
1/10000	0.5	0.4	0.3	0.2	0.1																																					

Table 15. Summary of Operator Remnant Characteristics in C

INVESTIGATOR	GENERAL CONTROL TASK INCLUDING CONTROLLED ELEMENT DYNAMICS (GAIN NOT SHOWN)	FORCING FUNCTION	AVERAGE LINEAR CORRELATION	ALL REMNANT ASSUMED DUE TO NOISE INJECTED THE OPERATOR'S IN $\Phi_{nn} = \frac{1}{ H ^2} \int_0^\infty \Phi_{11} d\omega$
RUSSELL	Simple tracker, handwheel type control with no restraints $Y_c = 1$	Random appearing superposition of 4 sinusoids 	0.9	
FLKIND	Simple following with pip trapper $Y_c = 1$	Random appearing function made up of 40-120 sinusoids, giving any desirable rectangular spectra $f_{co} = .16, .24, .4, .64, .96, 1.6, 2.4$ cps or $\omega_{co} = 1, 1.5, 2.5, 4, 6, 10, 15$ rad/sec 	R.16 = 0.995 R.24 = .99 R.40 = .995 R.64 = .98 R.96 = .92 R1.6 = .75 R2.4 = .58	White noise, $\Phi_{nn}(\omega) \leq \frac{1}{ H ^2} \int_0^\infty \Phi_{11} d\omega$ valid for R.16 - R.64 only
GOODYEAR	Simulated longitudinal aircraft control in pitching mockup; stick with inertial, spring, and damping restraints $Y_c = \frac{I_c s + 1}{s(T_1 s + 1)(s/\omega_n)^2 + 2\zeta s/\omega_n + 1}$ $1/T_1 = 1.37, 1/T_1 = 2.4$ $\omega_n = 4.17, \zeta = 0.52$	Random appearing 		
FRANKLIN	Simulated F-80A in tail chase; aileron and elevator controlled $Y_{11} = \frac{(s + 0.242)(s + 2.92 + 1)(s/4.11 + 1)(s/8.32 + 1)}{s^2(s/0.0017 + 1)(s/5.65 + 1)[(s/3.88)^2 + 2(0.084)s/3.88 + 1]}$ $Y_{12} = \frac{(s/0.28 + 1)(s/1.58 + 1)}{s^2[(s/3.08)^2 + 2(0.56)s/3.08 + 1]}$	Random appearing white noise through third order binomial filter giving available corner frequencies of 1, 2, and 4 rad/sec 	Elevator, $p_e \approx 0.6$ Aileron, $p_a \approx 0.5$ (p was a strong function of ω_{co})	ALYN

of Operator Remnant Characteristics in Compensatory Tasks.

AVERAGE LINEAR CORRELATION	REMNANT SOURCES and BEST FIT DATA			
	ALL REMNANT ASSUMED TO BE DUE TO NOISE INJECTED AT THE OPERATOR'S INPUT $\Phi_{nnr} = \frac{1}{ f ^2} \int_0^\infty \Phi_{nn} df$	ALL REMNANT ASSUMED TO BE DUE TO NOISE INJECTED AT THE OPERATOR'S OUTPUT $\Phi_{nnr} = \frac{ Y_p ^2}{ f ^2} \int_0^\infty \Phi_{nn} df$	ALL REMNANT ASSUMED TO BE DUE TO NONSTEADY OPERATOR BEHAVIOR	NONLINEAR OPERATION AND DITHER
0.9				$\Phi_{nnr} = A_d^2 [\delta(\omega - \omega_d) + \delta(\omega + \omega_d)]$ $\omega_d = 7.75 \text{ cps}$
.16 - 0.995 .24 - .99 .40 - .995 .64 - .98 .96 - .92 1.6 - .75 2.4 - .58	White noise, $\Phi_{nnr}(f) = \frac{1}{f} \int_0^\infty \Phi_{nn} df$ valid for R.16 - R.64 only	$\Phi_{nnr}(\omega) = 2T\sigma_{\Delta}^2 [(\sin \frac{1}{2}\omega T)/(\frac{1}{2}\omega T)]^2$ or $R_{nnr}(r) = \sigma_{\Delta}^2 (1 - r /T)$ $T = 0.75/f_{co} \text{ (All cases)}$ $\frac{\sigma_{\Delta}^2}{\int_0^\infty \Phi_{nn} df} = \frac{1.75}{\sqrt{f_{co}}} \text{ (R.40 - R.2.4)}$	$R_{\Delta H \Delta H}(r) = \sigma_{\Delta H}^2 (1 - r /T)$ where: $T_1 = \frac{0.5}{\omega_{co}} = 0.25 \text{ sec}$ $\sigma_{\Delta H}^2 = 0.7 f_{co}$ and $R_{\Delta H \Delta H}(r) = \lim_{T \rightarrow \infty} \frac{1}{T} \int_{-T}^T \Lambda_H(t) \Lambda_H(t+r) dt$	No dither observed; Small threshold nonlinearity is possibly present
2				$\Phi_{nnr} = 2T_A(E_A/2)^2 [(\sin \frac{1}{2}\omega T_A)/(\frac{1}{2}\omega T_A)]^2$ $+ \pi A_d^2 [\delta(\omega_d + \omega) + \delta(\omega_d - \omega)]$ $T_A = 2.7 \text{ sec}, \quad \omega_d = 8.8 \text{ rad/sec}$  COMPUTER MECHANIZATION
Elevator, $p_s = 0.6$ Aileron, $p_s = 0.5$ p was a strong function of ω_{co}	ALTHOUGH THE FRANKLIN F-80 DATA REMNANT POWER IS CONSISTENT WITH ALL OF THESE MODELS, IT IS NOT UNEQUIVOCALLY ASSIGNABLE TO ANY ONE SOURCE			

seconds for random appearing visual inputs. There also appears to be a fairly steady progression of decreasing r values from about 0.30 to 0.25 seconds for widely separated step inputs, to about 0.20 seconds for more closely spaced and random appearing discrete steps, and finally to the 0.15 seconds cited above for random appearing forcing functions. On both single-input, single-output systems and two-input, two-output systems with random appearing forcing functions, r does not appear to be a distinct function of either forcing function or controlled element characteristics. Whatever variability does exist in values of r appears to be on an intrasubject basis. It is probable that these variations are similar in both scope and form to those found in applicable reaction time experiments to discrete stimuli, since r is certainly a closely related quantity to certain classical reaction times.

The hypothetical linear model for continuous control, visual, compensatory tasks should then always include an e^{-T_d} term in the describing function to account for the reaction time delay, with r given approximately as

$$r \doteq 0.15 \pm 0.03 \text{ seconds} \quad (\text{IX-1})$$

2. Neuromuscular Lags

The dynamic portion of the data from step forcing functions for $Y_c = 1$ and that obtained for the non-synchronous phases of sine wave forcing functions for $Y_c = 1$ have a fair degree of similarity, and are presumably indicative of the actuator (neuromuscular) portion of the human response. The neuromuscular system involved in the particular measurements was that of the arm in following, and the describing numbers would be somewhat different for other neuromuscular systems. This actuator portion of the human responses is not directly apparent in the other describing function data since the effect would be minor at the frequencies used for determining them. It will be recalled, however, that much of the data required, as a minimum, the addition of a high frequency lag (beyond the measurement bandwidth), to stabilize the system.

We should also note that Elkind's higher forcing function bandwidths will scarcely admit of very large values for neuromuscular lags (because they would have to be subtracted from the already small values of r), unless they are associated with the very low frequency lag break point probably present; or unless both a lead and lag exist beyond the measurement bandwidth. The evidence for the second possibility is mixed (Section V-C), and the possibility of the low frequency lag being truly due to the neuromuscular system is extremely unlikely.

Since much of the evidence available at the higher frequencies (particularly those from step function inputs), indicates the existence of neuromuscular lags, and most of the other data implies their probable presence, a hypothetical model of the operator should include the effect. If really due to the neuromuscular system, these lag terms should be at least of the second order variety. About the only numerical value that one can derive from the data, however, is a first approximation consisting of a first order lag. Such a single lag will be used in the hypothetical model, but one should not attach too much physical significance to either the numerical values or, for that matter, the name.

3. Indifference Threshold

In the Goodyear studies the concept of an "indifference threshold" of response was derived as a serial member of the operator's transfer characteristic. Elkind's variable amplitude experiment data are also compatible with this result, so it does appear that the effect exists and should be taken into account, at least in principle. This can be done by using a threshold describing function, $K_T(a_T/\sigma_T)$, in series with the other elements of the transfer function. This is given approximately by.

$$K_T \left(\frac{a_T}{\sigma_T} \right) = 1 - \Phi \left(\frac{a_T}{\sqrt{2} \sigma_T} \right) + \sqrt{\frac{2}{\pi}} \frac{a_T}{\sigma_T} e^{-\left(\frac{a_T}{\sqrt{2} \sigma_T} \right)^2} \doteq 1 - 2 \sqrt{\frac{2}{\pi}} \frac{a_T}{\sigma_T}; \quad \frac{a_T}{\sigma_T} \ll 1 \quad (\text{IX-2})$$

Equation (IX-2) has only a slight change from unity for the relatively small values of a_T/σ_T observed. It can therefore be considered as a second order effect within the realm covered by present data.

4. Equalization

A most important thing to be noted regarding the transfer function form is the equalizing ability of the operator. This is shown by the occasional presences of a first order lead, a low frequency first order lag, and the probable existence of a variable high frequency lag (which may be part of the neuromuscular system).

Considering only non-moving mockups with pure visual inputs, a single low frequency lag term *always* appears to be present when *all* of the following conditions apply:

- a. When the introduction of a low frequency first order lag would improve the low frequency system response;
- b. When the low frequency system response is important because of the low bandwidth of the input.
- c. When the controlled element characteristics are such that the introduction of the low frequency lag will not result in higher frequency destabilizing effects incapable of being overcome by a single first order lead.

When these conditions do not apply, the low frequency lag does not appear.

When the controlled element characteristics, coupled with the "unalterable" reaction time delay term of the operator, are such that a lead term would be desirable from either a system stability or low frequency system performance standpoint, then the operator will generate a first order lead.

It is probable that either a second low frequency lag or a second lead term is difficult or impossible for the operator to generate when confronted with only visual, random appearing inputs. Several of the systems studied could have used such terms to advantage and there is no indication of their existence.

It should be pointed out, however, that a second order lead does appear to be possible under special circumstances. For example, the highly trained Navy jet pilots used as subjects by Goodyear were able to generate quadratic lead terms while operating in a moving simulator.

Expressed mathematically the operator's equalization characteristic, with only visual inputs, can take on the following forms.

$$K_p \left(\frac{a T_I s + 1}{T_I s + 1} \right) \quad a > 1 \quad (\text{LEAD-LAG}) \quad (a)$$

$$K_p \left(\frac{a T_I s + 1}{T_I s + 1} \right) \quad a < 1 \quad (\text{LAG-LEAD}) \quad (b)$$

$$K_p (T_I s + 1) \quad (\text{SIMPLE LEAD}) \quad (c)$$

$$\frac{K_p}{T_I s + 1} \quad (\text{SIMPLE LAG}) \quad (d)$$

$$K_p \quad (\text{PURE GAIN}) \quad (e) \quad (IX-3)$$

This ability to adapt the form of equalizing characteristic can be referred to as the *adaptive* behavior of the operator.

It should be recalled that the final transfer function obtained in a given task is a strong function of the operator training in the particular control task. All of the describing function data considered in this report were valid *after* the learning period. Therefore, adaptive behavior refers to what the operator can do after he has achieved some familiarity with the particular control process. The length of the trial and error process involved in achieving the final transfer function form is, of course, quite dependent upon the forcing function and controlled element characteristics and the background of the operator. For example, in Section VI we noted Russell's comment that only a few seconds to a minute or so were required to adapt properly for variations in controlled element characteristics during a run; much longer times were required on the F-80 simulator simply to achieve familiarity with the simulator. Goodyear noted that as much as 20 hours was required by one of their subjects (a non pilot) before he attained any reasonable degree of proficiency in controlling the simulator.

5. Gain Adjustment and Optimizing Behavior

From all of the data it is apparent that operator gain is a highly adjustable parameter. On essentially all of the more complex tasks with controlled element dynamics, the gain was set to values giving quite low phase margins, of the order of 30 degrees or less. This was also true of the Elkind rectangular spectra forcing function data for inputs to $f_{co} = 0.96$ cps. The gain value adopted by an operator also appears to be a distinct function of individual motivation and training in the particular task.

In addition to gain adjustment, all the evidence available indicates that the operator is not only *adaptive* in selecting the form of his equalization function within the rough limits set above, but also adjusts the value of some of the constants within the transfer function adapted.

Some insight into this behavior can be obtained by considering the simple tracker data as a function of forcing function bandwidth. From the Franklin data it appears that the lead time constant, T_L , is considerably reduced as the bandwidth is increased, indicating that the operator is attempting to increase his bandwidth as the presented information requires such an increase. A similar trend is seen in the Russell and Elkind data, except that there the operator changes his low frequency lag time constant and gain, e.g., $K \approx 9.42 T_L$ for Elkind's data. Both of these characteristics show a distinct tendency on the part of the operator to adjust his parameters in an endeavor to follow the forcing function and to minimize the effects of other signals present in his input.

This behavior is similar to that expected of an "optimizing" servo system, i.e., one that adjusts the values of its constants as a function of its inputs. Although we would be hard put to specify the precise optimum toward which the subject strives, we can assert that the human operator is both "adaptive" (within a relatively fixed form), and "optimizing" (to some internal criterion). In fact, the human operator is the very prototype of an adaptive, optimizing servo system. Unfortunately the human does much more than the more prosaic optimizing servos in that a large quantity of "unwanted" output motion is also supplied by him in the control process!

Having noted the optimizing characteristics, it becomes a matter of interest to speculate upon the criteria used to adjust these variable parameters. For simple systems, such as Elkind's, it was shown in Section V that the classical minimization of the rms error (operator's input) has some merit, at least in terms of giving a rough idea of the general type of compromise being performed between following of the forcing function and the noise. It will be recalled in this regard that a bugaboo exists in that the operator "generates" his own noise, which is, in turn, related to his transfer characteristic.

A similar optimizing behavior is exhibited at the other end of the range of difficulty by the F-80 simulator results. Here there is a reduction in α and an increase in $1/T_L$ in both the lateral and longitudinal operator describing functions as the forcing function bandwidth increases. Within the limitations of the possible form of operator's describing function, both of these changes tend to reduce functions of the absolute value of the error (operator's input). However, a rather remarkable difference exists between the F-80 and Elkind results. It will be recalled that the mean square error (and error spectrum) found in Elkind's experiments *increased* with task difficulty, i.e., with input bandwidth. The F-80 simulator results, on the other hand, show that the error spectra in a particular axis are *not* strong functions of the forcing function characteristics, but are similar for all three input bandwidth conditions differing mainly in their bandwidths. A considerable difference does exist, however, between lateral and longitudinal error spectra. In other words, the error spectra on the F-80 simulator appear to be largely functions of either the controlled element characteristics, or the attachment, by the operator, of differing degrees of importance to controlling aileron and elevator. This situation does not detract too much from the conjecture that the operator's tracking criterion is akin to the servo criterion of mean square error minimization. This is so because, in systems containing controlled elements as complex as the F-80 simulator and in view of the restricted operator transfer function form, the mean square error variation with operator parameters is relatively slight over the range of values allowable from the stabilization standpoint.

Taking all of the data, then, it appears that the operator does adjust his parameters as some function of the magnitude of his presented input. Further, he tends to modify his transfer characteristics until he has achieved either a performance which he accepts or, perhaps, a performance level which represents the limit of his abilities. It should be pointed out that the operator action tending to create the second of these possibilities was generally requested by the experimenter. Other experimental conditions, e.g., when the operator is asked to keep his signal within a rigidly defined set of limits shown on the display, may not yield similar results to those given here. Actually, we only have glimmers of the operator's criterion for optimization, and we are forced to note simply the consistency of his actions with other well defined criteria rather than being able to derive his rationale for acting.

6. Hypothetical Transfer Function Model

From all of the above it is now possible to hypothesize a linear adaptable model of the human operator, for random appearing visual inputs and motion outputs, which is consistent with all of the data available. In equation form:

$$Y_p = \frac{K_p e^{-\tau s} (T_L s + 1)}{(T_I s + 1)(T_N s + 1)} K_T \left(\frac{u_T}{\sigma_T} \right) = \frac{K_p e^{-\tau s} (a T_I s + 1)}{(T_I s + 1)(T_N s + 1)} K_T \left(\frac{a_T}{\sigma_T} \right) \quad (IX-4)$$

where: Reaction time delay, " τ ", is: $0.12 < \tau < 0.20$ seconds.

Neuromuscular lag, " T_N ", is partially adjustable for task.

Equalization, " $\frac{(a T_I s + 1)}{(T_I s + 1)}$ ", is adjustable with forcing function and controlled element.

Gain, " K_p ", is adjustable for overall system stability and low frequency performance.

Indifference Threshold, " $K_T \left(\frac{a_T}{\sigma_T} \right)$ ", is a second order effect with adjustment and values not known.

Within the limitations of the above form the operator adapts his describing function (lag-lead, lead-lag, pure lead, pure lag, or pure gain) to obtain what he considers to be an optimum controller, controlled-element system response in the presence of the forcing function. The describing function form adapted is one consistent with stability and good low frequency control of the overall system. The constants are adjusted to some criteria akin to that of the rms minimization criterion of servo theory. In most cases with forcing functions having a fairly low frequency content, the overall system probably exhibits marginally stable high frequency control. In other words, the operator transfer function for a given task is very similar to the one that a servo engineer would select if he were given an element to control together with a "black box," having within it elements making up the describing function given by Eq. (IX-3), and knobs on the outside for adjustment of a , T_I , and K_p .

C. HYPOTHETICAL REMNANT MODELS

In the course of this study several models have been proposed to "explain" that portion of the operator's output which is not "linearly coherent" with the system forcing function. In terms of the operator's uncorrelated output power, three of the models considered appear to have descriptive merit. These are listed below in the order of their appearance in the previous sections of the report, and are illustrated in Figure 146.

1. A "noise" or error superimposed upon the operator's linear output. As shown in Figure 146a, this noise is effectively injected into the system. As presently conceived this description assumes that:

a. The humans output response, $c(t)$, can be approximated by a series of discrete steps. Each step consists of two components, i.e.

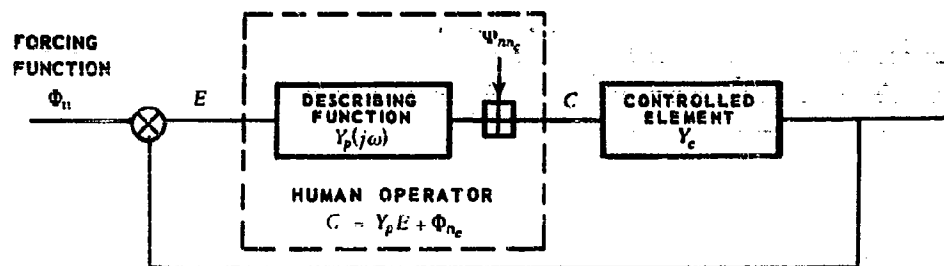
(1) A part, Δe_0 , linearly related to the forcing function;

(2) A part, $n_c(t)$, representing random error or noise, which is not linearly coherent with the forcing function, and which is independent of all other output steps.

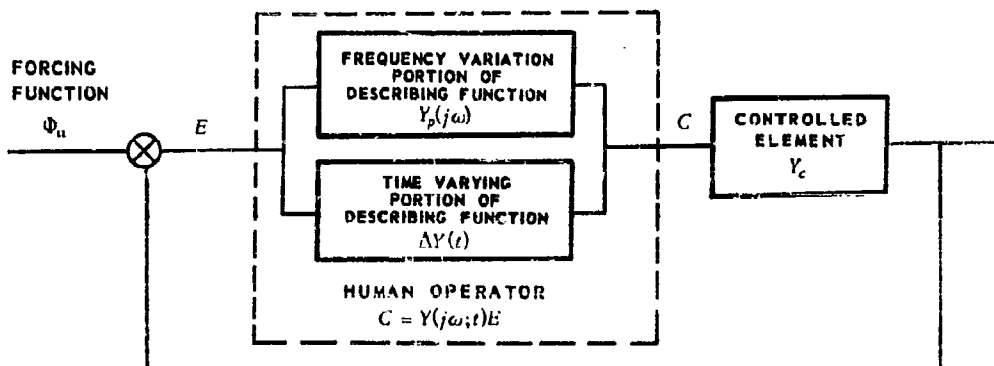
b. The mean-square noise may be proportional, in some fashion, to the mean square value of Δe_0 , i.e., $n_c^2 \sim \{\Delta e_0^2\}^k$.

The data fits made using assumption 1-a imply that the equivalent noise injected has a boxcar like time structure, with average "switching" from one value to another which is roughly proportional to operator input signal axis crossings. Assumption 1-b is not imperative for this interpretation.

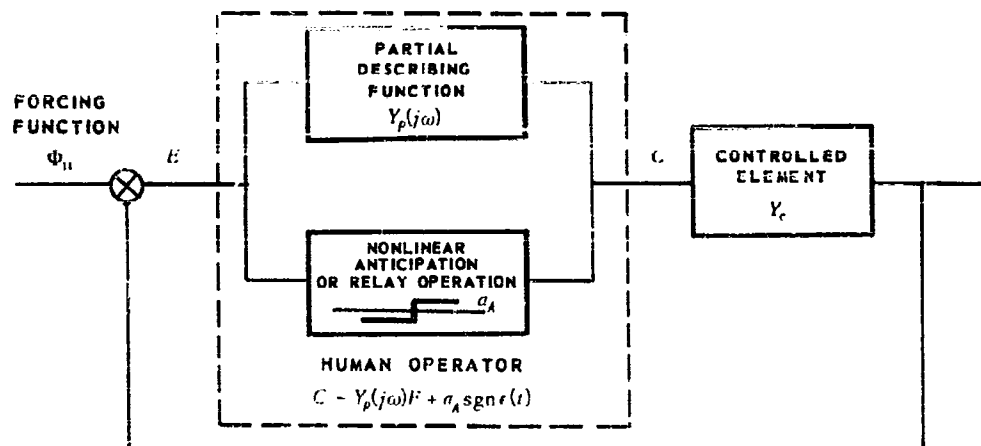
2. Nonsteady behavior of the operator. This concept is based on the notion that the operator's transfer characteristic is essentially linear but time varying in some random fashion. The time-varying portion of the closed loop transfer function, $\Delta H(t)$, would possess a box-car like structure, and its rms value would increase almost directly with the demands imposed by the task. The equivalent open-loop



a. Output Noise Injection Remnant Model.



b. Nonsteady Operator Behavior Remnant Model.



c. Linear With Parallel Sgn Function Operator Description.

Figure 146. Possible Forms of the Operator Model.

time-varying characteristic, $\Delta Y(t)$, would have an rms value not so drastically dependent upon the task demands, possibly being nearly constant. Such a nonsteady transfer characteristic will act in parallel with a describing function which is frequency variant only, as shown in Figure 145b.

3. An "anticipation" or sgn function operating on the input signal in parallel with a quasi-linear describing function. The portion of the operator's output due to the sgn function will be a square wave of constant amplitude, a_T . The axis crossings will be identical to those of the error (operator's input).

As implied in the statement preceeding this recapitulation, there is little to choose between these three concepts in terms of the existing data on uncorrelated operator output power. On this basis all three are effectively equivalent models. In addition, all "explain", to some extent at least, the quasi-periodic behavior observed on time records of human responses.

When more detailed factors are examined, such as the point-by-point output time function check between the Goodyear analog and actual pilot, the third (perfect parallel relay), description becomes very enticing. Unfortunately, this description is based upon only one set of controlled-element, forcing-function characteristics. The other remnant data could be explained to a large extent by such an "anticipation" model (and vice-versa, of course), but a limiting case tends to make us wary of the outright assertion that this is the best model. This limiting condition will occur when the task is very difficult, so that the parallel, nearly linear, describing function is very small relative to $K_A(a_A/a_T)$, the describing function of the sgn transfer characteristic. Under these conditions, the overall operator describing function would tend to be a pure gain, with no reaction time delay. For the Franklin F-80 studies in longitudinal control for $\omega_{co} = 1, 2$ radians/second the describing function does appear to approach a condition where it is effectively a pure gain, whereas for $\omega_{co} = 4$ radians/second for which p is greater than for $\omega_{co} = 1$, or 2 radians/second, $Y_c \approx K_A e^{-0.25s}$.

With all of these points in mind, it is probably expedient for us to assert that all three points have equal merit. However, we hold the following opinions:

1. The nonsteady model is best from the point of view that the curve fits upon which it is based were the most adequate ones made;
2. The noise injection model is best from the standpoint of simplicity in using the hypothetical describing function data for system stability predictions and general servo analysis;
3. The parallel sgn function, or perfect relay, model is best from the viewpoint of point by point prediction of the operator's output and in creating an intuitive physical view of the operator's actions.

Because of the approximate equivalence of the three models, as regards their manifest effects in the data, and the points enumerated above, we feel that the eclectic view is the most practical at this stage. By accepting this viewpoint, the choice of remnant model can be left to the engineer or psychologist analyzing a particular problem. The model can then be selected on the basis of convenience for the particular job at hand. Of course, due caution and restraint should be used in not exceeding the bounds imposed by the experimental conditions for which the models were originally derived. An experimenter's ingenuity would be challenged in designing appropriate experiments to choose between the possible remnant models. The nonsteady model is most amenable to experimental study.

In part B of this section we were able to outline a hypothetical transfer function model which can be used as a reasonable basis for crude prediction in overall system calculations. As matters now stand, this model should be suitable for engineering analyses of system stability, and for use as a guide for system equalization synthesis. This is the case because the reaction time delay and possible types of operator equalization within the restricted adaptive form are fairly well tied down. These two items usually dominate the scene when one is performing a stability analysis. The criteria that might be used for adjusting the operator's variable parameters (leads, lags, etc.) are not known, but this state of affairs detracts little from the general statements above.

Now in this part of the section, it would be very nice if we could prescribe a reasonable remnant model to go along with the hypothetical adaptive and optimizing transfer function. Unfortunately, the dearth of remnant data and the dependence of that available on both controlled element and forcing function details make this impossible. There is just barely enough data to allow us to make the above statements on the probable equivalence of

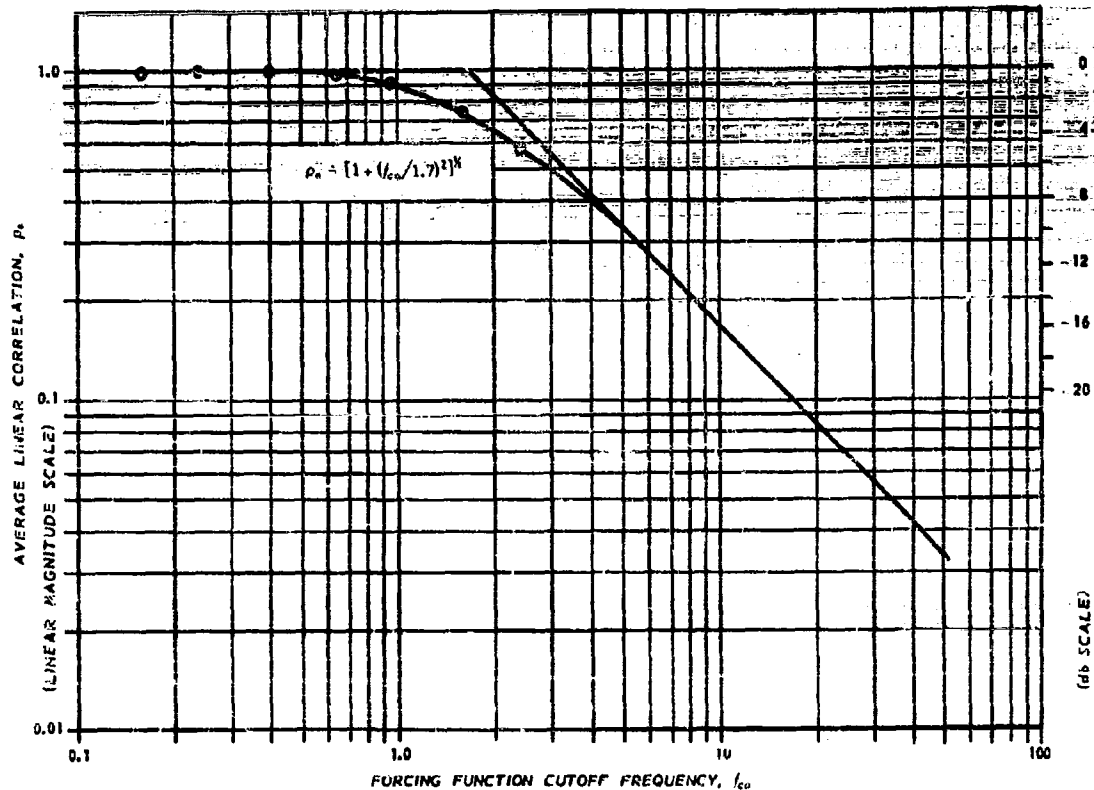


Figure 147. Variation of Average Linear Correlation with Task Difficulty.
(Elkind Rectangular Spectra Forcing Function.)

$$R(\tau) = \int_0^\infty \Phi(f) \cos 2\pi f \tau df \quad (IX-9)$$

If $\Phi(f)$ is continuous,

$$R''(\tau) = -(2\pi)^2 \int_0^\infty f^2 \Phi(f) \cos 2\pi f \tau df \quad (IX-10)$$

so that

$$R''(0) = -(2\pi)^2 \int_0^\infty f^2 \Phi(f) df \quad (IX-11)$$

Since $R(0) = \int_0^\infty \Phi(f) df$, then β_f will become

$$\begin{aligned} \beta_f &= \frac{1}{\pi} \left[\frac{-(2\pi)^2 \int_0^\infty f^2 \Phi(f) df}{\int_0^\infty \Phi(f) df} \right]^{1/2} = 2 \left[\frac{\int_0^\infty f^2 \Phi(f) df}{\int_0^\infty \Phi(f) df} \right]^{1/2} \\ &= \frac{2}{\sigma_f} \left[\int_0^\infty f^2 \Phi(f) df \right]^{1/2} \end{aligned} \quad (IX-12)$$

All of these forms, β_f , \bar{f} and σ_f , should result in about the same type of relationship as Equation (IX-5) for the Elkind rectangular spectrum data since, in that case, all are strong direct functions of f_{co} . The same thing

cannot be said of situations with dominant controlled element dynamics, such as the F-80 simulator. On the other hand, we can say that Elkind's higher f_{co} tasks were nearing the limits of human capability. For example, his subjects were unable to track the next higher forcing function $f_{co} = 4$ cps. Therefore, it may not be unreasonable to speculate that an equation of the form of (IX-5), with some more fundamental error spectra quantity substituted for f_{co} , will give a rough estimate of ρ_a for a given task. If we accept average error signal axis crossings, β_t , as this quantity (only as a guess, of course), then Eq. (IX-5) can be modified to

$$\rho_a = \frac{1}{\sqrt{1 + \left(\frac{\beta_t}{4.8}\right)^2}} \quad (IX-13)$$

since β_t in Elkind's case is approximately $2\sqrt{2}f_{co}$ for the higher cutoff forcing functions.

Section X

PREFERRED FORM OF OPERATOR'S DESCRIBING FUNCTION IN COMPENSATORY TASKS — AN INTERIM BASIS FOR MANUAL CONTROL SYSTEM DESIGN

In the preceding sections of this report consideration was given to how the operator actually performs in particular tasks, and an adaptive, optimizing model was hypothesized to characterize his behavior. This model can probably be used with some confidence to predict qualitatively the performance of a given man-machine system. While all of this information is very useful in an analysis problem, it is also desirable, for synthesis purposes, to know how the operator should be *allowed* to perform, i.e., what is the best type of describing function for the human? If the operator is more precise when he adopts a particular describing function than when he assumes other transmission properties, it would then seem desirable to design the nonhuman elements of the control system in such a fashion as to use the human in his most competent role.

To perform an intelligent controls design on this basis, the engineer requires a knowledge of an operator form which is "preferred" from the standpoint of performance. To derive an operator characteristic which is presumably the "best" for him to adopt, in the performance sense, we can use data of two varieties. The first, of course, is the describing function and remnant data which we have previously summarized. From these data we can draw some conclusions about those controlled element and forcing function conditions which tend to be more desirable than others from the overall system performance standpoint. Then, having the desirable controlled element and forcing function conditions well in mind, we can go directly to a preferred form.

The second form of data giving us leads in finding preferred operator characteristics is the experimental determination of some system performance measure, such as rms error, etc., as a function of controlled element and forcing function conditions. This latter approach, emphasizing particularly the controlled element characteristics, has been used extensively by Taylor and Birmingham and their colleagues [6, 7, 30, 42]. As a result of their efforts using this approach, they hypothesized a preferred form of operator model which is discussed in detail in Reference 6. Since this is such a lucid account, and because aspects of the Taylor-Birmingham model still appear applicable, some of the following is taken verbatim from that source. This section is not, however, a repetition of Reference 6 since we now have much more data to lead us to an appropriate model than was available to Birmingham and Taylor. The section is more in the nature of an extension of later results into a framework which bears some distinct similarities with the Birmingham-Taylor hypothetical preferred form model.

In the preceding sections it was pointed out that the human operator can be represented by the following, outwardly equivalent, general forms:

$$\begin{aligned} C(j\omega) &= Y_p(j\omega)E + N_s(j\omega) \\ \text{or} \\ C(j\omega) &= Y_p(j\omega_1 t)E \\ \text{or} \\ \bar{C}(j\omega) &= Y_p(j\omega)E + u_T \operatorname{sgn} t(t) \end{aligned} \quad (\text{X-1})$$

On a closed loop basis all of the above forms can be put into quantities which are more easily measured (at least by the quasi-linear methods), and which, in this sense, are more fundamental. In closed loop form,

$$\Phi_{ce} = |H|^2 \Phi_n + \Phi_m \quad (\text{X-2})$$

From the previous data summarized in this report we can further say that the remnant, Φ_m , term was of major importance in determining the average performance (such as rms error, time on target, etc.) while the $|H|^2 \Phi_n$ term was of greater importance in determining system stability and dynamic or transient performance. When we speak of tracking precision in the usual sense, we are concerned with such things as the rms tracking error, so the reduction of the Φ_m term is a major key to precision performance. The definition of the "optimum" operator linear form for precise average control can then be said to be that form of Y_p which minimizes Φ_m . If the Φ_m term was due to an operator induced noise which was uncorrelated with both Y_p and the forcing function, the preceding statement would have little practical meaning since Φ_m would be no function of Y_p . On the other hand, if Φ_m is dependent upon

Y_p in some fashion, then changes in the controlled element transfer function calling for a different form of operator describing function should result in a change in Φ_m and hence in tracking precision.

From the preceding sections it is evident that controlled element transfer characteristics and forcing function conditions are the major quantifiable components of task difficulty. It is also apparent that the more "difficult" either or both of these characteristics become, the larger the remnant. All of this can be cited as evidence of the fact that the operator is best when his task demands the least of him. This leaves us with the problem of defining minimal demands. When this has been done, a rational design scheme can be presented which will specify the human operator's role so that he will generate these characteristics at which he is best.

Both of these problems, i.e., first defining a "minimum demands" operator transfer characteristic form and then a consequent rational design procedure, have been attacked by Taylor and Birmingham. Their premises were made without the benefit of the mass of data included in this report, but it is worthwhile to present their argument in detail as a basis for the subsequent revision to certain parts. In the words of Reference 6, "It becomes, therefore, a fundamental assumption of this paper that the more complex the human task, the less precise and the more variable becomes the man. It is assumed that, within limits, the higher the number of integrations and/or differentiations required of the man the poorer will he perform. Conversely, it is hypothesized that the more the human operator is freed from the tasks of integration and differentiation the more regular and precise will become the human output. Human control behavior, it is asserted, reaches the optimum when the man becomes the analogue of a simple amplifier (with pure time delay) as shown in the following equation:

$$\theta_0(s) = Ke^{-\tau s}\theta_i(s) \quad \text{or} \quad \theta_0(t + \tau) = K\theta_i(t) \quad (X-3)$$

where t represents a value in time, and τ equals the human reaction time.

"In contrast to the poor performance of complex tasks hypothesized for the human operator is the fact that machines can be built to perform intricate computations with remarkably high precision and low variability. It is true that stability and accuracy are not obtained without effort, but for such tasks as double or triple integration and/or differentiation it seems unquestionable that electronic or mechanical components can be made to be more precise and repeatable than man.

"If this is the case, and if precision is required, it follows that when a man-machine system must integrate, differentiate, or perform other higher-order computations, these should be supplied by the nonhuman components of the system whenever possible. This is tantamount to saying that the human should be required to do no more than operate as a simple amplifier. Broadening this somewhat, adding to it a statement as to human bandwidth, and phrasing it as a general design principle, the following emerges: Design the man-machine system so that (1) the bandpass required of the man never exceeds three radians per second and (2) the transfer function required of the man is, mathematically, always as simple as possible, and, wherever practicable, no more complex than that of a simple amplifier.

"In line with this principle two matters require general comment. First of all, it is essential to describe a basic condition which must be observed if the ultimate intent of the design principle is to be achieved. Second, it is necessary to answer the obvious question of why, after designing the system so that only amplification is required of the man, one should not take the final step of dispensing with him entirely by substituting an actual amplifier in his place.

"As to the first, in order to obtain optimum performance from the control system, it is necessary, not only to design the system so that amplification is all that is required of the operator, but it is also necessary to insure that the operator adopts this, and no other, mode of response. It appears that when placed in a control loop, the human goes through a trial-and-error process wherein he varies his transfer function until he achieves a condition of minimum average error as it is reflected to him via the display. It follows from this that to insure the adoption by the operator of a mode of action equivalent to simple amplification, it is necessary to so design the non-human components that the operator will achieve minimum error at the display when he acts as an amplifier. If, through inadvertence, the design of the control loop permits the operator to reduce the displayed error more by acting as an integrator, differentiator, or a combination of one or more of these than as an amplifier, then, most certainly, he will do so.

"In regard to the question of why the design principle does not lead logically to employing an amplifier to supersede the man, one can only say that it does lead to precisely that—whenever it is feasible. Under some circumstances the best man-machine system design will demand the removal of the human from the system. But in many other circumstances it would be impractical to automatize completely.

"Finally, in many situations, it is not feasible to simplify the operator's task to the point of requiring of him only simple amplification. In some systems the man is used precisely because he can do more in a tracking loop than amplify. In these circumstances it would be self-defeating to attempt to carry the simplification process too far. This would be true, for example, in the case of handlebar tracking systems which utilize the man, not only as an error detector and analogue computer, but as the power drives as well. In such cases, complete redesign of the system would be required if one sought to supplant the human element entirely. In these cases, one must be satisfied with the more modest, yet still very appreciable, improvements to be brought about through task simplifications which stop short of the ultimate."

The Birmingham-Taylor thesis quoted above is given some detailed quantitative support in Reference 7. This paper reports the results of a series of tests where the operator is provided with instantaneous knowledge of the effects of his own motions in such a way as to make it unnecessary for the operator to generate either a lead term or an integration. In the actual experiment, the controlled element proper had a transfer function K/s^3 , while the effective controlled element, as seen by the pilot, could be adjusted to take either the form

$$\frac{K(T_1s + 1)(T_2s + 1)(T_3s + 1)}{s^3}$$

or K/s^3 .

In the referenced experiment a four-coordinate tracking task was employed. The subject manipulated two joysticks to keep within view two target data on a two-gun cathode ray tube. Each dot was free to move in both the vertical and horizontal directions.

"Painted in white outline on the face of the cathode-ray tube are two adjacent 2-inch squares which served as the boundaries of the tracking area. To position the spot horizontally within the left square, the subject manipulated the left stick and made left-right movements, while for vertical positioning, the same stick was moved back and forth. The spot could also be moved from any position within the square back to center directly by a movement which is the vector sum of the horizontal and vertical components. The right stick provided similar control over the spot within the right square. The subject's forearms were supported by armrests while tracking.

"In a remote room, an EASE (Electronic Analogue Simulating Equipment) computer was used to simulate the control system which included the three cascaded integrators in each channel (horizontal and vertical for both sticks). The experimenter sat in this room to observe and record the subject's performance on two cathode-ray monitoring scopes.

"Four experimental conditions were used. The conditions may be described as follows:

- Condition A.** Simulated system output is presented directly to the subject who operates in one channel. Only the spot in the left square moves and this only in the horizontal direction. It is controlled by left-right movements of the left joystick.
- Condition B.** Again, unmodified system output is presented directly to the subject, but in this condition he operates in two channels. Movement of the left spot, both horizontal and vertical, is controlled respectively by left-right and back-and-forth movement of the left joystick.
- Condition C.** The subject again operates in two channels with system output presented directly. The left spot is free to move only horizontally and the right spot only vertically. Left-right movement of the left joystick controls the left spot, while back-and-forth movement of the right joystick moves the right spot.
- Condition D.** In this condition all four channels are in operation. The system output is not presented directly, but instead the display had the lead terms added. In each channel the position of the spot is a function, not of system output alone, but of output plus terms obtained from joystick displacement and from each of the intermediate integrators.

"The subject's task was to hold system output at its initial value. Noise in the system and slight initial displacements of the control stick from center caused the spot to drift out of the field in 5 to 15 seconds if the operator did not attempt to hold it." [These two inputs were the only forcing function sources.]

"The subject was instructed to manipulate the stick (or sticks) so as to keep the spot(s) within the square(s) on the cathode-ray-tube face. A time-on-target score was used as the index of performance. The experimenter selected the appropriate condition and told the subject which task he was to perform. The experimenter signalled to the subject that the computer switch was closed, and started a stopwatch. The subject tracked until either (a) a spot drifted outside the boundaries of the square, or (b) two minutes of time elapsed. The subject's score was taken as the number of seconds that the spot was held within the prescribed square(s)."

The results show that a majority of the subjects were able to perform the task perfectly with added lead terms. Without the added lead terms these same subjects were never able to control the dot in two dimensions, though some of the subjects learned, over a period of time, to exert sufficient control of the dot in one coordinate to materially increase their score.

This experiment indicates the general effect of allowing the operator to function as a simple amplifier and pure time delay (though whether he actually did so or not is not known, since describing functions were not measured). As such, it adds to that considerable body of data taken on specific tracking, fire control, flight control systems, etc. where "aided tracking", "quickenings", "null steering", "zero reading", etc. terms, (similar to the lead terms introduced here) added considerably to the precision of control. These experiments are all consistent with the Taylor-Birmingham hypothesis advanced earlier in this section that the operator should be allowed to operate with a transfer function Ke^{-Ts} .

Now that we have summarized the Taylor-Birmingham approach to the "preferred" operator characteristic problem it becomes appropriate to discuss possible modifications in the light of the data reviewed and presented in this report.

First, with regard to the "optimum" operator form, it appears that some modification may be desirable. There is little question that the required presence of lead terms in the operator transfer characteristic is connected with an increase in the remnant, and hence decreases the tracking precision. Direct evidence on this score is available from the Franklin and Russell data. To some extent, the Goodyear stationary simulator results also corroborate this statement, since on those tests the indifference threshold characteristic was associated with the presence of the lead term in the operator. Based upon all of these data, then, we can conclude that the "preferred" operator form should contain no lead equalization.

In the general case with finite bandwidth forcing functions, the need to do away with a low frequency operator lag appears questionable. For example, in Russell's data with variable controlled elements, he showed that the very best performance, in terms of rms tracking error, in all his tests occurred when a filter having a transfer function of $1/(Ts + 1)$ was inserted in the postfilter location (to smooth the high frequencies of the remnant power), and then a lead-lag of $(Ts + 1)/(Ts + 10)$ in the prefilter position to cancel out the lag introduced by the postfilter. The net controlled element transfer function, for a $T = .5$ seconds, was $Y_c = 1/(.05s + 1)$. This controlled element transfer characteristic was shown in other tests to be effectively that of a simple tracker. The human transfer characteristic which existed with this controlled element configuration is best approximated by $Y_p = K_p e^{-T_p s} / (T_I s + 1)$,* and the mean square error was reduced about a factor of two below that of the simple tracker. In addition to these data, Russell also showed that insertion of a lag in the controlled element characteristic (to effectively "replace" the operator's lag T_I), with or without a lead in the controlled element, resulted in more output noise power than was the case with $Y_c = 1$. From these data we are led to suggest:

* The form for Y_p which we have specified is the simplest reasonable form. Were we to strive for a more general form we would choose either Equation (V-40): $Y_p = \frac{Ke^{-T_p s}(aT_I s + 1)}{(T_I s + 1)}$ or Equation (V-42): $Y_p = \frac{Ke^{-T_p s}(T_I s + 1)}{(T_I s + 1)(T_H s + 1)}$. In most cases, the choice is a matter of taste (see footnote to the discussion following Equation (V-40) in Section V), and the presence of lead terms is not strongly supported by the data.

(1) A low frequency operator lag term is desirable, at least when a forcing function is present. Further, interpreted in terms of "effective" desirable controlled element characteristics, the above data also support the premise that:

(2) The overall controlled element transfer characteristic should appear to be somewhere between

$$1 \leq Y_c \leq \frac{1}{0.05s + 1} \quad (X-4)$$

(3) The postfilter can be made effective as a filter to attenuate high frequency remnant power. This will probably be most effective in those instances where a dither signal is an important aspect of the remnant.

The above suggested modifications to the "simple amplifier" preferred form is a relatively minor change. On the other hand it should be stated that consideration of forcing function effects on the remnant can result in much more important modifications. Much of the background for the Taylor-Birmingham thesis was based upon forcing functions which were either non-existent or composed of extremely low frequency components. We can, however, consider the modifications imposed upon the preferred model by higher frequency forcing functions by the following reasoning:

(1) The modified preferred operator model should be of the form $Ke^{-Ts}/(T_I s + 1)$; or alternatively, the effective controlled element should be essentially a perfect tracker.

(2) Under these conditions, we can resort directly to Elkind's data to find the effects of forcing function.

Following these points through, we can see from Figure 30 that it is desirable to have as low a bandwidth forcing function as possible, and further that the rms error expected will be approximately proportional to the square of the effective forcing function bandwidth. If we would prefer to establish "good" low frequency system response to the forcing function as a criteria, i.e. high dc gain, we would like to restrict the forcing function bandwidth to some value somewhat less than that equivalent to a rectangular forcing function spectra cutoff of 0.64 cps. [This is based, of course, upon the somewhat arbitrary criterion that a dc gain of 15 db or so yields "good" low frequency response of a system having the overall open-loop transfer function $Ke^{-Ts}/(T_I s + 1)$.] In any event, by accepting the above modifications to the preferred form, one can use Elkind's data directly to get a firm notion of the best expected system performance.

With regard to the rest of the Birmingham-Taylor design procedure, it can be considered to be generally valid if the above preferred form and forcing function comments are inserted. This leads us to the following suggested design procedure:

1. Adjust* the effective controlled element transfer function to that of a simple tracker, i.e. within the limits (exclusive of gains):

$$1 \leq Y_c \leq \frac{1}{0.05s + 1} \quad (X-4)$$

a. In this adjustment due care should be taken to filter as much of the operator high frequency remnant power as is possible in the circumstances.

b. The arrangement of equalizing elements, etc. used in modifying the initial controlled element to that of the form above should be such that the operator input bandwidth is as small as practicable.

* The term "adjustment" as used here means the addition of equalizing devices into the system in such a way as to make the effective controlled element the form shown above. These equalizing means can consist of series or parallel compensating networks, additional loop closures, etc. These are all straightforward servo techniques, and need not be discussed here.

2. The human transfer characteristic will then be of the approximate form:

$$Y_p = \frac{K_p e^{-\tau s}}{(T_1 s + 1)(T_{hs} + 1)}$$

a. When the actual system forcing function is put into the form of an "effective" forcing function operating on a simple tracker system (which can be done with the aid of a little block diagram algebra), then the "effective" forcing function spectra can be found. Using Elkind's data as approximations to this forcing function, upper bound estimates for K_p and $1/T_1$ can be made from the forcing function spectral characteristics.

b. The remnant characteristics can also be estimated using either of the remnant models previously fitted to Elkind's data to obtain lower limits for the remnant power.

3. Using these items of information, the system performance can be estimated in detail by normal servo methods. The quantities obtained will always be optimistic since the basic (Elkind) operator data used in the analysis is probably an upper limit of human performance.

The approach outlined above is our best estimate of preferred operator forms extended to a rational design procedure. It would not be realistic, however, to assert that the procedure should be used indiscriminately. There are several possible pitfalls that should be mentioned. The first, and most obvious one, is that of application to areas beyond those where the fundamental assumptions used in the derivation of the model are valid. For example, the system should be one where the operator is continuously tracking only visual inputs on his display, and other inputs (including those effectively "set" into the operator by past experience), must be negligible. The second pitfall is commonly encountered in servo practice, and involves the problem of system reliability and over-complication. As an example consider the case of a human pilot-airframe system, where, of course, inputs "set" into the operator are not negligible in general, although we may disregard them in special instances. The effective controlled element transfer function, i.e., the equivalent airframe, can be put, at least approximately, into the form where $Y_c \approx 1$. This could be done by judicious design of artificial feel systems, stability augmenters, and compensation of various sorts in a display. Presumably everything would be satisfactory and a relatively naive operator could "fly" the aircraft quite well. However, the instant some element of the system fails, all bets are off, —the effective controlled element is no longer approximately free of dynamics, and the possible overall effects could be catastrophic. On this same point, we should further note that the application of this design procedure can often result in an overdesigned system. An important matter of judgment is the ability to recognize when a control system is good enough.

Section XI

COMPARISON OF COMPENSATORY AND PURSUIT TRACKING

A. INTRODUCTION

In the body of this report we have limited our discussion almost exclusively to compensatory tracking. The reasons for this are: firstly, most manual control devices of practical importance embody a compensatory display; secondly, most previous research concentrated on compensatory displays; thirdly, it is extremely difficult to measure open loop describing functions in pursuit tracking, and this has not yet been done.

In Section I we presented a discussion of pursuit and compensatory tracking. As can be noted by referring to the block diagrams in Figures 3a and b, the basic difference between pursuit and compensatory tracking (in the framework of a linear model), is that the operator generates one describing function, Y_p , which operates on $E(s)$ in the case of a compensatory display; and two describing functions, Y_{p1} , which operates in $I(s)$, and Y_{p2} , which operates on $E(s)$, for the pursuit display. This additional describing function provides the operator with the opportunity to improve his adaptive and optimizing behavior. Equations (I-1) and (I-2), which are repeated here (as (XI-1) describing compensatory tracking and (XI-2) for pursuit tracking), indicate how both $C(s)$ and $E(s)$ may be modified by the availability of two describing functions instead of just one.

$$\begin{aligned} C(s) &= \frac{Y_p(s) I(s) + N_c(s)}{1 + Y_p(s) Y_c(s)} \\ E(s) &= \frac{I(s) - Y_p(s) N_c(s)}{1 + Y_p(s) Y_c(s)} \end{aligned} \quad (XI-1)$$

$$\begin{aligned} C(s) &= \frac{[Y_{p1}(s) + Y_{p2}(s)] I(s) + N_c(s)}{1 + Y_{p2}(s) Y_c(s)} \\ E(s) &= \frac{[1 - Y_{p1}(s) Y_c(s)] I(s) - Y_c(s) N_c(s)}{1 + Y_{p2}(s) Y_c(s)} \end{aligned} \quad (XI-2)$$

B. COMPENSATORY VERSUS PURSUIT TRACKING WITHOUT HUMAN DYNAMICS MEASUREMENTS

The possibilities implicit in Equation (XI-2) have been sensed on a more intuitive level by Poulton, Senders and Cruzan, Chernikoff et al., and others, and many experiments using various forms of average error criteria were performed [17, 18, 19, 63, 64, 72]. Poulton demonstrated [64] that the tracking of a compensatory display error alone could be improved considerably by adding a pointer driven by $i(t)$, the forcing function input. The addition of a pointer driven by $c(t)$, the operator's output, had no significant effect. Senders and Cruzan [72] conducted an ingenious experiment to compare pursuit and compensatory tracking as well as contrived combinations of the two. Pursuit tracking was always better, and the reason given was that the display provided more information on which the operator could base predictive actions. This is, of course, a verbal statement of the meaning of Fig. 3b, and Equation (XI-2). A series of recent reports by the engineering psychologists of the Naval Research Laboratory has been devoted to comparisons of pursuit and compensatory tracking for problems with and without dynamics, with different types of aiding, and with different course frequencies. Almost invariably pursuit displays have been associated with lower tracking errors. An interesting exception is presented in [82] for a course composed of three sine waves of frequencies approximately 0.28, 0.47, and 0.70 radians/second, and whose respective amplitudes were inversely proportional to these frequencies. The manual control was a flexible steel bar and the control element dynamics could assume one of the following forms:

$$\begin{aligned} (a) \quad Y_c &= 1 \\ (b) \quad Y_c &= \frac{1}{s} \\ (c) \quad Y_c &= \frac{0.5 s + 1}{s} \end{aligned}$$

The pursuit display resulted in less error for $Y_c = 1$, but the compensatory display was more accurate for $Y_c = 1/s$ and for $Y_c = (0.5s + 1)/s$. The essential reason advanced by Chernikoff et al. in Reference 19 for the superiority of compensatory tracking when Y_c assumed values (b) and (c) was that the introduction of the aiding dynamics made the task so simple that the subject needed no more information than was provided by the error signal alone. The additional information in the pursuit display was deemed gratuitous, and, in fact, detrimental to the operator's performance. It is difficult for us to assess this situation in terms of the models essayed in this report since we do not have measures of either describing functions or error spectra for the NRL data presented in Reference 19. Chernikoff et al. make the procedural point that many pursuit vs. compensatory tracking comparisons are not adequate since rarely are both displays used in an optimum fashion. Since, from a practical viewpoint, the compensatory display allows a greater error magnification for a display of given physical dimensions, and the pursuit display has the advantages inherent in Eq. (XI-2), it appears that tracking displays, either presently or in the near future, will emphasize an empirical mixture of compensatory and pursuit components. This is much as Poulton implied and Senders and Cruzan achieved.

C. COMPENSATORY VERSUS PURSUIT TRACKING WITH MEASURED HUMAN DYNAMICS

The only data on the comparison of compensatory and pursuit tracking from the viewpoint of human dynamics were obtained by Elkind [23]. The experiments of Elkind described in Sections V and VII were, save for one minor example, carried out for pursuit as well as for compensatory tracking. It is not our purpose to present Elkind's pursuit data in the same detail as the data for compensatory tracking. We will attempt to point up similarities and contrasts, and leave it to the reader to refer to the original source for further detail. Since the open loop pursuit system describing function would have been obtainable only after great difficulty, only closed loop functions are available.

In Section VII we summarized Elkind's findings on the variability of the closed loop describing function, $W(f)$, and relative Φ_{ff} and Φ_{nn} . Since there was essentially no difference in the conclusions of the variability study for compensatory tracking from the conclusions for pursuit tracking, the discussion in Section VII need not be extended in this section.

In Section V we presented the general experimental results for Elkind's experiments: II - Amplitude, III - Bandwidth, and IV - Shape. The pursuit tracking parallels for these experiments were procedurally identical except that the pursuit display enabled the subjects to track a 4.0 cps cutoff rectangular spectrum which was impossible with a compensatory display. We will discuss these experiments in order.

Experiment II — Amplitude

In Figure 148 mean closed loop describing functions for each of the three rms amplitudes 0.1, 0.32 and 1.0 inches rms are shown. This figure is the comparison piece to Figure 28. Several differences are obvious. The phase lag for the pursuit tracking is much less than for compensatory tracking, and the magnitude of $H(f)$ increases sharply with frequency in the pursuit case as against a mild increase for compensatory tracking. These two observations indicate that the human operator is acting as a predictor, and this behavior characterizes pursuit tracking. Also, the extent of the invariance of the closed loop describing function $H(f)$ with input amplitude is not as great for pursuit tracking as it was for compensatory tracking. For pursuit, we are limited to a measured 10 db range from 0.3 to 1.0 inches rms, as compared to the measured range of 20 db for compensatory tracking. There is reason to believe that these ranges may be extended on the high end. A perceptual problem in extracting the derivative of $i(t)$ for very small amplitudes may be at the root of this. We cannot blame a manipulatory response for the difference in the response to the 0.1 inches rms amplitude input since the manual tracking responses for compensatory and pursuit are the same.

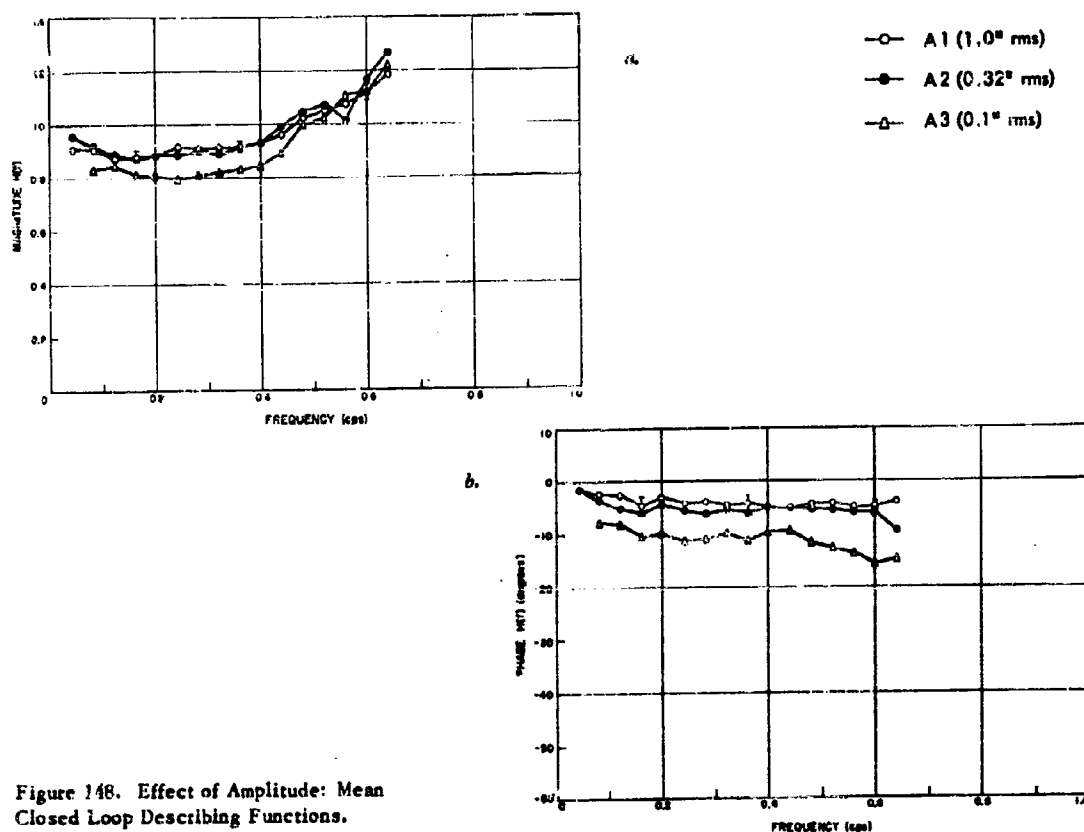


Figure 148. Effect of Amplitude: Mean Closed Loop Describing Functions.
(Reference 23, Fig. 4-6 a, b.)

Experiment III — Bandwidth

These results (see Section V and Reference 23) may be summarized as follows. Figure 149 presents a comparison of compensatory and pursuit tracking closed loop describing functions for rectangular spectra forcing functions of cutoff frequencies from 0.16 to 0.96 cps. Figure 150 presents a similar comparison for cutoff frequencies from 0.96 to 2.4 cps in compensatory tracking, while in pursuit tracking the upper end was pushed to 4.0 cps by the subjects. As was noted before, the pursuit describing functions indicate the presence of a lead term in the tracker's output.

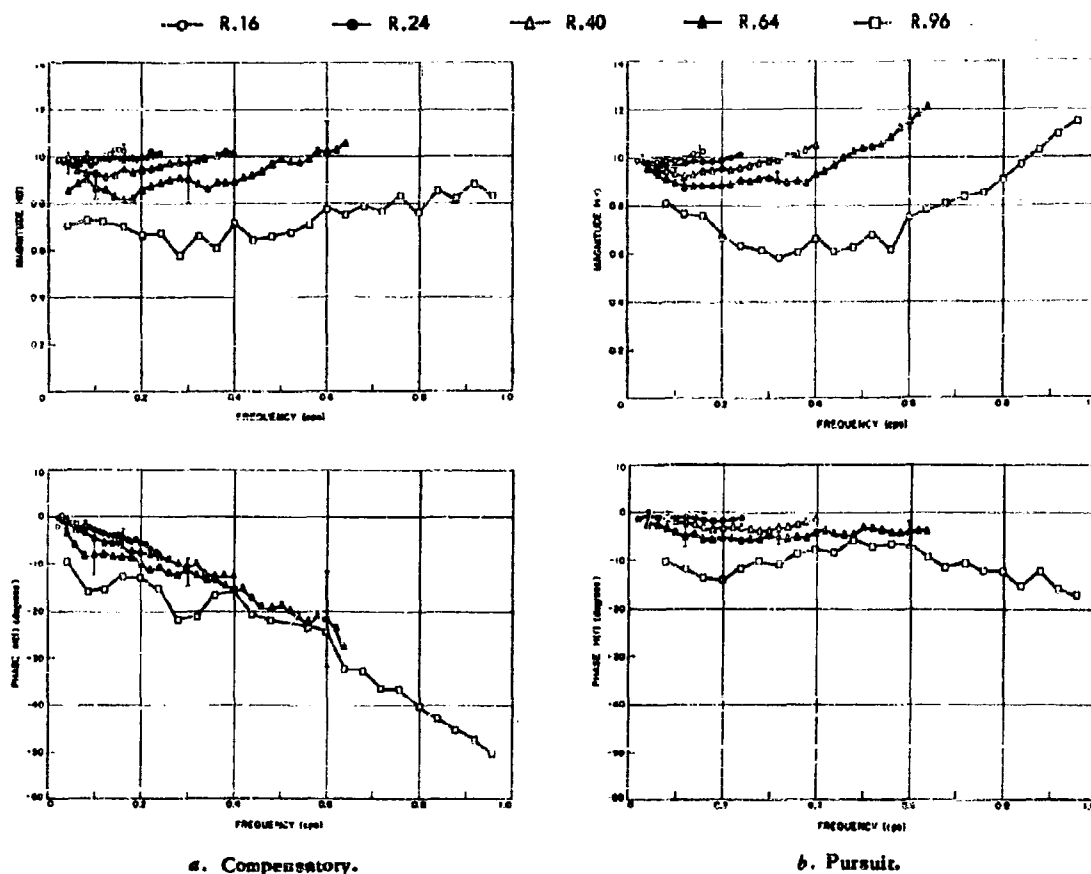


Figure 149. Comparison of Closed-Loop Describing Functions for Bandwidth Experiment.
(Reference 23, Figures 4-7 a, b and 4-9 a, b.)

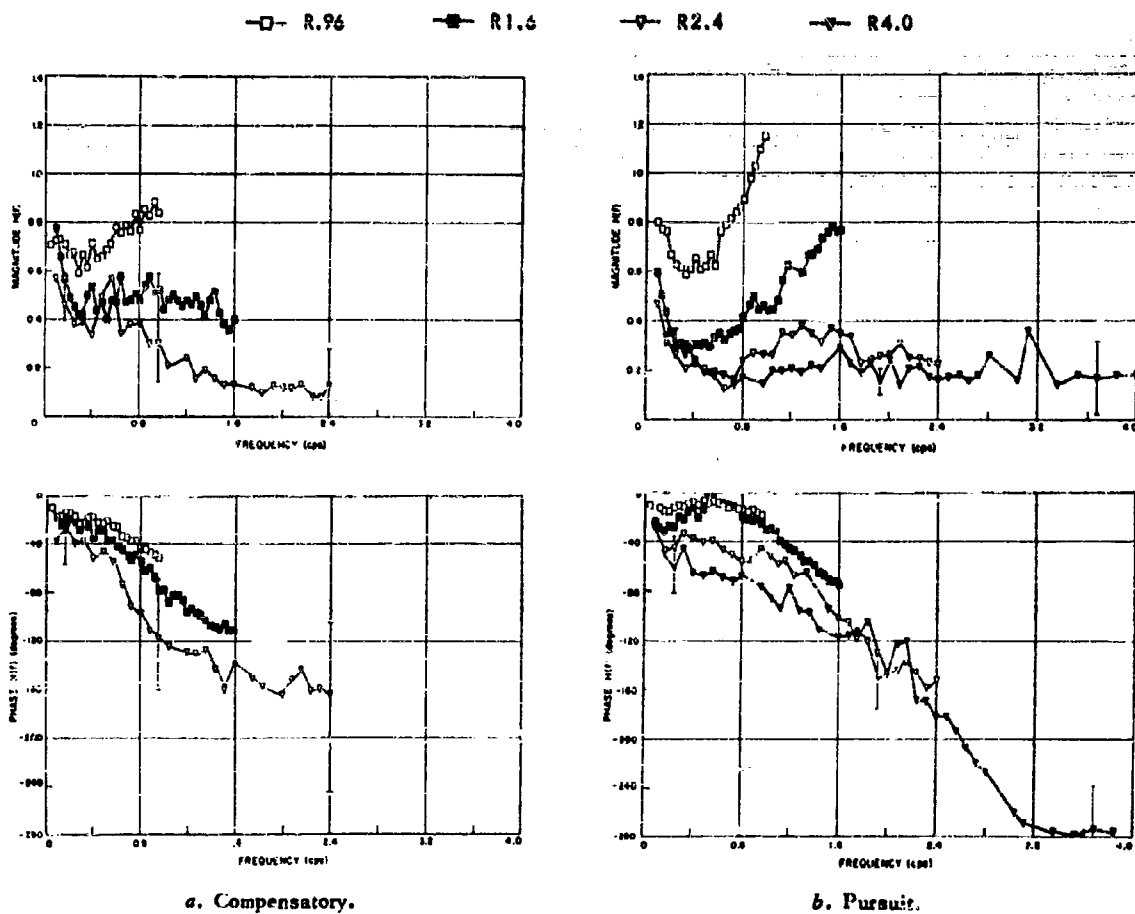


Figure 150. Comparison of Closed-Loop Describing Functions for Bandwidth Experiment.
(Reference 23, Figures 4-8 a,b and 4-10 a,b.)

Experiment IV — Shape

The describing function obtained with the set of RC filtered input spectra and the rectangular spectrum (see Figure 27) are presented in Figure 151. The differences between the describing function for the two displays are in the same direction as we might expect after seeing the previous data. Similarly an examination of selected band and band reject spectra demonstrates the lower phase lag, and greater closed loop gain, of the pursuit display. The most striking demonstration of the prediction ability of the human operator is obtained with the bandpass inputs, B-7 through B-10. As Elkind notes, bandpass random signals closely resemble a carrier modulated in both amplitude and phase by random noise. In pursuit tracking the human operator can extract this carrier from the input, as it were, and synchronize his response with it. The compensatory display does not allow such predictive ability. Figure 152 illustrates this effect.

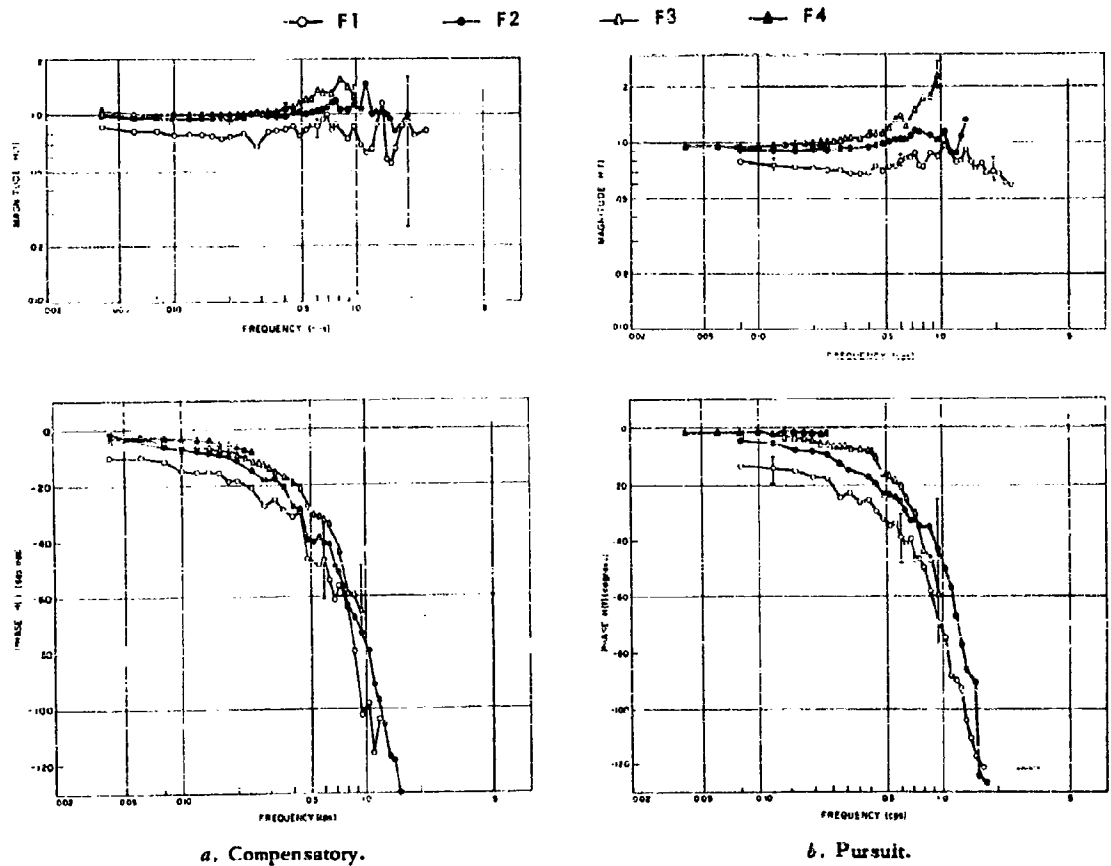
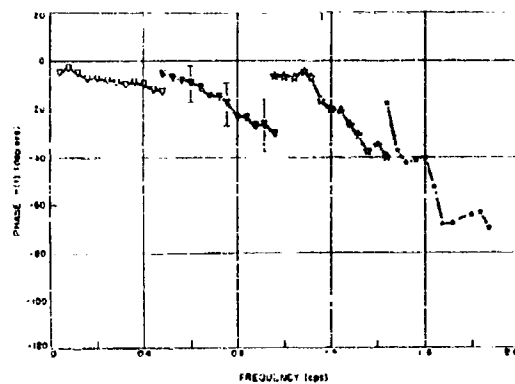
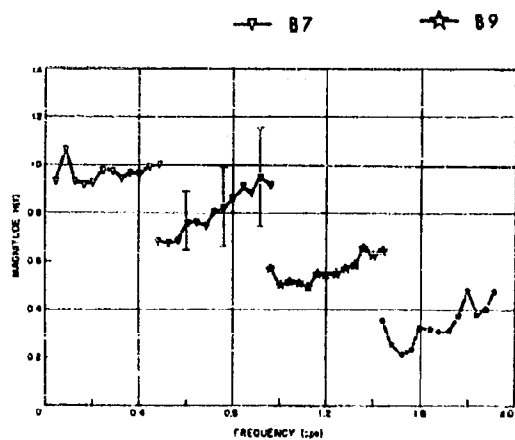
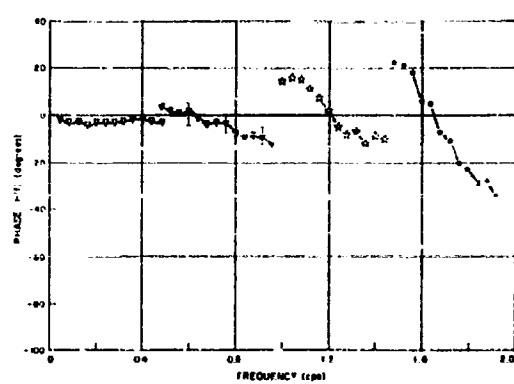
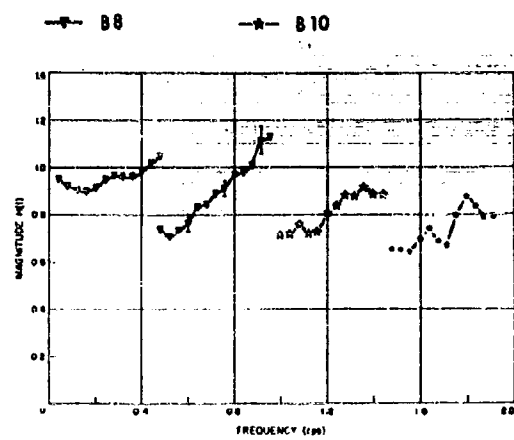


Figure 151. Comparison of Closed-Loop Describing Functions for Shape Experiment.
(Reference 23, Figures 4-13 a,b and 4-14 a,b.)



a. Compensatory.



b. Pursuit.

Figure 152. Comparison of Closed-Loop Describing Functions for Shape Experiment, Selected Bands.
(Reference 23, Figures 4-19 a,b and 4-22 a,b.)

Linear Correlations and Error Spectra

Save for an exception in Experiment III for input R2.4, the error spectra for pursuit tracking had lower values than the corresponding spectra for compensatory systems. The linear correlation squared, ρ^2 , was somewhat smoother and higher for the pursuit system than for the compensatory system but there were no striking differences.

In Experiment II the 0.1 inches rms amplitude run of Figure 153 was evidently different from the other inputs in the experiment. Figure 154, a comparison piece to Figure 52, illustrates the deterioration in ρ^2 as the task difficulty increases.

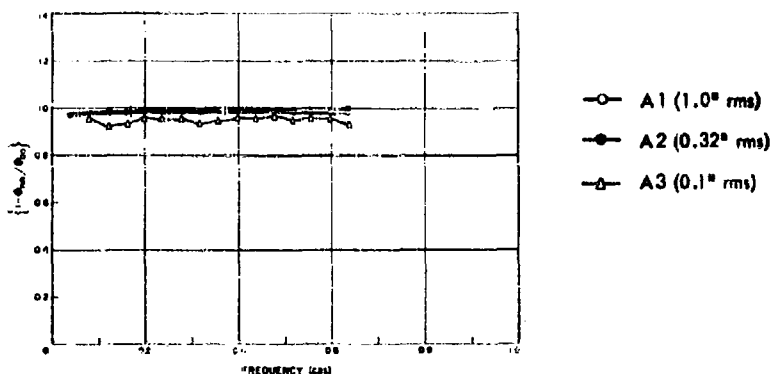


Figure 153. Linear Correlation Squared for Study of an Input Amplitude.
(Reference 23, Figure 4-6c.)

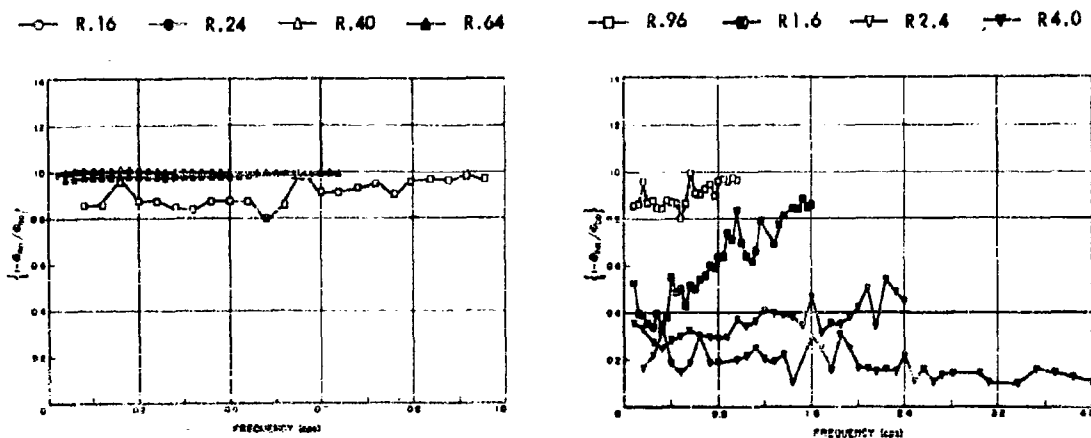


Figure 154. Linear Correlation Squared for Study of Bandwidths.
(Reference 23, Figures 4-7c and 4-10c.)

Models

As can be seen from Equation (XI-2) and Figure 3a, the extraction of Y_{p_i} and Y_{p_e} is an experimental problem. Elkind suggests the following technique, but understandably he did not carry it out. The method suggested is to add to $e(t)$ a second noise input $i_2(t)$ which is statistically independent of $i(t)$, having a spectrum similar to $\Phi_{ii}(\omega)$, and a small amplitude. Presumably, this additional input signal would not change the operator's pursuit tracking characteristics. Using Equation (III-52), measuring the power spectrum Φ_{ii} , and Φ_{ie} , it would be possible to obtain Y_{p_i} . From Y_{p_e} and the closed loop describing function $H(\omega)$, obtained from (XI-2),

$$H(\omega) = \frac{Y_{p_i} + Y_{p_e}}{1 - Y_{p_i} Y_{p_e}} \quad (\text{XI-3})$$

it would be possible to compute Y_{p_i} .

Elkind has associated a prediction element with Y_{p_i} and in his notation $P_i G_i = Y_{p_i}$, and $P_i G_2 = Y_{p_e}$ (see Figure 155, which is equivalent to Figure 3b). He then proceeded to construct a reasonable G_i from step responses, using the \log_e , τ , measured in compensatory tracking. G_2 then was approximated by the describing function of the compensatory system. Using a minimum mean square error criterion and the following assumptions:

- (a) the human operator makes use of only input displacement and velocity to predict the input;
- (b) the human operator does not consider his own noise when establishing an optimum P_i ;
- (c) G_2 can be neglected when computing P_i .

Elkind was able to approximate P_i by $P_i(f) = b_0 + b_1(2\pi jf)$, which only applies to low frequencies.

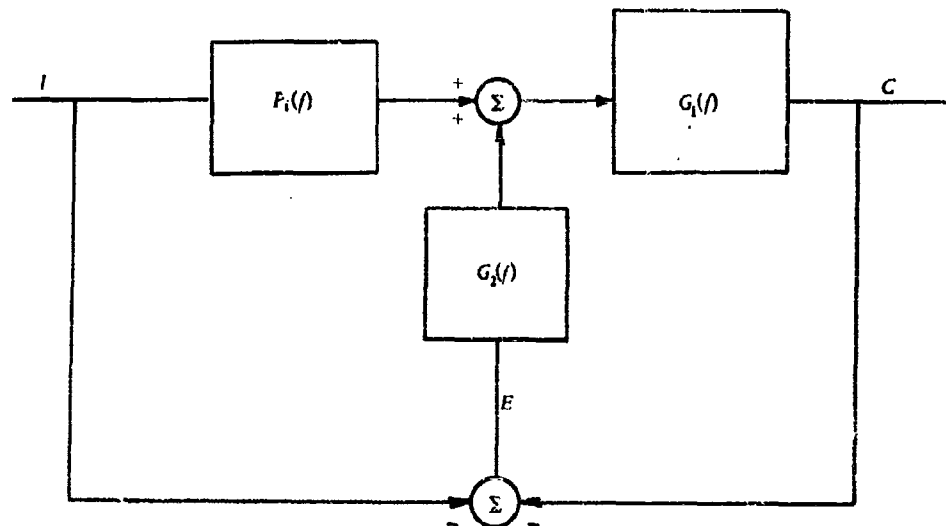


Figure 155. Pursuit Tracking Configuration with Unity Controlled Element Dynamics.
(Reference 23, Figure 5-10.)

Within the limits of these assumptions, i.e., in particular a simple tracking task, and $G_2 \approx 0$, the equation of $P_1 G_1$ to H produces a good fit for the RC filtered input, F_1 . Considering the tenuous assumptions, the other fits were surprisingly good. Usually, the prediction demonstrated by the human operator falls short of the mean square optimum; and it is postulated that noise in the visual process causes this degradation. Since there are no direct measurements of the describing function associated with pursuit tracking, further elaboration is tenuous at this time.

Our summary statement on pursuit tracking could be no more than a repetition of the Elkind results which clearly demonstrate the advantages, and limits, of the human operator's predictive abilities, the resulting phase response, and the attendant overall improvement in performance.

REFERENCES

1. Abelson, R. P.; *Spectral Analysis and the Study of Individual Differences in the Performance of Routine, Repetitive Tasks*; Ph.D. Thesis Princeton Univ. 1953, ONR Project NR 150-088, Educational Testing Service Res. Bulletin 53-2, March 1953.
2. Barnes, G. H.; *Data Reduction Equipment for the Analysis of Human Tracking*; Franklin Institute Report F-2333, AF 33(616)-270, May 1953.
3. Barnes, G. H.; *A Cross Spectrum Analyzer*; WADC TR 55-445, November 1955.
4. Bartlett, M. S.; *Periodogram Analysis and Continuous Spectra*; Biometrika, Vol. 37, 1950.
5. Benepe, O. J., Narasimhan, R. and Ellison, D. G.; *An Experimental Evaluation of Harmonic Analysis to the Tracking Behavior of the Human Operator*; Indiana Univ., TR-53-384, WADC, May 1954.
6. Birmingham, H. P. and Taylor, F. V.; *A Human Engineering Approach to the Design of Man-Operated Continuous Control Systems*; NRL Report 4333, 7 April 1954.
7. Birmingham, H. P., Kahn, A., and Taylor, F. V.; *A Demonstration of the Effects of Quickening in Multiple-Coordinate Control Tasks*; NRL Report 4380, 23 June 1954.
8. Blackman, R. B.; *Introduction to Spectra of Time Series*; Bell Telephone Laboratories; August 1951.
9. Booton, R. C. Jr.; *Nonlinear Control Systems with Statistical Inputs*; MIT DACL Report No. 61, March 1952.
10. Booton, R. C. Jr.; *The Analysis of Nonlinear Control Systems with Random Inputs*; Proceedings of the Symposium of Nonlinear Circuit Analysis, Brooklyn Polytechnic Institute, April 1953.
11. Booton, R. C. Jr., Seifert, W. W., and Mathews, M. V.; *Nonlinear Servomechanisms with Random Inputs*; MIT DACL Report No. 70, August 1953.
12. Booton, R. C. Jr.; *Nonlinear Control Systems with Random Inputs*; Trans. of the IRE PGCT, Vol. CT-1, No. 1, March 1954.
13. Booton, R. C. Jr.; *The Measurement and Representation of Nonlinear Systems*; Trans. of the IRE PGCT, Vol. CT-1, No. 4, December 1954.
14. Chaffin, D. L. C.; *A Study of the Characteristics of Human Pilot Control Response to Stimulated Aircraft Lateral Motions*; NACA RM L52C17, May 1952. Superseded by NACA Report 1197, same title, 1954.
15. Chen, K.; *Quasi-Linearization Techniques for Transient Study of Nonlinear Feedback Control Systems*; Trans. AIEE, Part II, Applications and Industry, No. 22, January 1956.
16. Chemikoff, R. and Taylor, F. V.; *Reaction Time to Kinesthetic Stimulation Resulting from Sudden Arm Displacement*; NRL Report 3387, November 19, 1951.
17. Chemikoff, R., Birmingham, H. P., and Taylor, F. V.; *A Comparison of Pursuit and Compensatory Tracking under Conditions of Aiding and No Aiding*; J. exp. Psychol., 1955, 49, 55-59.
18. Chemikoff, R., Birmingham, H. P., and Taylor, F. V.; *A Comparison of Pursuit and Compensatory Tracking in a Simulated Aircraft Control Loop*; J. appl. Psychol., 1956, 40, 47-52.

19. Chernikoff, R. and Taylor, F. V.; *Effects of Course Frequency and Aided Time Constant on Pursuit and Compensatory Tracking*; Journal of Experimental Psychology, 1957, Vol. 53, No. 5.
20. Craik, K. J. W.; *Theory of the Human Operator in Control Systems*; British Journal of Psychology, Vol. 38, Parts 2 and 3; December 1947 and March 1948.
21. Davis, R.; *The Limits of the "Psychological Refractory Period"*; Quarterly Journal Exp. Psychology, VIII, pp 24-38, February 1956.
22. Elkind, Jerome I.; *Tracking Response Characteristics of the Human Operator*; Human Factors Operation Research Laboratories Report HFORL Memo No. 40, PEP-2; September 1953.
23. Elkind, Jerome I.; *Characteristics of Simple Manual Control Systems*; Technical Report No. 111; MIT Lincoln Laboratory; April 6, 1956.
24. Ellson, D. G. and Gray, F.; *Frequency Responses of Human Operators Following a Sine Wave Input*; Memo Report MCRN 694-28, USAF AMC, 1949.
25. Ellson, D. G. and Hill, H.; *The Interaction of Response to Step Function Stimuli: 1. Opposed Steps of constant Amplitude*; AMC Memorandum Report No. MCRN 694-29, November 19, 1948.
26. Ellson, D. G., and Wheeler, L.; *The Runge Effect*; AF Technical Report 5813, May 1949.
27. Ellson, D. G.; *The Application of Operational Analysis to Human Motor Behavior*; Psychology Review, 57, pp 9-17, 1949.
28. Epple, R. G. E.; *The Human Pilot Response to Aircraft Input Devices*; Report AF-4011, August 1954.
29. Fenn, W. O.; *The Mechanics of Muscular Contraction in Man*; J. Appl. Physiol., 1948, pp. 11-17.
30. Garvey, W. D. and Mitnick, J. L.; *An Analysis of Tracking Behavior in Terms of Lead-Lag Error*; NRC Report 4707, 16 February 1956.
31. Glasman, L.; *A Dynamic Model of the Human Operator in a Control System*; Report of the AF Pilot School, 1954.
32. *A Proposal to Study the Dynamic Characteristics of the Human Operator in a Control System*; Goodyear Aircraft Corp., Report No. GER-3006-A; May 1952.
33. *Final Report: Human Dynamic Study*; Goodyear Aircraft Corp. Report No. GER-4750, April 8, 1952.
34. *Investigation of Vestibular and Body Reactions to the Response of a Human Operator*; Final Report; Report GEP-3352, 15 November 1953.
35. *Investigation of Control "Feel" Effects on the Response of a Human Operator*; Report of a Pilot School; Corporation Report GER 6726; 21 April 1954.
36. Greenwood, I. A., Holdam, J. V., and MacRae, P.; *Dynamic Instruments*; McGraw-Hill, pp. 194, 1948.
37. Grenander, U. and Rosenblatt, M.; *Comments on the Spectral Analysis of Human Behavior*; Swedish Akustikskrift, Haft 3-4, pp. 187-202, 1953 (in English).
38. Grenander, U. and Rosenblatt, M.; *Statistical Analysis of Human Behavior*; John Wiley & Sons, New York, 1957.